

**Dynamics of Sperm Maturation Markers and  
Capacitation in Relation to Hyaluronic Acid Binding**

**Forough Torabi Baghkomeh**

Submitted in accordance with the requirements for the degree of  
Doctor of Philosophy

The University of Leeds  
School of Medicine

August 2017

## Statement

The candidate confirms that the work submitted is her own, except where work which has formed part of jointly authored publications has been included. The contribution of the candidate and the other authors to this work has been explicitly indicated below. The candidate confirms that appropriate credit has been given within the thesis where reference has been made to the work of others.

The work in Chapter two and five of the thesis have appeared in publication as follows:

- Sedimentation properties in density gradients correspond with levels of sperm DNA fragmentation, chromatin compaction and binding affinity to hyaluronic acid, 2016, Torabi, F. Binduraihem, A. Miller, D. *Reprod Biomed Online* 34 (3), 298-311.
- Zona pellucida-binding protein 2 (ZPBP2) and several proteins containing BX7B motifs in human sperm may have hyaluronic acid binding or recognition properties, 2017, Torabi, F. Bogle, OA. Estanyol, JM. Oliva, R. Miller, D. *Mol Hum Reprod* 1; 23 (12): 803-816.

The candidate, Forough Torabi Baghkomeh, was responsible for the concept and design of the study, undertook the vast majority of the work that appeared in the publication, statistical analysis, writing of the manuscript and correction checking. Binduraihem A assisted with the optimisation of Acridine Orange staining and helping with some statistical analysis in the first publication.

Bogle OA, Estanyol JM and Oliva R were responsible for optimising and running the LC-MS/MS process used for the proteomic aspects of this study.

David Miller contributed to the concept and design of the study, supervised the laboratory work, reviewed and provided critical reading of the manuscript. He is also a participant in the Marie Curie ITN, 'Reprotrain' and is a NIHR-EME grant holder.

This copy has been supplied on the understanding that it is copyright material and that no quotation from the thesis may be published without proper acknowledgement.

© 2017 The University of Leeds and Forough Torabi Baghkomeh

## **Acknowledgments**

My work would not have been possible without the support and advice of a number of people from within the University of Leeds, and from outside organisations.

I would firstly like to thank Dr David Miller. He has provided me with so much support, not only with my research but also in settling into a new city, university and country. Without the essential support that he has provided over the last four years it would not have been possible to complete this project. The kindness, support and trust that Dr Miller has shown, enabled me to develop both personally and professionally, for which I will always be eternally grateful.

My co-supervisor Prof Paul Millner, was always on hand to provide additional guidance and support when I needed it. He was also a great support during the early stages of my study in Leeds.

I wish to thank Dr Orleigh Bogle and Dr Rafael Oliva for their continuous support in relation to my secondment in at the University of Barcelona.

I would like to thank Dr Gisela Lorente Marina, Dr Adel Binduraihem, Panagiotis Ntostis, Dr Chutima Topipat, Erika Berenyi, Dr Roberto de la Fuente Pita, who have supported the scientific progress of this project by assisting in answering questions and queries that I have raised. Additionally, they all supported my personal happiness with a friendly and supportive atmosphere which has been important for my academic development.

I am also appreciative of the support that I have received from the members of the Reproduction and Early Development group at the University of Leeds; Prof Helen Picton, Dr John Huntriss, Dr Jianping Lu, Dr Karen Forbes, Dr Niamh Forde, Dr Paul McKeegan, Dr John Dalton, Riitta Partanen, Philip Warburton and Christina Coll. The positive atmosphere they created was a real benefit to my work.

I would like to thank my postgraduate tutor Karen Porter for all of the support and advice that she has provided during the course of this project. She has always made time for the queries that I have raised for which I am grateful.

I would not have been able to take up this position within the University of Leeds, had it not been for the significant support from the European Commission, the Marie Skłodowska-Curie actions and the Reprotrain network. I am grateful for the faith they placed in me and the opportunity that they have given me.

I would have not been able to make it as far as I have, if it had not been for the amazing support of my family, especially whilst studying in Iran. My father was a real driving force behind my academic progression and I would never have reached this point without his amazing support. When he passed away I lost one of the biggest influences in my life and without the support of my family I would not have been able to manage this alongside my work commitments. I will never forget the sacrifices that he made for me and the opportunities that I have had as a result of his hard work, his love and his support.

The daily support that I have received from my mother, brothers and sister have been unquantifiable. They have always been there for me both whilst in Iran and also whilst in the UK. I cannot begin to explain how much they mean to me and how much their love and support have helped me.

My fiancé Paul Harvey has been with me during this project and some of the most difficult personal circumstances of my life. Without his constant support I would not have been able to come through these and complete this project. His parents have also shown me such kindness and support for which I am so grateful.

I would also like to thank my best friends Zohreh Naeimi, Zahra Naeimi, Raziye Abooshahab and Azadeh Esfandiary. I am indebted to them for their continual positive support which has been a key factor in completing my PhD.

To all of those that have supported me, kept me focussed and helped me to relax, I am forever grateful. The love and support I have received from so many people has been really touching and is something that I will never forget.

## **Publications, oral presentations and posters from this thesis**

### **Publications**

- Torabi F, Binduraihem A, Miller D. Sedimentation properties in density gradients correspond with levels of sperm DNA fragmentation, chromatin compaction and binding affinity to hyaluronic acid. *Reprod Biomed Online* (2016).
- Zona pellucida-binding protein 2 (ZPBP2) and several proteins containing BX7B motifs in human sperm may have hyaluronic acid binding or recognition properties, 2017, Torabi, F. Bogle, OA. Estanyol, JM. Oliva, R. Miller, D. *Mol Hum Reprod* 1; 23 (12): 803-816.

### **Oral presentation**

- Identification of putative sperm Hyaluronic Acid Binding Proteins (HABPs) by mass spectrometry. British Andrology Society (BAS) Annual Meeting. June 2017. London, United Kingdom.
- A complementary relationship exists between sperm affinity for hyaluronic acid and sedimentation properties in density gradients as defined by sperm chromatin integrity. *Fertility* 2017. January 2017, Edinburgh.
- Capacitation affects the affinity of spermatozoa for hyaluronic acid (HA). BAS Annual Meeting. June 2016. London, United Kingdom.
- Dynamics of sperm maturation markers and capacitation in relation to HA binding. *Frontiers in male infertility research (In the Framework of REPRO-TRAIN, a Marie Curie Initial Training Network Funded by the European Commission under the 7th Framework Program)*. November 2015, Barcelona, Spain.
- Hyaluronic acid binding proteins in human and bovine sperm: relevance for ICSI. BAS Annual Meeting. July 2015. London, United Kingdom.

**Poster Presentations**

- Sperm affinity for hyaluronic acid relates to sedimentation properties in density gradients and to sperm chromatin integrity. European Society of Human Reproduction and Embryology (ESHRE) Annual Congress. July 2017. Geneva, Switzerland.
  
- Dynamics of hyaluronic acid (hyaluronan) binding proteins in relation to sperm capacitation and the acrosome reaction. Society for Reproduction and Fertility (SRF) Annual Congress. July 2015. Oxford, United Kingdom.
  
- Hyaluronic acid binding proteins in human and bovine sperm: relevance for ICSI. 5th Florence-Utah International Symposium on Genetics of Male Infertility. September 2013. Florence, Italy.

## **Abstract**

### **Introduction**

Mature spermatozoa recognise and bind hyaluronic acid (HA) in the extracellular matrix via Hyaluronic Acid Binding Proteins (HABPs). HA-binding may be important in supporting the sperms' progress in the female genital tract. Information on sperm HABPs is limited, however and the current study investigated their expression in human and bovine sperm.

### **Materials and methods**

The ability of differential density gradient centrifugation (DDGC) processed human sperm to bind HA was evaluated. DDGC sperm populations (90% and 45% fractions) and sperm interacting with HA were assessed for DNA fragmentation and chromatin compaction using acridine orange (AO) and aniline blue (AB) staining, respectively. Additionally, the effect of capacitation on HA-binding was assessed. Expression of HABPs in bovine and human sperm was also investigated alongside changes in their distribution following capacitation and the acrosome reaction. Proteomics was used to monitor changes in the human sperm proteome (including HABPs) following capacitation and the acrosome reaction. Following a protein panning procedure, proteomics was also used to help identify HABPs in both HA-binding and non-binding fractions. The presence of HA-binding motifs (BX7B and Link module, common in several well-known HABPs) was also evaluated in both fractions. Increasing the sensitivity of HABP isolation and detection was attempted using biotinylation of sperm surface proteins alongside HA-affinity chromatography.

### **Results**

Sperm recovered from 90% fractions had significantly higher HA-binding ability, lower levels of DNA fragmentation and higher levels of chromatin compaction. The reverse was true for sperm from the 45% fractions. HA-binding showed higher efficiency at selecting sperm with higher DNA integrity and chromatin compaction than DDGC. Capacitation enhanced HA binding, which may reflect associated changes in sperm HABPs. Immunocytochemistry localised CD44 to the acrosome and equatorial segment of non-capacitated human sperm and on the anterior acrosome and post-acrosomal sheath of non-capacitated bovine



sperm. CD44 was more confined to the equatorial segment following capacitation in human sperm and to the post-acrosomal sheath of bovine sperm. Acrosomal labelling of CD44 was highly reduced after the acrosome reaction. Hyaluronic acid-TRITC (tetramethylrhodamine isothiocyanate) labelled the sperm membrane and the neck region, particularly strongly after capacitation and in acrosome reacted bovine sperm.

Qualitative and quantitative characteristics of 121 proteins altered by capacitation and the acrosome reaction is also reported. Differentially regulated proteins are involved in sperm metabolism, energy production, cell signaling, sperm-oocyte recognition and sperm motility. Following capacitation, mass spectrometry (MS) detected an increase in cilia and flagella associated protein 20, containing two potentially HA-binding BX7B motifs. Analysis of the proteomics data from the panning fractions resulted in the identification of 28 proteins in HA-binding fractions with PDBsum and SAS server highlighting structural similarities between ZPBP2 (found only in HA-binding fractions) and the HA-binding domain of CD44. Data also showed that 50% of binding (including ADAM32 and cilia-and flagella associated protein 20 amongst others) and 34.5% of non-binding proteins contained BX7B motifs, indicating a likely selective enrichment of putative HABPs by the panning technique. Western blot analysis confirmed these results. Isolation of HABPs from bovine sperm using HA affinity chromatography followed by SDS PAGE revealed distinct protein bands of molecular masses 58 and 78 kDa, possibly corresponding to CD44 and RHAMM, respectively, were detected. Other protein bands detected at 16, 27, 38, 42 and 47 may be novel HABPs, including ZPBP2 (molecular mass 38 kDa).

## **Conclusion**

In conclusion, ZPBP2, ADAM32, Midkine and cilia and flagella associated protein 20 may have HA binding properties. This is also the first study which has brought together compelling evidence for the relationship between excising methods of enriching good quality sperm (DDGC) and HA-binding. Sperm DNA fragmentation and chromatin compaction status, therefore, reflects this relationship and supports claims for a positive sperm quality benefit for HA-based sperm selection particularly for ICSI, where the choice of sperm is more critical. In this regard, the use of more specific, anti-HABP-based methods for sperm

selection (initially targeting RHAMM, CD44 and SPAM1) should also be considered.

## Table of Contents

<b>Statement</b> .....	<b>II</b>
<b>Acknowledgments</b> .....	<b>II</b>
<b>Publications, oral presentations and posters from this thesis</b> .....	<b>VIII</b>
<b>Abstract</b> .....	<b>VIII</b>
<b>Table of contents</b> .....	<b>II</b>
<b>List of tables</b> .....	<b>XVIVII</b>
<b>List of figures</b> .....	<b>XVII</b>
<b>List of abbreviations</b> .....	<b>XX</b>
<b>Symbols</b> .....	<b>XXI</b>
<b>List of Appendices</b> .....	<b>XXII</b>
<b>Chapter 1: Introduction</b> .....	<b>1</b>
1.1. Physiology of male reproductive system and spermatogenesis .....	1
1.1.1. Mechanism of spermiogenesis .....	4
1.1.2. Sperm transport from seminiferous tubules to urethra .....	6
1.1.3. Acquisition of fertility potential by the sperm .....	7
1.1.3.1. Epididymal maturation .....	7
1.2. Capacitation .....	8
1.3. Acrosome reaction .....	11
1.4. Capacitation and acrosome reaction-related changes in the organisation of sperm surface antigens .....	13
1.5. Relationship between sperm structure and function .....	14
1.6. The hormonal control of male reproductive function .....	16
1.7. Sperm metabolism .....	17
1.8. Physiology of fertilisation .....	21
1.9. Male infertility .....	23
1.10. Routine sperm analysis and separation methods .....	24
1.10.1. Visual measurement of semen parameters .....	24
1.10.2. Differential Density Gradient Centrifugation (DDGC) .....	25
1.10.3. The Swim-up procedure .....	25
1.11. The need for improvements in the efficiency of ART .....	26
1.11.1. Development of ART .....	26
1.11.2. Limitations of ART and the importance of sperm selection using more advanced methods .....	27
1.12. Hyaluronic Acid (HA) .....	29
1.12.1. Structural properties, synthesis and cleavage of HA .....	29
1.12.2. Digestion of HA .....	30
1.12.3. Hyaluronic acid binding proteins (HABPs) .....	30
1.12.4. Hyaluronic acid, its binding proteins and their role in reproductive system ...	35
1.12.5. Pregnancy outcomes using sperm selection by HA-binding .....	41
1.13. Sperm DNA fragmentation and male infertility .....	43
1.14. Assessing sperm DNA fragmentation and chromatin compaction .....	46
1.14.1. Acridine orange assay .....	47
1.14.2. Terminal deoxynucleotidyl transferase mediated fluorescein-dUTP nick end labelling (TUNEL) .....	48
1.14.3. The sperm chromatin dispersion (SCD) assay .....	48
1.14.4. Comet assay .....	48
1.14.5. Aniline blue staining .....	49
1.14.6. Chromomycin A3 staining .....	49
1.15. Epigenetics and male (in)fertility .....	49

<b>Thesis hypothesis, aims and objectives .....</b>	<b>51</b>
<b>Chapter 2: Investigating relationships between DDGC-separated sperm and their corresponding levels of sperm DNA fragmentation, chromatin compaction and binding affinity to hyaluronic acid .....</b>	<b>52</b>
2.1. Introduction .....	52
2.2. Hypothesis and objectives .....	54
2.3. Materials and Methods .....	56
2.3.1. Reagents used.....	56
2.3.2. Patient Samples .....	56
2.3.3. Differential Density Gradient Centrifugation (DDGC) .....	56
2.3.4. Counting spermatozoa .....	57
2.3.5. Spermatozoa binding to HA-coated slides .....	57
2.3.6. Induction of capacitation .....	58
2.3.7. Evaluation of capacitation efficiency by induction of acrosome reaction .....	59
2.3.8. FITC- <i>Pisum sativum</i> Agglutinin (PSA) labelling .....	59
2.3.9. Assessment of hyperactive motility after capacitation .....	60
2.3.10. Changes in HA binding ability after capacitation .....	61
2.3.11. Isolation of HA-bound and unbound sperm.....	61
2.3.12. Acridine orange staining and quantitation .....	61
2.3.13. Aniline blue staining and quantitation .....	62
2.3.14. Statistical Analysis .....	65
2.4. Results .....	67
2.4.1. Semen analysis of volunteers contributing to this study.....	67
2.4.2. HA-binding affinity in pelleted (90%) and interface (45%) spermatozoa.....	67
2.4.3. Evaluation of capacitation using PSA-FITC labelling.....	68
2.4.3. Evaluation of capacitation using assessment of hyperactive motility .....	70
2.4.5. Changes in HA binding after capacitation .....	72
2.4.6. DNA fragmentation in spermatozoa recovered from DDGC fractions.....	73
2.4.7. DNA fragmentation in spermatozoa recovered from HA-bound and unbound populations .....	76
2.4.8. Chromatin compaction in spermatozoa recovered from DDGC fractions.....	79
2.4.9. Chromatin compaction in spermatozoa recovered from HA-bound and unbound populations .....	81
2.4.10. A comparison between DDGC and HA-binding assay in selecting sperm with less DNA fragmentation and high chromatin maturity .....	82
2.5. Discussion .....	85
2.6. Conclusion.....	88
<b>Chapter 3: Investigating the appearance of and changes in HABPs of human and bovine spermatozoa during capacitation and the acrosome reaction.....</b>	<b>89</b>
3.1. Introduction.....	89
3.2. Hypothesis and Objectives.....	91
3.3. Materials and methods .....	92
3.3.1. Reagents used.....	92
3.3.2. Human sperm preparation .....	92
3.3.3. Bovine sperm Preparation .....	93
3.3.4. Detection of sperm HABPs in sperm.....	94
3.3.4.1. Detection of sperm HABPs in PC3 cells.....	95
3.3.5. Evaluation of HABPs in human spermatozoa before and after capacitation...	95
3.3.6. Evaluation of HABPs in bovine spermatozoa before and after capacitation ...	95
3.3.7. Evaluation of HABPs before and during acrosome reaction.....	96
3.3.8. FITC- <i>Pisum Sativum</i> Agglutinin (PSA) labelling.....	96
3.3.9. Evaluation of HABPs in bovine sperm recovered from 90% and 45% fractions .....	97
3.4. Results .....	99

3.4.1. Microscopic evaluation of HABPs in human sperm .....	99
3.4.2. Microscopic evaluation of HABPs in human sperm during capacitation and acrosome reaction.....	103
3.4.3. Assessing the efficiency of capacitation and acrosome reaction using PSA-FITC labelling.....	105
3.4.4. Microscopic evaluation of HABPs in bovine sperm.....	106
3.4.5. Microscopic evaluation of HABPs in bovine sperm during capacitation and acrosome reaction.....	108
3.4.6. Evaluation of HABPs in bovine sperm recovered from 90% and 45% fractions .....	110
3.5. Discussion .....	111
3.6. Conclusion.....	112

#### **Chapter 4: Using proteomics to investigate dynamic changes in protein expression during capacitation and the acrosome fraction .....**

<b>4.1. Introduction.....</b>	<b>113</b>
4.2. Hypothesis and objectives .....	116
4.3. Material and methods .....	117
4.3.1. Reagents used.....	117
4.3.2. Sample acquisition, processing and analysis .....	117
4.3.2.1. Sperm processing .....	118
4.3.2.2. Induction of capacitation .....	118
4.3.2.3. Induction of acrosome reaction.....	118
4.3.3. Sperm motility assessment.....	118
4.3.4. FITC- <i>Pisum sativum</i> Agglutinin (PSA) labelling .....	119
4.3.5. Sperm protein extraction .....	119
4.3.6. Peptide preparing and labelling with TMT isobaric mass tags .....	119
4.3.6.1. Preparing protein extracts and trypsin digestion .....	119
4.3.6.2. Peptide labelling.....	120
4.3.7. Liquid chromatography–tandem mass spectrometry (LC-MS/MS).....	120
4.3.8. Protein identification and quantification .....	123
4.3.9. Statistical analysis and data analysis.....	123
4.3.10. Differential protein annotation and Bioinformatics.....	124
4.4. Results .....	125
4.4.1. Semen characteristics of donors.....	125
4.4.2. Assessment of sperm capacitation and acrosome reaction using PSA-FITC.....	125
4.4.3. Motility assessment of spermatozoa after capacitation and acrosome reaction .....	127
4.4.4. TMT 6-plex labelling and protein identification .....	128
4.4.5. Changes from Pre-Capacitation to Capacitation in sperm.....	148
4.4.6. Changes from capacitation to acrosome reaction.....	150
4.4.7. Changes from Pre-Capacitation to acrosome reaction.....	152
4.4.8. Evidence for novel HABPs.....	155
4.5. Discussion .....	156
4.6. Conclusion.....	162

#### **Chapter 5: Identification and characterisation of putative sperm HABPs using mass spectrometry .....**

<b>5.1. Introduction.....</b>	<b>163</b>
5.2. Hypothesis and objectives .....	165
5.3. Materials and methods .....	166
5.3.1. Reagents used.....	166
5.3.2. Semen analysis .....	166
5.3.3. Sperm preparation .....	167
5.3.4. Protein extraction .....	168

5.3.5. Isolation of HA-binding and non-binding proteins.....	168
5.3.6. Protein precipitation using TCA.....	170
5.3.7. Liquid chromatography–tandem mass spectrometry (LC-MS/MS).....	170
5.3.8. Protein identification and quantification .....	170
5.3.9. Western blot confirming the results of LC-MS/MS .....	173
5.4. Results .....	175
5.4.1. Identification of proteins in HA-binding and non-binding fractions.....	175
5.4.2. Alignment of the sequences of HA-binding and non-binding proteins using PDBsum and SAS.....	181
5.4.3. Western blotting to confirm the results of proteomics.....	193
5.5. Discussion .....	194
5.6. Conclusion.....	196
<b>Chapter 6: Isolation of hyaluronic acid binding proteins from bovine sperm using affinity chromatography .....</b>	<b>197</b>
6.1. Introduction.....	197
6.2. Hypothesis and objectives .....	199
6.3. Materials and methods .....	200
6.3.1. Reagents used.....	200
6.3.2. Sample preparation.....	200
6.3.3. Biotinylation of sperm surface proteins .....	201
6.3.4. Detection of biotin labelled sperm using streptavidin-FITC.....	201
6.3.5. Extraction of biotinylated sperm surface proteins.....	201
6.3.6. Protein quantification using Bradford assay.....	202
6.3.7. Sodium Dodecyl Sulphate Polyacrylamide Gel Electrophoresis (SDS-PAGE) .....	202
6.3.8. Silver staining.....	202
6.3.9. Western blotting.....	203
6.3.10. Hyaluronic acid-agarose affinity chromatography column .....	203
6.3.10.1. Digestion of HA to oligomers .....	203
6.3.10.2. Preparation of HA affinity chromatography column .....	203
6.3.10.3. Affinity chromatography .....	205
6.3.11. Measurement of protein concentration using BCA assay.....	205
6.3.12. SDS-PAGE and silver staining on proteins recovered from HA-agarose column .....	206
6.3.13. Western blotting on proteins recovered from HA-agarose column.....	206
6.4. Results .....	208
6.4.1. Biotinylation.....	208
6.4.1.1. Fluorescent labelling of biotinylated bovine sperm surface proteins.....	208
6.4.1.2. Quantification of biotinylated bovine sperm surface proteins.....	208
6.4.1.3. Silver staining on non-biotinylated and biotinylated bovine sperm proteins	210
6.4.1.4. Western blot on non-biotinylated and biotinylated bovine sperm proteins .	210
6.4.2. Affinity chromatography.....	212
6.4.2.1. Measurement of protein content obtained from HA-agarose column following affinity chromatography .....	212
6.4.2.2. SDS-PAGE and silver staining on proteins recovered from HA-agarose column .....	213
6.4.2.3. Western blotting on proteins recovered from HA-agarose column.....	214
6.5. Discussion .....	215
6.6. Conclusion.....	217
<b>Chapter 7. General Discussion .....</b>	<b>218</b>
7.1. HA-binding and its changes during capacitation.....	219
7.2. Relationships between DNA fragmentation, chromatin maturity and sperm separation methods (DDGC and HA-binding).....	221

7.3. Evaluation of HABPs and their changes during capacitation and acrosome reaction .....	223
7.4. The proteomics of sperm capacitation and the acrosome reaction .....	225
7.5. Isolation of sperm HABPs and their identification by mass spectrometry and HA affinity chromatography column .....	226
7.6. Conclusion.....	231
7. 7. Future research .....	232
<b>References .....</b>	<b>234</b>
<b>Appendices .....</b>	<b>272</b>

## List of Tables

<b>Table 1.1.</b> Semen parameters and acceptable related reference values (WHO, 2010)...	25
<b>Table 1.2.</b> HA-binding motif BX7B identified in some HABPs.....	35
<b>Table 2.1.</b> Semen assessment of volunteers contributing to the study.....	67
<b>Table 2.2.</b> Changes in hyperactive motility following capacitation.....	71
<b>Table 3.1.</b> Semen assessment of volunteers contributing to the study.....	93
<b>Table 4.1.</b> Characteristics of ejaculates from four normozoospermic donors.....	125
<b>Table 4.2.</b> List of proteins (n=121) detected at significantly different levels by One-Way ANOVA with repeated measure in <i>in vitro</i> matured sperm.....	132
<b>Table 4.3.</b> Functional Annotation Clustering by DAVID of differentially regulated proteins (N=121) involved in CAP and AR analysed by one-way ANOVA with repeated measures.....	145
<b>Table 4.4.</b> Functional annotation clustering of differentially regulated proteins (N=30) found between Pre-CAP and CAP groups by One-Way ANOVA (Tukey's test).....	149
<b>Table 4.5.</b> Functional annotation clustering of differentially regulated proteins (N=27) found between CAP and AR groups by One-Way ANOVA (Tukey's test).....	151
<b>Table 4.6.</b> Functional annotation clustering of differentially regulated proteins (N=46) found between Pre-Cap and AR groups by One-Way ANOVA (Tukey's test).....	153
<b>Table 5.1.</b> Semen parameters of young male volunteers (unproven fertility) participating in the study.....	167
<b>Table 5.2.</b> Proteins found in both HA-binding fractions and no overlap with non-binding fractions.....	177
<b>Table 5.3.</b> Functional annotation clustering on HA-binding proteins using DAVID Bioinformatics Resources 6.8.....	178
<b>Table 5.4.</b> Functional annotation clustering on HA non-binding proteins using DAVID Bioinformatics Resources 6.8.....	179
<b>Table 5.5.</b> PDB codes matching to ZBP2 ( <a href="http://www.ebi.ac.uk/thornton-srv/databases/cgi-bin/pdbsum/GetPage.pl?pdbcode=index.html">http://www.ebi.ac.uk/thornton-srv/databases/cgi-bin/pdbsum/GetPage.pl?pdbcode=index.html</a> ).....	182
<b>Table 5.6.</b> Relationships of Link module superfamily proteins*, ZBP2 and HA non-binding <sup>†</sup> proteins with PDB codes.....	185
<b>Table 6.1.</b> Semen parameters of the bull sample used in the study.....	200
<b>Table 6.2.</b> Table showing protein concentrations of different protein fractions obtained from HA-agarose column, measured using the BCA assay.....	212



## List of Figures

<b>Figure 1.1.</b> Schematic representation of male reproductive system.....	2
<b>Figure 1.2.</b> Diagram illustrating mammalian spermatogenesis.....	4
<b>Figure 1.3.</b> Developmental changes during spermiogenesis.....	6
<b>Figure 1.4.</b> Schematic representation of important changes during sperm capacitation.....	11
<b>Figure 1.5.</b> Schematic illustration of important events during acrosome reaction.....	13
<b>Figure 1.6.</b> A model representing the main regions of a mature human sperm.....	15
<b>Figure 1.7.</b> Hormonal regulation of male reproductive system.....	17
<b>Figure 1.8.</b> Metabolic pathways in sperm cells.....	20
<b>Figure 1.9.</b> Diagram showing mammalian fertilisation.....	23
<b>Figure 1.10.</b> Chemical structure of hyaluronic acid.....	29
<b>Figure 1.11.</b> Synthesis of hyaluronic acid.....	30
<b>Figure 1.12.</b> The Link module superfamily of HABPs.....	31
<b>Figure 1.13.</b> Alignment of the Link module from some members of Link module superfamily.....	32
<b>Figure 1.14.</b> Hyaluronic acid-binding domain of CD44.....	33
<b>Figure 1.15.</b> The non-Link module superfamily of HABPs.....	20
<b>Figure 1.16.</b> Diagram of sperm penetration through the cumulus oophorus matrix.....	37
<b>Figure 1.17.</b> A model of normal and diminished maturation of human sperm.....	38
<b>Figure 1.18.</b> A model of HA synthesis, digestion and function in the reproductive system.....	41
<b>Figure 1.19.</b> Schematic illustration of major changes during chromatin compaction and chromatin unpacking in spermiogenesis and fertilisation, respectively.....	44
<b>Figure 2.1.</b> Neubauer chamber for sperm counting.....	57
<b>Figure 2.2.</b> The image presenting a HA-coated slide.....	58
<b>Figure 2.3.</b> Flow diagram outlining the approach used in the current study.....	64
<b>Figure 2.4.</b> Flow diagram outlining the approach for separation of HA-bound and unbound spermatozoa.....	65
<b>Figure 2.5.</b> Assessing of HA-binding in sperm recovered from DDGC fractions.....	68
<b>Figure 2.6.</b> Demonstrating the efficiency of capacitation by inducing the acrosome reaction and subsequent PSA-FITC labelling.....	69

<b>Figure 2.7.</b> Confirming the efficiency of capacitation by inducing acrosome reaction and subsequent PSA-FITC labelling.....	70
<b>Figure 2.8.</b> Assessment of hyperactive motility in non-capacitated and capacitated sperm.....	72
<b>Figure 2.9.</b> Assessment of HA-binding in relation to capacitation in washed sperm and sperm from 90% fractions.....	73
<b>Figure 2.10.</b> Examples of AO stained sperm from DDGC fractions.....	75
<b>Figure 2.11.</b> Plots of AO category data from DDGC fractions.....	76
<b>Figure 2.12.</b> Examples of AO staining on HA-bound and unbound sperm.....	77
<b>Figure 2.13.</b> Plots of AO category data from HA-bound and un-bound fractions.....	78
<b>Figure 2.14.</b> Examples of AB stained sperm from DDGC fractions.....	79
<b>Figure 2.15.</b> Plots of AB category data from DDGC fractions.....	80
<b>Figure 2.16.</b> Examples of AB stained sperm from HA-binding assay.....	81
<b>Figure 2.17.</b> Plots of AB category data from HA-bound and unbound fractions.....	82
<b>Figure 2.18.</b> Plots of AO category data from 90% and HA-bound fractions.....	83
<b>Figure 2.19.</b> Plots of AB category data from 90% and HA-bound fractions.....	84
<b>Figure 3.1.</b> Flow diagram representing the approach used in the current study.....	98
<b>Figure 3.2.</b> Immunofluorescence images of human sperm probed with reagents targeting HABPs.....	100
<b>Figure 3.3.</b> Immunofluorescence images of human sperm (non-capacitated) pre-incubated with HA (50 kDa) and probed with reagents targeting HABPs.....	101
<b>Figure 3.4.</b> Immunofluorescence images of PC3 cells probed with reagents targeting HABPs as positive controls.....	102
<b>Figure 3.5.</b> Immunofluorescence images of human sperm probed with reagents targeting HABPs during capacitation and acrosome reaction.....	104
<b>Figure 3.6.</b> Illustrating the efficiency of capacitation and acrosome reaction in bovine sperm by PSA-FITC labelling.....	105
<b>Figure 3.7.</b> Illustrating the efficiency of capacitation and acrosome reaction in human sperm by PSA-FITC labelling.....	106
<b>Figure 3.8.</b> Immunofluorescence images of bovine sperm probed with reagents targeting HABPs.....	107
<b>Figure 3.9.</b> Immunofluorescence images of bovine sperm probed with reagents targeting HABPs during capacitation and acrosome reaction.....	109
<b>Figure 3.10.</b> Targeting of HABPs in good and bad quality bovine sperm.....	110
<b>Figure 4.2.</b> Schematic outlining the approach used in the present study.....	122

<b>Figure 4.3.</b> Assessment of acrosome status using PSA-FITC labelling.....	126
<b>Figure 4.4.</b> Confirming the efficiency of capacitation by inducing the acrosome reaction followed by PSA-FITC labelling.....	127
<b>Figure 4.5.</b> Motility assessment of sperm following capacitation and acrosome reaction.....	128
<b>Figure 4.6.</b> Classification of the differential proteins identified by One-Way ANOVA with repeated measures according to their subcellular localisation (A) and main cellular function (B) using the information available at the UniportKB/Swiss-Prot website.....	129
<b>Figure 4.7.</b> Differentially regulated proteins in Pre-Cap, Cap and AR sperm using One-Way ANOVA (Tukey's test).....	154
<b>Figure 5.1.</b> A schematic illustration of density gradient centrifugation using ProInsert-Nidacon columns.....	168
<b>Figure 5.2.</b> Schematic illustration of Amicon Ultra-15 centrifugal filter units.....	169
<b>Figure 5.3.</b> Flow diagram outlining the approach used in the current study.....	172
<b>Figure 5.4.</b> Venn diagram to illustrate HA-binding and non-binding proteins from two different samples.....	175
<b>Figure 5.5.</b> Venn diagram showing HA-binding (A) and non-binding proteins (B) merged from two different samples.....	176
<b>Figure 5.6.</b> Residue alignment of ZPBP2 with 2i83. Residues implicated in ligand binding are bordered by boxes.....	183
<b>Figure 5.7.</b> Predicted secondary structure (helices and strands) of ZPBP2 with the confidence for helix and strand predictions denoted by green shading.....	183
<b>Figure 5.8.</b> Western blotting on HA-binding and non-binding proteins using antibodies against ZPBP2 and ADAM32.....	193
<b>Figure 6.1.</b> Mechanism of HA binding to Affi-Gel 102 amino-terminal crosslinked agarose gel.....	204
<b>Figure 6.2.</b> Flow diagram outlining the approach used in the current study.....	207
<b>Figure 6.3.</b> Fluorescence images of sperm probed with streptavidin-FITC following biotinylation of bovine sperm surface proteins.....	208
<b>Figure 6.4.</b> Standard protein curve generated from Bradford assay.....	209
<b>Figure 6.5.</b> Silver staining on biotinylated and non-biotinylated proteins after SDS electrophoresis in polyacrylamide gels.....	210
<b>Figure 6.6.</b> Western blotting on non-biotinylated and biotinylated bovine sperm proteins using HRP-streptavidin.....	211
<b>Figure 6.7.</b> Standard protein curve generated from BCA assay.....	212
<b>Figure 6.8.</b> Silver staining on protein content obtained from HA-agarose column.....	213
<b>Figure 6.9.</b> Western blotting on proteins recovered from HA-agarose column.....	214

## List of Abbreviations

ADAM32	A Disintegrin and Metalloproteinase Domain 32
AO	Acridine Orange
APS	Ammonium Persulfate
ART	Assisted Reproductive Technology
ATP	Adenosine-Triphosphate
BSA	Bovine Serum Albumin
CaCl <sub>2</sub>	Calcium Chloride
CAMP	Cyclic Adenosine Monophosphate
CK	Creatine Kinase
CO <sub>2</sub>	Carbon Dioxide
DAPI	4', 6' Diamino-2-Phenylindole
DMSO	Dimethyl Sulfoxide
DNA	Deoxyribonucleic Acid
DTT	Dithiothreitol
ECM	Extracellular Matrix
ERK1	Extracellular Regulated Kinase1
FAK	Focal Adhesion Kinase
FITC	Fluorescein Isothiocyanate
HA	Hyaluronic Acid
HABPs	Hyaluronic Acid Binding Proteins
IVF	In-vitro Fertilisation
ICC	Immunocytochemistry
KCl	Potassium Chloride
kDa	Kilo Dalton
NaCl	Sodium Chloride
NaH <sub>2</sub> PO <sub>4</sub>	Sodium mono phosphate
NaHCO <sub>3</sub>	Sodium Bicarbonate
NaOH	Sodium Hydroxide
PAGE	Polyacrylamide Gel Electrophoresis
PBS	Phosphate Buffer Solution
PI3K	Phosphatidylinositol 3-kinase
PMSF	Phenylmethylsulfonyl Fluoride
PSA	Pisum Sativum Agglutinin
PVP	Polyvinylpyrrolidone
RHAMM	Receptor for Hyaluronic Acid-Mediated Motility
RPM	Revolutions per Minute
RT	Room Temperature
SDS	Sodium Dodecyl Sulfate
Sp-TALP	Sperm Tyrode's Albumin-Lactate-Pyruvate
TEMED	Tetramethylethylenediamine
TK	Tyrosine Kinase
TRITC	Tetramethylrhodamine isothiocyanate
WHO	World Health Organization
ZPBP2	Zona Pellucia Binding Protein2

## Symbols

%	Percentage
M	Molar
mM	Millimolar
$\mu$ M	Micromolar
L	Litre
mL	Millilitre
mg/mL	Milligram per millilitre
$^{\circ}$ C	Degree Celsius
$10^6$ /mL	Million per millilitre

## List of Appendices

<b>Appendix Figure 3.1.</b> Optimisation of anti CD44 antibody in human sperm.....	272
<b>Appendix Figure 3.2.</b> Optimisation of the right dilution of streptavidin-FITC.....	273
<b>Appendix Figure 3.3.</b> Optimisation of HA-TRITC in human sperm.....	273
<b>Appendix Figure 3.4.</b> Optimisation of the anti CD44 antibody using fixation with PFA in human sperm.....	274
<b>Appendix Figure 3.5.</b> Optimisation of the anti CD44 antibody in bovine sperm.....	275
<b>Appendix Table 5.1.</b> Mass spectrometry data for hyaluronic acid-binding fraction (sample D70).....	276
<b>Appendix Table 5.2.</b> Mass spectrometry data for hyaluronic acid non-binding fraction (sample D70).....	282
<b>Appendix Table 5.3.</b> Mass spectrometry data for hyaluronic acid-binding fraction (sample D31).....	303
<b>Appendix Table 5.4.</b> Mass spectrometry data for hyaluronic acid non-binding fraction (sample D31).....	311
<b>Appendix Table 5.5.</b> Proteins found in both non-binding fractions and no overlap with HA-binding fractions.....	332

## **Chapter 1: Introduction**

### **1.1. Physiology of male reproductive system and spermatogenesis**

The male reproductive system produces, stores, nourishes and transports sperm. Its most important internal structures include the vas deference, testes, bulbourethral gland, prostate gland and seminal vesicles (Mohanty and Singh, 2017). The testicular mass is composed mainly of a convoluted set of tubules called seminiferous tubules which differentiate from testicular cords (containing primordial germ cells) during fetal development (Hai et al., 2014; Nel-Themaat et al., 2011). The seminiferous tubules are populated by Sertoli cells connected via tight junctions (Mruk and Cheng, 2010).

Testosterone is produced by Leydig cells located in the connective tissue surrounding the seminiferous tubules and under the influence of pituitary FSH. Smooth muscles help propel sperm through the seminiferous tubules (Romano et al., 2005).

Spermatogenesis is a complex and highly regulated process taking place in the seminiferous tubules of testis (Song and Wilkinson, 2012) which are surrounded by different layers of adventitial cells, forming the lamina propria of the tubules (Davidoff et al., 1990). Within the tubules, there are two major types of cells called Sertoli cells and the germ cells (spermatogonia). These germ cells form the seminiferous epithelium. The majority of the germ cells in this epithelium are in a constant state of division and successive stages in their differentiation occur closer to the lumen of the tubule, so that a series of differentiating cells can be seen converging towards the lumen. Cells layered in this way produce a stratified epithelium (Glover et al., 1990).

Sertoli cells are testis-specific somatic cells which are attached to the basement membrane of the seminiferous tubules where their main role is to support and nourish the developing and differentiating germ cells (Hai et al., 2014; Nel-Themaat et al., 2011; Rebourcet et al., 2014). The most interesting characteristic of Sertoli cells, however, is their specialised junctional complexes providing a selective barrier to the transfer of specific substances from blood stream into the lumen of the seminiferous tubules (Glover et al., 1990). Sertoli cells divide the seminiferous epithelium into two parts: a basal compartment surrounding by Leydig cells that covers the area from the tight junction (the linkage between two

Sertoli cells) towards the basement membrane and a luminal compartment encompassing germ cells in the later stages of spermatogenesis which extends from the tight junction towards the lumen of the seminiferous tubule (Figure 1.1) (Smith and Braun, 2012). It is known that immature germ cells are localised closer to the basement membrane and those with higher maturity are located closer to the lumen of the seminiferous tubules (O'Donnell et al., 2011). Figure 1.1 shows a schematic representation of male reproductive system with the main focus on the testes.

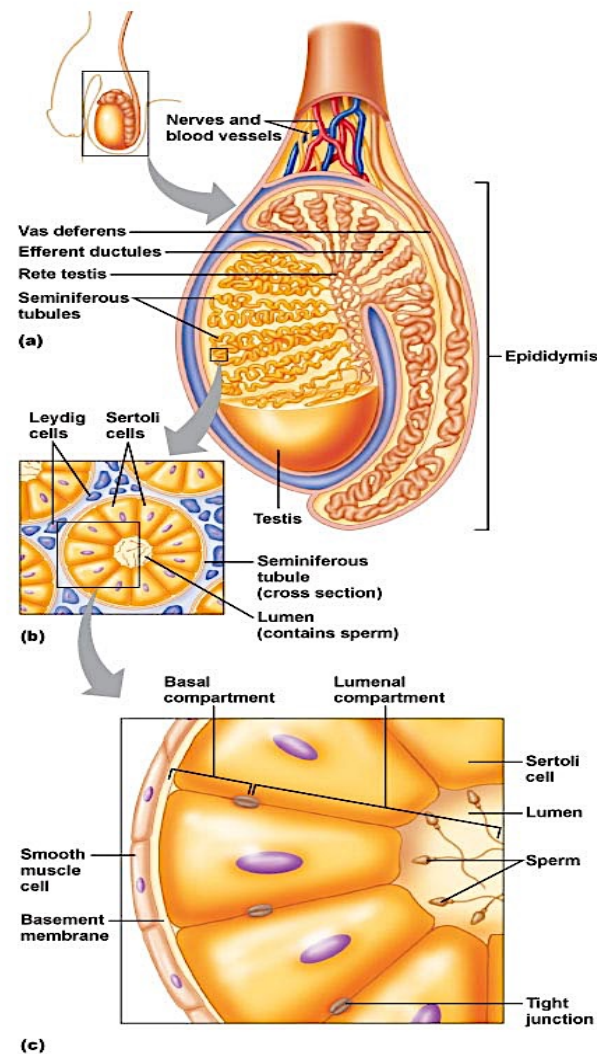


**Figure 1.1. Schematic representation of male reproductive system.**

a) A cross-section through a testis.  
b, c, d) Seminiferous tubule cross-sections.  
(Available from: [http://droualb.faculty.mjc.edu/Course%20Materials/Physiology%20101/Chapter%20Notes/Fall%202007/chapter\\_22%20Fall%2007.htm](http://droualb.faculty.mjc.edu/Course%20Materials/Physiology%20101/Chapter%20Notes/Fall%202007/chapter_22%20Fall%2007.htm)).

As mentioned above, spermatozoa are produced by spermatogenesis in which a series of mitotic, meiotic and post meiotic phases of cellular division are involved. The process of spermatogenesis itself can be divided into four stages, namely spermatocytogenesis, meiosis, spermiogenesis and spermiation (Amann and Schanbacher, 1983).



Spermatogenesis begins with mitotic division of spermatogonial germ cells localised at the basement membrane of the seminiferous tubules (Nikolic et al., 2016). Different types of spermatogonia including type A (dark), type A (pale) and type B have been identified by microscopic observation (Phillips et al., 2010). Type A (dark) are spermatogonial stem cells with the ability to mitotically proliferate and replace cells committed to undergo mitosis for further spermatogenesis (type A pale) with these cells then committing to mitosis (type B) generating primary spermatocytes (diploid) that migrate across the tight junctions between two Sertoli cells (Gilbert, 2000).

Once primary spermatocytes have traversed the tight junctions they start to enlarge by increasing their cytoplasm. They then initiate the process of meiosis, which unlike mitosis, has two sequential cellular divisions following DNA replication prior to meiosis I by which the chromosome copy number decreases by half to form haploid gametes that can restore the species-specific ploidy ( $n$ ) number upon fertilisation of and fusion with the oocyte, forming a diploid zygote (Griswold, 2016; Phillips et al., 2010). Secondary spermatocytes with 23 chromosomes in sister chromatid configuration form as a result of meiosis I. These cells will then undergo meiosis II and produce four spermatids with 23 single chromatids for each chromosome (Alberts et al., 2002). Male and female gametes are haploid because after fertilisation when sperm and egg nuclei fuse, they create a set of 23 pairs of chromosomes (one set from the father and the other from mother). Figure 1.2 illustrates the process of mammalian spermatogenesis.

In the male, haploid round spermatids are the first outcomes of the completion of meiosis but are immature and so incapable of fertilisation. These round cells condense in order to acquire all the features of mature spermatozoa, a process that requires elongation of the cell, removal of most of the cytoplasm and acrosome formation. This phase of spermatogenesis is known as spermiogenesis (Cheng and Mruk, 2010; O'Donnell, 2014). The duration of spermatogenesis in human is approximately 68-74 days and 39-40 days in mouse (Hess and Renato de Franca, 2008).

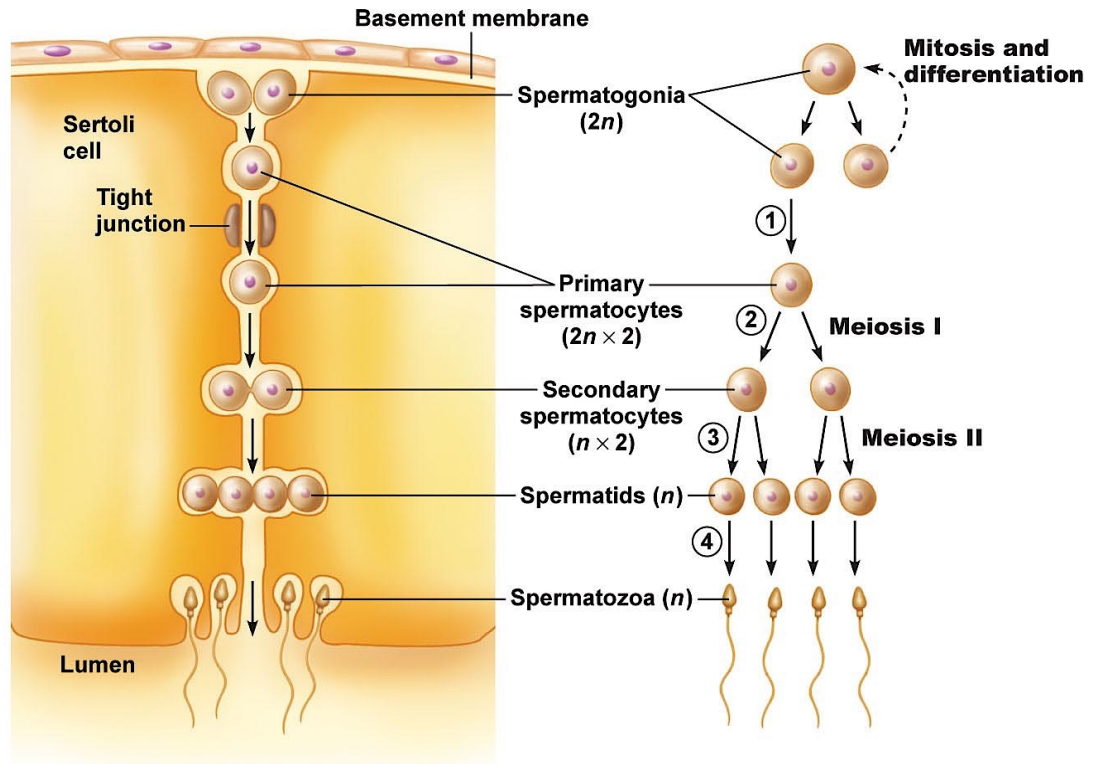


**Figure 1.2. Diagram illustrating mammalian spermatogenesis.**

Available from:

([http://droualb.faculty.mjc.edu/Course%20Materials/Physiology%20101/Chapter%20Notes/Fall%202007/chapter\\_22%20Fall%202007.htm](http://droualb.faculty.mjc.edu/Course%20Materials/Physiology%20101/Chapter%20Notes/Fall%202007/chapter_22%20Fall%202007.htm)).

### 1.1.1. Mechanism of spermiogenesis

As discussed above, spermiogenesis is the final stage of spermatogenesis when spermatozoa are formed as a result of morphological differentiation from round spermatids. The alteration in the shape of spherical spermatid leads to the formation of a streamlined head with a compact nucleus, an acrosome and a tail that is required for sperm motility. Spermatids depending on the development of their acrosome are categorised into different phases of Golgi, cap, acrosome and maturation phases (Cooper, 2011).

Spermatids in Golgi phase have a Golgi apparatus which produces membrane-bound granules containing acrosomal enzymes. As shown in Figure 1.3 a, during Golgi phase, the formation of acrosomal vesicle occurs at the upper surface of the nucleus by fusion of small vesicles and the tail begins to elongate. The acrosomal vesicle will then extend down the upper surface of the nucleus to provide the cap phase of acrosomal development (Glover et al., 1990). It is during the other two phases of acrosomal development (acrosome and maturation

phases) that the final acrosomal shape is proceeded. During cap phase, distinct changes occur to the nucleus and it shifts from the central part of the spermatid to the periphery and spermatid elongates gradually. At the same time during the cap phase, nuclear pores move to the caudal extremity of the nucleus (Figure 1.3 b).

Additionally, the chromatin of spermatids becomes condensed by replacing histones with protamines that will be further discussed. The mitochondria of spermatids have distinctive features such as extra cristae. During spermiogenesis the mitochondria move to the periphery of the spermatid and later to the caudal part of the nucleus where the sperm tail begins to develop. The formation of a chromatid body from mitochondrial clusters in spermatid cytoplasm is another remarkable feature of spermatid development during spermiogenesis (Sun and Yang, 2010).

The acrosomal cap extends over the nucleus in the acrosome and maturation phases at which the chromatid body migrates towards the caudal extremity of the nucleus and form the annulus which ultimately moves to the end of the midpiece (Figure 1.3 c). The centrioles also move to the caudal region of the nucleus. The proximal centriole creates a link with the fibers of the axoneme. As the tail starts to extend, a group of cytoplasmic microtubules accumulates around the developing axoneme and creates a ring of microtubules around the tail called the manchette. This structure is partially associated with spermatid nuclear elongation and early development of the tail (Glover et al., 1990). Before sperm are released into the lumen of seminiferous tubules, most of the spermatid cytoplasm is left behind as residual bodies that will ultimately become digested by Sertoli cells. Some residual cytoplasm, however, remains attached after spermiation in the form of cytoplasmic droplets. The cytoplasmic droplet contains extensive remnants of the endoplasmic reticulum and high levels of alkaline phosphates associated with several membrane phenomena (Cooper, 2011). Following maturation of spermatids into spermatozoa, they are released into the lumen of the seminiferous tubules, a process known as spermiation (Manku and Culty, 2015). Further maturation, however, occurs during transport through the epididymis (Cooper, 1995).

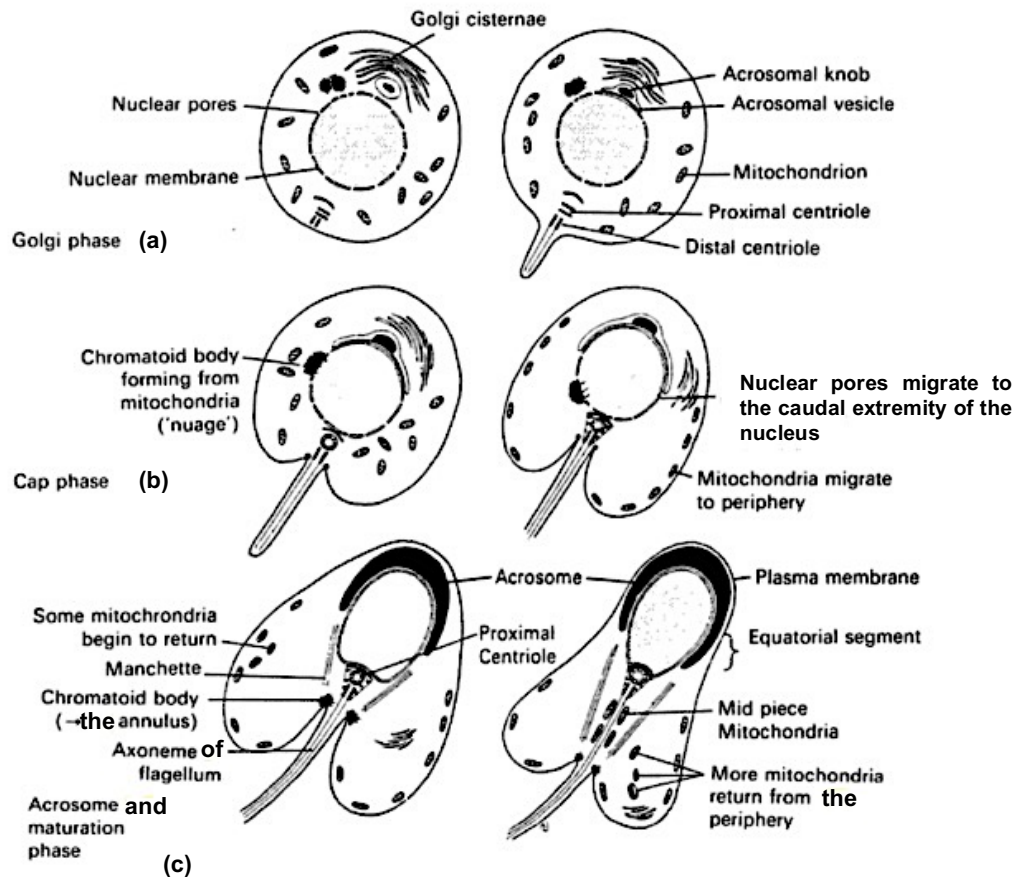


**Figure 1.3. Developmental changes during spermiogenesis.**  
Available from: (Taken from T.D. Glover et al, 1990).

### 1.1.2. Sperm transport from seminiferous tubules to urethra

After spermatozoa are released into the lumen of the seminiferous tubules, they will travel through rete testis and enter the efferent ductules (Figure 1.1). This is the point at which they exit the testis and enter the epididymis where they undergo further maturation (Cooper, 1995). At this stage sperm transport occurs due to peristaltic contractions of smooth muscles of the epididymides. Ultimately, spermatozoa enter the vas deferens that is connected with seminal vesicles to form the ejaculatory duct. At this point sperm is mixed with the fluid originating from the seminal vesicle. The ejaculatory duct penetrates through the prostate gland to join the urethra. As such, sperm reach the urethra which receives secretions from the bulbourethral glands (Mohanty and Singh, 2017).

### **1.1.3. Acquisition of fertility potential by the sperm**

#### **1.1.3.1. Epididymal maturation**

Spermatozoa obtained from the testis are unable to naturally fertilise the egg. Therefore, sperm maturation in the epididymis is a crucial step required for the acquisition of fertilising ability. It is known that mature spermatozoa from the epididymal tail (cauda) are vigorously motile, whereas immature sperm from the caput are very slow and testicular sperm are entirely immotile (Nijs et al., 1996). Spermatozoa passing into epididymides are incapable of gene expression, and so maturation occurs by sperm interaction with secreted proteins such as CRISP proteins, beta-hexosaminidase, ADAM7, clusterin, Glycerylphosphorylcholine (an organic osmotic regulator), carnitine (associated with phospholipid metabolism), glutamic acid, sialic acid and lipoproteins in the epididymal lumen (Cornwall, 2009; Kratzschmar et al., 1996; Miranda et al., 1995). Epididymal migration confers several important changes during sperm maturation including the acquisition of forward progressive motility, changes in surface charge, changes in sperm agglutination pattern, acrosomal remodelling, migration of the cytoplasmic droplet along the tail, further chromatin compaction (cross-linking of protamines) and remodelling of the plasma membrane and sperm tail (Jones, 1989; Sellami et al., 2013; Cooper, 2011; Enciso et al., 2011).

Plasma membrane remodeling includes uptake of glycoproteins secreted by the epididymis, elimination or consumption of certain phospholipids from the inner section of the membrane, processing of glycoproteins using enzymes such as endoproteolysis and re-locating of lipids and proteins to different membrane domains (Jones, 1998). All these changes occur consecutively in different parts of the epididymis (see below) (Aitken *et al*, 2007), which is divided into three parts namely the caput (head), corpus (body) and cauda (tail). Early sperm maturation occurs in the caput. Sperm motility from the caput toward the corpus is slow, but it increases rapidly when sperm are in the corpus. At this stage, sperm are not fully matured and they acquire full maturation and are stored temporarily in the cauda prior to ejaculation via the vas deferens (Cornwall, 2009; van Der Horst et al., 1999). Even at the point of ejaculation, spermatozoa only become capable of fertilisation following ejaculation into the female reproductive tract during their transport across the female reproductive tract (Suarez and Pacey, 2006) .

## 1.2. Capacitation

The fertilising ability of spermatozoa is acquired only after transformation and maturation, which normally occurs in the female genital tract. This final stage of sperm maturation is called capacitation (CAP), which is essential for sperm to undergo the acrosome reaction (AR) (De Jonge, 2005). Capacitation facilitates a series of molecular and physiological changes that sperm must undergo to acquire fertilising potential (Yanagimachi, 1969; Austin and Bishop, 1958; Bernabo et al., 2015; Ded et al., 2010). Despite its importance, the fundamental cellular and molecular mechanisms and identification of key players driving CAP and AR processes are still poorly understood. Independent studies first revealed the importance of CAP (Austin, 1951; Chang, 1951) by showing that sperm needed a certain amount of time in the oviduct to acquire fertilising ability.

Capacitation can be induced *in vitro* when sperm are incubated in an appropriate medium containing suitable energy sources (pyruvate and glucose), a protein source (like bovine serum albumin), Sodium bicarbonate ( $\text{HCO}_3^-$ ) and calcium ( $\text{Ca}^{2+}$ ) (Visconti et al., 1999; De Jonge, 2005). Different media components have different effects on capacitation depending on the species. Glucose containing media, for example, induce sperm capacitation in human, mouse and hamster but has an inhibitory effect on the sperm of other species such as bovine and dog (Travis et al., 2004; Ferramosca and Zara, 2014). All the following events involved in the capacitation process ultimately relate to the potential of sperm to acrosome react (Aitken and Nixon, 2013).

The main changes during capacitation are as follows:

- Removal of decapacitation factors (DFs) that leads to increased levels of intracellular  $\text{Ca}^{2+}$  (Fraser, 1998a; Adeoya-Osiguwa and Fraser, 1996).
- Cholesterol efflux from sperm plasma membrane and an increase in membrane fluidity (Davis et al., 1979; Aitken and Nixon, 2013).
- Protein kinase A (PKA)-dependent changes in lipid architecture of plasma membrane due to increased levels of  $\text{HCO}_3^-$  (Gadella and Harrison, 2000; Flesch et al., 2001; de Vries et al., 2003).
- Alteration in sperm membrane permeability to different ions (Visconti et al., 2011; Ickowicz et al., 2012).
- Protein tyrosine phosphorylation (Leahy and Gadella, 2011a; Aitken and Nixon, 2013; Reid et al., 2011).

- Lipid raft formation and movement and consequently, the aggregation of proteins/molecules necessary for binding to the zona pellucida (Bou Khalil et al., 2006; Reid et al., 2011).
- Sperm hyper-activation, which is a cyclic-AMP (cAMP)-mediated event associated with high levels of tyrosine phosphorylation in the sperm flagellum (Nassar et al., 1999; Leahy and Gadella, 2011a).
- Acquisition of the ability to bind to the zona pellucida by remodelling/translocation or post-translational modification of existing proteins (Reid et al., 2011).
- Acquisition of the ability to undergo the acrosome reaction which is the final step of the capacitation process. The acrosome reaction is triggered by the release of intracellular  $\text{Ca}^{2+}$  when sperm bind to the zona pellucida (Baibakov et al., 2007; Mayorga et al., 2007).

The completion of capacitation and the acrosome reaction is time (and site)-sensitive in sperm and therefore, measuring the sperm population that is capable of undergoing proper maturation, and their associated protein changes provide potential biomarker opportunities to measure semen quality. *In vivo*, ejaculated sperm begin the capacitation process in the female reproductive tract whereby albumin removes cholesterol from the plasma membrane altering lipid membrane domains, fluidity and the membrane becomes more permeable to calcium and bicarbonate ions (Travis and Kopf, 2002; Leahy and Gadella, 2015).

Cholesterol efflux (cholesterol removal) was reported as one of the first changes detected during capacitation (Aitken and Nixon, 2013). Changes in sperm membrane lipid/phospholipids and increasing the plasma membrane fluidity are considered to be important features favouring sperm capacitation. Cholesterol efflux is stimulated by exposure of sperm to cholesterol sinks (such as albumin) and leads to an increase in the fluidity of the plasma membrane (Davis, 1981; Martinez and Morros, 1996; Reid et al., 2011). Cholesterol efflux can also increase sperm membrane permeability to different ions such as  $\text{HCO}_3^-$  and  $\text{Ca}^{2+}$  (Sheriff and Ali, 2010; Baldi et al., 1996; Ickowicz et al., 2012; Reid et al., 2011). The net intake of these ions causes an increase in intracellular pH and also activates a soluble adenylyl cyclase (sAC), which subsequently increases the levels of cAMP leading to activation of PKA (Ickowicz et al., 2012; Aitken and

Nixon, 2013). Activation of PKA leads to activation of tyrosine kinase (s) (TK) and as a result tyrosine phosphorylation of different proteins. The rise in tyrosine phosphorylation is associated with hyper-activation (Osheroff et al., 1999; Baldi et al., 2000; Ickowicz et al., 2012; Naz and Rajesh, 2004; Breitbart, 2003).

Increases in protein tyrosine phosphorylation during capacitation are blocked when PKA is inhibited and confirms that cAMP-dependent PKA activation is an important event during capacitation (Lawson et al., 2008). More recently, the modulatory effect of nitric oxide (NO) and reactive oxygen species (ROS) has also been revealed (Baldi et al., 2000; de Lamirande and O'Flaherty, 2008). An increase in intracellular  $\text{Ca}^{2+}$  is another main feature of sperm capacitation. When sperm are ejaculated, they are surrounded by decapacitation factors (DF) such as uteroglobin and transglutaminase (Luconi et al., 2000). Before capacitation occurs, DFs are attached to the sperm surface and keep the intracellular calcium levels low by activation of an intracellular  $\text{Ca}^{2+}$ -ATPase (a  $\text{Ca}^{2+}$  extrusion pump). DFs are released, during capacitation and the concentration of intracellular  $\text{Ca}^{2+}$  increases (Baldi et al., 2000). The intracellular  $\text{Ca}^{2+}$  also increases due to: (i) activation of CatSper channels following hyperpolarisation of the plasma membrane (Shukla et al., 2012; Navarro et al., 2008), (ii) a transient influx of  $\text{Ca}^{2+}$  through the CatSper channels (cation channel of spermatozoa) and (iii) the combined activity of the different  $\text{Ca}^{2+}$ -specific channels of the mitochondria (Bravo et al., 2015). The rise in the levels of intracellular  $\text{Ca}^{2+}$  is crucial for the acrosome reaction to occur. Figure 1.4 shows an overview of the most important events occurring during capacitation.



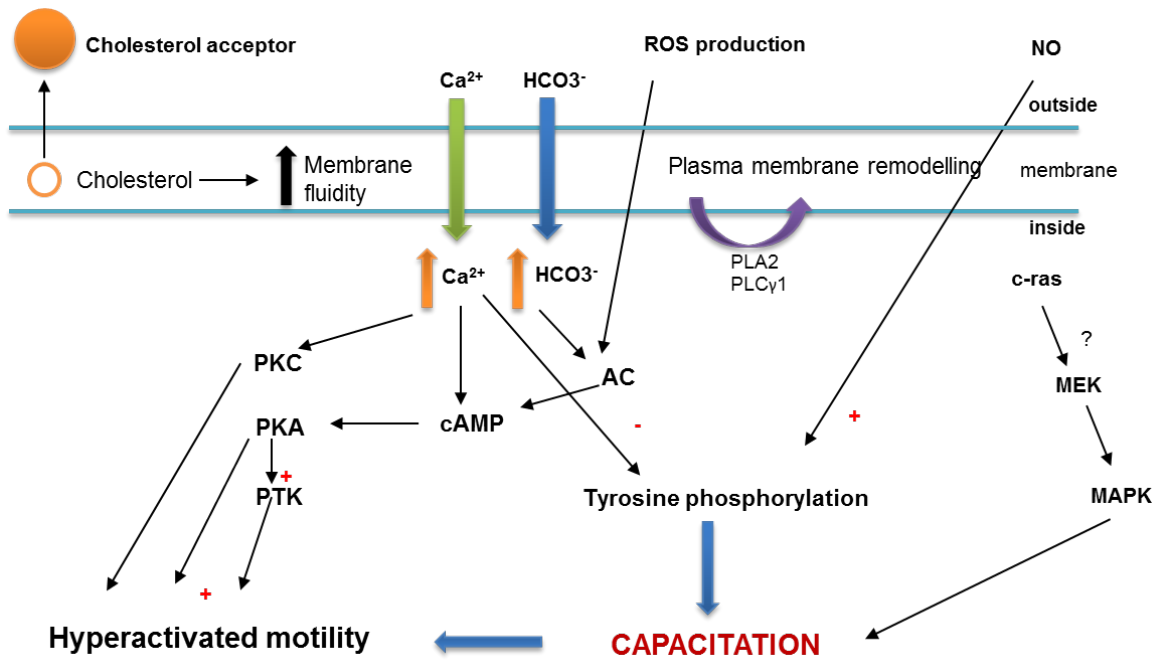


**Figure 1.4. Schematic representation of important changes during sperm capacitation (reproduced from Baldi E et al, 2000).**

Cholesterol efflux, increases in membrane fluidity, influx of different ions (such as  $\text{Ca}^{2+}$  and  $\text{HCO}_3^-$ , changes sperm membrane phospholipids and stimulation of phospholipases (including PLA2 and PLC $\gamma$ 1), activation of adenylyl cyclase (AC), increased production of cAMP, activation of protein kinase A (PKA) and tyrosine kinase (TK) have been shown. The inhibitory effect of  $\text{Ca}^{2+}$  and modulatory effect of reactive oxygen species (ROS) and nitric oxide (NO) on tyrosine phosphorylation have also been pointed.

### 1.3. Acrosome reaction

The acrosome reaction (AR) is a crucial exocytotic event for spermatozoa to be able to fertilise the egg. Only acrosome-reacted spermatozoa have the ability to penetrate the zona pellucida and bind the oocyte plasma membrane (Yanagimachi, 1994a). The acrosome is a flattened, membrane-bound vesicle that contains many digestive enzymes including hyaluronidase. It is located over the anterior portion of the nucleus. The acrosome reaction is accompanied by membrane structure transformation and loss of acrosomal content (Baldi et al., 1996; Patrat et al., 2000). To acquire the ability to undergo the acrosome reaction, spermatozoa must first complete their capacitation process (Saling and Storey, 1979).

The AR also leads to alterations of plasma membrane proteins at the equatorial and post-acrosomal regions of the sperm head (Patrat et al., 2000). The AR is initiated by spermatozoa binding to zona pellucida (ZP) and involves the release

of hydrolytic enzymes including acrosin and hyaluronidase to allow spermatozoa access to and penetration through the oocyte envelopes and fusion with the oocyte membrane (Baldi et al., 1996; Patrat et al., 2000). As a result of the AR, the outer acrosomal and plasma membranes fuse, allowing the inner acrosomal membrane to be exposed to the zona pellucida glycoprotein ZP3 or to progesterone (a cofactor for the occurrence of AR) and leads to the release of the acrosomal contents, induction of a cascade of intracellular signals and exposure of critical membrane domains for fertilisation (Witte and Schafer-Somi, 2007; Patrat et al., 2000).

There are several receptors on the sperm plasma membrane known to bind zona pellucida glycoproteins. In humans, for example, Gi- protein coupled and tyrosine kinase receptors (TKR) bind to the ZP glycoproteins. The Gi-coupled protein acts as an activator for phospholipase C (PLC) and has a regulatory effect on adenylate cyclase (AC) leading to the production of cAMP and activation of phospholipase A (Witte and Schafer-Somi, 2007). As a result of TKR binding to the zona pellucida, a  $\text{Ca}^{2+}$  transporter becomes phosphorylated and increases the influx of  $\text{Ca}^{2+}$  which leads to activation of phospholipase  $\text{C}\gamma 1$  and as a consequence, the generation of Inositol triphosphate (InsP3) and diacylglycerol (DAG). Activation of InsP3-cascade opens a voltage-dependent  $\text{Ca}^{2+}$  channel in the outer acrosome membrane and releasing  $\text{Ca}^{2+}$  from the interior of the acrosome to the cytosol (Patrat et al., 2000). The increase in the levels of intracellular  $\text{Ca}^{2+}$  leads to the occurrence of AR.

Intracellular levels of  $\text{Ca}^{2+}$  are also increased by the stimulation of G-proteins, a consequence of the binding of the sperm to the zona pellucida. Such molecular interaction, in turn, increases the intracellular pH and plasma membrane depolarisation leading to the release of  $\text{Ca}^{2+}$ . The increased levels of intracellular  $\text{Ca}^{2+}$  lead to the phosphorylation of different proteins and as a consequence, results in the AR (Figure 1.5) (Breitbart and Spungin, 1997; Patrat et al., 2000; Witte and Schafer-Somi, 2007).

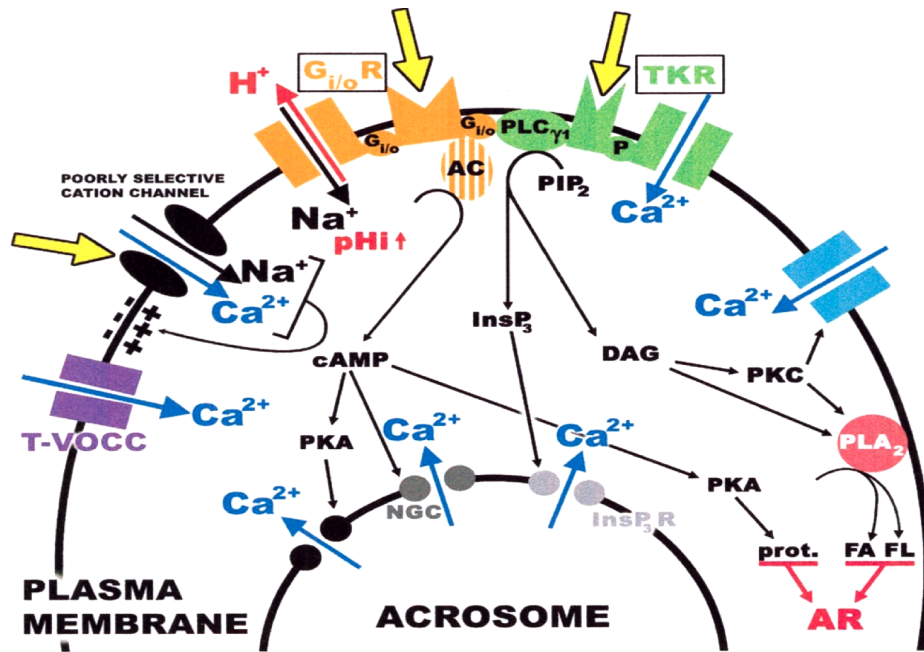


Figure 1.5. Schematic illustration of important events during acrosome reaction (From Patrat et al., 2000).

Evaluation of the acrosome reaction and capacitation can be used to predict fertilisation success and can be of great help in choosing the most appropriate technique of assisted reproductive technology (ART) (Henkel et al., 1993; Sandro and Sidney, 2011).

#### 1.4. Capacitation and acrosome reaction-related changes in the organisation of sperm surface antigens

The sperm membrane is a dynamic structure of proteins and phospholipids which react to developmental and environmental signals to modify particular cellular functions (Myles and Primakoff, 1984b). CAP and AR, as discussed change the fluidity of sperm membrane which leads to migration of different antigens to the surface and changing the membrane topography (Okabe et al., 1987). Different studies have reported changes in the appearance of antigenic sites located on the sperm head during CAP and AR. The localisation of PH-20 (SPAM1) for example changes from the posterior acrosome to the anterior acrosome after AR (Myles and Primakoff, 1984b). PH-20 is a highly conserved and multifunctional protein located on sperm surface. It acts as a hyaluronidase in acrosome intact sperm to support sperm penetration through the cumulus oophorus matrix. Its

second function in acrosome reacted sperm involves sperm-zona binding (secondary binding) (Hunnicuttt et al., 1996; Kimura et al., 2009). Its third function involves the HA receptor domain of PH-20 located in the N-terminus involving in signaling of  $\text{Ca}^{2+}$  that accompanies acrosome reaction (Zhang et al., 2004). Research carried out by Francou et.al (2014) demonstrated the changes in immunodistribution of other proteins such alpha tubulin during capacitation and the acrosome reaction. They showed that the percentage of sperm with immunoreactive flagellum for  $\alpha$ -tubulin increased during capacitation and the acrosome reaction (Francou et al., 2014).

Proteomic analysis (Kongmanas et al 2015) revealed changes in the distribution of some acrosomal proteins such as zona pellucida binding protein 1 (ZPBP1), zonadhesin, proacrosin/acrosin and acrosin-binding protein (ACRBP) in capacitated sperm. These and other proteins are involved in sperm-ZP binding, suggesting that changes in their distribution and perhaps availability may occur during capacitation (Kongmanas et al., 2015).

It is known that tyrosine phosphorylation of proteins occurring during capacitation has an important role in sperm-zona binding (Asquith et al., 2005). Different proteins including tubulin, voltage-dependent anion-selective channel proteins (VDAC), pyruvate dehydrogenase (PDH) E1  $\beta$  chain, glutathione S-transferase, NADH dehydrogenase (ubiquinone) Fe-S protein 6, acrosin binding protein precursor, proteasome subunit alpha type 6b, and cytochrome b-c1 complex undergo tyrosine phosphorylation during capacitation (Arcelay et al., 2008). Heat shock protein 1 (HSPD1) and tumor rejection antigen 1 (TRA1, belonging to heat shock protein 90 family) are another two important proteins which become phosphorylated during capacitation and disappeared after acrosome reaction (Asquith et al., 2005; Nixon and Aitken, 2009).

### **1.5. Relationship between sperm structure and function**

In nature, mature spermatozoa of different species present a wide variety of sizes and shapes. Common to all and as seen in Figure 1.6, mammalian spermatozoa consist of the head, neck, midpiece and tail (Alberts et al., 2002). The head contains a large nucleus that has the crucial hereditary information in the form of condensed chromatin in which histones are replaced by protamines (Castillo et

al., 2015). The head also has an enzyme-filled vesicle known as acrosome that covers two-thirds of the head. The acrosome is located over the anterior portion of the nucleus and contains different lysosomal enzymes such as hyaluronidases and proteases that facilitate sperm penetration into the oocyte. The acrosome is bound by an inner acrosomal membrane facing the nucleus and an outer membrane in close contact with sperm plasma membrane (Tanphaichitr et al., 2015). The neck (the area between the head and the midpiece) contains proximal and distal centrioles. The proximal centriole plays a role in the first zygotic cleavage (except rodents) and the distal centriole gives rise to the axial filament of sperm tail (Schatten and Sun, 2009). The midpiece of sperm consists of mitochondria that provide energy for sperm movement and is surrounded by a thin cytoskeletal sheath known as the manchette. The tail or flagellum consists of an axial filament containing a core of microtubules enabling the sperm to swim and reach the oocyte (Lehti and Sironen, 2016). Figure 1.6 represents the main regions of a mature spermatozoon.

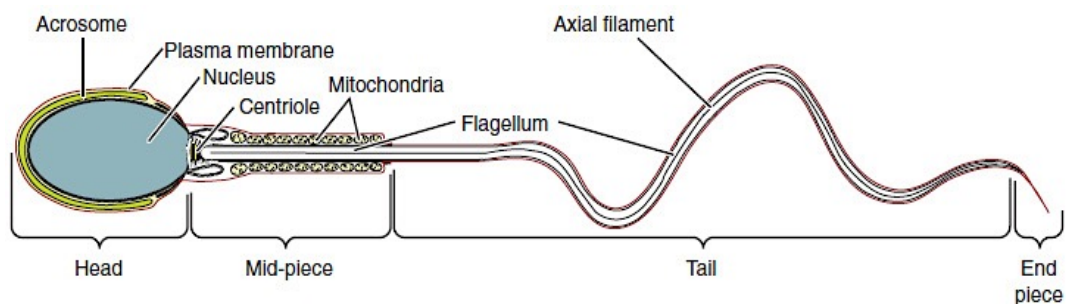


**Figure 1.6. A model representing the main regions of a mature human sperm.**  
([https://cnx.org/resources/63e4c7b77be4e97c88b4c649fd6c6472cf58466/Figure\\_28\\_01\\_05.jpg](https://cnx.org/resources/63e4c7b77be4e97c88b4c649fd6c6472cf58466/Figure_28_01_05.jpg)).

Different studies have been conducted to help correlate fertility to sperm nuclear shape, flagellar length, sperm head dimension, and midpiece length in different species (Saoud et al., 1984; Ostermeier et al., 2001; Mossman et al., 2013). For example, sperm from infertile humans showed higher sperm head width and lower ratio of length/width (Katz et al., 1986). In stallions, significantly higher numbers of sperm with bigger head length is reported in subfertile populations (Casey et al., 1997). In boar, higher sperm head and length, and lower width and width/length ratio are related to infertility (Hirai et al., 2001).

In rabbits, fertile male populations have bigger sperm heads and volume (de Paz et al., 2011). In bovine and canine species, an association between head length (indirect) and head width (direct) and DNA fragmentation is reported (Sailer et al., 1996; Nunez-Martinez et al., 2007). Research on goat sperm showed that dead sperm had smaller head length and width compared with live sperm after cryopreservation (Marco-Jimenez et al., 2006). In addition, human sperm with smaller acrosomes are more sensitive to damage and also non-physiological acrosomal loss (Menkveld et al., 2003).

### **1.6. The hormonal control of male reproductive function**

The male reproductive system is responsible for two main functions including sperm production and maintenance of secondary sexual characteristics both highly regulated by hormones. The hypothalamus act as the first stage of control over male reproduction by producing a hormone known as gonadotropin-releasing hormone (GnRH) (Pitteloud and Dwyer, 2014). The increased levels of GnRH stimulates the anterior pituitary to release follicle stimulating hormones (FSH) and luteinizing hormone (LH). These are the gonadotrophins that exist in both male and female reproductive systems (Courot, 1976). In male, LH stimulates the interstitial cells located between the seminiferous tubules of testes that are responsible for production and secretion of androgens such as testosterone by Leydig cells. Therefore, the obvious role of LH is to initiate the production of testosterone (Ramaswamy and Weinbauer, 2014).

The FSH stimulates the seminiferous tubules of testes responsible for spermatogenesis. Therefore, there are several levels of control of spermatogenesis. Testosterone is important in initiating and maintaining spermatogenesis, however, it is the coordinated secretion of FSH and LH that are ultimately responsible for the continual production of sperm (Ramaswamy and Weinbauer, 2014). Inhibin produced by seminiferous tubules negatively feeds back and inhibits the anterior pituitary from producing FSH. This ultimately stops the stimulation of seminiferous tubules and slows down spermatogenesis when high levels of inhibin are present in the blood. Testosterone also negatively feeds back and inhibits the anterior pituitary from releasing more LH meaning that high levels of testosterone in the blood can reduce the secretory activity of the

interstitial cells of testes and decrease the production of testosterone. The negative feedback mechanisms help to maintain the proper levels of sperm and testosterone production in the male reproductive system (O'Donnell et al., 2000). Figure 1.7 represents the hormonal regulation of male reproductive system.

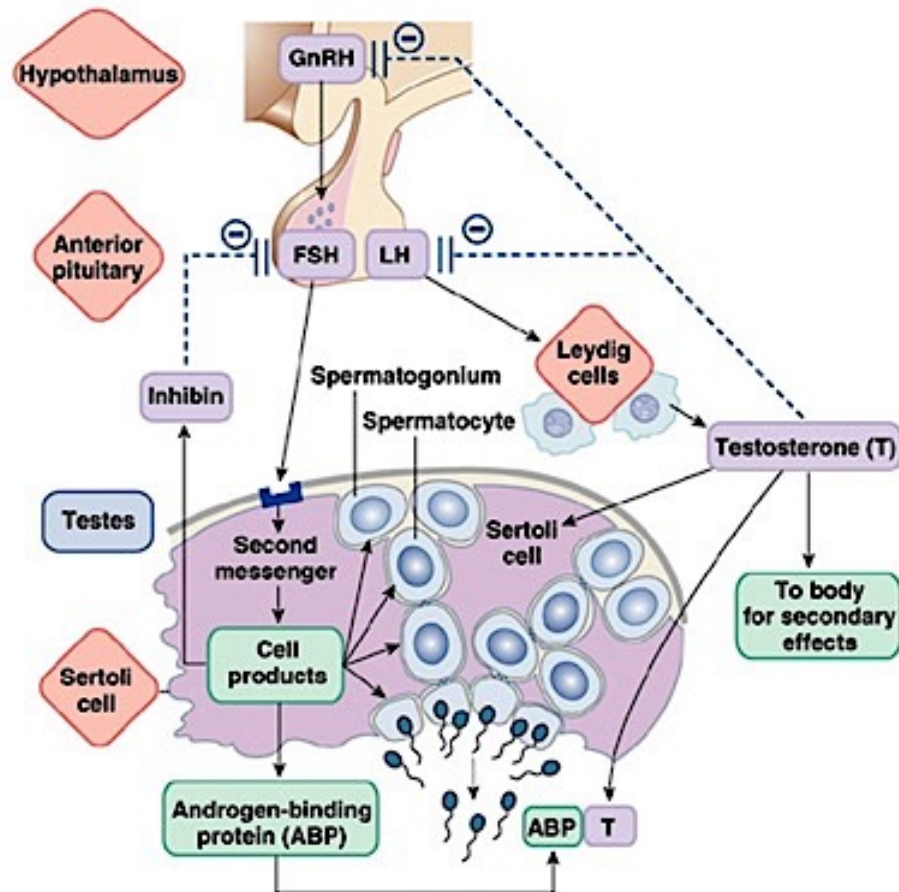


**Figure 1.7. Hormonal regulation of male reproductive system.**

Available from:

(<http://www.austincc.edu/apreview/PhysText/Reproductive.html>).

### 1.7. Sperm metabolism

An optimal sperm metabolism and bioenergetics are crucial for the male fertility and successful spontaneous/assisted pregnancy. It is not only required for the proper function of the sperm in the males but also in the females, en route to fertilisation (Visconti, 2012). The development of germ cells inside the testis depends on the metabolic support from the Sertoli cells, whereas, mature sperm cells can independently carry out the metabolic processes using external nutrients (Miki, 2007; Boussouar and Benahmed, 2004). The testicular

developing germ cells are not able to metabolise glucose but can efficiently use lactate (produced by Sertoli cells) to generate the high energy molecules, ATP (Adenosine triphosphate). Whereas, mature sperm have their own metabolic machinery to utilise several substrates; such as glucose, fructose, mannose, lactate, amino acids to produce ATP. Moreover, the ejaculated sperm cells obtain these nutrient molecules from seminal plasma and the female reproductive tract, once deposited. ATP produced during sperm metabolism is mainly used for sperm motility, acrosome reactions, transportation of molecules through membranes and signaling pathways (Miki, 2007).

Metabolic pathways mainly, glycolysis and mitochondrial oxidative phosphorylation (OXPHOS), are responsible for producing ATP in sperm cells (Goodson et al., 2012; Miki et al., 2004; Huang et al., 2017; Visconti, 2012; Williams and Ford, 2001). Nonetheless, these metabolic pathways are confined to different cellular compartments of sperm. Mitochondrial oxidative phosphorylation occurs in midpiece which is characterised by the presence of mitochondrial sheath, whereas glycolysis takes place in the principal piece of the sperm tail (fibrous sheath of the flagellum) where glycolytic enzymes are mainly located (Ford, 2006; Krisfalusi et al., 2006). Moreover, sperm membrane is equipped with different glucose transporters (GLUTs) for the smooth trafficking of glucose (and other hexose), which is a main substrate for glycolysis (Bucci et al., 2011). The GLUT family consists of 14 proteins which can be classified into three classes depending on hexose affinity, tissue distribution, and structural homogeneity. Numerous studies reported importance of GLUTs 1, 2, 3, 4, 5, 8, and 9 in mature sperm including human revealed various mechanisms involved in producing energy (Bucci et al., 2010; Burant et al., 1992; Angulo et al., 1998; Haber et al., 1993). In human sperm, various GLUTs are located in the acrosome (GLUT1, GLUT2), midpiece (GLUT3, GLUT5), principal piece (GLUT1, GLUT2, GLUT5) and endpiece (GLUT1, GLUT2) highlighting its role in metabolic processes. Another glucose transporter called sodium-coupled glucose transporters (SGLTs) also exists in sperm membrane which require energy to actively transport the sugar molecules. However, GLUTs are the passive transporter of sugars with no requirement of energy consumption (Scheepers et al., 2004).



Hexose metabolism in the sperm is a key process for its function and motility. As stated above, two metabolic processes (glycolysis and OXPHOS) can be accomplished in conjunction or independently to acquire the required energy (Storey, 2008). However, for complete and aerobic oxidation of glucose, both processes work in conjunction, wherein glycolysis serves as a preliminary pathway to the OXPHOS by mitochondria. These pathways are particularly operational in males for attaining sperm motility and in females for completing the fertilisation, in addition to other metabolic process such as pentose phosphate pathways (PPP).

The glycolysis and OXPHOS pathways in sperm are similar to the somatic cells. During glycolysis, glucose from seminal plasma/female reproductive tract enters cellular sperm compartment and is decomposed by different enzymes to produce two molecules of ATP, NADH, and pyruvate. Knocking out of glycolytic enzymes in mice resulted in infertile males. GAPDHS (glyceraldehyde 3-phosphate dehydrogenase, spermatogenic), a sperm-specific glycolytic enzyme is crucial for sperm motility and male fertility potential (Miki et al., 2004). Similarly, a null mouse for phosphoglycerate kinase 2 (PGK2) also exhibited alike infertile phenotype (Danshina et al., 2010). Pyruvate produced during glycolysis either enters the mitochondria or catabolised by LDH (lactate dehydrogenase) generating lactic acid (Peterson and Freund, 1971; Reynolds et al., 2017). Similar to glycolysis, fructolysis is also initiated when fructose is present in the environment with the help of a battery of fructose specific catabolising enzymes also resulting in production of pyruvate and lactate (Douard and Ferraris, 2008). Inside the mitochondria, pyruvate is oxidised and decarboxylated by PDH (pyruvate dehydrogenase enzyme) resulting in production of acetyl- CoA, which can initiate the tricarboxylic acid cycle (TCA cycle). The complete TCA cycle together with mitochondrial electron transport chain will produce enough ATPs to accomplish the sperm functions. Apart from this, sperm also possesses different enzymatic machinery to complete its metabolic activities in the absence or presence of the oxygen, reflecting sperm's metabolic plasticity. Intracellular lipids, glycogen, and other endogenous glucose's sources may serve as the source of energy when obligatory energy sources are absent (Misro and Ramya, 2012; Travis et al., 2001). In fact, sperm may obtain ATP by metabolising long chain fatty acids using mitochondrial and peroxisomal pathways (Amaral et al., 2013). Apart from this,

sperm can also oxidise amino acids to meet their energy requirements. In addition to these two metabolic pathways, PPP is necessarily required during the fertilisation, specifically to facilitate the sperm entry inside the oocyte (Urner and Sakkas, 1999). A study by Goodson et al. (2012) has evidently shown the contribution of glycolysis and OXPHOS by using variously glycolysable and nonglycolysable metabolites. The study further observed that ATP produced in different sub-cellular compartments plays different roles, particularly ATP produced in the principal piece can be efficiently used for hyperactivation of sperm during sperm capacitation. Bioinformatic analysis of combined human sperm proteins has resulted in different metabolic pathways that support the earlier studies and need further studies to establish new pathways (Amaral et al., 2014a). An alteration in the metabolism regulation *in vivo* or due to a pathological condition can result in compromised sperm quality and function. Sperm metabolism can be negatively influenced in diabetic males as well as in varicocele-associated male infertility (Guido et al., 2011; Dias et al., 2014; Agbaje et al., 2007; Ding et al., 2015). Thus, sperm metabolism studies have enough potential to assess male fertility and their implications in assisted reproduction or treatments to improve sperm quality and functionality. Figure 1.8 represents the main metabolic pathways in sperm cells.

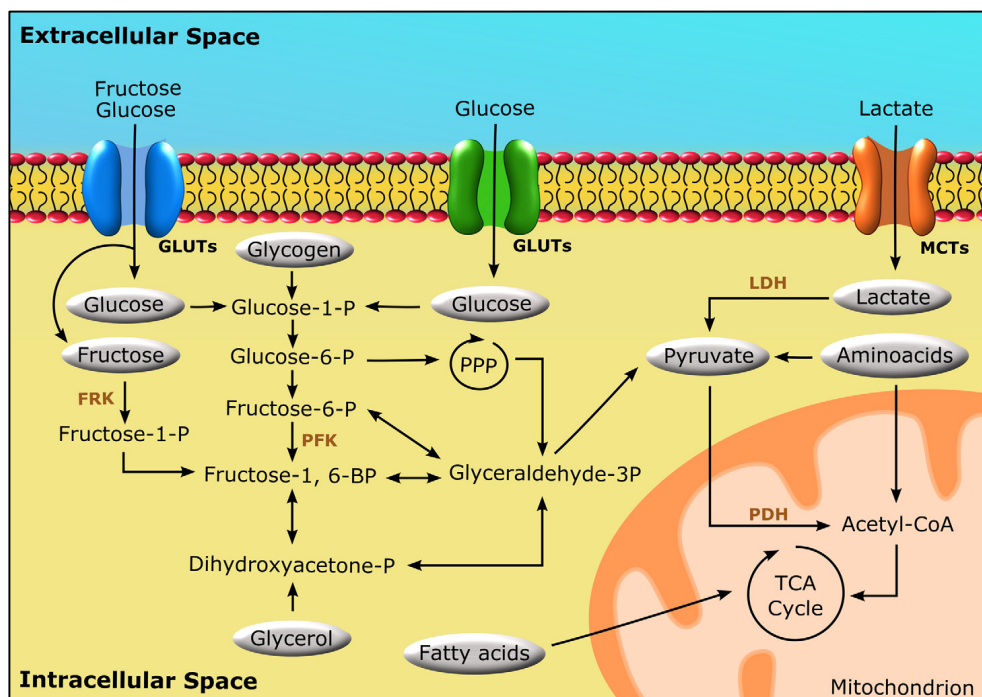


**Figure 1.8. Metabolic pathways in sperm cells (adapted from (Dias et al., 2014)).**

### **1.8. Physiology of fertilisation**

Sperm exist solely to safely deliver the paternal genetic material into the oocyte. Similar to the sperm, the egg contains its share of genetic material ready to combine during fertilisation. To fertilise the egg, spermatozoa have to travel through the female reproductive tract to the oviduct where fertilisation occurs (Coy et al., 2012). The process of capacitation that leads to sperm hyperactive motility takes place during this passage. The oviduct consists of three main parts including the uterotubal junction (UTJ), the isthmus and the ampulla. After spermatozoa are passed through the UTJ, they are held in the isthmus until the time of ovulation. It is known that in cows, binder of sperm protein (BSP) on the surface of sperm (such BSPA1/A2, BSPA3 and BSPA30K) and annexin family of proteins on the epithelium of oviduct are important elements for sperm storage in the isthmus (Ikawa et al., 2010). By releasing unknown female factors, spermatozoa leave the reservoir and migrate to ampulla at the time of ovulation. Sperm hyperactive motility as a result of capacitation also facilitates the release of sperm from the isthmus epithelium (Demott and Suarez, 1992). The slow release of sperm assists the reduction in the number of spermatozoa at the time of fertilisation as polyspermy is incompatible with embryo development (Hunter, 1996).

After sperm migration into the ampulla, the sperm locate the cumulus cell complex (COC) composed of ovulated eggs covered up by zona pellucida (ZP) and multicellular cumulus oophorus and hyaluronic acid (Ikawa et al., 2010). After interaction with COC, sperm penetrates through the cumulus oophorus matrix comprised of a complex of proteins (pentraxin, inter-alpha-trypsin and TNF- $\alpha$ -induced protein 6, all enmeshed in a matrix or glycocalyx of hyaluronic acid (Ikawa et al., 2010; Relucenti et al., 2005). After migration through the cumulus oophorus, capacitated sperm face the zona pellucida as the last barrier before encountering the egg. The main components of mammalian zona pellucida are glycoproteins namely ZP1 to ZP3 in mice and ZP1 to ZP4 in humans. The induction of the AR begins upon sperm binding to zona pellucida. The ZP3 is thought to be the primary sperm receptor that can induce the AR, while ZP2 acts as a secondary receptor for acrosome reacted sperm (Clift and Schuh, 2013). Different sperm proteins such as B4galt1, Clgn, Ace, Adam1a, Adam2, and Adam3 are known to be required for binding to zona pellucida. Sperm meet

the egg soon after penetration of the zona pellucida (Stein et al., 2004). It is known that only acrosome reacted spermatozoa are capable of fusing with the egg and it is due to the exposure or activation of sperm antigens. For example, Izumo1 an important sperm antigen for sperm binding to the egg relocates from the anterior acrosome to the equatorial segment after acrosome reaction (Sebkova et al., 2014).

However, very little is known about the mechanism that facilitates gamete fusion, the necessity of binding between sperm Izumo1 and its egg receptor Juno during sperm-egg binding has been confirmed. *Izumo1*<sup>-/-</sup> sperm do not fuse with the egg and therefore male mice deleted for *Izumo1* are sterile. Female mice deleted for *Juno* are infertile and *Juno*<sup>-/-</sup> eggs are not able to fuse with sperm (Chalbi et al., 2014). After sperm-egg fusion, the egg continues meiosis by which half of the sister chromatids are segregated into a second polar body. The increased levels of intracellular calcium result in exit from meiosis and formation of a female pronucleus. In the meantime sperm chromatin undergoes decompaction by replacing protamines with histones. It also undergoes DNA demethylation as part of epigenetic reprogramming (Clift and Schuh, 2013). The female and male haploid pronuclei combine their chromosomes and form zygote with a diploid nucleus (Alberts et al., 2002). Blastomeres will then form as a result of a series of mitotic divisions. Blastomeres attach to each other in the 8 cell stage to produce morula that eventually form blastocyst (Clift and Schuh, 2013). Figure 1.9 illustrates the process of mammalian fertilisation.

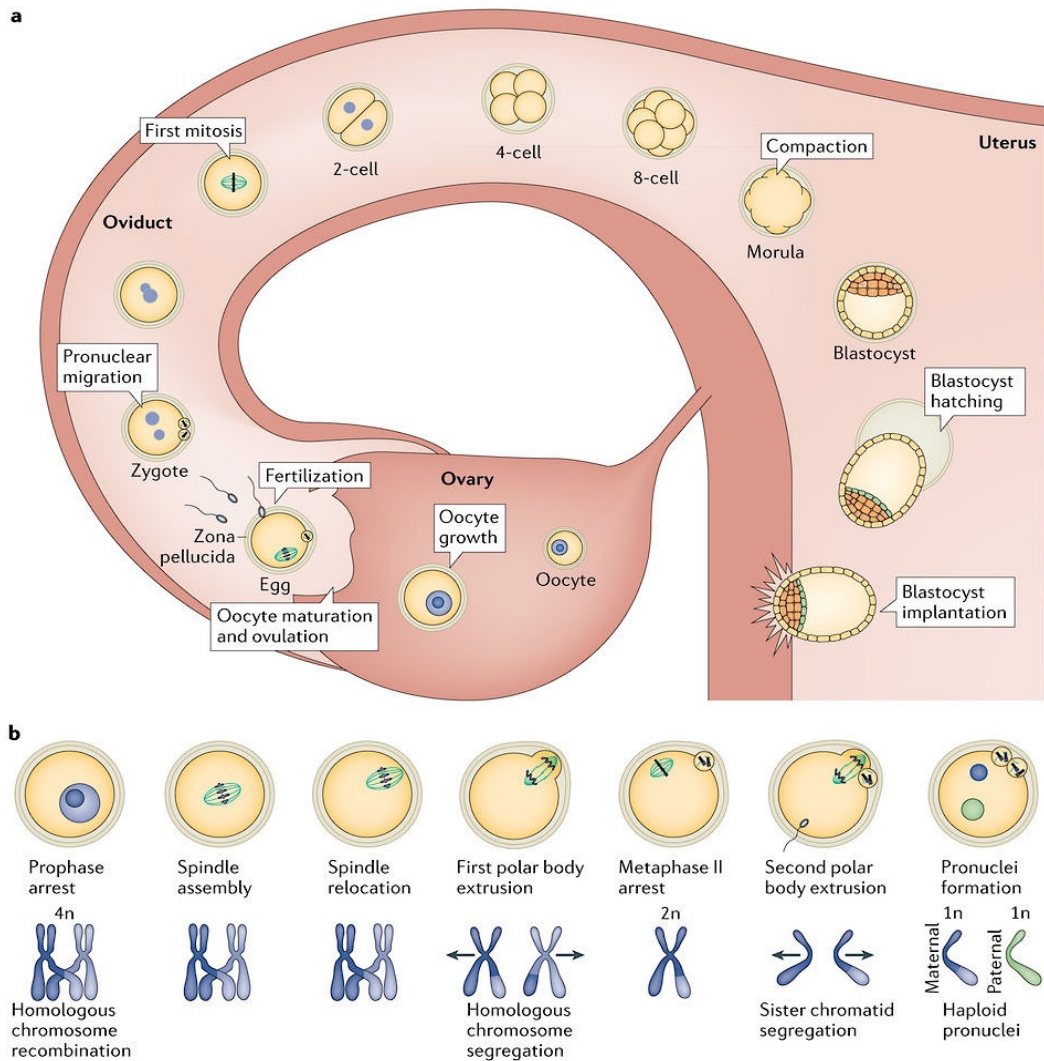


**Figure 1.9. Diagram showing mammalian fertilisation.**

a): An overview of preimplantation development. b): oocyte maturation (from Clift and Schuh 2013).

### 1.9. Male infertility

Infertility is defined as the inability to conceive after regular unprotected coitus for twelve months in the absence of identified reproductive disorders (Zegers-Hochschild et al., 2009). According to World Health Organisation (WHO), 15% of reproductive-age couples are infertile (WHO 2010). Research undertaken by Human Fertilisation and Embryology Authority (HFEA) has shown that the percentage of couples looking for infertility treatment is increasing (HFEA, 2011). This rise in infertility is due to alterations in living standards, delays in planning for motherhood, financial problems and other reasons (Dunson et al., 2004; Sharma et al., 2013). It is believed that approximately 40-50% of infertility cases is due to male factor infertility (Kumar and Singh, 2015; Poongothai et al., 2009).

The major causes of male infertility are pre-testicular (PrT), testicular (T) and post-testicular (PoT):

- Pre-testicular causes: congenital hypogonadotropic hypogonadism, hyperprolactinemia, obesity, medications, aging, drugs, alcohol, genetic disorders (such as a Robertsonian translocation) and epigenetics (such as DNA methylation) (Fraietta et al., 2013; Teerds et al., 2011; Frydman et al., 2001; Dada et al., 2012; Cocuzza et al., 2013).
- Testicular causes: genetic disorders such as Klinefelter Syndrome, mitochondrial DNA mutations, Y chromosome microdeletions, testicular cancer, radiation therapy, acrosomal abnormalities, varicoceles and idiopathic causes (McLachlan et al., 1998; Diez-Sanchez et al., 2003; Poongothai et al., 2009; Liu et al., 2016; Paduch, 2006; Sreenivasa et al., 2012; Kupis et al., 2015; Cocuzza et al., 2013).
- Post-testicular causes: obstruction of vas deferens and the ejaculatory duct and physical abnormalities in the male reproductive tract (Cocuzza et al., 2013).

Due to the complex aetiology of male infertility, males will need a comprehensive andrological evaluation to acquire a precise diagnosis (Barroso et al., 2009; Weber et al., 2005) and there have always been debates in the field regarding how to assess normal and abnormal semen parameters. Thus, WHO developed a standardised procedure of semen analysis to assess conventional sperm parameters including sperm count, morphology and motility (WHO, 2010b). It is thought that the function of sperm may extend beyond the early stages of fertilisation leading to abnormal embryogenesis and implantation failure (Barroso et al., 2009). Therefore the enrichment or selection of high quality sperm with low levels of DNA fragmentation is likely to be an important requirement for successful assisted reproductive technology (ART) treatment.

## **1.10. Routine sperm analysis and separation methods**

### **1.10.1. Visual measurement of semen parameters**

The first step towards the evaluation of male infertility is semen analysis, which involves visual assessment of semen parameters (Table 1.1) using Hoffman contrast microscopy (400x objective) (Oliveira et al., 2011). The obtained figures are compared with those published by the WHO (2010).

**Table 1.1.** Semen parameters and acceptable related reference values (WHO, 2010).

<b>Semen Parameters</b>	<b>Normal</b>	<b>95% Confidence Interval</b>
<b>Liquefaction</b>	≤ 60 minutes	None
<b>Appearance of ejaculate</b>	Grey-opalescent	None
<b>Volume (mL)</b>	1.5	1.4-1.7
<b>pH</b>	7.2	None
<b>Total motility (%)</b>	40	38-42
<b>Progress motility (%)</b>	32	31-34
<b>Vitality (%)</b>	58	55-63
<b>Sperm concentration (million/mL)</b>	15	12-16
<b>Total sperm number (million)</b>	39	33-46
<b>Normal morphology (%)</b>	4	3-4

### 1.10.2. Differential Density Gradient Centrifugation (DDGC)

Differential Density Gradient Centrifugation (DDGC) is routinely used to separate spermatozoa for ART procedures including Intra-Cytoplasmic Sperm Injection (ICSI) and *In Vitro* Fertilisation (IVF). Coated silica-based density gradients are usually used for this purpose (Lee et al., 2009). Percoll, for example consists of polyvinylpyrrolidone (PVP) coated silica particles. During sperm separation by Percoll, a lower concentration solution is underlaid with higher concentration solution. Semen is then introduced to the upper layer. After centrifugation, due to the fertile sperm having higher density and motility, spermatozoa with better fertilising potential sediment to the bottom of the tube forming a pellet from which they can be recovered (Henkel and Schill, 2003). DDGC is thought to enrich for better quality spermatozoa and products for the processing of human sperm, such as PureSperm, SupraSperm and PureCeption, are now routinely used by clinics for this purpose (Soderlund and Lundin, 2000; Malvezzi et al., 2014).

### 1.10.3. The Swim-up procedure

Swim-up is another regularly used method for sperm separation. By using this method, spermatozoa are separated based on their motility (Allamaneni et al., 2005). Briefly, spermatozoa are centrifuged out of seminal plasma in a tube and

pellets are then over-laid with a small volume of culture medium. The tube is then angled to 45° before being incubated for up to one hour at 37°C, 5% CO<sub>2</sub>. The supernatant containing the highly motile spermatozoa will then be washed and can be used in ARTs (Jameel, 2008).

### **1.11. The need for improvements in the efficiency of ART**

ART is the use of reproductive technology for treatment of infertility by manipulating both sperm and egg, and it accounts for 1% of live births in the UK each year (Larcher, 2007). The most common ART techniques include *in vitro* fertilisation (IVF), Gamete Intrafallopian Transfer (GIFT), Zygote Intrafallopian Transfer (ZIFT), Intracytoplasmic Sperm Injection (ICSI) and Laser-Assisted Hatching (Mirza et al., 2016).

#### **1.11.1. Development of ART**

ART has received extensive attention since the birth of Louis Brown, the first baby born using IVF in 1978 (Kamel, 2013). Since then, the ART has gone through extensive improvements. The main developments of ART listed below:

- *In vitro* maturation (IVM) for fertilising morphologically immature oocytes was reported in 1983 (Veeck et al., 1983).
- The first pregnancy using GIFT was reported in 1984 (Asch et al., 1984).
- The first successful pregnancy following ZIFT was reported in 1986 (Devroey et al., 1986).
- For the first time, a new technique called SUZI (sub-zonal injection) was introduced in 1987 that would help couples with persistent failed IVF cycles by injection of a single sperm under the zona pellucida (Laws-King et al., 1987).
- The first successful fertilisation using microsurgical epididymal sperm aspiration (MESA) in men with congenital absence of vas deferens was reported in 1988 (Patrizio et al., 1988).
- The biopsies taken from pre-implanted embryos and sex detection by DNA amplification were reported in 1989 (Handyside et al., 1989).
- A pregnancy was reported after using IVM of donor oocytes collected from non-stimulated cycles in 1991 (Cha et al., 1991).



- The birth of the first baby born after intrauterine insemination (IUI) which involves the insertion of sperm into the uterus at the time of ovulation was announced in 1992 (Cohen et al., 2005).
- The first successful pregnancy after ICSI was also reported in 1992 (Palermo et al., 1992). ICSI involves the injection of a single sperm into the cytoplasm of the egg and can be used in male with poor sperm quality, epididymal or testicular sperm samples, high titres of anti-sperm antibodies, or following a failed fertilisation using IVF (Check et al., 2000; Wong and Ledger, 2013).
- Pregnancies using Testicular Sperm Extraction (TESE) and ICSI procedures in men with non-obstructive azoospermia were announced in 1993 (Devroey et al., 1995).
- Pregnancies by using cryopreserved testicular sperm and ICSI were reported in 1996 (Gil-Salom et al., 1996).

### **1.11.2. Limitations of ART and the importance of sperm selection using more advanced methods**

In natural reproductive cycles, ejaculated spermatozoa encounter physiological selection pressures during their journey across the female reproductive tract, where defective sperm encounter several biological 'checkpoints', probably ensuring that only the 'fitter' sperm reach the oocyte (Suarez and Pacey, 2006; Ikawa et al., 2010). In ART, the success of embryo development and pregnancy outcome also depends on sperm quality (Sakkas et al., 2000a) and the selection of viable sperm, including sperm with high DNA integrity and chromatin maturity is crucial for ART (Hekmatdoost et al., 2009). These requirements are normally met by routine sperm sorting techniques such as swim up and DDGC although their effectiveness is still uncertain (Akerlof et al., 1987; Said and Land, 2011). To a large extent, sperm selection for ART, particularly with ICSI will depend on the embryologist's experience on picking the best sperm and is based on microscopic parameters of sperm motility, viability and morphology. Therefore, sperm abnormalities, especially those occurring at the molecular level cannot be detected by microscopic observation alone (Palermo et al., 1992).

Research has showed sperm with normal motility and morphology may have DNA fragmentation and ICSI provides no barrier for sperm with chromatin and other

defects to participate in the fertilisation process (Celik-Ozenci et al., 2004; Schulte et al., 2010; Avendano and Oehninger, 2011). Functional properties of DDGC or swim up that could explain the improved fertility using sperm processed by these methods may involve DNA integrity and chromatin maturity; but these are usually not measured by the usual assessment techniques (Avendano and Oehninger, 2011). Available evidence suggests that spermatozoa prepared using these methods have generally lower levels of DNA fragmentation or compromised chromatin and are therefore suitable for use in ART. Such preparations, however, may not exclude sperm that are compromised in these regards (Brahem et al., 2011; Henkel, 2012; Mortimer and Mortimer, 2013). Indeed, sperm with normal motility and morphology may still have unacceptably high levels of DNA fragmentation (Celik-Ozenci et al., 2004; Schulte et al., 2010; Avendano and Oehninger, 2011; Seli and Sakkas, 2005)

This situation raises concerns related to the increased risk of ART failure that will include fertilisation failure, failure to implant, miscarriage, an increased risk of congenital abnormalities and childhood cancer (Halliday, 2012; Gopalkrishnan et al., 2000; Larsen et al., 2013). In this regard, various studies have shown that clinical pregnancy rate (CPR), live birth rates (LBR) and also miscarriage in IVF and ICSI are affected when using DNA fragmented spermatozoa (Zini et al., 2001; Zini et al., 2008; Carrell et al., 2003; Simon et al., 2010). These issues have led to calls for the development of new methods of sperm selection, particularly for ICSI based on functional properties and potentially mimicking the natural processes occurring in the reproductive tract of healthy individuals. These methods can be classified as follows:

- Non-apoptotic sperm selection (Magnetic activated cell sorting - MACS) (Said et al., 2008; Grunewald et al., 2001).
- Selection of spermatozoa based on ability to bind with zona pellucida (hemi zona assay) (Said et al., 2008; Ainsworth et al., 2005).
- Selection by differential sperm surface charge (electrophoretic separation and zeta potential) (Ainsworth et al., 2005; Chan et al., 2006; Kheirollahi-Kouhestani et al., 2009).
- Selection based on sperm ultra-morphologic criteria (motile sperm organelle morphology examination (MSOME), intracytoplasmic morphologically selected sperm injection (IMSI) and ICSI using

polarization microscopy) (Bartoov et al., 2002; Bartoov et al., 2003; Gianaroli et al., 2008; Oliveira et al., 2009).

Sperm binding to hyaluronic acid (hyaluronan) is another procedure of sperm selection where sperm are selected on the basis of their membrane maturity (Huszar et al., 1997; Huszar et al., 2003; Nasr-Esfahani et al., 2008; Parmegiani et al., 2010c; Parmegiani et al., 2010a; Torabi et al., 2016; Cayli et al., 2003).

## 1.12. Hyaluronic Acid (HA)

### 1.12.1. Structural properties, synthesis and cleavage of HA

Hyaluronic acid is a high molecular mass ( $10^5$ - $10^7$  Da) and negatively charged glycosaminoglycan (Toole, 2004; Fakhari and Berklund, 2013). It is an extracellular matrix component with numerous biological functions, composed of a repeating disaccharide of N-acetylglucosamine and glucuronic acid [ $-\beta(1,4)$ -GlcUA- $\beta(1,3)$ -GlcNAc-] $_n$  (Figure 1.10). In the body, HA is highly concentrated in several soft connective tissues, including skin, synovial fluid and vitreous humour and also in brain, lung, kidney and muscle tissues (Chen and Abatangelo, 1999).

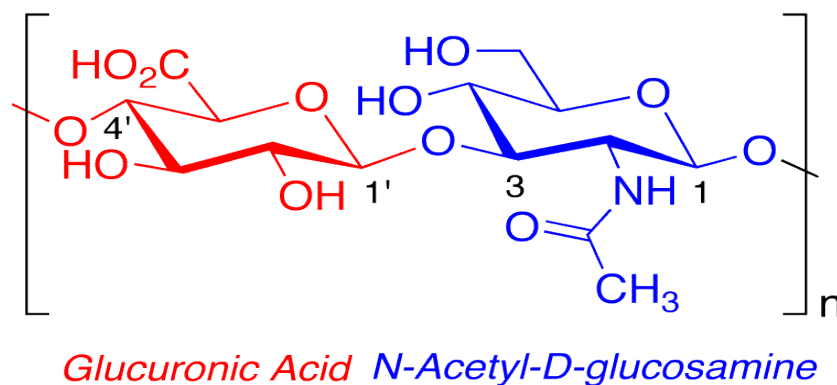
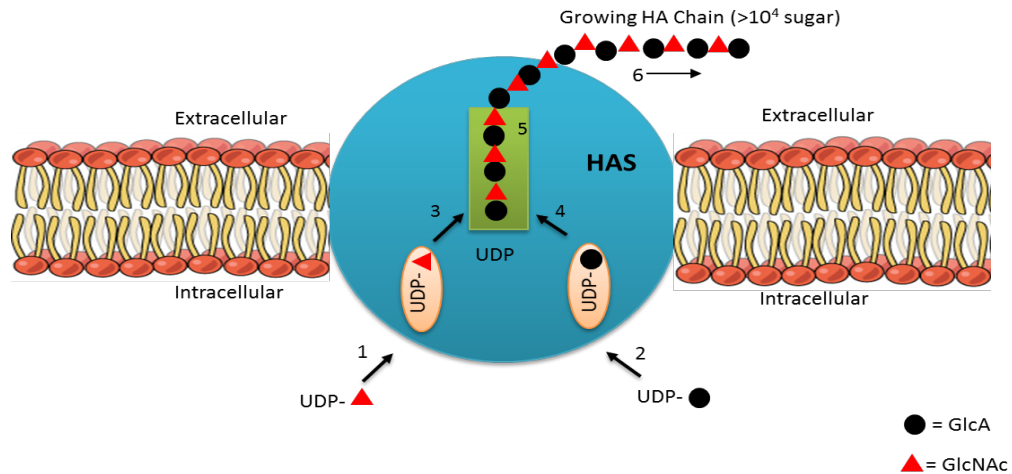


Figure 1.10. Chemical structure of hyaluronic acid (Toole, 2004).

A class of integral membrane proteins called hyaluronan synthases (HAS) produce HA (Necas et al., 2008). There are three different isoforms of these synthases in vertebrates: HAS1, HAS2, and HAS3. These enzymes are located on the inner surface of the plasma membrane and synthesise HA by adding N-acetylglucosamine (GlcNAc) and glucuronic acid (GlcA) to the growing

polysaccharide. The HA is transported through the plasma membrane onto the cell surface or into the extracellular space (Figure 1.11) (Weigel et al., 1997; Toole, 2004; Hascall and Esko, 2009; Weigel, 2015).



**Figure 1.11. Synthesis of hyaluronic acid (Reproduced from Weigel, 2015).**

1) UDP-GlcNAc binding site, 2) UDP-GlcA binding site, 3) beta (1, 4) GlcNAc transferase, 4) beta (1, 3) GlcA transferase, 5) HA (acceptor) binding site, 6) HA transfer (translocation).

### 1.12.2. Digestion of HA

In mammals,  $\beta$ -N-acetyl-hexosaminidase,  $\beta$ -D-glucuronidase and hyaluronidase (hyase) are involved in degradation of HA. In general, high molecular weight HA is cleaved into smaller oligosaccharides by hyases and degradation of fragmented oligosaccharides occurs using  $\beta$ -D-glucuronidase and  $\beta$ -N-acetyl-hexosaminidase by removing non-reducing terminal sugars (J. Necas, 2008). To date, six hyaluronidase-like genes have been identified in the human genome. Three of these genes are clustered on chromosome 3p21.3 including *HYAL1*, *HYAL2* and *HYAL3* which their products are HYAL-1, HYAL-2 and HYAL-3, respectively. The other hyaluronidases are clustered on chromosome 7q31.3 (*HYAL4* and *SPAM1*) and produce HYAL-4 and PH-20 (Csoka et al., 2001).

### 1.12.3. Hyaluronic acid binding proteins (HABPs)

Hyaluronic acid plays many important roles in the extracellular matrix (ECM) by interaction with several hyaluronic acid-binding proteins (HABPs) called hyaladherins (Sengupta et al., 2005). In general, HABPs are divided into two different superfamilies including the Link module and non-Link module

superfamily (Day and Prestwich, 2002). Figure 1.12 summarises the known HABPs belonging to the Link module superfamily.

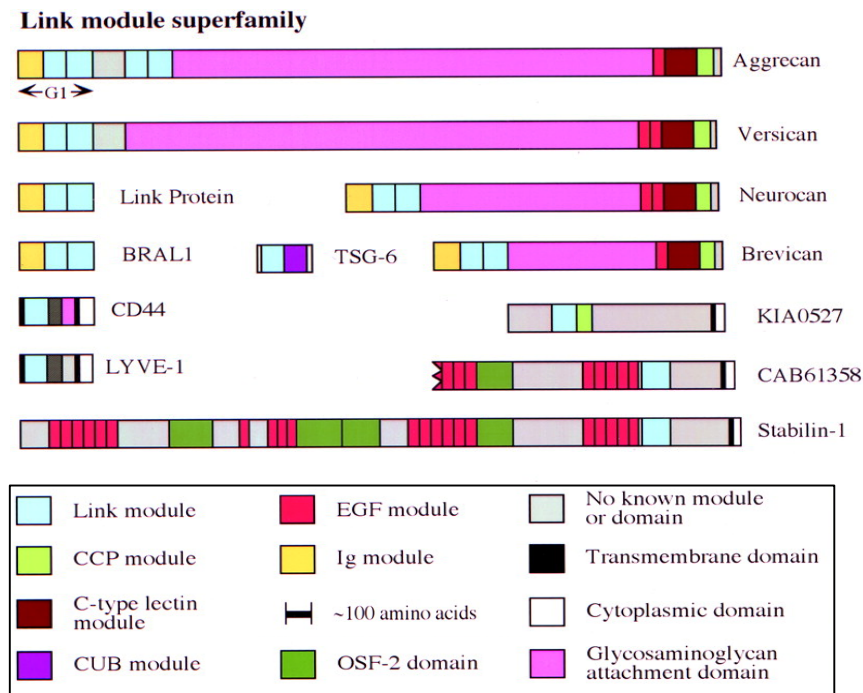


**Figure 1.12. The Link module superfamily of HABPs (Day and Prestwich, 2002).**

The Link module consists of approximately 100 amino acids with two  $\alpha$ -helices and two triple-stranded anti-parallel  $\beta$ -sheets (Kohda et al., 1996). Furthermore, it has two disulphide bonds between Cys1-Cys4 and Cys2-Cys3 (<http://www.expasy.org/prosite/PDOC00955>).

TSG-6 protein a member of the Link module superfamily is secreted in response to inflammatory stimuli and its Link module can be considered as representative of the other superfamily members (Day and Prestwich, 2002; Kahmann et al., 2000). Figure 1.13 presents a schematic illustration of the Link module from different Link module-containing hyaluronic acid binding proteins.



**Figure 1.13. Alignment of the Link modules from some members of Link module superfamily (from Day; <http://glycoforum.gr.jp/science/hyaluronan/HA16/HA16E.pdf>).** LP, A1, B1 (R), V1, 61358 and 0527 are link proteins, aggrecan, brevican, versican, CAB61358 and KIA0527, respectively. Cysteine and other conserved residues forming the Link module consensus sequence (CON) are highlighted in yellow and pink, respectively. The location of secondary structure residues (SS), identified in TSG-6 are presented below the alignment (a =  $\alpha$ -helix, b =  $\beta$ -strand, ^ = bulge).

The best characterised HABP belonging to the Link module superfamily is CD44 (Bajorath et al., 1998; Day and Prestwich, 2002) which is a cell surface glycoprotein with a molecular mass ranging from 70 to > 220 kDa. This HABP is involved in cell-cell interactions, cell adhesion and migration (Martegani et al., 1999; Ahrens et al., 2001). There is significant variation in the size of CD44 molecules expressed in different cell types due to varied levels of glycosylation and also differential splicing of several exons (approximately 10 in mammals) in the membrane proximal region of the extracellular domain (Peach et al., 1993; Oliferenko et al., 2000). As shown in Figure 1.14, CD44 binds HA through a disulphide-bond stabilized HA-binding domain (HABD) included within the Link module (residues 32-124) and some additional residues at the N-terminal (residues 21-31) and C-terminal ends (residues 125-178) which are known to be important for binding to HA (Takeda et al., 2006).

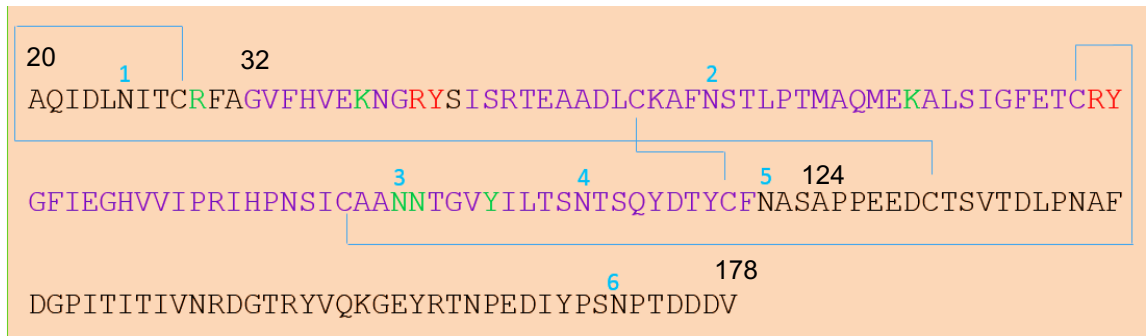


**Figure 1.14. Hyaluronic acid-binding domain of CD44 (reproduced from Day; <http://glycoforum.gr.jp/science/hyaluronan/HA16/HA16E.pdf>).**

The Link module is indicated in purple.

The black residues are N- and C-terminal segments which are connected via a disulphide bond. The important residues for binding to HA are labelled in green and red. Six N-linked glycosylation sites (N1-N6) are available.

The non-Link module superfamily is another category of HABPs that do not contain a Link module. RHAMM (receptor for hyaluronic-acid-mediated motility) is one of the better known HABPs belonging to this superfamily and is expressed in many cell types such as endothelial cells, nerve cells, fibroblasts, macrophages, smooth muscle cells, sperm and malignant tumours. Like CD44, alternative splicing generates different RHAMM isoforms expressed in the cytoplasm, nucleus and on the cell surface (Turley et al., 2002; Nedvetzki et al., 2004; Kouvidi et al., 2011; Day and Prestwich, 2002). In addition to RHAMM other intracellular HABPs including vertebrate CDC37, IHABP4, P-32 (also known as HABP-1) have been described. Figure 1.15 shows the members of this superfamily identified to date.

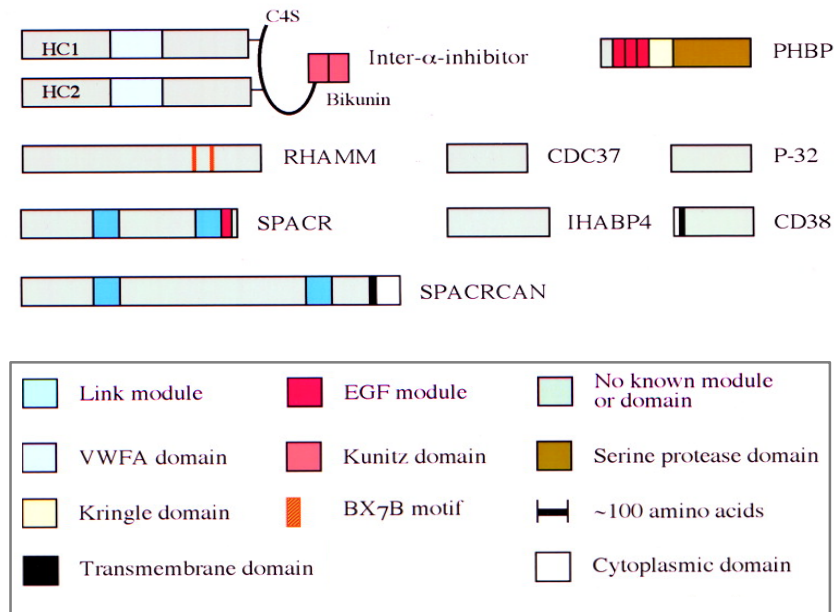


**Figure 1.15. The non-Link module superfamily of HABPs (Day and Prestwich, 2002).**

The main HA binding motif in RHAMM is the BX7B motif (where “B” is arginine (R) or lysine (K) and “X” is any non-acidic amino acid with at least one basic amino acid). RHAMM BXB7 is located near the carboxyl-terminus of the protein (Yang et al., 1994; Day and Prestwich, 2002). The same motif can be found in some other HABPs such as CD44, Link protein, TSG-6, versican and may be crucial for binding to HA (Table 1.2) (Yang et al., 1994; Misra et al., 2015; Naor, 2016).

In general, the interactions of HA with CD44 and RHAMM are of obvious physiological importance, and their normal activities seem to be disrupted in cancer cells. The interactions of HA with CD44 and RHAMM give rise to many cellular responses, which involve protein kinase C (PKC), focal adhesion kinase (FAK), tyrosine kinases (TK), phosphatidylinositol 3-kinase (PI3K), mitogen-activated protein kinase and nuclear factor- $\kappa$ B to name a few (Turley et al., 2002; Ponta et al., 2003).



**Table 1.2.** HA-binding motif BX7B identified in some HABPs (Reproduced from Yang *et al.*, 1994).

Proteins	Binding region	Amino acid sequence	Binding confirmed
RHAMM	401-411	<sup>401</sup> KQKIKHVVKL <sup>411</sup>	+
RHAMM	423-432	<sup>423</sup> KLKSQLVKRK <sup>432</sup>	+
Link protein	103-112	<sup>103</sup> RKSYGKYQGR <sup>112</sup>	
Link protein	316-325	<sup>316</sup> RYPISRPRKR <sup>325</sup>	+
CD44	38-46	<sup>38</sup> KNGRYSISR <sup>46</sup>	+
CD44	150-162	<sup>150</sup> RDGTRYVQKGEYR <sup>162</sup>	+
CD44	292-300	<sup>29</sup> 2RRRCGQKKK <sup>300</sup>	+
HAse	96-104	<sup>96</sup> RGTRSGSTR <sup>104</sup>	+
HAse	106-117	<sup>106</sup> RRRKKIQGRSKR <sup>117</sup>	+
Versican	25-33	<sup>25</sup> KVGKSPVVR <sup>33</sup>	
Versican	2319-2327	<sup>2319</sup> KTFGKMKPR <sup>2327</sup>	
Aggrecan	71-79	<sup>71</sup> RIKWSRVSK <sup>79</sup>	
Aggrecan	2109-2117	<sup>2109</sup> KRTMRPTRR2 <sup>2117</sup>	
TSG-6	39-48	<sup>39</sup> HREARSGKYK <sup>48</sup>	

#### 1.12.4. Hyaluronic acid, its binding proteins and their role in reproductive system

Compared with female, very little is known about HA and its binding proteins in the male reproductive system. Geipel et al (1992) reported higher HA concentration in human seminal fluid compared with serum (Geipel et al., 1992). They also showed a negative correlation between HA concentrations in seminal fluid with ejaculate volume and sperm concentration. Higher levels of HA in patients with oligozoospermia and azoospermia were the other findings of their

study. Research by Tammi et al (1994) revealed high concentrations of HA in different segments of the bovine reproductive system including the epididymis, seminal vesicles, prostate, Cowper's gland. Only traces of HA were found in testes (Tammi et al., 1994). These data suggest that HA in seminal fluid originates from the male accessory sex glands. Hyaluronic acid is also found in the seminal fluids of other species, including alpaca, llama and pigs (Bravo et al., 2000; Sakairi et al., 2007).

Additionally, HA is abundant in the female reproductive tract including the oviduct, uterus and cervix and is thought to be involved in sperm-egg interactions (Ghosh et al., 2002). The cumulus oophorus complex (COC), consisting of 3000-5000 cumulus cells in the periphery of the oocyte is also HA-rich (Zhuo and Kimata, 2001) and HA also permeates the zona pellucida and the perivitelline space of mammalian oocytes (Figure 1.16) (Vandevoort et al., 1997). The formation of specific receptors involved in sperm-egg fusion including zona pellucida receptors and HABPs occurs during sperm plasma membrane remodelling (Sakkas et al., 2015). During *in vivo* fertilisation, mature spermatozoa bind HA in the extracellular matrix of the COC via specific HA-binding proteins (including CD44) and by releasing hyaluronidase (for example, SPAM1) on interaction with the zona pellucida. Immature spermatozoa, however, do not bind to HA or bind to it more weakly (Nasr-Esfahani et al., 2008; Huszar et al., 2003). Reports suggest that only mature spermatozoa bind efficiently to hyaluronic acid and subsequent sperm hyper-activation facilitates sperm penetration of the cumulus shell to give access to the zona pellucida and fertilisation of the oocyte (Parmegiani et al., 2010a; Witt et al., 2016). Research has also demonstrated that spermatozoa binding to HA *in vitro* have completed nuclear maturation, cytoplasmic extrusion and plasma membrane remodelling (Huszar et al., 2003; Rengan et al., 2012).

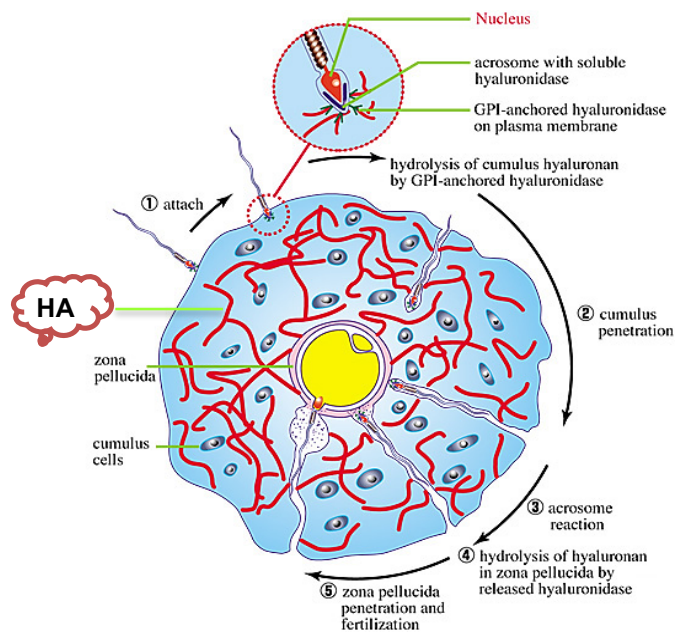


**Figure 1.16. Diagram of sperm penetration through the cumulus oophorus matrix (reproduced from Salustri and Fulop, 1998).**

The current theory for the processing that gives rise to the sperm's ability to bind HA involves the heat shock protein HSPA2 which is expressed in spermatozoa during late spermiogenesis. In normal sperm maturation HSPA2 is involved in plasma membrane remodelling, cytoplasmic extrusion, and the formation of the zona pellucida binding domains and hyaluronic acid binding proteins (Figure 1.17). In contrast, sperm with diminished maturity lack HSPA2 expression which leads to meiotic defects and a higher rate of retention of cytoplasmic enzymes, as well as increased levels of lipid peroxidation (LP) and consequent DNA fragmentation, abnormal sperm morphology and deficiency in zona and HA binding (Figure 1.17) (Huszar et al., 1997; Huszar et al., 2000; Nixon et al., 2015).

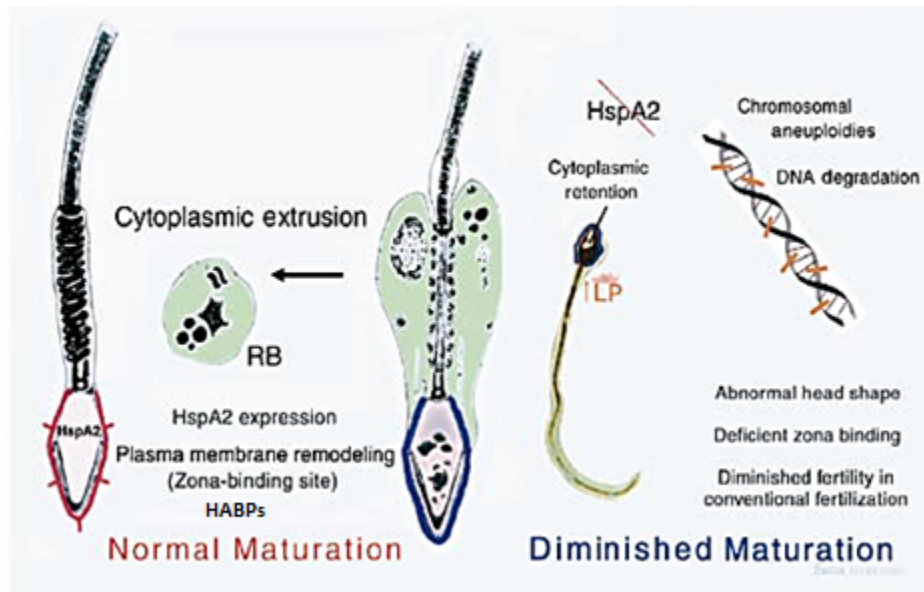


Figure 1.17. A model of normal and diminished maturation of human sperm (Huszar et al, 2000).

In these studies, HA-binding spermatozoa had better morphology and motility than spermatozoa prepared by DDGC or spermatozoa in unprocessed semen. It has also been reported that HA-binding spermatozoa have improved morphology based on Tygerberg (strict) scoring criteria (Prinosilova et al., 2009; Parmegiani et al., 2010b; Petersen et al., 2010). In addition, it has been confirmed that HA-selected spermatozoa are mature, viable, non-acrosome reacted and devoid of cytoplasmic retention. Furthermore, HA-binding sperm seem to have less DNA fragmentation, fewer chromosomal aneuploidies and lower levels of apoptotic markers such as caspase-3 (Huszar et al., 2003; Tarozzi et al., 2009; Parmegiani et al., 2010b). A previous study has also reported the expression of CD44 on human spermatozoa (Bains et al., 2002).

Hyaluronic acid is reported to be involved in induction of capacitation in bovine sperm by the activation of membrane-associated adenylate cyclase and in dog sperm by an increasing influx of  $Ca^{2+}$  into the cytoplasm and the elevated production of cAMP (Kawakami et al., 2006; Fernandez and Cordoba, 2014). Hyaluronic acid also enhances the acrosome reaction in bovine and porcine sperm (Gutnisky et al., 2007; Suzuki et al., 2002).

The addition of HA to human sperm during sample preparation (swim-up) increases sperm motility and decreases the number of sperm with high DNA fragmentation (Saylan and Duman, 2016). Additionally, HA can counteract the negative impact of sperm motility and viability resulting from cryopreservation of human, mouse, rooster and boar sperm (Sbracia et al., 1997; Bakhtiari et al., 2007; Lotfi et al., 2017; Qian et al., 2016). In human, the HA-induced increase in sperm motility is associated with protein phosphorylation including the phosphorylation of HABPs (Ranganathan et al., 1995). Different HABPs including CD44, RHAMM, hyaluronic acid binding protein 1 (HABP1) and SPAM1 have been reported in sperm. Research by Bain et al (2002) led to identification of CD44 in human sperm with the protein's distribution reported on the sperm membrane and acrosome (Bains et al., 2002). In addition, CD44 has been reported on the surface of sperm of other species including bovine, boar and ram (Tienthai et al., 2003; Huszar et al., 2003; Bergqvist et al., 2006). CD44 has also been reported in human cervical, uterine and ovarian tissues (Lopez et al., 2013), ovine cervix (Perry et al., 2010), bovine oviductal epithelium (Bergqvist et al., 2005) and mare ovarian, oviduct and uterine tissues (Rodriguez Hurtado et al., 2011).

The interaction between HA and CD44 initiates different signaling pathways involved in oocyte development, sperm-egg interaction (Kimura et al., 2007; Schoenfelder and Einspanier, 2003) and cancer (Toole, 2009; Misra et al., 2015). The interaction between HA and CD44 stimulates intracellular signaling through extracellular regulated kinase (ERK), phosphoinositide 3-kinase (PI3K), Ras and Rac in different cells (Fouladi-Nashta et al., 2017). Research by Marei et al (2013) revealed that small HA fragments (20 kDa) enhanced MAPK1/3 (mitogen-activated protein kinase 1/3) phosphorylation, leading to increased blastocyst formation. This was inhibited by blocking CD44 with specific antibodies (Marei et al., 2013).

Receptor for hyaluronan-mediated motility (RHAMM) is known to be located in the human sperm head, midpiece and tail. Its role in regulation of sperm motility was investigated with anti RHAMM antibodies (Kornovski et al., 1994). The presence of RHAMM in sperm from other species remains unknown. This HABP also plays an important role in different cellular events including mitosis with high

expression in the G2/M phase of the cell cycle, and in cell proliferation and migration. HA-RHAMM interaction leads to mitotic stimulation and activation of MAPK1/3 via its phosphorylation (Fouladi-Nashta et al., 2017).

Research in mice has shown that RHAMM deficiency disrupts spindle orientation in dividing granulosa cells and folliculogenesis resulting in female hypofertility (Li et al., 2015). In the human, RHAMM is expressed during all stages of pre-implantation embryogenesis from the two-cell stage to blastocysts (Choudhary et al., 2007). Bovine embryos showed highest RHAMM expression at their blastocyst stage (Stojkovic et al., 2003). RHAMM, therefore, supports mitotic division during embryogenesis and the development of blastocysts with high cell numbers (Fouladi-Nashta et al., 2017). Hyaluronic acid binding protein 1 (HABP1) is also involved in sperm-oocyte interactions and its presence on sperm of different species including human, rat, mouse and bull has been confirmed (Ghosh et al., 2007; Ranganathan et al., 1994). A decrease in the expression of HABP1 is associated with diminished sperm motility (Ghosh et al., 2007) and resulted in the development of the HA-binding assay (Cayli et al., 2003).

As well as HABPs, the presence of hyaluronidases including HYAL5 and SPAM1 (PH20) are reported in sperm. These proteins are localised in the testis or epididymis of different species including human, pig and mouse (Fouladi-Nashta et al., 2017). SPAM1 is a glycosylphosphatidylinositol-anchored hyaluronidase expressed on the sperm surface and involved in digestion of HA into tetra and hexasacharide units. The protein is secreted during epididymal maturation (Martin-DeLeon, 2006). It is the main hyaluronidase in human sperm and exhibits its enzymatic activity at neutral and acidic pHs (Zhang et al., 2004). Insoluble membrane-bound SPAM1, facilitates penetration of sperm through the HA-rich ECM of cumulus cells, whereas the soluble protein is released after the AR and may interact with the zona pellucida (Myles and Primakoff, 1997). SPAM1 contains a HA receptor domain located in the N-terminal. The interaction between HA and SPAM1 results in  $Ca^{2+}$  signaling that accompanies the AR (Cherr et al., 2001). SPAM1 is synthesised in epididymis of different species including rat, dog, human and mouse (Zhang et al., 2004). The role of mouse SPAM1 in sperm penetration through the cumulus matrix and binding to zona pellucida has been reported (Cherr et al., 2001). Research by Reddy et al 1980 showed that HYAL

inhibitors inhibited fertilisation as a result of a decreased disaggregation of the cumulus oophorus complex (Reddy et al., 1980).

HA-mediated signaling is driven mainly by smaller molecules of HA (20kDa). The high molecular weight HA is space filling, has immunosuppressive effects and can induce cell cycle arrest (Fouladi-Nashta et al., 2017). In reproduction, the size of the HA molecule is dictated by the structural elements and physiological status of the tissue. In females, as shown in Figure 1.18, estradiol (E2) induces the expression of hyaluronic synthase 2 (HAS2) that synthesizes high molecular weight HA to support ovulation and fertilisation. The expression of CD44, production of small HA fragments (by HAS3) and depolymerisation of HA into small fragments (by Hyal2) are all up-regulated by progesterone (P4)-dominated secretory phase of the cycle. Small HA fragments support early embryo development and stimulate the expression of adhesion molecules and the signaling pathways necessary for blastocyst attachment to the uterine luminal epithelium and pregnancy (Fouladi-Nashta et al., 2017).

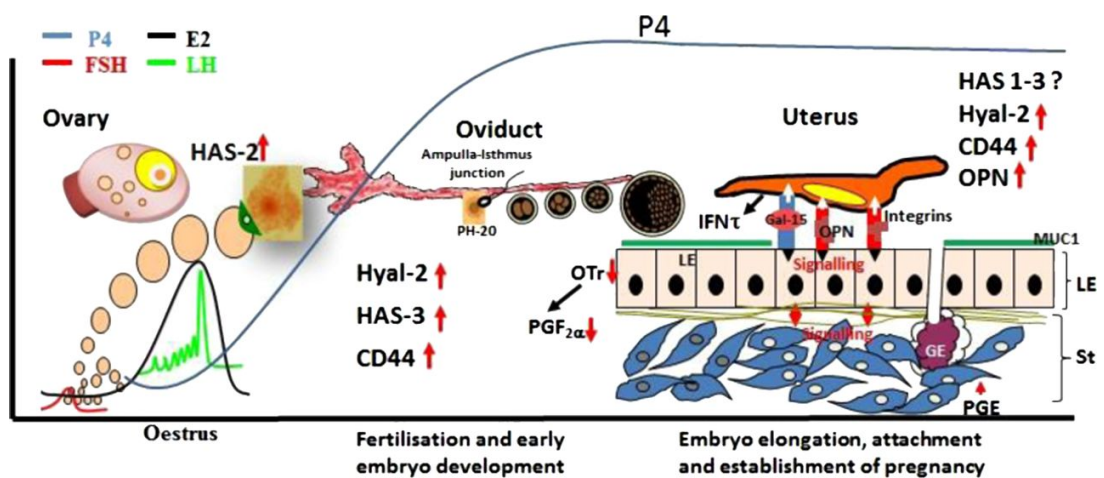


**Figure 1.18. A model of HA synthesis, digestion and function in the reproductive system (from Fouladi-Nashta et al. 2017).**

FSH: follicle-stimulating hormone, GE: glandular epithelium, LH: luteinising hormone, IFN $\tau$ : interferon tau, MUC1: mucin 1, OPN: osteopontin, OTr: oxytocin receptor, PGE: prostaglandin E, St: uterine stroma cell.

### 1.12.5. Pregnancy outcomes using sperm selection by HA-binding

Based on the likely importance of HA in the fertilisation process Huszar et al developed the PICSI (physiological ICSI) process (Huszar et al., 2003). In this procedure, washed spermatozoa are introduced to a HA-coated surface and sperm that bind are then collected and used for injection. It is thought that the

heads of motile mature spermatozoa presenting adequate numbers of HABPs bind to the HA coated surface while immature spermatozoa do not have sufficient numbers of HABPs and continue to move around freely (Huszar et al., 2003). Until recently, ART data had not shown significant correlations between sperm HA-binding and fertilisation rate, embryo quality, miscarriage and pregnancy. Newer studies, however, have reported significantly higher fertilisation and pregnancy rates after ICSI using spermatozoa selected by HA (Nasr-Esfahani et al., 2008; Tarozzi et al., 2009; Nijs et al., 2010). Other ICSI studies using HA-binding spermatozoa revealed higher embryo quality and cleavage rates compared with spermatozoa selected by routine methods such as DDGC (Tarozzi et al., 2009; Parmegiani et al., 2010a; Parmegiani et al., 2010b). A multicenter randomised study by WorriLOW et al (2013) showed higher implantation and clinical pregnancy rates in the PICSi compared with the control (ICSI) group (WorriLOW et al., 2013). The same study revealed significantly lower miscarriage rates in the PICSi group.

A randomised study in relation to the effect of HA sperm selection on ICSI outcomes by Majmbar et al (2013) revealed lower miscarriage rate in the PICSi group of patients with unexplained infertility and normal semen parameters. However, they did not find any difference in fertilisation rate and the number of high quality embryos between two groups. They concluded that patients with unexplained infertility and normal semen parameters may not benefit from HA-binding assay before ICSI (Majumdar and Majumdar, 2013). A systematic review and meta-analysis in relation to HA binding technique by Beck-Fruchter et al (2016) showed an increase in implantation rate and embryo quality after PICSi (Beck-Fruchter et al., 2016). The most recent study on HA-binding (Erberelli et al (2017) reported enhanced clinical and chemical pregnancy rates in PICSi cycles associated with male factor infertility (Erberelli et al., 2017). This study recommended including HA-based sperm selection to avoid the use of immature sperm with high DNA fragmentation in ICSI cycles.

The reasoning behind the use of a treatment-associated HA-binding assay, is that sperm with the ability to recognise and bind HA have a greater chance of successfully fertilizing the egg. However further studies are needed (Sakkas et al., 2015).



### 1.13. Sperm DNA fragmentation and male infertility

Histones (~10-15%) and protamines (~85%) are the main and the most abundant proteins in the sperm nucleus (Figure 1.19) (Marino-Ramirez et al., 2005; Balhorn, 2007; Oliva, 2006). The replacement of histones with protamines during spermatogenesis leads to higher sperm chromatin compaction and if incomplete, DNA becomes susceptible to damage. Indeed, abnormally high levels of histones in sperm are associated with sperm immaturity (Schulte et al., 2010). Hence, protamination is a crucial step for sperm DNA re-packaging as it helps to protect the DNA against exogenous assaults (Barratt et al., 2010). Despite this protection, some levels of DNA fragmentations can be still found in infertile men (Sakkas and Alvarez, 2010) and there is the possibility that the less densely compacted histone-bound DNA, naturally retained by sperm may be differentially susceptible (Stuppia et al., 2015; Kumar et al., 2013c). In this regard, in addition to ejaculated spermatozoa, DNA fragmentation has also been found in spermatozoa retrieved from testis and the epididymis. As spermatozoa are transcriptionally and translationally silent, DNA fragmentation can only be partially repaired by sperm while it is developing and post ejaculation, will rely on the oocyte or early embryo for more complete repair (Menezo et al., 2010; Aitken, 2014). Oocytes and embryos however, may not be able to repair all sperm DNA fragmentations (Gonzalez-Marin et al., 2012).

Sperm DNA fragmentation has been found to be associated with male infertility phenotype in human and other mammals (Aitken et al., 2013; Moretti et al., 2017; Simon et al., 2014a; Durmaz et al., 2014). Both spontaneous and assisted reproduction outcome is affected due to a high level of sperm DNA fragmentation (Zhao et al., 2014; Osman et al., 2014; Ramos-Ibeas et al., 2014; Simon et al., 2013). DNA fragmentation in sperm may originate during *in vivo* spermatogenesis as well mature sperm transportation from testis. The underlying mechanisms for DNA fragmentation are cell apoptosis during production and maturation of sperm, chromatin remodeling during histone to protamine transition, exposure to free radicals during sperm transport and epididymal maturation, and adverse lifestyle together with exposure to environment toxicants (Sakkas and Alvarez, 2010; Delbès et al., 2010).

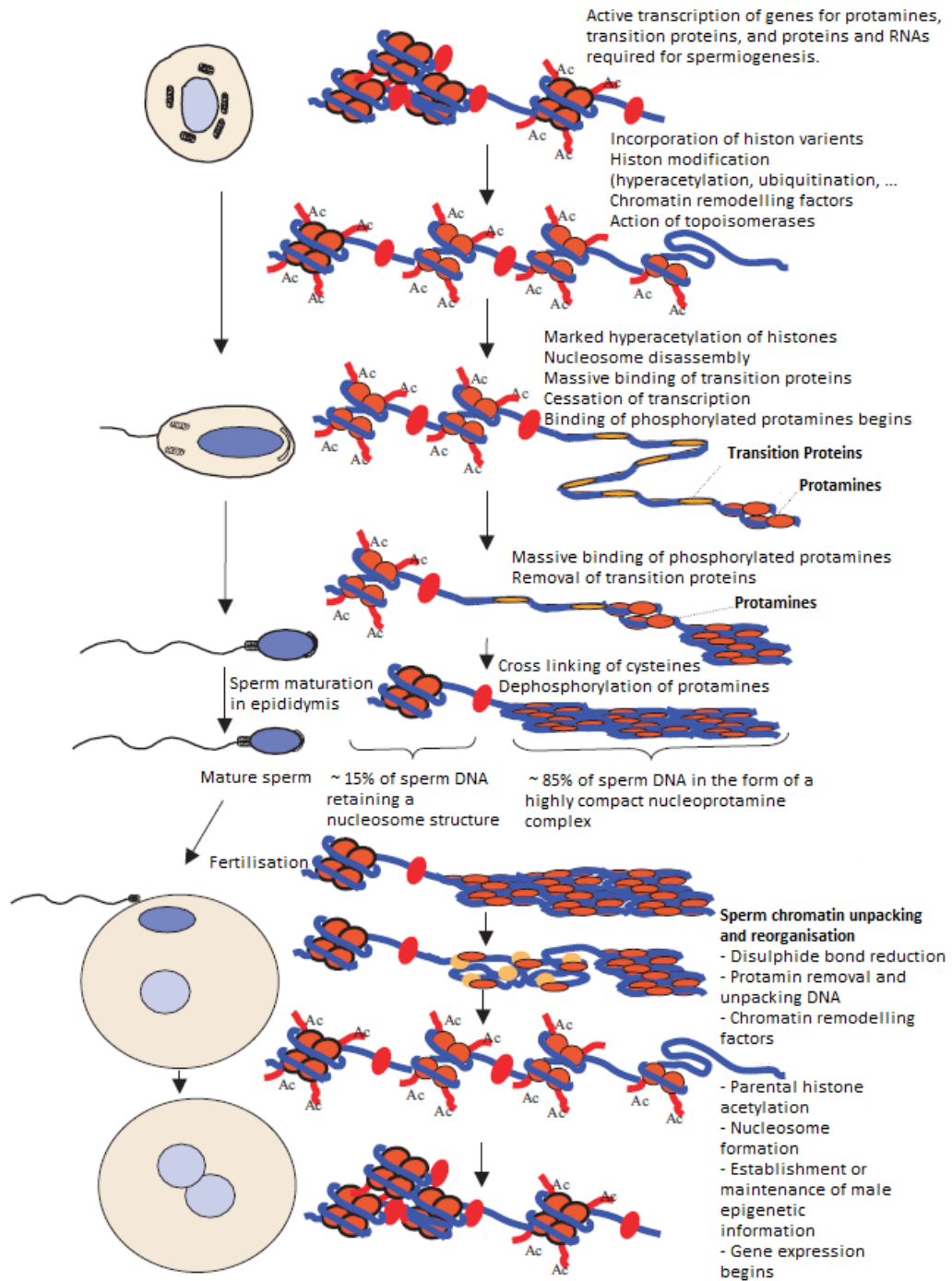


**Figure 1.19. Schematic illustration of major changes during chromatin compaction and chromatin unpacking in spermiogenesis and fertilisation, respectively (Oliva, 2006).**

One of the most accepted and documented cause of the sperm DNA fragmentation in infertile men is oxidative stress (OS): a condition where oxidants (also free radicals) exceed antioxidants (Aitken et al., 2010; Wright et al., 2014;

Chen et al., 2013; Cambi et al., 2013). Indeed, studies have reported OS mediated sperm DNA fragmentation amounts to 30-80% of infertile cases (Shen and Ong, 2000; Aitken et al., 2013). As sperm plasma membrane is rich in polyunsaturated fatty acids, it makes sperm prone to OS-induced injuries, consequently affecting sperm function and DNA integrity (Agarwal et al., 2014). A common adduct of OS is 8-hydroxy-2-deoxyguanosine (8-OH-2-deoxyguanosine) which is confirmed as a main biomarker of oxidative-induced sperm DNA fragmentation in infertile men (Cambi et al., 2013). Moreover, 8OHdG formation and DNA fragmentation are highly correlated to each other which in combination negatively affect ART success rate (Aitken et al., 2010). Also, infertile men opting for IUI treatment having normal semen parameters were diagnosed with high sperm DNA fragmentation (Alkhalaf et al., 2013). DNA breaks such as double-strand DNA breaks (dsDNA) also causes sperm DNA fragmentation and poor sperm quality. A study found a significant difference in sperm dsDNA breaks between normozoospermic and oligozoospermic men (Derijck et al., 2007). Consequently, OS has been linked with the generation of the dsDNA breaks in sperm as confirmed by formation of  $\gamma$ H2AX due to *in vitro* OS (Li et al., 2006). A higher level of sperm dsDNA breaks were observed in asthenoteratozoospermia (ATZ), oligoasthenoteratozoospermia, and ATZ with varicocele cases in comparison to fertile donors (Ribas-Maynou et al., 2012a). In addition, dsDNA breaks in sperm are associated with male infertility, poor ART outcome, idiopathic recurrent miscarriage and compromised future offspring's health (Morris et al., 2002; Baulch et al., 2007; Ribas-Maynou et al., 2012c). This is further evident by the presence of significantly higher H2AX fragmentation indices and percentages (to indicate dsDNA breaks) in non-pregnant couples than pregnant couples following ICSI (Garolla et al., 2015). The decline in sperm quality of sperm with ageing is also associated with increased dsDNA breaks (Singh et al., 2003). In fact, ageing has been a major confounder for the reduced male fertility potential (Sharma et al., 2015; Zitzmann, 2013; Krausz and Chianese, 2010; Baird et al., 2005). Therefore, high sperm DNA fragmentation is a characteristic of infertile men and associated with poor ART outcomes due to reduced fertilisation rates, asymmetric pre- and post-implantation embryo development and lower implantation rates (Simon, 2012; Meseguer et al., 2008). Even upon successful fertilisation by poor quality sperm DNA, it may adversely affect the EEG (early embryo genome) expression as well as early post-natal

survival of offspring (Brevik et al., 2012; Kumar et al., 2013a). This further evident by recurrent miscarriage in cases of spontaneous and assisted conception, due to sperm DNA fragmentation (Kumar et al., 2012a; Bungum et al., 2007; Esbert et al., 2011). Moreover, a recent meta-analysis study analysing 2969 couples reported a significant association of sperm DNA fragmentation with increased miscarriage rate (Robinson et al., 2012).

In all those aspects, poor quality sperm with compromised DNA integrity can affect the fertilisation rate, clinical pregnancy and increase miscarriages in couples treated with assisted reproduction techniques. Conventional semen analysis remains the only andrological technique for the evaluation of the sperm parameters. The semen analysis, however, provides information that can only be useful for the initial examination of the (in)fertile male, it is not a clinical test of fertility. Such analysis of semen is unable to measure the functional competency of the sperm and thus require a more robust diagnostic and prognostic tests. As stated above, sperm DNA fragmentation testing looks promising and should now be incorporated in the routine clinical evaluation of infertile men. Quantifying sperm DNA fragmentation can be a useful adjunct to semen analysis in a clinical setting for better diagnosis of infertile men.

#### **1.14. Assessing sperm DNA fragmentation and chromatin compaction**

As indicated, sperm selection for ICSI depends on the subjective judgement of the embryologist to choose the best sperm based on classical parameters such as concentration, motility and morphology. Different studies have shown that sperm with poor DNA quality remains in sperm populations selected using DDGC and swim-up (Simon et al., 2010; Parmegiani et al., 2010b). Different studies have shown the importance of assessing sperm DNA fragmentation to obtain better results in natural conception and ART. A threshold value of 20-30% fragmentation has been reported in infertile men suggesting that no pregnancy will occur if DNA fragmentation is much above this threshold (Schulte et al., 2010; Venkatesh et al., 2011). Male patients originally diagnosed with idiopathic infertility are subsequently found to have higher levels of sperm DNA fragmentation (Saleh et al., 2003). The importance of DNA integrity in fertilisation and embryo implantation has been the main focus of different studies as there is a positive correlation between DNA fragmentation and miscarriage rates,

unexplained recurrent miscarriage and abnormal embryo development. (Tomsu et al., 2002; Simon et al., 2014b; Robinson et al., 2012; Loutradi et al., 2006; Kumar et al., 2012b; Coughlan et al., 2015). In another study by Zini et al. (2005), no significant difference was seen in pregnancy rates between different groups when sperm DNA fragmentation was 0–15%, 15–30%, and >30%, but higher abortion and multinucleation of blastomeres were detected when DNA fragmentation was >30% (Zini et al., 2005).

In general, different intrinsic and extrinsic factors contribute to sperm DNA fragmentation. The intrinsic factors involved in induction of sperm DNA fragmentation including deficiencies in recombination during spermatogenesis, protamine deficiency, apoptosis and ROS (Mengual et al., 2003; Oliva, 2006; Aitken et al., 2012a; Aitken et al., 1998). The main extrinsic factors include sperm collection and preparation methods for ART, cryopreservation, testicular hyperthermia, chemotherapy, smoking, genital tract inflammation, varicoceles and bacterial infection (Jimenez-Rabadan et al., 2012; Jackson et al., 2010; Gallegos et al., 2008). Sperm DNA fragmentation is linked with reduced fertility potential and ART outcomes (Guerin et al., 2005). Furthermore, if low quality paternal DNA is delivered to the oocyte, regardless of a successful fertilisation it may later influence the early embryo gene expression and early post-natal survival of offspring (Kumar et al., 2013b). Therefore, it is important to develop a good strategy for testing the levels of DNA fragmentation. In this regard, depending on the type of DNA fragmentation, different methods have been used for the assessment of sperm DNA fragmentation and chromatin compaction.

#### **1.14.1. Acridine orange assay**

The SCSA (sperm chromatin structure assay) was first developed by Evenson et al., 1980 (Evenson et al., 1980). Using this method, the DNA is denatured by heating spermatozoa to 100°C followed by staining with acridine orange (AO) prior to analysis with flow cytometry. Acridine orange is a metachromatic dye and following excitation with a monochromatic 488 nm blue light, AO emits red fluorescence when linked with single-stranded DNA (wavelength: 600 nm), while double-stranded DNA emits green fluorescence (wavelength: 530 nm) (Shamsi et al., 2011). As a result, DNA fragmentation index (DFI) is determined by measuring the ratio of red fluorescence to overall nuclear fluorescence (red +

green) (Evenson et al., 1980). The results of AO staining can also be seen under a fluorescent microscope.

#### **1.14.2. Terminal deoxynucleotidyl transferase mediated fluorescein-dUTP nick end labelling (TUNEL)**

This method detects both single and double stranded DNA breaks by transferring a labelled nucleotide to the 3'OH group of a broken DNA strand using a terminal deoxynucleotidyl transferase (TdT) (Evenson and Wixon, 2006). The results obtained using this method are often variable as this method relies on the activity of an enzyme for detection of DNA breaks. This method associates well with SCSA, but it is still under optimisation (Shamsi et al., 2011).

#### **1.14.3. The sperm chromatin dispersion (SCD) assay**

This assay works using the simple principle of chromatin decondensation and relaxation. Using this method, intact DNA spermatozoa show a “halo” around the head while spermatozoa with fragmented DNA fail to show any halo. More accurately, under acid denaturation, spermatozoa with fragmented DNA fail to make a diffuse chromatin halo as shown by intact DNA (Fernandez et al., 2003). This method still needs to be more validated using ART studies as some studies show that it does not correlate with pregnancy outcomes in ART (Muriel et al., 2006).

#### **1.14.4. Comet assay**

The comet assay is a single cell gel electrophoretic assay used for quantification of DNA breaks in individual sperm. This method can be performed under two different conditions. Under alkaline condition ( $\text{pH} \geq 13$ ), it can assess single and double stranded DNA breaks while natural comet assay quantifies double strand breaks (Ribas-Maynou et al., 2012b). The main advantage of this method is that not many sperm are needed for analysis and it can be easily used for oligozoospermic semen or testicular samples. It has been reported that in couples with successful live births using IVF, DNA fragmentation (measured by comet assay) is significantly lower than in couples with no live births (Simon et al., 2011).

#### **1.14.5. Aniline blue staining**

Aniline blue (AB) is an acidic dye, and it is used for assessment of chromatin compaction. Due to its high affinity to lysine-rich histones, immature spermatozoa uptake the dye and stain blue whereas arginine and cysteine-rich mature sperm do not react to the dye and remain unstained (Auger et al., 1990).

#### **1.14.6. Chromomycin A3 staining**

Chromomycine A3 (CMA3) is a guanine-cytosine (GC)-specific fluorochrome competing with protamines in binding to DNA. Therefore, it is used for assessment of chromatin compaction. The intensity of this dye is higher in immature sperm with low levels of protamination (Agarwal et al., 2016).

### **1.15. Epigenetics and male (in)fertility**

Epigenetics describes the mechanisms that control gene activity predominantly through chromatin modification rather than intrinsic DNA sequences. The epigenetic state is inherited from parents through cell division and can be susceptible to environmental changes altering an individual's risk for chronic disease (Chen et al., 2015; Zeh et al., 2012). Sperm epigenetic changes have been extensively studied and linked to male fertility potential, abnormal sperm functioning/pathology and early embryo development (Luense et al., 2016; Jenkins et al., 2016a; Urduingio et al., 2015; O'Doherty and McGettigan, 2015; Schagdarsurengin et al., 2012; Hammoud et al., 2011; Jenkins and Carrell, 2012; Filipponi and Feil, 2009). The main epigenetic mechanisms in the sperm include DNA methylation, core histone's modification, chromatin remodelling, and regulation through noncoding RNAs. Sperm histones are mainly modified by ubiquitination, lysine acetylation, monomethylation, dimethylation of lysines and arginines. Studies have shown that precise and accurate acetylation of histones are crucial for sperm development whereas abnormal histone acetylation causes impaired spermatogenesis (Song et al., 2011; Faure et al., 2003; Luense et al., 2016; Hazzouri et al., 2000). For example, H3K9ac play an essential role in human sperm development and serve as an epigenetic signal required for gene expression after fertilisation (Steilmann et al., 2011). Indeed, such modified histones are significantly placed at genetic loci of developmental significance rather than non-random distribution (Arpanahi et al., 2009; Hammoud et al., 2009). The hyperacetylated H4 is specifically recognised by bromodomain testis-

specific protein (BRDT) and facilitates its binding. However, an impaired binding of BRDT to modified histones was associated with infertile men (Steilmann et al., 2010). Like acetylation, sperm histone methylation can also act as a potential epigenetic signal associated with transcriptionally active and inactive genes. For example, H3K27me can act as an activator whereas H3K4me as a repressor (Carrell and Hammoud, 2010). Also, the role of histone ubiquitination during spermatogenesis have been reported. Ubiquitinated histones act as a transient process for the histone removal during chromatin remodelling (Baarends et al., 1999; Sheng et al., 2014). Moreover, inactivation of ubiquitin-conjugating enzyme, HR6B in male mice causes infertility due to inadequate chromatin remodelling (Roest et al., 1996). Sperm DNA methylation is yet another form of epigenetic modification that is often marked as a gene silencer. Methylation are often tagged at CpG islands within the genome leading to reduced gene transcription. DNA methyltransferases (DNMTs) facilitates addition of methyl groups to cytosine residues of CpG islands. DNMTs can be divided into different types of mammals: DNMT1, DNMT2 and DNMT3. A genome-wide epigenetic analysis of testicular tissue revealed that it is 8 times more hypomethylated than somatic cells (Oakes et al., 2007). An aberrant sperm DNA methylation both confined to specific gene locus and globally were observed to be associated with idiopathic male infertility, abnormal semen parameters and pregnancy failure (Benchaib et al., 2005; Houshdaran et al., 2007; Urdinguio et al., 2015). Even an altered sperm DNA methylation pattern is associated with decreased infertility in humans (Jenkins et al., 2016b).

Moreover, hypermethylation of promoters of methylenetetrahydrofolate reductase (*MTHFR*) and *DAZL* has been associated with unexplained male infertility (Wu et al., 2010; Navarro-Costa et al., 2010). Furthermore, *MTHFR* promoter hypermethylation has also been observed in about half of non-obstructive azoospermic men, but could not be confirmed in men with obstructive azoospermia (Khazamipour et al., 2009). Also, a specific methylation pattern of *MTHFR* promoter has been also reported in oligoasthenozoospermia (Botezatu et al., 2014). Furthermore, since epigenetics are largely influenced by environment, paternal diet play a crucial role in regulating the unique sperm epigenetic landscape for better sperm quality and offspring health (Schagdarsurengin and Steger, 2016).



Epigenetic modulation through noncoding RNAs: microRNAs (miRNAs) are small (~21–25 nucleotides) non-coding RNAs that are recognized as cellular modulators of gene expression in a variety of eukaryotic organisms. These small RNAs function mainly post-transcriptionally by affecting the stability of target mRNAs as well as by translational repression. Studies have identified a set of germinal miRNAs and their roles in the normal spermatogenesis (Kotaja, 2014; Salas-Huetos et al., 2016) and different infertile population including but not limited to oligoasthezoospermia, normozoospermic infertile men, idiopathic asthenozoospermia, and teratozoospermia (Abu-Halima et al., 2016; Munoz et al., 2015). Future studies are required to discover how these epigenetic signatures are associated with reproductive potential and identifying the mechanisms affecting trans-generational effects in offspring.

### **Thesis hypothesis, aims and objectives**

The main and overarching hypothesis for the work reported herein is that hyaluronic acid binding proteins including potentially novel forms will be shown to behave dynamically and purposefully in relation to sperm function and vitality. Considering the recent interest in the use of hyaluronic binding as a sperm selection method for ICSI, it is becoming increasingly important to examine and characterise sperm hyaluronic acid binding proteins (HABPs), as they are an integral part of the selection. Therefore, the main objectives of the current study are as follows:

- To investigate the relationship between HA-binding and sperm function tests including sperm DNA fragmentation and chromatin maturity.
- To evaluate the dynamic changes of HABPs in non-capacitated, capacitated and acrosome reacted human and bovine spermatozoa.
- To apply a proteomic approach to identify protein changes including HABPs during capacitation and acrosome reaction.
- To investigate the dynamics of sperm capacitation in relation to HA binding.
- To identify and characterise sperm HABPs using mass spectrometry and HA affinity chromatography.

Chapter 2: Investigating relationships between DDGC-separated sperm and their corresponding levels of sperm DNA fragmentation, chromatin compaction and binding affinity to hyaluronic acid

### 2.1. Introduction

Male reproductive dysfunction was more effectively treatable from the early 1990s as a result of the introduction of ICSI (Palermo et al., 1992; Wang et al., 1997). However, the success of assisted reproductive techniques, as measured by 24% of cycles (including ICSI), achieving a term pregnancy ( $\geq 37$  weeks) has remained relatively unchanged since its introduction (HFEA, 2015). As indicated earlier, sperm must undergo capacitation before they become capable of fertilising the egg naturally. *In vivo* sperm capacitation occurs in the female reproductive tract. *In vitro*, capacitation, requires sperm to be washed free of seminal plasma (Mortimer and Mortimer, 2013). Different studies have shown that extended exposure to seminal plasma can negatively affect sperm function (Yanagimachi, 1994b; Mortimer, 2000; Rogers et al., 1983) and indicating that they should be separated from seminal plasma as efficiently as possible after semen liquefaction and before carrying out any clinical procedure such as IVF, ICSI, IUI or any diagnostic procedures (Mortimer and Mortimer, 2013).

A raft of techniques have been developed to enrich for more viable, mature and fertile sperm populations (HFEA, 2008) including washing and separating techniques such as DDGC, which is the most widely-used procedure (Akerlof et al., 1987; Mortimer, 2000; Bjorndahl et al., 2010). This method separates sperm according to their density (mass/volume or specific gravity) and as a result, spermatozoa are distributed at gradient levels that match their density (Mortimer and Mortimer, 2013).

It is known that mature morphologically normal and immature sperm have densities of  $> 1.2$  g/mL and between 1.06 and 1.09 g/mL, respectively (Oshio et al., 1987). Different research has shown that processing by DDGC leads to separation of sperm with higher motility, viability, morphology, DNA integrity and mitochondrial potential (Jayaraman et al., 2012; Donnelly et al., 2000; Sakkas et al., 2000b; Marchetti et al., 2002). Other studies have revealed that DDGC enriches for a population of sperm with a low percentage of apoptotic and necrotic sperm compared with the original semen sample (Ricci et al., 2009; Amiri et al.,

2012). Others have reported that DNA fragmentation can remain high after processing by DDGC (Stevanato et al., 2008; Gosalvez et al., 2010). Research by Zeini et al (2000) showed that detrimental effect of DDGC on sperm DNA is associated with the initial quality of the semen sample (Zini et al., 2000).

In general, sperm separation methods such as DDGC and swim-up enrich for more fertile sperm based on the classical parameters as set out by WHO guidelines including sperm motility, morphology, viability and concentration (WHO, 2010a; Xue et al., 2014; Yamanaka et al., 2016). Functional characteristics of sperm populations obtained from DDGC (DNA integrity and chromatin maturity) that may explain the enhanced fertility of these populations, are usually not evaluated. This is a particular issue for ICSI where sperm selection relies almost exclusively on the embryologist's judgement. Therefore, evaluation of sperm DNA integrity has been suggested for the assessment of male infertility. DNA fragmentation can occur in single and double DNA strands (Marchlewska et al., 2016). Various reports on sperm DNA fragmentation have shown that a DNA fragmentation threshold value more than 30% is linked with decreased rate of pregnancy and increased risk of early miscarriage (Agarwal and Esteves, 2011).

Celik-Ozenci (2004) demonstrated that sperm with normal motility and morphology may have DNA fragmentation; therefore, IVF and ICSI using sperm with normal motility and morphology may provide a chance for sperm with chromatin defects, DNA fragmentation, apoptosis and membrane malformation to participate in the fertilisation process. This situation raises concerns related to the increased risk of childhood cancer and miscarriage in pregnancies achieved by IVF and ICSI (Celik-Ozenci et al., 2004; Moskovtsev et al., 2010). Therefore, in response to this demand, numerous innovative techniques have been introduced and are continuing to be improved, with the aim of isolating or enriching higher quality sperm with respect to DNA integrity and maturity, morphology and motility (Zhao et al., 2014; Yetunde and Vasiliki, 2013; Said and Land, 2011). One such method, HA-binding is being proposed as a possible, non-destructive selection technique as a result of its ability to select mature sperm with low DNA fragmentation and chromosomal aneuploidies levels (Huszar et al., 2006; Jakab et al., 2005). It is suggested that HA plays an important role in

fertilisation by 'capturing' spermatozoa which express HABPs with the ability to bind HA directly (such as CD44; (Bains et al., 2002)) or facilitating sperm penetration through the cumulus via a hyaluronidase activity (such as SPAM1) which then leads to accessing and binding to the zona pellucida (McLeskey et al., 1998). In this regard, it has been reported that spermatozoa capable of binding to HA *in vitro* have improved markers of nuclear maturation, cytoplasmic extrusion and plasma membrane remodelling compared to spermatozoa that do not bind to HA (Huszar et al., 2003; Rengan et al., 2012; Parmegiani et al., 2010a).

It has also been shown that there is a relationship between the ability of spermatozoa to bind to HA and their viability. In fact, having completed their plasma membrane remodelling, mature spermatozoa express receptors that enable them to recognise and bind HA (Cayli et al., 2003; Huszar et al., 2003; Parmegiani et al., 2010a). Protocols have been developed based on the likely functional aspects of HA and HABPs in the fertilisation process, in which spermatozoa are able to interact with and bind to an HA-coated surface followed by collection for ICSI (Nasr-Esfahani and Marziyeh, 2013; Jakab et al., 2005). A number of reports indicate some efficiency for the procedure in regards to miscarriage, clinical pregnancy and more recently live birth rates by using PICSI platform (Worrilow et al., 2013; Mokanszki et al., 2014; Parmegiani et al., 2010a; Nasr-Esfahani et al., 2008; Beck-Fruchter et al., 2016).

## **2.2. Hypothesis and objectives**

Assuming that HA binding is related to sperm vitality, it was hypothesised that there would be a relationship between the sedimentation properties of sperm during DDGC with their capacity to bind HA and their ability to capacitate. Also, if HA binding selects mature sperm, then there should be a relationship between HA-binding and the properties of sperm fractionated by DDGC. It can, therefore, be hypothesised that HA-selected and DDGC fractionated sperm will have related levels of DNA fragmentation and chromatin compaction. The main objectives of this study, therefore, were to:

- Investigate the HA binding capacity of 90% and 45% sperm fractions following DDGC.
- Investigate changes in binding of sperm from these fractions to HA after capacitation.
- Examine the levels of chromatin maturity and DNA integrity in 90% and 45% sperm fractions.
- Assess the levels of chromatin maturity and DNA integrity in HA-binding and non-binding fractions.
- Compare HA-binding assay and DDGC regarding their ability in separating spermatozoa with high DNA integrity and chromatin maturity.

## **2.3. Materials and Methods**

### **2.3.1. Reagents used**

SupraSperm™, Quinn's (HEPES-buffered) sperm washing medium and Hyaluronic acid coated slides (HBA® slides) were supplied by Origio, Denmark. Calcium ionophore A23187, Bovine serum albumin (BSA, fatty acid free, ≥96%), Sodium bicarbonate, Sodium lactate, Sodium pyruvate, Lectin from *Pisum sativum* (pea) FITC conjugate (PSA-FITC), Dimethyl sulphoxide (DMSO) solution, Aniline blue solution (2.5% w/v) in 2% acetic acid (v/v), DAPI, Methanol and Acetic acid were obtained from Sigma-Aldrich, UK. 2% (w/v) Acridine orange (ready-to-use) DNA interacting dye and hyaluronic acid coated dishes were purchased from Polysciences Inc (USA) and Biocoat (USA), respectively. Phosphate buffered saline (PBS, pH:7.2) and Ham's F-10 nutrient mix (HEPES) were purchased from Gibco, ThermoFisher Scientific (UK). Poly-L-Lysine coated slides were purchased from VWR, UK. Vectashield mounting medium with DAPI was purchased from Vector Laboratories, UK.

### **2.3.2. Patient Samples**

Sixteen human semen samples were ethically obtained from young male donors (of unproven fertility) by masturbation after a minimum of three days' abstinence into sterile, tissue culture grade universal containers. The study was considered and nationally approved by the relevant UK Integrated Research Application System (IRAS) ethics committee (NRES 12\_NE\_0192) and locally approved by the University of Leeds' School of Medicine Research Ethics Committee (SoMREC/13/017) (Torabi et al., 2016). Collected semen samples were liquefied for 30 minutes at 37°C. Only those samples with normal semen parameters as defined by WHO (2010) criteria were included in the study. The patients were aged between 19 and 36 years with a mean age ( $\pm$  standard deviation (SD)) of  $22.43 \pm 4.25$  years, and only those with normal semen parameters as defined by WHO (2010) criteria were included in the study. A more complete description of the volunteer semen profiles is presented in Table 2.1 (Result section 2.4.1).

### **2.3.3. Differential Density Gradient Centrifugation (DDGC)**

A two-layer density gradient of 90% and 45% SupraSperm™ (a silane-coated colloidal silica-based HEPES-buffered density gradient medium) was utilised to process the samples. Briefly, 2 mL of 90% SupraSperm™ (Origio) was placed in

a 15 mL polypropylene centrifuge tube and carefully overlaid with 2mL 45% SupraSperm™ and 1 mL semen sample. Following centrifugation at 300 ×g for 20 min at RT, spermatozoa were taken from the 90% pellets and 45%-90% interface fractions. These fractions are referred to as 90% and 45% fractions. Spermatozoa obtained from both fractions were washed with Quinn's sperm washing medium by centrifugation at 300 × g for 10 minutes (two consecutive washes). They were then resuspended in the same medium. Sperm total motility and concentration were evaluated using a Leitz Laborlux 12 light microscope.

#### 2.3.4. Counting spermatozoa

Estimates of sperm concentration were obtained using a Neubauer haemocytometer. To ease counting, spermatozoa were first diluted and killed in hot (60°C) water and then loaded onto the Neubauer haemocytometer. Sperm in the four large square as shown in Figure 2.1 (red squares) were counted, and the concentration was calculated as below:

Concentration (sperm/mL) = number of sperm in red squares /4 x dilution factor x  $10^4$

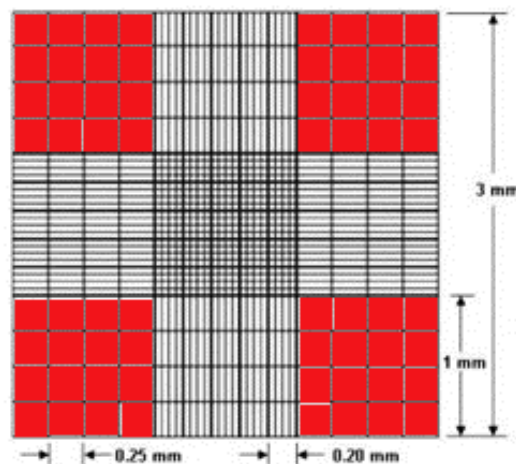


**Figure 2.1. Neubauer chamber for sperm counting.**

#### 2.3.5. Spermatozoa binding to HA-coated slides

Hyaluronic acid coated slides (HBA® slides, Origio) were used to check the ability of sperm to bind HA according to the manufacturer's protocol. Each slide has two chambers and a viewing circle for assessment of sperm HA-binding (Figure 2.2).



**Figure 2.2. The image presenting a HA-coated slide.**

(From: <http://www.origio.com/en/products/all-products/hbar-assay>).

The experiment was performed according to manufacturer's instruction (Origio). Briefly, after sperm separation by DDGC approximately  $1 \times 10^6$  (10  $\mu$ L) spermatozoa (90% and 45%) were placed onto the assay chamber and incubated for 15 min at room temperature (RT). Motile spermatozoa with HA receptors are able to bind to the HA-coated slide, while immotile spermatozoa and spermatozoa lacking HA receptors are not able to bind to the HA. The percentage of HA-bound spermatozoa (in pelleted and interface fractions) was calculated as follows:

$$\% \text{ bound} = \frac{\text{bound motile spermatozoa}}{\text{bound motile spermatozoa} + \text{unbound motile spermatozoa}} \times 100$$

### 2.3.6. Induction of capacitation

Capacitation of sperm obtained directly following centrifugation and washing of semen or from DDGC pellets was performed in accordance with the guidelines as set out by WHO (WHO, 2010). Briefly, spermatozoa were separated as explained earlier. Capacitation was then induced by incubating pelleted spermatozoa (approx.  $10^6$ ) for 3 hours in 1 mL of a HEPES-buffered Ham's F10 solution supplemented with 0.36% (w/v) sodium lactate, 0.2% (w/v)  $\text{NaHCO}_3$ , 0.003% (w/v) sodium pyruvate, 5 mM  $\text{CaCl}_2$  and 3.5% (w/v) BSA at  $37^\circ\text{C}$  with gentle continual rotation (Torabi et al., 2016). Following the period of incubation, capacitated spermatozoa were harvested by centrifugation at  $300 \times g$  for 10 minutes and washed with PBS (x2). It should be noted that the pellet contains capacitated sperm. To check the efficiency of capacitation, the acrosome reaction



was induced, and PSA-FITC labelling was performed. The level of capacitation was also monitored by assessment of hyperactive motility.

Different buffers such as Biggers-Whitten-Whittingham (BWW) for 1h (Jaiswal et al., 1998), BWW for 2h (Cohen-Dayag et al., 1995) and Krebs-Ringer's bicarbonate (Choi et al., 2008a) were examined to optimise the protocol for induction of capacitation. Additionally, different time points (1h, 5h, 10h and 20h) using supplemented HEPES-buffered Ham's-F10 (recommended by WHO 2010) were checked. None of the above buffers gave satisfactory results. For example, by using BWW for 1h and 2h and supplemented Ham's F10 for 1h, the process of capacitation was not completed. The time points of 5h and 10h were not ideal as sperm motility dropped down dramatically and the number of dead spermatozoa increased. After 20h incubation in supplemented Ham's F10, the majority of sperm were dead. The best results were obtained after sperm incubation for 3h in HEPES-buffered Ham's F10 solution supplemented with sodium lactate, sodium bicarbonate, sodium pyruvate, calcium chloride and BSA as recommended by WHO 2010.

### **2.3.7. Evaluation of capacitation efficiency by induction of acrosome reaction**

As the AR is more efficiently accomplished by capacitated spermatozoa, it was used to check the efficiency of capacitation. To induce the AR, 10  $\mu\text{L}$  of  $\text{Ca}^{2+}$  ionophore A23187 (stock solution 1.0 mM in 100% DMSO) was added to  $\sim 10^6$  capacitated spermatozoa in 1 mL (final concentration 0.01 mM) and incubated at 37°C for 15 minutes. To stop the reaction 70% ethanol was added and spermatozoa were recovered as indicated above (Torabi et al., 2016).

Capacitated spermatozoa incubated with 10  $\mu\text{L}$  DMSO alone and spermatozoa incubated in buffer supporting capacitation for 0hr (non-capacitated) and subsequent acrosome reaction were used as controls for further PSA-FITC labelling. The reason for using incubated sperm in DMSO (as control) is that  $\text{Ca}^{2+}$  ionophore A23187 stock solution was prepared in DMSO.

### **2.3.8. FITC-*Pisum sativum* Agglutinin (PSA) labelling**

PSA-FITC (*Pisum sativum* agglutinin conjugated with fluorescein isothiocyanate) labelling was carried out to check the acrosome status after capacitation and

acrosome reaction. This fluorescent probe binds to the alpha-methyl mannose and labels the acrosomal content of sperm (Benoff et al., 1993).

Briefly, 10  $\mu\text{L}$  aliquot of non-capacitated (control), capacitated, acrosome reacted and capacitated sperm incubated with 1 mL of 1% v/v DMSO (control) were cytopspun on Poly-L-Lysine coated slides. The slides were fixed in 95% (v/v) ethanol (in a coplin jar containing 30 mL ethanol) for 30 minutes and then left at RT to dry rapidly. The slides were then immersed in a solution of 25  $\mu\text{g}/\text{mL}$  PSA-FITC in PBS (in a copling jar containing 30 mL PSA-FITC) for 1 hour at 4°C. The slides were then washed in distilled water for at least 15 min. Coverslips (Fisher Scientific) were mounted with a drop of Vectashield mounting medium containing 1.5  $\mu\text{g}/\text{mL}$  DAPI (4, 6-diamidino-2-phenylindole). The slides were examined immediately with a Leica LEITZ DMRB fluorescence microscope (Mazurek Optical Services, UK) using FITC and DAPI filters with excitation/emission wavelengths 495 nm/520 nm and 358 nm/461 nm, respectively. The images were taken using SmartCapture 3 software. According to Cross and Meizel (1989), sperm showing PSA-FITC binding to the anterior part of the head throughout the acrosomal region were marked as intact acrosome (not-acrosome reacted) and spermatozoa with no fluorescence in the acrosome or a band of fluorescence localised to the equatorial segment were regarded as acrosome-reacted. Any other signal between intact acrosome and acrosome reacted was considered as partially intact (Cross and Meizel, 1989). Figure 2.6 shows some examples of each category (intact AR, partially intact AR and acrosome reacted). A minimum of 150 sperm were counted per slide. In total, 8 samples were evaluated for validation of capacitation and the AR using PSA-FITC labelling.

### **2.3.9. Assessment of hyperactive motility after capacitation**

In addition to PSA-FITC labelling, sperm hyperactive motility was evaluated after capacitation. To this end, hyperactivity was assessed in spermatozoa incubated in capacitation supporting media for 0h (non-capacitated) and after 3h capacitation (capacitated). To make the counting process easier, 10  $\mu\text{L}$  spermatozoa from four different donors were loaded on HA-coated slides. Hyperactive motility was recorded as more vigorous with an asymmetrical beating tail. A minimum of 150 sperm were counted per slide.

### **2.3.10. Changes in HA binding ability after capacitation**

After capacitation was accomplished and its efficiency was checked, binding of non-capacitated and capacitated spermatozoa to HA was assessed. Briefly,  $1 \times 10^6$  ( $10 \mu\text{L}$ ) of each non-capacitated and capacitated spermatozoa (prepared in Section 2.3.3 and 2.3.6) were incubated on the HBA<sup>®</sup> slides for 15 min at RT and the percentages of HA-bound spermatozoa in each fraction were calculated as described in Section 2.3.5.

### **2.3.11. Isolation of HA-bound and unbound sperm**

HA-coated dishes were used as the number of HA-bound sperm obtained from HA-coated slides were not sufficient for AO and AB staining. Human semen samples were washed with, and resuspended in Quinn's sperm washing medium as stated previously in Section 2.3.3. Spermatozoa at the concentration of  $50 \times 10^6$  / mL were loaded on to a specially prepared HA-coated dish (Biocoat). Following an incubation period of 15 min at  $37 \text{ }^\circ\text{C}$  ( $5\% \text{ CO}_2$ ), HA-unbound spermatozoa were detached by a gentle rinsing of the dish with Quinn's sperm washing medium for 2 min with constant pipetting (Torabi et al., 2016).

Sperm bound to the plates were recovered by more vigorous washing, and both bound and unbound spermatozoa were then centrifuged for 15 min at  $300 \times g$  and washed twice with PBS.

To optimise the protocol for sperm binding to HA-coated dishes, different temperatures were examined. That was due to the failure of the protocol used for sperm HA-binding (using HAB<sup>®</sup> slides at RT) in sperm binding to HA-coated dishes. More accurately, sperm motility dropped dramatically when the experiment was performed at RT as recommended for HAB<sup>®</sup> slides. Therefore, different temperatures of  $30$  and  $37 \text{ }^\circ\text{C}$  ( $5\% \text{ CO}_2$ ) were examined. In addition, various washing methods such as a gentle washing and a more vigorous washing were tried to detach HA-unbound sperm. The best population of HA-unbound sperm was obtained only after applying the more vigorous washing.

### **2.3.12. Acridine orange staining and quantitation**

Approximately  $1 \times 10^6$  spermatozoa resolved by HA-binding ability (Section 2.3.11) and/or DDGC (Section 2.3.3) were cytopspun on Poly-L-Lysine coated slides (supplied by VWR, UK). To do cytopspin, slides were inserted into a cytoclip

and covered with a single cytofunnel. A volume of 100  $\mu\text{L}$  containing  $1 \times 10^6$  sperm was pipetted into the slide through the cytofunnel. Centrifugation was performed at 200 x g for 15 min. The slides were removed and fixed with 30 mL of an altered Carnoy's solution (methanol and glacial acetic acid at a ratio of 9:1) for 2 hours at RT (Yagci et al., 2010). Slides were then stained with 100  $\mu\text{L}$  of a solution of 12  $\mu\text{g}/\text{mL}$  AO for 5 min at RT and then washed with double-distilled water. Spermatozoa incubated with 100  $\mu\text{M}$   $\text{H}_2\text{O}_2$  for 60 min at RT were served as a positive control for DNA fragmentation.

To evaluate the levels of DNA fragmentation, three different AO groupings were derived comprising all red (--), mixed red/green and yellow ( $\pm$ ) and all green (++) fluorescence corresponding to high, medium and low DNA fragmentation were used. Examples can be seen in Figures 2.10 and 2.12. A minimum of 150 spermatozoa per sample were grouped by two independent observers using a Zeiss LSM510-META confocal microscope.

AO from different suppliers was tested before settling on a 2% w/v solution from Polyscience Inc. Different concentrations (9, 15 and 18  $\mu\text{g}/\text{mL}$ ) of this stock were applied to sperm smears on slides for different time points (3, 5, 10, 15 min) to obtain optimal incubation conditions (12  $\mu\text{g}/\text{mL}$  for 5 min) using  $\text{H}_2\text{O}_2$  (100  $\mu\text{M}$ ) as an inducer of DNA fragmentation.

Originally, a Carnoy's fixative (methanol/acetic acid, 3 : 1) was used but due to its severity, it was changed to a modified Carnoy's solution (Methanol/acetic acid 9:1).

### **2.3.13. Aniline blue staining and quantitation**

Excessive histone retention (indicating defective chromatin compaction and therefore maturity) was evaluated in spermatozoa resolved by HA-binding ability (Section 2.3.11) and/or by DDGC (Section 2.3.3) using aniline blue (AB) staining. To do this, approximately  $1 \times 10^6$  spermatozoa were placed on Poly-L-Lysine coated slides (supplied by VWR, UK) as outlined in section 2.3.12. The slides were then fixed with 30 mL of a solution of methanol and acetic acid at the ratio of 3:1 in a coplin jar for 1 hour at RT. A solution of 2.5% AB (w/v) in 2% acetic acid (v/v) was then used to stain the slides for 5 min at RT (Huszar et al., 2003). A minimum of 150 sperm were assessed per sample by two independent

observers using a Leica LEITZ DMRB brightfield light microscope under oil immersion (100x objective) using SmartCapture 3 software. Spermatozoa with extensively stained (++), moderately stained ( $\pm$ ) and unstained (--) nuclei were counted as sperm with weakly, partially and fully compacted chromatin (Torabi et al., 2016). Examples can be seen in Figure 2.14 and 2.16.

Different fixatives were used to help optimise the method including 4% formalin and 2% glutaraldehyde (Wong et al., 2008; Santiago-Moreno et al., 2009). Additionally, different staining solutions including 5% w/v aniline blue in 4% v/v acetic acid (pH 3.5) were used (Kim et al., 2013). The best results were obtained when using methanol/acetic (3:1) as the fixative and 2.5% w/v AB in 2% v/v acetic acid as the staining solution.

Figure 2.3 and 2.4 represent the flow diagrams of the approach used in the present chapter.

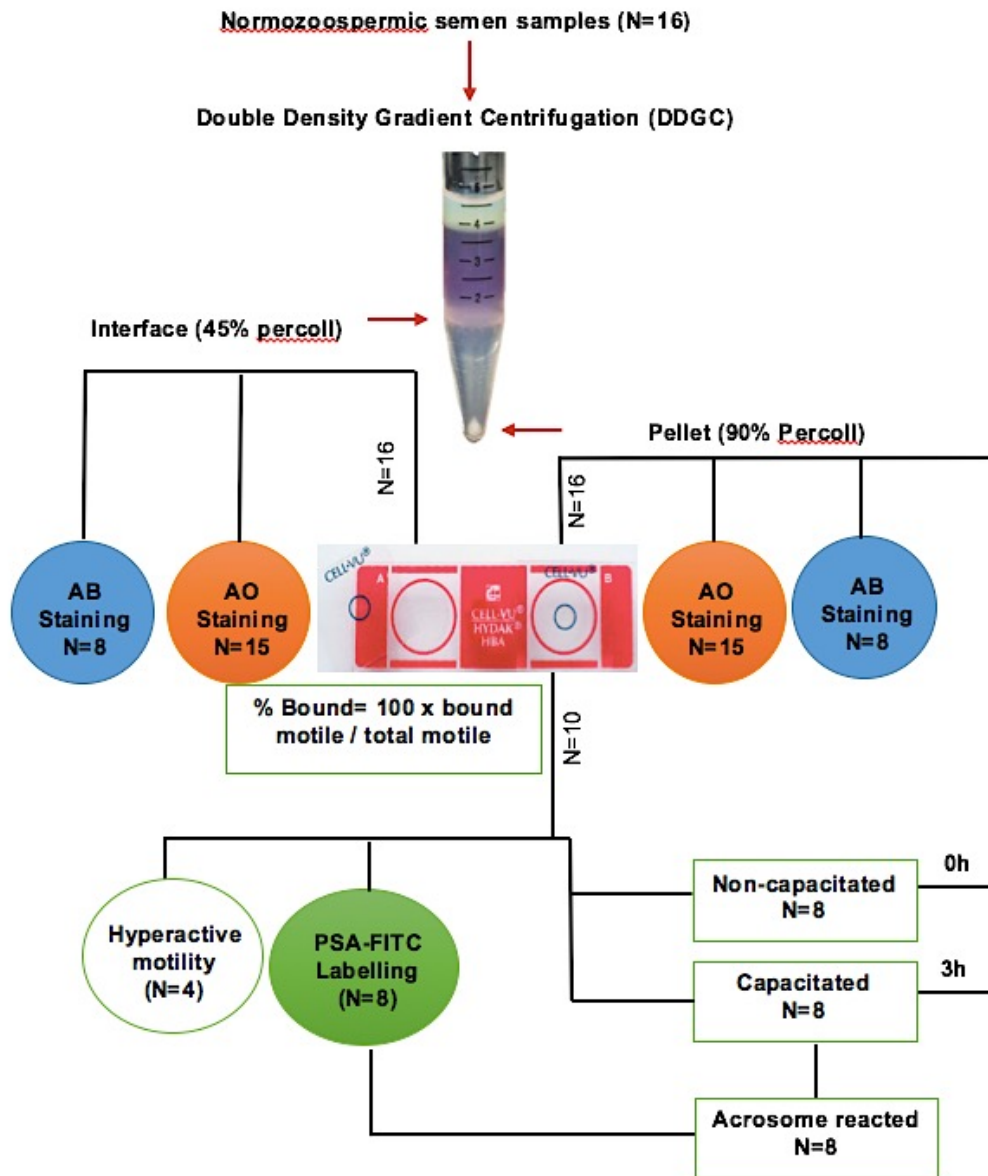


**Figure 2.3. Flow diagram outlining the approach used in the current study.**

Sperm from 16 normozoospermic donors were separated using DDGC. Sperm obtained from interface and pellet fractions were checked for DNA integrity and chromatin compaction using AO and AB staining, respectively. The percentage of HA-binding was assessed using HBA<sup>®</sup> slides.

Capacitation of pelleted sperm was performed in a capacitation supportive media for 3h. Acrosome reaction was induced on capacitated sperm using Ca<sup>2+</sup> ionophore.

Non-capacitated sperm were used as controls. The efficiency of capacitation was checked by measuring sperm hyperactive motility and PSA-FITC labelling. The HA-binding ability of capacitated and non-capacitated sperm was evaluated using HBA<sup>®</sup> slides. Different sample sizes (N) were used due to the low sperm count after sample processing, poor quality of separated sperm and the loss of sperm during processing or very high background masking sperm visibility.

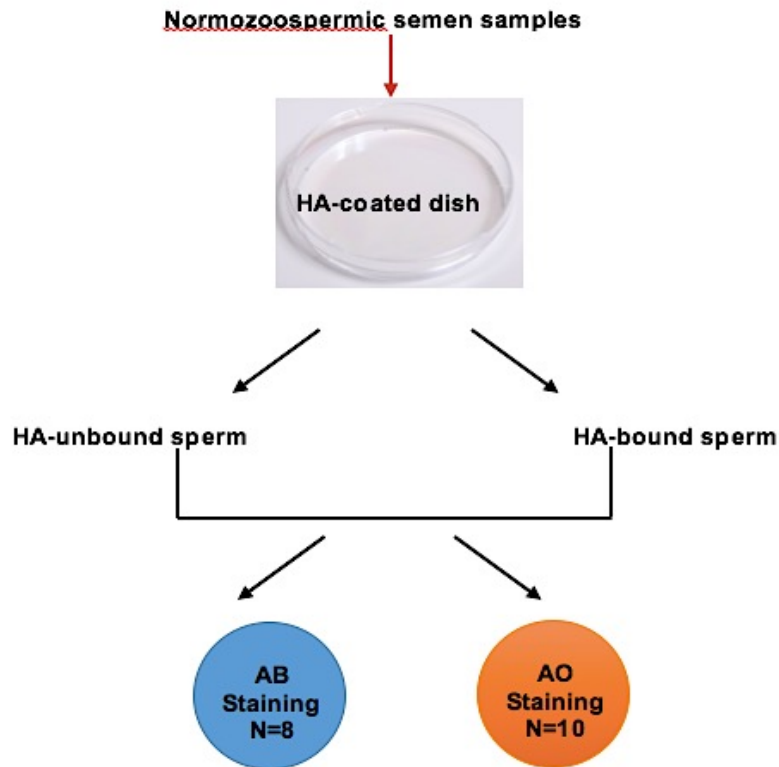


**Figure 2.4. Flow diagram outlining the approach for separation of HA-bound and unbound spermatozoa.**

Sperm from normozoospermic donors were washed using Quinn's sperm washing medium and incubated on HA-coated dishes. HA-bound and unbound sperm were separated and checked for DNA integrity and chromatin maturity using AO and AB staining, respectively. Different sample sizes (N) were used due to the low sperm count after sample processing, poor quality of separated sperm and the loss of sperm during processing or very high background masking sperm visibility.

#### **2.3.14. Statistical Analysis**

GraphPad Prism (version 6) was used to analyse experimental data. Mann-Whitney U-test was used to analyse the data obtained from HA-binding assay in the 90% and 45% DDGC fractions (variable: % HA-binding) and the data related to hyperactive motility after capacitation (variable: % hyperactive motility). PSA-FITC labelling data was analysed using Two-way ANOVA followed by Tukey's post-hoc test (independent variables: capacitation and the AR, measurement variable: % PSA-FITC labelling).

All other group-based comparisons (variables: % HA-binding in capacitated and acrosome reacted sperm, % DNA fragmentation and % chromatin maturity) were analysed using Kruskal–Wallis (K-W) analysis of variance with Dunn’s post-hoc multiple comparisons test applied to compare groups. The P-values for median rank differences are indicated in all figures as a (0.0001) > b (0.001) > c (0.01) > d (0.05) (Torabi et al., 2016). Mann-Whitney U-test was also used for the comparison between HA-binding assay and DDGC regarding DNA fragmentation and chromatin maturity. The data were tested for normal distribution using D’Agostino-Pearson, Shapiro-Wilk and Kolmogorov-Smirnov tests (GraphPad-Prism 6).



## 2.4. Results

### 2.4.1. Semen analysis of volunteers contributing to this study

Donors for this study were a cohort of healthy males (N=16) from the student population at the University of Leeds from an age range of 19-36 (Table 2.1).

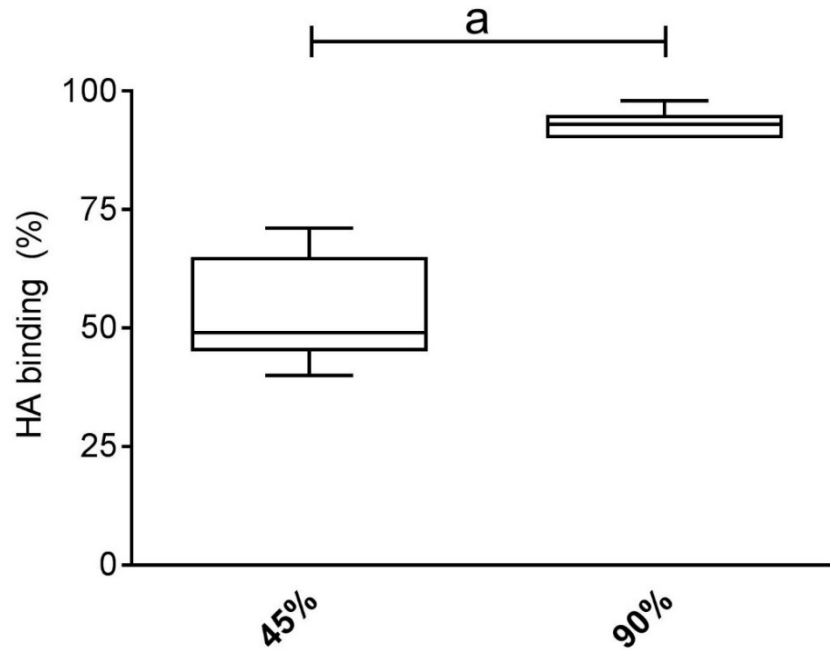
The age range of the participants and also general semen assessment data are presented in Table 2.1.

Table 2.1. Semen assessment of volunteers contributing to the study.

Sample	Donor Age	Sperm concentration (million/mL)	Total sperm count ( $\times 10^6$ )	Semen volume (mL)	Total motility (%)
D11	20	159	238.5	1.5	56
D27	21	69	345	5	94
D30	22	122	244	2	70
D31	36	200	300	1.5	90
D43	21	56	224	4	67
D49	21	120	360	3	86
D56	20	156	93.6	0.6	85
D62	19	120	240	2	70
D70	28	233	349.5	1.5	92
D84	24	185	370	2	75
D101	21	90	270	3	65
D104	24	36	108	3	85
D107	19	251	1204.8	4.8	87
D115	20	179	716	4	61
D116	22	154	385	2.5	83
D117	21	55	330	6	75
<b>Mean <math>\pm</math> SD</b>	<b>22.4 <math>\pm</math> 4.2</b>	<b>136.6 <math>\pm</math> 64.5</b>	<b>361 <math>\pm</math> 264.53</b>	<b>2.9 <math>\pm</math> 1.5</b>	<b>77.5 <math>\pm</math> 11.7</b>

### 2.4.2. HA-binding affinity in pelleted (90%) and interface (45%) spermatozoa

As the results showed there was a significant difference ( $p < 0.0001$ ) between the percentage of HA-binding in spermatozoa from 90% compared to 45% fractions (with the mean average  $\pm$  SD of  $93.2\% \pm 2.59\%$  and  $53.4\% \pm 10.4\%$ , respectively; Figure 2.5).



**Figure 2.5. Assessing of HA-binding in sperm recovered from DDGC fractions.** Box-whisker plots show quartiles and outliers (%) with 'a' representing significance ( $p < 0.0001$ ; Mann-Whitney U test) (N=16).

#### 2.4.3. Evaluation of capacitation using PSA-FITC labelling

To check the efficiency of capacitation procedure spermatozoa recovered from 90% fraction were incubated in capacitation supportive media for 0 hour (control) and 3 hours and then acrosome reacted using  $\text{Ca}^{2+}$  ionophore prior to labelling with PSA-FITC. Capacitated spermatozoa incubated with DMSO alone were also used as controls.

Figure 2.6 illustrates changes in non-capacitated, capacitated and acrosome reacted (AR) sperm based on PSA-FITC staining.

Approximately 78% of the population of sperm incubated for 3 hours under capacitation supportive conditions had completely reacted acrosomes (Figure 2.6C), which was significantly higher than non-capacitated (Figure 2.6A) and capacitated but not acrosome reacted (Figure 2.6B) groups confirming the efficiency of capacitation. (Figure 2.7;  $P < 0.0001$ ).

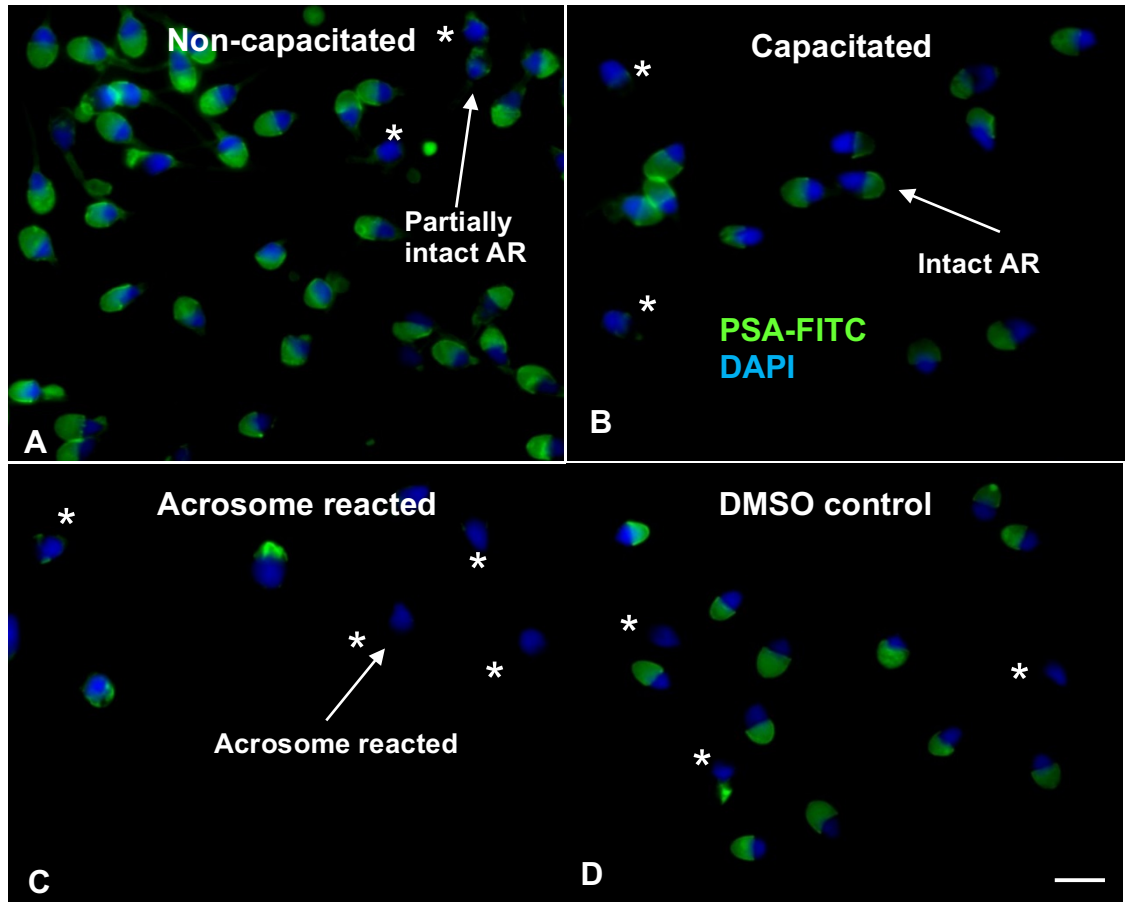


**Figure 2.6. Demonstrating the efficiency of capacitation by inducing the acrosome reaction and subsequent PSA-FITC labelling.**

A: non-capacitated spermatozoa (incubated for 0h in capacitation supportive buffer).

B: Capacitated spermatozoa (incubated for 3h in capacitation supportive buffer).

C: Acrosome reacted spermatozoa.

D: Capacitated spermatozoa incubated with DMSO as an AR control.

Acrosome reacted sperm are indicated by a star '\*'. The scale bar is 5  $\mu\text{m}$ .

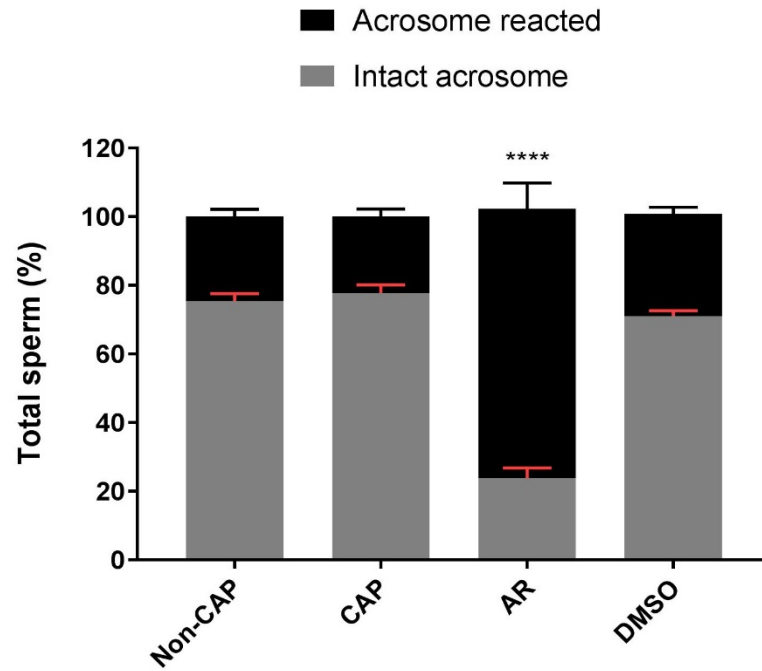


**Figure 2.7. Confirming the efficiency of capacitation by inducing acrosome reaction and subsequent PSA-FITC labelling.**

Data was analysed by two-way ANOVA followed by Tukey's post-hoc test. Asterisks (\*\*\*\*) indicate significantly different values ( $p < 0.000$ ) from all other groups (N=8).

#### 2.4.3. Evaluation of capacitation using assessment of hyperactive motility

In addition to the assessment of capacitation efficacy using PSA-FITC labelling after induction of the acrosome reaction, hyperactive motility was also assessed. A large increase in hyperactive motility (more vigorous and more clearly defined asymmetrical tail beating) was observed with sperm binding to the HA-coated surface after 3h incubation in capacitation supportive buffer but not after 0 hr incubation (Table 2.2).

Table 2.2. Changes in hyperactive motility during capacitation.

Sample	Sperm motility (%)	Motility after DDGC (90%) (%)	Hyperactive motility in washed semen at 0 hr cap (%)	Hyperactive motility in washed semen at 3 hr cap (%)	Hyperactive motility after DDGC (90%) at 0 hr cap (%)	Hyperactive motility after DDGC (90%) at 3hr cap (%)	Hyperactive motility at 3 hr incubation in cap supportive conditions (%)
D62	70	88	0.53	44.5	0.6	47.5	47.5
D43	67	81.5	0.2	41.0	0.4	43.4	43.4
D101	65	84.3	0.4	39.8	0.4	44.0	44
D115	61	79	0.27	42.8	0.3	39.6	39.6
<b>Mean ± SD</b>	65.8 ±3.8	83.2 ±3.9	0.35 ±0.2	42 ± 2.01	0.43 ± 0.13	43.6 ±3.23	43.63 ± 3.23

As shown in Figure 2.8 there is a significant difference ( $p < 0.05$ ) between the percentage of hyperactive motility in non-capacitated (from washed semen and DDGC separated populations) compared to capacitated (washed semen and DDGC separated) spermatozoa. These results in addition to PSA-FITC labelling results confirmed the efficiency of capacitation.

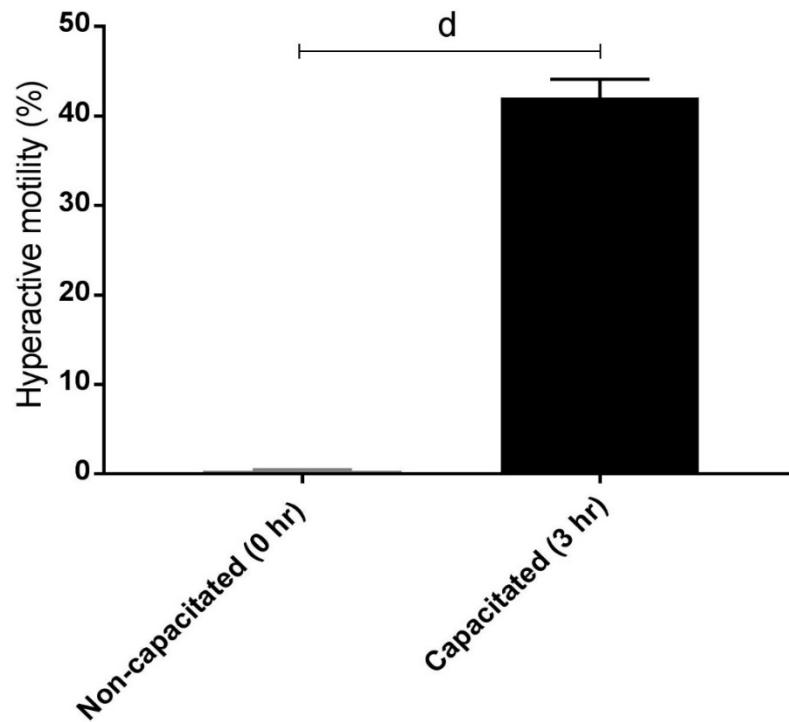


**Figure 2.8. Assessment of hyperactive motility in non-capacitated and capacitated sperm.**

The graph shows the significant difference (“d” indicates  $p < 0.05$ ) between the percentage of hyperactive motile spermatozoa in non-capacitated and capacitated spermatozoa, in 4 human semen samples using Mann-Whitney U test.

#### 2.4.5. Changes in HA binding after capacitation

HA-coated slides were used to investigate the effect of capacitation on sperm binding to HA. Whilst recovering higher numbers of capacitated sperm with the ability of binding to HA from washed samples, non-capacitated controls revealed lower HA-binding ability. The difference between them was not statistically significant.

The most significant difference in HA binding was between washed, non-capacitated sperm and 90% capacitated sperm (Figure 2.9). A clear increase in HA-binding of washed sperm was noted following capacitation but this was not

statistically significant. DDGC, however, promoted HA-binding, at least in the 90% fractions, regardless of the conditions for capacitation being favourable or not. This implies that 90% fractions contain higher levels of sperm competent to bind to HA and that induction of capacitation on these fractions make only a slight difference to their HA-binding. The data also suggests that capacitation supportive conditions might improve HA-binding in samples of only buffer washed sperm.

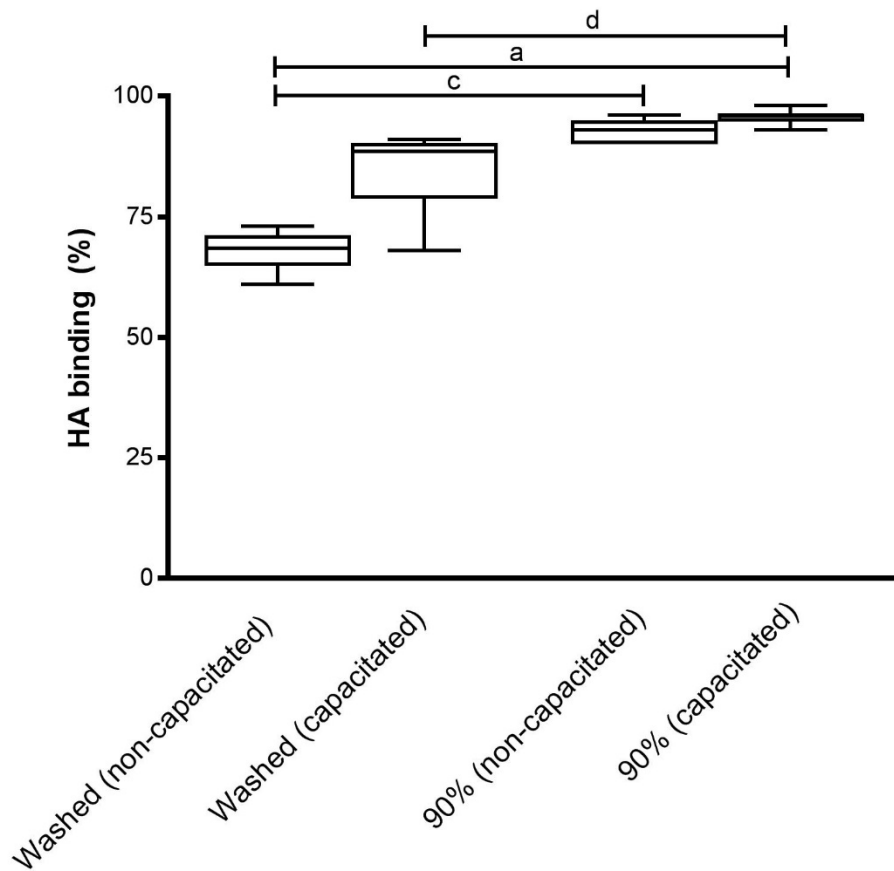


**Figure 2.9. Assessment of HA-binding in relation to capacitation in washed sperm and sperm from 90% fractions.**

The Kruskal–Wallis test (K-W), post-hoc Dunn’s test assigns the significance alpha between group medians hierarchically with a (0.0001) > b (0.001) > c (0.01) > d (0.05) (N=10).

#### 2.4.6. DNA fragmentation in spermatozoa recovered from DDGC fractions

As discussed, a significantly higher number of spermatozoa from 90% fractions bound HA. To evaluate the importance of this relationship to sperm viability, the levels of DNA fragmentation (by AO staining) and chromatin compaction (by AB

staining) were assessed in spermatozoa from 90% and 45% DDGC fractions and also in HA-bound and unbound populations of washed spermatozoa.

Examples of DNA fragmentation levels in spermatozoa recovered from 90% and 45% fractions can be seen in Figure 2.10. The AO staining produced predominantly green (++) fluorescence in 90% fractions suggesting sperm with relatively low levels of DNA fragmentation compared with more mixed colours (++, ±, --) in 45% fraction.

Significant relationships between sperm DNA fragmentation and sedimentation are presented in Figure 2.11. These findings were expected given the known ability of DDGC in differentiating between good and poor quality spermatozoa according to their motility and density. Therefore, compared with the 45% fractions, a significantly higher number of spermatozoa with low (++) and medium (±) DNA fragmentation levels were found in the 90% fractions (as shown by the almost uniform AO colour in Figure 2.10A/B and 2.10C/D).



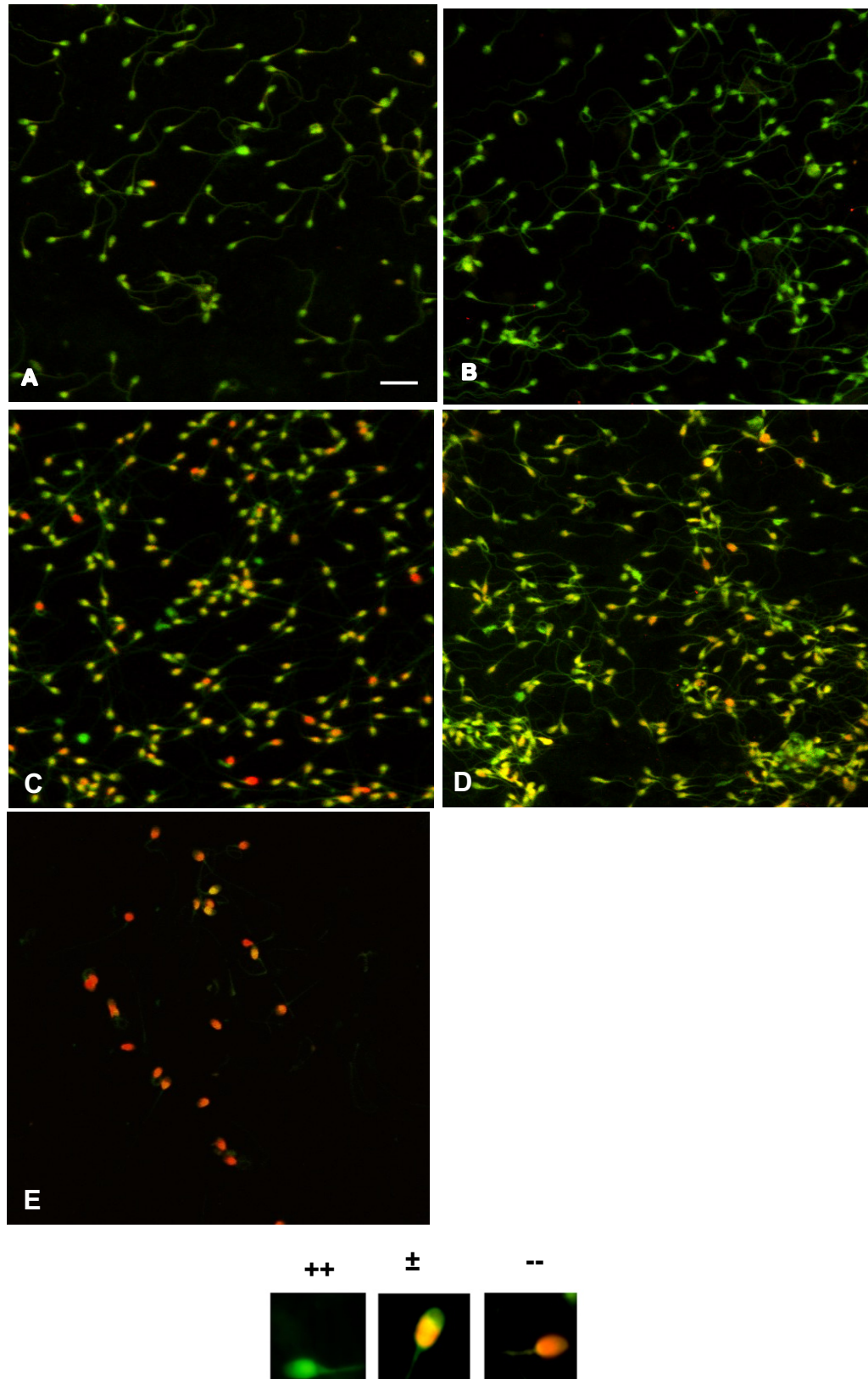


**Figure 2.10. Examples of AO stained sperm from DDGC fractions.**

A-B: Sperm recovered from 90% DDGC fraction.

C-D: Sperm recovered from 45% DDGC fraction.

E: Sperm incubated with H<sub>2</sub>O<sub>2</sub> as a positive control.

The panels below image A-D represent the subjective scoring method used to assign three different categories including low (++), medium (±) and high (--) DNA fragmentation to each sample. The scale bar is 20 μm (A-D).

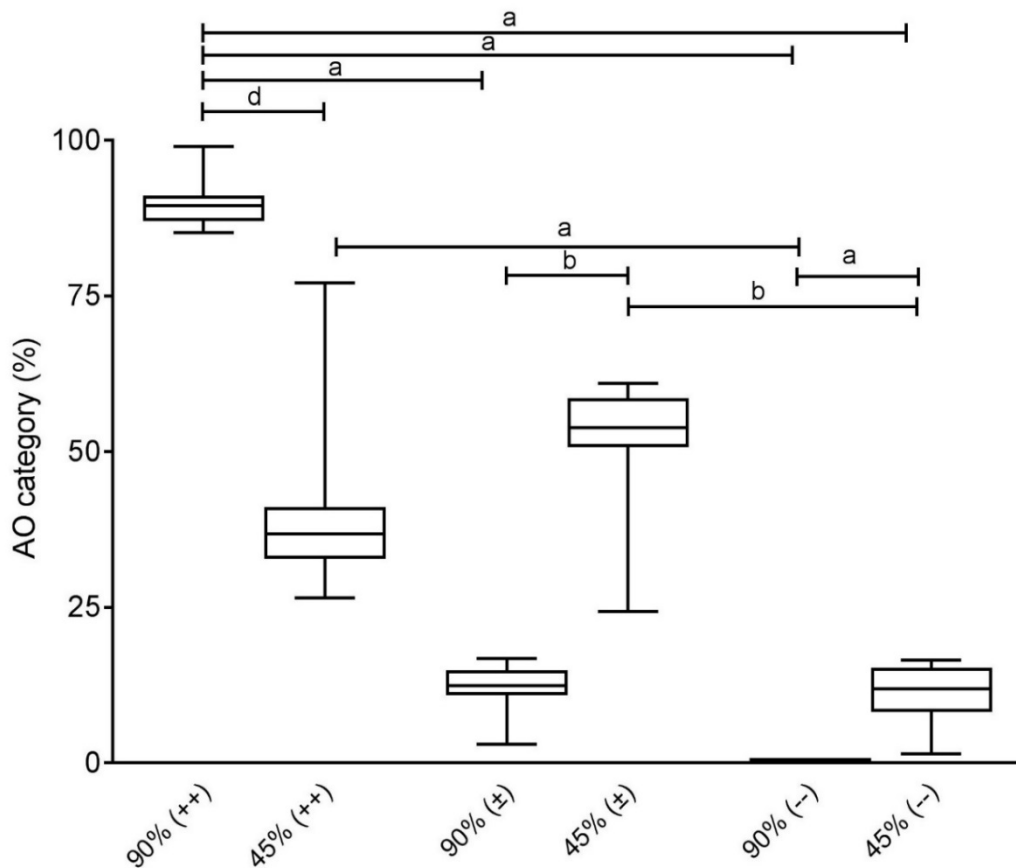


**Figure 2.11. Plots of AO category data from DDGC fractions.**

The K-W, post-hoc Dunn's test assigns the significance alpha between group medians hierarchically with a (0.0001) > b (0.001) > c (0.01) > d (0.05) (N=15).

Low, medium and high DNA fragmentation are indicated as ++, ± and --, respectively. Note the inverse relationships between sedimentation profile and staining categories.

#### 2.4.7. DNA fragmentation in spermatozoa recovered from HA-bound and unbound populations

DNA fragmentation was also assessed in relation to HA binding capacity where sperm with little or no fragmentation dominated HA-binding populations (Figure 2.13) and an almost complete clearance of sperm from HA-bound populations with medium or higher levels of DNA fragmentation. Figure 2.12 shows some examples of AO staining on HA-bound and unbound sperm.

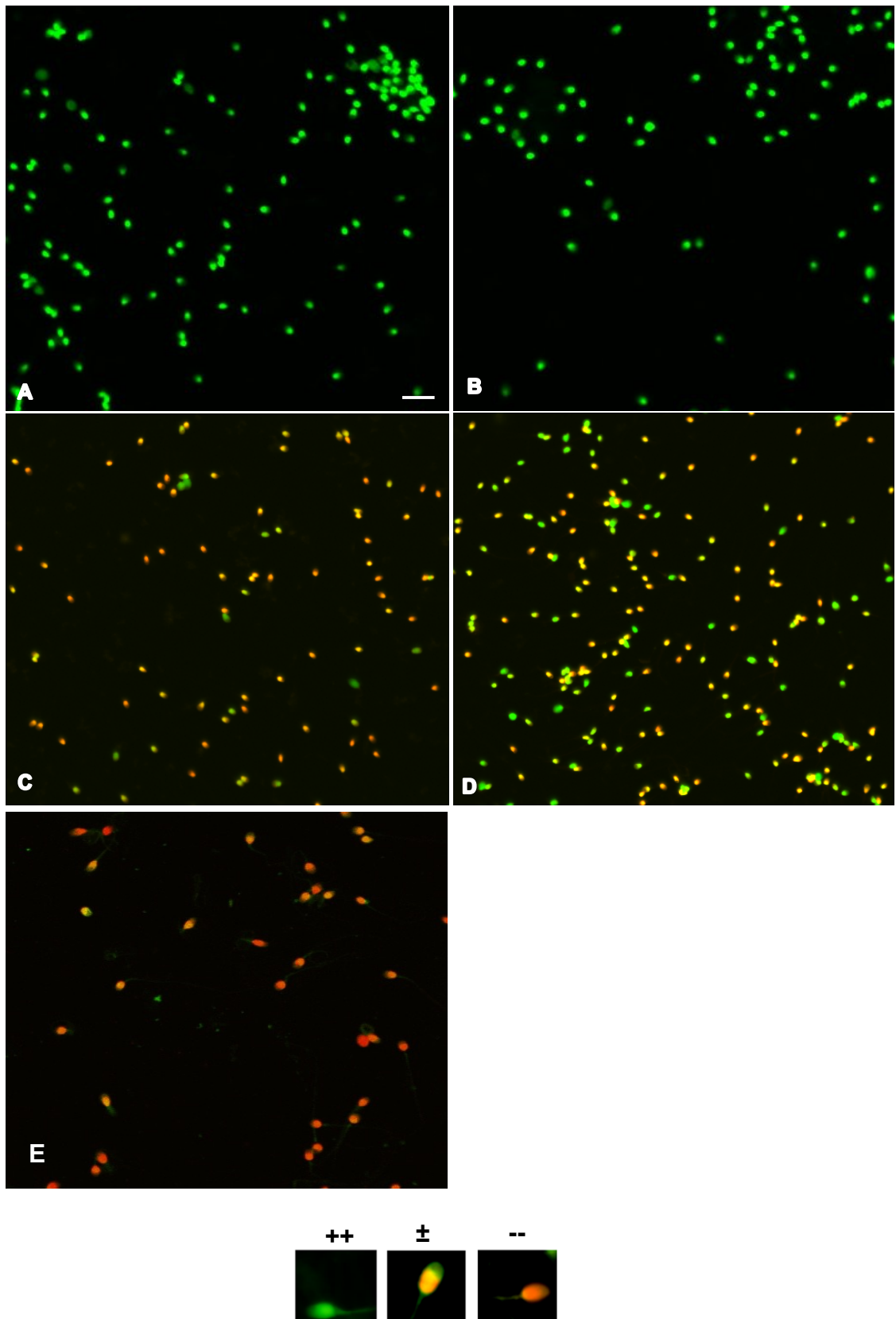


**Figure 2.12. Examples of AO staining on HA-bound and unbound sperm.**

A-B: HA-bound spermatozoa.

C-D: HA-unbound spermatozoa.

E: Sperm incubated with H<sub>2</sub>O<sub>2</sub> as a positive control.

The panels below image A-D represent the subjective scoring method used to assign three different categories including low (++), medium (±) and high (--) DNA fragmentation to each sample. The scale bar is 20 μm (A-D).

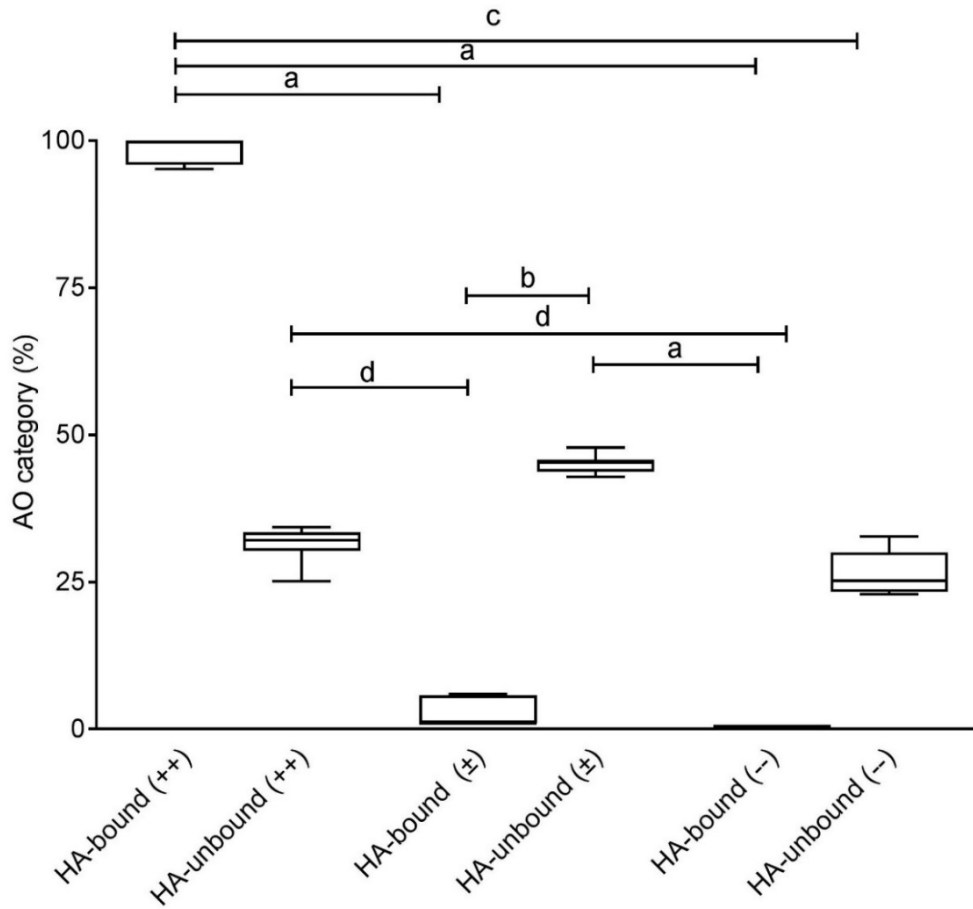


**Figure 2.13. Plots of AO category data from HA-bound and un-bound fractions.**

The K-W, post-hoc Dunn's test assigns the significance alpha between group medians hierarchically with a (0.0001) > b (0.001) > c (0.01) > d (0.05) (N=10). Low, medium and high DNA fragmentation are indicated as ++, ± and --, respectively. Note the inverse relationships between HA-binding profile and staining categories.

#### 2.4.8. Chromatin compaction in spermatozoa recovered from DDGC fractions

Aniline blue staining was carried out to evaluate incomplete protamination and chromatin compaction levels in DDGC fractionated and HA-binding and non-binding sperm populations. Examples of each are shown in Figure 2.14.

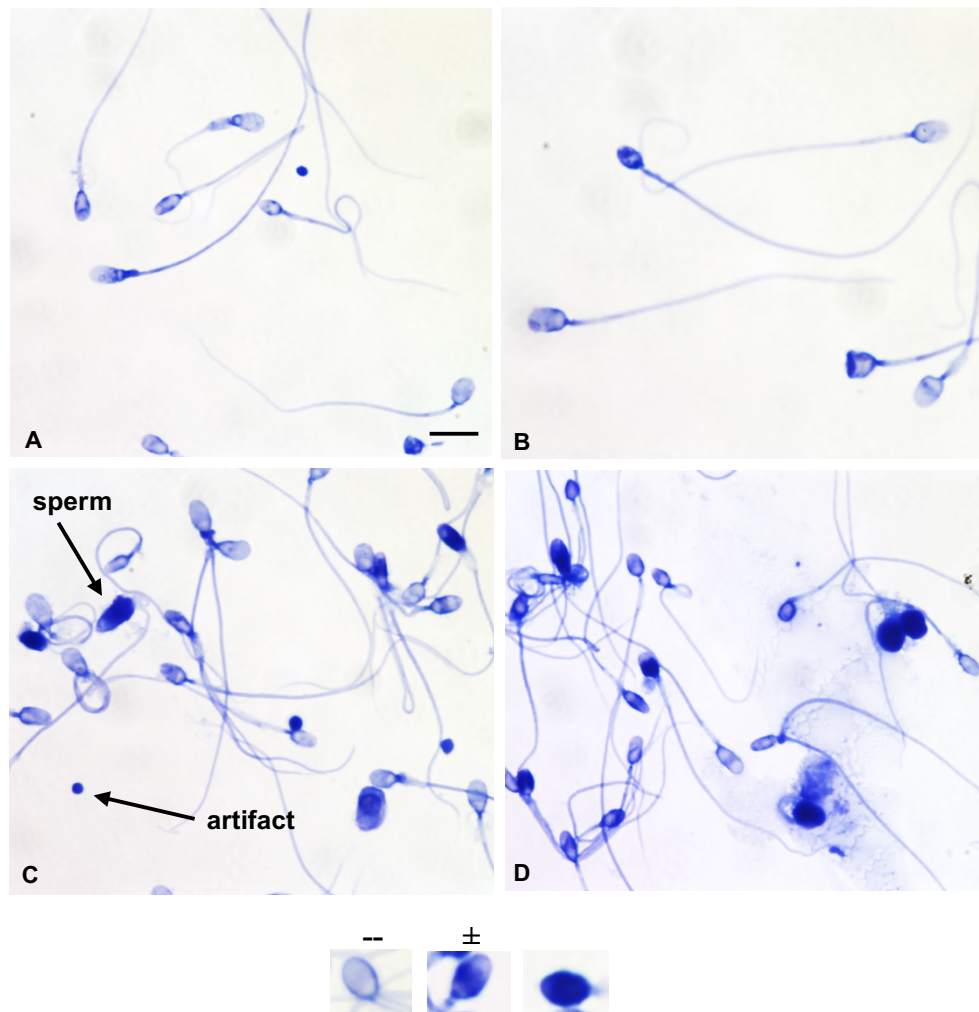


**Figure 2.14. Examples of AB stained sperm from DDGC fractions.**

A-B: Sperm recovered from 90% DDGC fraction.

C-D: Sperm recovered from 45% DDGC fraction.

The panels below image A-D represent the subjective scoring method used to assign three different categories including fully (--), partially ( $\pm$ ) and weakly (++) compacted chromatin to each sample. The scale bar is 10  $\mu$ m (A-D).

Very low proportions of spermatozoa with incomplete protamination (highly stained; ++)) were found in 90% fractions which were instead dominated by spermatozoa with highly compact chromatin (unstained, --; Figure 2.15).

Whilst higher levels of highly stained spermatozoa were found in 45% fractions, differences were not statistically significant when compared to the other groups and weakly stained ( $\pm$ ) or unstained spermatozoa showing good chromatin compaction were well represented in 45% fractions. Proportions of weakly stained sperm essentially mirrored those of strongly stained sperm in both DDGC fractions.

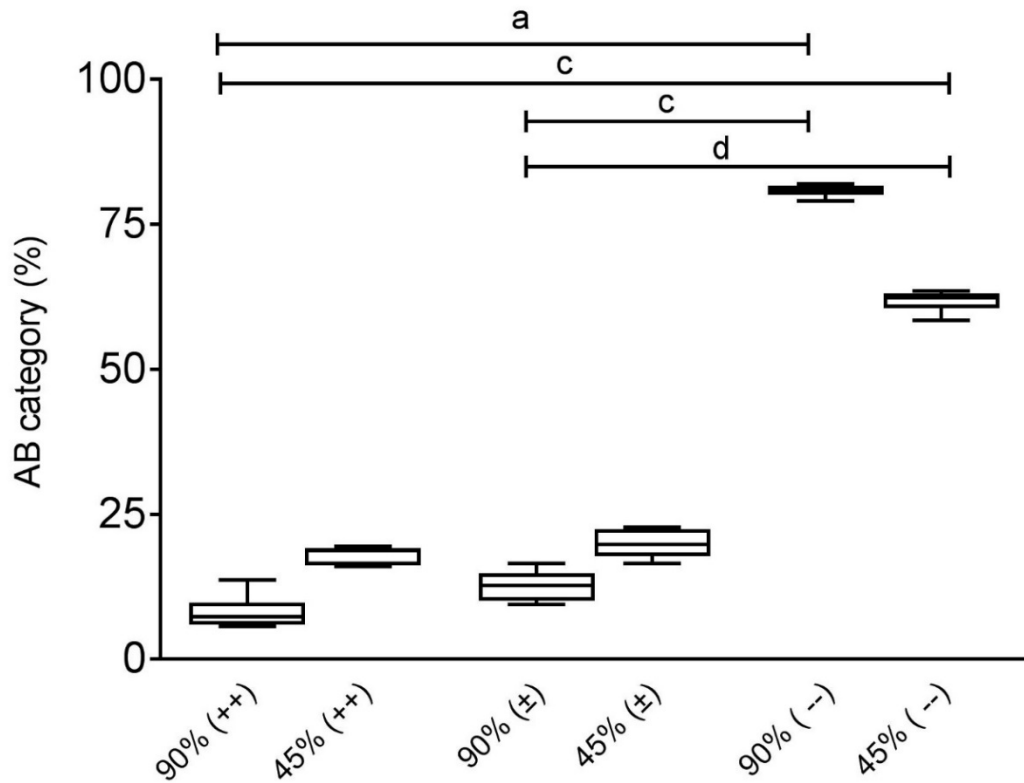


**Figure 2.15. Plots of AB category data from DDGC fractions.**

The K-W, post-hoc Dunn's test assigns the significance alpha between group medians hierarchically with a (0.0001) > b (0.001) > c (0.01) > d (0.05) (N=8). Fully, partially and weakly compacted chromatin are indicated as --,  $\pm$  and ++, respectively. Note the inverse relationships between sedimentation profile and staining categories.

#### 2.4.9. Chromatin compaction in spermatozoa recovered from HA-bound and unbound populations

Similar to the previous findings on DDGC and chromatin compaction, spermatozoa with  $\pm$  and  $++$  AB staining characteristics were more abundant in HA-unbound populations with unstained sperm ( $--$ ) dominating the bound fractions (Figure 2.16 and 2.17). In general, AO and AB staining essentially mirrored each other in relation to DNA fragmentation and chromatin compaction with each indicating better quality sperm in 90% DDGC fractions and HA-binding sperm from washed samples.

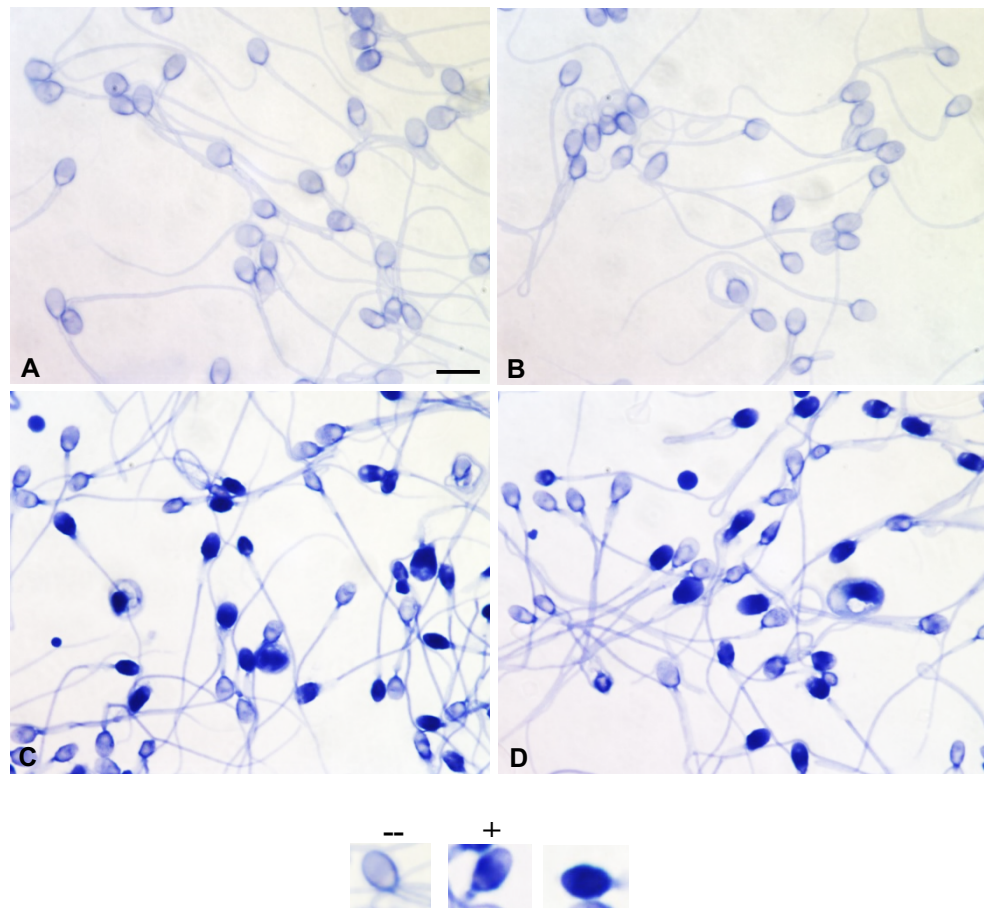


**Figure 2.16. Examples of AB stained sperm from HA-binding assay.**

A-B: HA-bound spermatozoa.

C-D: HA-unbound spermatozoa.

The panels below image A-D represent the subjective scoring method used to assign three different categories including fully ( $--$ ), partially ( $\pm$ ) and weakly ( $++$ ) compacted chromatin to each sample. The scale bar is 10  $\mu\text{m}$  (A-D).

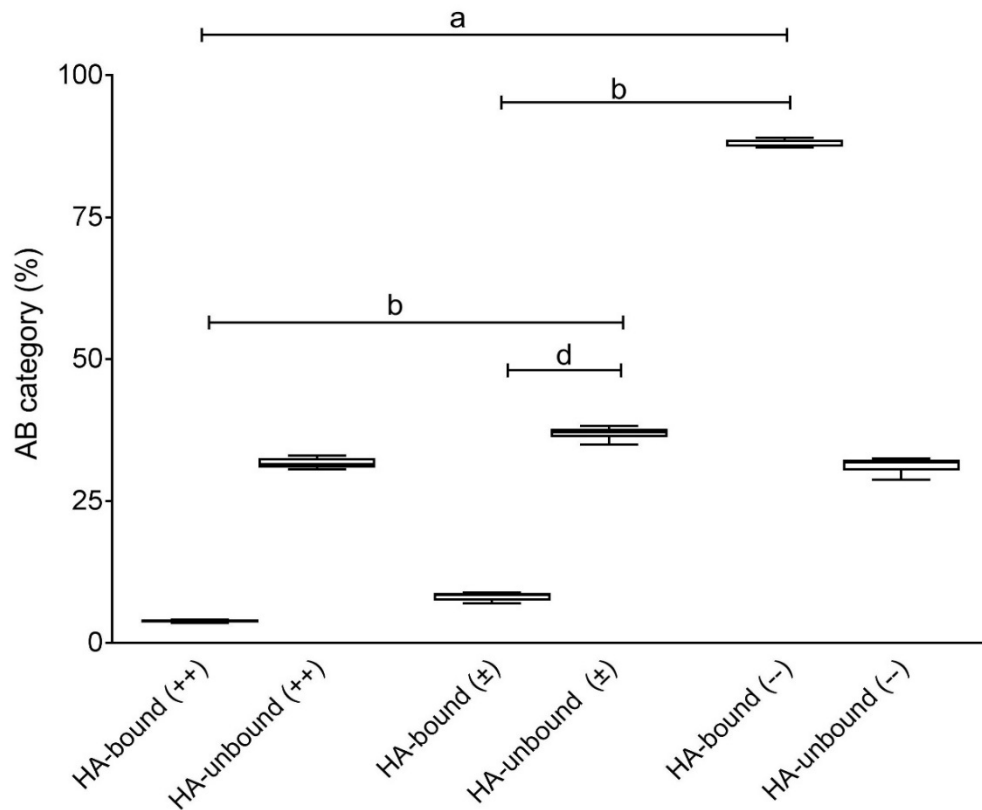


**Figure 2.17. Plots of AB category data from HA-bound and unbound fractions.**

The K-W, post-hoc Dunn's test assigns the significance alpha between group medians hierarchically with a (0.0001) > b (0.001) > c (0.01) > d (0.05) (N=8). Fully, partially and weakly compacted chromatin are indicated as --, ± and ++, respectively. Note the inverse relationships between HA-binding profile and staining categories.

#### **2.4.10. A comparison between DDGC and HA-binding assay in selecting sperm with less DNA fragmentation and high chromatin maturity**

A comparison between HA-binding and DDGC was performed to evaluate what method would be the best in selecting better quality sperm regarding their DNA and chromatin status.

As Figure 2.18 shows HA-binding is more powerful than DDGC is separating intact DNA (++) sperm. It also shows that 90% fractions have significantly higher levels of sperm with medium levels of DNA fragmentation (±).



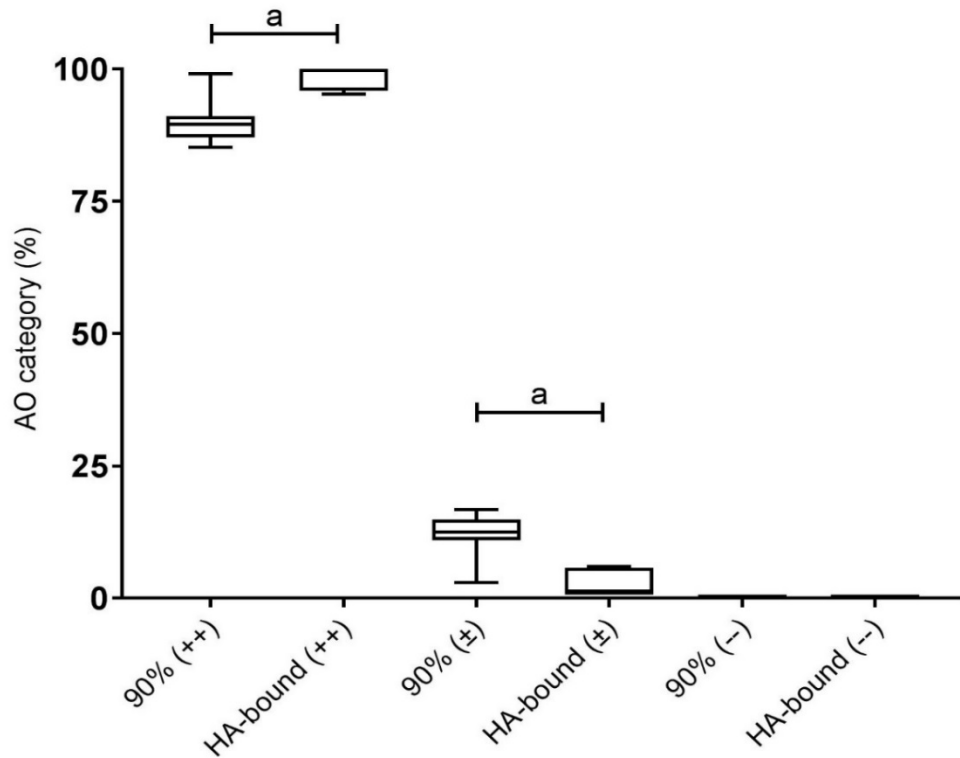


**Figure 2.18. Plots of AO category data from 90% and HA-bound fractions.** Semi-quantitative data for AO staining in relation to HA-binding (N=10) and sedimentation through a 90% DDGC gradient (N=15). Low, medium and high DNA fragmentation are indicated as ++, ± and --, respectively. The data was analysed using *Mann-Whitney* U-test (a= p<0.0001).

As mentioned above spermatozoa separated using DDGC and HA-binding assay were also compared regarding their chromatin status.

The results presented in Figure 2.19 show that HA-binding assay is a better choice in selecting spermatozoa with fully compacted chromatin (--). The results also demonstrate that 90% fractions have significantly higher percentage of spermatozoa with partially (±) and weakly (++) compacted chromatin.

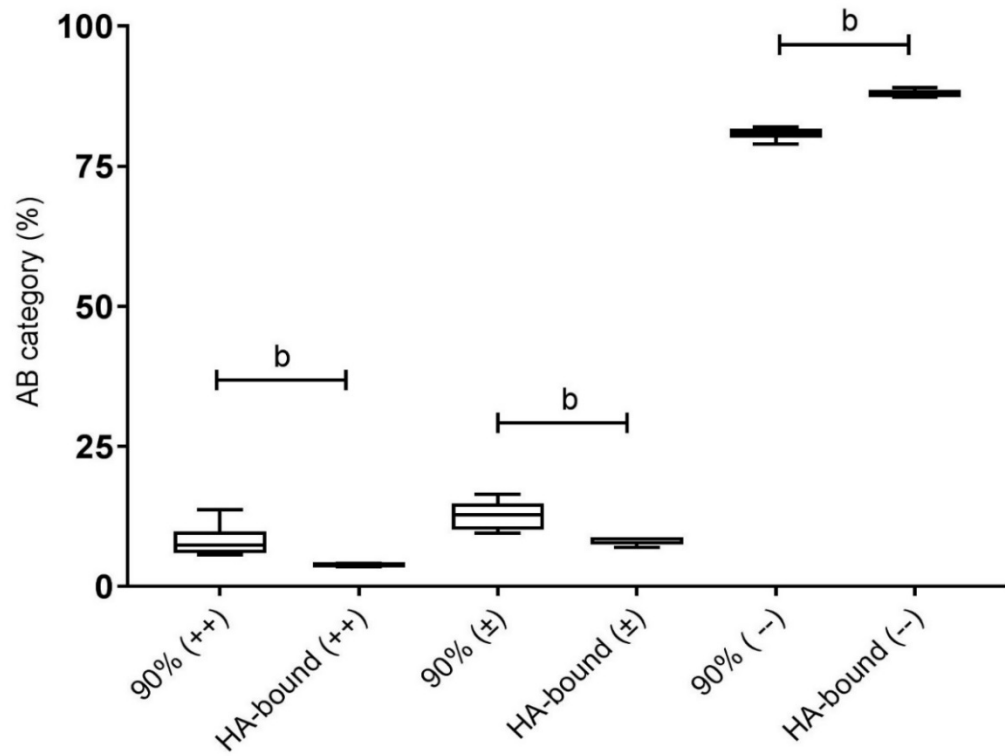


**Figure 2.19. Plots of AB category data from 90% and HA-bound fractions.**

Semi-quantitative data for AB staining in relation to HA-binding and sedimentation through a 90% DDGC gradient (N=8).

Fully, partially and weakly compacted chromatin are indicated as --, ± and ++, respectively.

The data was analysed using *Mann-Whitney U-test* ("b" indicates  $p < 0.05$ ).

## 2.5. Discussion

In the Western world approximately 5% of births are currently achieved by ARTs such as IVF and ICSI (Lewis and Kumar, 2015) and some checkpoints of natural fertilisation are bypassed when using ICSI. This results in selecting spermatozoa of low quality such as those with low motility, abnormal morphology, aneuploidy, damaged DNA and poor zona binding ability that are not usually able to participate in natural fertilisation (Tournaye, 2003; Alukal and Lamb, 2008; Cummins and Jequier, 1995).

Recent clinical evidence has shown that a high proportion of infertile men possess substantially higher levels of damaged sperm DNA compared to fertile males (Zhang et al., 2008). Since spermatozoa do not have any mechanism for repairing DNA fragmentation, sperm with fragmented DNA could be transferred to the oocyte during ICSI, and will be reliant on the oocyte to be repaired (Lewis and Kumar, 2015). In this regard, sperm with increased levels of DNA fragmentation could contribute to embryonic mortality and affect assisted reproductive outcomes (Marchesi et al., 2010; Heytens et al., 2009; Bonduelle et al., 2002; Jakab et al., 2005). Therefore, new methods of selecting sperm with optimum quality are being developed for use in ART. These include electrical (flow cell, Zeta potential), morphological (IMSI, MSOME) and cell sorting methods (FACS, MACS) (Sakkas, 2013; Nasr-Esfahani et al., 2012; Delaroche et al., 2013; Chan et al., 2006; Teixeira et al., 2013).

Studies have suggested that spermatozoa with the ability of binding to endocervical mucus have better morphology and that selecting spermatozoa with good morphology should also select for sperm with other good parameters including progressive motility and high DNA integrity (Yagci et al., 2010; Sati et al., 2008; Prinosilova et al., 2009). A possible relationship between spermatozoal viability and HA-binding was established in the 1990s (Cayli et al., 2003; Vandervoort et al., 1997). This work and related studies have suggested that spermatozoa with the ability of binding to HA completed the maturation process, more specifically chromatin compaction and plasma membrane remodelling and therefore have a higher fertilising capacity (Cayli et al., 2003; Huszar et al., 2003; Mokanszki et al., 2014). Other studies have shown that HA-binding improves embryo quality and development following ICSI, however these studies have

been relatively small (Parmegiani et al., 2010b; Parmegiani et al., 2010a; Nasr-Esfahani et al., 2008; Mokanszki et al., 2014; Beck-Fruchter et al., 2015).

DDGC, which is now a widely adopted procedure for sperm preparation for ART (WHO 2010) is thought to enrich for higher quality spermatozoa with a higher density and motility due to prior cytoplasmic extrusion and greater chromatin condensation. These denser and more motile, mature cells can more readily (and rapidly) sediment through high-density silica-based media (Bolton and Braude, 1984; Mortimer and Mortimer, 2013). In this regard, sperm populations from 90% fractions had significantly higher HA binding abilities than 45% fractions, implying that HABPs are more abundant or have a greater affinity for HA in sperm from 90% fractions and supporting the likelihood of these sperm being more cytoplasmically mature.

Spermatozoa undergo capacitation during their journey through the female genital tract, which involves hyperactive motility, protein tyrosine phosphorylation and the dramatic re-distribution of membrane proteins and lipids including the efflux of membrane cholesterol (Liu et al., 2007; Gadella et al., 2008; Leahy and Gadella, 2011b; Zaneveld et al., 1991). Other changes might also have an impact on the distribution of HABPs in preparation for encountering the descending egg mass (Baldi et al., 2000). In the current study, higher HA-binding was reported in capacitated spermatozoa, suggesting greater accessibility of HABPs to their ligands in keeping with the likely redistribution of membrane components (Leahy and Gadella, 2011b).

Capacitation was originally reported by Yanagimachi (1969) using hamster sperm and is currently a broadly recognised phenomenon associated with acquisition of hyperactive motility (Bailey, 2010; Fraser, 1998b; Suarez, 2008). The redistribution of HABPs observed in the present study accords with research showing that actively motile and cytoplasmically mature sperm have completed their plasma membrane remodelling, which probably includes the redistribution of HABPs (Cayli et al., 2003; Huszar et al., 2003; Parmegiani et al., 2010a; Prinosilova et al., 2009; Yagci et al., 2010). Hyperactive motility is not an absolute requirement for sperm binding to HA, but it may be a requirement for sperm penetration of the HA-rich, cumulus complex surrounding the oocyte *in vivo*

(Hong et al., 2009). It is likely that the higher HA-binding scores in capacitated sperm reflect this process *in vitro*.

As discussed earlier, ARTs help to bypass the natural barriers of the fertilisation process and potentially allow spermatozoa with damaged DNA to fertilise the oocyte, which can have deleterious effects on embryo development (Agarwal and Allamaneni, 2004). In this regard, more efficient separation methods may be needed to obtain spermatozoa with lower levels of DNA fragmentation and higher levels of chromatin maturity. In the present study, spermatozoa were separated using DDGC or following brief incubation on surfaces coated with HA and were assayed for their levels of DNA integrity and chromatin maturity.

The results confirmed that sperm populations from 90% fractions had significantly lower DNA fragmentation and higher levels of chromatin maturity than 45% fractions. It was also clear that HA-binding is highly efficient in eliminating spermatozoa with higher DNA fragmentation and lower chromatin compaction. The post-hoc Dunn's test reports the most significant ranking differences between group medians following K-W (Kruskal–Wallis) ANOVA. Whilst the differences in chromatin compaction and DNA fragmentation between unpaired 90% and 45% fractions or between HA-bound and unbound fractions were not significant on some occasions, there were still clearly visible trends. The results are supported by other research showing higher normal morphology and chromatin compaction in sperm from 90% fractions of DDGC processed samples (Brahem et al., 2011; Le Lannou and Blanchard, 1988; Sakkas et al., 2000b; Tomlinson et al., 2001).

Whilst the data from the current study was obtained from men of unproven fertility, the results remain relevant when considering ART for infertile males, where higher sperm DNA fragmentation might be correlated with enhanced risks of early pregnancy failure after ICSI and IVF (Osman et al., 2015; Robinson et al., 2012; Zhao et al., 2014; Zini et al., 2008). In this regard, earlier studies showed that compared to spermatozoa recovered following a standard washing process, sperm from the same sample which bound to HA were more mature with respect to their cytoplasmic and nuclear condensation (Huszar et al., 2003; Yagci et al., 2010) and that HA-selected sperm from crude semen samples had low DNA

fragmentation (Yagci et al., 2010). These sets of data suggest that HA-binding might be a beneficial alternative or augmentation to DDGC for semen sample preparation prior to ICSI and potentially other IVF procedures, specifically where sperm concentration is very low for DDGC. The results also showed that HA-binding assay is more efficient in separating sperm with better quality DNA and chromatin. Clinical support for these findings, however, is equivocal. Whilst the study carried out by Nijs et al., (2009) established a clear link between routine sperm assessment techniques and more advanced methods including those for evaluation of DNA fragmentation and chromatin compaction, it could not link these connections through to sample HA-binding capacity (Nijs et al., 2009). A further study by Nijs et al., (2010) appeared to uphold this disconnect (Nijs et al., 2010).

A meta-analysis by of numerous studies Zini et al (2008) that included the use of an HA-selection step prior to ICSI have so far also failed to support efficacy with the caveat that the studies concerned were relatively small (Zini et al. 2008). The biggest study so far has shown a significant drop in miscarriage, although it unfortunately did not report birth outcomes (Worrilow et al., 2013). A significant improvement in live births was shown in a recent report, however due to the lack of raw data, it was not included in a later meta-analysis which recommended the requirement for better clinical trials with full data reporting (Mokanszki et al., 2014; Beck-Fruchter et al., 2015).

## **2.6. Conclusion**

In conclusion, this study has brought together convincing evidence for the first time, of a relationship between a standard sperm processing technique (DDGC) and the affinity of sperm for HA. In this regard, this relationship is reflected by the status of chromatin compaction and DNA fragmentation. Whether this benefit translates into significantly improved live birth outcomes for ICSI remains to be determined.

## **Chapter 3: Investigating the appearance of and changes in HABPs of human and bovine spermatozoa during capacitation and the acrosome reaction**

### **3.1. Introduction**

Hyaluronic acid plays an essential role in natural fertilisation and is normally present in the extracellular matrix (ECM) of the cumulus oophorus surrounding the oocyte (Parmegiani et al., 2010a). During *in vivo* fertilisation, mature spermatozoa binds to HA in the extracellular matrix of cumulus cells via HABPs (Petersen et al., 2010; Jakab et al., 2005). To date, CD44 and RHAMM (receptor for hyaluronic-acid-mediated motility) are the best studied HABPs and are known to affect cell motility, survival and proliferation (Toole, 2004). The main physiological role of CD44 is to assist with organ and tissue structural integrity through cell-cell and cell-matrix adhesion (Goodison et al., 1999). Post-translational modifications of CD44 such as glycosylation control the binding of HA to CD44. Specific variant isoforms of CD44 (CD44v) can participate in lymphocyte activation, homing and the presentation of chemical factors and hormones to various cell types (Goodison et al., 1999; Dzwonek and Wilczynski, 2015). For example, increased levels of CD44v and N-linked glycosylation leading to changes in the binding of CD44 to HA have been investigated in chronic lymphocytic leukaemia (CLL) (Gutjahr et al., 2015). The presence of CD44 is also known to be associated with the initiation of arthritis and in mice with a genetic deficiency of CD44, disease severity is increased (Misra et al., 2015). Different studies have shown that RHAMM, another well-known HABP mediates HA-dependent migration of various cells, such as breast tumour cells and vascular smooth muscle (Assmann et al., 1998; Goueffic et al., 2006).

The inherent uniqueness of the mammalian spermatozoon is embodied by its formation, shape and exclusive requirement to complete the maturation process outside its host. As discussed previously, for successful fertilisation, mammalian spermatozoa must undergo maturation in the female reproductive tract. The final stages of sperm maturation involve two sequential, multifaceted phases: capacitation and the AR (Ikawa et al., 2010; De Jonge, 2005). In ART, sperm acquire fertilising ability by being incubated in specific media for 3-24 hours. During capacitation and AR, there is a redistribution, change in enzyme activity,

and quite possibly *de novo* translation of nuclear-encoded proteins by mitochondrial-type ribosomes that prepare the cell for fertilisation (Zhao et al., 2009; Gur and Breitbart, 2006). Thus, the general consensus is that the acquisition of fertilising ability during capacitation is very much dependent on post-translational modifications of pre-existing proteins.

The completion of capacitation and the AR is time and site-sensitive in sperm and therefore, measuring the sperm population that is capable of undergoing proper maturation and their associated protein changes provide potential biomarker opportunities to measure semen quality. During capacitation, the membrane proteins and lipid microdomain organisation change dramatically which allow the sperm to bind to the zona pellucida and instantly after that to acrosome react (Gadella et al., 2008). Certain sperm surface regions have specific roles in fertilisation. For example, the apical ridge participates in the binding of sperm to the zona pellucida and has particular zona binding proteins that do not exist or at least not functional in other regions of the sperm surface (Flesch and Gadella, 2000). The localisation and distribution of different antigens also change during capacitation. For example, a positive correlation between the expression of fibronectin, laminin and vitronectin is reported during sperm capacitation in hamster and human (de Lamirande et al., 1997).

Huszar et al reported that HA-binding spermatozoa displayed the highest proportion of tyrosine phosphorylation (TP) in contrast to sperm with arrested development and cytoplasmic retention assayed by the presence of surplus creatine kinase (CK) (Sati et al., 2014). It is possible that the observed increased ability of sperm to bind HA during capacitation (Chapter 2) is due to similar changes in the expression and distribution of HABPs. To this end, the HABPs in non-capacitated, capacitated and acrosome reacted spermatozoa were investigated in human and bovine sperm. This study is the first to evaluate dynamic changes of HABPs during capacitation and acrosome reaction.

Initially, frozen human sperm were used in the study, but they were replaced by fresh samples (Table 3.1) due to the very poor quality of thawed sperm such as high numbers of dead sperm and very low motility even after DDGC. Frozen



bovine sperm were also used to check whether or not the distribution and localisation of HABPs are similar amongst different species.

### **3.2. Hypothesis and Objectives**

The main hypothesis is that the expression and distribution of sperm HABPs change dynamically with capacitation. The objectives of the study are as follows:

- To look for and identify HABPs in human and bovine sperm.
- To investigate how capacitation and the acrosome reaction affect the distribution of HABPs in human and bovine sperm.

### **3.3. Materials and methods**

#### **3.3.1. Reagents used**

Percoll™ was purchased from GE Healthcare, Sweden. Polyvinyl alcohol (PVP) mounting medium with DABCO, HEPES, Sodium dihydrogen phosphate ( $\text{NaH}_2\text{PO}_4$ ), Magnesium chloride ( $\text{MgCl}_2$ ), 4', 6-Diamidino-2-phenylindole dihydrochloride (DAPI), Penicillin-Streptomycin and T-75 cell culture flasks were obtained from Sigma-Aldrich, UK. Potassium chloride (KCl) and calcium chloride ( $\text{CaCl}_2$ ) were purchased from BDH, UK. Sodium chloride (NaCl) was obtained from Fisher Scientific, UK. Hyaluronic acid (50 and 1500 kDa) and HA-TRITC (hyaluronic acid-tetramethyl rhodamine isothiocyanate 1500kDa) were supplied by Creative PEGWorks, USA. Biotinylated monoclonal anti-CD44 antibody and streptavidin-FITC conjugate were obtained from Abcam (UK) and BD Pharmingen (UK), respectively. RPMI 1640 medium (GlutaMAX™ Supplement) and FBS (Fetal Bovine Serum) were purchased from Gibco, ThermoFisher Scientific (UK).

#### **3.3.2. Human sperm preparation**

Human spermatozoa were ethically obtained and prepared as described previously in Chapter 2. Different ejaculates of the same volunteers as used in Chapter 2 (N=10) were also used in the current Chapter. Table 3.1 presents a more complete description of the volunteer semen profiles.

**Table 3.1. Semen assessment of volunteers contributing to the study.**

<b>Sample</b>	<b>Donor Age</b>	<b>Sperm concentration (million/mL)</b>	<b>Total sperm count (<math>\times 10^6</math>)</b>	<b>Semen volume (mL)</b>	<b>Sperm motility (%)</b>
<b>D11</b>	20	153	306	2	61
<b>D27</b>	21	72	324	4.5	93
<b>D30</b>	22	120	204	1.7	74
<b>D43</b>	21	54	189	3.5	69
<b>D49</b>	21	120	336	2.8	86
<b>D56</b>	20	159	111.3	0.7	85
<b>D62</b>	19	120	252	2.1	70
<b>D70</b>	28	232	324.8	1.4	92
<b>D84</b>	24	186	409	2.2	75
<b>D116</b>	22	153	398	2.6	88
<b>Mean <math>\pm</math> SD</b>	<b>22 <math>\pm</math> 4</b>	<b>137 <math>\pm</math> 65</b>	<b>361 <math>\pm</math> 265</b>	<b>3 <math>\pm</math> 2</b>	<b>78 <math>\pm</math> 12</b>

### 3.3.3. Bovine sperm Preparation

Frozen bovine semen samples were obtained from Genus, Cheshire, UK. 500  $\mu$ L straws of frozen bovine semen sample were thawed at 39 °C for 30 seconds in water bath prior to use. Spermatozoa were separated using a two-layer Percoll gradient (90% and 45%). Motile (high quality) and less motile (lower quality) spermatozoa were recovered from 90% (pellet) and 45% (interface) fractions, respectively. To prepare gradients, 2.0 mL of 90%(v/v) Percoll was placed at the bottom of a polypropylene centrifuge tube with 2.0 mL of a 45% (v/v) solution carefully layered over the top. The 500  $\mu$ L of thawed semen was placed over the 90-45% gradient. Ninety percent Percoll was prepared by adding 1mL of 10x stock buffer (1000 mM NaCl, 31.0 mM KCl, 3.0 mM NaH<sub>2</sub>PO<sub>4</sub> and 100.0 mM HEPES (pH 7.3) to 9 mL of Percoll medium supplemented with 0.40 mM MgCl<sub>2</sub>, 25.0 mM NaHCO<sub>3</sub>, 2.0 mM CaCl<sub>2</sub>, and 21.6 mM Lactic acid (C<sub>3</sub>H<sub>6</sub>O<sub>3</sub>). Forty-five percent Percoll was prepared by mixing the 90% Percoll solution 1:1 with Sperm Tyrode's Albumin-Lactate-Pyruvate (SP-TALP) (100 mM NaCl, 10 mM HEPES, 0.3 mM NaH<sub>2</sub>PO<sub>4</sub>, 3.1 mM KCl, 25 mM NaHCO<sub>3</sub>, 21.6 mM Lactic acid, 2 mM CaCl<sub>2</sub>, 0.40 mM MgCl<sub>2</sub>, 1 mM pyruvate, 1% BSA pH 7.3). Centrifugation was performed at 700 x g for 30 min. Fresh SP-TALP were used for each experiment. Spermatozoa were recovered from 90% and 45% fractions, respectively and

washed in SP-TALP separately by centrifugation at 700 x g for 10 min (two repeat washes). A Neubauer haemocytometer was used to count sperm as described in Chapter 2 (Section 2.3.4).

### **3.3.4. Detection of sperm HABPs in sperm**

Human and bovine spermatozoa were prepared as described above. Spermatozoa recovered from 90% fractions were resuspended in 1x PBS and were placed on Poly-L-Lysine coated slides. To block non-specific binding, after air drying, 100  $\mu$ L of 3% BSA (w/v) in PBS were placed on the slides and incubated for 60 min at RT. To detect HABPs, slides were first incubated with 100  $\mu$ L (10  $\mu$ g/mL) of HA-TRITC (a generic probe for HABPs) for 75 min in a humid chamber at RT and then washed by immersing in 30 mL PBS prior to incubation with 100  $\mu$ L of a biotinylated monoclonal anti-CD44 antibody raised in mouse (1:100 dilution of 0.5 mg/mL, in PBS) for 90 min in a humid chamber at RT. Slides were then washed (x3) with PBS (30 mL in a coplin jar) for 15 min each and then incubated with 100  $\mu$ L of a mixture of streptavidin-FITC (1:1000 dilution of 0.5 mg/mL in PBS) and DAPI (1:5000 dilution) for 60 min in a humid chamber at RT in the dark and then washed with PBS (see above). Coverslips (Fisher Scientific) were mounted with a drop of polyvinyl alcohol (PVA) mounting medium. A Leica LEITZ DMRB fluorescence microscope (Mazurek Optical Services, UK) was used to view the samples. The microscope was equipped with FITC, TRITC and DAPI filters with excitation/emission at 495 nm/520 nm, 541 nm/572 nm and 358 nm/461 nm, respectively. SmartCapture 3 software was used to image the slides. To act as controls for non-specific fluorescence, spermatozoa were incubated with 1500 and also 50 kDa unlabelled HA or exposed to streptavidin-FITC without the primary antibody. The experiment was performed on 10 human and 8 bovine samples.

Different concentrations of HA-TRITC (1, 5, 10, 20, 50 and 100  $\mu$ g/mL), anti CD44 antibody (1/20, 1/50, 1/1000) and streptavidin-FITC (1/2000, 1/15000, 1/1000, 1/500) as well as different time points for each reagent were examined before the above final protocol was optimised. In addition, 4% paraformaldehyde (PFA) was used to check the effect of fixation on HA-TRITC and anti CD44 antibody/streptavidin-FITC signals. Some results obtained during protocol optimisation are shown in Appendix Figures 3.1-3.5.

#### **3.3.4.1. Detection of sperm HABPs in PC3 cells**

PC-3 cells (human prostate cancer cell line), originally from the American Type Culture Collection (ATCC) were used as a positive control for HABP expression. These cells also express CD44. Briefly, frozen cells were thawed in a 37°C water bath. The cells were then transferred to a 75 cm<sup>2</sup> tissue (T-75) culture flask and diluted with RPMI 1640 medium containing 10% (v/v) FBS, 100 units/mL penicillin, 100 µg/mL streptomycin, 2mM L-glutamine at 37°C with 5% CO<sub>2</sub> in T-75 culture flasks. The cells were subcultured when they were 80% confluent. To subculture the cells, the culture media was removed and the cell layer was rinsed with PBS (3x). To detach the cells from the flask, 3 mL solution of 0.025% trypsin and 0.01% EDTA was added. After the cells were detached, 8 mL of the culture media was added to the cell suspension. Aliquots of the cell suspension were added to new culture flasks appropriately. The flasks were incubated at 37°C with 5% CO<sub>2</sub>. Collected cells were fixed with 4% (w/v) PFA and labelled with HA-TRITC and the anti CD44 antibody as indicated in Section 3.3.4. Sperm labelled with only streptavidin-FITC were served as a negative control for the experiment (Figure 3.3).

#### **3.3.5. Evaluation of HABPs in human spermatozoa before and after capacitation**

Capacitation was accomplished as described previously in Chapter 2 (Section 2.3.6). Pelleted spermatozoa re-suspended in the buffer supporting capacitation, incubated for 0 hour (non-capacitated), were used as a control. Spermatozoa were then placed on Poly-L-Lysine coated slides and labelled with HA-TRITC and biotinylated anti-CD44 as described earlier. Additional slides were prepared to check the efficiency of capacitation (after acrosome reaction) using PSA-FITC labelling. This experiment was performed on 10 human and 8 bovine samples.

#### **3.3.6. Evaluation of HABPs in bovine spermatozoa before and after capacitation**

Motile bovine spermatozoa were recovered from 90% Percoll as described above and washed with Sp-TALP media. To induce capacitation, pelleted spermatozoa ( $2 \times 10^6$ ) were incubated in 1mL Sp-TALP media supplemented with 25 mM

NaHCO<sub>3</sub>, 2.0 mM CaCl<sub>2</sub> and 10 mg/mL BSA (pH=7.3) at 37°C and 5% CO<sub>2</sub> for 3 hour. Capacitated spermatozoa were recovered by centrifugation at 500 ×g for 10 minutes and washed with PBS (x2). Spermatozoa were then placed on Poly-L-Lysine coated slides and labelled with HA-TRITC and a biotinylated anti-CD44 antibody as described above. Additional slides (two slides per each condition of non-cap, cap, AR and DMSO control) were used to evaluate the efficiency of capacitation using PSA-FITC labelling. Pelleted spermatozoa re-suspended in the buffer supporting capacitation, incubated for 0 h (non-capacitated), were used as a control. As shown in Figure 3.1, 10 different human samples and 8 different bovine samples were used throughout the current chapter.

### **3.3.7. Evaluation of HABPs before and during acrosome reaction**

The AR was induced as described previously in Chapter 2 (Section 2.3.7). Acrosome reacted sperm were then placed on Poly-L-Lysine coated slides and labelled with HA-TRITC and biotinylated anti-CD44 as described above. As mentioned above, 10 human samples and 8 bovine samples were used.

### **3.3.8. FITC-*Pisum Sativum* Agglutinin (PSA) labelling**

PSA-FITC labelling was performed to evaluate the acrosome status in human and bovine sperm during capacitation and the AR. Ten (10) µL aliquots of non-capacitated, capacitated and acrosome reacted spermatozoa were washed with 200 µL PBS and spermatozoa were placed on Poly-L-Lysine slides. The slides were air-dried and labelled with PSA-FITC was performed as discussed previously (Chapter 2). Non-capacitated sperm (incubated in the capacitation buffer for 0h) and capacitated sperm incubated with DMSO only were used as controls. After labelling, the slides were examined immediately with a Leica LEITZ DMRB fluorescence microscope. The microscope was equipped with FITC, TRITC and DAPI filters with excitation/emission filter 495 nm/520 nm, 541 nm/572 nm and 358 nm/461 nm, respectively. SmartCapture 3 software was used to image the slides.

### **3.3.9. Evaluation of HABPs in bovine sperm recovered from 90% and 45% fractions**

The purpose of doing this experiment was to check whether or not the distribution of HABPs changes in high quality (recovered from 90% fractions) and low quality (recovered from the 45% fractions) spermatozoa. Bovine spermatozoa were prepared as described in Section 3.3.3 and recovered from 90% and 45% layers following washing with PBS (x2) at 300 ×g for 10 minutes. Spermatozoa were then placed on Poly-L-Lysine coated slides and probed with HA-TRITC and biotinylated anti-CD44 as described in Section 3.3.4. Eight (8) different bovine samples were used for this experiment. Figure 3.1 represents a flow diagram of the approach used in the present study.

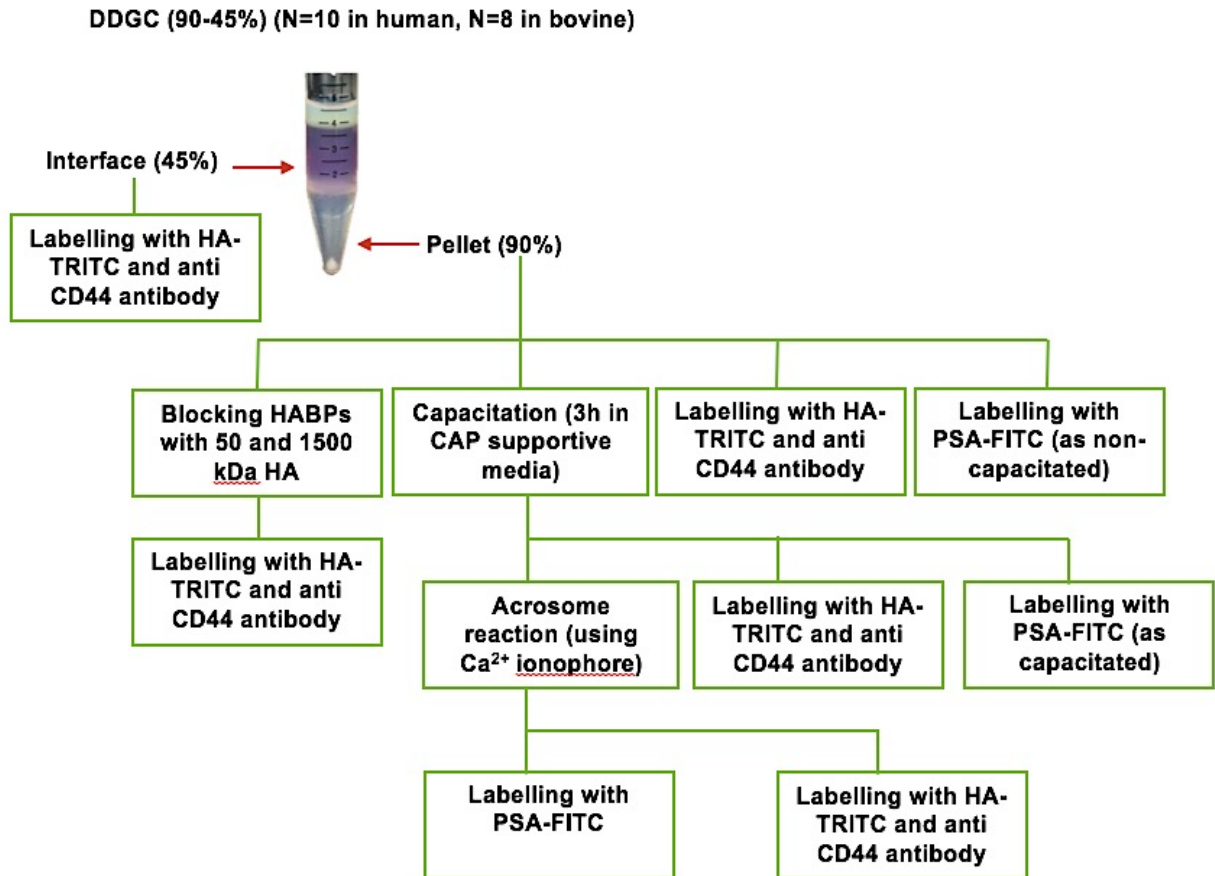


**Figure 3.1. Flow diagram representing the approach used in the current study.**

Human (N=10) and bovine (N=8) sperm were separated using DDGC. Sperm recovered from 45% and 90% fractions were labelled with HA-TRITC and anti-CD44 biotin/streptavidin-FITC. To check the accuracy of the results, HABPs were blocked using 50 and 1500 kDa HA and sperm were labelled with HA-TRITC and anti-CD44 biotin/streptavidin-FITC. The changes in HABPs during capacitation were evaluated by induction of capacitation on pelleted sperm. Capacitated sperm were then labelled with HA-TRITC and anti-CD44 biotin/streptavidin-FITC. The effect of acrosome reaction on distribution of HABPs was evaluated by induction of acrosome reaction on capacitated sperm using  $\text{Ca}^{2+}$  ionophore. Acrosome reacted sperm were then labelled with HA-TRITC and anti-CD44 biotin/streptavidin-FITC. Labelling with PSA-FITC was performed to check the efficiency of capacitation and acrosome reaction.



### **3.4. Results**

#### **3.4.1. Microscopic evaluation of HABPs in human sperm**

To investigate the general presence, capacity and conditions for sperm to recognise and bind HA, spermatozoa were recovered from 90% fractions and incubated with TRITC-labelled HA (a generic detection reagent for HABPs) and an antibody to the common HABP, CD44 and counterstained with DAPI (Figure 3.2). HA-TRITC (red) labelled the acrosome and the tail and more strongly, the neck region (3.2A1, 3.2A4) while an antibody to CD44 (green) decorated the equatorial segment and the acrosome (3.2A2, 3.2A4). On repeating the experiment with samples pre-incubated with excess unlabelled soluble HA as controls, signals for both CD44 (3.2B2, 3.2B4) and HA-TRITC (3.2B1, 3.2B4) were strongly reduced showing that HABPs exist on sperm surface and they were blocked due to the interaction between excess HA and HABPs. Therefore, it confirms that the signals from anti CD44 antibody/streptavidin-FITC and HA-TRITC are specific signals due to the presence of HABPs in sperm. The other control to show the specificity of anti CD44 antibody/streptavidin-FITC is spermatozoa incubated only with streptavidin-FITC. This experiment was performed on 10 human sample (Table 3.1) and 9 of them showed the same pattern. One of them had very low count and as a consequent difficult to judge the results.

To check if blocking of HABPs was not due to masking them with high molecular weigh HA (1500kDa), a smaller HA fragment (50 kDa) was also used. Similar results using 50 kDa were obtained as with 1500 kDa HA (Figure 3.3). This reassures the presence of HABPs in sperm and their specific interaction with HA. Sperm incubation with secondary antibody (streptavidin-FITC) alone as a control to confirm the specificity of the anti CD44 antibody did not elicit a fluorescent signal (Figure 3.2C). The experiment was performed on 10 samples and they all showed very similar labelling patterns.

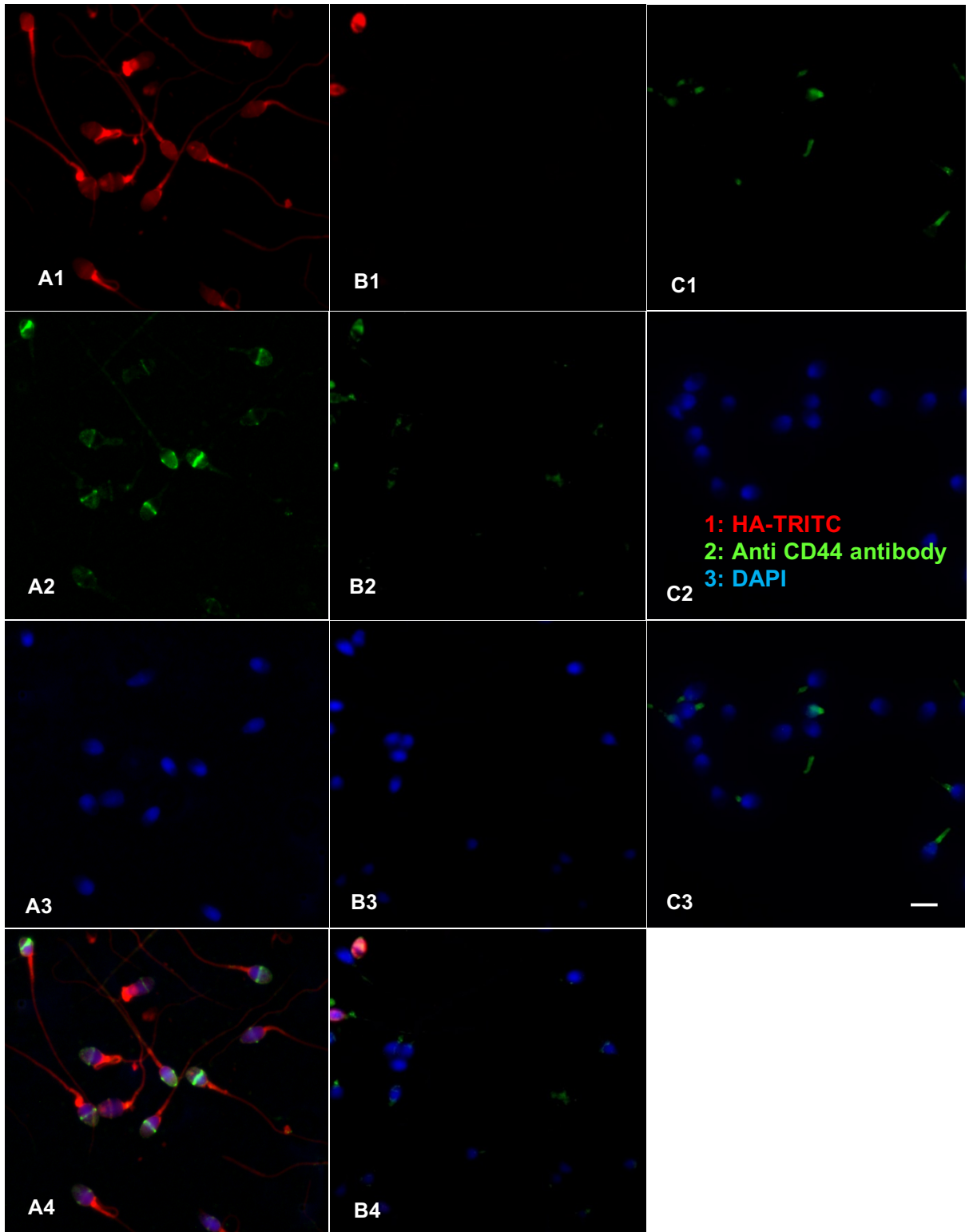


**Figure 3.2. Immunofluorescence images of human sperm probed with reagents targeting HABPs.**

A): Non-capacitated spermatozoa, B): Non-capacitated spermatozoa pre-incubated with excess unlabelled 1500 kDa HA (control), C): Non-capacitated spermatozoa only probed with streptavidin-FITC and DAPI (control).

Panels A4, B4 and C3 show the corresponding merged images. The scale bar is 5  $\mu$ m (A1-C3).

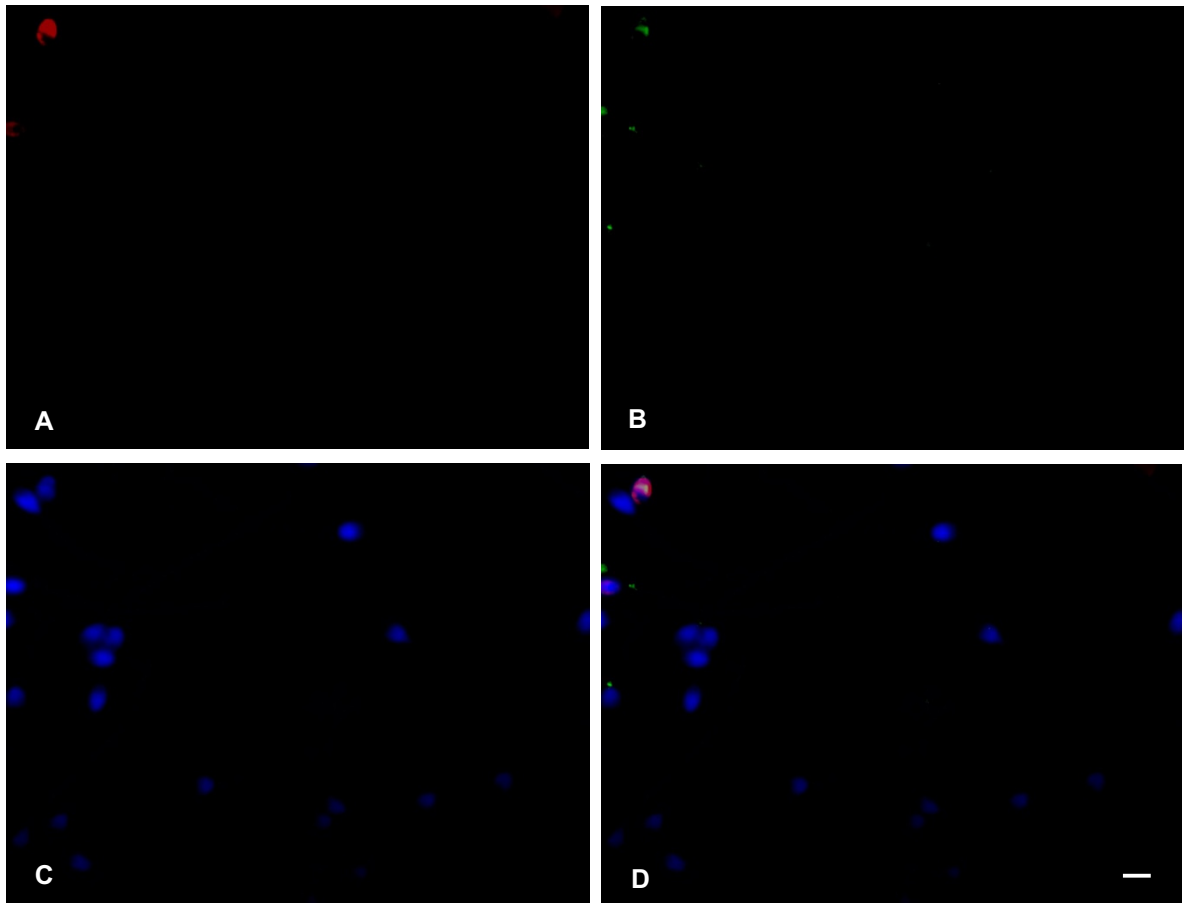


**Figure 3.3. Immunofluorescence images of human sperm (non-capacitated) pre-incubated with HA (50 kDa) and probed with reagents targeting HABPs.**

A): Non-capacitated sperm pre-incubated with excess HA (50 kDa) and probed with HA-TRITC.  
 B): Non-capacitated sperm pre-incubated with excess HA 50 (kDa) and probed with anti-CD44/streptavidin-FITC.  
 C): Non-capacitated sperm pre-incubated with excess HA 50 (kDa) and probed with DAPI.  
 Panel D shows the corresponding merged image. The scale bar is 5  $\mu\text{m}$  (A-D).

PC3 cells were used as positive controls, as they are known to express different HABPs (Figure 3.4). As the figure shows PC3 cells are labelled with HA-TRITC and anti CD44/streptavidin-FITC (Figure 3.4B) confirming the results obtained in human sperm. PC3 cells only probed with streptavidin-FITC did not emit any green fluorescence confirming the specificity of the antibody used for detection of CD44.

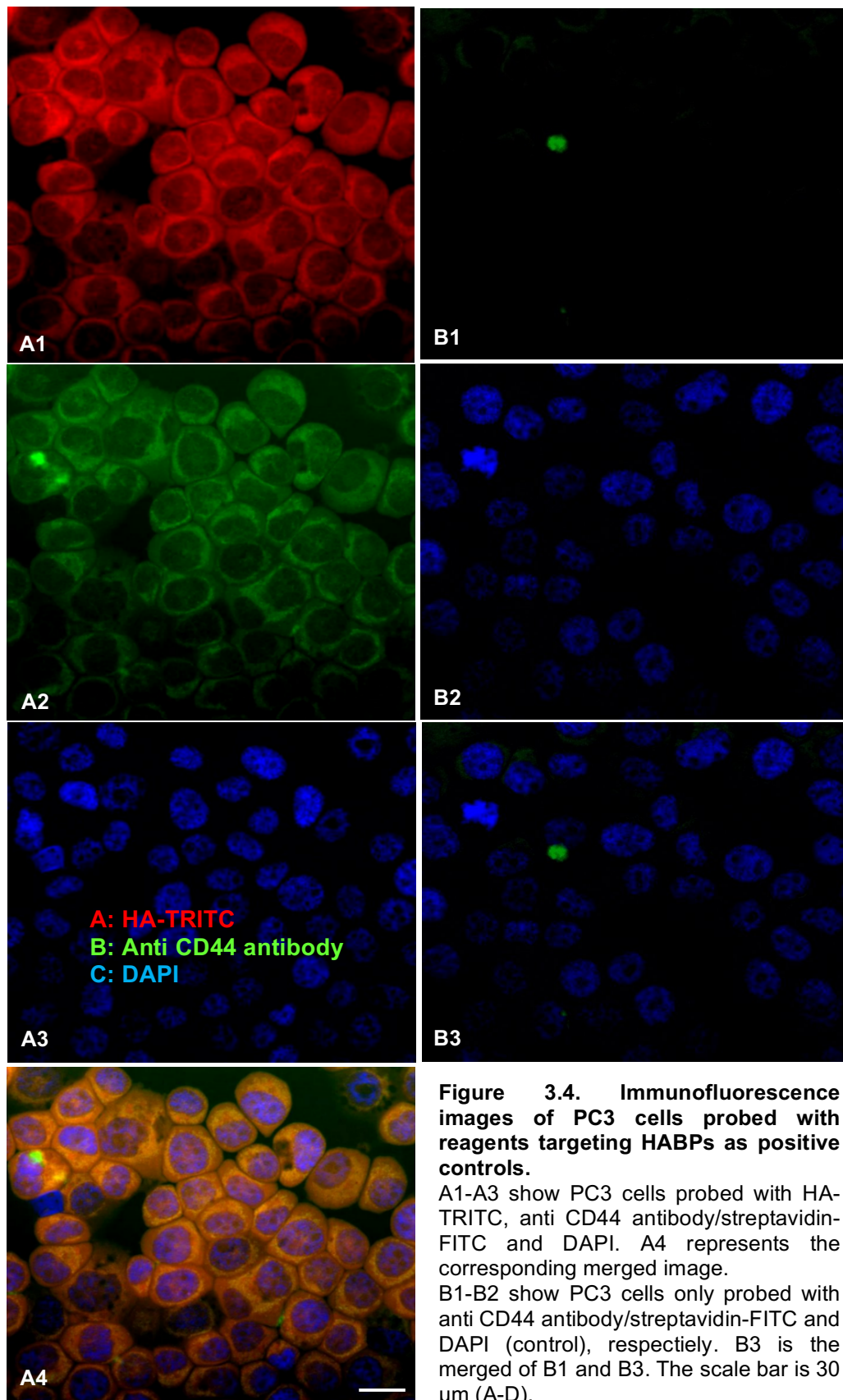


**Figure 3.4. Immunofluorescence images of PC3 cells probed with reagents targeting HABPs as positive controls.**

A1-A3 show PC3 cells probed with HA-TRITC, anti CD44 antibody/streptavidin-FITC and DAPI. A4 represents the corresponding merged image.

B1-B2 show PC3 cells only probed with anti CD44 antibody/streptavidin-FITC and DAPI (control), respectively. B3 is the merged of B1 and B3. The scale bar is 30  $\mu\text{m}$  (A-D).

### **3.4.2. Microscopic evaluation of HABPs in human sperm during capacitation and acrosome reaction**

The changes in HA binding in response to sperm capacitation and the acrosome reaction were evaluated. Non-capacitated sperm were used as controls. As mentioned above (and see Figure 3.5) in non-capacitated sperm, HA-TRITC labelled the acrosome and the tail and (more strongly, the neck region (3.5A1, 3.5A4) while CD44 was located on the equatorial segment and the acrosome (3.53A2, 3.5A4).

During capacitation as Figure 3.5 shows, CD44 acrosomal labelling was slightly reduced and more restricted to the equatorial segment (3.5B2, 3.5B4) and was reduced further during the acrosome reaction (3.5C2, 3.5C4). Labelling with TRITC-tagged HA, however, intensified during capacitation (compare 3.5A1, 3.5A4 with 3.5B1, 3.5B4), particularly on the neck region. These results suggest that capacitation and the acrosome reaction changes the distribution of HABPs. Repeating the experiment on 10 different human sample resulted in very similar labelling pattern as seen in Figure 3.5.

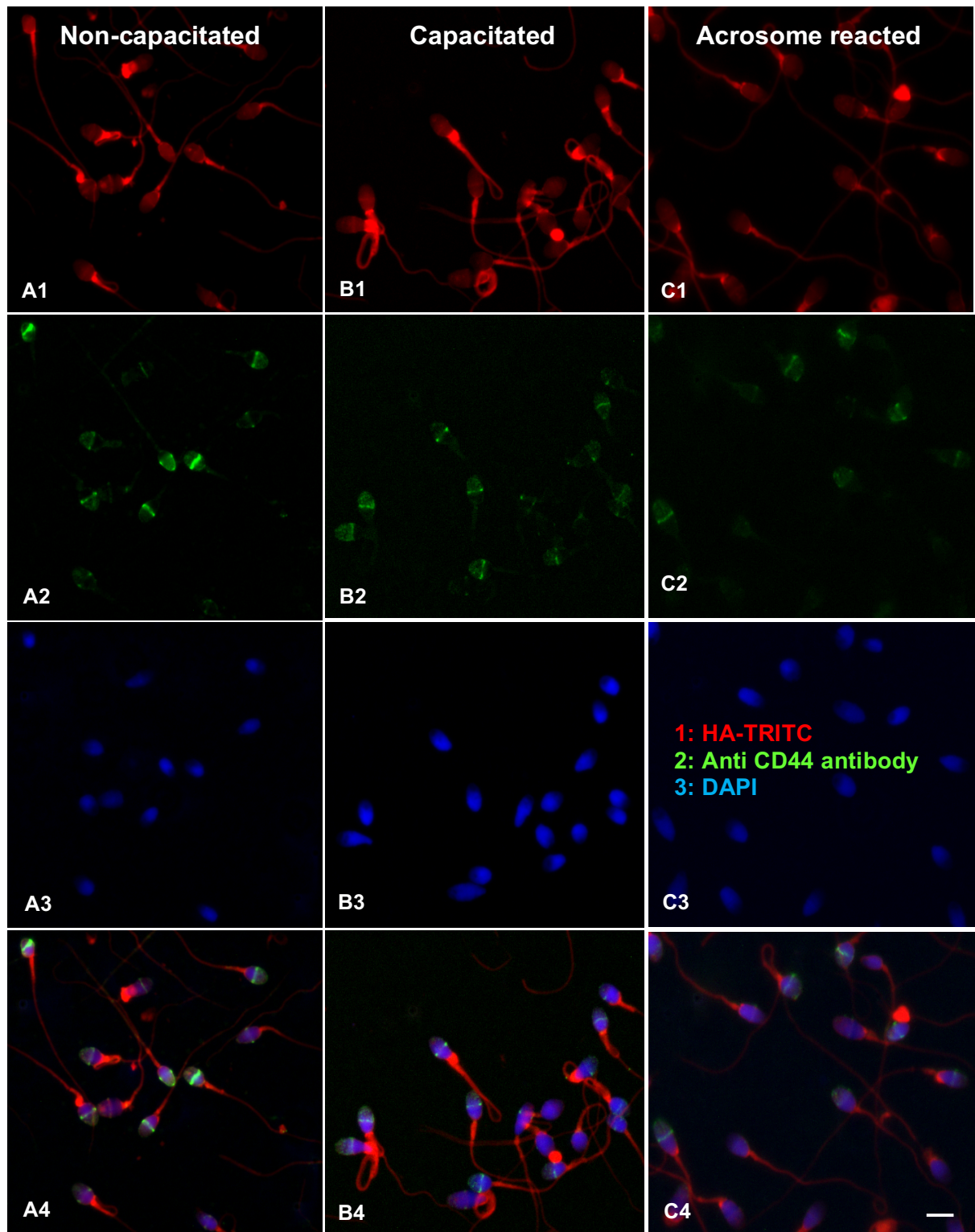


**Figure 3.5. Immunofluorescence images of human sperm probed with reagents targeting HABPs during capacitation and acrosome reaction.**

Panels A4, B4 and C4 show the corresponding merged image. The scale bar is 5  $\mu\text{m}$  (A1-C4).

### 3.4.3. Assessing the efficiency of capacitation and acrosome reaction using PSA-FITC labelling

Human and bovine spermatozoa recovered from 90% fractions were incubated in capacitation supportive media for 0 hour (non-capacitated) and 3 hours (capacitated) and then acrosome reacted using  $\text{Ca}^{2+}$  ionophore prior to labelling with PSA-FITC. Non-capacitated sperm and capacitated sperm incubated with DMSO were used as controls. The reason for using incubated sperm in DMSO (as control) is that  $\text{Ca}^{2+}$  ionophore A23187 stock solution was prepared in DMSO. As seen in Figure 3.6, PSA-FITC signal dramatically reduced after spermatozoa were acrosome reacted (Figure 3.6C, 3.7C) confirming the efficiency of capacitation and acrosome reaction as AR is more efficiently accomplished by capacitated spermatozoa (Figure 3.6 and 3.7). The experiment on 10 human and 8 bovine samples showed very similar labelling patterns with PSA-FITC.

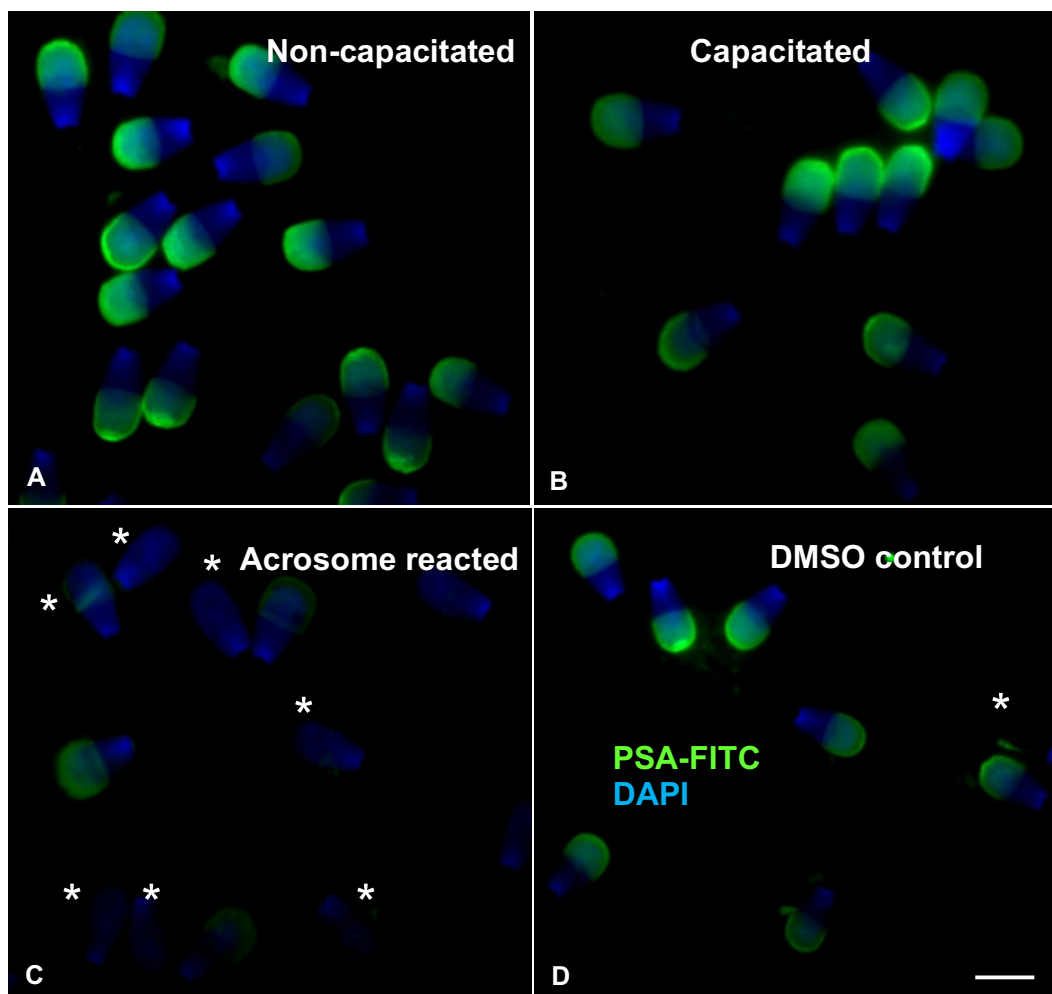


**Figure 3.6. Illustrating the efficiency of capacitation and acrosome reaction in bovine sperm by PSA-FITC labelling.**

Acrosome reacted sperm are indicated by a star '\*'. The scale bar is 20  $\mu\text{m}$  (A-D).

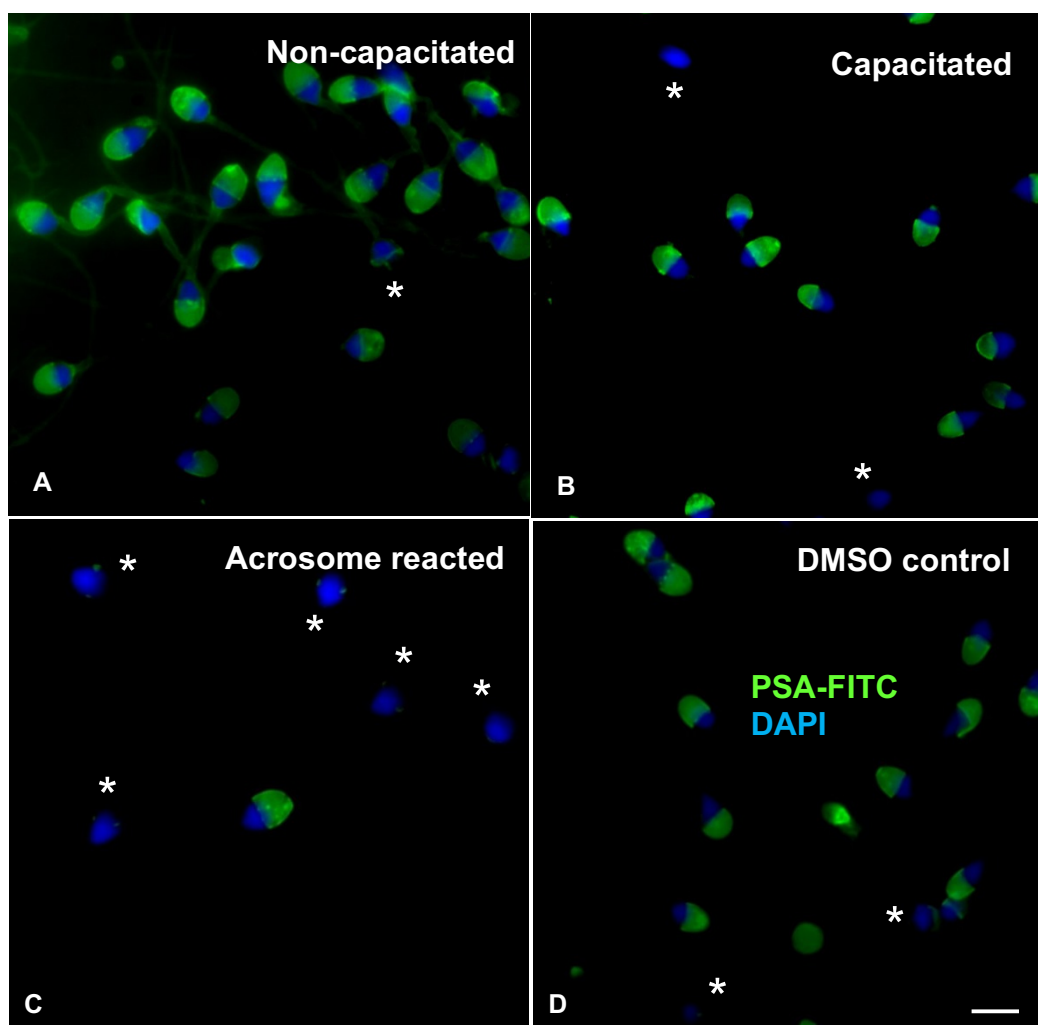


**Figure 3.7. Illustrating the efficiency of capacitation and acrosome reaction in human sperm by PSA-FITC labelling.**

Acrosome reacted sperm are indicated by a star '\*'. The scale bar is 5  $\mu\text{m}$  (A-D).

#### 3.4.4. Microscopic evaluation of HABPs in bovine sperm

To evaluate HABPs, Percoll washed bovine spermatozoa were labelled with HA-TRITC and a biotinylated anti CD44 antibody. As the results show, HABPs labelled with HA-TRITC are located on the sperm plasma membrane, more strongly in the post-acrosomal sheath and the neck of bovine spermatozoa (Figure 3.8A1, 3.6A4) and CD44 is clearly located on the anterior acrosome and post-acrosomal sheath (Figure 3.8A2, 3.8A4). Controls included spermatozoa treated with excess unlabelled HA prior to incubation with HA-TRITC and the anti CD44 antibody. As for human sperm, bovine spermatozoa incubated with streptavidin-FITC in the absence of anti-CD44 antibody were used as negative



controls. As shown in Figure 3.8C these spermatozoa lacked any specific fluorescent signal. It should be noted that the labelling in midpiece (observed in 3.8C2) was non-specific signal. Out of 8 bovine samples, 7 showed similar labelling patterns. Approximately 200 sperm were evaluated per each sample.

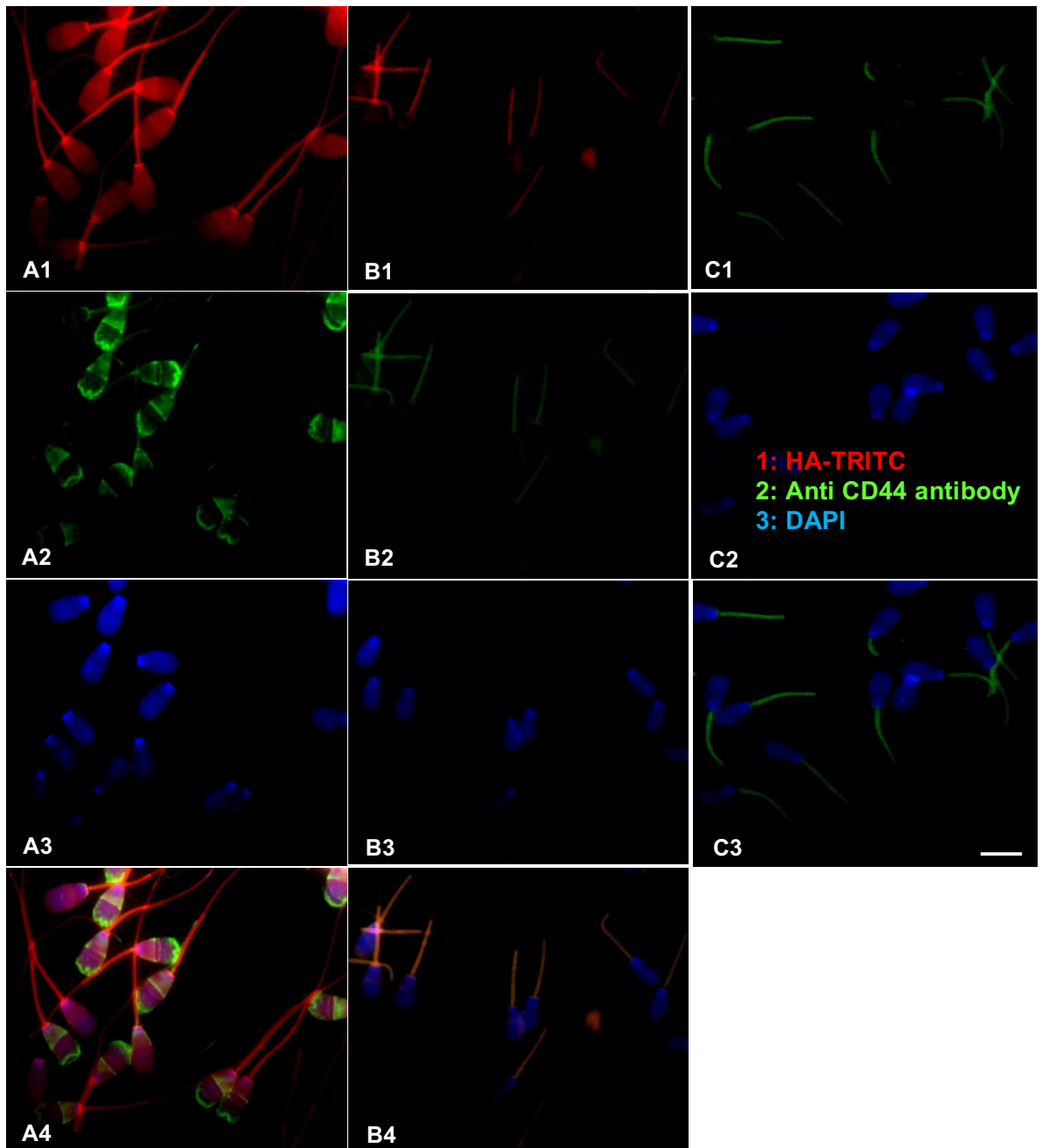


**Figure 3.8. Immunofluorescence images of bovine sperm probed with reagents targeting HABPs.**

A): Non-capacitated spermatozoa, B): Non-capacitated spermatozoa pre-incubated with excess unlabelled HA, C): Non-capacitated spermatozoa only probed with streptavidin-FITC and DAPI (control).

Panels A4, B4 and C3 show the corresponding merged images. The scale bar is 20  $\mu$ m (A1-C3).

#### **3.4.5. Microscopic evaluation of HABPs in bovine sperm during capacitation and acrosome reaction**

Similar to human sperm, the changes in distribution of HABPs during capacitation and acrosome reaction was evaluated in bovine sperm. As the results show, CD44 is clearly located on the anterior acrosome and post-acrosomal sheath of non-capacitated bovine spermatozoa (Figure 3.9A2, 3.9A4). In addition, the presence of CD44 becomes more restricted to post-acrosomal sheath in capacitated spermatozoa (Figure 3.9B2, 3.9B4) and is essentially reduced during the acrosome reaction (Figure 3.9C2, 3.9C4). HA-TRITC strongly labelled the sperm plasma membrane and the post-acrosomal sheath of non-capacitated sperm (Figure 3.9A1, 3.9A4). HA-TRITC labelling was most intense on the plasma membrane of capacitated spermatozoa (Figure 3.9B1, 3.9B4) and was particularly strong on acrosome reacted sperm (Figure 3.9C1, 3.9C4). These results suggest that HABPs (detected by HA-TRITC) additional to CD44 are located on the plasma and sub-acrosomal membranes and are only accessible to labelling by HA-TRITC during the acrosome reaction when these membranes fuse. This experiment was performed on 8 bovine samples and 7 showed similar results as shown in Figure 3.9.

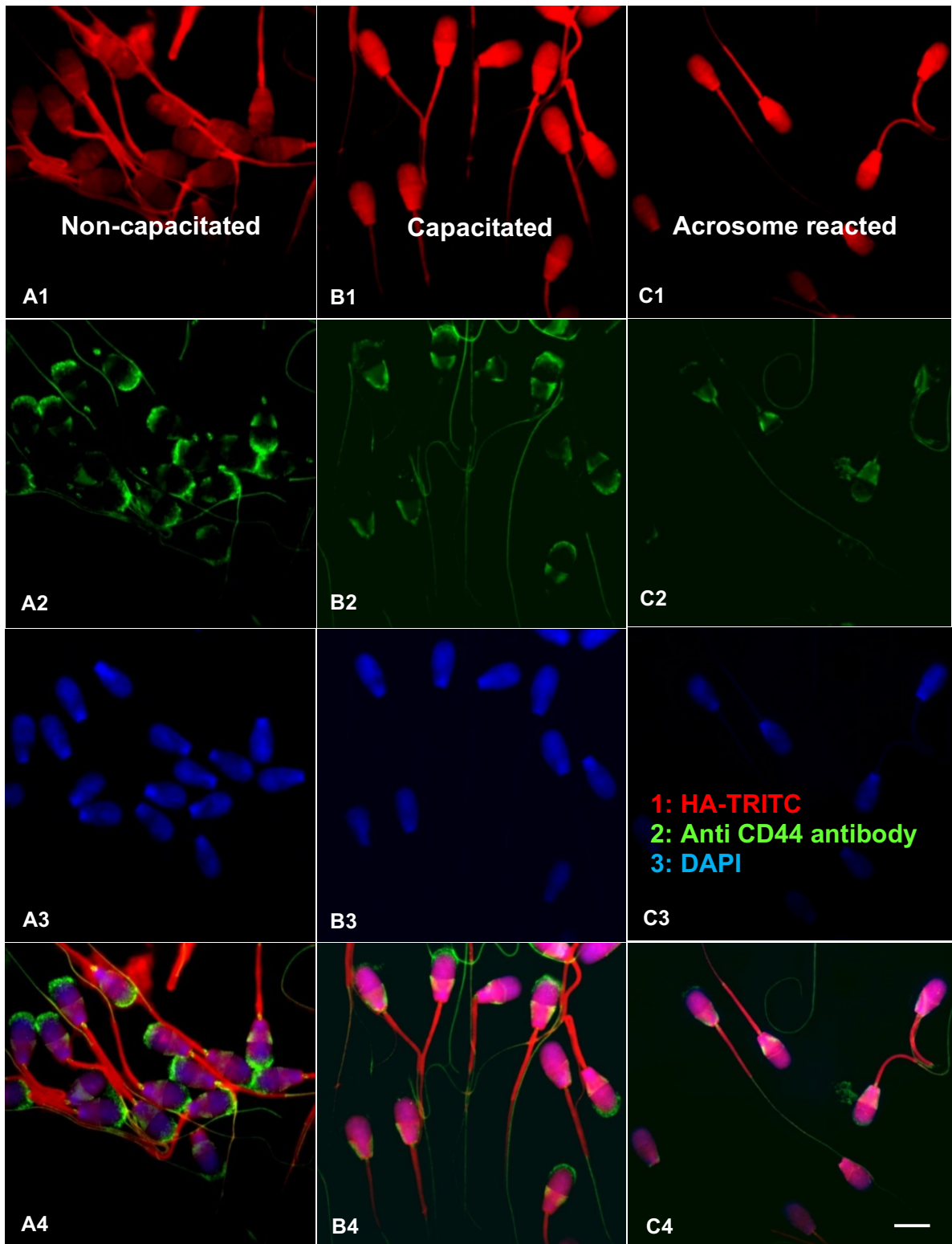


**Figure 3.9. Immunofluorescence images of bovine sperm probed with reagents targeting HABPs during capacitation and acrosome reaction.** Panels A4, B4 and C4 show the corresponding merged images. The scale bar is 20  $\mu\text{m}$  (A1-C4).

### 3.4.6. Evaluation of HABPs in bovine sperm recovered from 90% and 45% fractions

Bovine sperm of higher quality (recovered from 90% fractions) and lower quality sperm (recovered from 45% fractions) were probed with reagents targeting HABPs. As shown in Figure 3.10, sperm from 90% fractions are more intensely labelled with HA-TRITC (3.10A1, 3.10A2) compared to sperm from 45% fractions (3.10B1, 3.10B2). Regarding CD44, the results show that CD44 is located on the anterior acrosome and post-acrosome of higher quality sperm (3.10A1, 3.10A2) while the labelling in lower quality sperm is weaker, specifically on the anterior acrosome (3.10B1, 3.10B2). This experiment was carried out on 8 bovine samples and 7 showed similar labelling patterns as shown in Figure 3.10. This experiment was also performed on human sperm but it was difficult to interpret the results due to the very bad quality of human sperm recovered from 45% and also the smaller size of human sperm compared with bovine sperm.

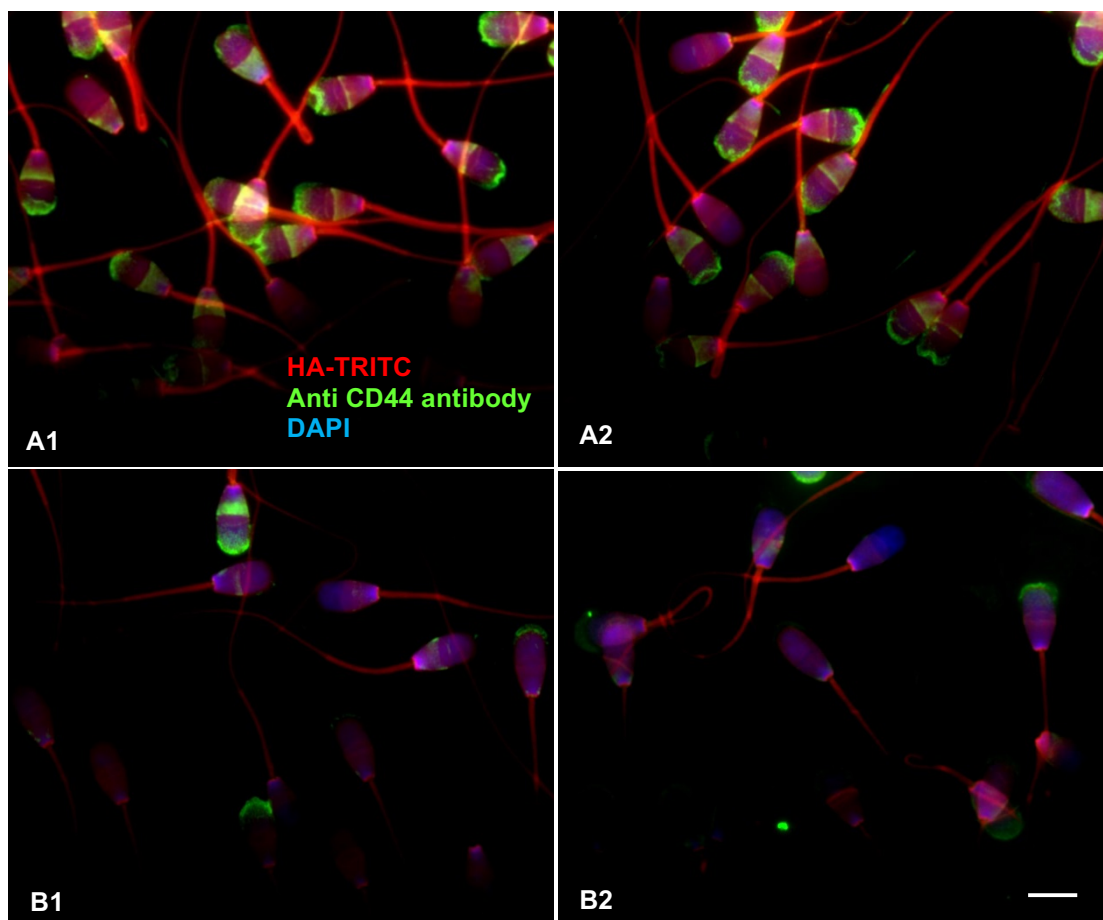


**Figure 3.10. Targeting of HABPs in good and bad quality bovine sperm.**

Sperm were recovered from the 90% (A1, A2) and 45% (B1, B2) fractions and probed with HA-TRITC (red), anti CD44-Biotin/streptavidin-FITC (green) and DAPI. The scale bar is 20  $\mu$ m (A1-B2).

### 3.5. Discussion

Binding of sperm to HA in the female genital tract is probably an important feature of natural fertilisation (Henkel, 2012). Therefore the current study was conducted to monitor and characterise HAPBs on the spermatozoa surface that may be involved in sperm selection by HA binding. Initially, microscopy was used to detect HAPBs including CD44 on human and bovine sperm, which was detected on the acrosome (including equatorial segment) in human sperm as has been reported elsewhere (Bains et al., 2002) and on the anterior acrosome and post-acrosomal sheath of bovine spermatozoa, which was a novel finding. Compared with CD44, however, the signals obtained with a fluorescently tagged probe for generic HA binding (HA-TRITC), appeared to be more widely distributed over the sperm surface with some localised areas of high intensity, particularly in the neck region of human sperm and in the acrosome and the neck of bovine sperm. In this regard, signals for CD44 and HAPBs in general were both substantially quenched by incubating sperm with excess HA (1500 kDa) beforehand. These results confirm previous reports that HAPBs (CD44 amongst them) are present on human and bovine sperm (Cherr et al., 2001; Kornovski et al., 1994; Bains et al., 2002; Kim et al., 2008; Martin-Deleon, 2011; Ranganathan et al., 1994). Loss of the fluorescence signal was most likely due to competition between molar excess unlabeled high (~1500kDa) or low (~50 kDa) molecular mass HA with TRITC-labelled HA for the same HAPBs. A similar signal reduction was observed with anti CD44 in competition with molar excess unlabeled HA (of both varieties). The failure to completely abolish labelling of HAPBs following incubation with excess HA may reflect the transient interaction of HA with its receptors compared with the stronger and more stable interaction between antibodies and their ligands (Plazinski and Knys-Dzieciuch, 2012). Other background signals may be due to non-specific interaction of small amounts of free TRITC with 'sticky' sperm surfaces.

As discussed, during transit through the female genital tract sperm undergo capacitation, which involves protein tyrosine phosphorylation, hyperactive motility and the dramatic re-distribution of membrane proteins and lipids including the efflux of membrane cholesterol (Liu et al., 2007; Gadella et al., 2008; Leahy and Gadella, 2011b; Zaneveld et al., 1991). Other changes may also affect the

distribution of HABPs in preparation for encountering the descending egg mass (Baldi et al., 2000).

In the current study, striking changes in the labelling of HABPs was observed following incubation under conditions favouring capacitation and following the acrosome reaction. General fluorescence, particularly with HA-TRITC increased during capacitation and the acrosome reaction, suggesting greater accessibility of this detection reagent to its ligands in keeping with the likely redistribution of membrane components (Leahy and Gadella, 2011b). The observed redistribution of HABPs accords with reports showing that cytoplasmically mature and actively motile spermatozoa have completed their plasma membrane remodelling, which probably includes the redistribution of HABPs (Cayli et al., 2003; Huszar et al., 2003; Parmegiani et al., 2010a; Prinosilova et al., 2009; Yagci et al., 2010).

### **3.6. Conclusion**

In conclusion the current study supports the presence of HABPs in human and bovine sperm and their higher expression in good quality sperm compared with poor quality sperm. The findings of the study also support that capacitation and the acrosome reaction alters the presence of sperm HABPs and increases the likelihood of their interaction with and binding to HA.

## **Chapter 4: Using proteomics to investigate dynamic changes in protein expression during capacitation and the acrosome fraction**

### **4.1. Introduction**

Sperm capacitation is associated with the redistribution of and the expression of specific surface proteins enhancing the fertilisation process in mammals and other species (Torabi et al., 2017; Cohen et al., 2007; Bailey, 2010; Nandi et al., 2012; Piehler et al., 2006). The studies regarding the human sperm proteome during capacitation are very few and limited by proteome technology. Most of the previously sperm proteomic studies were based on conventional approaches, i.e. gel-based proteomics. The gel-based technology has a limitation in detecting the proteins of commonly varying concentration. It is also criticised for its reproducibility and drawback in resolving protein size and detecting hydrophobic proteins. Thus, mass spectrometry-based differential proteomics study of sperm is useful in overcoming the gel-based limitations and defining sperm proteome to the next level, which is of physiological and functional importance.

As discussed previously, HABPs may play a role in sperm-zona binding (Ranganathan et al., 1994; Cherr et al., 2001; Huszar et al., 2006). Evidence presented elsewhere in this thesis (Chapter 3) showed that the distribution of HABPs labelled with a generic probe (HA-TRITC) appeared to change during capacitation and acrosome reaction alongside an apparent increase in their overall expression. Evidence for changes in the distribution and localisation of CD44 during capacitation and acrosome reaction was also obtained (see Chapter 3). These experiments suggested that some sperm surface proteins, potentially including HABPs were redistributed by capacitation and the acrosome reaction. Mass spectrometry using isobaric mass tags was therefore used to help identify the proteins giving rise to these changes. The methods used were standardised elsewhere (Oliva laboratory, Barcelona, Spain) as part of collaborative effort (Azpiazu et al., 2014; Amaral et al., 2014b) and employed tandem mass tags (TMT)-labelling coupled with liquid chromatography mass spectrometry (LC-MS/MS).

Isobaric tagging is a high throughput proteomic technique for studying proteins having similar masses and chemical characteristics to the peptides followed by LC-MS/MS (Amaral et al., 2014b; Thompson et al., 2003; Bai et al., 2017). These

TMTs are so named to specify their use in association with tandem mass spectrometry (MS/MS) (Thompson et al., 2003). Most commercially available isobaric mass tag reagents are composed of a mass reporter (tag) with a unique isotopic characteristic such as  $^{13}\text{C}$ . A mass normalizer balances the tag's mass (helps in sample identification) with an amine-reactive NHS-ester group. In general, the TMT labelling procedure includes reduction followed by alkylation of the protein extracts and further protein digestion and labelling with TMT. Depending upon the type of TMT multiplexing (6-plex, 8-plex or 10-plex), it allows simultaneous identification and quantitation of several biological samples (4, 6, 8, 10) in parallel without affecting the identification capabilities (McAlister et al., 2012). Therefore, because of these benefits, in this study, TMT 6-plex was used to study the sperm proteome under different conditions.

Several proteomic studies (using different techniques) have been documented in various mammals including human that have compared proteins associated with sperm capacitation and the AR (Secciani et al., 2009a; Baker et al., 2010b; Dorus et al., 2010; Kwon et al., 2014; Kota et al., 2009; Choi et al., 2008a).

Previously, proteomic studies compared sperm from infertile and fertile normozoospermic men and identified differentially expressed proteins ( $\approx 24$ ) with known involvement in sperm maturation and fertilisation processes (Xu et al., 2012). Proteomic studies have also reported several proteins that are differentially expressed in globozoospermia, asthenozoospermic and in sperm samples from men with IVF failure (Azpiazu et al., 2014; Amaral et al., 2014b; Liao et al., 2009).

Since sperm are transcriptionally and translationally inactive, sperm functionality depends heavily on cognate proteins and their PTMs (post-translational modification) during the capacitation and fertilisation processes. In depth comparison of sperm mRNAs and proteins, observed only 29% of identified proteins (Wang et al., 2013). This shows that residual RNAs not only participate in translation but may function actively during capacitation and fertilisation. During sperm capacitation, nuclear RNAs are thought to be translated by mitochondrial ribosomes (Gur and Breitbart, 2006).



comparative study of freshly ejaculated and capacitated human normozoospermic samples demonstrated differential expression of specific proteins in the capacitated sperm. The capacitation led to decreases in the level of certain proteins associated with flagellar organisation (TBB2C, ODFP1), metabolic enzymes (ATPA, ASGL1), heat shock proteins (HSP72) and enzymes involved in cell metabolism notably, energy production (Secciani et al., 2009a). In contrast, clusterin (CLUS) and prolactin-inducible protein (PIP) expression were increased following capacitation. A similar study in boar spermatozoa resulted in the identification of 224 proteins of which 10 were differentially expressed along with the increased tyrosine-phosphorylation of proteins (a type of PTM). This study showed that ACRBP (Acrosin-binding protein) expression was increased in association with sperm penetration of the oocyte by releasing acrosin from the acrosome. In another study on porcine sperm, an increase in cytochrome c was observed during sperm capacitation and the acrosome reaction, among 56 differentially expressed proteins (Choi et al., 2008a). Consequently, surface protein profiles of ejaculated and capacitated porcine sperm showed quantitative and qualitative differences having the presence of zona pellucida protein candidates (Zigo et al., 2013). Moreover, the expression of at least 11 different tyrosine phosphoproteins were observed during bovine sperm capacitation, confirming sperm proteins' translational modification role during capacitation (Jagan Mohanarao and Atreja, 2011). This further confirms the role of sperm proteins' PTMs during capacitation. A proteomic approach to investigating proteins and PTMs during capacitation has also been reported in murine spermatozoa (Baker et al., 2010b). Among 52 differentially expressed proteins in this study, 10 and 11 proteins were associated with glycolysis and mitochondrial metabolism respectively.

The role of mitochondrial proteins in capacitation and acrosome reaction has been further appreciated and investigated by various studies. Mitochondrial proteins may regulate capacitation and the acrosome reaction through protein phosphorylation. Depending on the species, several sperm mitochondrial proteins undergo tyrosine phosphorylation during capacitation and the acrosome reaction (Shivaji et al., 2009). Also, mitochondrial rather than cytoplasmic ribosome are thought to translate sperm mRNAs beneficial for the sperm-egg fusion during capacitation including 26 proteins involved in gamete fusion (Zhao

et al., 2009). Along with other previously reported proteins, Mups (Major urinary proteins) presence was confirmed during acrosome and capacitated mouse sperm. Dorus et al., hypothesized that evolutionary pressures induces positive and intense selection for expression of genes involved in sperm-egg fusion and the physical restructuring of the sperm membrane and acrosome to accommodate this feature (Dorus et al., 2010). Analysis of the proteome of mouse sperm at the site of sperm-oocyte fusion revealed 100 proteins that may participate in gamete fusion (Stein et al., 2006a). Moreover, a study of mouse acrosomal matrix also identified 501 proteins and proposed their role in various biological processes crucial during fertilisation (Guyonnet et al., 2012).

Alongside a specific set of capacitation-related proteins, a role for the 26S sperm proteasome during capacitation and fertilisation, targeting ubiquitinated proteins has been proposed (Zimmerman and Sutovsky, 2009; Guyonnet et al., 2012) and the prediction of male fertility status using this subset of sperm capacitation-associated proteins has been proposed (Rahman et al., 2017).

In the current study, potential changes in the expression of known HABPs, including CD44 and RHAMM were also investigated. As explained in Chapter 1, HABPs can be divided into three different categories, which include those containing a Link module, a BX7B motif, a covalent bond or combinations thereof (Yang et al., 1994; Day and Prestwich, 2002; Amemiya et al., 2005). Therefore, the presence of the Link module and BX7B motif were evaluated in proteins obtained from pre-capacitated, capacitated and acrosome reacted sperm.

#### **4.2. Hypothesis and objectives**

The working hypothesis is that different proteins become up-regulated and down-regulated during sperm maturation where sperm undergoes capacitation and acrosome reaction. Therefore, the main goal of the current chapter is as follows:

- To investigate qualitative and quantitative changes in the human sperm proteome including HABPs during capacitation and the acrosome reaction.

### **4.3. Material and methods**

#### **4.3.1. Reagents used**

F-10 Ham nutrient mixture 10x was purchased from Biological Industries. Sodium bicarbonate was obtained from Merck. Sodium dodecyl sulphate (SDS), Phenylmethylsulfonyl fluoride (PMSF) and anhydrous acetonitrile were supplied by Sigma-Aldrich™. CryoSperm™ was obtained from Origio. Vectashield (mounting medium for fluorescence with DAPI) was purchased from Vector Laboratories. Pierce™ Reducing Agent Compatible BCA Protein Assay Kit, TMTsixplex™ Isobaric Label Reagent Set, TEAB (triethyl ammonium bicarbonate) and Pierce C18 Spin Columns were purchased from Thermo Scientific.

#### **4.3.2. Sample acquisition, processing and analysis**

Four human semen samples were obtained from normozoospermic (according to WHO, 2010) patients by masturbation at the Assisted Reproduction Unit of the Hospital Clinic, Barcelona, Spain after a minimum of 3 days abstinence (Castillo et al., 2014). All semen samples were processed and used according to the ethical and Internal Review Board guidelines of the Hospital Clinic, Barcelona, Spain. The experiments were carried out in the context of the collection of samples entitled “Proteòmica i Genòmica de l’Espermatozoide (Proteomics and Genomics of the spermatozoa)” approved by the research committee of the Hospital Clinic from Barcelona, Spain, on November 22, 2012”.

Prior to processing, all samples were liquefied for at least 30 min at 37°C. After liquefaction, samples were checked for volume, pH, sperm concentration and sperm morphology. Potential round cell contamination of processed samples was minimised by centrifugation on a Percoll cushion (Section 4.3.2.1, 400 x g) (WHO, 2010). Table 4.1 (Section 4.4.1) represents the initial spermogram of the four ejaculates used in the current chapter.

#### **4.3.2.1. Sperm processing**

For these experiments, a 60% Percoll cushion containing HEPES-buffered Ham's F10 medium was prepared and used to separate sperm from any round cells present in the samples. Washing medium consisted of the same buffer supplemented with sodium bicarbonate (0.2% w/v), sodium pyruvate (0.003% w/v) and sodium DL lactate (0.36% v/v). For centrifugation, 1 mL of 60% Percoll was carefully overlaid with 1 mL of semen in a 15 mL polypropylene tube. Sperm were pelleted by centrifugation at 400 x g for 20 minutes (RT). The supernatant was removed and sperm pellets were washed twice for 10 min with 2 mL washing medium at 400 x g.

#### **4.3.2.2. Induction of capacitation**

Approximately  $10 \times 10^6$  sperm were incubated in 1 mL of capacitation medium (see Chapter 2, Section 2.3.6) for 3 hours at 37°C with constant rotation. Sperm motility was checked following capacitation. Aliquots of  $20 \times 10^6$  sperm (established in Oliva's laboratory) were used for protein extraction and the remainder of the sample underwent an ionophore-induced acrosome reaction (see below).

#### **4.3.2.3. Induction of acrosome reaction**

The acrosome reaction was induced as described previously in Chapter 2 (Section 2.3.7). Control samples were incubated with DMSO only (vehicle control) for the same amount of time (De Jonge and Barratt, 2013). Sperm motility was assessed after the acrosome reaction. Aliquots of  $20 \times 10^6$  sperm from each sample was used for protein extraction.

#### **4.3.3. Sperm motility assessment**

The total motility of sperm was checked after each treatment (in Pre-CAP, CAP and AR sperm). Ten (10)  $\mu$ L of each sample was placed onto a glass slide and covered with a coverslip. Total sperm motility was then assessed under Olympus CX41 Upright Microscope. To assess total motility, sperm with progressive motility (active moving) and non-progressive motility (all other patterns of motility) were counted. Additional care and attention was given to avoid double counting of any sperm. At least 200 spermatozoa were checked per slide.

#### **4.3.4. FITC-*Pisum sativum* Agglutinin (PSA) labelling**

PSA-FITC labelling was performed to evaluate the status of the acrosome in Pre-Cap, CAP, AR and control (DMSO) as explained in Chapter 2. The slides were examined immediately using an Olympus BX50 fluorescent microscope equipped FITC and DAPI filters with excitation/emission wavelengths 495 nm/520 nm and 358 nm/461 nm, respectively. A minimum of 150 sperm from each donor were counted per slide by two different observers.

#### **4.3.5. Sperm protein extraction**

Proteins were extracted by incubating Pre-Cap, CAP and AR spermatozoa ( $20 \times 10^6$  sperm) with 50  $\mu$ L of lysis solution containing 2% SDS (w/v) and 1 mM PMSF dissolved in distilled water for 30 minutes at RT with constant shaking. Lysates were centrifuged at 16000 x g for 10 min at 4°C. The supernatant containing the solubilised proteins were collected and quantified using Pierce™ Reducing Agent Compatible BCA Protein Assay Kit according to manufacturer's instruction (Thermo Scientific). Briefly, 10  $\mu$ L of each protein sample was loaded into a microplate well (Greiner Bio-One, Germany) as duplicates and measured alongside different concentration of BCA as standard (125-2000  $\mu$ g/mL). The absorption was then measured at 595 nm. A standard curve was generated, and protein concentration was calculated based on the standard curve (see Section 6.3.11). As there were four donors contributing to the study, the assay was performed 4 times on proteins extracted from pre-Cap, CAP and AR samples.

#### **4.3.6. Peptide preparing and labelling with TMT isobaric mass tags**

##### **4.3.6.1. Preparing protein extracts and trypsin digestion**

The method for TMT-6-plex labelling was performed according to the manufacturer's instructions (Thermo Scientific, Rockford, IL, USA) with minor modifications. In preparation for TMT labelling, 10  $\mu$ g protein from different fractions (Pre-CAP, CAP and AR) were suspended in 200 mM TEAB (triethyl ammonium bicarbonate; pH 8.5) in order to have a final concentration of 0.50  $\mu$ g/ $\mu$ L in each tube. Protein quantification was repeated to ensure all samples had the same concentration. Three (3)  $\mu$ L of 200 mM TCEP (tris (2-carboxyethyl) phosphine) was added and the sample mixture was incubated for one hour at 55°C.

A working solution of 375 mM iodoacetamide was prepared by dissolving 9 mg iodoacetamide with 132  $\mu$ L of 200mM TEAB. Three (3)  $\mu$ L of 375 mM iodoacetamide was added to each tube and incubated for 30 min in the dark at RT. Six-volumes of pre-chilled acetone (-20°C) was added to each tube and precipitated at -20°C overnight. The samples were centrifuged at 17,500 x g for 10 min at 4°C. The acetone was removed and the pellet was left to dry for 2-3 minutes. Acetone-precipitated proteins were redissolved in 10  $\mu$ L of 200 mM TEAB. Trypsin was added to each tube at a 1:20 protease-to-protein ratio and the mixture was incubated overnight at 37°C with constant shaking.

#### **4.3.6.2. Peptide labelling**

As an internal control, equal quantities of peptides from aliquots of samples (from each run) were combined prior to labelling. Experiments included pre-CAP, CAP, AR fractions and control sample in each run. All fractions and controls contained approximately 10  $\mu$ g of digested peptides. Peptides were labelled with the TMT isobaric tags as follows. Before use, TMT label reagents (0.8 mg each) were equilibrated at RT and dissolved in 41  $\mu$ L of anhydrous acetonitrile for 5 minutes at RT. Five (5)  $\mu$ L of prepared reagent were added to the peptides. All 6 TMT tags were used for the first run (tags: 126, 127,128, 129, 130, 131; Figure 4.2) but tag 131 was excluded in the second run. The samples were then incubated for 1 hour at RT and after that, the reaction was quenched by incubating the samples for 15 min with 0.95  $\mu$ L of 8% hydroxylamine. The TMT-labelled samples were combined at equal volumes so that run 1 consisted of 5 samples and 1 control sample (see above), and run 2 consisted of 4 samples and 1 control sample (see above). Labelled peptides were dried in a vacuum centrifuge to near dryness and dissolved in 20  $\mu$ L of 0.5% trifluoroacetic acid (TFA) in 5% acetone before processing with Pierce C18 Spin Columns (Thermo Scientific).

#### **4.3.7. Liquid chromatography–tandem mass spectrometry (LC-MS/MS)**

LC-MS/MS was carried out in the proteomics facility at the University of Barcelona. The proteomics procedures used in the current study consisted of the same standard that has been published by Amarel et al (Amaral et al., 2014b). Labelled peptides were analysed via LC-MS/MS with an LTQ-Orbitrap Velos (Thermo-Fisher Scientific) interfaced with an Eksigent nanoLC ultra 2D plus system (AB Sciex, Switzerland). Peptides were injected onto a Pepmap 100 trap

column (300  $\mu\text{m}$  x 5 mm, 5 $\mu\text{m}$ , 100  $\text{\AA}$ ) at a flow rate of 400 nL/min. For analytical separation, the trap was switched inline to an Acclaim Pepmap C18 column (75  $\mu\text{m}$  x 15 cm, 3  $\mu\text{m}$ , 100  $\text{\AA}$ ) using a 140 min linear gradient from 5 to 30% acetonitrile in 0.1% formic acid at a flow rate of 400 nL/min. MS/MS analyses were performed using an LTQ Orbitrap Velos (ThermoFisher Scientific) with a nanoelectrospray ion source. The LTQ-Orbitrap Velos settings included one 30 000 resolution scan for precursor ions followed by MS2 scans of the 20 most intense precursor ions in positive ion mode (Beck et al., 2011). MS/MS data acquisition was completed using Xcalibur 2.1 (ThermoFisher Scientific). For identification of TMT-labelled peptides, higher energy collisional dissociation (HCD) (Azpiazu et al., 2014) with 40% fixed collision energy (CE) was the fragmentation method.

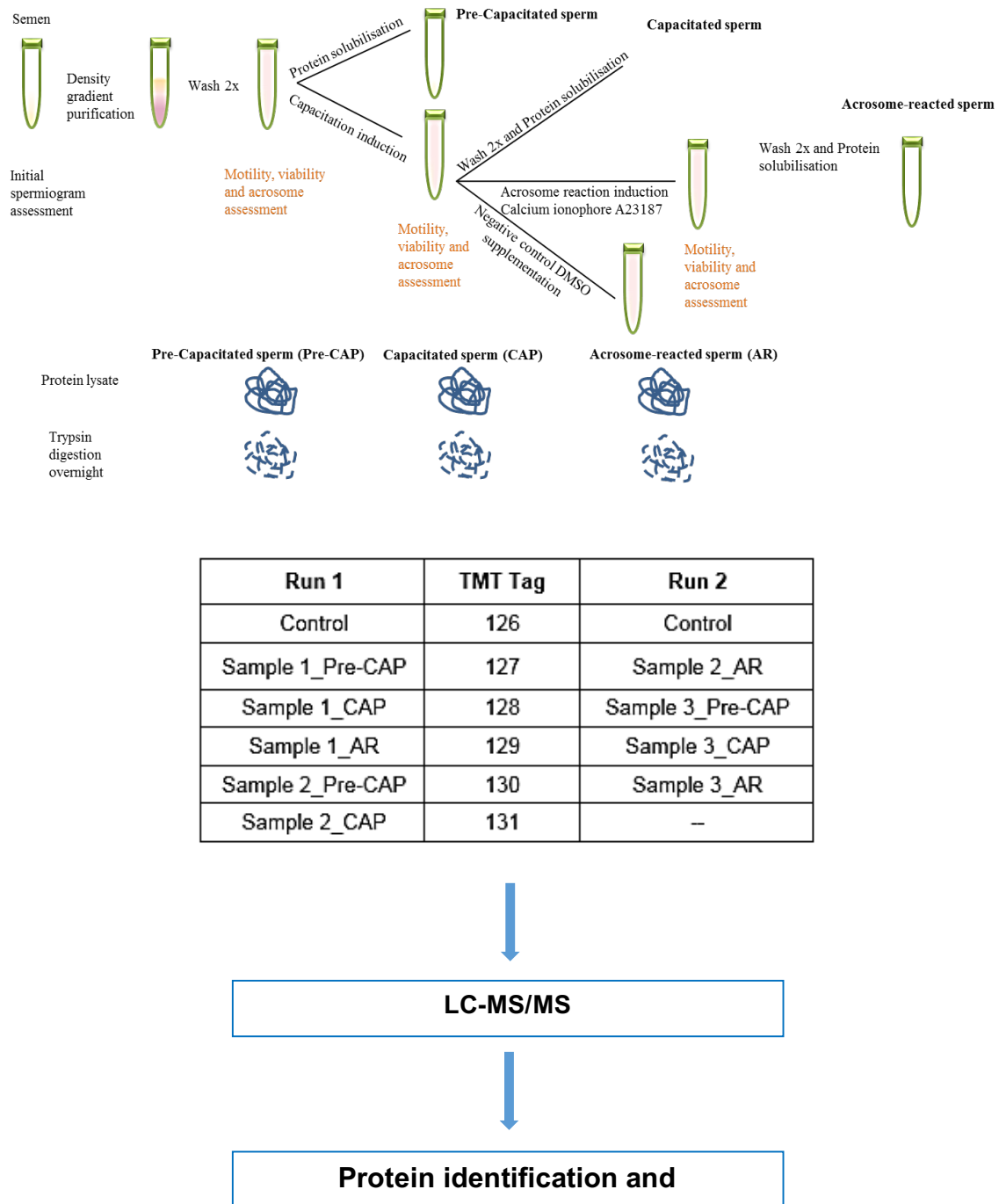


**Figure 4.2. Schematic outlining the approach used in the present study.**

Sperm from three fertile donors were used and analysed individually (one sample was not used due to high number of dead sperm after capacitation and the AR). Sperm from ejaculate were assessed under three sequential conditions: washed or pre-capacitated, capacitated and acrosome reacted. Sperm were solubilized, quantified, alkylated and reduced before enzymatically digested overnight with trypsin. Samples were labelled by TMT-6 plex, pooled into 2 multiplexes and analysed by LC-MS/MS.



#### **4.3.8. Protein identification and quantification**

The protein identification and quantification used in the present study consisted of the same standard that has been published by Bogle et al (Bogle et al., 2017). Proteome Discoverer 1.4 (ThermoFisher Scientific) was used to identify proteins. Database searching included all entries from the *Homo sapiens* UniProtKB/Swiss-Prot database using SEQUEST version 28.0 (Thermo Fisher Scientific). Searches were carried out using the following settings: 2 maximum miss-cleavage for trypsin, TMT-labelled in N-Terminal, lysine(+229.163 Da) and methionine oxidation (+15.995 Da) as dynamic modifications, cysteine carbamidomethylation (+57.021 Da) as static modification, 20 ppm precursor mass tolerance, 0.05 mmu fragment mass tolerance, 5 mmu peak integration tolerance, and most confident centroid peak integration method. A 1% FDR (false discovery rate) and a minimum of one peptide match per protein were the criteria used for protein identification (Amaral et al., 2014b). The dissociated or 'ungrouping' of proteins from their respective families was used during the quantification process in order to avoid the possible ambiguity associated with different isoforms of the same protein (Bogle et al., 2017). Peptide spectral matches (PSMs) were filtered by Proteome Discoverer 1.4 with parameters including Min. Precursor Mass: 300 Da, Max. Precursor Mass: 5000 Da. Reporter ion quantification of HCDMS2 spectra was used, and TMT-6plex was set as quantification method. The quantification values were obtained from the ratio between the reporter ions intensities and the reporter ion intensity from m/z 126.1, and were corrected according to the isotopic purities of the reporter ions provided by the manufacturer (Bogle et al., 2017). The data was then exported to Microsoft Excel, and only those proteins with quantification values were used for further analysis. Proteins were excluded from analyses if protein quantification was based on one spectra and high variability among spectra.

#### **4.3.9. Statistical analysis and data analysis**

Data from four individual samples were used for statistical analyses of PSA-FITC labelling and sperm motility. Due to high numbers of dead sperm after capacitation and the AR, one sample was excluded from TMT labelling and subsequent protein analyses. Therefore, LS-MS/MS was performed on three samples.

All data sets are expressed as mean  $\pm$  SEM. Statistical Analyses were performed using GraphPad Prism 7. One-way ANOVA with repeated measures analysis and Two-way ANOVA were used to analyse changes in total sperm motility and AR amongst groups (Pre-cap, CAP and AR), respectively. One-way ANOVA with repeated measures analysis was also used to identify differentially expressed proteins with similar variance among Pre-CAP, CAP and AR groups. Multiple comparison using One-Way ANOVA (Tukey's test) was carried out to compare individual changes associated only with capacitation (Pre-CAP to CAP) and acrosome reaction (CAP to AR or Pre-CAP to AR). P-value that was  $\leq 0.05$  was considered significant. The data were tested for normal distribution using D'Agostino-Pearson, Shapiro-Wilk and Kolmogorov-Smirnov tests (GraphPad-Prism 6).

#### **4.3.10. Differential protein annotation and Bioinformatics**

For all annotation, proteins that were present at statistically different levels in the fractions or tending towards statistical difference were reported. Functional Annotation Clustering (FAC) of differential proteins was carried out using DAVID Bioinformatics Resources 6.7. FACs were reported using settings at High Classification Stringency, Multiple Linkage Threshold of 0.50 and an ease score of 0.001. All proteins that were statistically different or had a tendency towards significance were used for classification according to subcellular location and biological processes by UniProt Knowledgebase. Enriched or overrepresented pathways were visualised by Gene Ontology Terms.

## 4.4. Results

### 4.4.1. Semen characteristics of donors

Initial spermogram assessments of the four ejaculates used in the current chapter are shown in Table 4.1. All sample are normozoospermic according to WHO 2010 (also see Table 1.1).

**Table 4.1.** Characteristics of ejaculates from four normozoospermic donors.

Sample	Age	Concentration (10 <sup>6</sup> /mL)	Volume (mL)	Total motility (%)	Normal morphology (%)
6436	24	68.2	4.0	83.1	64.4
6437	35	353.5	2.7	96.5	63.3
6438	30	134.8	2.3	75.7	66.8
6439	30	190.9	6.5	88.7	68.7
<b>Mean ± SEM</b>	30 ± 2	187 ± 55	4 ± 1	86 ± 3	66 ± 1

### 4.4.2. Assessment of sperm capacitation and acrosome reaction using PSA-FITC

PSA-FITC labelling was performed to assess the acrosomal status of spermatozoa in washed (Pre-CAP), capacitated (CAP) and acrosome reacted (AR) spermatozoa. As discussed in Chapter 2, based on the PSA-FITC signal, 3 different categories namely intact acrosome, partially intact acrosome and acrosome reacted were considered. Figure 4.3 shows an example of each category and Figure 4.4 illustrates changes in Pre-CAP, CAP and AR sperm based on their PSA-FITC labelling pattern. Approximately 75% of the population of sperm had completely reacted-acrosomes in the AR group which was significantly higher than both Pre-CAP and CAP populations ( $P < 0.0001$ ). This observation demonstrates that an enriched population of acrosome reacted sperm was obtained.

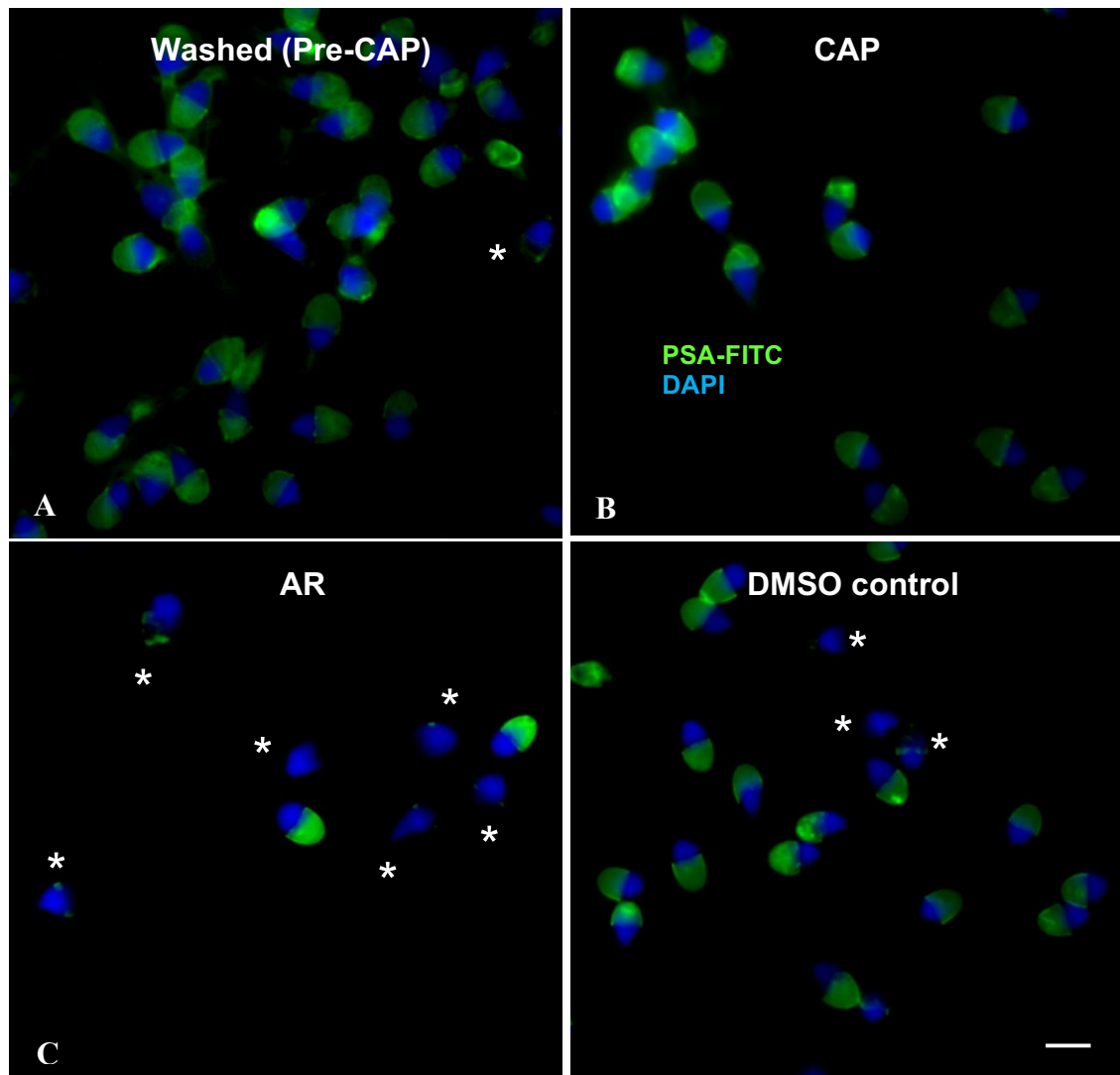


**Figure 4.3. Assessment of acrosome status using PSA-FITC labelling (sample 6438).** Acrosome reaction was induced *in vitro* by calcium ionophore A21387 and visualised by PSA-FITC labelling. Acrosome reacted sperm are indicated by a star '\*'. The scale bar is 5  $\mu$ m.

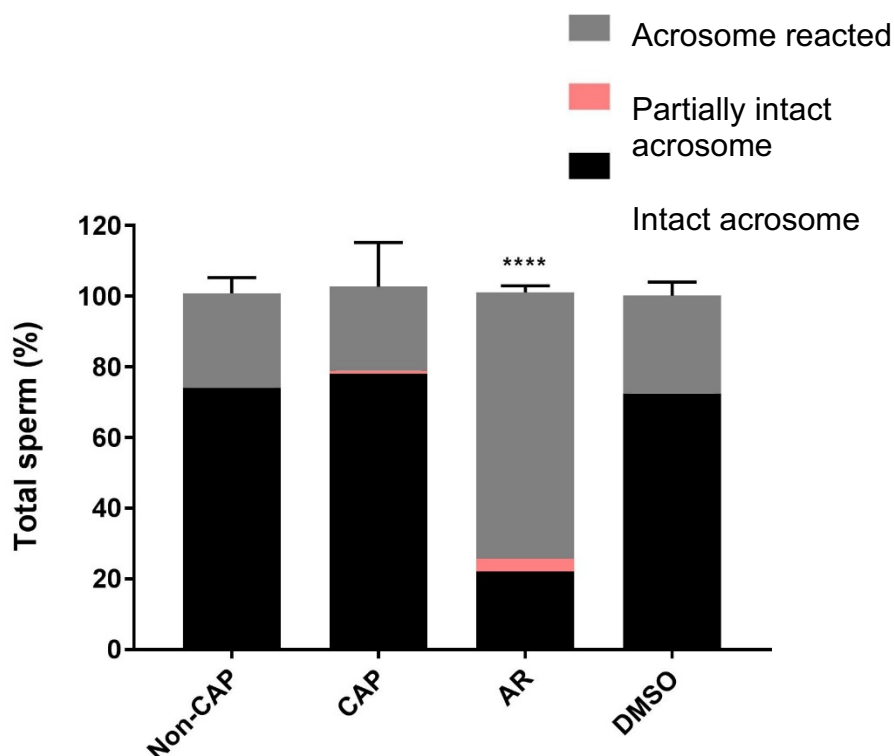


**Figure 4.4. Confirming the efficiency of capacitation by inducing the acrosome reaction followed by PSA-FITC labelling.**

Data was analysed by ANOVA followed by Tukey's post-hoc test. Asterisks (\*\*\*\*) indicate significantly different from all other groups. Data sets are an average of 4 ejaculates from different men ( $P < 0.0001$ ).

#### **4.4.3. Motility assessment of spermatozoa after capacitation and acrosome reaction**

The total motility was assessed in Pre-CAP, CAP and AR sperm to make sure that capacitation and acrosome reaction were performed on motile sperm for highest efficacy. As Figure 4.5 shows, the total sperm motility decreased slightly from washed to the acrosome reacted sperm, but the change was not significantly different ( $P = 0.2$ ).

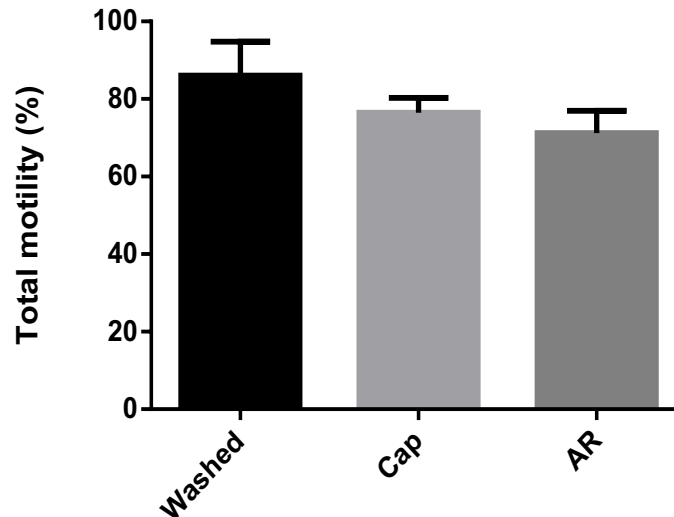


**Figure 4.5. Motility assessment of sperm following capacitation and acrosome reaction.** There is no significant decrease in the motility of sperm before and after acrosome reaction. The data was analysed using One-way ANOVA with repeated measures (N=4).

#### 4.4.4. TMT 6-plex labelling and protein identification

For protein analysis, three of the four ejaculates were used for direct comparison of changes to the same ejaculate under the pre-capacitated, capacitated and acrosome reacted conditions. A total of 1003 proteins were identified, and 571 were used for quantification based on the selection criteria described earlier. Comparisons of the proteomes from Pre-CAP to AR sperm by one-way ANOVA with repeated measures resulted in the identification of 121 proteins (Table 4.2). In agreement with previous studies, several of the differential proteins identified have been characterised in relation to either capacitation or acrosome reaction (Table 4.2). As explained previously, BX7B motif is a characteristic of HABPs. Therefore, the presence of BX7B motif as a binding domain to HA was also investigated (Table 4.2). As shown in Table 4.2, out of 121 differentially regulated proteins, 31 proteins were novel to the current study. The results showed that 30 (14 upregulated, 16 downregulated), 27 (11 upregulated, 16 downregulated) and 46 (21 upregulated, 25 downregulated) proteins were differentially regulated from pre-capacitated to cap, cap to AR and pre-cap to AR, respectively.

The subcellular location of the differentially regulated proteins derived by UniProt demonstrates that the *in vitro* maturation process involves changes in both the

sperm head and tail, which lead to the reorganisation and release of acrosomal content (Figure 4.6A). Approximately 18% of the differential proteins were localised to the mitochondria and flagella/cytoskeleton which reflect the acquisition or change in sperm motility (Figure 4.6A). Correspondingly, approximately 7% of the known proteins have a known role in sperm motility (Figure 4.6B). Throughout sperm maturation, a majority of the identified proteins play a role in energy production and cell metabolism (17%; Figure 4.6B).

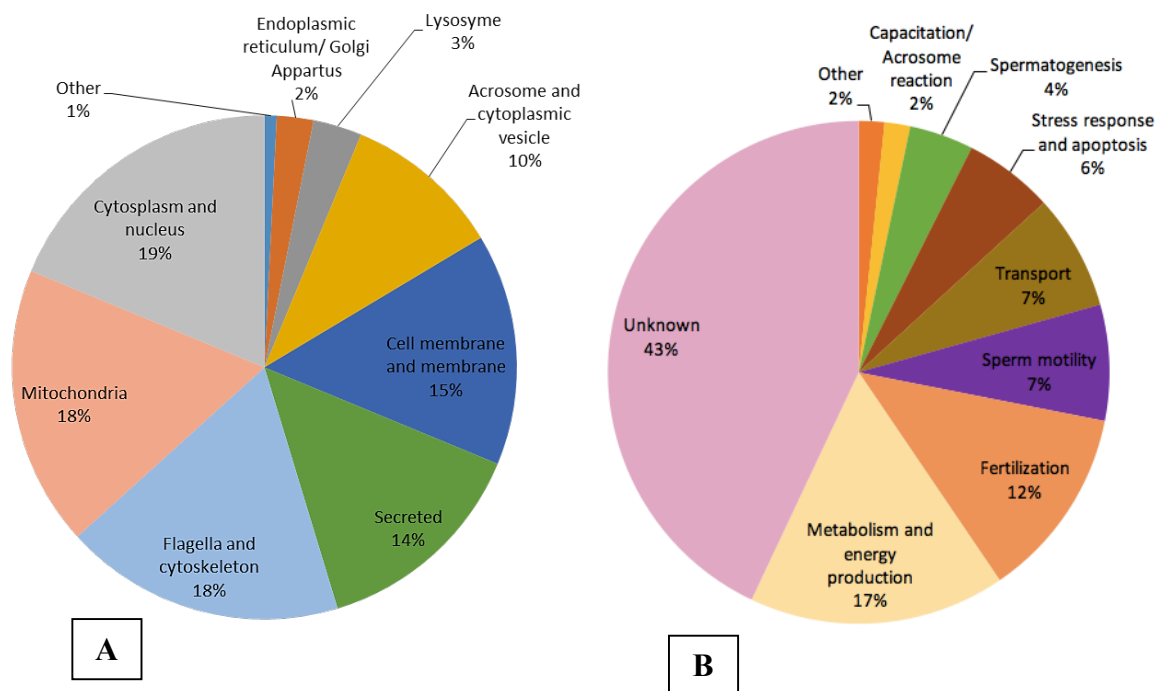


**Figure 4.6.** Classification of the differentially regulated proteins identified by One-Way ANOVA with repeated measures according to their subcellular localisation (A) and main cellular function (B) using the information available at the UniportKB/Swiss-Prot website.

Several proteins involved in the electron transport chain and ATP production via oxidative phosphorylation through complexes III -V were identified. These include ATP synthase subunit alpha (ATP5A1), ATP synthase subunit delta (ATP5D), ATP synthase subunit g (ATP5L), ATP synthase subunit d (ATP5H) of Complex V, cytochrome c oxidase subunit 2 (MT-CO2) and subunit 7A2 (COX7A2) of complex IV; and cytochrome b-c1 complex 7 (UQCRB) of complex III. These results were further confirmed with DAVID and Gene Ontology Knowledge bases (Table 4.2). Functional Annotation Clustering Analysis identified 9 clusters with an enrichment score greater than 3.0. Similar to data compiled by UniProt

Knowledgebase, a large proportion of differential proteins were localised to the mitochondria and cytoplasmic vesicle/acrosome. Glucose metabolism, hydrogen transport and oxidative phosphorylation were principal pathways for energy production (Table 4.2).



**Table 4.2.** List of proteins (n=121) detected at significantly different levels by One-Way ANOVA with repeated measure in *in vitro* matured sperm (P-value ≤ 0.05 was considered significant, and 0.05 > P-value ≤ 0.1 were viewed as a tendency to significant).

Accession	Description	Gene name	Pre-CAP ±SEM	CAP ±SEM	AR ±SEM	P-value	Pre-CAP to CAP	CAP to AR	Pre-CAP to AR	Previously cited	No of BX7B
P26436	Acrosomal protein SP-10	<i>ACRV1</i>	1.22±0.019	1.04±0.008	0.73±0.007	0.002	↓ *	↓ ****	↓ **	CAP and AR (Foster et al., 1994)	N/D
P15259	Phosphoglycerate mutase 2	<i>PGAM2, PGAMM</i>	1.06±0.024	1.04±0.019	0.93±0.019	0.002	-	↓ *	↓ **	CAP (Kongmanas et al., 2015)	N/D
Q96KW9	Sperm acrosome-associated protein 7	<i>SPACA7, C13orf28</i>	1.11±0.044	1.09±0.051	0.93±0.059	0.004	-	↓ *	↓ *	AR (Nguyen et al., 2014)	N/D
P39656	Dolichyl-diphosphooligosaccharide--protein glycosyltransferase 48 kDa subunit	<i>DDOST, KIAA0115, OST48</i>	0.96±0.045	1.00±0.034	1.06±0.041	0.004	-	↑ *	↑ *	Present study	1
Q8IXA5	Sperm acrosome membrane-associated protein 3	<i>SPACA3, LYC3, LYZL3, SLLP1, SPRASA</i>	1.09±0.027	1.05±0.030	0.91±0.033	0.006	↓ *	↓ **	↓ *	Fertilisation (Herrero et al., 2005)	N/D
Q8NEB7	Acrosin-binding protein	<i>ACRBP</i>	1.12±0.025	1.08±0.017	0.91±0.020	0.006	-	↓ **	↓ *	CAP (Kongmanas et al., 2015)	2
O00330	Pyruvate dehydrogenase protein X component, mitochondrial	<i>PDHX, PDX1</i>	0.94±0.018	1.00±0.018	1.05±0.025	0.006	-	-	↑ **	*CAP/Motility (Amaral et al., 2014b; Kumar et al., 2006; Baker et al., 2010a)	1







P07900	Heat shock protein HSP 90-alpha	<i>HSP90AA1, SP90A, HSPC1, HSPCA</i>	1.07±0.043	1.04±0.051	0.98±0.046	0.007	-	↓ ***	-	CAP (Baker et al., 2010c; Baker et al., 2006)	3
P07864	L-lactate dehydrogenase C chain	<i>LDHC, LDH3, LDHX</i>	1.02±0.018	1.02±0.014	0.97±0.010	0.008	-	↓ *	-	Motility (Odet et al., 2008)	N/D
Q53QW1	Uncharacterised protein C2orf57	<i>C2orf57</i>	0.94±0.031	0.97±0.024	1.07±0.030	0.008	-	↑ **	↑ *	CAP (Baker et al., 2010c)	N/D
P49755	Transmembrane emp24 domain-containing protein 10	<i>TMED10, TMP21</i>	0.99±0.138	0.99±0.120	1.14±0.146	0.009	-	-	-	Membrane remodelling (Kinoshita and Fujita, 2016)	N/D
O95831	Apoptosis-inducing factor 1, mitochondrial	<i>AIFM1, AIF, PDCD8</i>	0.94±0.016	0.97±0.021	1.01±0.023	0.009	-	↑ *	↑ *	Motility (Amaral et al., 2014b)	2
P67812	Signal peptidase complex catalytic subunit SEC11A	<i>SEC11A, SEC11L1, SPC18, SPCS4A</i>	0.92±0.015	0.99±0.003	1.06±0.019	0.009	-	-	↑ *	Present study	N/D
Q6J272	Protein FAM166A	<i>FAM166A</i>	1.15±0.076	1.06±0.065	0.98±0.073	0.009	↓ *	-	↓ *	Fertilisation (Frapsauce et al., 2014)	N/D
P49913	Cathelicidin antimicrobial peptide	<i>CAMP, CAP18, FALL39</i>	1.27±0.075	0.84±0.017	0.91±0.059	0.009	↓ *	-	↓ **	*Fertilisation (Hammami-Hamza et al., 2001)	N/D
O75969	A-kinase anchor protein 3	<i>AKAP3, AKAP110, SOB1</i>	83±0.039	1.30±0.0940	0.85±0.065	0.010	↑ *	-	↓ **	CAP (Baker et al., 2010c; Li et al., 2011)	2






Q6UW49	Sperm equatorial segment protein 1	<i>SPESP1</i>	1.05 ± 0.036	1.03±0.027	0.96±0.023	0.011	-	↓ *	↓ *	AR (Fujihara et al., 2010; Baker et al., 2010a)	N/D
Q8TEM1	Nuclear pore membrane glycoprotein 210	<i>NUP210, KIAA0906</i>	0.97±0.038	1.03±0.041	1.08±0.039	0.011	↑ *	↑ *	↑ *	Implantation (Ledee et al., 2011)	3
P10323	Acrosin	<i>ACR, ACRS</i>	1.05±0.024	1.04±0.023	0.86±0.008	0.013	-	↓ *	↓ *	AR/ Fertilisation (Yamagata et al., 1998; Adham et al., 1997)	N/D
P02656	Apolipoprotein C-III	<i>APOC3</i>	0.25±0.014	1.11±0.022	1.51±0.141	0.014	↑ **	↑ *	↑ *	*CAP (Kwon et al., 2014)	N/D
Q9UL16	Cilia- and flagella-associated protein 45	<i>CFAP45</i>	0.94±0.018	0.98±0.024	1.03±0.031	0.014	-	-	↑ *	Present study	1
P25705	ATP synthase subunit alpha, mitochondrial	<i>ATP5A1, ATP5A, ATP5AL2, ATPM</i>	0.98±0.003	1.02±0.006	1.05±0.007	0.015	↑ *	-	↑ *	CAP/Motility (Amaral et al., 2014b; Secciani et al., 2009a; Baker et al., 2010a)	3
P30049	ATP synthase subunit delta, mitochondrial	<i>ATP5D</i>	0.91±0.034	0.97±0.019	1.05±0.022	0.017	↑ *	↑ *	↑ *	*CAP (Secciani et al., 2009a)	1
Q9UL15	BAG family molecular chaperone regulator 5	<i>BAG5, KIAA0873</i>	1,02±0,063	0,99±0,067	1,02±0,066	0.018	↓ *	↑ **	-	Present study	2
P21266	Glutathione S-transferase Mu 3	<i>GSTM3, GST5</i>	1.10±0.089	0.95±0.092	0.92±0.075	0.018	↓ *	-	↓ *	CAP/Fertilisation (Petit et al., 2013; Baker et al., 2010a)	

P47756	F-actin-capping protein subunit beta	<i>CAPZB</i>	1.08±0.041	1.01±0.033	1.02±0.044	0.020	↓ *	-	↓ *	*CAP (Brener et al., 2003; Baker et al., 2010a)	N/D
P00403	Cytochrome c oxidase subunit 2	<i>MT-CO2, COII, COXII, MTCO2</i>	0.95±0.036	0.97±0.053	1.05±0.048	0.021	-	↑ *	↑ *	*Motility (Amaral et al., 2014b)	N/D
Q9BUN1	Protein MENT	<i>MENT, C1orf56</i>	1.07±0.003	1.04±0.024	0.96±0.021	0.025	-	-	-	Present study	2
Q71U36	Tubulin alpha-1A chain	<i>TUBA1A, TUBA3</i>	0.94±0.036	1.01±0.017	1.02±0.032	0.026	-	↑ *	-	*CAP (Secciani et al., 2009a)	N/D
Q5JQC9	A-kinase anchor protein 4	<i>AKAP4, AKAP82</i>	0.72±0.034	1.59±0.155	0.77±0.039	0.027	↑ *	-	↓ *	CAP (Secciani et al., 2009a)	2
P19367	Hexokinase-1	<i>HK1</i>	1.04±0.066	1.05±0.068	0.97±0.051	0.028	-	-	-	CAP (Kongmanas et al., 2015)	3
Q8IYK2	Coiled-coil domain-containing protein 105	<i>CCDC105</i>	0.96±0.010	0.96±0.007	1.00±0.006	0.028	-	↑ **	↑ **	Present study	3
Q99623	Prohibitin-2	<i>PHB2, BAP, REA</i>	0.95±0.017	0.99±0.033	1.04±0.019	0.029	-	-	↑ *	Present study	1
O15173	Membrane-associated progesterone receptor component 2	<i>PGRMC2, DG6, PMBP</i>	0.85±0.100	0.99±0.042	1.14±0.105	0.029	-	-	↑ *	Present study	1

Accession	Protein Name	Gene	Value 1	Value 2	Value 3	P-value	Direction	Significance	Other	Source	Count	
Q5BJF6	Outer dense fiber protein 2	<i>ODF2</i>	0.97±0.063	1.11±0.063	0.95±0.039	0.030	↑	**	-	-	CAP/Fertilisation (Secciani et al., 2009a; Petit et al., 2013)	1
A6NM11	Leucine-rich repeat-containing protein 37A2	<i>LRRC37A2</i>	1.02±0.085	0.99±0.064	0.88±0.086	0.030	-	-	↓	*	Present study	4
Q9BZX4	Ropporin-1B	<i>ROPN1B</i>	0.80±0.056	1.29±0.072	0.93±0.096	0.031	↑	**	-	-	*CAP (Zhao et al., 2009; Baker et al., 2010c; Kwon et al., 2014)	N/D
Q8NCR6	Spermatid-specific manchette-related protein 1	<i>SMRP1, C9orf24, CBE1</i>	1.18±0.043	0.93±0.023	0.91±0.088	0.032	↓	*	-	-	Present study	N/D
Q9BS86	Zona pellucida-binding protein 1	<i>ZPBP, ZPBP1</i>	1.05±0.028	1.06±0.029	0.98±0.013	0.032	-	-	-	-	CAP (Kongmanas et al., 2015; Baker et al., 2010a)	1
P04179	Superoxide dismutase [Mn], mitochondrial	<i>SOD2</i>	0.97±0.026	0.98±0.017	1.02±0.029	0.033	-	-	↑	*	CAP (Kwon et al., 2014)	N/D
O75951	Lysozyme-like protein 6	<i>LYZL6, LYC1</i>	1.21±0.094	1.05±0.050	0.81±0.038	0.033	-	-	-	-	Fertilization (Stein et al., 2006a)	N/D
O75964	ATP synthase subunit g, mitochondrial	<i>ATP5L</i>	0.97±0.021	1.02±0.026	1.04±0.017	0.034	-	-	-	-	* CAP/Motility (Amaral et al., 2014b; Secciani et al., 2009a)	N/D

Q9BVK6	Transmembrane emp24 domain-containing protein 9	<i>TMED9, GP25L2</i>	0.96±0.124	0.97±0.120	1.13±0.158	0.035	-	-	-	*Membrane remodelling (Kinoshita and Fujita, 2016)	N/D
Q96QE4	Leucine-rich repeat-containing protein 37B	<i>LRRC37B</i>	1.04±0.017	1.05±0.014	0.96±0.029	0.036	-	-	-	Present study	1
P13987	CD59 glycoprotein	<i>CD59, MIC11, MIN1, MIN2, MIN3, MSK21</i>	1.05±0.033	1.01±0.014	0.88±0.022	0.038	-	-	↓ *	Fertilisation (Fenichel et al., 1994)	N/D
Q15363	Transmembrane emp24 domain-containing protein 2	<i>TMED2, RNP24</i>	0.87±0.050	0.98±0.067	1.04±0.031	0.038	-	-	↑ *	*Membrane remodelling (Kinoshita and Fujita, 2016)	N/D
P62857	40S ribosomal protein S28	<i>RPS28</i>	1.10±0.043	0.90±0.029	0.75±0.044	0.038	↓ *	-	-	Present study	1
P16562	Cysteine-rich secretory protein 2	<i>CRISP2, GAPDL5, TPX1</i>	1.09±0.078	1.04±0.063	0.93±0.088	0.038	-	-	-	Fertilisation (Busso et al., 2007)	N/D
Q9UFH2	Dynein heavy chain 17, axonemal	<i>DNAH17, DNAHL1, DNEL2</i>	0.96±0.006	1.00±0.003	1.01±0.010	0.040	-	-	-	*Motility (Neesen et al., 2001)	5
P54652	Heat shock-related 70 kDa protein 2	<i>HSPA2</i>	1.03±0.055	1.01±0.058	0.96±0.058	0.041	-	↓ *	↓ *	CAP/Motility (Amaral et al., 2014b; Secciani et al., 2009a)	1
P14927	Cytochrome b-c1 complex subunit 7	<i>UQCRB, UQBP</i>	0.98±0.040	1.00±0.039	1.05±0.039	0.041	-	-	↑ *	*CAP (Arcelay et al., 2008)	




Q9P225	Dynein heavy chain 2, axonemal	<i>DNAH2, DNAHC2, DNHD3, KIAA1503</i>	0.84±0.055	0.90±0.077	0.99±0.047	0.042	-	-	-	*Motility (Neesen et al., 2001)	12	
Q8NEP4	Uncharacterized protein C17orf47	<i>C17orf47</i>	1.00±0.035	1.02±0.054	0.93±0.056	0.043	-		*	-	CAP (Chung et al., 2014)	1
P00918	Carbonic anhydrase 2	<i>CA2</i>	1.06±0.015	0.98±0.041	0.97±0.035	0.044	-	-	-	-	*Motility (bicarbonate transport) (Breton, 2001)	1
Q6UW68	Transmembrane protein 205	<i>TMEM205</i>	0.74±0.082	1.01±0.064	1.05±0.009	0.044		*	-	-	Motility (Amaral et al., 2014b)	N/D
P59282	Tubulin polymerization-promoting protein family member 2	<i>TPPP2, C14orf8</i>	1.08±0.052	0.96±0.064	0.88±0.041	0.045	-	-		**	CAP (Kongmanas et al., 2015)	N/D
P52209	6-phosphogluconate dehydrogenase, decarboxylating	<i>PGD, PGDH</i>	1.08±0.018	1.04±0.012	0.97±0.021	0.046	-	-	-	-	CAP/Fertilisation (Cordoba et al., 2008; Urner and Sakkas, 2005)	2
Q15631	Translin	<i>TSN</i>	1.04±0.026	1.01±0.021	0.96±0.007	0.046		*	-	-	Motility (Amaral et al., 2014b)	N/D
Q16891	MICOS complex subunit MIC60	<i>IMMT, HMP, MIC60, MINOS2</i>	0.95±0.020	0.98±0.004	1.04±0.028	0.047	-	-		*	Present study	2
Q9UI46	Dynein intermediate chain 1, axonemal	<i>DNAI1</i>	0.91±0.033	0.98±0.043	0.99±0.049	0.048		*	-	-	*Motility (Hendrickson et al., 2004)	N/D



Q5JRM2	Uncharacterized protein CXorf66	<i>CXorf66</i>	0.99±0.045	0.84±0.013	1.20±0.041	0.048	-	 *	-	Present study	3
Q8N4E7	Ferritin, mitochondrial	<i>FTMT</i>	0.91±0.083	1.03±0.033	1.10±0.050	0.048	-	-	-	CAP/AR (Kwon W-S. et al., 2015)	1
Q96QH8	Sperm acrosome-associated protein 5	<i>SPACA5, LYZL5, SPACA5A, SPACA5B</i>	1.09±0.031	1.04±0.041	0.89±0.056	0.049	-	 *	-	*Fertilization (Herrero et al., 2005; Zheng et al., 2015)	N/D
Q6X784	Zona pellucida-binding protein 2	<i>ZPBP2, ZPBPL</i>	0.99±0.066	1.00±0.084	0.90±0.059	0.049	-	-	 *	Fertilisation (Stein et al., 2006a)	N/D
Q969V4	Tektin-1	<i>TEKT1</i>	1,02±0,018	0,95±0,028	1,00±0,024	0.049	-	-	-	Present study	N/D
Q8TC99	Fibronectin type III domain-containing protein 8	<i>FNDC8</i>	1,04±0,034	0,90±0,049	0,98±0,025	0.05	 *	-	-	Present study	1
Q9NQ60	Equatorin	<i>EQTN, AFAF, C9orf11</i>	1.04±0.041	1.01±0.057	0.92±0.043	0.050	-	-	 *	AR/Fertilisation (Manandhar and Toshimori, 2001; Toshimori et al., 1998)	N/D
P14406	Cytochrome c oxidase subunit 7A2, mitochondrial	<i>COX7A2</i>	0.98±0.015	0.98±0.014	1.07±0.031	0.051	-	-	-	Present study	1
O75947	ATP synthase subunit d, mitochondrial	<i>ATP5H, My032</i>	0.94±0.008	0.97±0.012	1.04±0.015	0.051	-	-	-	* CAP/Motility (Amaral et al., 2014b; Secciani et al., 2009a)	N/D









Q9Y581	Insulin-like peptide INSL6	<i>INSL6, RIF1</i>	1.23±0.013	1.17±0.040	0.90±0.053	0.051	-	-	-	*CAP/AR (Miah et al., 2011; Miah AG. et al., 2008)	1
O60309	Leucine-rich repeat-containing protein 37A3	<i>LRRC37A3</i>	0.94±0.024	0.95±0.021	0.88±0.020	0.052	-	-	-	Present study	5
P07205	Phosphoglycerate kinase 2	<i>PGK2, PGKB</i>	1.04±0.055	0.99±0.060	0.93±0.033	0.054	↓ *	-	-	CAP (Secciani et al., 2009a)	N/D
Q5JQC4	Cancer/testis antigen 47A	<i>CT47A1, CT47A2, CT47A3, CT47A4, C</i>	0.82±0.017	1.15±0.100	1.10±0.088	0.054	-	-	-	Present study	N/D
P20155	Serine protease inhibitor Kazal-type 2	<i>SPINK2</i>	1.08±0.055	1.03±0.030	0.85±0.048	0.054	-	-	-	CAP/AR (Yi et al., 2012; Lin et al., 2008)	N/D
Q99497	Protein deglycase DJ-1	<i>PARK7</i>	1.02±0.013	1.00±0.025	0.94±0.034	0.055	-	↓ *	-	Motility/Infertility (Amaral et al., 2014b; Agarwal et al., 2015; Hosseinifar et al., 2013)	N/D
Q96KX2	F-actin-capping protein subunit alpha-3	<i>CAPZAac3, CAPAA3, GSG3</i>	1.07±0.078	0.93±0.070	0.92±0.036	0.055	-	-	-	*CAP (Brener et al., 2003)	N/D
Q96RQ9	L-amino-acid oxidase	<i>IL4I1, FIG1</i>	1.01±0.022	1.05±0.035	0.97±0.017	0.055	-	-	↓ *	Present study	1
Q6UWU2	Beta-galactosidase-1-like protein	<i>GLB1L</i>	1.07±0.021	1.08±0.013	0.95±0.019	0.055	-	-	-	Fertilisation (Stein et al., 2006a)	N/D

Q9UKF2	Disintegrin and metalloproteinase domain-containing protein 30	<i>ADAM30</i>	1.14±0.054	1.08±0.035	0.94±0.087	0.056	-	-	-	*Fertilisation (Stein et al., 2006a)	2
P04279	Semenogelin-1	<i>SEMG1, SEMG</i>	1.05±0.179	0.87±0.148	0.88±0.122	0.056	-	-	-	CAP (de Lamirande and Lamothe, 2010; de Lamirande et al., 2001)	N/D
Q96FJ2	Dynein light chain 2, cytoplasmic	<i>DYNLL2, DLC2</i>	1.03±0.031	1.05±0.014	0.91±0.027	0.057	-	-	↓ *	*Motility (Porter and Sale, 2000)	N/D
Q6ZU69	Protein FAM205A	<i>FAM205A, C9orf144B</i>	1.08±0.083	0.92±0.054	0.96±0.066	0.057	-	-	↓ *	Present study	2
P42765	3-ketoacyl-CoA thiolase, mitochondrial	<i>ACAA2</i>	0.89±0.017	1.01±0.014	1.11±0.043	0.059	↑ *	-	-	Present study	N/D
P13861	cAMP-dependent protein kinase type II-alpha regulatory subunit	<i>PRKAR2A, PKR2, PRKAR2</i>	1.02±0.006	1.01±0.012	0.98±0.008	0.061	-	-	↓ **	*CAP (Secciani et al., 2009a)	1
Q96M29	Tektin-5	<i>TEKT5</i>	1.25±0.069	0.92±0.030	0.86±0.047	0.061	-	-	-	Motility (Amaral et al., 2014b)	1
P02768	Serum albumin	<i>ALB</i>	0.41±0.033	1.17±0.240	1.24±0.234	0.061	↑ *	-	↑ *	Motility (Amaral et al., 2014b)	2
Q02383	Semenogelin-2	<i>SEMG2</i>	1.20±0.241	0.63±0.176	0.76±0.150	0.062	↓ *	-	-	*CAP (de Lamirande and Lamothe, 2010; de Lamirande et al., 2001)	N/D

O75694	Nuclear pore complex protein Nup155	<i>NUP155, KIAA0791</i>	0.95±0.012	0.95±0.011	1.02±0.029	0.066	-	-	-	Present study	N/D
P98164	Low-density lipoprotein receptor-related protein 2	<i>LRP2</i>	1.12±0.072	1.01±0.069	0.99±0.032	0.067	-	-	-	Present study	4
Q0VFZ6	Coiled-coil domain-containing protein 173	<i>CCDC173, C2orf77</i>	0,96±0,023	0,92±0,010	1,03±0,015	0.068	-	-	 *	*Motility (Schwarz et al., 2017; Inaba, 2011)	1
P17174	Aspartate aminotransferase, cytoplasmic	<i>GOT1</i>	1.03±0.020	1.01±0.025	0.97±0.007	0.069	-	-	-	Motility (Amaral et al., 2014b)	N/D
Q96D96	Voltage-gated hydrogen channel 1	<i>HVCN1</i>	0.87±0.058	1.00±0.085	1.06±0.026	0.070	-	-	-	CAP/AR (Lishko and Kirichok, 2010; Visconti et al., 2011; Buffone et al., 2012)	N/D
Q9UBX1	Cathepsin F	<i>CTSF</i>	1.00±0.019	1.00±0.028	0.92±0.010	0.070	-	-	-	*AR (Tulsiani et al., 1998)	2
P18859	ATP synthase-coupling factor 6, mitochondrial	<i>ATP5J, ATP5A, ATPM</i>	0.95±0.023	1.03±0.016	1.02±0.000	0.070	 *	-	-	CAP/Motility (Amaral et al., 2014b; Secciani et al., 2009a)	N/D
O75952	Calcium-binding tyrosine phosphorylation-regulated protein	<i>CABYR, CBP86, FSP2</i>	1.03±0.050	0.95±0.049	1.00±0.038	0.072	 ***	-	-	CAP (Naaby-Hansen et al., 2002)	N/D
P07195	L-lactate dehydrogenase B chain	<i>LDHB</i>	1.01±0.032	1.02±0.025	0.96±0.032	0.073	-	-	-	*Motility (Odet et al., 2008)	1

P78406	mRNA export factor	<i>RAE1, MRNP41</i>	1.06±0.030	0.99±0.019	0.94±0.029	0.073	-	-	-	Present study	N/D
P63167	Dynein light chain 1, cytoplasmic	<i>DYNLL1, DLC1, DNCL1, DNCLC1, HDLC1</i>	1.09±0.035	1.03±0.009	0.93±0.012	0.074	-	-	-	*Motility (Porter and Sale, 2000)	N/D
P63104	14-3-3 protein zeta/delta	<i>YWHA,</i>	1.05±0.029	1.01±0.034	0.95±0.022	0.076	-	-	-	CAP (Kongmanas et al., 2015)	N/D
Q9Y6A4	Cilia- and flagella-associated protein 20	<i>CFAP20, BUG22, C16orf80</i>	0.94±0.011	1.00±0.011	1.03±0.021	0.076		*	-	Motility (Mendes Maia et al., 2014; Meng et al., 2014)	3
P24752	Acetyl-CoA acetyltransferase, mitochondrial	<i>ACAT1, ACAT, MAT</i>	0.99±0.015	0.99±0.013	1.01±0.020	0.077	-	-	-	Present study	N/D
Q5T5A4	Uncharacterized protein C1orf194	<i>C1orf194</i>	1.01±0.049	1.01±0.032	1.14±0.073	0.077	-	-	-	Motility/Infertility (Amaral et al., 2014b; McReynolds et al., 2014)	1
Q9H1E5	Thioredoxin-related transmembrane protein 4	<i>TMX4, KIAA1162, TXNDC13</i>	0.97±0.057	0.98±0.064	1.06±0.048	0.078	-	-	-	Present study	N/D
Q92820	Gamma-glutamyl hydrolase	<i>GGH</i>	1.08±0.067	1.02±0.035	0.91±0.018	0.079	-		*	Present study	N/D
P31937	3-hydroxyisobutyrate dehydrogenase, mitochondrial	<i>HIBADH</i>	0.99±0.031	1.06±0.005	1.10±0.016	0.080	-	-	-	Motility (Tasi et al., 2013)	N/D

Q7L266	Isoaspartyl peptidase/L-asparaginase	<i>ASRGL1, ALP, CRASH</i>	1.03±0.014	1.04±0.015	1.00±0.014	0.082	-	-	-	CAP (Schulte et al., 2010)	N/D
A4D1T9	Probable inactive serine protease 37	<i>PRSS37, TRYX2</i>	1.06±0.076	1.09±0.037	0.98±0.048	0.086	-	 *	-	Fertilisation (Shen et al., 2013)	N/D
P62829	60S ribosomal protein L23	<i>RPL23</i>	1.03±0.010	0.91±0.028	0.90±0.036	0.087	-	-	-	Present study	2
P06702	Protein S100-A9	<i>S100A9, CAGB, CFAG, MRP14</i>	0.96±0.309	0.94±0.301	0.84±0.270	0.088	-	-	-	Motility (Martinez-Heredia et al., 2008)	N/D
P36873	Serine/threonine-protein phosphatase PP1-gamma catalytic subunit	<i>PPP1CC</i>	1.05±0.037	1.00±0.008	0.95±0.030	0.090	-	-	 *	Fertility (Forgione et al., 2010)	2
P35663	Cylicin-1	<i>CYLC1, CYL, CYL1</i>	1.16±0.094	1.09±0.047	0.98±0.049	0.090	-	 ****	-	Present study	6
P62826	GTP-binding nuclear protein Ran	<i>RAN, ARA24</i>	1.02±0.141	0.95±0.129	0.96±0.129	0.091	-	-	-	Present study	1
Q9BWH2	FUN14 domain-containing protein 2	<i>FUNDC2, HCBP6</i>	0.97±0.071	0.95±0.064	1.01±0.072	0.092	-	-	 *	Present study	N/D
Q8TC56	Protein FAM71B	<i>FAM71B</i>	1.07±0.022	1.01±0.023	1.00±0.017	0.092	 *	-	-	Present study	5
P00441	Superoxide dismutase [Cu-Zn]	<i>SOD1</i>	1.00±0.024	0.96±0.010	0.94±0.007	0.093	-	-	-	Fertilisation (Tsunoda et al., 2012)	N/D

O95757	Heat shock 70 kDa protein 4L	<i>HSPA4L, APG1, OSP94</i>	1.02±0.020	0.98±0.036	0.96±0.018	0.093	-	-		*	*CAP/Motility (Amaral et al., 2014b; Secciani et al., 2009a)	1
Q9UJZ1	Stomatin-like protein 2, mitochondrial	<i>STOML2, SLP2</i>	0.91±0.059	0.94±0.042	1.06±0.022	0.094	-	-	-	-	Present study	N/D
P30041	Peroxiredoxin-6	<i>PRDX6, AOP2, KIAA0106</i>	1.04±0.042	0.99±0.052	0.97±0.043	0.095	-	-	-	-	CAP/Motility (Amaral et al., 2014b; O'Flaherty, 2015)	N/D
P09972	Fructose-bisphosphate aldolase C	<i>ALDOC, ALDC</i>	0.93±0.025	0.96±0.023	1.04±0.058	0.095	-	-	-	-	*Fertilisation (Petit et al., 2013)	N/D
Q86VQ3	Thioredoxin domain-containing protein 2	<i>TXNDC2, SPTRX, SPTRX1</i>	0.99±0.085	0.97±0.076	0.95±0.071	0.098	-	-	-	-	Present study	N/D
P00492	Hypoxanthine-guanine phosphoribosyltransferase	<i>HPRT1, HPRT</i>	1.01±0.032	1.03±0.048	0.98±0.047	0.099	-	-	-	-	Motility (Aliaga and Ren, 2006)	2

Note: citation involves a related member and not the specific protein.

\* (P<0.05), \*\* (P<0.01), \*\*\* (P<0.001), \*\*\*\* (P<0.0001).

N/D: Not Detected.

**Table 4.3.** Functional Annotation Clustering by DAVID of differentially regulated proteins (N=121) involved in CAP and AR analysed by one-way ANOVA with repeated measures.

<b>Annotation Cluster 1</b>		<b>Enrichment score: 7.57</b>				
<b>Category</b>	<b>Term</b>	<b>Identifier</b>	<b>P-Value</b>	<b>Number of proteins</b>	<b>Bonferro ni</b>	<b>FDR</b>
GOTERM_CC_FAT	organelle envelope	GO:0031967	2.08E-08	22	3.95E-06	2.59E-05
GOTERM_CC_FAT	Envelope	GO:0031975	2.20E-08	22	4.18E-06	2.74E-05
GOTERM_CC_FAT	mitochondrial envelope	GO:0005740	4.22E-08	18	8.03E-06	5.25E-05
<b>Annotation Cluster 2</b>		<b>Enrichment score: 6.78</b>				
<b>Category</b>	<b>Term</b>	<b>Identifier</b>	<b>P-Value</b>	<b>Number of proteins</b>	<b>Bonferro ni</b>	<b>FDR</b>
GOTERM_CC_FAT	cytoplasmic membrane-bounded vesicle	GO:0016023	7.99E-08	20	1.52E-05	9.93E-05
GOTERM_CC_FAT	membrane-bounded vesicle	GO:0031988	1.32E-07	20	2.51E-05	1.64E-04
GOTERM_CC_FAT	cytoplasmic vesicle	GO:0031410	1.87E-07	21	3.55E-05	2.32E-04
GOTERM_CC_FAT	Vesicle	GO:0031982	3.70E-07	21	7.03E-05	4.60E-04
<b>Annotation Cluster 3</b>		<b>Enrichment score: 6.33</b>				
<b>Category</b>	<b>Term</b>	<b>Identifier</b>	<b>P-Value</b>	<b>Number of proteins</b>	<b>Bonferro ni</b>	<b>FDR</b>
GOTERM_CC_FAT	mitochondrial envelope	GO:0005740	4.22E-08	18	8.03E-06	5.25E-05
GOTERM_CC_FAT	mitochondrial part	GO:0044429	2.72E-07	20	5.16E-05	3.38E-04
GOTERM_CC_FAT	mitochondrial membrane	GO:0031966	6.46E-07	16	1.23E-04	8.02E-04
GOTERM_CC_FAT	mitochondrial inner membrane	GO:0005743	1.14E-06	14	2.17E-04	0.001418
GOTERM_CC_FAT	organelle inner membrane	GO:0019866	2.55E-06	14	4.85E-04	0.003175
<b>Annotation Cluster 4</b>		<b>Enrichment score: 5.55</b>				
<b>Category</b>	<b>Term</b>	<b>Identifier</b>	<b>P-Value</b>	<b>Number of proteins</b>	<b>Bonferro ni</b>	<b>FDR</b>
GOTERM_BP_FAT	glucose catabolic process	GO:0006007	6.98E-08	8	6.97E-05	1.10E-04
GOTERM_BP_FAT	hexose catabolic process	GO:0019320	2.37E-07	8	2.36E-04	3.74E-04
GOTERM_BP_FAT	monosaccharide catabolic process	GO:0046365	2.89E-07	8	2.88E-04	4.57E-04
GOTERM_BP_FAT	carbohydrate catabolic process	GO:0016052	3.94E-07	9	3.94E-04	6.23E-04
GOTERM_BP_FAT	alcohol catabolic process	GO:0046164	7.19E-07	8	7.17E-04	0.001135

Category	Term	Identifier	P-Value	Number of proteins	Bonferroni	FDR
GOTERM_BP_FAT	cellular carbohydrate catabolic process	GO:0044275	1.00E-06	8	9.97E-04	0.001579
GOTERM_BP_FAT	glucose metabolic process	GO:0006006	5.13E-06	9	0.005111	0.00811
SP_PIR_KEYWORDS	Glycolysis		7.77E-06	6	0.001731	0.009911
GOTERM_BP_FAT	Glycolysis	GO:0006096	1.08E-05	6	0.01076	0.017122
GOTERM_BP_FAT	hexose metabolic process	GO:0019318	2.69E-05	9	0.026511	0.042517
GOTERM_BP_FAT	monosaccharide metabolic process	GO:0005996	7.54E-05	9	0.072467	0.118993
KEGG_PATHWAY	Glycolysis / Gluconeogenesis	hsa00010	1.64E-04	6	0.010626	0.167368
<b>Annotation Cluster 5</b>						
<b>Enrichment score: 4.70</b>						
Category	Term	Identifier	P-Value	Number of proteins	Bonferroni	FDR
GOTERM_MF_FAT	hydrogen ion transmembrane transporter activity	GO:0015078	1.39E-06	8	3.33E-04	0.001797
SP_PIR_KEYWORDS	mitochondrion inner membrane		3.43E-06	10	7.64E-04	0.004375
GOTERM_MF_FAT	monovalent inorganic cation transmembrane transporter activity	GO:0015077	3.69E-06	8	8.82E-04	0.004763
GOTERM_BP_FAT	oxidative phosphorylation	GO:0006119	3.41E-05	7	0.033504	0.053921
GOTERM_MF_FAT	inorganic cation transmembrane transporter activity	GO:0022890	4.24E-05	8	0.010083	0.054678
GOTERM_CC_FAT	mitochondrial membrane part	GO:0044455	7.00E-05	8	0.013213	0.086966
KEGG_PATHWAY	Parkinson's disease	hsa05012	1.11E-04	8	0.007202	0.113265
KEGG_PATHWAY	Oxidative phosphorylation	hsa00190	1.23E-04	8	0.007939	0.124909
<b>Annotation Cluster 6</b>						
<b>Enrichment score: 4.07</b>						
Category	Term	Identifier	P-Value	Number of proteins	Bonferroni	FDR
GOTERM_CC_FAT	mitochondrial proton-transporting ATP synthase complex	GO:0005753	1.46E-05	5	0.002769	0.018135
GOTERM_CC_FAT	proton-transporting ATP synthase complex	GO:0045259	2.23E-05	5	0.004219	0.027653
GOTERM_BP_FAT	proton transport	GO:0015992	3.92E-05	6	0.038408	0.061969
GOTERM_BP_FAT	hydrogen transport	GO:0006818	4.59E-05	6	0.044786	0.072495
GOTERM_BP_FAT	energy coupled proton transport, down electrochemical gradient	GO:0015985	1.12E-04	5	0.105445	0.176206
GOTERM_BP_FAT	ATP synthesis coupled proton transport	GO:0015986	1.12E-04	5	0.105445	0.176206



Category	Term	Identifier	P-Value	Number of proteins	Bonferroni	FDR
SP_PIR_KEYWORDS	Hydrogen ion transport		2.27E-04	5	0.049314	0.288885
GOTERM_BP_FAT	ion transmembrane transport	GO:0034220	2.48E-04	5	0.219236	0.390932
GOTERM_CC_FAT	proton-transporting two-sector ATPase complex	GO:0016469	4.77E-04	5	0.086641	0.591069
<b>Annotation Cluster 7</b>						
<b>Enrichment score: 4.02</b>						
Category	Term	Identifier	P-Value	Number of proteins	Bonferroni	FDR
GOTERM_BP_FAT	multicellular organism reproduction	GO:0032504	4.99E-05	13	0.048556	0.078748
GOTERM_BP_FAT	reproductive process in a multicellular organism	GO:0048609	4.99E-05	13	0.048556	0.078748
GOTERM_BP_FAT	spermatogenesis	GO:0007283	1.32E-04	10	0.123465	0.208352
GOTERM_BP_FAT	male gamete generation	GO:0048232	1.32E-04	10	0.123465	0.208352
GOTERM_BP_FAT	gamete generation	GO:0007276	1.79E-04	11	0.163269	0.281728
<b>Annotation Cluster 8</b>						
<b>Enrichment score: 3.61</b>						
Category	Term	Identifier	P-Value	Number of proteins	Bonferroni	FDR
INTERPRO	Thioredoxin-like	IPR017936	5.97E-05	5	0.013703	0.076603
SP_PIR_KEYWORDS	Redox-active center		1.34E-04	5	0.029496	0.171131
INTERPRO	Thioredoxin fold	IPR012335	3.38E-04	6	0.075081	0.432531
INTERPRO	Thioredoxin, conserved site	IPR017937	4.79E-04	4	0.104827	0.613131
GOTERM_BP_FAT	cell redox homeostasis	GO:0045454	6.52E-04	5	0.478467	1.025042
<b>Annotation Cluster 9</b>						
<b>Enrichment score: 3.18</b>						
Category	Term	Identifier	P-Value	Number of proteins	Bonferroni	FDR
SMART	LYZ1	SM00263	2.73E-04	3	0.007334	0.225615
INTERPRO	Glycoside hydrolase, family 22, lysozyme	IPR000974	7.20E-04	3	0.153288	0.919864
INTERPRO	Glycoside hydrolase, family 22, conserved site	IPR019799	9.56E-04	3	0.198304	1.22003
INTERPRO	Glycoside hydrolase, family 22	IPR001916	9.56E-04	3	0.198304	1.22003

#### **4.4.5. Changes from Pre-Capacitation to Capacitation in sperm**

The multiple comparison using One-Way ANOVA (Tukey's test) was carried out to investigate protein changes and key differentially regulated proteins found between Pre-CAP and CAP groups. From this comparison 30 proteins were detected to be differentially regulated with 14 of them up-regulated in capacitated sperm (Table 4.2). The results showed that A-kinase anchoring proteins (AKAPs) which are involved in activation of several protein kinases were up-regulated during capacitation. It is known that protein phosphorylation and hyper-activation are the most important events during capacitation. In the current study the up-regulation of ROPN1B was also investigated. Changes in AKAPs and ROPN1B are associated with hyper-activation. The up-regulation of other proteins such as serum albumin and apolipoproteins was also reported.

According to Gene Ontology, acrosome related structures and the flagellum had the greatest fold enrichment (Table 4.4). Biological processes associated with this translational process involves calcium ion-dependent exocytosis, fertilisation and energy coupled proton transport amongst others (Table 4.4).

**Table 4.4.** Functional annotation clustering of differentially regulated proteins (N=30) found between Pre-CAP and CAP groups by One-Way ANOVA (Tukey's test).

<b>Annotation Cluster 1</b>		<b>Enrichment Score: 3.66</b>			
<b>Category</b>	<b>Term</b>	<b>Identifier</b>	<b>P-Value</b>	<b>Benjamini</b>	<b>FDR</b>
GOTERM_CC_FAT	secretory granule	GO:0030141	5.94E-07	6.00E-05	6.60E-04
GOTERM_CC_FAT	cytoplasmic membrane-bounded vesicle	GO:0016023	3.33E-04	0.011151	0.369711
GOTERM_CC_FAT	membrane-bounded vesicle	GO:0031988	3.96E-04	0.00995	0.439422
GOTERM_CC_FAT	cytoplasmic vesicle	GO:0031410	7.59E-04	0.010901	0.841226
GOTERM_CC_FAT	Vesicle	GO:0031982	9.50E-04	0.010613	1.051706
GOTERM_CC_FAT	acrosomal vesicle	GO:0001669	0.001985	0.016587	2.185622
<b>Annotation Cluster 2</b>		<b>Enrichment Score: 3.6</b>			
<b>Category</b>	<b>Term</b>	<b>Identifier</b>	<b>P-Value</b>	<b>Benjamini</b>	<b>FDR</b>
GOTERM_CC_FAT	Flagellum	GO:0019861	1.24E-06	6.24E-05	0.001375
GOTERM_BP_FAT	single fertilization	GO:0007338	1.20E-04	0.045032	0.166604
GOTERM_BP_FAT	acrosome reaction	GO:0007340	1.65E-04	0.031105	0.228438
GOTERM_BP_FAT	Fertilization	GO:0009566	2.72E-04	0.034194	0.377007
GOTERM_BP_FAT	calcium ion-dependent exocytosis	GO:0017156	6.26E-04	0.058166	0.863678
GOTERM_BP_FAT	sexual reproduction	GO:0019953	7.11E-04	0.053014	0.980744
GOTERM_CC_FAT	microtubule-based flagellum	GO:0009434	7.66E-04	0.009625	0.848295
GOTERM_CC_FAT	cell projection	GO:0042995	0.001168	0.011734	1.291141
GOTERM_CC_FAT	Cilium	GO:0005929	0.001534	0.014	1.693046
<b>Annotation Cluster 3</b>		<b>Enrichment Score: 2.81</b>			
<b>Category</b>	<b>Term</b>	<b>Identifier</b>	<b>P-Value</b>	<b>Benjamini</b>	<b>FDR</b>
GOTERM_MF_FAT	hydrogen ion transporting ATP synthase activity, rotational mechanism	GO:0046933	2.95E-04	0.029357	0.327524
GOTERM_CC_FAT	mitochondrial proton-transporting ATP synthase complex	GO:0005753	5.20E-04	0.010449	0.576586
GOTERM_MF_FAT	proton-transporting ATPase activity, rotational mechanism	GO:0046961	6.18E-04	0.03072	0.684713
GOTERM_CC_FAT	proton-transporting ATP synthase complex	GO:0045259	6.37E-04	0.01067	0.706121
GOTERM_MF_FAT	cation-transporting ATPase activity	GO:0019829	0.001519	0.049881	1.675902
GOTERM_BP_FAT	energy coupled proton transport, down electrochemical gradient	GO:0015985	0.001897	0.114144	2.597263
GOTERM_BP_FAT	ATP synthesis coupled proton transport	GO:0015986	0.001897	0.114144	2.597263
KEGG_PATHWAY	hsa05016:Huntington's disease		0.002142	0.027492	1.409669
SP_PIR_KEYWORDS	Hydrogen ion transport		0.002372	0.222508	2.629094
GOTERM_BP_FAT	ion transmembrane transport	GO:003422	0.002835	0.14386	3.858115
GOTERM_CC_FAT	proton-transporting two-sector ATPase complex	GO:0016469	0.002925	0.022504	3.205374
GOTERM_BP_FAT	proton transport	GO:0015992	0.00436	0.188741	5.875742
GOTERM_BP_FAT	hydrogen transport	GO:0006818	0.004643	0.179681	6.247026

#### **4.4.6. Changes from capacitation to acrosome reaction**

The multiple comparison using One-Way ANOVA (Tukey's test) was carried out to understand the biochemical changes occurring in the sperm cell as it transitions from capacitation to acquire fertilisation capability during the acrosome reaction. Of the 27 identified differential proteins, 16 were down-regulated in the AR group in comparison to the CAP group (Table 4.2). A decrease in the protein levels of those localised to the acrosome, are indicative of the shedding or reorganisation occurring in that region (Table 4.2). These include Acrosomal protein SP 10 (ACRV1), acrosin (ACR), acrosin binding protein (ACRBP), Sperm acrosome-associated protein 7 (SPACA7), sperm acrosome-associated protein 5 (SPACA5), sperm acrosome membrane associated protein 3 (SPACA5), cylicin-1 (CYLC1) and zona-pellucida -binding protein 2 (ZPBP2). Gene Ontology revealed that cellular components including acrosomal vesicle, secretory granule, plasma membrane amongst others had the greatest fold enrichment (Table 4.5).

**Table 4.5.** Functional annotation clustering of differentially regulated proteins (N=27) found between CAP and AR groups by One-Way ANOVA (Tukey's test).

<b>Annotation Cluster 1</b>	<b>Enrichment Score: 4.43</b>				
<b>Category</b>	<b>Term</b>	<b>Identifier</b>	<b>P-Value</b>	<b>Benjamini</b>	<b>FDR</b>
GOTERM_CC_FAT	acrosomal vesicle	GO:0001669	4.19E-07	3.64E-05	4.53E-04
GOTERM_CC_FAT	secretory granule	GO:0030141	1.14E-05	4.94E-04	0.012275
GOTERM_CC_FAT	cytoplasmic membrane-bounded vesicle	GO:0016023	2.55E-05	7.39E-04	0.027543
GOTERM_CC_FAT	membrane-bounded vesicle	GO:0031988	3.14E-05	6.82E-04	0.033897
GOTERM_CC_FAT	cytoplasmic vesicle	GO:0031410	6.86E-05	0.001194	0.074158
GOTERM_CC_FAT	vesicle	GO:0031982	9.00E-05	0.001304	0.097176
SP_PIR_KEYWORDS	cytoplasmic vesicle		0.003941	0.117549	4.247926
<b>Annotation Cluster 2</b>	<b>Enrichment Score: 2.41</b>				
<b>Category</b>	<b>Term</b>		<b>P-Value</b>	<b>Benjamini</b>	<b>FDR</b>
GOTERM_BP_FAT	sexual reproduction	GO:0019953	0.003353	0.49262	4.583412
GOTERM_BP_FAT	multicellular organism reproduction	GO:0032504	0.00418	0.431113	5.682957
GOTERM_BP_FAT	reproductive process in a multicellular organism	GO:0048609	0.00418	0.431113	5.682957

#### **4.4.7. Changes from Pre-Capacitation to acrosome reaction**

Finally, to obtain a globalised overview of dynamic changes occurring in the sperm cell in preparation for fertilisation, One-Way ANOVA (Tukey's test) was carried out to compare protein changes between Pre-CAP and AR groups (Table 4.2). The results revealed that 46 proteins were differentially regulated in Pre-cap and AR sperm. Twenty-one proteins were found to be upregulated in AR sperm compared to Pre-cap sperm.

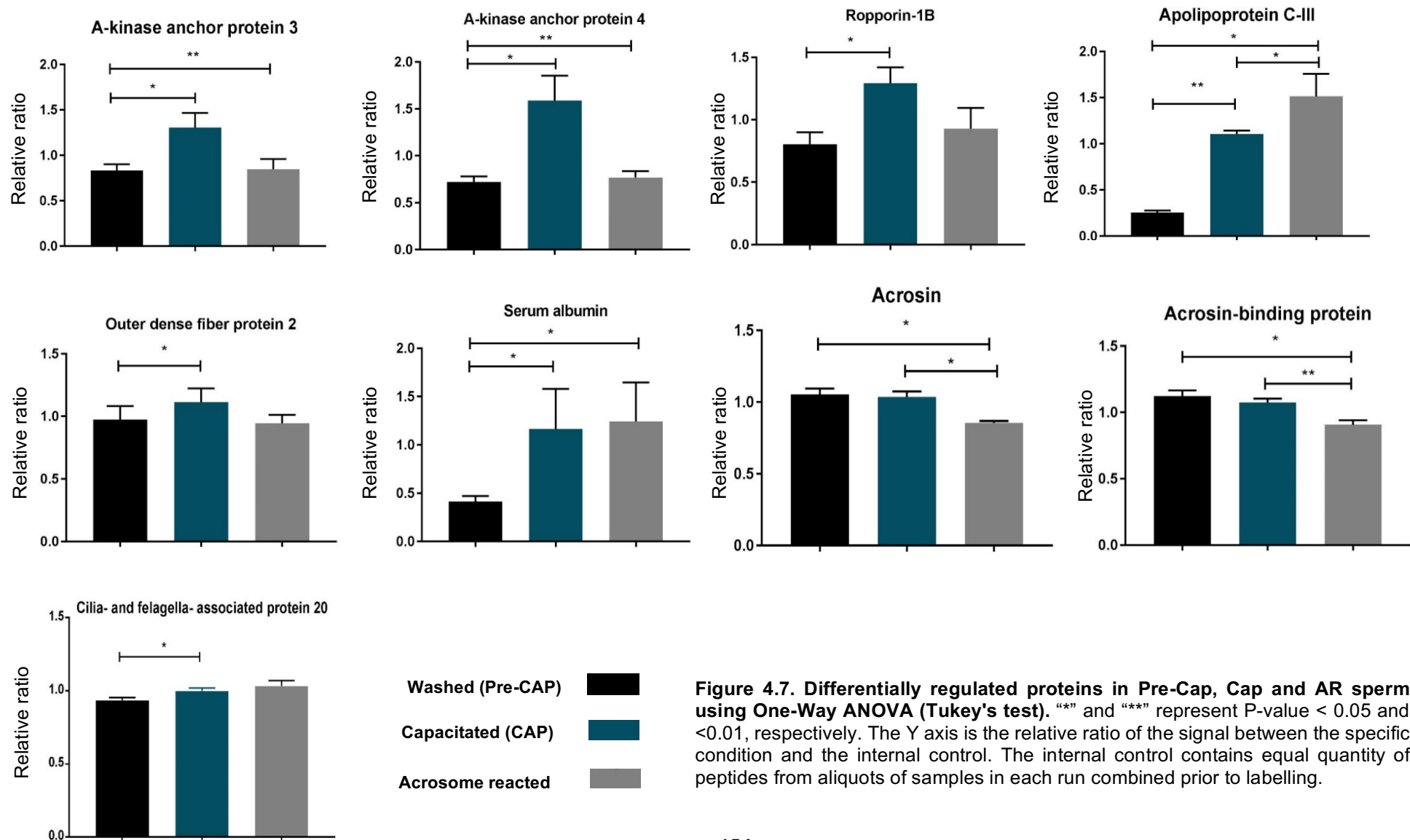
Gene Ontology showed that differentially regulated proteins were localised to the mitochondria, acrosome and secretory granule (Table 4.6). As seen in Table 4.6, energy production is one of the main biological process enriched.

Figure 4.7 shows some of the important differentially regulated proteins during capacitation and acrosome reaction.

The relative ratio in Figure 4.7 represents the ratio of the signal obtained from TMT-taq (127, 128, 129, 130 or 131) in the peptide in any specific condition (pre-CAP, CAP, AR) divided by the signal of the TMT-taq (126) of the peptide in the internal control.

**Table 4.6:** Functional annotation clustering of differentially regulated proteins (N=46) found between Pre-Cap and AR groups by One-Way ANOVA (Tukey's test).

<b>Annotation Cluster 1</b>	<b>Enrichment Score: 5.4</b>				
<b>Category</b>	<b>Term</b>	<b>Identifier</b>	<b>P-Value</b>	<b>Benjamini</b>	<b>FDR</b>
GOTERM_CC_FAT	secretory granule	GO:0030141	2.04E-09	2.64E-07	2.38E-06
GOTERM_CC_FAT	acrosomal vesicle	GO:0001669	7.19E-08	4.64E-06	8.36E-05
SP_PIR_KEYWORDS	cytoplasmic vesicle		1.60E-05	0.002228	0.01891
GOTERM_CC_FAT	cytoplasmic membrane-bounded vesicle	GO:0016023	2.52E-05	0.001084	0.029324
GOTERM_CC_FAT	membrane-bounded vesicle	GO:0031988	3.25E-05	0.001048	0.037807
GOTERM_CC_FAT	cytoplasmic vesicle	GO:0031410	8.44E-05	0.002175	0.098104
GOTERM_CC_FAT	vesicle	GO:0031982	1.17E-04	0.002515	0.136094
<b>Annotation Cluster 2</b>	<b>Enrichment Score: 3.04</b>				
<b>Category</b>	<b>Term</b>		<b>P-Value</b>	<b>Benjamini</b>	<b>FDR</b>
GOTERM_CC_FAT	mitochondrial envelope	GO:0005740	2.02E-04	0.003724	0.235158
GOTERM_CC_FAT	mitochondrion	GO:0005739	2.24E-04	0.003612	0.260606
GOTERM_CC_FAT	mitochondrial part	GO:0044429	2.98E-04	0.004258	0.345654
GOTERM_CC_FAT	organelle envelope	GO:0031967	3.93E-04	0.005057	0.456042
GOTERM_CC_FAT	envelope	GO:0031975	4.02E-04	0.004699	0.465991
GOTERM_BP_FAT	generation of precursor metabolites and energy	GO:0006091	4.07E-04	0.108382	0.594861
SP_PIR_KEYWORDS	mitochondrion		5.26E-04	0.024073	0.617842
SP_PIR_KEYWORDS	oxidative phosphorylation		0.0029	0.096006	3.36483
GOTERM_BP_FAT	energy derivation by oxidation of organic compounds	GO:0015980	0.003184	0.301697	4.56182
GOTERM_CC_FAT	organelle membrane	GO:0031090	0.004048	0.039448	4.607246
UP_SEQ_FEATURE	transit peptide:Mitochondrion		0.004224	0.14768	4.934734
SP_PIR_KEYWORDS	transit peptide		0.004458	0.116798	5.128586



**Figure 4.7. Differentially regulated proteins in Pre-Cap, Cap and AR sperm using One-Way ANOVA (Tukey's test). “\*” and “\*\*” represent P-value < 0.05 and <0.01, respectively. The Y axis is the relative ratio of the signal between the specific condition and the internal control. The internal control contains equal quantity of peptides from aliquots of samples in each run combined prior to labelling.**



#### **4.4.8. Evidence for novel HABPs**

The presence of the BX7B motif in many HABPs including CD44 and RHAMM was investigated. Several differentially regulated proteins were shown to contain the motif (Table 4.2) with Cilia and flagella-associated protein 20 being the most interesting. In Chapter 3, the changes in localisation and distribution of HABPs was investigated. It was also shown that the intensity of labelling with HA-TRITC (a generic probe for detecting of HABPs) increased during capacitation and the acrosome reaction. The results of the current study for the first time revealed that Cilia and flagella-associated protein 20 containing 2 BX7B motifs increased during capacitation. Therefore, these proteins might represent novel HABPs which increase during capacitation.

#### 4.5. Discussion

A key goal of the present study was to identify dynamic changes of HABPs during capacitation and the AR. Therefore, a comprehensive proteomic profiling of human sperm was performed to evaluate dynamic changes in protein expression including HABPs, throughout the *in vitro* maturation process, which includes capacitation and the AR. Proteins were highlighted that help shed light on dynamic changes in sperm membrane proteins accompanying preparation for fertilisation (Baker et al., 2010a; Zhao et al., 2009).

In an attempt to elucidate the natural changes in the distribution of membrane proteins occurring during sperm maturation, sperm from three donors of proven fertility were used and in support of previous studies, proteins related to intracellular signaling, metabolism, motility and membrane remodelling were identified (Table 4.2, Figure 4.6). The interpretation of these changes in protein abundance is through a combination of protein turnover, acrosomal exocytosis, post-translational modifications (phosphorylation), protein folding and potentially *de novo* protein translation by mitochondrial-type ribosomes (Zhao et al., 2009).

As explained above, the study was intended to look at the changes in the accessibility of HABPs following capacitation and the AR (that indirectly indicates changes in their distribution), however, surprisingly, neither CD44 nor RHAMM were reported in Pre-Cap, CAP and AR fractions. The absence of these HABPs might be associated with the failure of the extraction buffer to access these proteins. It should be noted that CD44 is not reported in the most updated sperm proteome list (Amaral et al., 2014a). It is therefore possible that CD44 and RHAMM have very low abundance in sperm homogenates that could not be detected by the LC-MS/MS. It is also possible that the buffer used for protein extraction was unable to access these proteins, which were lost in the insoluble pellets following sperm homogenisation.

The results also showed that Cilia and flagella-associated protein 20 containing 2 BX7B motifs increased during capacitation. As discussed previously, a family of HABPs contain BX7B motif. It will be further discussed in Chapter 5 that Cilia and flagella-associated protein 20 might have HA binding properties. This protein is involved in axonemal structure organisation and motility (Mendes Maia et al.,

2014). As hyperactivation is a main feature of capacitation process, therefore, the protein might be involved in hyperactive motility of sperm during capacitation (Jin and Yang, 2017). The results in previous chapters confirmed that HA-binding increased after capacitation. It was also shown that HA-TRITC labelling was intensified during capacitation. Therefore, Cilia- and flagella-associated protein 20 might be a putative HABP that increases during capacitation.

Some of the findings of the current chapter (Table 4.2) have previously been shown to change or play a role either during capacitation or the AR (Zhao et al., 2009; Baker et al., 2010c; Baker et al., 2010a; Kwon et al., 2014; Secciani et al., 2009b; Arcelay et al., 2008). Therefore, the results of this study support previous reports that sperm capacitation involves changes in cholesterol efflux, reorganisation of the plasma membrane, changes in intracellular ion concentration and protein phosphorylation. The activation of calcium channels in the outer acrosome membrane occurs via PKA. Phosphorylation is a principle pathway activated during capacitation (Breitbart, 2003; Brenner et al., 2003; Marin-Briggiler et al., 2005). PKA is a ubiquitous multifunctional signaling molecule that interacts with and is anchored to specific cellular compartments through the interaction with A-kinase anchoring proteins (AKAPs) in the fibrous sheath. It is believed that AKAPs act as a scaffolding molecule that coordinates the actions of several kinases and phosphatases within one cellular compartment. Similar to previous reports, it was found that capacitation involved the activation of A-Kinase anchor proteins 3 (AKAP3) and 4 (AKAP4) (Carr and Newell, 2007; Ficarro et al., 2003; Luconi et al., 2004). In addition, ropporins have been shown to interact with AKAPs. Collectively, the phosphorylation and signaling of these molecules have all been implicated in sperm motility. As such, the change in AKAP3, AKAP4 and ROPN1B (reported in the current study) have been characterised in hyperactivation and sperm motility during the capacitation process (Carr and Newell, 2007). The tyrosine-phosphorylated state of such proteins during sperm capacitation could be critical for signal transduction and energy generation. Research has demonstrated capacitation-dependent tyrosine phosphorylation occurring in structural proteins including outer dense fiber proteins, cAMP-dependent protein kinase, HSP70 (HSPA2), F-actin-capping protein, Glutathione S-transferase Mu 3 and tubulin (Baker et al., 2010a; Choi et al., 2008b; Mariappa et al., 2010; Francou et al., 2014). Therefore, it is likely that the changes observed

in these proteins reflect phosphorylated activation states, which collectively contribute to capacitation and altered sperm motility.

In this study, differential expression of mitochondrial proteins during capacitation and the acrosome reaction was the most significant feature of the full data set. For example, ATP5A, ATP5D, ATP5J are all involved in energy production and were detected in all the studied groups. These enzymes belong to the mitochondrial membrane multi-protein complex ATP synthase that produces ATP from ADP (through electron transport chain). During capacitation, sperm require more energy for hyperactivation, a requisite step for fertilisation. The present study showed that the ATP synthase subunit delta (ATP5D) was in abundance in the capacitated group and AR human sperm compared to the pre-capacitated group. ATP5D is located in the membrane enriched fraction in ram sperm showing its function during the AR (van Tilburg et al., 2013). Also, the alpha subunit, ATP5A1 was increased in capacitated sperm as reported previously (Baker et al., 2010b). This further suggests that the mitochondrial ATP synthesizing machinery is required or involved in capacitation and the acrosomal reaction. However, a study in mouse sperm using gel-based proteome technology found reduced expression of ATP5A1 (Zhao et al., 2009). Differences may be explained by the different technologies employed to study the sperm proteome.

Moreover, mitochondrial cytochrome c oxidase subunit 2 expression was differentially increased in sperm completing the acrosome reaction compared to pre-capacitated sperm. Cytochrome c oxidase is involved in mitochondrial electron transport and reducing oxygen to water during oxidative phosphorylation. Its subunits have been associated with human sperm motility (Amaral et al., 2014b). However, as observed in the present study, an abundance of cytochrome c also plays a crucial role in capacitation and acrosome reaction (Choi et al., 2008a). Using porcine sperm, Choi et al (2008) demonstrated a significant relationship between increased cytochrome c and capacitated sperm ultimately determining the fate of the sperm cell. They proposed that cytochrome c-tyrosine phosphorylation is involved in the acrosome reaction, which was supported by the presence of 3 major sets of tyrosine phosphorylated proteins (18, 28 and 48 kDa) (Choi et al., 2008a). Furthermore, increased levels of

cytochrome c oxidase were also present in capacitated mouse sperm (Baker et al., 2010b).

A positive role of ROS (such as superoxide anion and nitric oxide) regulating capacitation has also been suggested (Griveau et al., 1995; de Lamirande and Gagnon, 1993; Aitken and Nixon, 2013; de Lamirande and Lamothe, 2009). Indeed, tyrosine phosphorylation associated with capacitation process is induced by hydrogen peroxide in various species (Roy and Atreja, 2008; Griveau et al., 1994) ultimately initiating the acrosome reaction (O'Flaherty et al., 2003; O'Flaherty et al., 1999). Nonetheless, ROS can act as a two-edged sword depending on their nature and quantity (Griveau and Le Lannou, 1997). Sperm are vulnerable to oxidative stress that can compromise both sperm quality and function. Also, mitochondria make notable contributions to oxidative stress (superoxide) in the abnormal/defective human sperm (Koppers et al., 2008). Certain sperm metabolites, like electrophilic aldehydes (4-hydroxynonenal) activate production of mitochondrial ROS production (Aitken et al., 2012b). Nonetheless, a lower level of mitochondrial ROS has been linked with good sperm quality and functionality (Marques et al., 2014). In the present study, superoxide dismutase (SOD2) was observed in abundance in acrosome reacted sperm compared to pre-capacitated sperm. The high level of SOD2 could be related to a reduction in the oxidative stress if happens during/after acrosome reaction process. Moreover, SOD1 was found in decreased level following cryopreservation, proposing an increase in ROS like events (Bogle et al., 2017). Levels of a few apoptotic proteins were different in acrosome reacted sperm compared with capacitated and pre-capacitated sperm. Proteomic analysis showed an increased level of mitochondrial apoptosis-inducing factor 1, (AIFM1) which is crucial for mitochondrial-mediated apoptosis in response to stress. It activates caspase-independent chromatin decondensation causing a high level of DNA fragmentation ultimately leading to apoptosis inside the nucleus. As explained in the above section ROS may initiate the capacitation and apoptosis when produced in the excess. Fragmentation of flagellar proteins during capacitation of human sperm has been reported (Secciani et al., 2009a). This apoptotic like effect could lead to the loss of sperm movement. Thus, sperm capacitation and apoptosis may occur simultaneously during sperm conditioning (Aitken, 2011).

Interestingly, in this study, Prohibitin-2 (PHB2) was highly expressed in acrosome reacted sperm compared to pre-capacitated sperm. The finding is in accordance with other studies where its roles have been associated with the acrosome reaction in various species (Choi et al., 2008a; Jin et al., 2016). PHB2 resides in the inner mitochondrial membrane and is involved in different biological processes including signal transduction, mitochondrial stability and apoptosis (Mishra et al., 2006; Chowdhury et al., 2014). PHB2 plays an important role in acrosome formation and nuclear shaping. These functions are facilitated by PHB2 mediated mitochondrial ubiquitination (Hou et al., 2017). Furthermore, the high expression level of PHB2 in sperm is negatively associated with mitochondrial ROS level and can regulate sperm function controlling ROS production inside mitochondria (Chai et al., 2017). In this study, mitochondrial SOD2 and PHB2 were highly upregulated in acrosome reacted sperm that shows their essential role in acrosome reaction by combating oxidative stress occurring during the process.

The level of protein deglycase DJ-1(PARK7), another mitochondrial protein was significantly decreased in acrosome reacted sperm compared to capacitated sperm. PARK7 is critical for mitochondrial function and preventing mitochondrial damage-induced cell death (Ooe et al., 2005; Hao et al., 2010). PARK7 has been hypothesised to play a role in sperm function (Bansal et al., 2015; Sun et al., 2014), and oxidative stress management (Taira et al., 2004). PARK7 has been reported in the acrosomal matrix of the mouse (Guyonnet et al., 2012). Transcriptomic studies showed that PARK7 transcripts were upregulated in the sperm of asthenozoospermic men (Bansal et al., 2015). Moreover, down-regulation of PARK7 in sperm from asthenozoospermic men resulted in impaired mitochondrial function compromising sperm motility (Sun et al., 2014). Another study in the same group of patients (asthenozoospermic), however, found decreased levels of expression (An et al., 2011). It remains to be established whether PARK7 is essential for the acrosome reaction. Since sperm motility ceases after acrosome reaction, the decreased level in this study was an interesting finding.

The expression of other mitochondrial proteins was either decreased or increased. For example, mitochondrial 3-ketoacyl-CoA thiolase (ACAA2)

expression was increased in the capacitated group compared to pre-capacitated group whereas no significant differential expression was observed in acrosome reacted sperm fraction. This protein is specifically involved in the pathway of fatty acid metabolism to produce energy during capacitation. To our knowledge, this study is first to link ACAA2 expression with the capacitation status of the sperm.

In the present study the up-regulation of tubulin a main axonemal phosphoprotein was also revealed. Tubulins are essential for sperm functionality as they are associated with sperm motility (Francou et al., 2014; Secciani et al., 2009b). It is known that phosphorylation of tubulin is regulated by cAMP and it might be involved in sperm hyperactivation during capacitation (Francou et al., 2014).

Serum albumin and apolipoproteins have been reported to induce cholesterol efflux in spermatozoa (Therien et al., 2001; Langlais J. and Roberts KD., 1985; Go and Wolf, 1985). Recently, one study presented a link between protein kinases and lipoproteins during capacitation. During capacitation, PKA activation phosphorylates apolipoprotein A-I binding protein and its subsequent release (Jha et al., 2008). Serum albumin removes cholesterol from the plasma membrane altering lipid membrane domains, fluidity and the membrane becomes more permeable to calcium and bicarbonate ions. Correspondingly, in the present study both capacitated and acrosome-reacted sperm showed an approximately 3-fold increase in serum albumin and apolipoprotein C-III (APOC3) compared with pre-capacitated sperm.

Recently, using a high-throughput proteomic approach, several proteins were identified that may be biomarkers for unexplained infertility, while the men providing the semen samples were classified as normozoospermic (Azpiazu et al., 2014). Several of these proteins changed during the maturation process, indicating their potential importance during normal sperm function. F-actin-capping protein submit alpha -3, mitochondrial Acetyl-CoA acetyltransferase, semenogelin 2 and serum albumin were in lower abundance in infertile samples and all of these proteins are thought to be important in the maturation process (Azpiazu et al., 2014).

#### **4.6. Conclusion**

The findings of the current chapter revealed some of the important differentially regulated proteins including mitochondrial proteins during *in vitro* maturation. No clear evidence of known HABPs such CD44 or RHAMM was seen. The levels of Cilia and flagella-associated protein 20 as a potential novel HABPs increased following capacitation.



## **Chapter 5: Identification and characterisation of putative sperm HABPs using mass spectrometry**

### **5.1. Introduction**

Negative effects on ICSI outcomes of the use of poor quality sperm may include miscarriage, an increased risk of congenital abnormalities and childhood cancer (Celik-Ozenci et al., 2004; Halliday, 2012; Gopalkrishnan et al., 2000; Larsen et al., 2013; Jaleel and Khan, 2013). As discussed, these issues have led to the development of new methods of sperm selection for ICSI based on functional properties, potentially mimicking the natural processes occurring in the reproductive tract of healthy individuals. Sperm binding to hyaluronic acid is one such alternative method of sperm selection.

As discussed in Chapter 1, different HABPs including CD44, RHAMM, HABP1 have been identified in various contexts. RHAMM is highly expressed in arthritis and advanced cancers but not in normal tissue. It was first identified by cloning a cDNA encoding RHAMM from GT11 3T3 (fibroblasts) cDNA library and caused fibroblast transformation when it was overexpressed (Hardwick et al., 1992). This protein is considered as a nuclear and cytoplasmic protein that can interact with centromeres, microtubules and the mitotic spindle proposing that it is a multifunctional protein (Hamilton et al., 2007). RHAMM is also involved in cell motility. Activation of various mitogenic signaling pathways, including Ras and ERK1,2 occurs upon HA-RHAMM interaction (Hall et al., 1995; Wang et al., 1998).

CD44 was first identified as a glycoprotein in SV-3T3 cells using a monoclonal antibody, designated K-3. The antibody specifically immunoprecipitated CD44 from baby hamster kidney (BHK) cells (Underhill et al., 1987). It was then shown that CD44 was a HABP in placenta cells when their binding to HA was blocked using an antibody against CD44. To date, several domains including extracellular (7), transmembrane (1) cytoplasmic (1) domains are identified for CD44 (Misra et al., 2015). CD44 is involved in various cellular functions including cell aggregation, tumor metastasis, releasing chemokines and growth factors, lymphocyte activation amongst others (Haynes et al., 1991).

In 1994, a 68 kDa HABP was identified in sperm of different species including mouse, rat, bovine and human using Western blotting and immunocytochemistry. This protein was distributed on sperm head, midpiece and tail. The same study showed phosphorylation of 68 kDa HABP in motile sperm and also the failure of sperm-zona interaction due to pre-treatment of sperm with the anti-HABP antibody. Therefore, it may be involved in sperm motility and fertilisation (Ranganathan et al., 1994).

Mature sperm express several HABPs including CD44 (Underhill, 1992; Bajorath et al., 1998) and RHAMM (Yang et al., 1993; Hardwick et al., 1992). HABPs are categorised into three groups based on the nature of their HA binding properties: namely, those proteins containing a Link domain or module, a BX7B motif, a covalent bond or combinations thereof (Yang et al., 1994; Day and Prestwich, 2002; Amemiya et al., 2005). CD44 belongs to the Link module superfamily of HABPs (See Chapter 1). CD44 also contains the BX7B motif, also thought to confer HA-binding properties (See Chapter 1) (Yang et al., 1994; Day and Prestwich, 2002). The cumulus oophorus complex and the zona pellucida can be considered part of a 'capture' mechanism for sperm binding and requires the expression of HABPs on the sperm surface (Hong et al., 2004). Investigating sperm HABPs is therefore justified with regard to understanding male infertility and the fertilisation potential of sperm.

The complexity of HABP expression in human spermatozoa and enhancement of sperm binding to HA during capacitation were investigated (Chapter 2 and 3). The results of the previous chapters also suggested the presence of sperm HABPs other than CD44 and RHAMM, justifying further investigation. To this end, ejaculated human sperm were homogenised and extracted proteins were subjected to panning on an HA-coated surface (Amemiya et al., 2005). Non-binding proteins were washed from the substrate and recovered and binding proteins were stripped from the substrate using a modified pre-heated Laemmli buffer. Both bound and unbound fractions were characterised by tandem mass spectrometry (LC-MS/MS).

## **5.2. Hypothesis and objectives**

The hypothesis states that loading sperm homogenates on a surface coated with HA is effective in partitioning HA-binding and non-binding proteins. To this end, the main objectives of the current study were to:

- Isolate HA-binding and non-binding proteins using an HA affinity process.
- Sequence proteins from HA-binding and non-binding fractions by LC-MS/MS and to identify novel HABPs.
- Verify the results of LC-MS/MS experiments using Western blotting.

### 5.3. Materials and methods

#### 5.3.1. Reagents used

Ethylenediaminetetraacetic acid (EDTA), Triton-X100, Phenylmethylsulfonyl fluoride (PMSF), Acrylamide/Bis-acrylamide, 30% solution, Sodium dodecyl sulfate (SDS), Ammonium persulfate (APS) and *N,N,N',N'*-Tetramethylethylenediamine (TEMED) were obtained from Sigma-Aldrich (UK). Polyvinylidene (PVDF) membranes and Amicon Ultra-0.5 mL and 15 mL centrifugal filter units were obtained from Millipore (UK). Pierce BCA protein assay kit, Pierce™ Protein-Free (PBS) Blocking Buffer and were obtained from Thermo Fisher Scientific (UK). Tris Base and NaCl were purchased from Fisher Scientific (UK). Protease inhibitor cocktail was purchased from Cell Signaling Technology (UK). ColorPlus prestained protein ladder (10-230 kDa) was acquired from New England Biolabs (UK). Clarity™ western ECL substrate and Bradford protein assay reagent were purchased from Bio-Rad (UK). HA-coated dishes were purchased from Biocoat (USA). The monoclonal anti-ZPBP2 antibody was purchased from antibodies-online. The monoclonal anti-ADAM32 (sc-376738) and anti-Alpha tubulin (SC-5286) antibodies were obtained from Santa Cruz Biotechnology. For mass spectrometry the Water with 0.1% (v/v) formic acid (LC-MS Chromasolv®) was from Honeywell (Seelze, Germany) and the acetonitrile from Fluka. The rest of the reagents were supplied by Sigma-Aldrich (St. Louis, MO) unless otherwise stated.

#### 5.3.2. Semen analysis

SupraSperm™ and Quinn's sperm washing medium were obtained from Origio (Denmark). ProInsert-Nidacon tubes were purchased from Nidacon (Sweden). Human semen samples were obtained and liquefied as described in Chapter 2. The semen parameters related to each sample are shown in Table 5.1. After liquefaction, the samples were checked for volume, sperm concentration, sperm morphology and the number of round cells according to the WHO criteria (2010). Only those with normal semen parameters as defined by WHO criteria were included in the study (WHO 2010). Briefly, samples with  $\geq 50\%$  progressive motility,  $\geq 200 \times 10^6$  sperm cells and  $\leq 0.1\%$  round cell contamination (after double DDGC) were used.

**Table 5.1.** Semen parameters of young male volunteers (unproven fertility) participating in the study.

Sample	Volunteer Age	Sperm concentration (million/mL)	Total sperm count ( $\times 10^6$ )	Semen volume (mL)	Sperm motility (%)
D70	28	233	349.5	1.5	92
D31	36	200	300	1.5	90
D107	19	251	1204.8	4.8	87
D115	20	179	716	4	61
<b>Mean <math>\pm</math> SD</b>	26 $\pm$ 8	216 $\pm$ 33	643 $\pm$ 418	3 $\pm$ 2	83 $\pm$ 15

### 5.3.3. Sperm preparation

After liquefaction of 4 semen samples, sperm were separated using a 60% density cushion of SupraSperm™ and to remove any round cell contamination, ProInsert-Nidacon tubes were used for sperm separation. Briefly, 2 mL SupraSperm™ with a density of 60% was loaded to the outer channel of the tube. SupraSperm™ is able to reach the bottom of the tube due to the presence of a hole at the bottom of the chamber. A 500  $\mu$ L semen sample was then layered on top and the tube was centrifuged at 300  $\times$ g for 20 min. A pellet retrieval pipette (from the ProInsert kit) was used to aspirate sperm pellets via the central channel (Figure 5.1). Sperm pellets were then resuspended and washed in PBS (pH: 7.2) and centrifuged at 300  $\times$  g for 10 minutes (two repeated washes). They were then used for further protein extraction. To obtain sufficient protein for analysis, combined ejaculates from two individuals (sample D70 and sample D31) were used. It should be noted that 2 samples (D70 and D31) were used for LC-MS/MS and 4 samples (D31, D70, D107, D115) were used for Western blotting to verify the results of LC-MS/MS.

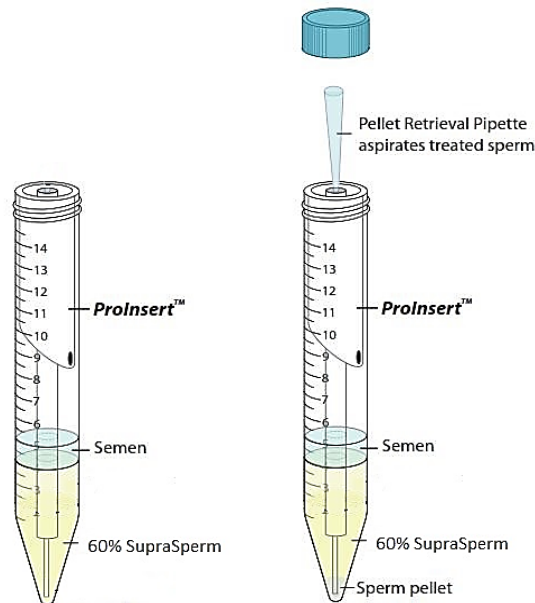


**Figure 5.1. A schematic illustration of density gradient centrifugation using Prolinsert-Nidacon columns (n=4).**

#### 5.3.4. Protein extraction

Proteins from  $\sim 2 \times 10^8$  sperm were extracted in 500  $\mu\text{L}$  of a mild lysis buffer (150 mM NaCl, 20 mM Tris-HCl (pH: 8), 2mM EDTA, 1mM PMSF, 1x protease inhibitor cocktail, 0.5% Triton X-100) (D'Cruz et al., 1993). Eppendorf<sup>®</sup> safe-lock microcentrifuge tubes (sigma) were used. The suspension was sonicated on ice for 15 seconds on, 40 seconds off, at an amplitude of 10 microns . The sonication was repeated four times. Samples were incubated on ice for 1 hour with constant shaking. To recover extracted soluble proteins, samples were centrifuged at 16000  $\times g$  for 20 minutes and supernatants were aspirated and transferred into fresh tubes. Pellets were discarded. Protein quantification was performed using the Pierce BCA protein assay kit according to manufacturer's instruction (Thermo Fisher Scientific, UK).

#### 5.3.5. Isolation of HA-binding and non-binding proteins

HA-coated dishes (Biocoat, USA) were used to isolate proteins with an affinity for HA. To block non-specific binding, dishes were treated with 1.5 mL of Pierce<sup>™</sup> protein-free (PBS) blocking buffer (Thermo Fisher Scientific, UK) for 30 min at RT with gentle shaking. Dishes were then washed twice with 2 mL of PBS. Extracted proteins from the sperm of two different men were used and loaded on to

separate HA-coated dishes at a concentration of 1.5 mg/mL. Dishes were incubated for 75 min at RT with gentle shaking after which, non-binding proteins were decanted for frozen storage and further experiments.

To minimise non-specific contamination of the binding fraction, dishes were washed with 1.5 mL PBS (four times for one minute each wash). Bound proteins were then recovered by incubating the plate surface with 400  $\mu$ L of pre-heated (95°C) Laemmli-based buffer containing 0.125 M Tris-HCL (pH: 6.8), 4%w/v SDS and 10%v/v 2-mercaptoethanol for 5 minutes with gentle shaking. The bound proteins were aspirated using a pipette. Both protein fractions (HA-binding and non-binding) were dialysed against PBS using Amicon Ultra-15 mL Centrifugal Filters (3 kDa) according to manufacturer's instruction (Millipore, UK) (Figure 5.2). Briefly, 400  $\mu$ L of each protein fraction and 14.6 mL PBS were added to each filter device and centrifuged at 4,000  $\times$  g for 40 min at 25°C. The proteins were recovered after dialysis using a pipette from the bottom of the filter and were concentrated using Amicon Ultra-0.5 mL Centrifugal Filters according to manufacturer's instruction (Millipore, UK).

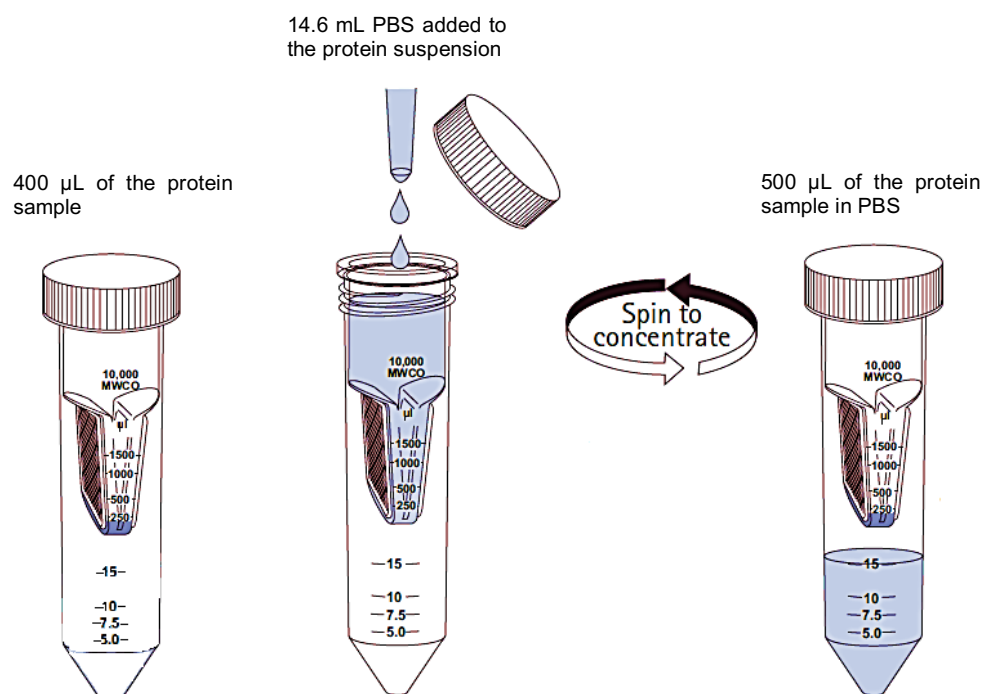


**Figure 5.2. Schematic illustration of Amicon Ultra-15 centrifugal filter units.**

A final volume (40  $\mu$ L) was obtained after concentration and 30  $\mu$ L aliquots of concentrated HA-binding and non-binding proteins from each sample were

precipitated using TCA-acetone (see below). Ten (10  $\mu$ l) aliquots were stored at  $-80^{\circ}\text{C}$  for Western blot analysis (see below).

### **5.3.6. Protein precipitation using TCA**

To precipitate soluble proteins from both HA-binding and non-binding samples, one volume of 100% (w/v) TCA was added to four volumes of the protein solution (final conc of 20% TCA). All samples were incubated for 20 min at  $4^{\circ}\text{C}$  and centrifuged at 19000 xg for 5 min. Supernatants were discarded. Pellets were washed with 200  $\mu$ L of ice cold acetone and centrifuged at 19000 xg for 5 min at  $4^{\circ}\text{C}$  (twice, with washing between). Pellets were dried and stored at  $-80^{\circ}\text{C}$  before sequencing by LC-MS/MS as outlined below.

### **5.3.7. Liquid chromatography–tandem mass spectrometry (LC-MS/MS)**

Digestion of proteins was performed using trypsin (Promega, Madison, WI) at  $37^{\circ}\text{C}$  overnight according to the manufacturer's instructions. Mass spectrometry analysis was accomplished as described elsewhere (Amaral et al., 2013). Trypsin-derived peptides were separated through a nano liquid chromatography by an Eksigent NanoLC AS2 ultra (AB SCIEX; flow rate of 400 nL/min), an EASY C18 trap column (5  $\mu$ m, 120  $\text{\AA}$ , 100  $\mu$ m inner diameter  $\times$  2 cm in length) and an EASY C18 analytical column (3  $\mu$ m, 120  $\text{\AA}$ , 75  $\mu$ m inner diameter  $\times$  10 cm in length). The obtained linear gradient, by Solvent B (97% acetonitrile, 0.1% formic acid) and Solvent A (3% acetonitrile, 0.1% formic acid), was employed. MS/MS analysis was carried out by using an LTQ Orbitrap Velos (Thermo Fisher Scientific) with a nano-electrospray ion source with precursor ion selection in the Orbitrap at 30,000 of resolution, choosing the 15 most intense precursor ions, with a collision energy of 35 in positive ion mode. The completion of MS/MS data acquisition was accomplished using Xcalibur 2.1 (Thermo Fisher Scientific).

### **5.3.8. Protein identification and quantification**

Proteome Discoverer 1.4. (ThermoFisher Scientific) was used to analyse identified proteins. Database searching included all entries from the *Homo sapiens* UniProtKB/Swiss-Prot database (release 2015-02) using SEQUEST version 28.0 (Thermo Fisher Scientific). A 1% FDR and at least one unique peptide per protein were the criteria used for protein identification. The



dissociated or 'ungrouping' of proteins from their respective families was used during the quantification process in order to avoid possible ambiguities associated with different isoforms of the same protein (Bogle et al., 2017).

Identified proteins in binding and non-binding fractions from the two individual samples were compared and checked against the whole human sperm proteome (Amaral et al., 2014a) and only those present in this database were included for further analysis. Additional information about the identified proteins was obtained using UniProtKB/Swiss-Prot, and BioMart - Ensembl. DAVID Bioinformatics Resources 6.8 was used for functional ontological annotation clustering.

PDBsum was used to align amino acid sequences of identified proteins with sequences for which structural information is available (Laskowski, 2001; Laskowski et al., 2005; Laskowski, 2009). The SAS (Sequences annotated by structure) server was then used (<http://www.ebi.ac.uk/thornton-srv/databases/sas/>) to determine the structural similarities between identified proteins in HA-binding and non-binding fractions with the hyaluronic acid binding domain of CD44 (highlighted by PDBsum).

SAS annotates protein residues according to residue type (polar, non-polar, aliphatic and aromatic), secondary structure ( $\alpha$ -helix,  $\beta$ -strand, turn and coil), inter-molecular contacts (number of hydrogen bonds, total contacts, nucleic acid contacts and metal ions contacts to ligand), active sites and residue similarity (Milburn et al., 1998). Sequence similarities were computed using the PAM250 log odds scores matrix with FASTA used as the sequence search method and the alignment presented as a simple pile-up from the resulting pairwise comparisons. The colouring of residue similarity signifies identical amino acid types (red) down to conservative, semi-conservative and dissimilar residues using a spectrum ranging from orange through to blue. In addition, a Z-score and an E-value for sequence similarity was computed (Pagni and Jongeneel, 2001). Figure 5.3 represents a flow diagram of the approach used in the present study.

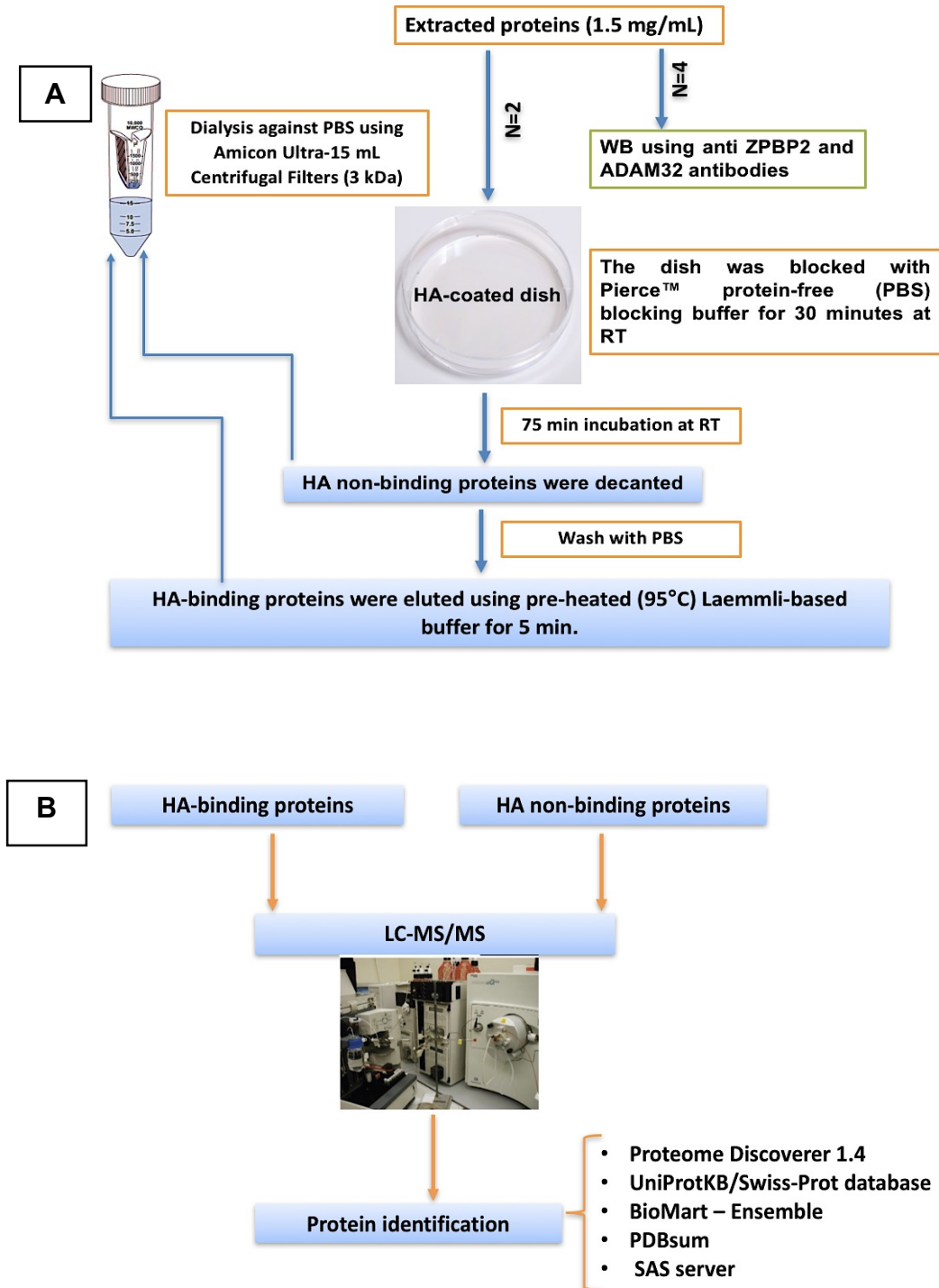


**Figure 5.3. Flow diagram outlining the approach used in the current study.**

Sperm from 4 normozoospermic donors were separated using 60% DGC. Protein extraction was performed. As shown in 5.3A, proteins from 2 samples were loaded on HA-coated dishes and incubated for 75 min at RT. Unbound proteins were decanted. Bound proteins were separated using a Laemmli-based buffer. Both HA-bound and unbound fractions were dialysed against PBS. As shown in 5.3B, LC-MS/MS and protein identification were performed after dialysis and concentration on both HA-bound and unbound fractions.

### 5.3.9. Western blot confirming the results of LC-MS/MS

To verify the results of LC-MS/MS experiments, samples (15 µg each) of HA-binding and non-binding proteins isolated from D31, D70, D107 and D115 were resolved by SDS-PAGE and Western blotted. Samples were dissolved and diluted 1:1 with 2x Laemmli buffer (4% SDS (w/v), 10% 2-mercaptoethanol (v/v), 20% glycerol (v/v), 0.004% bromophenol blue (w/v), 0.125 M Tris-HCl (pH: 6.8)) and boiled for 5 min at 95°C. The proteins were separated on a 10% gel at 120 V for 100 min in 1x SDS running buffer (25 mM Tris-base, 190 mM Glycine, 0.1% SDS w/v). Proteins were then transferred to PVDF membranes at 250 mA for 90 min in 1x transfer buffer (25 mM Tris-base, 190 mM Glycine, and 20% methanol (v/v)). The membrane was blocked with Pierce™ protein-free (TBS) (Thermo Fisher Scientific, UK) blocking buffer for 1 hour at RT with constant shaking. It was then probed with monoclonal antibodies (raised in mouse) to two proteins specific to the binding fraction, zona pellucida binding protein 2 (ZPBP2) and ADAM32 (200 µg/mL) at a primary antibody concentration of 1/500 and 1/200, respectively overnight at 4°C. A monoclonal (raised in mouse) alpha tubulin antibody (200 µg/mL at a final concentration of 1/2000) was used as a control for proteins present in both fractions and as a loading control. Membranes were washed three times with TBS containing 0.1% Tween-20 (v/v) for 15 minutes each and incubated with 1:1000 dilution of relevant HRP-conjugated secondary antibodies for 1 hour at RT (all primary and secondary antibodies were diluted in Pierce™ protein-free (TBS)). Membranes were washed as described above and the ECL Clarity western ECL substrate was used to visualise protein bands (Bio-Rad, UK).

To optimise the protocol, different concentrations of each antibody as well as different time points for each were examined. Initially various dilutions of 1/000, 1/500 and 1/200 were checked for anti ZPBP2 antibody. The best results only obtained at 1/500 dilution. The bands for CD44 at 1/1000 were very weak and the background was too high at 1/200 dilution.

In relation to ADAM32, different dilutions of 1/1000, 1/800, 1/500 and 1/200 were examined. The bands obtained at 1/000, 1/800 and 1/500 were not strong enough. Therefore, higher concentration (1/200 v/v) was also tested where the best results obtained. To check the accuracy of the results, alpha tubulin antibody was used as an internal control.

In spite of its detection on the sperm surface by immunocytochemistry, CD44 was not reported in the total sperm protein homogenate data obtained by mass spectrometry. Moreover, western blotting using the same anti-CD44 antibodies also failed to detect this protein. Very low concentrations of CD44 in the mass-spec samples could have been responsible for the detection failure. Failure to detect the protein by western blotting is more likely to have been due to the antibodies' inability to recognise the denatured form of the protein resolved by SDS PAGE. Had time permitted, renaturation of the protein on the membrane *in situ* may have helped in to visualise it.

## 5.4. Results

### 5.4.1. Identification of proteins in HA-binding and non-binding fractions

LC-MS/MS data resulted in the identification of 180 (sample D70) and 227 (sample D31) proteins in HA-binding fractions and 466 (sample D70) and 563 (sample D31) proteins in non-binding fractions (Figure 5.4).

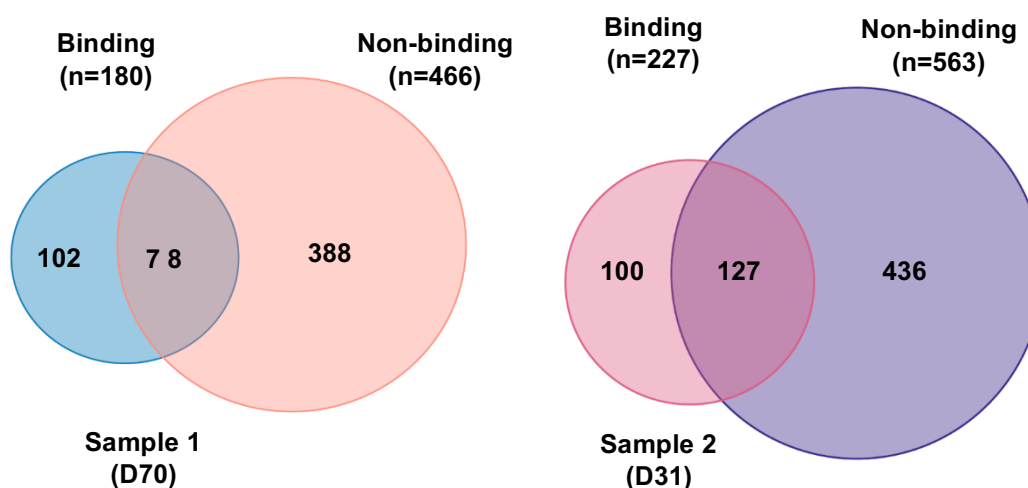


**Figure 5.4.** Venn diagram to illustrate HA-binding and non-binding proteins from two different samples.

As shown in Figure 5.5A, 45 proteins were common and specific (no overlaps with non-binding fractions) to both HA-binding fractions and 28 of them with  $\geq 1$  unique peptide per protein had records in the human sperm proteome database (Amaral et al., 2014a). Two hundred and twenty-five (225) proteins were common to both non-binding fractions with 81 of them with  $\geq 1$  unique peptide and recorded in the human sperm proteome database (Figure 5.5B). A list of mass spectrometry data can be found in Appendix Tables 5.1- 5.4.

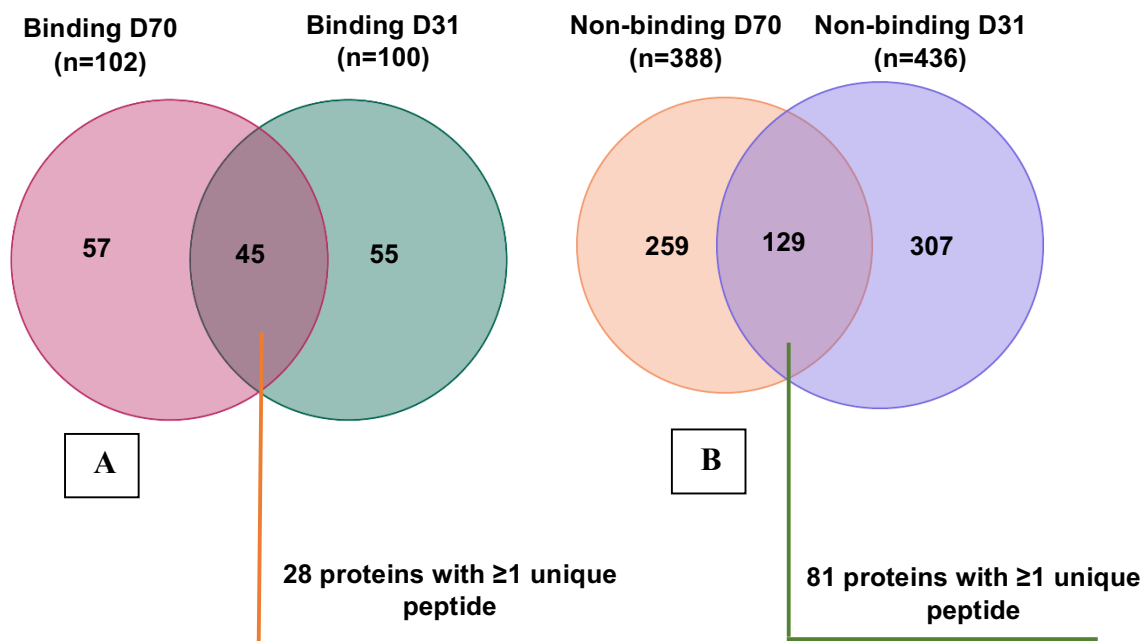


**Figure 5.5. Venn diagram showing HA-binding (A) and non-binding proteins (B) merged from two different samples.**

In binding fractions there is no overlap from non-binding and in non-binding fractions there is no overlap from binding.

Additional information about the identified proteins was obtained using UniProtKB/Swiss-Prot and BioMart - Ensembl. Table 5.2 lists proteins in the binding fractions. The list from the non-binding fractions is shown in Appendix Table 5.5.

**Table 5.2.** Proteins found in both HA-binding fractions and no overlap with non-binding fractions.

UniProt/SwissProt Accession	Description	UniProt Gene Name	Potential HA-binding domain (N)
A4D1T9	protease, serine, 37	PRSS37	BX7B(1)
P03973	Antileukoproteinase, secretory leukocyte peptidase inhibitor	SLPI	BX7B (1)
P05109	S100 calcium binding protein A8	S100A8	BX7B (1)
P13647	Keratin, type II cytoskeletal 5	KRT5	N/D
P20155	serine protease inhibitor, Kazal type 2 (acrosin-trypsin inhibitor)	SPINK2	N/D
P21741	midkine (neurite growth-promoting factor 2)	MDK	BX7B (4)
P35663	cylicin, basic protein of sperm head cytoskeleton 1	CYLC1	BX7B (6)
P62987	ubiquitin A-52 residue ribosomal protein fusion product 1	UBA52	BX7B (1)
P99999	cytochrome c, somatic	CYCS	BX7B (1)
Q00796	sorbitol dehydrogenase	SORD	N/D
Q13618	cullin 3	CUL3	BX7B (2)
Q16568	CART prepropeptide	CARTPT	N/D
Q16836	hydroxyacyl-CoA dehydrogenase	HADH	N/D
Q6NUT2	Probable C-mannosyltransferase	DPY19L2	BX7B (2)
Q6P4A8	phospholipase B domain containing 1	PLBD1	BX7B (1)
Q6UWM5	GLIPR1-like protein 1	GLIPR1L1	N/D
Q6X784	zona pellucida binding protein 2	ZPBP2	Link-like domain
Q86YZ3	Hornerin	HRNR	N/D
Q8N5Q1	family with sequence similarity 71, member E2	FAM71E2	BX7B (3)
Q8TC27	ADAM metallopeptidase domain 32	ADAM32	BX7B (2)
Q8WZ59	transmembrane protein 190	TMEM190	N/D
Q96KX0	lysozyme-like 4	LYZA	N/D
Q96QH8	sperm acrosome associated 5B	SPACA5	N/D
Q9BVA1	tubulin, beta 2B class IIb	TUBB2B	N/D
Q9BWH2	FUN14 domain containing 2	FUNDC2	BX7B (1)
Q9NPJ3	acyl-CoA thioesterase 13	ACOT13	N/D
Q9UII2	ATPase inhibitory factor 1	ATPIF1	N/D
Q9Y6A4	cilia and flagella associated protein 20	CFAP20	BX7B (2)

N/D: Not detected.

An ontological analysis was undertaken to determine whether binding and non-binding proteins carried any functional signatures and whether these were distinct or similar. Following submission to DAVID, results suggested distinct signatures with the binding fraction containing a weak enrichment for secreted proteins compared with stronger enrichment of chaperone and chaperone-like proteins in the non-binding fraction (Table 5.3 and 5.4).

**Table 5.3.** Functional annotation clustering on HA-binding proteins using DAVID Bioinformatics Resources 6.8.

<b>Annotation Cluster 1</b>	<b>Enrichment Score: 1.93</b>				
Category	Term	Count	P-Value	Benjamini	FDR
UP_KEYWORDS	Secreted	10	6.16E-04	0.049262	0.655983
UP_SEQ_FEATURE	signal peptide	11	0.006566	0.549394	7.294336
UP_KEYWORDS	Signal	12	0.01183	0.386094	11.93837
UP_KEYWORDS	disulfide bond	10	0.026459	0.519518	24.90958
UP_SEQ_FEATURE	disulfide bond	7	0.166538	0.999984	87.68431
<b>Annotation Cluster 2</b>	<b>Enrichment Score: 0.74</b>				
Category	Term	Count	P-Value	Benjamini	FDR
UP_KEYWORDS	Mitochondrion	5	0.056326	0.695313	46.17043
KEGG_PATHWAY	hsa01100:Metabolic pathways	3	0.217781	0.999764	88.46748
UP_KEYWORDS	Acetylation	6	0.474806	0.982787	99.89717
<b>Annotation Cluster 3</b>	<b>Enrichment Score: 0.50</b>				
Category	Term	Count	PValue	Benjamini	FDR
UP_KEYWORDS	Isopeptide bond	4	0.183541	0.907023	88.54006
UP_KEYWORDS	Ubl conjugation	4	0.389801	0.974835	99.48931
UP_KEYWORDS	Disease mutation	5	0.434581	0.979683	99.77378
<b>Annotation Cluster 4</b>	<b>Enrichment Score: 0.004</b>				
Category	Term	Count	P-Value	Benjamini	FDR
UP_KEYWORDS	Membrane	6	0.987437	1	100
UP_KEYWORDS	Transmembrane helix	4	0.989198	1	100
UP_KEYWORDS	Transmembrane	4	0.989446	1	100
GOTERM_CC_DIRECT	integral component of membrane	4	0.991776	1	100
UP_SEQ_FEATURE	transmembrane region	3	0.994882	1	100



**Table 5.4.** Functional annotation clustering on HA non-binding proteins using DAVID Bioinformatics Resources 6.8.

Annotation Cluster 1	Enrichment Score: 7.26				
Category	Term	Count	P-Value	Benjamini	FDR
UP_KEYWORDS	Chaperone	11	5.74E-09	4.99E-07	7.02E-06
GOTERM_BP_DIRECT	GO:0006457~protein folding	10	7.29E-08	3.78E-05	1.05E-04
GOTERM_MF_DIRECT	GO:0051082~unfolded protein binding	8	3.88E-07	7.57E-05	4.85E-04
Annotation Cluster 2	Enrichment Score: 5.76				
Category	Term	Count	P-Value	Benjamini	FDR
UP_SEQ_FEATURE	transit peptide:Mitochondrion	14	5.50E-08	1.77E-05	7.43E-05
UP_KEYWORDS	Transit peptide	14	1.40E-07	8.14E-06	1.72E-04
UP_KEYWORDS	Mitochondrion	18	1.10E-06	4.80E-05	0.001351
GOTERM_CC_DIRECT	GO:0005739~mitochondrion	20	2.90E-06	1.57E-04	0.00351
GOTERM_CC_DIRECT	GO:0005743~mitochondrial inner membrane	9	6.41E-04	0.017167	0.773065
Annotation Cluster 3	Enrichment Score: 3.01				
Category	Term	Count	P-Value	Benjamini	FDR
KEGG_PATHWAY	hsa05016:Huntington's disease	11	1.47E-07	1.22E-05	1.58E-04
UP_KEYWORDS	Mitochondrion	18	1.10E-06	4.80E-05	0.001351
UP_KEYWORDS	Mitochondrion inner membrane	8	8.69E-05	0.003019	0.106357
KEGG_PATHWAY	hsa00190:Oxidative phosphorylation	7	1.35E-04	0.005581	0.1443
KEGG_PATHWAY	hsa05012:Parkinson's disease	7	1.93E-04	0.005332	0.206722
KEGG_PATHWAY	hsa05010:Alzheimer's disease	7	4.79E-04	0.0099	0.512174
GOTERM_CC_DIRECT	GO:0005743~mitochondrial inner membrane	9	6.41E-04	0.017167	0.773065
KEGG_PATHWAY	hsa04260:Cardiac muscle contraction	5	0.001049	0.01441	1.117337
GOTERM_BP_DIRECT	GO:0006119~oxidative phosphorylation	3	0.001372	0.132787	1.967284
GOTERM_CC_DIRECT	GO:0005750~mitochondrial respiratory chain complex III	3	0.001403	0.028033	1.684693

GOTERM_BP_DIRECT	GO:0006122~mitochondrial electron transport, ubiquinol to cytochrome c	3	0.001836	0.146983	2.625407
GOTERM_BP_DIRECT	GO:0009060~aerobic respiration	3	0.008785	0.278999	11.99127
UP_KEYWORDS	Respiratory chain	3	0.025007	0.35638	26.66763
GOTERM_BP_DIRECT	GO:1902600~hydrogen ion transmembrane transport	3	0.028196	0.54217	33.90157
KEGG_PATHWAY	hsa01100:Metabolic pathways	13	0.057059	0.456404	46.6956
KEGG_PATHWAY	hsa04932:Non-alcoholic fatty liver disease (NAFLD)	4	0.063235	0.452514	50.31744
UP_KEYWORDS	Electron transport	3	0.066202	0.548213	56.7819
Annotation Cluster 4					
Annotation Cluster 4		Enrichment Score: 2.62			
Category	Term	Count	P-Value	Benjamini	FDR
GOTERM_MF_DIRECT	GO:0051082~unfolded protein binding	8	3.88E-07	7.57E-05	4.85E-04
GOTERM_BP_DIRECT	GO:0050821~protein stabilization	8	1.86E-06	4.83E-04	0.002693
INTERPRO	IPR017998:Chaperone tailless complex polypeptide 1 (TCP-1)	3	9.82E-04	0.173511	1.217609
INTERPRO	IPR027413:GroEL-like equatorial domain	3	0.00155	0.139703	1.91612
INTERPRO	IPR027409:GroEL-like apical domain	3	0.001767	0.108073	2.181575
INTERPRO	IPR002423:Chaperonin Cpn60/TCP-1	3	0.001767	0.108073	2.181575
UP_KEYWORDS	Stress response	3	0.05784	0.523124	51.79582
UP_KEYWORDS	Nucleotide-binding	11	0.154563	0.767937	87.20886
GOTERM_MF_DIRECT	GO:0005524~ATP binding	8	0.441966	0.995558	99.93116
UP_KEYWORDS	ATP-binding	7	0.457619	0.956322	99.9443

#### 5.4.2. Alignment of the sequences of HA-binding and non-binding proteins using PDBsum and SAS

Ontological analysis provided only limited information on the properties of proteins in the binding and non-binding fractions. To augment and improve the analysis, the amino acid sequences of the 28 proteins in the HA-binding fractions were submitted to PDBsum, which generates lists of structural features (PDB codes) conserved between proteins. Common features of HABPs include a Link domain and/or one or more BX7B motifs, both of which are thought to confer an affinity for HA (Misra et al., 2015). One protein (ZPBP2) from the binding fraction contained a sequence motif bearing some similarity to the Link module of CD44, while 14 other proteins (50% in total; Table 5.2) contained BX7B sequences, also thought to be involved in HA binding. Twenty-eight (28) proteins (34.5%; Appendix Table 5.5) from the non-binding fraction also contained the BXB7 motif but no protein containing a sequence similar to the Link domain was present. Proteins with multiple ( $\geq 2$ ) BX7B motifs, including Midkine (Uniprot P21741), which can bind other glycosaminoglycans including HA (<http://www.ebi.ac.uk/QuickGO/GProtein?ac=P21741>) and Cilia and flagella-associated protein 20 were more abundant in the binding (25%) versus the non-binding fractions (15%). ADAM32, for example has two BX7B motifs. Hence, HA binding motifs may have had some effect on the partitioning of the two populations.

Charge differences between proteins were also explored as an alternative partitioning mechanism. Net charge is dictated by a protein's pI and basic proteins with a net positive charge could interact electrostatically with the HA substrate. HA carries a net negative charge at pH 8.0 (the pH of the extraction buffer). Based on their pI values at pH 8.0, twenty (71.4%) of the proteins in the binding fraction compared with 21 (26%) in the non-binding fraction were likely to carry a net positive charge, suggesting that a charge effect may also have influenced the partitioning of proteins into binding and non-binding fractions.

Of all the proteins in the binding fraction, ZPBP2 was flagged as one of the more interesting. ZPBP2 contains a sequence motif with similarities to the Link module found in CD44. Figure 5.6 shows the similarity between ZPBP2 and CD44 (PDB code 2i83 residues 21 – 178) with a 32.7% sequence identity and 69% overall

similarity covering a 55 amino acid overlap. There were no equivalent proteins with a sequence resembling the Link module in the non-binding fraction. The 2i83 PDB code comparison is drawn because it corresponds with the CD44's HA-binding form although other valid codes across a similar residue overlap are available (Table 5.5) (Liu and Finzel, 2014a; Teriete et al., 2004; Takeda et al., 2006).

**Table 5.5.** PDB codes matching to ZPBP2 (<http://www.ebi.ac.uk/thornton-srv/databases/cgi-bin/pdbsum/GetPage.pl?pdbcode=index.html>).

PDB code	Model	Length	%-identity	a.a. overlap	z-score	Protein name
<b>4pz3</b> (A)	X-ray 1.08Å	150	32.7	55	116.4	High-resolution crystal structure of the human CD44 hyaluron domain complex with undefined peptides
<b>1uuh</b> (A)	X-ray 2.20Å	150	32.7	55	116.4	Hyaluronan binding domain of human CD44
<b>4pz4</b> (A)	X-ray 1.60Å	154	32.7	55	116.2	High-resolution crystal structure of the human CD44 hyaluron domain in new space group
<b>2i83</b> (A)	NMR	158	32.7	55	116.1	Hyaluronan-binding domain of CD44 in its ligand-bound form
<b>1poz</b> (A)	NMR	159	32.7	55	116.0	Solution structure of the hyaluronan binding domain of human CD44

As ZPBP2 may have HA binding properties based on sequence similarities with the Link domain, further structural similarities were investigated using the Sequences Annotated by Structure (SAS) server (Milburn et al., 1998). This resource checks for the number of contacts between the protein and its presumptive ligand based on secondary structure prediction and was used to scan the homologous HA binding motif on ZPBP2. Results are shown in Figure 5.5 with the PROSITE secondary structure alignment (PS01241) for HA-binding domain of CD44 in its ligand-bound form (2i83) on ZPBP2 shown in Figure 5.7 (<http://prosite.expasy.org/cgi-bin/prosite/prosite-search-ac?PS01241>).

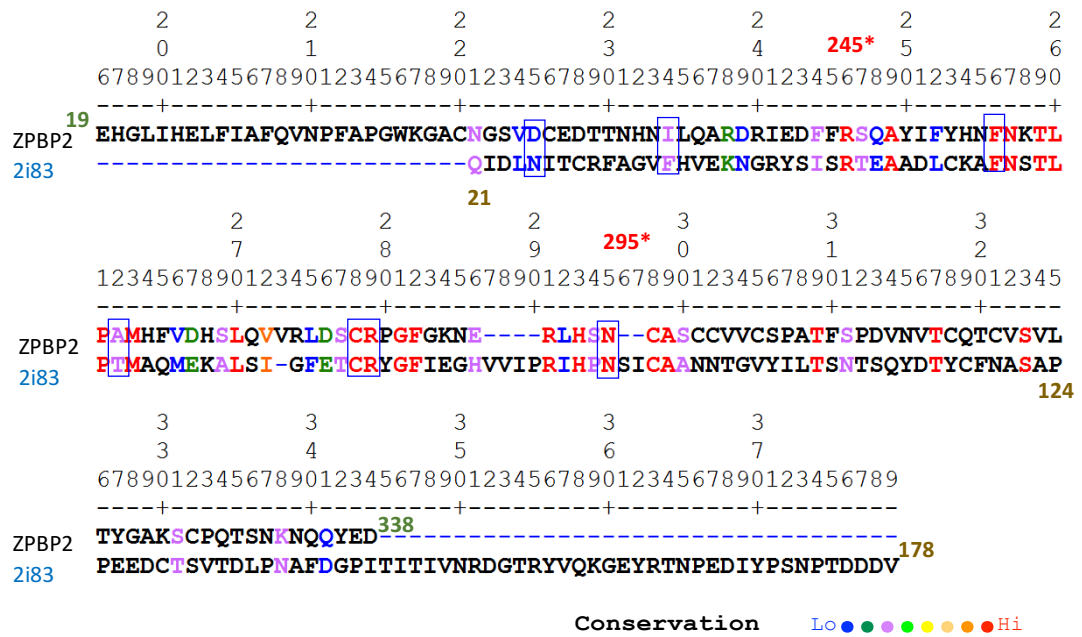


**Figure 5.6.** Residue alignment of ZPBP2 with 2i83. Residues implicated in ligand binding are bordered by boxes. Residue conservation is denoted by colours ranging from red (identical) to least conserved (blue).

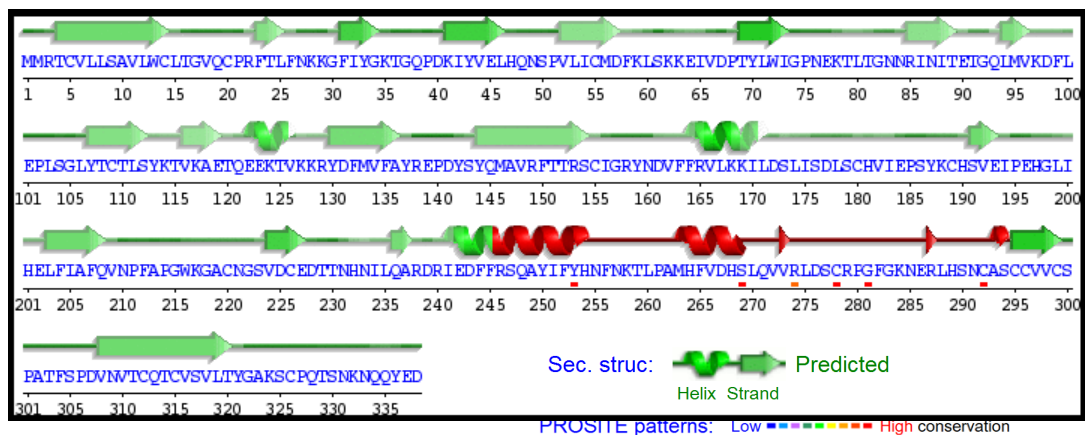


**Figure 5.7.** Predicted secondary structure (helices and strands) of ZPBP2 with the confidence for helix and strand predictions denoted by green shading (darker shade means higher confidence). Red shading signifies the Link domain signature of CD44 with the small shaded bars indicating the strongest drivers of predicted secondary structure.

PDB was used to check whether putative HA binding motifs that could influence the partitioning of proteins into binding and non-binding fractions were present in any of the 81 proteins common to the non-binding fraction. None returned a PDB code with a match to HA binding domains. The sequence alignment was also performed on ten known HA-binding proteins containing the Link module (Table 5.6\*) and eleven, randomly selected proteins from the non-binding fraction (Table 5.6<sup>†</sup>) without evidence for a Link module. SAS was then used to look for any existing structural similarities between them and the CD44 motif flagged by the PDB codes, (4pz3, 4pz4, 1uuh, 1poz and 2i83; Table 5.5). When aligned with any of PDB codes, the first seven proteins in the list had the highest Z-scores (123-321) and smallest E-values ( $4.5e^{-16}$ - $2.2e^{-5}$ ). The next three proteins (also belonging to the Link module superfamily) had lower Z-scores (50.6 -112.1) and higher E-values ( $1.9e^{-4}$ -0.38).

The eleven proteins in the non-binding fraction (Table 5.6<sup>†</sup>) occasionally showed higher percentage identities with the CD44 HA-binding domain while having no evidence for a Link module in their sequence. For example, compared with ZPBP2 with 32.7% identity following alignments with 4pz3, 4pz4, 1uuh, 2i83 and 1poz, PLIN3 has 39% identity while the corresponding Z-scores were lower and E-values higher. Similarly, Human Axonemal dynein light intermediate polypeptide 1 (O14645) also showed a high % identity with PDB codes 4pz3 and 1uuh but with a low Z-score and high E-value. The data shows that in the present study, relative Z-scores or E-values gave more accurate predictions of relationships between proteins than percentage identity. Hence, unlike any of the non-HA binding proteins, ZPBP2 has some structural similarities with the Link module of CD44.

**Table 5.6.** Relationships of Link module superfamily proteins\*, ZPBP2 and HA non-binding<sup>†</sup> proteins with PDB codes.

PDB code	Smith Waterman Score	% Identity	a.a Overlap	Seq length	Z-score	E-value	Protein name/UniProt accession number
4pz4 (a.a 18-171)	227	35	120	227	279.5	9.2e-14	TSG6_Human tumor necrosis factor-inducible gene 6 protein (P98066) *
4pz3(a.a 18-170)	227	35	120	227	279.9	8.8e-14	
1uuh(a.a 20-178)	227	35	120	227	279.9	8.8e-14	
2i83 (a.a 21-178)	227	35	120	227	279.2	9.6e-14	
1poz (a.a 20-178)	227	35	120	227	279.1	9.7e-14	
4pz4 (a.a 18-171)	259	32.6	138	322	317.6	7e-16	LYVE1_Human Lymphatic vessel endothelial hyaluronic acid receptor 1 (Q9Y5Y7) *
4pz3(a.a 18-170)	259	32.6	138	322	318	6.7e-16	
1uuh(a.a 20-178)	259	32.6	138	322	318	6.7e-16	
2i83 (a.a 21-178)	262	32.3	158	322	321	4.5e-16	
1poz (a.a 20-178)	262	32.3	158	322	320	4.6e-16	
4pz4 (a.a 18-171)	148	26.2	103	862	173	7.9e-08	Human putative uncharacterized protein DKFZp434E0321 (Fragment)( CAB61358) (Q9UF98) *
4pz3(a.a 18-170)	148	26.2	103	862	173.4	7.5e-08	
1uuh(a.a 20-178)	148	26.2	103	862	173.4	7.5e-08	
2i83 (a.a 21-178)	148	26.2	103	862	172.7	8.3e-08	

PDB code	Smith Waterman Score	% Identity	a.a Overlap	Seq length	Z-score	E-value	Protein name/UniProt accession number
1poz (a.a 20-178)	148	26.2	103	862	172.6	8.4e-08	
4pz4 (a.a 18-171)	154	29.8	94	2415	173.1	7.8e-08	Human Aggrecan core protein (P16112) *
4pz3(a.a 18-170)	154	29.8	94	2415	173.5	7.4e-08	
1uuh(a.a 20-178)	154	29.8	94	2415	173.5	7.4e-08	
2i83 (a.a 21-178)	154	29.8	94	2415	172.6	8.3e-08	
1poz (a.a 20-178)	154	29.8	94	2415	172.5	8.4e-08	
4pz4 (a.a 18-171)	123	26.1	88	340	149.6	1.6e-06	Human Hyaluronan and proteoglycan link protein 2 (BRAL1) (Q9GZV7) *
4pz3(a.a 18-170)	123	26.1	88	340	150	1.5e-06	
1uuh(a.a 20-178)	123	26.1	88	340	150	1.5e-06	
2i83 (a.a 21-178)	123	26.1	88	340	123	1.7e-06	
1poz (a.a 20-178)	123	26.1	88	340	149.2	1.7e-06	
4pz4 (a.a 18-171)	182	31.4	102	2570	207.2	9.9e-10	HUMAN Stabilin-1 (Q9NY15) *
4pz3(a.a 18-170)	182	31.4	102	2570	207.6	9.3e-19	
1uuh(a.a 20-178)	182	31.4	102	2570	207.6	9.3e-10	
2i83 (a.a 21-178)	182	31.4	102	2570	206.7	1e-09	
1poz (a.a 20-178)	182	31.4	102	2570	206.7	1e-09	



PDB code	Smith Waterman Score	% Identity	a.a Overlap	Seq length	Z-score	E-value	Protein name/UniProt accession number
4pz4 (a.a 18-171)	115	25.5	94	1321	129.3	2.2e-05	Human Neurocan core protein (O14594) *
4pz3(a.a 18-170)	115	25.5	94	1321	129.7	2e-05	
1uuh(a.a 20-178)	115	25.5	94	1321	129.7	2e-05	
2i83 (a.a 21-178)	115	25.5	94	1321	128.9	2.3e-05	
1poz (a.a 20-178)	115	25.5	94	1321	128.8	2.3e-05	
4pz4 (a.a 18-171)	123	24.3	107	911	65.4	0.075	Human Brevican core protein (Q96GW7) *
4pz3(a.a 18-170)	123	24.3	107	911	65.8	0.071	
1uuh(a.a 20-178)	123	24.3	107	911	65.8	0.071	
2i83 (a.a 21-178)	123	24.3	107	911	65.1	0.078	
1poz (a.a 20-178)	123	24.3	107	911	65	0.079	
4pz4 (a.a 18-171)	123	27.8	108	3396	111.6	0.00021	Human Versican core protein (P13611) *
4pz3(a.a 18-170)	123	27.8	108	3396	112.1	0.00019	
1uuh(a.a 20-178)	123	27.8	108	3396	112.1	0.00019	
2i83 (a.a 21-178)	123	27.8	108	3396	111.2	0.00022	
1poz (a.a 20-178)	123	27.8	108	3396	111.2	0.00022	

PDB code	Smith Waterman Score	% Identity	a.a Overlap	Seq length	Z-score	E-value	Protein name/UniProt accession number
4pz4 (a.a 18-171)	61	26.2	61	629	51	0.39	Human Sushi domain-containing protein 5 (KIAA0527) (O60279) *
4pz3(a.a 18-170)	61	26.2	61	629	51.4	0.38	
1uuh(a.a 20-178)	61	26.2	61	629	51.4	0.38	
2i83 (a.a 21-178)	61	26.2	61	629	50.6	0.4	
1poz (a.a 20-178)	61	26.2	61	629	50.6	0.41	
<b>4pz4 (a.a 18-171)</b>	<b>88</b>	<b>32.7</b>	<b>55</b>	<b>316</b>	<b>107</b>	<b>3.7e-04 (0.00037)</b>	Zona pellucida binding protein 2 (ZBP2 ) (Q6X784) *
<b>4pz3(a.a 18-170)</b>	<b>88</b>	<b>32.7</b>	<b>55</b>	<b>316</b>	<b>107.5</b>	<b>3.5e-4</b>	
<b>1uuh(a.a 20-178)</b>	<b>88</b>	<b>32.7</b>	<b>55</b>	<b>316</b>	<b>107.5</b>	<b>3.5e-4</b>	
<b>2i83 (a.a 21-178)</b>	<b>88</b>	<b>32.7</b>	<b>55</b>	<b>316</b>	<b>106.8</b>	<b>3.8e-04</b>	
<b>1poz (a.a 20-178)</b>	<b>88</b>	<b>32.7</b>	<b>55</b>	<b>316</b>	<b>106.7</b>	<b>3.9e-04</b>	
4pz4 (a.a 18-171)	40	20.7	29	215	38	0.93	Human sperm acrosome membrane-associated protein 3 (Q81XA5) †
4pz3(a.a 18-170)	40	20.7	29	215	38.3	0.92	
1uuh(a.a 20-178)	40	20.7	29	215	38.3	0.92	
2i83 (a.a 21-178)	40	20.7	29	215	37.7	0.93	
1poz (a.a 20-178)	40	20.7	29	215	37.6	0.94	

PDB code	Smith Waterman Score	% Identity	a.a Overlap	Seq length	Z-score	E-value	Protein name/UniProt accession number
4pz4 (a.a 18-171)	58	25	92	548	39.8	0.88	Human T-complex protein 1 subunit theta (P50990) <sup>‡</sup>
4pz3(a.a 18-170)	58	25	92	548	40.1	0.86	
1uuh(a.a 20-178)	58	25	92	548	40	0.86	
2i83 (a.a 21-178)	58	225	92	548	39.4	0.89	
1poz (a.a 20-178)	58	25	92	548	39.3	0.89	
4pz4 (a.a 18-171)	46	23.4	64	170	52.7	0.33	CAMP_Human Cathelicidin antimicrobial peptide (P49913) <sup>‡</sup>
4pz3(a.a 18-170)	46	23.4	64	170	53	0.32	
1uuh(a.a 20-178)	46	23.4	64	170	53	0.32	
2i83 (a.a 21-178)	46	23.4	64	170	52.4	0.34	
1poz (a.a 20-178)	46	23.4	64	170	52.3	0.34	
4pz4 (a.a 18-171)	39	23.5	34	258	42.4	0.77	Human Axonemal dynein light intermediate polypeptide 1 (O14645) <sup>‡</sup>
4pz3(a.a 18-170)	34	55.6	9	258	42.7	0.76	
1uuh(a.a 20-178)	34	55.6	9	258	42.7	0.76	
2i83 (a.a 21-178)	39	23.5	34	258	42.1	0.79	
1poz (a.a 20-178)	39	23.5	34	258	42	0.79	

PDB code	Smith Waterman Score	% Identity	a.a Overlap	Seq length	Z-score	E-value	Protein name/UniProt accession number
4pz4 (a.a 18-171)	49	38.9	18	434	33	0.99	PLIN3_HUMAN Perilipin-3 O60664 ‡
4pz3(a.a 18-170)	49	38.9	18	434	33.4	0.99	
1uuh(a.a 20-178)	49	38.9	18	434	33.4	0.99	
2i83 (a.a 21-178)	49	38.9	18	434	32.7	0.99	
1poz (a.a 20-178)	49	38.9	18	434	32.6	0.99	
4pz4 (a.a 18-171)	53	23.9	67	148	71.5	0.035	LYZL6_HUMAN Lysozyme-like protein 6 (O75951) ‡
4pz3(a.a 18-170)	50	28.1	64	148	63.2	0.099	
1uuh(a.a 20-178)	50	28.1	64	148	63.2	0.099	
2i83 (a.a 21-178)	50	28.1	64	148	62.6	0.11	
1poz (a.a 20-178)	50	28.1	64	148	62.5	0.11	
4pz4 (a.a 18-171)	38	25	32	150	52.8	0.32	Human Cytochrome c oxidase subunit 5A, mitochondrial (P20674) ‡
4pz3(a.a 18-170)	38	25	32	150	53.1	0.31	
1uuh(a.a 20-178)	38	25	32	150	53.1	0.31	
2i83 (a.a 21-178)	38	25	32	150	52.6	0.33	
1poz (a.a 20-178)	38	25	32	150	52.5	0.33	

PDB code	Smith Waterman Score	% Identity	a.a Overlap	Seq length	Z-score	E-value	Protein name/UniProt accession number
4pz4 (a.a 18-171)	45	23.3	43	381	50.1	0.43	Human Putative heat shock protein HSP 90-beta 2 (Q58FF8) ‡
4pz3(a.a 18-170)	45	23.3	43	381	50.4	0.41	
1uuh(a.a 20-178)	45	23.3	43	381	50.4	0.41	
2i83 (a.a 21-178)	45	23.3	43	381	49.8	0.44	
1poz (a.a 20-178)	45	23.3	43	381	49.7	0.44	
4pz4 (a.a 18-171)	33	17.4	46	369	24.5	1	Human Hsc70-interacting protein (P50502) ‡
4pz3(a.a 18-170)	33	17.4	46	369	24.8	1	
1uuh(a.a 20-178)	33	17.4	46	369	24.8	1	
2i83 (a.a 21-178)	36	19.4	36	369	40.2	0.86	
1poz (a.a 20-178)	36	19.4	36	369	40.1	0.86	
4pz4 (a.a 18-171)	41	25.4	59	378	30.4	1	Human Hsp90 co-chaperone Cdc37 (Q16543) ‡
4pz3(a.a 18-170)	41	25.4	59	378	30.8	1	
1uuh(a.a 20-178)	41	25.4	59	378	30.8	1	
2i83 (a.a 21-178)	41	25.4	59	378	30.1	1	
1poz (a.a 20-178)	41	25.4	59	378	30	1	

PDB code	Smith Waterman Score	% Identity	a.a Overlap	Seq length	Z-score	E-value	Protein name/UniProt accession number
4pz4 (a.a 18-171)	41	24	75	507	24.4	1	ARSA_HUMAN Arylsulfatase A (P15289) ‡
4pz3(a.a 18-170)	38	22	50	507	39.5	0.88	
1uuh(a.a 20-178)	38	22	50	507	39.5	0.88	
2i83 (a.a 21-178)	42	23.7	76	507	40	0.87	
1poz (a.a 20-178)	42	23.7	76	507	39.9	0.87	

### 5.4.3. Western blotting to confirm the results of proteomics

To confirm the results obtained by tandem mass spectrometry (LC-MS/MS), Western blotting using antibodies against ZPBP2 and ADAM32 was performed on HA-binding and non-binding fractions from 4 individual samples (Figure 5.8). ZPBP2 and ADAM32 were chosen because of the structural similarities between a sequence in ZPBP2 and the hyaluronic acid binding domain of CD44 and ADAM32 has two BX7B motifs. Antibodies against ZPBP2 and ADAM32 detected protein bands at approximately 38 kDa and 85 kDa, respectively in HA-binding fractions (Lanes 2, 4, 6, 8), consistent with the sequencing data. Additional bands at ~36 kDa and 42 kDa were revealed using the antibody to ZPBP2. No protein bands were observed in non-binding fractions (Lanes 1, 3, 5, 7). An antibody against Alpha-tubulin (as a loading control) detected a single band at approximately 50 kDa in all samples from both fractions.

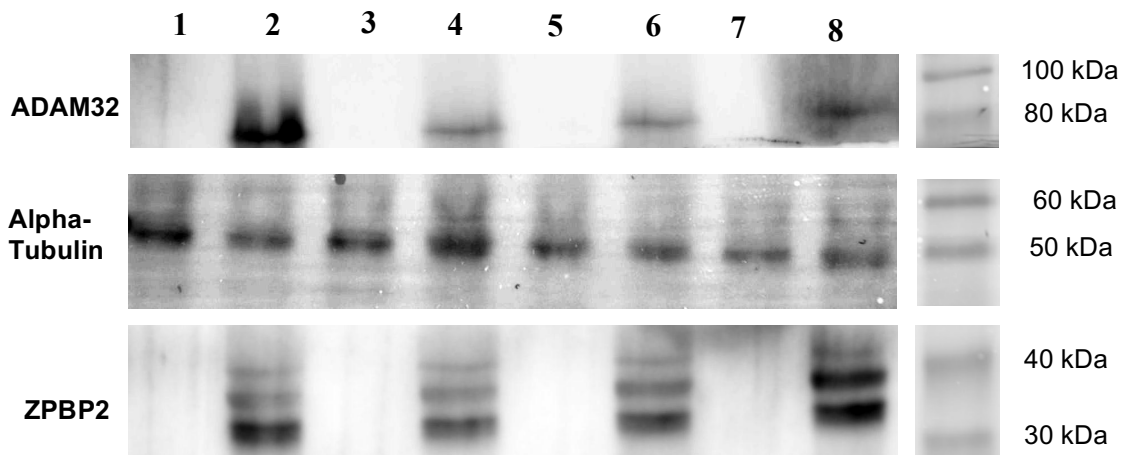


**Figure 5.8.** Western blotting on HA-binding and non-binding proteins using antibodies against ZPBP2 and ADAM32. Lanes 1, 3, 5 and 7 represent HA non-binding fractions. HA-binding fractions were loaded in wells 2, 4, 6 and 8. Alpha-tubulin was used as a loading control.

## 5.5. Discussion

In addition to its presence in the cumulus oophorus complex, HA also permeates and is an integral part of the zona pellucida and the perivitelline space of mammalian oocytes (Vandevoort et al., 1997). HA is a non-sulphated glycosaminoglycan and the zona pellucida is composed of a reticular meshwork of sulphated glycoproteins (ZP2, ZP3 and ZP1/ZP4; (Lin et al., 2007). The present study was conducted to search for novel HABPs in human sperm by allowing the soluble proteins extracted from homogenised sperm to interact with an HA-coated surface before their recovery and characterisation by LC-MS/MS. This panning process (Amemiya et al., 2005) resulted in the identification of 28 proteins (HA-binding fraction) with a range of functions based on their gene ontology and one protein (ZPBP2), with evidence for a sequence related to the HA-binding domain of CD44 (Takeda et al., 2006; Liu and Finzel, 2014a; Teriete et al., 2004; Torabi et al., 2017b). Based on the proportion of positively charged proteins in the binding versus non-binding fractions of extracted sperm proteins, additional interactions may have arisen via electrostatic attraction (Lenormand et al., 2008; Purcell et al., 2014).

ZPBP2 is a paralogue of the acrosomal matrix protein ZPBP1 located in the rostral ridge of the acrosome (Lin et al., 2007) and was first identified when looking for genes associated with ZNFN1A3 (Zinc Finger Protein, Subfamily 1a; (Kato and Kato, 2003). ZPBP1 and 2 belong to the immunoglobulin like domain containing family (Lin et al., 2007) and are co-designated by sequence similarity. In humans, ZPBP2 has at least two known isoforms of 338 (38.6 kDa) and 316 (36.2 kDa) amino acids, respectively, both of which have an N-terminal signal peptide and 15 conserved cysteines. These, and an additional band at ~42 kDa were only detected in the binding fraction by Western blotting (Figure 5.8). The additional ~42 kDa band may represent a novel isoform of this protein (Lin et al., 2007). The 36 kDa isoform has 23 fewer residues (18-39) and alongside the 38.6 kDa isoform, has four N-glycosylation sites and shares approximately 37% identity with ZPBP1. Both ZPBP1 and ZPBP2 are located on the acrosome and the role of the former in binding the zona pellucida is well documented (Mori et al., 1993; Mori et al., 1995). Absence of ZPBP1 causes male sterility with abnormal head morphology while ZPBP2 knockout



mice are sub-fertile mice with sperm showing head deformation and reduced zona penetration. The consensus is that ZPBPs are important acrosomal proteins involved in interaction with the zona pellucida during sperm penetration (Lin et al., 2007).

SAS determines and applies unique identifiers from different crystallographic (X-ray or Nuclear Magnetic Resonance) submissions, which in the case of the ZPBP2 covered five records (PDB codes 4pz3, 1uuh, 4pz4, 2i83 and 1poz) relating to the HA-binding (Link) domain of CD44 (Teriete et al., 2004; Liu and Finzel, 2014a; Takeda et al., 2006). The structural similarities highlighted between ZPBP2 and CD44 did not extend to ZPBP1. CD44 is one of the better understood HA binding proteins and is a type I transmembrane protein located on the surface of many different cell types including mammalian sperm as reported previously (Bains et al., 2002). The location of CD44 on the sperm surface has also been shown to alter during and following capacitation and the acrosome reaction (Torabi et al., 2016). CD44 binds HA through a disulphide-bond stabilized HA-binding domain (HABD) including the Link module (residues 32-124) and some additional residues at the N-terminal (residues 21-31) and C-terminal ends (residues 125-178) (Takeda et al., 2006). CD44 has many different isoforms due to alternative splicing of several exons in the proximal region of the extracellular domain and also post-translational modifications (Toole, 2004; Oliferenko et al., 2000). The HABD is highly conserved amongst CD44 isoforms (Liu and Finzel, 2014b). The exact identities of the CD44 isoforms of spermatozoa are not known.

ADAM32 (disintegrin and metalloproteinase domain-containing 32) belongs to the ADAM family of metalloproteases. ADAMs are widely expressed proteins with potential functions in cell adhesion and ADAM32 has been identified as a type I non-catalytic metalloprotease-like transmembrane protein (Wolfsberg et al., 1995). Western blot analysis confirmed that this protein (~85 kDa) was confined to the HA binding fraction. Due to the presence of an active metalloprotease domain, these proteins may also have protease activity (Glasse and Civetta, 2004). To date 29 ADAMs have been identified of which 15 are expressed in testis (Primakoff and Myles, 2000). This suggests a specific relationship between ADAM function,

spermatogenesis and fertilisation. ADAM1 (fertilin alpha), ADAM2 (fertilin beta) and ADAM3 (cyritestin) interact with integrin in the egg plasma membrane of mouse oocytes (Wassarman et al., 2001). ADAM32 is synthesised during spermatogenesis and processed during epididymal maturation to become localised on the sperm surface (Kim et al., 2006).

HABPs bind HA through a variety of motifs including the Link module of CD44, TSG-6, versican, link protein, brevican, aggrecan and neurican. The BX7B motif has been reported in RHAMM, CD44 and HABP1 among many others (Yang et al., 1994; Day and Prestwich, 2002). Midkine (MK) is a secreted growth factor rich in basic amino acids and cysteine with a molecular weight of approximately 13 kDa (Jono and Ando, 2010). The two BX7B motifs in ADAM32 and Cilia- and flagella-associated protein 20 and the four in Midkine may help explain the presence of these proteins in the binding fraction although to date, neither protein has been reported to have HA binding properties (Zaleski et al., 2006; Yang et al., 1994).

Work is in progress to modify the HA substrate in order to improve its capacity to recognise and bind HABPs.

## **5.6. Conclusion**

Different proteins were identified in the HA-binding and non-binding fractions. As determined by LC-MS/MS and verified using Western blotting, ZPBP2 and ADAM32 were found only in the HA-binding fraction and both could therefore be considered as novel HABPs. Midkine and Cilia- and flagella-associated protein 20 may also have HABP properties.

## **Chapter 6: Isolation of hyaluronic acid binding proteins from bovine sperm using affinity chromatography**

### **6.1. Introduction**

As discussed several alternative methods for sperm selection have been introduced. Methods for selecting higher quality sperm that might augment or replace standard procedures. As one of the main components of the cumulus oophorus complex (Hong et al., 2009), HA-binding is being used as a diagnostic tool for evaluation of sperm maturity. In the second chapter it was shown that HA-binding is able to separate sperm with high DNA integrity and chromatin maturity which is important to be considered as an indicator for assessment of a good sperm separation method.

Hyaluronic acid plays its diverse biological function through the interaction with its HABPs (Dicker et al., 2014). HABPs are ubiquitous proteins in nature with various cellular functions including cell signaling, tumour invasion, sperm motility/maturity and cell adhesion (Ranganathan et al., 1994; Rao et al., 1996). They are also involved in successful fertilisation following penetration through the cumulus oophorus matrix enveloping the oocyte and binding with the zona pellucida; a complex and essential process which can only take place following spermatogenesis, maturation and capacitation (Reid et al., 2011; Gadella, 2010). Sperm from different species are reported to express HABPs on their surface including hyaluronidase PH-20 (SPAM1) and hyaluronic acid binding protein 1 (HABP1) (Hunnicuttt et al., 1996; Kimura et al., 2009; Ghosh et al., 2007).

CD44 and the receptor for hyaluronic acid mediated motility (RHAMM), however, are the best described HABPs on the human sperm surface and their presence in bovine sperm was investigated for the first time in this study. CD44 is a broadly expressed cell surface glycoprotein with many different isoforms ranging 70 to > 220 kDa (Thorne et al., 2004; Martegani et al., 1999; Ahrens et al., 2001). CD44 is present in many human tissues including cervical epithelium (Woerner et al., 1995), endometrium (Saegusa et al., 1998; Albers et al., 1995), oocyte/cumulus oophorus complex and early embryos (Furnus et al., 2003). Different isoforms of CD44

including 68 kDa and 73 kDa have been reported on human sperm (Ranganathan et al., 1994; Bains et al., 2002).

RHAMM is an intracellular protein (with the ability to be transported to the cell membrane) and its interaction with microtubules and actin filaments may play an essential role in cytoskeletal configuration (Hall et al., 1994; Zhang et al., 1998). Different isoforms of human RHAMM including 58, 60, 64, 70, and 84 kDa variants have been reported (Hofmann et al., 1998). To date, RHAMM with molecular masses of 58 and 64 kDa have been identified on human sperm and more specifically on sperm head, midpiece and tail (Kornovski et al., 1994). The interaction between hyaluronic acid and RHAMM results in phosphorylation of different intracellular proteins including the focal adhesion kinase pp125<sup>FAK</sup>, which leads into the reorganisation of actin filament and the extracellular matrix that are essential for cell movement (Turley et al., 1994; Assmann et al., 1999; Hall et al., 1994).

As very little is known about HABPs in bovine sperm, the current study focused on their presence and changes in their localisation and distribution following capacitation and the acrosome reaction (Chapter 3). This chapter details results of attempts to couple HA to agarose for affinity chromatography purification of bovine sperm HABPs, aimed ideally at subsequent proteomic analysis.

Several different methods have been introduced for identification of cell surface proteins including ultra-centrifugation, sequential extraction, two-phase partitioning and biotinylation of cell surface proteins (Huber et al., 2003; McCarthy et al., 2009; Schindler and Nothwang, 2006; Rybak et al., 2005; Scheurer et al., 2005).

As biotinylation is one of the most efficient methods for tagging and recovering proteins (Elia, 2012; Elia, 2008), affinity chromatography and biotinylation of sperm surface proteins were both investigated for this purpose. Initially, capture of HABPs was explored using a bespoke agarose-based affinity column following activation of HA and coupling to sepharose beads (Tengblad, 1979). In parallel, biotinylation of sperm surface proteins was achieved using a water-soluble EZ-Link Sulfo-NHS-LC-

biotin analogue (Elia, 2008). This reagent had several unique advantages that made it an ideal candidate for labelling of cell surface proteins. First it is highly soluble in aqueous buffers. Second, due to the presence of sodium sulfonate groups, the reagent cannot permeate the cell membrane and is particularly well suited for only labelling surface proteins with primary amines. Third, the presence of a long spacer arm in this reagent enhances binding to avidin-based supports. Ultimately, the disulphide bridge located in the linker could easily be cleaved during protein extraction using reducing agents (Elia, 2012).

The main aim of the experiment was to use HA-affinity to enrich HABPs from a solution of biotinylated proteins from the sperm extracts and then use a streptavidin-coated bead complex (Chivers et al., 2011) to recover the affinity enriched proteins for subsequent analysis.

## **6.2. Hypothesis and objectives**

The working hypothesis is that HA affinity chromatography is effective at resolving HA-binding from non-binding proteins. In this regard, the main objective of the current study was to attempt an isolation of those proteins for subsequent analysis using an affinity chromatography based approach.

### 6.3. Materials and methods

#### 6.3.1. Reagents used

Hyaluronic acid (1500 kDa) was obtained from Creative PEGWorks (USA). FITC-streptavidin was purchased from BD Pharmingen (UK). Hyaluronidase was obtained from Sigma-Aldrich (UK). EZ-Link Sulfo-NHS-LC-Biotin, Pierce BCA protein assay kit and HRP-streptavidin were obtained from Thermo Fisher Scientific (UK). Affi-Gel 102, 1-ethyl-3-(3-dimethylaminopropyl) carbodiimide hydrochloride (EDAC), Bradford protein assay reagent and Glass Econo-Columns were obtained from Bio-Rad (UK). To avoid repetition, the reagents that were used in the other chapters are not listed.

#### 6.3.2. Sample preparation

Six straws of a frozen bovine semen were thawed at 39 °C for 30 seconds in water bath prior to use. Table 6.1 describes the semen parameters related to each straw. Seminal plasma and debris were removed by washing the samples with PBS at 500 x g for 10 min (x3).

**Table 6.1.** Semen parameters of the bull sample used in the study.

Bull name	Bull no.	Sperm count/mL	Motility %	Semen volume per straw (µL)
Classic (straw 1)	116218	28.5 x 10 <sup>6</sup>	69	250
Classic (straw 2)	116218	27.4 x 10 <sup>6</sup>	67.5	250
Classic (straw 3)	116218	28 x 10 <sup>6</sup>	71	250
Classic (straw 4)	116218	27 x 10 <sup>6</sup>	66	250
Classic (straw 5)	116218	27.8 x 10 <sup>6</sup>	69.3	250
Classic (straw 6)	116218	28.3 x 10 <sup>6</sup>	65	250

### **6.3.3. Biotinylation of sperm surface proteins**

Cold PBS (2 mL) was used to wash sperm from seminal plasma (500  $\mu$ L) at 500 x g for 10 min. Biotinylation was performed according to manufacturer's instruction (Thermo Fisher Scientific). Approximately  $25 \times 10^6$  sperm were re-suspended in 1 mL PBS and 1 mg Sulfo-NHS-LC-Biotin was added. The reaction mixture was incubated for 30 min at RT with constant shaking. In order to quench and remove additional biotin, sperm were washed with a solution of 100 mM glycine in PBS followed by centrifugation at 500 x g for 15 minutes (all centrifugation steps were performed at 4°C). Supernatants were discarded. Fluorescent labelling of biotinylated sperm with streptavidin-FITC was performed to validate the efficiency of biotinylation process.

### **6.3.4. Detection of biotin labelled sperm using streptavidin-FITC**

About  $1 \times 10^6$  of biotinylated and non-biotinylated (as a negative control) sperm were resuspended in PBS and cytospun on Poly-L-Lysine coated slides. After air drying, 50  $\mu$ L of 3% (w/v) bovine serum albumin (fatty acid free,  $\geq 96\%$ ) in PBS was placed on the slides and incubated for 60 min at RT to block non-specific binding. The slides were then washed with PBS prior to incubation with 100  $\mu$ L of a mixture of streptavidin-FITC (1:1000 dilution of 0.5 mg/mL in PBS) and DAPI (1:5000 dilution) for 60 min at RT in a humid chamber in darkness. The slides were then washed with 30 mL PBS in a coplin jar three times and each time for 15 min. The slides were viewed with a Leica LEITZ DMRB fluorescence microscope. The microscope was equipped with FITC, TRITC and DAPI filters with excitation/emission filter 495 nm/520 nm, 541 nm/572 nm and 358 nm/461 nm, respectively. SmartCapture 3 software was used to image the slides.

### **6.3.5. Extraction of biotinylated sperm surface proteins**

400  $\mu$ L of the lysis buffer containing 20 mM Tris, 150 mM NaCl, 2 mM EDTA, 1% Triton X-100 and 1 mM PMSF were added to  $100 \times 10^6$  biotinylated sperm in an Eppendorf tube (1.5 mL). The suspension was sonicated on ice 15 seconds on, 40 seconds off, at an amplitude of 15 microns. The sonication was repeated 5 times and the suspension was incubated for 1h at 4°C. Solubilised proteins were collected

from the supernatant by centrifugation at 16000 x g for 20 min at 4°C. The same procedure was used to extract proteins from non-biotinylated sperm as a control for further experiments.

### **6.3.6. Protein quantification using Bradford assay**

Coomassie blue interacts with proteins and leads to a shift in absorption from 365 nm to 595 nm. The reagent was used according to the manufacturer's microplate assay protocol (Quick Start™ Bradford Protein Assay, BioRad). Five (5) µL of 2, 1, 0.5, 0.25 and 0.125 mg/mL of BSA (fatty acid free, ≥96%) were added to separate wells of a 96 microplate (Greiner Bio-One, Germany) as standard. Five (5) µL of the lysis buffer (Section 6.3.5) was used as the blank. Five (5) µL of non-biotinylated and biotinylated proteins were used for protein quantification. 250 µL of Bradford dye solution was added to each well and mixed. The absorption was then measured at 595 nm in a spectrophotometer (Varioskan, Thermo Science). A standard curve was generated, and protein concentration was calculated based on the standard curve.

### **6.3.7. Sodium Dodecyl Sulphate Polyacrylamide Gel Electrophoresis (SDS-PAGE)**

SDS-PAGE (10% resolving and 4% stacking gels) followed by silver staining of resolved proteins (see Section 6.3.8) was performed to check the presence of extracted proteins. Non-biotinylated proteins (negative control) were used to show that bands developed after addition of HRP-streptavidin were specifically due to biotinylated proteins. To check the presence of biotinylated proteins, different concentrations of biotinylated proteins (10, 30, 50 and 100 µg/mL) were diluted with 2x Laemmli buffer (Chapter 5) and boiled for 5 min at 95°C. Non-biotinylated proteins with the same concentrations were used as controls. The samples were then loaded onto the gel and run at 120 V for 100 min in 1x SDS-PAGE running buffer as described in Chapter 5.

### **6.3.8. Silver staining**

Gel silver staining was performed (Morrissey, 1981). Briefly, the gel was fixed for 30 minutes at RT using a solution of 5% acetic acid (v/v) and 5% ethanol (v/v). After



fixation, the gel was washed with distilled water and incubated in a mixture of solution 1 (1 mL 2 M NaOH, 20 mL pure H<sub>2</sub>O, 1.3 mL ammonia) and solution 2 (3 mL of 10% silver nitrate (w/v), 17 mL pure H<sub>2</sub>O) for 60 min. After staining, the gel was thoroughly washed with water (x3) and then incubated in developer solution containing 1 mL of 1% citric acid (w/v) and 100 µL formaldehyde in 100 mL pure H<sub>2</sub>O until bands appeared. After the development step, the process was stopped by immersing the gel in stop solution containing 2% acetic acid (v/v).

### **6.3.9. Western blotting**

Western blot was performed to monitor the presence of biotinylated proteins. The same transfer procedure as explained in Chapter 5 was followed. Briefly, proteins were transferred to a PVDF membrane at 250 mA for 75 min. Following 1h blocking of the membrane in 3% (w/v) non-fat milk in TBS containing 0.5% Tween (v/v, TBS.T) at RT, HRP-streptavidin (1:1000 dilution of 0.5 mg/mL, in PBS) was introduced for 1h at RT. Following washing with TBS.T, the bands were visualised as explained in Chapter 5.

### **6.3.10. Hyaluronic acid-agarose affinity chromatography column**

#### **6.3.10.1. Digestion of HA to oligomers**

In order to bind HA to a solid matrix (Affi-Gel 102 amino-terminal crosslinked agarose gel), it was digested to smaller oligomers with a hyaluronidase from bovine testes (Banerjee and Toole, 1991). Briefly, 8 mL of 0.05 M C<sub>2</sub>H<sub>3</sub>NaO<sub>2</sub> and 0.15 M NaCl (pH 5) were added to 50 mg HA. The HA solution was digested by adding 4000 units of bovine testicular hyaluronidase (pre-dissolved in above buffer) and incubated for 5h at 37°C.

#### **6.3.10.2. Preparation of HA affinity chromatography column**

Hyaluronic acid binding to Affi-Gel 102 amino-terminal crosslinked agarose gel was performed according to Tengblad (Tengblad, 1979) and the manufacturer's instructions (Bio-Rad, UK) using 1-ethyl-3-(3-dimethylaminopropyl) carbodiimide hydrochloride coupling reagent (EDAC). The mechanism of this reaction involves two steps including 1) activation of carboxyl groups on HA using EDAC and 2)

reaction between activated carboxyl groups with amino groups in Affi-Gel 102 amino-terminal crosslinked agarose gel. Figure 6.1 illustrates the mechanism of this reaction.

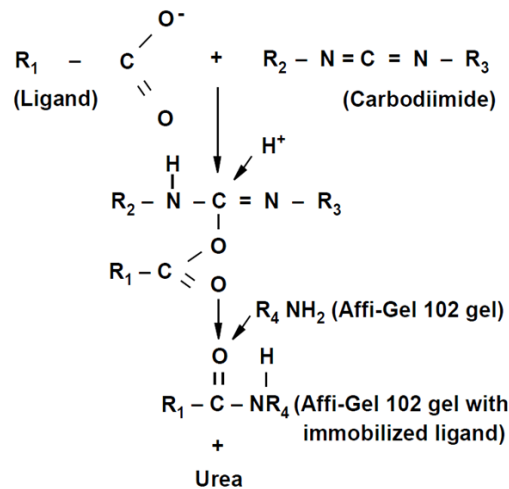


**Figure 6.1.** Mechanism of HA binding to Affi-Gel 102 amino-terminal crosslinked agarose gel (taken from <http://www.bio-rad.com/webroot/web/pdf/lsr/literature/LIT329.pdf>).

Briefly, 50 mg hyaluronic acid (pre-digested) were added to 10 mL Affi-Gel 102 amino-terminal crosslinked agarose gel and the pH was reduced to 4.8-5 using 1M HCl. Ten (10) mg EDAC were added and the pH was adjusted to 4.8-5. The solution was left at room temperature overnight with constant shaking. The excess amino groups were blocked by incubating the mixture with 1 mL acetic acid for 3h at RT. Packing of the gel into a Bio-Rad glass column (length: 20 cm, inner diameter: 1.5 cm) was performed following sequential washes (x3 times 10 bed volumes each, approximately 100 mL) with 500 mM NaCl, 100 mM C<sub>2</sub>H<sub>3</sub>NaO<sub>2</sub>, pH 4.0 followed by 100 mM Tris-HCl and 500 mM NaCl, pH 8.3 (Choi-Miura et al., 1996).

### **6.3.10.3. Affinity chromatography**

The column was washed with PBS (10 bed volumes). Biotinylated proteins were added to the column (flow rate: 30 mL/h) and then incubated for 60 min at room temperature. Pharmacia P-1 peristaltic pump with feature of low pulsation flow from 0.6-500 mL/h was used to adjust the flow rate. The flow-through proteins were collected and the volume was measured using an electronic pipette to make sure that the flow rate was adjusted to 30 mL/h. Non-binding proteins were removed by washing the column with 5 mL of the same lysis buffer (4 times) used for protein extraction (20 mM Tris, 150 mM NaCl, 2 mM EDTA, 1% Triton X-100 (v/v), 1 mM PMSF and 1x protease inhibitor cocktail). A solution of 0.2 M glycine-HCl (pH 2.5) was then used to elute HA-binding proteins and the pH was immediately adjusted to 7.2. Protein fractions were dialysed against PBS using Amicon Ultra-15 centrifugal device (Millipore) as described in Section 5.3.5. Amicon Ultra-0.5 mL centrifugal filters were then used to concentrate the proteins at 14000g for 30 min after dialysis. Protein quantification was then performed on each fraction.

### **6.3.11. Measurement of protein concentration using BCA assay**

A BCA (bicinchoninic acid) assay was used instead of the Bradford assay for protein quantification as after eluting the proteins from the column the resulting solution was not compatible with the reagents used for Bradford assay. Ninety-six (96) well microplates (Greiner Bio-One, Germany) were used for protein measurement using BCA assay according to manufacturer's instruction (Pierce BCA Protein Assay Kit, Thermo Scientific). Briefly, 10  $\mu$ L of each protein sample was loaded into a microplate well (as duplicates) and measured alongside different concentration of BCA as standard (125-2000  $\mu$ g/mL). Two hundred (200)  $\mu$ L of the working solution (50:1, Reagent A: B) was added, and the plate incubated at 37°C for 30 min. The absorption was measured at 562 nm in a spectrophotometer (Varioskan, Thermo Science) and the protein concentration was calculated using the standard protein curve.

### **6.3.12. SDS-PAGE and silver staining on proteins recovered from HA-agarose column**

Different protein fractions recovered from the column were separated using SDS-PAGE and silver stained as described previously (Sections 6.3.7 and 6.3.8). It should be noted that HRP-streptavidin was used for detection of biotinylated proteins.

### **6.3.13. Western blotting on proteins recovered from HA-agarose column**

Western blotting was carried out on different protein fractions recovered from the HA-agarose column including flow-through, non-binding and binding proteins as described in Section 6.3.9. It should be noted that no antibody was used for this experiment. The reason is that biotinylated proteins were separated using SDS-PAGE and as a result, HRP-streptavidin was needed to detect biotinylated proteins. Figure 6.2 shows flow diagram of the approach used in the present study.

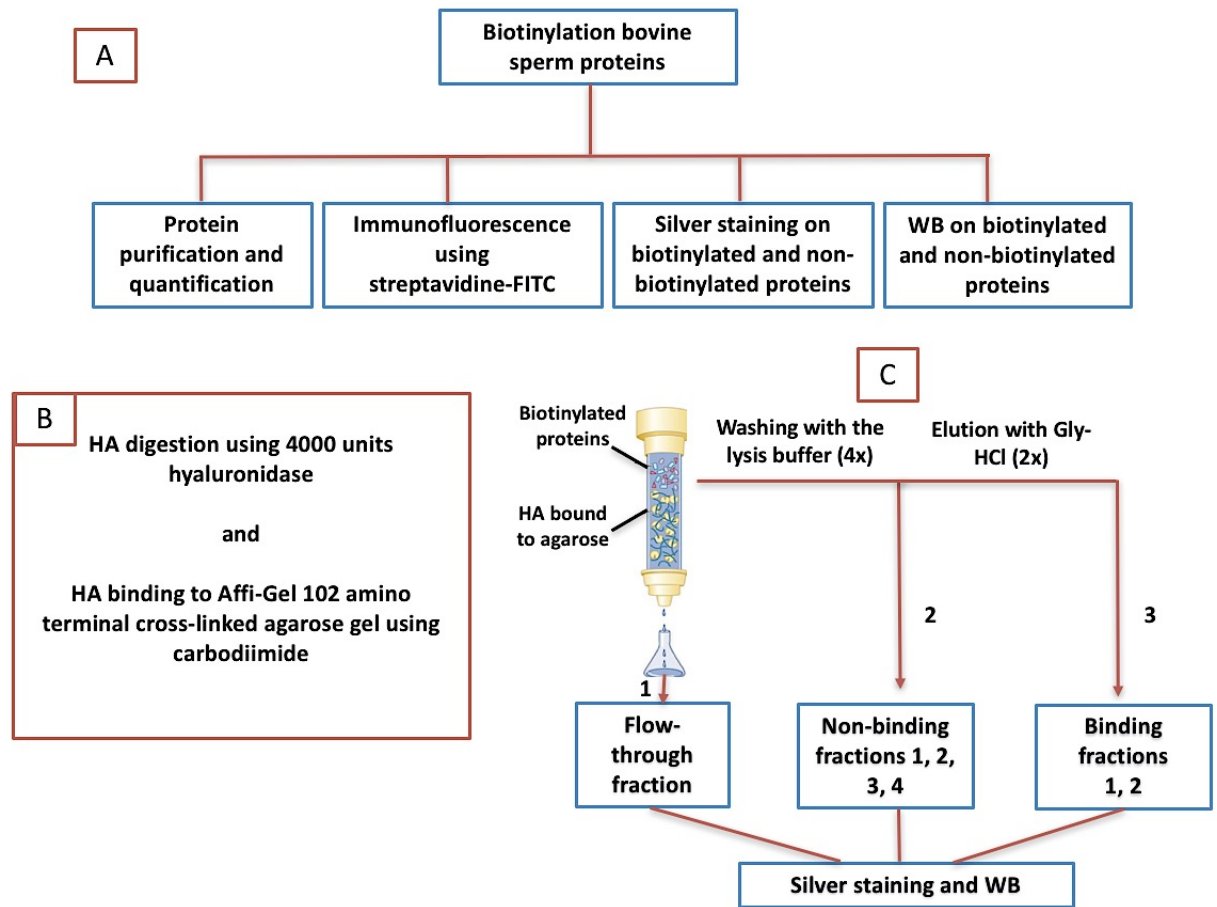


**Figure 6.2. Flow diagram outlining the approach used in the current study.**

Bovine sperm were biotinylated and the efficiency of biotinylation was checked using streptavidin-FITC. Biotinylated proteins were then extracted for further SDS-PAGE, silver staining and WB analysis (6.2A).

Hyaluronic acid was digested using a hyaluronidase and HA fragments were bound to Affi-Gel 102 amino terminal cross-linked agarose gel using carbodiimide (6.2B). Biotinylated proteins were then added to the HA-agarose column. Different flow-through, non-binding and binding fractions were collected for further silver staining and WB (6.2C).

## 6.4. Results

### 6.4.1. Biotinylation

#### 6.4.1.1. Fluorescent labelling of biotinylated bovine sperm surface proteins

In order to confirm successful biotinylation of sperm surface proteins, fluorescent tagging was carried out using FITC conjugated streptavidin on samples of biotinylated and non-biotinylated (control) sperm.

Green fluorescence was emitted only from different regions of biotinylated sperm including the head, tail and neck and not from any non-biotinylated sperm. Therefore, it confirms that the method used for biotinylation of sperm surface proteins was successful. This experiment was performed on sperm obtained from each straw (Table 6.1) and each showed similar labelling patterns. Representative examples are shown in Figure 6.3.

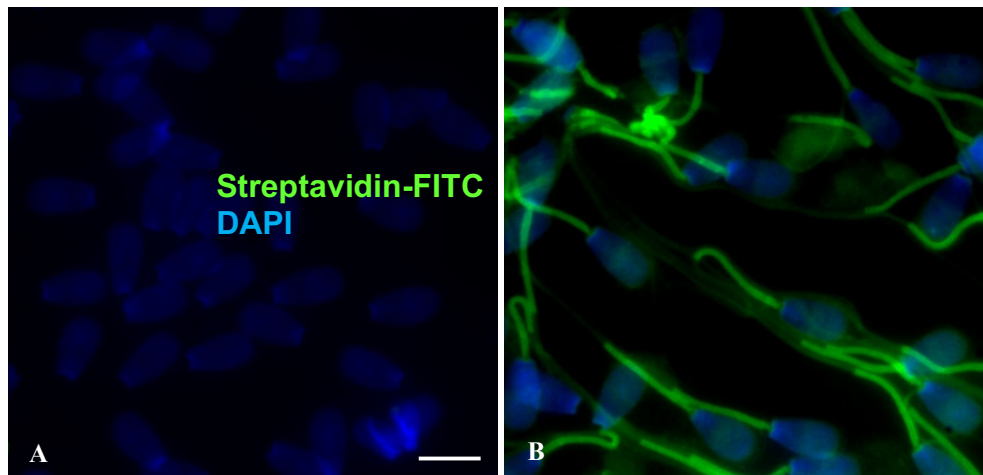


**Figure 6.3. Fluorescence images of sperm probed with streptavidin-FITC following biotinylation of bovine sperm surface proteins.**

A: Non-biotinylated bovine sperm, B: biotinylated bovine sperm. The scale bar is 20  $\mu\text{m}$ .

#### 6.4.1.2. Quantification of biotinylated bovine sperm surface proteins

As shown in Figure 6.4, the standard curve was generated by plotting optical density (OD) values (at 595 nm) against protein concentration (BSA: mg/mL). The Bradford assay indicated an insufficient amount of protein available from sperm in a single straw; therefore, 6 straws (Table 6.1) were pooled in order to obtain sufficient

material for biotinylation and subsequent analysis. Samples (standards, biotinylated proteins, non-biotinylated, blank) were measured in duplicate. The final concentrations of non-biotinylated and biotinylated proteins were calculated at 1.84 mg/mL and 1.85 mg/mL, respectively.

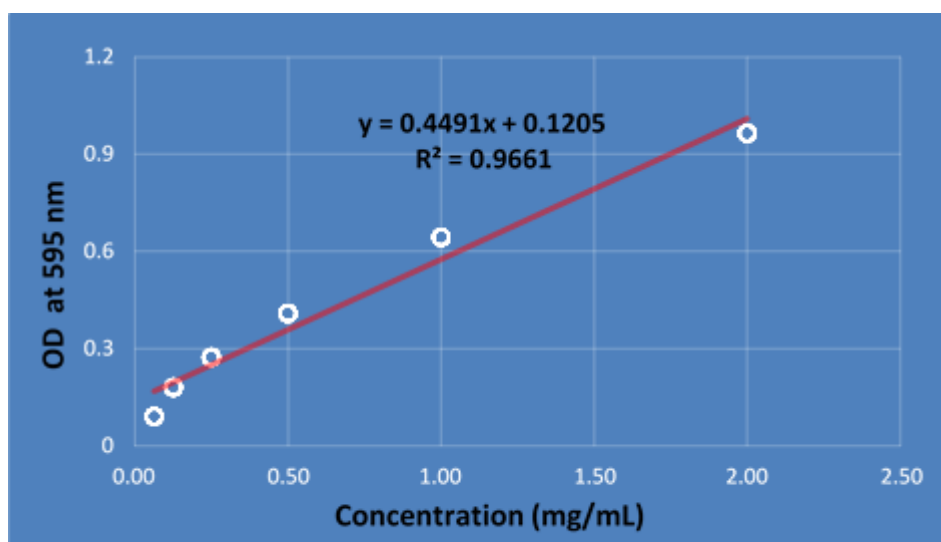


**Figure 6.4.** Standard protein curve generated from Bradford assay.

### 6.4.1.3 Silver staining on non-biotinylated and biotinylated bovine sperm proteins

Different concentrations of non-biotinylated and biotinylated bovine sperm proteins were resolved by SDS-PAGE and the proteins visualised by silver staining. As presented in Figure 6.5, very similar protein bands were identified in both non-biotinylated and biotinylated fractions showing that the biotinylation process did not affect protein extraction. To test whether or not some of these proteins were biotinylated, Western blotting using HRP-streptavidin was performed. This experiment was examined 3 times and similar results were obtained each time.

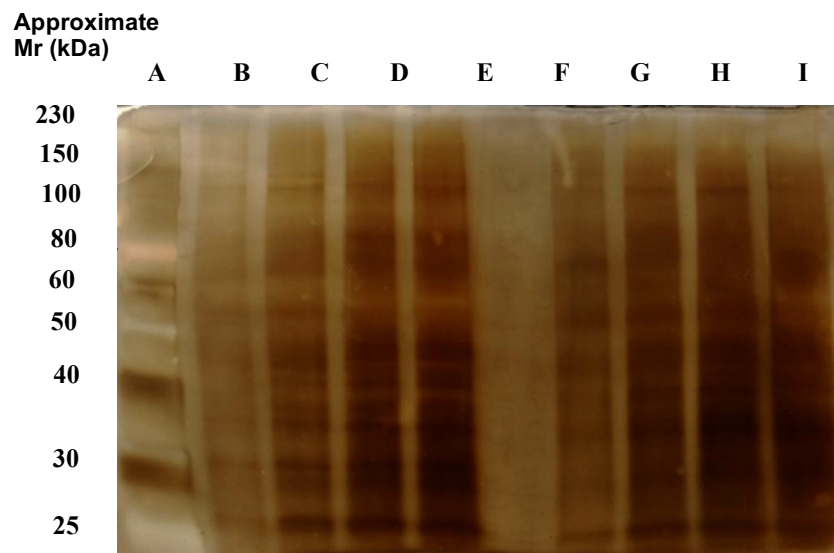


**Figure 6.5. Silver staining on biotinylated and non-biotinylated proteins after SDS electrophoresis in polyacrylamide gels.**

A) Protein ladder (10-230 kDa), B-E) Non-biotinylated proteins (10, 30, 50 and 100 µg, respectively), F) Empty lane, G-I) Biotinylated proteins (10, 30, 50 and 100 µg, respectively).

### 6.4.1.4. Western blot on non-biotinylated and biotinylated bovine sperm proteins

The existence of biotinylated proteins was confirmed by the emission of chemiluminescence (Figure 6.6, lanes F-H), whereas no chemiluminescence was emitted from non-biotinylated proteins (lanes B-D). Similar to Section 6.4.1.3, this experiment was carried out 3 times and each time chemiluminescence was omitted only from biotinylated sperm confirming the success of biotinylation protocol.



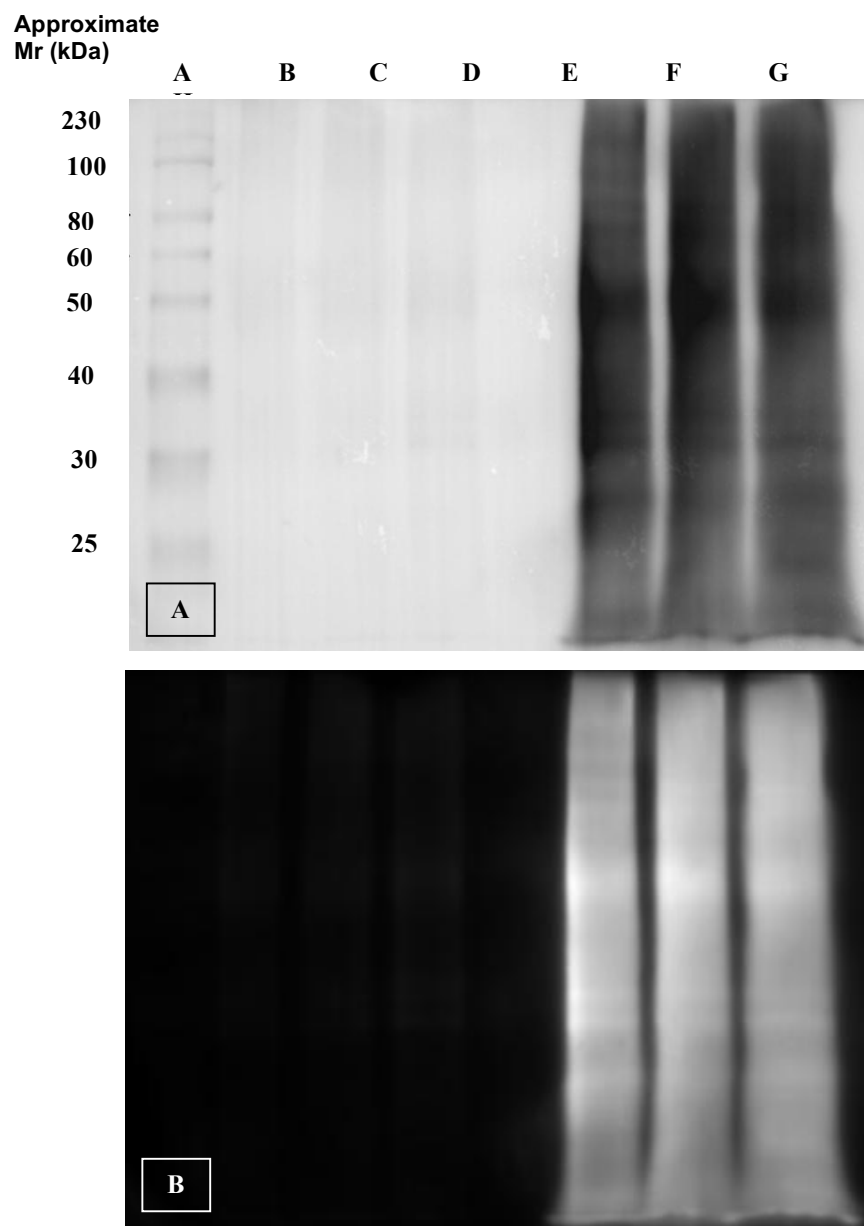


**Figure 6.6. Western blotting on non-biotinylated and biotinylated bovine sperm proteins using HRP-streptavidin.**

A) Protein ladder (10-230 kDa), B-D) Non-biotinylated proteins (10, 30 and 50 µg, respectively), E) Empty lane, F-H) Biotinylated proteins (10, 30 and 50 µg, respectively). Figure 6B is the inverted version of 6A.

## 6.4.2. Affinity chromatography

### 6.4.2.1. Measurement of protein content obtained from HA-agarose column following affinity chromatography

Biotinylated proteins were passed through the HA-agarose chromatography column. Flow-through, non-binding and binding fractions were collected and protein concentration was measured using BCA protein assay. Figure 6.7 shows the standard curve from which the protein concentration from each fraction was obtained. The OD and concentration of different protein fractions are presented in Table 6.2. It should be noted that one BCA assay was carried out and each sample (flow through, non-binding 1/2/3/4, binding 1/2, blank) was loaded as duplicate.

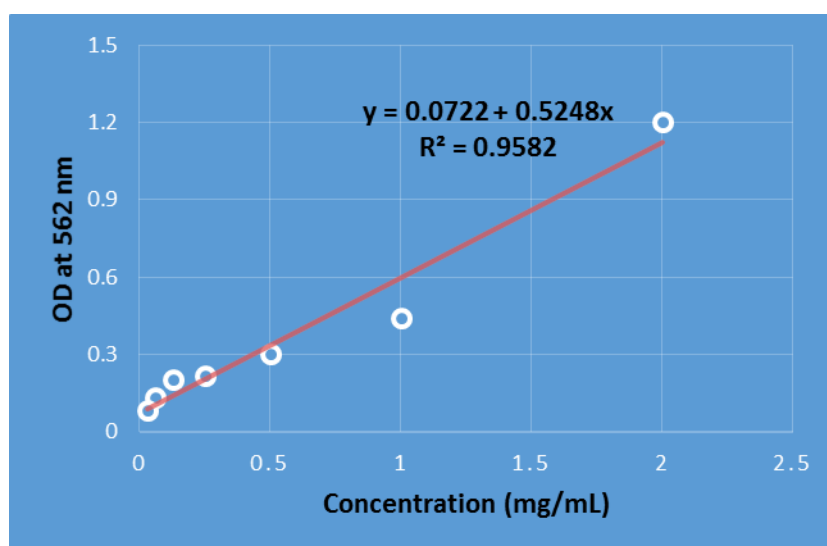


**Figure 6.7.** Standard protein curve generated from BCA assay.

**Table 6.2.** Table showing protein concentrations of different protein fractions obtained from HA-agarose column, measured by BCA assay.

Protein fraction	Optical density (OD) at 595 nm	Protein concentration (mg/mL)
Flow-through	0.76	1.31
Non-binding 1	0.29	0.42
Non-binding 2	0.16	0.17
Non-binding 3	0.19	0.22
Non-binding 4	0.09	0.03
Binding 1	0.16	0.167
Binding 2	0.25	0.34

#### 6.4.2.2. SDS-PAGE and silver staining on proteins recovered from HA-agarose column

Following protein measurement, different protein fractions recovered from the HA-agarose column including flow-through, non-binding (fractions 1 and 4) and binding proteins at appropriate concentrations of each fraction were separated using SDS-PAGE and the gel was silver stained. As Figure 6.8 shows protein bands were identified in all lanes apart from lane F, which corresponds with the fourth wash to remove non-binding proteins. The enlarged lane H, represents the second elution of binding proteins using glycine-HCl and shows the presence of three different bands with molecular masses of approximately 27, 58 and 78 kDa. Some other less distinct bands were detected with molecular masses of 16, 38, 42 and 47 kDa.

This experiment was performed 3 times, but due to the insufficient recovery of material from the column (particularly the binding fraction), only one gel (Figure 6.8) gave clear results after silver staining. Insufficient recovery from the column was the biggest challenge for this aspect of the study.

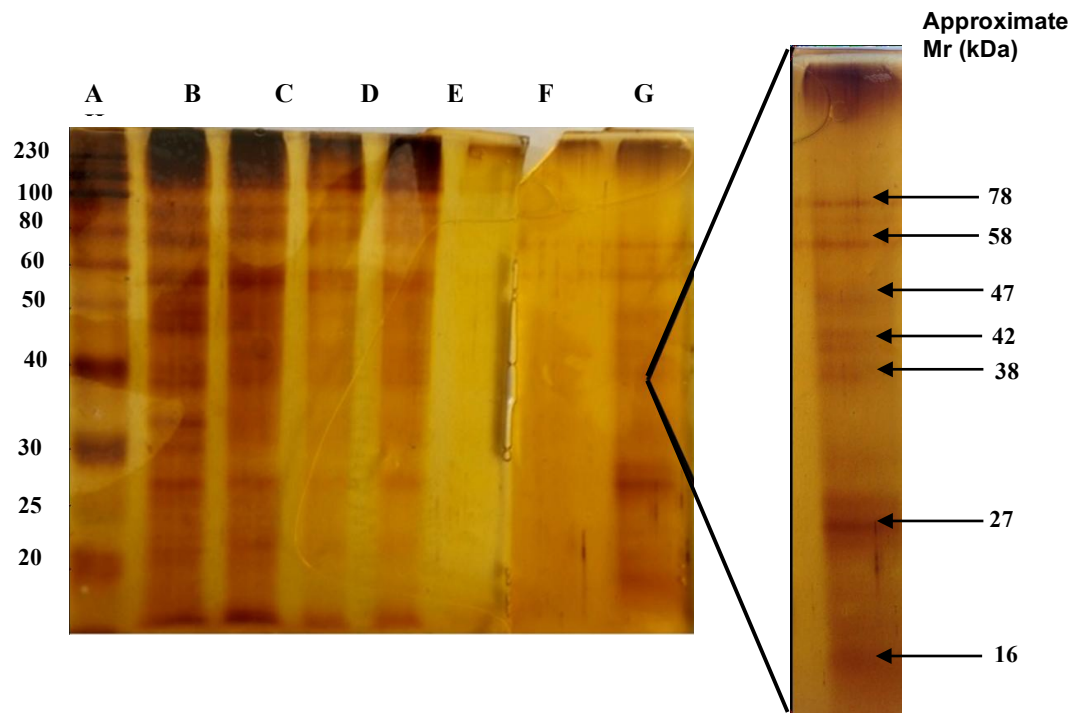


**Figure 6.8. Silver staining on protein content obtained from HA-agarose column.** A) Protein ladder (10-230 kDa), B) Non-biotinylated proteins, C) Biotinylated proteins, D) Flow-through fraction, E-F) Non-binding fractions, G-H) Binding fractions. Lane 8 is enlarged in order to increase clarity of identified bands.

### 6.4.2.3. Western blotting on proteins recovered from HA-agarose column

Western blotting of a duplicate gel was also carried out and as shown in Figure 6.9, different protein bands were identified in lanes C-F containing biotinylated proteins, flow-through fraction, non-binding fraction1 and 2. No protein bands were seen in the third (lane G) and fourth (lane H) washes to remove non-binding proteins. First and second elutions (lanes I and J) show proteins that were probably HA-column bound. The arrows highlight some distinct protein bands at molecular masses of 27, 32, 47 and 78 kDa. The protein band at 78 kDa might be corresponding to CD44.

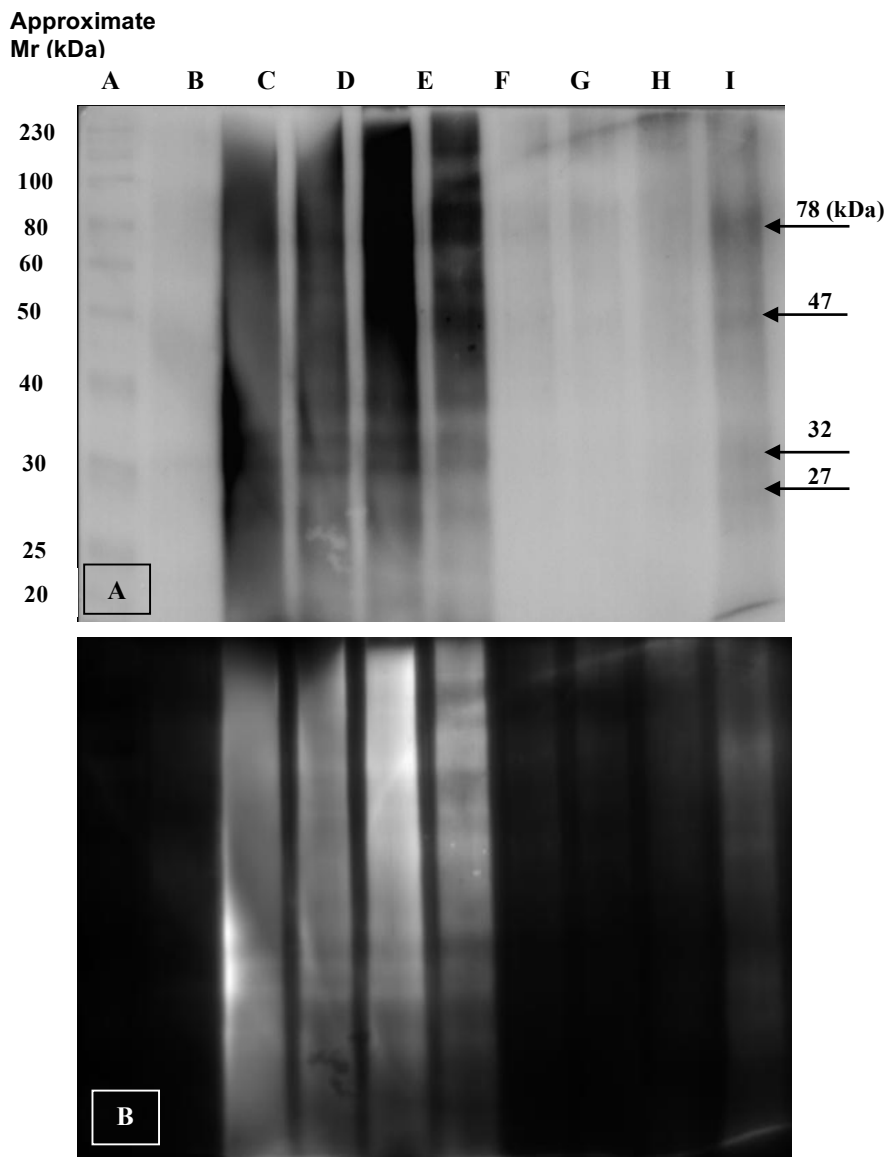


**Figure 6.9. Western blotting on proteins recovered from HA-agarose column.**

A) Protein ladder (10-230 kDa), B) Non-biotinylated proteins, C) Biotinylated proteins, D) Flow-through fraction, E-H) Non-binding fractions, I-J) Binding fractions. Figure 9B is the inverted version of 9A.

## 6.5. Discussion

The HABPs have important roles in sperm motility and maturity and their presence is linked to successful fertilisation (Ranganathan et al., 1994; Bains et al., 2002; Ghosh et al., 2002). More specifically, spermatozoa expressing HABPs on their surface are viable and more mature with no cytoplasmic retention and as a result can bind the zona pellucida more effectively (Huszar et al., 1990; Huszar et al., 2003). Hyaluronic acid may play an important role in fertilisation by 'capturing' spermatozoa expressing hyaluronic acid binding proteins including CD44, RHAMM (Bains et al., 2002; Kornovski et al., 1994) and SPAM1 (McLeskey et al., 1998). Deficiency of HABPs such as SPAM1 (PH-20) and HABP1 can decrease fertilisation potential or lead to male infertility (Zheng et al., 2001; Ghosh et al., 2007). Therefore, it is important to understand sperm HABPs and their roles in sperm-egg recognition and zona pellucida binding.

In Chapter 3, the presence of HABPs and their dynamic changes following capacitation and acrosome reaction on human and bovine sperm membrane were shown. Other than CD44 and RHAMM, for which there is some evidence in human sperm, there are no studies with clear evidence of these or other HABPs in bovine sperm or sperm from any other species. The main objective therefore was to isolate and characterise surface-expressed HABPs from bovine sperm. To that end, bovine sperm membrane proteins were biotinylated. Biotinylation allows both the tracking of proteins through the process (including the HA chromatography column) and permits an additional route for recovering processed proteins using streptavidin-mediated binding.

The HA-agarose column was constructed and biotinylated proteins were passed through it with the likelihood that HABPs would either bind to or be retarded by their interaction with the HA. The proteins with high affinity to HA were then eluted using Gly-HCl. To check the efficiency of biotinylation, fluorescent labelling was carried out using FITC-conjugated streptavidin. The absence of green signal in non-biotinylated sperm as shown in Figure 6.3 confirms that biotinylation of sperm was successful and that biotinylated proteins are localised in the acrosome, the tail and equatorial

segment. The efficacy of biotinylation was further confirmed by carrying out Western blot analysis. As seen in Figure 6.6, after incubation with streptavidin-HRP, different protein bands were developed in biotinylated samples whereas no bands were identified in non-biotinylated samples. Similar results are shown in Figure 6.9, where biotinylated proteins were passed through the HA-agarose column and Western blotting was performed on HA non-binding and binding proteins. The chemiluminescence revealed from potentially HA-binding proteins at the molecular masses of 27, 32, 47 and 78 kDa confirms that binding proteins were successfully biotinylated and therefore likely to be located on the sperm surface and consequently might be considered as HABPs.

In the current study, biotinylation together with silver staining and Western blotting permitted the detection of sperm surface proteins. Detection of proteins with very low concentration can be performed using silver staining and as seen in Figure 6.8, it was able to detect proteins in all lanes apart from lane F which corresponds for the forth wash through of non-binding proteins. The results from silver staining and Western blot analysis (Figure 6.9) suggested that all non-binding biotinylated proteins were removed from the column after the final wash with the lysis buffer and eluted bound proteins using Gly-HCl (lane J) are biotinylated proteins with high affinity for HA. The bands detected at 78 kDa (Figure 6.9, lane H; Figure 6.9, lane J) may be CD44 as suggested by work carried out by Bains in 2002 on CD44, who estimated molecular masses of 70-95 kDa for various isoforms of CD44 (Bains et al., 2002). Similar to CD44, the clear band at 58 kDa (Figure 6.9, lane H) may represent RHAMM with an estimated molecular mass of 58-64 kDa (Kornovski et al., 1994).

The weaker signals for bands with a wide-range of molecular masses estimated at between 16 and 47 kDa do not match other well-known HABPs in human and mouse sperm (such as HAPB1 and SPAM1), but these proteins may not have been located on the cell surface at the time of sampling. It is tempting to speculate that one of these proteins may be the zona pellucida binding protein 2 (ZPBP2) with a molecular mass of 38 kDa (see Chapter 5). Unfortunately, although Western blotting using anti CD44 and anti RHAMM antibodies was performed on the HA-bound and eluted

fraction, no protein bands were detected, perhaps because of the low quantity of eluted proteins overall as can be seen in Figure 6.8 (Lanes G and H). As HA binding might improve ART outcomes and decrease the risk of genetic disorders in offspring, the interaction between HA and its binding proteins on sperm surface should be studied more extensively. The findings from such a study would facilitate a better understanding of, and may lead to the development of, more advanced methods for sperm selection in ART.

## **6.6. Conclusion**

In conclusion, the presence of different HABPs on the surface of bovine sperm was investigated with some intriguing but inconclusive evidence for the presence of novel proteins with high affinity for HA uncovered.

## Chapter 7. General Discussion

The main hypothesis for the study is that HABPs (including potentially novel forms) are present in sperm and behave dynamically and purposefully in relation to sperm maturation and function.

The main objectives of the present study were to:

- Evaluate the presence of sperm HABPs using human and bovine as model species.
- Investigate how capacitation and the acrosome reaction affect the distribution and localisation of HABPs.
- Examine the relationships between HA-binding affinity, DNA integrity and chromatin maturity.
- Look for evidence of novel HABPs in human and bovine sperm.
- Use proteomics to help characterise microscopically observed changes in the appearance and distribution of sperm HABPs during capacitation and the acrosome reaction.

Initially, HA-binding ability was assessed in human sperm recovered from 90% (pelleted) and 45% (interface) fractions using commercially available HA-coated slides (Chapter 2). The effect of capacitation on HA-binding was also evaluated as was the behavior of pelleted/interface and HA-binding/non-binding sperm in relation to DNA fragmentation (AO staining) and chromatin maturity (AB staining). The work described in Chapter 3 focused more closely on the distribution of HABPs including CD44 in mature sperm and the effects of both capacitation and the acrosome reaction on their distribution. To continue the investigation, based on the observations that capacitation and the acrosome reaction could alter the distribution of HABPs, among other unknown proteins, the identities of human sperm proteins were assessed in extracts prepared from pre-capacitated, capacitated and acrosome reacted sperm by tandem mass tags (TMT)-labelling followed by LC.MS/MS (Chapter 4). As an extension of this investigation, Chapter 5 described attempts to partition human sperm proteins into HA-binding enriched and non-enriched fractions using a simple panning (HA-coated dish) system. Finally, the specific isolation of HABPs from bovine sperm was attempted using affinity



chromatography on a bespoke HA-agarose conjugate column and their presence/recovery evaluated using a combination of silver staining and Western blotting. Bovine spermatozoa were used, due to the limited amount of human samples and the need for large protein quantities required in affinity chromatography.

### **7.1. HA-binding and its changes during capacitation**

As indicated throughout the thesis, approximately 5% of births in the Western world are supported by ARTs (Ebner et al., 2012; Lewis and Kumar, 2015). Sperm selection for ICSI depends on the subjective judgment of the embryologist and one of the main drawbacks of this set up is that low quality sperm including sperm with high levels of DNA fragmentation may be inadvertently selected for ICSI (Epe et al., 1993). Therefore, new techniques for sperm selection in ART, particularly for ICSI and IUI are being developed and gradually introduced. These methods include selection of spermatozoa based on their surface charge, apoptosis markers and ultra-morphology (Said and Land, 2011; McDowell et al., 2014). Selection of sperm by HA-binding is another method developed for separating spermatozoa based on their membrane maturity (Huszar et al., 2003; Huszar et al., 2007; McDowell et al., 2014).

A relationship between the affinity of spermatozoa for HA and their viability is now established (Huszar et al., 2003). The most likely explanation for this relationship is that compared with less vital or viable sperm, HA-binding is a marker of sperm maturity which requires essential plasma membrane remodelling and the formation of HA binding sites on or close to the sperm surface. HA binding probably helps sperm to interact with the HA-surrounded cumulus oophorus and zona pellucida (Cayli et al., 2003; Huszar et al., 2003; Parmegiani et al., 2010a; Sakkas et al., 2015). Supporting this explanation, recent reports suggest that better quality spermatozoa have low levels of DNA fragmentation, protamine deficiency and abnormal sperm morphology and that HA selection favours the enrichment of sperm with these qualities (Nasr-Esfahani et al., 2008). Other studies have indicated that injection of

HA-binding spermatozoa improved embryo quality after ICSI (Beck-Fruchter et al., 2016; Mokanszki et al., 2014; Nasr-Esfahani et al., 2008; Parmegiani et al., 2010b). Research carried out by Marie et al. (2012) revealed that HA produced by cumulus cells is crucial for expansion of cumulus cells, oocyte maturation and embryo development in bovine (Marei et al., 2012). This work also demonstrated that the presence of small HA fragments (20 kDa) is essential for increasing embryo development and blastocyst formation in ewes. In contrast, large HA fragments (500-750 kDa) interrupt oviductal environment and embryo development (Marei et al., 2016).

Considering that intermittent sperm binding to HA during their journey across the female genital tract may be an important aspect of normal fertility (Henkel, 2012), the current study was set up to investigate the dynamics of sperm HA-binding *in vitro* and the relationship between HA-binding and standard methods of sperm preparation for IVF (in this case, DDGC). Differences in the ability of pelleted (90%) and interphase (45%) human spermatozoa to bind HA were evaluated for the first time. The results showed a significantly higher HA-binding capacity in 90%, compared to the 45% subpopulations ( $p < 0.0001$ ), suggesting that sperm recovered from 90% fractions are either expressing more HABPs or that their binding affinity for HA is enhanced. Either outcome could arise through cytoplasmic maturity.

Sperm achieve fertilising ability after transit through the female genital tract which accommodates their capacitation accompanied by hyperactive motility, redistribution of membrane proteins and other biochemical changes (Liu et al., 2007; Gadella et al., 2008; Leahy and Gadella, 2011a; Zaneveld et al., 1991). Hence, changes in HA-binding after capacitation were also assessed. Results showed that hyperactive motility and HA-binding affinity correspondingly increased during capacitation suggesting that capacitation affects the distribution or HA-binding capacity of HABPs (Leahy and Gadella, 2011a).

## **7.2. Relationships between DNA fragmentation, chromatin maturity and sperm separation methods (DDGC and HA-binding)**

Evidence suggests that sperm with damaged DNA fertilising the egg can have adverse effects on embryo development (Zhang et al., 2008; Robinson et al., 2012; Zini et al., 2008; El Hachem et al., 2017). Therefore, various sperm selection methods are deployed (DDGC and swim-up) or are in development aimed at eliminating compromised sperm from the fertilising pool as far as possible. As such HA-binding is being introduced to select sperm based on functional characteristics and to minimise the selection of sperm with damaged DNA.

In the present study DNA fragmentation and chromatin maturity were also evaluated in spermatozoa fractionated into sub-populations using DDGC and/or HA-binding. The results showed that sperm recovered from the 45% fraction had significantly higher levels of fragmented DNA and poorer chromatin compaction compared to sperm from the 90% fraction. Although a significant difference in the levels of HA binding between DDGC processed interface (45%) and pelleted (90%) sperm subpopulations was found, this difference was not as great as the difference in the levels of DNA fragmentation between the two subpopulations (which were substantial). It was therefore assumed that HA-binding capability of the sperm is tolerant to low levels of sperm DNA fragmentation that are unlikely to affect fertilisation. At higher levels of DNA fragmentation, HA-binding is compromised.

As discussed, sperm from the 90% fraction revealed higher HA affinity compared to sperm recovered from the 45% fraction. It was also shown that HA-binding sperm had significantly higher DNA integrity and chromatin maturity than non-binding sperm. These results are supported by another study (Yagci 2010), showing that HA-binding spermatozoa isolated from unprocessed semen had low levels of DNA fragmentation (Yagci et al., 2010).

While DDGC processing of crude semen samples can certainly generate sperm subpopulations with better DNA integrity, the results of the current study also showed that HA-binding was more effective than DDGC in separating intact DNA (++) sperm.

The percentage of sperm with medium levels of DNA fragmentation ( $\pm$ ) was also significantly higher in 90% fraction compared to HA-binding fraction (Figure 2.18). A comparison in chromatin compaction status between sperm separated using HA-binding and DDGC was also carried out. The results showed that the HA-binding population had significantly higher levels of sperm with fully compacted chromatin (Figure 2.19).

In general, the data from the current study suggest a link between DNA integrity and chromatin maturity with HA binding and sperm density (and probably motility), ultimately increasing the probability of the least damaged sperm fertilising the oocyte. The results of the current study give further support that sperm with slightly damaged DNA are capable of fertilising the oocyte. Different studies have shown that mammalian oocytes and early embryos are able to repair sperm DNA fragmentation (Menezo et al., 2010; Gonzalez-Marin et al., 2012; Carroll and Marangos, 2013). Therefore, the low levels of DNA fragmentation observed in HA-binding sperm and sperm from 90% fraction might be repaired by the oocyte.

The combination of DDGC and HA-binding might be also useful in minimising DNA fragmentation. This would help older couples especially where the female is aged above 37, and their oocytes are less capable of repairing DNA fragmentation in their partner's sperm (Menezo et al., 2010; Gindoff and Jewelewicz, 1986).

The aetiology of DNA fragmentation in sperm is closely correlated with impaired spermiogenesis, which suggests that there is a disruption in up-regulation of HABPs during spermiogenesis, causing a decreased ability of the sperm to bind to HA (McPherson and Longo, 1993). More accurately, the appearance of HABPs is likely to be dependent on sperm maturity and that various things can happen during spermatogenesis that can compromise maturity (Huszar et al., 2006). These can include intrinsic problems arising in spermatogenesis itself such as apoptosis, deficiencies in recombination, protamine imbalances or oxidative stress and extrinsic problems caused by the environments sperm encounter (Gonzalez-Marin et al., 2012). Some sperm will be more resistant to extrinsic factors than others.

The data from the present study lend further support to the link between sperm DNA fragmentation and HA binding as both lower HA binding and higher levels of DNA fragmentation were uncovered in the interface, with a reciprocal relationship in sperm from the pellets. In conclusion, as the present study indicates links between sperm DNA integrity, chromatin maturity and HA binding, the HA binding assay may assist embryologists choose how best to treat male infertility and so hopefully decrease the levels of fertilisation failure and other complications of pregnancy.

### **7.3. Evaluation of HABPs and their changes during capacitation and acrosome reaction**

Given the presence of HA in the oocyte–cumulus complex (Sakkas et al., 2015) it is reasonable to consider that sperm expressing HABPs would be more successful in fertilising the egg. Therefore, in the present study, immunocytochemistry was carried out initially to monitor the presence of HABPs in human and bovine sperm. In the bovine, the fluorescence signal with HA-TRITC appeared to be evenly distributed on the sperm membrane, with some localised areas of high intensity, particularly in the post-acrosomal region and the neck. In human sperm, HA-TRITC preferentially labelled the acrosome, neck and the tail. These results show that different HABPs are expressed in sperm. CD44 was detected in the anterior acrosome and post-acrosomal sheath of bovine sperm and labelling in human sperm was more restricted to the acrosome and equatorial segment. These results are supported by work carried out by Bains et al. (2002), who identified CD44 in the acrosome of human spermatozoa alongside a variant of CD44 with an approximate molecular weight of 73 kDa by Western blot.

Sperm acquire the ability to fertilise the egg during their journey across the female genital track (Fraser, 1992; Ickowicz et al., 2012). During this time, sperm undergo capacitation, which is a pre-requisite for the AR. Despite the fact that capacitation and the AR are fundamental steps towards fertilisation, the changes that occur during these events are not yet fully understood. Capacitation is accompanied by acquisition of hyperactive motility, which aids sperm as they swim through the

oviductal mucus and assists their penetration of the zona pellucida after the AR (Yanagimachi, 1969; Ferramosca and Zara, 2014; Naz and Rajesh, 2004). Protein phosphorylation occurs during sperm capacitation in different regions of sperm (Jin and Yang, 2017; Ficarro et al., 2003). For example, tyrosine phosphorylation has been reported in the principal piece and neck and is thought to be essential for fertilisation (D. Sakkas et al., 2003). Phosphorylation also increases during capacitation (Carrera et al., 1996; D. Sakkas et al., 2003; Liu et al., 2006). Changes during sperm capacitation and the AR in the distribution of other proteins includes the hyaluronidase, PH-20 (SPAM1), actin and alpha-tubulin (Myles and Primakoff, 1984a; Francou et al., 2014). The current study examined whether the induction of capacitation and the AR in sperm would have any effect on distribution and localisation of HABPs.

The results revealed changes in the localisation and distribution of HABPs during capacitation and the AR in both human and bovine sperm, where HABPs (detected by HA-TRITC) increased during capacitation and the AR. This increase in the intensity of HA-TRITC labelling was higher in bovine sperm than in human sperm. It was also shown that the pattern of CD44 labelling changed after spermatozoa were capacitated and acrosome reacted, when the majority of capacitated bovine sperm lost their acrosomal labelling with anti CD44 antibody and the labelling became more restricted to the post-acrosomal region. This shows that membrane remodeling and the relocalisation of different proteins during capacitation and the the AR accompany the sperms' preparation for potential fertilisation. CD44 acrosomal labelling in human capacitated sperm was reduced and became more restricted to the equatorial segment. After the the AR, acrosomal labelling with anti-CD44 antibody was highly reduced in both human and bovine sperm. These results suggest that the location and/or the abundance of HABPs are affected by capacitation and the AR. One possible explanation for these observations lies with the re-distribution of membrane components which in turn, leads to altered accessibility of the HABP detection reagents (generic HA-TRITC and mono-specific antibodies) to their ligands (Leahy and Gadella, 2011b). The distribution and localisation of HABPs were also assessed in good quality (90%) and poor quality (45%) bovine sperm. The results showed that

in 90% sperm, the intensity of HA-TRITC was much higher than in sperm from 45% fraction. CD44 labelling was particularly weak in the anterior acrosome of sperm from 45% fraction. All these results provide additional evidence that sperm from 90% fraction (pellet) are highly mature and they have completed their plasma membrane re-modelling.

#### **7.4. The proteomics of sperm capacitation and the acrosome reaction**

By using TMT labelling of trypsin-derived peptides prior to LC-MS/MS, differentially regulated proteins were investigated in pre-capacitated, capacitated and acrosome reacted sperm. The changes in differential regulation of some of the identified proteins during capacitation and the AR were already known from mass spectrometry studies. These proteins included Acrosomal protein SP-10, Phosphoglycerate mutase 2, Acrosin-binding protein and Pyruvate dehydrogenase protein X component mitochondrial amongst others (Table 4.2) (Foster et al., 1994; Amaral et al., 2014b; Kongmanas et al., 2015).

It was also confirmed that during capacitation, several changes including cholesterol efflux and reorganisation of the plasma membrane, changes in intracellular ion concentration and protein phosphorylation occurred. The changes during the AR are associated with metabolism, energy production and an increase in acrosomal vesicle activity.

In addition, several mitochondrial proteins involved in capacitation and acrosome reaction were identified. The proteins were present in both increased and decreased level depending on the functional state of the sperm. The present study successfully corroborated the findings of previous studies where the role of mitochondrial proteins (mitochondrial Cytochrome c oxidase, PHB2, different ATP synthase proteins, AIFM1, SOD2, PARK7) have been linked to capacitation and acrosome reactions. Few additional mitochondrial proteins including ACAA2 that was not reported in previous studies was observed in this study. Most of the differentially expressed mitochondrial proteins were associated with energy metabolism, protection against (mitochondrial) ROS and cell apoptosis. All these process during capacitation and acrosome

reaction plays a crucial role in proper functioning of the sperm in female reproductive tract. However, more studies will be required to validate the proteins role in the different pathways and deciphering their role in sperm gamete fusion.

The results of the current study revealed some of the important differentially regulated proteins involved in capacitation and acrosome reaction (such as AKAPs, ATP synthases and serum albumin) but no clear evidence of known HABPs such as CD44 or RHAMM. In spite of the apparently wide distribution of HABPs, particularly in capacitating sperm as determined by immunocytochemistry, neither CD44 nor RHAMM were detected by LC-MS/MS. One possible reason for this is that the lysis solution used for protein extraction could not access these proteins sufficiently.

In the current study, levels of the Cilia and flagella-associated protein 20 increased following capacitation. This protein is involved in sperm motility and contains 2 BX7B motifs (common motifs amongst many of the previously characterised HABPs such as CD44 and RHAMM; (Yang et al., 1994; Day; Day and Prestwich, 2002). The results of Chapter 3 showed HABPs increased during capacitation and in Chapter 5, Cilia and flagella-associated protein 20 was found only in HA-binding fraction (explained below). Therefore it may also be considered as a putative HABP, abundance of which, may be affected by capacitation.

### **7.5. Isolation of sperm HABPs and their identification by mass spectrometry and HA affinity chromatography column**

One of the main objectives of the current study was to look for evidence of novel sperm HABPs. The chosen approaches relied on the likely affinity of HABPs for HA and used either a 'panning' method or affinity chromatography to achieve their selective enrichment. The panning experiment was performed by allowing human sperm protein homogenates to interact with a specially prepared HA-coated surface, before their recovery from the surface by washing. Twenty-eight proteins were recovered and characterized by LC-MS/MS including ADAM32 and cilia and flagella associated protein 20 with two BX7B motifs and midkine containing four BX7B



motifs. Another interesting protein identified in the recovered proteins was ZPBP2, which showed similarities to the Link module of CD44 (Takeda et al., 2006; Liu and Finzel, 2014a; Teriete et al., 2004). As explained throughout the thesis the Link module is a sequence of approximately 100 amino acids with two  $\alpha$ -helices and two triple-stranded anti-parallel  $\beta$ -sheets. In addition, it has two disulphide bonds between Cys1-Cys4 and Cys2-Cys3 (Kohda et al., 1996; Higman et al., 2014).

Although the partitioning of proteins achieved by panning could have been influenced by selective, direct HA-interaction, compared with the non-binding proteins from these experiments, the majority of recovered, HA-interacting proteins (Table 5.2) carried a net positive charge under experimental conditions. Hence, electrostatic interactions between positively charged proteins and negatively charged HA could offer an alternative explanation for why those proteins were found in the HA-binding fraction. Strictly speaking, an electrostatic interaction could apply to any positively charged proteins and indeed, the HA non-binding fractions contained a higher proportion of negatively charged proteins. However, it is known that electrostatic interactions can modulate hyaluronidase activity, suggesting that a de facto HA-ligand interaction on the panning surface cannot be discounted (Lenormand et al., 2008; Purcell et al., 2014).

ZPBP2 is a paralogue of the acrosomal matrix protein ZPBP1 and is localised to the rostral ridge of the acrosome (Lin et al., 2007). The role of ZPBP1 and ZPBP2 in binding the zona pellucida is understood (Mori et al., 1993; Mori et al., 1995). Research by Line et al. (2007) showed sub-fertility in mice lacking ZPBP2, alongside deformation of the sperm head and compromised zona penetration. ZPBPs, therefore are essential acrosomal proteins participating in zona pellucida binding (Lin et al., 2007).

By using the SAS server, five PDB records were identified for ZPBP2 including 4pz3, 1uuh, 4pz4, 2i83 and 1poz. All these records refer to the HA-binding domain of CD44 containing the Link module (Teriete et al., 2004; Liu and Finzel, 2014a; Takeda et al., 2006). The interaction between CD44 and HA is thought to be due to the

presence of a Link module (residues 32-124) containing two disulphide bonds and some additional residues at the N-terminal (residues 21-31) and C-terminal ends (residues 125-178) (Takeda et al., 2006). As indicated by the evidence presented in the present study, ZPBP2 (but not ZPBP1) contains sequences with some structural similarities to the HA-binding domain of CD44, suggesting that the HA-binding function (if active) arose in ZPBP2 and was lost during the gene duplication event that gave rise to ZPBP1 (Lin et al., 2007). It is tempting to speculate that originally, ZPBPs functioned as HABPs but have progressively lost that function over evolutionary timescales.

ADAM32 (disintegrin and metalloproteinase domain-containing 32) was another interesting protein found in HA-binding fractions. To date, 15 out of 29 well-known ADAMs are known to be expressed in testis, suggesting an important role for the ADAM family in spermatogenesis and fertilisation (Primakoff and Myles, 2000).

To confirm the proteomics results, Western blotting was carried out on HA-binding and non-binding fractions using anti-ZPBP2 and ADAM32 antibodies. In agreement with the proteomics results, the antibodies detected corresponding bands for ZPBP2 and ADAM32 in HA-binding fractions but no protein bands were found in non-binding fractions. These results suggest that ZPBP2, ADAM32 and other proteins found in HA-binding fraction (Table 5.2) may be novel HABPs.

The absence of known sperm HABPs, including CD44 (Underhill, 1992; Bajorath et al., 1998), RHAMM (Yang et al., 1993; Hardwick et al., 1992) and SPAM1 (Hunnicut et al., 1996; Vines et al., 2001) in HA-binding and non-binding fractions warrants further consideration. Firstly these proteins are present in sperm as reported elsewhere (Underhill, 1992; Bajorath et al., 1998; Yang et al., 1993; Hardwick et al., 1992) but were not detected in this study. As explained CD44 did not exist in the most updated human sperm proteome list by Amaral et al (2014 a). One explanation for that might be the very low quantity of CD44 and RHAMM in sperm homogenates and they could not be detected by the LC-MS/MS.

The absence of CD44 may also be explained by the transient and dynamic binding reported for CD44 to hyaluronic acid (Kohda et al., 1996; Misra et al., 2015; Liu and Finzel, 2014a). It is also possible that these proteins were not sufficiently abundant in any of the sperm homogenates to be detectable by the LC-MS/MS method used or that the extraction buffer was unable to access these proteins, which were lost in the insoluble pellets following sperm homogenisation. It is known that some proteins such as SPAM1 (a bifunctional glycosylphosphatidylinositol (GPI)-anchored membrane protein) need to be activated, otherwise they are unable to bind HA (Hunnicuttt et al., 1996; Vines et al., 2001). SPAM1 acts as a hyaluronidase in acrosome intact sperm where it undergoes proteolytic cleavage at its N-terminal and as a result interacts with HA for secondary binding to the zona (Hunnicuttt et al., 1996; Vines et al., 2001). This offers another potential explanation for the absence of well characterised HABPs in the present study.

Finally, the configuration of the HA substrate on the dishes used for panning sperm homogenates may have played a role. These plates were designed to enrich populations of motile, mature spermatozoa from mixed populations based on the expression of HABPs on their surface (Underhill, 1992; Bajorath et al., 1998; Yang et al., 1993; Hardwick et al., 1992; Ghosh et al., 2007) and may not have had the correct properties for binding to these HABPs in solution. Work is in progress to modify the HA substrate in order to improve its capacity to recognise and bind HABPs.

HA affinity chromatography was attempted as an alternative route to the isolation of HABPs. To assist with this process, bovine sperm surface proteins were biotinylated prior to their addition to the column and HA non-binding and binding proteins were collected in the flow-through and eluate fractions, respectively. Silver staining and Western blotting were performed to check for evidence of HABPs in the HA-binding fractions, revealing proteins with molecular masses of 27, 32, 47 and 78 kDa. These proteins were not found in the non-binding fractions (Figure 6.8 and 6.9). As different molecular masses have been reported for CD44 and RHAMM, including 70-95 kDa and 58-64 kDa respectively (Bains et al., 2002; Kornovski et al., 1994), the bands

detected at 78 kDa and 58 kDa (Figure 6.8 and 6.9) could be CD44 and RHAMM, respectively (Figure 6.8 and 6.9). Western blotting with antibodies specific to these proteins, however, failed to support this possibility. Similarly, although the analysis of HA-binding proteins using LC-MS/MS described in Chapter 5 suggested that ZPBP2 could be a potential HABPs and that the protein band at 37 kDa may have been ZPBP2, Western blot analysis failed to support this possibility. Failure to detect CD44, RHAMM and ZPBP2 using Western blotting may have been due to the very low concentrations on the blots and detection limits being reached. The transient interaction between HA and its binding proteins could have also been another reason for why CD44 and RHAMM were not detected on the blots. The efficiency of the antibodies was checked using extracted proteins from PC3 cells as positive controls.

There were several challenges faced during protein purification using HA affinity chromatography with the main challenge being protocol optimisation. Compared to human sperm, the membrane of bovine sperm is tougher and as a result less sensitive to the mild lysis buffer that was optimised for extraction of human sperm membrane proteins (Chapter 5). As the study required the preservation of protein interactions, the use of a mild lysis buffer was considered important to maintain native protein structure. Therefore, several protocols with different concentrations of salt and detergent were tried and discarded until the protocol was optimised. Another challenge posed by this study was the construction of the affinity chromatography column by immobilising HA on a matrix such as sepharose or agarose. Primarily, a protocol adapted from Ponting and Kumar (1995) was used, but even after extensive dialysis, eluted fractions contained high salt concentrations and interfered with protein separation on SDS-PAGE.

The use of Affi-Gel matrix, which is mainly for coupling proteins and not glycosaminoglycans was another challenge. Consequently, it took longer than expected to bind HA to agarose beads and provided insufficient material available for mass spectrometry. Assuming that only cell surface proteins are biotinylated, streptavidin beads were used to pull out biotinylated proteins from sperm

homogenates before passing them through the column. However, insufficient amount of protein was obtained after several attempts.

## **7.6. Conclusion**

In the present study, sperm recovered from 90% DDGC fractions (pelleted) had a greater affinity for HA than sperm recovered from 45% fractions (interface). Both pelleted and HA-binding sperm had lower levels of DNA fragmentation and higher levels of chromatin compaction than both 45% and non HA-binding sperm. HA-binding, however, appeared to be more efficient than DDGC and *quid pro quo*, better at excluding poor quality sperm from a sample. Therefore, these results suggest that HA binding (and / or a high HA binding score) are good measures for selecting mature spermatozoa with the highest potential for supporting clinical pregnancy. Under circumstances where sperm count is very low, or DDGC cannot be carried out, HA binding should be considered.

The presence of HABPs was confirmed in bovine and human sperm. The generic HABP-detection reagent (HA-TRITC), suggested that HABPs were more generally distributed on the sperm, indicating the likely presence of novel forms.

Capacitation influenced the distribution of HABPs and increased HA-binding which is known as one of the efficient sperm selection methods. Results suggest that permitting sperm capacitation in washed samples could improve sperm selection outcomes based on HA-binding. A mass spectrometry-based proteomic approach resulted in identification of important proteins involved in capacitation and acrosome reaction including AKAPs amongst others. The same data suggested that Cilia and flagella-associated protein 20 containing two HA-binding motifs (BX7B) could be considered as a putative HABP which its levels increased in capacitated sperm. The changes in HABPs following capacitation and acrosome reaction observed by using ICC, may not have been supported directly by the proteomics data. Indirectly, however, the fact that differences between non-capacitated, capacitated and acrosome reacted sperm (in the absence of gene expression) were revealed by proteomics shows that the principle which was followed (protein redistribution and

changes in solvent accessibility) was justified. Analysis of the proteomics data from the panning fractions (HA-binding and non-binding fractions) led us to identify several proteins including ZBP2, ADAM32, Midkine and Cilia and flagella-associated protein 20 (amongst others) which all contained HA-binding motifs and could be considered as novel HABPs.

Data obtained from this study supports the main hypothesis in that HABPs are present in sperm and respond dynamically and purposefully in relation to known markers of sperm function and viability, including capacitation and the acrosome reaction. The data also support the argument for further research into HA-based sperm selection, particularly for ICSI, where the choice of sperm is more critical.

#### 7. 7. Future research

The data from this study is preliminary and additional research is needed. For example, it was shown that the localisation and distribution of HABPs including CD44 changed during capacitation and the acrosome reaction. Future research should aim to investigate the dynamic changes of other sperm HABPs such as RHAMM and SPAM1 during capacitation and acrosome reaction to confidently conclude that the distribution and localisation of HABPs are affected by capacitation and the acrosome reaction. Increasing the sensitivity of Western blotting may also help.

In Chapter 5, 28 proteins including ZBP2, ADAM32, Cilia- and flagella-associated protein 20 and Midkine were considered as potential novel HABPs. The HA substrate used in Chapter 2 and 5 was designed for isolation of motile sperm and not for isolation of HABPs. It is possible that this contributed to the absence of CD44 (and other potential HABPs) in the HA-binding fraction from the panning experiments. The efficiency of the panning system could be improved by the development of a modified HA substrate with greater selective affinity for HABPs (Baranova et al., 2014). Similarly, the transient interaction between HA and its binding proteins could be altered by chemical modification of the HA to facilitate longer binding times and improving its suitability for affinity chromatography (Wolny et al., 2010; Richter et al.,

2007; Baranova et al., 2011; Baranova et al., 2014). Confirming the identities of eluted proteins (as HABPs) could be checked using more sensitive LC-MS/MS systems in development. An additional goal would be a matrix capable of selectively attracting better quality motile sperm for standard IVF procedures and thereby reducing reliance on the use of ICSI for treating male infertility.

## References:

- Abu-Halima, M.Ludwig, N.Hart, M.Leidinger, P.Backes, C.Keller, A.Hammadeh, M. and Meese, E. 2016. Altered micro-ribonucleic acid expression profiles of extracellular microvesicles in the seminal plasma of patients with oligoasthenozoospermia. *Fertil Steril.* **106**(5), pp.1061-1069 e3.
- Adeoya-Osiguwa, S.A. and Fraser, L.R. 1996. Evidence for Ca(2+)-dependent ATPase activity, stimulated by decapacitation factor and calmodulin, in mouse sperm. *Mol Reprod Dev.* **44**(1), pp.111-20.
- Adham, I.M.Nayernia, K. and Engel, W. 1997. Spermatozoa lacking acrosin protein show delayed fertilization. *Mol Reprod Dev.* **46**(3), pp.370-6.
- Agarwal, A. and Allamaneni, S.S. 2004. The effect of sperm DNA damage on assisted reproduction outcomes. A review. *Minerva Ginecol.* **56**(3), pp.235-45.
- Agarwal, A. and Esteves, S.C. 2011. Novel concepts in male infertility *International Brazilian Journal Urology.* **37**(1), pp.5-15.
- Agarwal, A.Majzoub, A.Esteves, S.C.Ko, E.Ramasamy, R. and Zini, A. 2016. Clinical utility of sperm DNA fragmentation testing: practice recommendations based on clinical scenarios. *Transl Androl Urol.* **5**(6), pp.935-950.
- Agarwal, A.Sharma, R.Durairajanayagam, D.Cui, Z.Ayaz, A.Gupta, S.Willard, B.Gopalan, B. and Sabanegh, E. 2015. Differential proteomic profiling of spermatozoal proteins of infertile men with unilateral or bilateral varicocele. *Urology.* **85**(3), pp.580-8.
- Agarwal, A.Virk, G.Ong, C. and du Plessis, S.S. 2014. Effect of oxidative stress on male reproduction. *World J Mens Health.* **32**(1), pp.1-17.
- Agbaje, I.M.Rogers, D.A.McVicar, C.M.McClure, N.Atkinson, A.B.Mallidis, C. and Lewis, S.E. 2007. Insulin dependant diabetes mellitus: implications for male reproductive function. *Hum Reprod.* **22**(7), pp.1871-7.
- Ahrens, T.Sleeman, J.P.Schempp, C.M.Howells, N.Hofmann, M.Ponta, H.Herrlich, P. and Simon, J.C. 2001. Soluble CD44 inhibits melanoma tumor growth by blocking cell surface CD44 binding to hyaluronic acid. *Oncogene.* **20**(26), pp.3399-408.
- Ainsworth, C.Nixon, B. and Aitken, R.J. 2005. Development of a novel electrophoretic system for the isolation of human spermatozoa. *Hum Reprod.* **20**(8), pp.2261-70.
- Aitken, R.J. 2011. The capacitation-apoptosis highway: oxysterols and mammalian sperm function. *Biol Reprod.* **85**(1), pp.9-12.
- Aitken, R.J. 2014. Age, the environment and our reproductive future: bonking baby boomers and the future of sex. *Reproduction.* **147**(2), pp.S1-S11.
- Aitken, R.J.Bronson, R.Smith, T.B. and De luliis, G.N. 2013. The source and significance of DNA damage in human spermatozoa; a commentary on diagnostic strategies and straw man fallacies. *Mol Hum Reprod.* **19**(8), pp.475-85.
- Aitken, R.J.De luliis, G.N.Finnie, J.M.Hedges, A. and McLachlan, R.I. 2010. Analysis of the relationships between oxidative stress, DNA damage and sperm vitality in a patient population: development of diagnostic criteria. *Hum Reprod.* **25**(10), pp.2415-26.
- Aitken, R.J.Gordon, E.Harkiss, D.Twigg, J.P.Milne, P.Jennings, Z. and Irvine, D.S. 1998. Relative impact of oxidative stress on the functional competence and genomic integrity of human spermatozoa. *Biol Reprod.* **59**(5), pp.1037-46.
- Aitken, R.J.Jones, K.T. and Robertson, S.A. 2012a. Reactive oxygen species and sperm function--in sickness and in health. *J Androl.* **33**(6), pp.1096-106.
- Aitken, R.J. and Nixon, B. 2013. Sperm capacitation: a distant landscape glimpsed but unexplored. *Mol Hum Reprod.* **19**(12), pp.785-93.



- Aitken, R.J., Whiting, S., De Luliis, G.N., McClymont, S., Mitchell, L.A. and Baker, M.A. 2012b. Electrophilic aldehydes generated by sperm metabolism activate mitochondrial reactive oxygen species generation and apoptosis by targeting succinate dehydrogenase. *J Biol Chem.* **287**(39), pp.33048-60.
- Akerlof, E., Fredricson, B., Gustafsson, O., Lundin, A., Lunell, N.O., Nylund, L., Rosenborg, L. and Pousette, A. 1987. Comparison between a swim-up and a Percoll gradient technique for the separation of human spermatozoa. *Int J Androl.* **10**(5), pp.663-9.
- Albers, A., Thie, M., Hohn, H.P. and Denker, H.W. 1995. Differential expression and localization of integrins and CD44 in the membrane domains of human uterine epithelial cells during the menstrual cycle. *Acta Anat (Basel).* **153**(1), pp.12-9.
- Alberts, B., Johnson, A., Lewis, J., Raff, M., Roberts, K. and Walter, P. 2002. *Molecular Biology of the Cell, 4th edition.* New York: Garland Science.
- Aliaga, A. and Ren, R. 2006. *Optimal sample sizes for two-stage cluster sampling in demographic and health surveys.* Calverton, Maryland, USA: ORC Macro.
- Alkhalaf, A., San Gabriel, M., Zeidan, K., Alrabeeh, K., Noel, D., McGraw, R., Bissonnette, F., Kadoch, I. and Zini, A. 2013. Sperm DNA and chromatin integrity in semen samples used for intrauterine insemination. *Journal of Assisted Reproduction and Genetics.* pp.1-6.
- Allamaneni, S.S., Agarwal, A., Rama, S., Ranganathan, P. and Sharma, R.K. 2005. Comparative study on density gradients and swim-up preparation techniques utilizing neat and cryopreserved spermatozoa. *Asian J Androl.* **7**(1), pp.86-92.
- Alukal, J.P. and Lamb, D.J. 2008. Intracytoplasmic sperm injection (ICSI)--what are the risks? *Urol Clin North Am.* **35**(2), pp.277-88, ix-x.
- Amann, R.P. and Schanbacher, B.D. 1983. Physiology of male reproduction. *J Anim Sci.* **57** Suppl 2, pp.380-403.
- Amaral, A., Castillo, J., Estanyol, J.M., Balleca, J.L., Ramalho-Santos, J. and Oliva, R. 2013. Human sperm tail proteome suggests new endogenous metabolic pathways. *Mol Cell Proteomics.* **12**(2), pp.330-42.
- Amaral, A., Castillo, J., Ramalho-Santos, J. and Oliva, R. 2014a. The combined human sperm proteome: cellular pathways and implications for basic and clinical science. *Hum Reprod Update.* **20**(1), pp.40-62.
- Amaral, A., Paiva, C., Attardo Parrinello, C., Estanyol, J.M., Balleca, J.L., Ramalho-Santos, J. and Oliva, R. 2014b. Identification of proteins involved in human sperm motility using high-throughput differential proteomics. *J Proteome Res.* **13**(12), pp.5670-84.
- Amemiya, K., Nakatani, T., Saito, A., Suzuki, A. and Munakata, H. 2005. Hyaluronan-binding motif identified by panning a random peptide display library. *Biochim Biophys Acta.* **1724**(1-2), pp.94-9.
- Amiri, I., Ghorbani, M. and Heshmati, S. 2012. Comparison of the DNA Fragmentation and the Sperm Parameters after Processing by the Density Gradient and the Swim up Methods. *J Clin Diagn Res.* **6**(9), pp.1451-3.
- An, C.N., Jiang, H., Wang, Q., Yuan, R.P., Liu, J.M., Shi, W.L., Zhang, Z.Y. and Pu, X.P. 2011. Down-regulation of DJ-1 protein in the ejaculated spermatozoa from Chinese asthenozoospermia patients. *Fertil Steril.* **96**(1), pp.19-23 e2.
- Angulo, C., Rauch, M.C., Droppelmann, A., Reyes, A.M., Slebe, J.C., Delgado-Lopez, F., Guaiquil, V.H., Vera, J.C. and Concha, II. 1998. Hexose transporter expression and function in mammalian spermatozoa: cellular localization and transport of hexoses and vitamin C. *J Cell Biochem.* **71**(2), pp.189-203.
- Arcelay, E., Salicioni, A.M., Wertheimer, E. and Visconti, P.E. 2008. Identification of proteins undergoing tyrosine phosphorylation during mouse sperm capacitation. *Int J Dev Biol.* **52**(5-6), pp.463-72.

- Arpanahi, A.Brinkworth, M.Iles, D.Krawetz, S.A.Paradowska, A.Platts, A.E.Saida, M.Steger, K.Tedder, P. and Miller, D. 2009. Endonuclease-sensitive regions of human spermatozoal chromatin are highly enriched in promoter and CTCF binding sequences. *Genome Res.* **19**(8), pp.1338-49.
- Asch, R.H.Ellsworth, L.R.Balmaceda, J.P. and Wong, P.C. 1984. Pregnancy after translaparoscopic gamete intrafallopian transfer. *Lancet.* **2**(8410), pp.1034-5.
- Asquith, K.L.Harman, A.J.McLaughlin, E.A.Nixon, B. and Aitken, R.J. 2005. Localization and significance of molecular chaperones, heat shock protein 1, and tumor rejection antigen gp96 in the male reproductive tract and during capacitation and acrosome reaction. *Biol Reprod.* **72**(2), pp.328-37.
- Assmann, V.Jenkinson, D.Marshall, J.F. and Hart, I.R. 1999. The intracellular hyaluronan receptor RHAMM/IHABP interacts with microtubules and actin filaments. *J Cell Sci.* **112** ( Pt **22**), pp.3943-54.
- Assmann, V.Marshall, J.F.Fieber, C.Hofmann, M. and Hart, I.R. 1998. The human hyaluronan receptor RHAMM is expressed as an intracellular protein in breast cancer cells. *J Cell Sci.* **111** ( Pt **12**), pp.1685-94.
- Auger, J.Mesbah, M.Huber, C. and Dadoune, J.P. 1990. Aniline blue staining as a marker of sperm chromatin defects associated with different semen characteristics discriminates between proven fertile and suspected infertile men. *Int J Androl.* **13**(6), pp.452-62.
- Austin, C.R. 1951. Observations on the penetration of the sperm in the mammalian egg. *Aust J Sci Res B.* **4**(4), pp.581-96.
- Austin, C.R. and Bishop, M.W. 1958. Capacitation of mammalian spermatozoa. *Nature.* **181**(4612), p851.
- Avendano, C. and Oehninger, S. 2011. DNA fragmentation in morphologically normal spermatozoa: how much should we be concerned in the ICSI era? *J Androl.* **32**(4), pp.356-63.
- Azpiazu, R.Amaral, A.Castillo, J.Estanyol, J.M.Guimera, M.Ballesca, J.L.Balash, J. and Oliva, R. 2014. High-throughput sperm differential proteomics suggests that epigenetic alterations contribute to failed assisted reproduction. *Hum Reprod.* **29**(6), pp.1225-37.
- Baarends, W.M.Roest, H.P. and Grootegoed, J.A. 1999. The ubiquitin system in gametogenesis. *Mol Cell Endocrinol.* **151**(1-2), pp.5-16.
- Bai, B.Tan, H.Pagala, V.R.High, A.A.Ichhaporia, V.P.Hendershot, L. and Peng, J. 2017. Deep Profiling of Proteome and Phosphoproteome by Isobaric Labeling, Extensive Liquid Chromatography, and Mass Spectrometry. *Methods Enzymol.* **585**, pp.377-395.
- Baibakov, B.Gauthier, L.Talbot, P.Rankin, T.L. and Dean, J. 2007. Sperm binding to the zona pellucida is not sufficient to induce acrosome exocytosis. *Development.* **134**(5), pp.933-43.
- Bailey, J.L. 2010. Factors regulating sperm capacitation. *Syst Biol Reprod Med.* **56**(5), pp.334-48.
- Bains, R.Adeghe, J. and Carson, R.J. 2002. Human sperm cells express CD44. *Fertil Steril.* **78**(2), pp.307-12.
- Baird, D.T.Collins, J.Egozcue, J.Evers, L.H.Gianaroli, L.Leridon, H.Sunde, A.Templeton, A.Van Steirteghem, A.Cohen, J.Crosignani, P.G.Devroey, P.Diedrich, K.Fauser, B.C.J.M.Fraser, L.Glasier, A.Liebaers, I.Mautone, G.Penney, G. and Tarlatzis, B. 2005. Fertility and ageing. *Human Reproduction Update.* **11**(3), pp.261-276.
- Bajorath, J.Greenfield, B.Munro, S.B.Day, A.J. and Aruffo, A. 1998. Identification of CD44 residues important for hyaluronan binding and delineation of the binding site. *J Biol Chem.* **273**(1), pp.338-43.
- Baker, M.A.Hetherington, L. and Aitken, R.J. 2006. Identification of SRC as a key PKA-stimulated tyrosine kinase involved in the capacitation-associated hyperactivation of murine spermatozoa. *J Cell Sci.* **119**(Pt 15), pp.3182-92.

- Baker, M.A.Reeves, G.Hetherington, L. and Aitken, R.J. 2010a. Analysis of proteomic changes associated with sperm capacitation through the combined use of IPG-strip pre-fractionation followed by RP chromatography LC-MS/MS analysis. *Proteomics*. **10**(3), pp.482-95.
- Baker, M.A.Reeves, G.Hetherington, L. and Aitken, R.J. 2010b. Analysis of proteomic changes associated with sperm capacitation through the combined use of IPG-strip pre-fractionation followed by RP chromatography LC-MS/MS analysis. *Proteomics*. **10**(3), pp.482-495.
- Baker, M.A.Smith, N.D.Hetherington, L.Taubman, K.Graham, M.E.Robinson, P.J. and Aitken, R.J. 2010c. Label-free quantitation of phosphopeptide changes during rat sperm capacitation. *J Proteome Res*. **9**(2), pp.718-29.
- Bakhtiari, M.Sobhani, A.Akbari, M.Pasbakhsh, P.Abbasi, M.Hedayatpoor, A.Amidi, F. and Sargolzaei, F. 2007. The effect of hyaluronic acid on motility, vitality and fertilization capability of mouse sperms after cryopreservation *Iranian Journal of Reproductive Medicine*. **5**(2), pp.45-50.
- Baldi, E.Luconi, M.Bonaccorsi, L.Krausz, C. and Forti, G. 1996. Human sperm activation during capacitation and acrosome reaction: role of calcium, protein phosphorylation and lipid remodelling pathways. *Front Biosci*. **1**, pp.d189-205.
- Baldi, E.Luconi, M.Bonaccorsi, L.Muratori, M. and Forti, G. 2000. Intracellular events and signaling pathways involved in sperm acquisition of fertilizing capacity and acrosome reaction. *Front Biosci*. **5**, pp.E110-23.
- Balhorn, R. 2007. The protamine family of sperm nuclear proteins. *Genome Biol*. **8**(9), p227.
- Banerjee, S.D. and Toole, B.P. 1991. Monoclonal antibody to chick embryo hyaluronan-binding protein: changes in distribution of binding protein during early brain development. *Dev Biol*. **146**(1), pp.186-97.
- Bansal, S.K.Gupta, N.Sankhwar, S.N. and Rajender, S. 2015. Differential Genes Expression between Fertile and Infertile Spermatozoa Revealed by Transcriptome Analysis. *PLoS One*. **10**(5), pe0127007.
- Baranova, N.S.Inforzato, A.Briggs, D.C.Tilakaratna, V.Engchild, J.J.Thakar, D.Milner, C.M.Day, A.J. and Richter, R.P. 2014. Incorporation of pentraxin 3 into hyaluronan matrices is tightly regulated and promotes matrix cross-linking. *J Biol Chem*. **289**(44), pp.30481-98.
- Baranova, N.S.Nileback, E.Haller, F.M.Briggs, D.C.Svedhem, S.Day, A.J. and Richter, R.P. 2011. The inflammation-associated protein TSG-6 cross-links hyaluronan via hyaluronan-induced TSG-6 oligomers. *J Biol Chem*. **286**(29), pp.25675-86.
- Barratt, C.L.Aitken, R.J.Bjorndahl, L.Carrell, D.T.de Boer, P.Kvist, U.Lewis, S.E.Perreault, S.D.Perry, M.J.Ramos, L.Robaire, B.Ward, S. and Zini, A. 2010. Sperm DNA: organization, protection and vulnerability: from basic science to clinical applications--a position report. *Hum Reprod*. **25**(4), pp.824-38.
- Barroso, G.Valdespin, C.Vega, E.Kershenovich, R.Avila, R.Avendano, C. and Oehninger, S. 2009. Developmental sperm contributions: fertilization and beyond. *Fertil Steril*. **92**(3), pp.835-48.
- Bartoov, B.Berkovitz, A.Eltes, F.Kogosovsky, A.Yagoda, A.Lederman, H.Artzi, S.Gross, M. and Barak, Y. 2003. Pregnancy rates are higher with intracytoplasmic morphologically selected sperm injection than with conventional intracytoplasmic injection. *Fertil Steril*. **80**(6), pp.1413-9.
- Bartoov, B.Berkovitz, A.Eltes, F.Kogosowski, A.Menezo, Y. and Barak, Y. 2002. Real-time fine morphology of motile human sperm cells is associated with IVF-ICSI outcome. *J Androl*. **23**(1), pp.1-8.
- Baulch, J.E.Li, M.W. and Raabe, O.G. 2007. Effect of ATM heterozygosity on heritable DNA damage in mice following paternal FO germline irradiation. *Mutat Res*. **616**(1-2), pp.34-45.

- Baumber, J.Sabeur, K.Vo, A. and Ball, B.A. 2003. Reactive oxygen species promote tyrosine phosphorylation and capacitation in equine spermatozoa. *Theriogenology*. **60**(7), pp.1239-47.
- Beck-Fruchter, R.Shalev, E. and Weiss, A. 2015. Clinical benefit using sperm hyaluronic acid binding technique in ICSI cycles: a systematic review and meta-analysis. *Reprod Biomed Online*.
- Beck-Fruchter, R.Shalev, E. and Weiss, A. 2016. Clinical benefit using sperm hyaluronic acid binding technique in ICSI cycles: a systematic review and meta-analysis. *Reprod Biomed Online*. **32**(3), pp.286-98.
- Beck, M.Schmidt, A.Malmstroem, J.Claassen, M.Ori, A.Szymborska, A.Herzog, F.Rinner, O.Ellenberg, J. and Aebersold, R. 2011. The quantitative proteome of a human cell line. *Mol Syst Biol*. **7**, p549.
- Benchaib, M.Braun, V.Ressnikof, D.Lornage, J.Durand, P.Niveleau, A. and Guerin, J.F. 2005. Influence of global sperm DNA methylation on IVF results. *Hum Reprod*. **20**(3), pp.768-73.
- Benoff, S.Hurley, I.Cooper, G.W.Mandel, F.S.Rosenfeld, D.L. and Hershlag, A. 1993. Head-specific mannose-ligand receptor expression in human spermatozoa is dependent on capacitation-associated membrane cholesterol loss. *Hum Reprod*. **8**(12), pp.2141-54.
- Bergqvist, A.S.Ballester, J.Johannisson, A.Hernandez, M.Lundeheim, N. and Rodriguez-Martinez, H. 2006. In vitro capacitation of bull spermatozoa by oviductal fluid and its components. *Zygote*. **14**(3), pp.259-73.
- Bergqvist, A.S.Yokoo, M.Bage, R.Sato, E. and Rodriguez-Martinez, H. 2005. Detection of the hyaluronan receptor CD44 in the bovine oviductal epithelium. *J Reprod Dev*. **51**(4), pp.445-53.
- Bernabo, N.Greco, L.Ordinelli, A.Mattioli, M. and Barboni, B. 2015. Capacitation-Related Lipid Remodeling of Mammalian Spermatozoa Membrane Determines the Final Fate of Male Gametes: A Computational Biology Study. *OMICS*. **19**(11), pp.712-21.
- Bjorndahl, L.Mortimer, D.Barratt, C.Castilla, J.Menkveld, R.Kvist, U.Alvarez, J.G. and Haugen, T.B. 2010. *A Practical Guide to Basic Laboratory Andrology*. Cambridge. Cambridge University Press.
- Bogle, O.A.Kumar, K.Attardo-Parrinello, C.Lewis, S.E.Estanyol, J.M.Ballesca, J.L. and Oliva, R. 2017. Identification of protein changes in human spermatozoa throughout the cryopreservation process. *Andrology*. **5**(1), pp.10-22.
- Bolton, V.N. and Braude, P.R. 1984. Preparation of human spermatozoa for in vitro fertilization by isopycnic centrifugation on self-generating density gradients. *Arch Androl*. **13**(2-3), pp.167-76.
- Bonduelle, M.Van Assche, E.Joris, H.Keymolen, K.Devroey, P.Van Steirteghem, A. and Liebaers, I. 2002. Prenatal testing in ICSI pregnancies: incidence of chromosomal anomalies in 1586 karyotypes and relation to sperm parameters. *Hum Reprod*. **17**(10), pp.2600-14.
- Botezatu, A.Socolov, R.Socolov, D.Iancu, I.V. and Anton, G. 2014. Methylation pattern of methylene tetrahydrofolate reductase and small nuclear ribonucleoprotein polypeptide N promoters in oligoasthenospermia: A case-control study. *Reproductive BioMedicine Online*. **28**(2), pp.225-231.
- Bou Khalil, M.Chakrabandhu, K.Xu, H.Weerachayanukul, W.Buhr, M.Berger, T.Carmona, E.Vuong, N.Kumarathanan, P.Wong, P.T.Carrier, D. and Tanphaichitr, N. 2006. Sperm capacitation induces an increase in lipid rafts having zona pellucida binding ability and containing sulfogalactosylglycerolipid. *Dev Biol*. **290**(1), pp.220-35.
- Boussouar, F. and Benahmed, M. 2004. Lactate and energy metabolism in male germ cells. *Trends Endocrinol Metab*. **15**(7), pp.345-50.
- Brahem, S.Mehdi, M.Elghzal, H. and Saad, A. 2011. Semen processing by density gradient centrifugation is useful in selecting sperm with higher double-strand DNA integrity. *Andrologia*. **43**(3), pp.196-202.

- Bravo, A.Treulen, F.Uribe, P.Boguen, R.Felmer, R. and Villegas, J.V. 2015. Effect of mitochondrial calcium uniporter blocking on human spermatozoa. *Andrologia*. **47**(6), pp.662-8.
- Bravo, P.W.Ccallo, M. and Garnica, J. 2000. The effect of enzymes on semen viscosity in Llamas and Alpacas. *Small Rumin Res*. **38**(1), pp.91-95.
- Breitbart, H. 2003. Signaling pathways in sperm capacitation and acrosome reaction. *Cell Mol Biol (Noisy-le-grand)*. **49**(3), pp.321-7.
- Breitbart, H. and Spungin, B. 1997. The biochemistry of the acrosome reaction. *Mol Hum Reprod*. **3**(3), pp.195-202.
- Brener, E.Rubinstein, S.Cohen, G.Shternall, K.Rivlin, J. and Breitbart, H. 2003. Remodeling of the actin cytoskeleton during mammalian sperm capacitation and acrosome reaction. *Biol Reprod*. **68**(3), pp.837-45.
- Breton, S. 2001. The cellular physiology of carbonic anhydrases. *JOP*. **2**(4 Suppl), pp.159-64.
- Brevik, A.Lindeman, B.Rusnakova, V.Olsen, A.K.Brunborg, G. and Duale, N. 2012. Paternal benzo[a]pyrene exposure affects gene expression in the early developing mouse embryo. *Toxicol Sci*. **129**(1), pp.157-65.
- Bucci, D.Isani, G.Spinaci, M.Tamanini, C.Mari, G.Zambelli, D. and Galeati, G. 2010. Comparative immunolocalization of GLUTs 1, 2, 3 and 5 in boar, stallion and dog spermatozoa. *Reprod Domest Anim*. **45**(2), pp.315-22.
- Bucci, D.Rodriguez-Gil, J.E.Vallorani, C.Spinaci, M.Galeati, G. and Tamanini, C. 2011. GLUTs and mammalian sperm metabolism. *J Androl*. **32**(4), pp.348-55.
- Buffone, M.G.Ijiri, T.W.Cao, W.Merdiushev, T.Aghajanian, H.K. and Gerton, G.L. 2012. Heads or tails? Structural events and molecular mechanisms that promote mammalian sperm acrosomal exocytosis and motility. *Mol Reprod Dev*. **79**(1), pp.4-18.
- Bungum, M.Humaidan, P.Axmon, A.Spano, M.Bungum, L.Erenpreiss, J. and Giwercman, A. 2007. Sperm DNA integrity assessment in prediction of assisted reproduction technology outcome. *Hum Reprod*. **22**(1), pp.174-9.
- Burant, C.F.Takeda, J.Brot-Laroche, E.Bell, G.I. and Davidson, N.O. 1992. Fructose transporter in human spermatozoa and small intestine is GLUT5. *J Biol Chem*. **267**(21), pp.14523-6.
- Busso, D.Goldweic, N.M.Hayashi, M.Kasahara, M. and Cuasnicu, P.S. 2007. Evidence for the involvement of testicular protein CRISP2 in mouse sperm-egg fusion. *Biol Reprod*. **76**(4), pp.701-8.
- Cambi, M.Tamburrino, L.Marchiani, S.Olivito, B.Azzari, C.Forti, G.Baldi, E. and Muratori, M. 2013. Development of a specific method to evaluate 8-hydroxy, 2-deoxyguanosine in sperm nuclei: relationship with semen quality in a cohort of 94 subjects. *Reproduction*. **145**(3), pp.227-35.
- Carr, D.W. and Newell, A.E. 2007. The role of A-kinase anchoring proteins (AKaps) in regulating sperm function. *Soc Reprod Fertil Suppl*. **63**, pp.135-41.
- Carrell, D.T. and Hammoud, S.S. 2010. The human sperm epigenome and its potential role in embryonic development. *Molecular Human Reproduction*. **16**(1), pp.37-47.
- Carrell, D.T.Liu, L.Peterson, C.M.Jones, K.P.Hatasaka, H.H.Erickson, L. and Campbell, B. 2003. Sperm DNA fragmentation is increased in couples with unexplained recurrent pregnancy loss. *Arch Androl*. **49**(1), pp.49-55.
- Carrera, A.Moos, J.Ning, X.P.Gerton, G.L.Tesarik, J.Kopf, G.S. and Moss, S.B. 1996. Regulation of protein tyrosine phosphorylation in human sperm by a calcium/calmodulin-dependent mechanism: identification of A kinase anchor proteins as major substrates for tyrosine phosphorylation. *Dev Biol*. **180**(1), pp.284-96.
- Carroll, J. and Marangos, P. 2013. The DNA damage response in mammalian oocytes. *Front Genet*. **4**, p117.
- Casey, P.J.Gravance, C.G.Davis, R.O.Chabot, D.D. and Liu, I.K. 1997. Morphometric differences in sperm head dimensions of fertile and subfertile stallions. *Theriogenology*. **47**(2), pp.575-82.

- Castillo, J.Amaral, A.Azpiazu, R.Vavouri, T.Estanyol, J.M.Ballesca, J.L. and Oliva, R. 2014. Genomic and proteomic dissection and characterization of the human sperm chromatin. *Mol Hum Reprod.* **20**(11), pp.1041-53.
- Castillo, J.Estanyol, J.M.Ballesca, J.L. and Oliva, R. 2015. Human sperm chromatin epigenetic potential: genomics, proteomics, and male infertility. *Asian J Androl.* **17**(4), pp.601-9.
- Cayli, S.Jakab, A.Ovari, L.Delpiano, E.Celik-Ozenci, C.Sakkas, D.Ward, D. and Huszar, G. 2003. Biochemical markers of sperm function: male fertility and sperm selection for ICSI. *Reprod Biomed Online.* **7**(4), pp.462-8.
- Celik-Ozenci, C.Jakab, A.Kovacs, T.Catalanotti, J.Demir, R.Bray-Ward, P.Ward, D. and Huszar, G. 2004. Sperm selection for ICSI: shape properties do not predict the absence or presence of numerical chromosomal aberrations. *Hum Reprod.* **19**(9), pp.2052-9.
- Cha, K.Y.Koo, J.J.Ko, J.J.Choi, D.H.Han, S.Y. and Yoon, T.K. 1991. Pregnancy after in vitro fertilization of human follicular oocytes collected from nonstimulated cycles, their culture in vitro and their transfer in a donor oocyte program. *Fertil Steril.* **55**(1), pp.109-13.
- Chai, R.R.Chen, G.W.Shi, H.J.O, W.S.Martin-DeLeon, P.A. and Chen, H. 2017. Prohibitin involvement in the generation of mitochondrial superoxide at complex I in human sperm. *J Cell Mol Med.* **21**(1), pp.121-129.
- Chalbi, M.Barraud-Lange, V.Ravaux, B.Howan, K.Rodriguez, N.Soule, P.Ndzoudi, A.Boucheix, C.Rubinstein, E.Wolf, J.P.Ziyyat, A.Perez, E.Pincet, F. and Gourier, C. 2014. Binding of sperm protein Izumo1 and its egg receptor Juno drives Cd9 accumulation in the intercellular contact area prior to fusion during mammalian fertilization. *Development.* **141**(19), pp.3732-9.
- Chan, P.J.Jacobson, J.D.Corselli, J.U. and Patton, W.C. 2006. A simple zeta method for sperm selection based on membrane charge. *Fertil Steril.* **85**(2), pp.481-6.
- Chang, M.C. 1951. Fertilizing capacity of spermatozoa deposited into the fallopian tubes. *Nature.* **168**(4277), pp.697-8.
- Check, M.L.Check, J.H.Katsoff, D. and Summers-Chase, D. 2000. ICSI as an effective therapy for male factor with antisperm antibodies. *Arch Androl.* **45**(3), pp.125-30.
- Chen, J.Wu, S.Wen, S.Shen, L.Peng, J.Yan, C.Cao, X.Zhou, Y.Long, C.Lin, T.He, D.Hua, Y. and Wei, G. 2015. The mechanism of environmental endocrine disruptors (DEHP) induces epigenetic transgenerational inheritance of cryptorchidism. *PLoS ONE.* **10**(6).
- Chen, S.J.Allam, J.P.Duan, Y.G. and Haidl, G. 2013. Influence of reactive oxygen species on human sperm functions and fertilizing capacity including therapeutical approaches. *Arch Gynecol Obstet.*
- Chen, W.Y. and Abatangelo, G. 1999. Functions of hyaluronan in wound repair. *Wound Repair Regen.* **7**(2), pp.79-89.
- Cheng, C.Y. and Mruk, D.D. 2010. The biology of spermatogenesis: the past, present and future. *Philos Trans R Soc Lond B Biol Sci.* **365**(1546), pp.1459-63.
- Cherr, G.N.Yudin, A.I. and Overstreet, J.W. 2001. The dual functions of GPI-anchored PH-20: hyaluronidase and intracellular signaling. *Matrix Biol.* **20**(8), pp.515-25.
- Chivers, C.E.Koner, A.L.Lowe, E.D. and Howarth, M. 2011. How the biotin-streptavidin interaction was made even stronger: investigation via crystallography and a chimaeric tetramer. *Biochem J.* **435**(1), pp.55-63.
- Chohan, K.R.Griffin, J.T. and Carrell, D.T. 2004. Evaluation of chromatin integrity in human sperm using acridine orange staining with different fixatives and after cryopreservation. *Andrologia.* **36**(5), pp.321-6.
- Choi-Miura, N.H.Tobe, T.Sumiya, J.Nakano, Y.Sano, Y.Mazda, T. and Tomita, M. 1996. Purification and characterization of a novel hyaluronan-binding protein (PHBP) from human plasma: it has three EGF, a kringle and a serine protease domain, similar to hepatocyte growth factor activator. *J Biochem.* **119**(6), pp.1157-65.

- Choi, Y.J.Uhm, S.J.Song, S.J.Song, H.Park, J.K.Kim, T.Park, C. and Kim, J.H. 2008a. Cytochrome c upregulation during capacitation and spontaneous acrosome reaction determines the fate of pig sperm cells: linking proteome analysis. *J Reprod Dev.* **54**(1), pp.68-83.
- Choi, Y.J.Uhm, S.J.Song, S.J.Song, H.Park, J.K.Kim, T.Park, C. and Kim, J.H. 2008b. Cytochrome c upregulation during capacitation and spontaneous acrosome reaction determines the fate of pig sperm cells: Linking proteome analysis. *Journal of Reproduction and Development.* **54**(1), pp.68-83.
- Choudhary, M.Zhang, X.Stojkovic, P.Hyslop, L.Anyfantis, G.Herbert, M.Murdoch, A.P.Stojkovic, M. and Lako, M. 2007. Putative role of hyaluronan and its related genes, HAS2 and RHAMM, in human early preimplantation embryogenesis and embryonic stem cell characterization. *Stem Cells.* **25**(12), pp.3045-57.
- Chowdhury, I.Thompson, W.E. and Thomas, K. 2014. Prohibitins role in cellular survival through Ras-Raf-MEK-ERK pathway. *J Cell Physiol.* **229**(8), pp.998-1004.
- Chung, J.J.Shim, S.H.Everley, R.A.Gygi, S.P.Zhuang, X. and Clapham, D.E. 2014. Structurally distinct Ca(2+) signaling domains of sperm flagella orchestrate tyrosine phosphorylation and motility. *Cell.* **157**(4), pp.808-22.
- Clift, D. and Schuh, M. 2013. Restarting life: fertilization and the transition from meiosis to mitosis. *Nat Rev Mol Cell Biol.* **14**(9), pp.549-62.
- Cocuzza, M.Alvarenga, C. and Pagani, R. 2013. The epidemiology and etiology of azoospermia. *Clinics (Sao Paulo).* **68 Suppl 1**, pp.15-26.
- Cohen-Dayag, A.Tur-Kaspa, I.Dor, J.Mashiach, S. and Eisenbach, M. 1995. Sperm capacitation in humans is transient and correlates with chemotactic responsiveness to follicular factors. *Proc Natl Acad Sci U S A.* **92**(24), pp.11039-43.
- Cohen, D.J.Da Ros, V.G.Busso, D.Ellerman, D.A.Maldera, J.A.Goldweic, N. and Cuasnicu, P.S. 2007. Participation of epididymal cysteine-rich secretory proteins in sperm-egg fusion and their potential use for male fertility regulation. *Asian J Androl.* **9**(4), pp.528-32.
- Cohen, J.Trounson, A.Dawson, K.Jones, H.Hazekamp, J.Nygren, K.G. and Hamberger, L. 2005. The early days of IVF outside the UK. *Hum Reprod Update.* **11**(5), pp.439-59.
- Cooper, T.G. 1995. Role of the epididymis in mediating changes in the male gamete during maturation. *Adv Exp Med Biol.* **377**, pp.87-101.
- Cooper, T.G. 2011. The epididymis, cytoplasmic droplets and male fertility. *Asian J Androl.* **13**(1), pp.130-8.
- Cordoba, M.Pintos, L. and Beconi, M.T. 2008. Variations in creatine kinase activity and reactive oxygen species levels are involved in capacitation of bovine spermatozoa. *Andrologia.* **40**(6), pp.370-6.
- Cornwall, G.A. 2009. New insights into epididymal biology and function. *Hum Reprod Update.* **15**(2), pp.213-27.
- Coughlan, C.Clarke, H.Cutting, R.Saxton, J.Waite, S.Ledger, W.Li, T. and Pacey, A.A. 2015. Sperm DNA fragmentation, recurrent implantation failure and recurrent miscarriage. *Asian J Androl.* **17**(4), pp.681-5.
- Courot, M. 1976. Hormonal regulation of male reproduction (with reference to infertility in man). *Andrologia.* **8**(3), pp.187-93.
- Coy, P.Garcia-Vazquez, F.A.Visconti, P.E. and Aviles, M. 2012. Roles of the oviduct in mammalian fertilization. *Reproduction.* **144**(6), pp.649-60.
- Cross, N.L. and Meizel, S. 1989. Methods for evaluating the acrosomal status of mammalian sperm. *Biol Reprod.* **41**(4), pp.635-41.
- Csoka, A.B.Frost, G.I. and Stern, R. 2001. The six hyaluronidase-like genes in the human and mouse genomes. *Matrix Biol.* **20**(8), pp.499-508.
- Cummins, J.M. and Jequier, A.M. 1995. Concerns and recommendations for intracytoplasmic sperm injection (ICSI) treatment. *Hum Reprod.* **10 Suppl 1**, pp.138-43.

- D'Cruz, O.J.Haas, G.G., Jr. and Lambert, H. 1993. Heterogeneity of human sperm surface antigens identified by indirect immunoprecipitation of antisperm antibody bound to biotinylated sperm. *J Immunol.* **151**(2), pp.1062-74.
- D. SakkasG. Leppens-LuisierH. LucasD. ChardonnensA. CampanaD.R. Franken and F. Urner. 2003. Localization of Tyrosine Phosphorylated Proteins in Human Sperm and Relation to Capacitation and Zona Pellucida Binding. *Biol Reprod.* **68**(4), pp.1463-1469.
- Dada, R.Kumar, M.Jesudasan, R.Fernandez, J.L.Gosalvez, J. and Agarwal, A. 2012. Epigenetics and its role in male infertility. *J Assist Reprod Genet.* **29**(3), pp.213-23.
- Danshina, P.V.Geyer, C.B.Dai, Q.Goulding, E.H.Willis, W.D.Kitto, G.B.McCarrey, J.R.Eddy, E.M. and O'Brien, D.A. 2010. Phosphoglycerate kinase 2 (PGK2) is essential for sperm function and male fertility in mice. *Biol Reprod.* **82**(1), pp.136-45.
- Davidoff, M.S.Breucker, H.Holstein, A.F. and Seidl, K. 1990. Cellular architecture of the lamina propria of human seminiferous tubules. *Cell Tissue Res.* **262**(2), pp.253-61.
- Davis, B.K. 1981. Timing of fertilization in mammals: sperm cholesterol/phospholipid ratio as a determinant of the capacitation interval. *Proc Natl Acad Sci U S A.* **78**(12), pp.7560-4.
- Davis, B.K.Byrne, R. and Hungund, B. 1979. Studies on the mechanism of capacitation. II. Evidence for lipid transfer between plasma membrane of rat sperm and serum albumin during capacitation in vitro. *Biochim Biophys Acta.* **558**(3), pp.257-66.
- Day, A.J. Understanding Hyaluronan-Protein Interction.
- Day, A.J. and Prestwich, G.D. 2002. Hyaluronan-binding proteins: tying up the giant. *J Biol Chem.* **277**(7), pp.4585-8.
- De Jonge, C. 2005. Biological basis for human capacitation. *Hum Reprod Update.* **11**(3), pp.205-14.
- De Jonge, C.J. and Barratt, C.L. 2013. Methods for the assessment of sperm capacitation and acrosome reaction excluding the sperm penetration assay. *Methods Mol Biol.* **927**, pp.113-8.
- de Lamirande, E. and Gagnon, C. 1993. A positive role for the superoxide anion in triggering hyperactivation and capacitation of human spermatozoa. *Int J Androl.* **16**(1), pp.21-5.
- de Lamirande, E. and Lamothe, G. 2009. Reactive oxygen-induced reactive oxygen formation during human sperm capacitation. *Free Radic Biol Med.* **46**(4), pp.502-10.
- de Lamirande, E. and Lamothe, G. 2010. Levels of semenogelin in human spermatozoa decrease during capacitation: involvement of reactive oxygen species and zinc. *Hum Reprod.* **25**(7), pp.1619-30.
- de Lamirande, E.Leclerc, P. and Gagnon, C. 1997. Capacitation as a regulatory event that primes spermatozoa for the acrosome reaction and fertilization. *Mol Hum Reprod.* **3**(3), pp.175-94.
- de Lamirande, E. and O'Flaherty, C. 2008. Sperm activation: role of reactive oxygen species and kinases. *Biochim Biophys Acta.* **1784**(1), pp.106-15.
- de Lamirande, E.Yoshida, K.Yoshiike, T.M.Iwamoto, T. and Gagnon, C. 2001. Semenogelin, the main protein of semen coagulum, inhibits human sperm capacitation by interfering with the superoxide anion generated during this process. *J Androl.* **22**(4), pp.672-9.
- de Paz, P.Mata-Campuzano, M.Tizado, E.J.Alvarez, M.Alvarez-Rodriguez, M.Herraez, P. and Anel, L. 2011. The relationship between ram sperm head morphometry and fertility depends on the procedures of acquisition and analysis used. *Theriogenology.* **76**(7), pp.1313-25.
- de Vries, K.J.Wiedmer, T.Sims, P.J. and Gadella, B.M. 2003. Caspase-independent exposure of aminophospholipids and tyrosine phosphorylation in bicarbonate responsive human sperm cells. *Biol Reprod.* **68**(6), pp.2122-34.
- Ded, L.Dostalova, P.Dorosh, A.Dvorakova-Hortova, K. and Peknicova, J. 2010. Effect of estrogens on boar sperm capacitation in vitro. *Reprod Biol Endocrinol.* **8**, p87.
- Delaroche, L.Yazbeck, C.Gout, C.Kahn, V.Oger, P. and Rougier, N. 2013. Intracytoplasmic morphologically selected sperm injection (IMSI) after repeated IVF or ICSI failures: a prospective comparative study. *Eur J Obstet Gynecol Reprod Biol.* **167**(1), pp.76-80.



- Delbès, G.Hales, B.F. and Robaire, B. 2010. Toxicants and human sperm chromatin integrity. *Molecular Human Reproduction*. **16**(1), pp.14-22.
- Demott, R.P. and Suarez, S.S. 1992. Hyperactivated sperm progress in the mouse oviduct. *Biol Reprod*. **46**(5), pp.779-85.
- Derijck, A.A.van der Heijden, G.W.Ramos, L.Giele, M.Kremer, J.A. and de Boer, P. 2007. Motile human normozoospermic and oligozoospermic semen samples show a difference in double-strand DNA break incidence. *Hum Reprod*. **22**(9), pp.2368-76.
- Devroey, P.Braeckmans, P.Smitz, J.Van Waesberghe, L.Wisanto, A.Van Steirteghem, A.Heytens, L. and Camu, F. 1986. Pregnancy after translaparoscopic zygote intrafallopian transfer in a patient with sperm antibodies. *Lancet*. **1**(8493), p1329.
- Devroey, P.Liu, J.Nagy, Z.Goossens, A.Tournaye, H.Camus, M.Van Steirteghem, A. and Silber, S. 1995. Pregnancies after testicular sperm extraction and intracytoplasmic sperm injection in non-obstructive azoospermia. *Hum Reprod*. **10**(6), pp.1457-60.
- Dias, T.R.Alves, M.G.Silva, B.M. and Oliveira, P.F. 2014. Sperm glucose transport and metabolism in diabetic individuals. *Mol Cell Endocrinol*. **396**(1-2), pp.37-45.
- Dicker, K.T.Gurski, L.A.Pradhan-Bhatt, S.Witt, R.L.Farach-Carson, M.C. and Jia, X. 2014. Hyaluronan: a simple polysaccharide with diverse biological functions. *Acta Biomater*. **10**(4), pp.1558-70.
- Diez-Sanchez, C.Ruiz-Pesini, E.Lapena, A.C.Montoya, J.Perez-Martos, A.Enriquez, J.A. and Lopez-Perez, M.J. 2003. Mitochondrial DNA content of human spermatozoa. *Biol Reprod*. **68**(1), pp.180-5.
- Ding, G.L.Liu, Y.Liu, M.E.Pan, J.X.Guo, M.X.Sheng, J.Z. and Huang, H.F. 2015. The effects of diabetes on male fertility and epigenetic regulation during spermatogenesis. *Asian Journal of Andrology*. **17**(6), pp.948-953.
- Donnelly, E.T.O'Connell, M.McClure, N. and Lewis, S.E. 2000. Differences in nuclear DNA fragmentation and mitochondrial integrity of semen and prepared human spermatozoa. *Hum Reprod*. **15**(7), pp.1552-61.
- Dorus, S.Wasbrough, E.R.Busby, J.Wilkin, E.C. and Karr, T.L. 2010. Sperm proteomics reveals intensified selection on mouse sperm membrane and acrosome genes. *Mol Biol Evol*. **27**(6), pp.1235-46.
- Douard, V. and Ferraris, R.P. 2008. Regulation of the fructose transporter GLUT5 in health and disease. *Am J Physiol Endocrinol Metab*. **295**(2), pp.E227-37.
- Dunson, D.B.Baird, D.D. and Colombo, B. 2004. Increased infertility with age in men and women. *Obstet Gynecol*. **103**(1), pp.51-6.
- Durmaz, A.Dikmen, N.Gunduz, C.Goker, E.N. and Tavmergen, E. 2014. Fluctuation of "sperm DNA integrity" in accordance with semen parameters, and it's relationship with infertility. *J Assist Reprod Genet*.
- Dzwonek, J. and Wilczynski, G.M. 2015. CD44: molecular interactions, signaling and functions in the nervous system. *Front Cell Neurosci*. **9**, p175.
- Ebner, T.Filicori, M.Tews, G. and Parmegiani, L. 2012. A plea for a more physiological ICSI. *Andrologia*. **44 Suppl 1**, pp.2-19.
- El Hachem, H.Crepaux, V.May-Panloup, P.Descamps, P.Legendre, G. and Bouet, P.E. 2017. Recurrent pregnancy loss: current perspectives. *Int J Womens Health*. **9**, pp.331-345.
- Elia, G. 2008. Biotinylation reagents for the study of cell surface proteins. *Proteomics*. **8**(19), pp.4012-24.
- Elia, G. 2012. Cell surface protein biotinylation for SDS-PAGE analysis. *Methods Mol Biol*. **869**, pp.361-72.
- Enciso, M.Johnston, S.D. and Gosalvez, J. 2011. Differential resistance of mammalian sperm chromatin to oxidative stress as assessed by a two-tailed comet assay. *Reprod Fertil Dev*. **23**(5), pp.633-7.

- Epe, B.Pflaum, M.Haring, M.Hegler, J. and Rudiger, H. 1993. Use of repair endonucleases to characterize DNA damage induced by reactive oxygen species in cellular and cell-free systems. *Toxicol Lett.* **67**(1-3), pp.57-72.
- Erberelli, R.F.Salgado, R.M.Pereira, D.H. and Wolff, P. 2017. Hyaluronan-binding system for sperm selection enhances pregnancy rates in ICSI cycles associated with male factor infertility. *JBRA Assist Reprod.* **21**(1), pp.2-6.
- Esbert, M.Pacheco, A.Vidal, F.Florensa, M.Riqueros, M.Ballesteros, A.Garrido, N. and Calderon, G. 2011. Impact of sperm DNA fragmentation on the outcome of IVF with own or donated oocytes. *Reprod Biomed Online.* **23**(6), pp.704-10.
- Evenson, D.P.Darzynkiewicz, Z. and Melamed, M.R. 1980. Relation of mammalian sperm chromatin heterogeneity to fertility. *Science.* **210**(4474), pp.1131-3.
- Evenson, D.P. and Wixon, R. 2006. Clinical aspects of sperm DNA fragmentation detection and male infertility. *Theriogenology.* **65**(5), pp.979-91.
- Fakhari, A. and Berkland, C. 2013. Applications and emerging trends of hyaluronic acid in tissue engineering, as a dermal filler and in osteoarthritis treatment. *Acta Biomater.* **9**(7), pp.7081-92.
- Falkenstein, E.Heck, M.Gerdes, D.Grube, D.Christ, M.Weigel, M.Buddhikot, M.Meizel, S. and Wehling, M. 1999. Specific progesterone binding to a membrane protein and related nongenomic effects on Ca<sup>2+</sup>-fluxes in sperm. *Endocrinology.* **140**(12), pp.5999-6002.
- Faure, A.K.Pivot-Pajot, C.Kerjean, A.Hazzouri, M.Pelletier, R.Peoc'h, M.Sele, B.Khochbin, S. and Rousseaux, S. 2003. Misregulation of histone acetylation in Sertoli cell-only syndrome and testicular cancer. *Mol Hum Reprod.* **9**(12), pp.757-63.
- Fenichel, P.Cervoni, F.Hofmann, P.Deckert, M.Emiliozzi, C.Hsi, B.L. and Rossi, B. 1994. Expression of the complement regulatory protein CD59 on human spermatozoa: characterization and role in gametic interaction. *Mol Reprod Dev.* **38**(3), pp.338-46.
- Fernandez, J.L.Muriel, L.Rivero, M.T.Goyanes, V.Vazquez, R. and Alvarez, J.G. 2003. The sperm chromatin dispersion test: a simple method for the determination of sperm DNA fragmentation. *J Androl.* **24**(1), pp.59-66.
- Fernandez, S. and Cordoba, M. 2014. Hyaluronic acid as capacitation inductor: metabolic changes and membrane-associated adenylate cyclase regulation. *Reprod Domest Anim.* **49**(6), pp.941-6.
- Ferramosca, A. and Zara, V. 2014. Bioenergetics of mammalian sperm capacitation. *Biomed Res Int.* **2014**, p902953.
- Ficarro, S.Chertihin, O.Westbrook, V.A.White, F.Jayes, F.Kalab, P.Marto, J.A.Shabanowitz, J.Herr, J.C.Hunt, D.F. and Visconti, P.E. 2003. Phosphoproteome analysis of capacitated human sperm. Evidence of tyrosine phosphorylation of a kinase-anchoring protein 3 and valosin-containing protein/p97 during capacitation. *J Biol Chem.* **278**(13), pp.11579-89.
- Filipponi, D. and Feil, R. 2009. Perturbation of genomic imprinting in oligozoospermia. *Epigenetics.* **4**(1), pp.27-30.
- Flesch, F.M.Brouwers, J.F.Nievelstein, P.F.Verkleij, A.J.van Golde, L.M.Colenbrander, B. and Gadella, B.M. 2001. Bicarbonate stimulated phospholipid scrambling induces cholesterol redistribution and enables cholesterol depletion in the sperm plasma membrane. *J Cell Sci.* **114**(Pt 19), pp.3543-55.
- Flesch, F.M. and Gadella, B.M. 2000. Dynamics of the mammalian sperm plasma membrane in the process of fertilization. *Biochim Biophys Acta.* **1469**(3), pp.197-235.
- Ford, W.C. 2006. Glycolysis and sperm motility: does a spoonful of sugar help the flagellum go round? *Hum Reprod Update.* **12**(3), pp.269-74.
- Forgione, N.Vogl, A.W. and Varmuza, S. 2010. Loss of protein phosphatase 1c{gamma} (PPP1CC) leads to impaired spermatogenesis associated with defects in chromatin condensation and acrosome development: an ultrastructural analysis. *Reproduction.* **139**(6), pp.1021-9.

- Foster, J.A.Klotz, K.L.Flickinger, C.J.Thomas, T.S.Wright, R.M.Castillo, J.R. and Herr, J.C. 1994. Human SP-10: acrosomal distribution, processing, and fate after the acrosome reaction. *Biol Reprod.* **51**(6), pp.1222-31.
- Fouladi-Nashta, A.A.Raheem, K.A.Marei, W.F.Ghafari, F. and Hartshorne, G.M. 2017. Regulation and roles of the hyaluronan system in mammalian reproduction. *Reproduction.* **153**(2), pp.R43-R58.
- Fraietta, R.Zylberstejn, D.S. and Esteves, S.C. 2013. Hypogonadotropic hypogonadism revisited. *Clinics (Sao Paulo).* **68 Suppl 1**, pp.81-8.
- Francou, M.M.Ten, J.Bernabeu, R. and De Juan, J. 2014. Capacitation and acrosome reaction changes alpha-tubulin immunodistribution in human spermatozoa. *Reprod Biomed Online.* **28**(2), pp.246-50.
- Frapsauce, C.Pionneau, C.Bouley, J.Delarouziere, V.Berthaut, I.Ravel, C.Antoine, J.M.Soubrier, F. and Mandelbaum, J. 2014. Proteomic identification of target proteins in normal but nonfertilizing sperm. *Fertil Steril.* **102**(2), pp.372-80.
- Fraser, L.R. 1992. Requirements for successful mammalian sperm capacitation and fertilization. *Arch Pathol Lab Med.* **116**(4), pp.345-50.
- Fraser, L.R. 1998a. Interactions between a decapacitation factor and mouse spermatozoa appear to involve fucose residues and a GPI-anchored receptor. *Mol Reprod Dev.* **51**(2), pp.193-202.
- Fraser, L.R. 1998b. Sperm capacitation and the acrosome reaction. *Hum Reprod.* **13 Suppl 1**, pp.9-19.
- Frydman, N.Romana, S.Le Lorc'h, M.Vekemans, M.Frydman, R. and Tachdjian, G. 2001. Assisting reproduction of infertile men carrying a Robertsonian translocation. *Hum Reprod.* **16**(11), pp.2274-7.
- Fujihara, Y.Murakami, M.Inoue, N.Satouh, Y.Kaseda, K.Ikawa, M. and Okabe, M. 2010. Sperm equatorial segment protein 1, SPESP1, is required for fully fertile sperm in mouse. *J Cell Sci.* **123**(Pt 9), pp.1531-6.
- Furnus, C.C.Valcarcel, A.Dulout, F.N. and Errecalde, A.L. 2003. The hyaluronic acid receptor (CD44) is expressed in bovine oocytes and early stage embryos. *Theriogenology.* **60**(9), pp.1633-44.
- Gadella, B.M. 2010. Interaction of sperm with the zona pellucida during fertilization. *Soc Reprod Fertil Suppl.* **67**, pp.267-87.
- Gadella, B.M. and Harrison, R.A. 2000. The capacitating agent bicarbonate induces protein kinase A-dependent changes in phospholipid transbilayer behavior in the sperm plasma membrane. *Development.* **127**(11), pp.2407-20.
- Gadella, B.M.Tsai, P.S.Boerke, A. and Brewis, I.A. 2008. Sperm head membrane reorganisation during capacitation. *Int J Dev Biol.* **52**(5-6), pp.473-80.
- Gallegos, G.Ramos, B.Santiso, R.Goyanes, V.Gosalvez, J. and Fernandez, J.L. 2008. Sperm DNA fragmentation in infertile men with genitourinary infection by Chlamydia trachomatis and Mycoplasma. *Fertil Steril.* **90**(2), pp.328-34.
- Garolla, A.Cosci, I.Bertoldo, A.Sartini, B.Boudjema, E. and Foresta, C. 2015. DNA double strand breaks in human spermatozoa can be predictive for assisted reproductive outcome. *Reprod Biomed Online.* **31**(1), pp.100-7.
- Geipel, U.Kropf, J.Krause, W. and Gressner, A.M. 1992. The concentration pattern of laminin, hyaluronan, and aminoterminal propeptide of type III procollagen in seminal fluid. *Andrologia.* **24**(4), pp.205-11.
- Ghosh, I.Bharadwaj, A. and Datta, K. 2002. Reduction in the level of hyaluronan binding protein 1 (HABP1) is associated with loss of sperm motility. *J Reprod Immunol.* **53**(1-2), pp.45-54.
- Ghosh, I.Chattopadhyaya, R.Kumar, V.Chakravarty, B.N. and Datta, K. 2007. Hyaluronan binding protein-1: a modulator of sperm-oocyte interaction. *Soc Reprod Fertil Suppl.* **63**, pp.539-43.
- Gianaroli, L.Magli, M.C.Collodel, G.Moretti, E.Ferraretti, A.P. and Baccetti, B. 2008. Sperm head's birefringence: a new criterion for sperm selection. *Fertil Steril.* **90**(1), pp.104-12.

- Gil-Salom, M.Romero, J.Minguez, Y.Rubio, C.De los Santos, M.J.Remohi, J. and Pellicer, A. 1996. Pregnancies after intracytoplasmic sperm injection with cryopreserved testicular spermatozoa. *Hum Reprod.* **11**(6), pp.1309-13.
- Gilbert, S. 2000. *Developmental Biology, 6th edition*. Sunderland, Massachusetts: Sinauer Associates, Inc.
- Gindoff, P.R. and Jewelewicz, R. 1986. Reproductive potential in the older woman. *Fertil Steril.* **46**(6), pp.989-1001.
- Glasse, B. and Civetta, A. 2004. Positive selection at reproductive ADAM genes with potential intercellular binding activity. *Mol Biol Evol.* **21**(5), pp.851-9.
- Glover, T.Barratt, C.Tyler, J. and Hennessey, J. 1990. *Human Male Fertility and Semen Analysis*. New York: Academic Press.
- Go, K.J. and Wolf, D.P. 1985. Albumin-mediated changes in sperm sterol content during capacitation. *Biol Reprod.* **32**(1), pp.145-53.
- Gonzalez-Marin, C.Gosalvez, J. and Roy, R. 2012. Types, causes, detection and repair of DNA fragmentation in animal and human sperm cells. *Int J Mol Sci.* **13**(11), pp.14026-52.
- Goodison, S.Urquidi, V. and Tarin, D. 1999. CD44 cell adhesion molecules. *Mol Pathol.* **52**(4), pp.189-96.
- Goodson, S.G.Qiu, Y.Sutton, K.A.Xie, G.Jia, W. and O'Brien, D.A. 2012. Metabolic substrates exhibit differential effects on functional parameters of mouse sperm capacitation. *Biol Reprod.* **87**(3), p75.
- Gopalkrishnan, K.Padwal, V.Meherji, P.K.Gokral, J.S.Shah, R. and Juneja, H.S. 2000. Poor quality of sperm as it affects repeated early pregnancy loss. *Arch Androl.* **45**(2), pp.111-7.
- Gosalvez, J.de la Torre, J.Lopez-Fernandez, C.Perez-Gutierrez, L.Ortega, L.Caballero, P. and Nunez, R. 2010. DNA fragmentation dynamics in fresh versus frozen thawed plus gradient-isolated human spermatozoa. *Syst Biol Reprod Med.* **56**(1), pp.27-36.
- Goueffic, Y.Guilluy, C.Guerin, P.Patra, P.Pacaud, P. and Loirand, G. 2006. Hyaluronan induces vascular smooth muscle cell migration through RHAMM-mediated PI3K-dependent Rac activation. *Cardiovasc Res.* **72**(2), pp.339-48.
- Griswold, M.D. 2016. Spermatogenesis: The Commitment to Meiosis. *Physiol Rev.* **96**(1), pp.1-17.
- Griveau, J.F. and Le Lannou, D. 1997. Reactive oxygen species and human spermatozoa: physiology and pathology. *Int J Androl.* **20**(2), pp.61-9.
- Griveau, J.F.Renard, P. and Le Lannou, D. 1994. An in vitro promoting role for hydrogen peroxide in human sperm capacitation. *Int J Androl.* **17**(6), pp.300-7.
- Griveau, J.F.Renard, P. and Le Lannou, D. 1995. Superoxide anion production by human spermatozoa as a part of the ionophore-induced acrosome reaction process. *Int J Androl.* **18**(2), pp.67-74.
- Grunewald, S.Paasch, U. and Glander, H.J. 2001. Enrichment of non-apoptotic human spermatozoa after cryopreservation by immunomagnetic cell sorting. *Cell Tissue Bank.* **2**(3), pp.127-33.
- Guerin, P.Matillon, C.Bleau, G.Levy, R. and Menezo, Y. 2005. [Impact of sperm DNA fragmentation on ART outcome]. *Gynecol Obstet Fertil.* **33**(9), pp.665-8.
- Guido, C.Perrotta, I.Panza, S.Middea, E.Avena, P.Santoro, M.Marsico, S.Imbrogno, P.Ando, S. and Aquila, S. 2011. Human sperm physiology: estrogen receptor alpha (ERalpha) and estrogen receptor beta (ERbeta) influence sperm metabolism and may be involved in the pathophysiology of varicocele-associated male infertility. *J Cell Physiol.* **226**(12), pp.3403-12.
- Gur, Y. and Breitbart, H. 2006. Mammalian sperm translate nuclear-encoded proteins by mitochondrial-type ribosomes. *Genes Dev.* **20**(4), pp.411-6.
- Gutjahr, J.C.Greil, R. and Hartmann, T.N. 2015. The Role of CD44 in the Pathophysiology of Chronic Lymphocytic Leukemia. *Front Immunol.* **6**, p177.

- Gutnisky, C., Dalvit, G.C., Pintos, L.N., Thompson, J.G., Beconi, M.T. and Cetica, P.D. 2007. Influence of hyaluronic acid synthesis and cumulus mucification on bovine oocyte in vitro maturation, fertilisation and embryo development. *Reprod Fertil Dev.* **19**(3), pp.488-97.
- Guyonnet, B., Zabet-Moghaddam, M., San Francisco, S. and Cornwall, G.A. 2012. Isolation and proteomic characterization of the mouse sperm acrosomal matrix. *Mol Cell Proteomics.* **11**(9), pp.758-74.
- Haber, R.S., Weinstein, S.P., O'Boyle, E. and Morgello, S. 1993. Tissue distribution of the human GLUT3 glucose transporter. *Endocrinology.* **132**(6), pp.2538-43.
- Hai, Y., Hou, J., Liu, Y., Yang, H., Li, Z. and He, Z. 2014. The roles and regulation of Sertoli cells in fate determinations of spermatogonial stem cells and spermatogenesis. *Semin Cell Dev Biol.* **29**, pp.66-75.
- Hall, C.L., Wang, C., Lange, L.A. and Turley, E.A. 1994. Hyaluronan and the hyaluronan receptor RHAMM promote focal adhesion turnover and transient tyrosine kinase activity. *J Cell Biol.* **126**(2), pp.575-88.
- Hall, C.L., Yang, B., Yang, X., Zhang, S., Turley, M., Samuel, S., Lange, L.A., Wang, C., Curpen, G.D., Savani, R.C., Greenberg, A.H. and Turley, E.A. 1995. Overexpression of the hyaluronan receptor RHAMM is transforming and is also required for H-ras transformation. *Cell.* **82**(1), pp.19-26.
- Halliday, J. 2012. Outcomes for offspring of men having ICSI for male factor infertility. *Asian J Androl.* **14**(1), pp.116-20.
- Hamilton, S.R., Fard, S.F., Paiwand, F.F., Tolg, C., Veiseh, M., Wang, C., McCarthy, J.B., Bissell, M.J., Koropatnick, J. and Turley, E.A. 2007. The hyaluronan receptors CD44 and Rhamm (CD168) form complexes with ERK1,2 that sustain high basal motility in breast cancer cells. *J Biol Chem.* **282**(22), pp.16667-80.
- Hammami-Hamza, S., Doussau, M., Bernard, J., Rogier, E., Duquenne, C., Richard, Y., Lefevre, A. and Finaz, C. 2001. Cloning and sequencing of SOB3, a human gene coding for a sperm protein homologous to an antimicrobial protein and potentially involved in zona pellucida binding. *Mol Hum Reprod.* **7**(7), pp.625-32.
- Hammoud, S.S., Nix, D.A., Hammoud, A.O., Gibson, M., Cairns, B.R. and Carrell, D.T. 2011. Genome-wide analysis identifies changes in histone retention and epigenetic modifications at developmental and imprinted gene loci in the sperm of infertile men. *Human Reproduction.* **26**(9), pp.2558-2569.
- Hammoud, S.S., Nix, D.A., Zhang, H., Purwar, J., Carrell, D.T. and Cairns, B.R. 2009. Distinctive chromatin in human sperm packages genes for embryo development. *Nature.* **460**(7254), pp.473-8.
- Handyside, A.H., Pattinson, J.K., Penketh, R.J., Delhanty, J.D., Winston, R.M. and Tuddenham, E.G. 1989. Biopsy of human preimplantation embryos and sexing by DNA amplification. *Lancet.* **1**(8634), pp.347-9.
- Hao, L.Y., Giasson, B.I. and Bonini, N.M. 2010. DJ-1 is critical for mitochondrial function and rescues PINK1 loss of function. *Proc Natl Acad Sci U S A.* **107**(21), pp.9747-52.
- Hardwick, C., Hoare, K., Owens, R., Hohn, H.P., Hook, M., Moore, D., Cripps, V., Austen, L., Nance, D.M. and Turley, E.A. 1992. Molecular cloning of a novel hyaluronan receptor that mediates tumor cell motility. *J Cell Biol.* **117**(6), pp.1343-50.
- Hascall, V. and Esko, J.D. 2009. Hyaluronan. In: Varki, A., et al. eds. *Essentials of Glycobiology*. 2nd ed. Cold Spring Harbor (NY).
- Haynes, B.F., Liao, H.X. and Patton, K.L. 1991. The transmembrane hyaluronate receptor (CD44): multiple functions, multiple forms. *Cancer Cells.* **3**(9), pp.347-50.
- Hazzouri, M., Pivot-Pajot, C., Faure, A.K., Usson, Y., Pelletier, R., Sele, B., Khochbin, S. and Rousseaux, S. 2000. Regulated hyperacetylation of core histones during mouse spermatogenesis: involvement of histone deacetylases. *Eur J Cell Biol.* **79**(12), pp.950-60.

- Hekmatdoost, A.Lakpour, N. and Sadeghi, M.R. 2009. Sperm chromatin integrity: etiologies and mechanisms of abnormality, assays, clinical importance, preventing and repairing damage. *Avicenna J Med Biotechnol.* **1**(3), pp.147-60.
- Hendrickson, T.W.Perrone, C.A.Griffin, P.Wuichet, K.Mueller, J.Yang, P.Porter, M.E. and Sale, W.S. 2004. IC138 is a WD-repeat dynein intermediate chain required for light chain assembly and regulation of flagellar bending. *Mol Biol Cell.* **15**(12), pp.5431-42.
- Henkel, R. 2012. Sperm preparation: state-of-the-art--physiological aspects and application of advanced sperm preparation methods. *Asian J Androl.* **14**(2), pp.260-9.
- Henkel, R.Muller, C.Miska, W.Gips, H. and Schill, W.B. 1993. Determination of the acrosome reaction in human spermatozoa is predictive of fertilization in vitro. *Hum Reprod.* **8**(12), pp.2128-32.
- Henkel, R.R. and Schill, W.B. 2003. Sperm preparation for ART. *Reprod Biol Endocrinol.* **1**, p108.
- Herrero, M.B.Mandal, A.Digilio, L.C.Coonrod, S.A.Maier, B. and Herr, J.C. 2005. Mouse SLLP1, a sperm lysozyme-like protein involved in sperm-egg binding and fertilization. *Dev Biol.* **284**(1), pp.126-42.
- Hess, R.A. and Renato de Franca, L. 2008. Spermatogenesis and cycle of the seminiferous epithelium. *Adv Exp Med Biol.* **636**, pp.1-15.
- Heytens, E.Parrington, J.Coward, K.Young, C.Lambrecht, S.Yoon, S.Y.Fissore, R.A.Hamer, R.Deane, C.M.Ruas, M.Grasa, P.Soleimani, R.Cuvelier, C.A.Gerris, J.Dhont, M.Deforce, D.Leybaert, L. and De Sutter, P. 2009. Reduced amounts and abnormal forms of phospholipase C zeta (PLCzeta) in spermatozoa from infertile men. *Hum Reprod.* **24**(10), pp.2417-28.
- HFEA. 2008. *A long term analysis of the HFEA Register data, 1991-2006.*
- HFEA. 2011. *Human Fertilisation & Embryology Authority (HFEA). 2011. Fertility Treatment In 2011: Trends and Figures.*
- HFEA. 2015. Latest UK fertility treatment data and figures: 2012-2013. [Online]. Available from: [http://www.hfea.gov.uk/docs/HFEA\\_Fertility\\_Trends\\_and\\_Figures\\_2013.pdf](http://www.hfea.gov.uk/docs/HFEA_Fertility_Trends_and_Figures_2013.pdf)
- Higman, V.A.Briggs, D.C.Mahoney, D.J.Blundell, C.D.Sattelle, B.M.Dyer, D.P.Green, D.E.DeAngelis, P.L.Almond, A.Milner, C.M. and Day, A.J. 2014. A refined model for the TSG-6 link module in complex with hyaluronan: use of defined oligosaccharides to probe structure and function. *J Biol Chem.* **289**(9), pp.5619-34.
- Hirai, M.Boersma, A.Hoeflich, A.Wolf, E.Foll, J.Aumuller, T.R. and Braun, J. 2001. Objectively measured sperm motility and sperm head morphometry in boars (*Sus scrofa*): relation to fertility and seminal plasma growth factors. *J Androl.* **22**(1), pp.104-10.
- Hofmann, M.Assmann, V.Fieber, C.Sleeman, J.P.Moll, J.Ponta, H.Hart, I.R. and Herrlich, P. 1998. Problems with RHAMM: a new link between surface adhesion and oncogenesis? *Cell.* **95**(5), pp.591-2; author reply 592-3.
- Hong, S.J.Chiu, P.C.Lee, K.F.Tse, J.M.Ho, P.C. and Yeung, W.S. 2004. Establishment of a capillary-cumulus model to study the selection of sperm for fertilization by the cumulus oophorus. *Hum Reprod.* **19**(7), pp.1562-9.
- Hong, S.J.Chiu, P.C.Lee, K.F.Tse, J.Y.Ho, P.C. and Yeung, W.S. 2009. Cumulus cells and their extracellular matrix affect the quality of the spermatozoa penetrating the cumulus mass. *Fertil Steril.* **92**(3), pp.971-8.
- Hosseinfar, H.Gourabi, H.Salekdeh, G.H.Alikhani, M.Mirshahvaladi, S.Sabbaghian, M.Modarresi, T. and Gilani, M.A. 2013. Study of sperm protein profile in men with and without varicocele using two-dimensional gel electrophoresis. *Urology.* **81**(2), pp.293-300.
- Hou, C.C.Weij, C.G.Lu, C.P.Gao, X.M.Yang, W.X. and Zhu, J.Q. 2017. Prohibitin-mediated mitochondrial ubiquitination during spermiogenesis in Chinese mitten crab *Eriocheir sinensis*. *Oncotarget.* **8**(58), pp.98782-98797.
- Houshdaran, S.Cortessis, V.K.Siegmund, K.Yang, A.Laird, P.W. and Sokol, R.Z. 2007. Widespread epigenetic abnormalities suggest a broad DNA methylation erasure defect in abnormal human sperm. *PLoS ONE.* **2**(12).

- Huang, Z.Danshina, P.V.Mohr, K.Qu, W.Goodson, S.G.O'Connell, T.M. and O'Brien, D.A. 2017. Sperm function, protein phosphorylation, and metabolism differ in mice lacking successive sperm-specific glycolytic enzymes. *Biol Reprod.* **97**(4), pp.586-597.
- Huber, L.A.Pfaller, K. and Vietor, I. 2003. Organelle proteomics: implications for subcellular fractionation in proteomics. *Circ Res.* **92**(9), pp.962-8.
- Hunnicuttt, G.R.Primakoff, P. and Myles, D.G. 1996. Sperm surface protein PH-20 is bifunctional: one activity is a hyaluronidase and a second, distinct activity is required in secondary sperm-zona binding. *Biol Reprod.* **55**(1), pp.80-6.
- Hunter, R.H. 1996. Ovarian control of very low sperm/egg ratios at the commencement of mammalian fertilisation to avoid polyspermy. *Mol Reprod Dev.* **44**(3), pp.417-22.
- Huszar, G.Jakab, A.Sakkas, D.Ozenci, C.C.Cayli, S.Delpiano, E. and Ozkavukcu, S. 2007. Fertility testing and ICSI sperm selection by hyaluronic acid binding: clinical and genetic aspects. *Reprod Biomed Online.* **14**(5), pp.650-63.
- Huszar, G.Ozenci, C.C.Cayli, S.Zavaczki, Z.Hansch, E. and Vigue, L. 2003. Hyaluronic acid binding by human sperm indicates cellular maturity, viability, and unreacted acrosomal status. *Fertil Steril.* **79 Suppl 3**, pp.1616-24.
- Huszar, G.Ozkavukcu, S.Jakab, A.Celik-Ozenci, C.Sati, G.L. and Cayli, S. 2006. Hyaluronic acid binding ability of human sperm reflects cellular maturity and fertilizing potential: selection of sperm for intracytoplasmic sperm injection. *Curr Opin Obstet Gynecol.* **18**(3), pp.260-7.
- Huszar, G.Sbracia, M.Vigue, L.Miller, D.J. and Shur, B.D. 1997. Sperm plasma membrane remodeling during spermiogenetic maturation in men: relationship among plasma membrane beta 1,4-galactosyltransferase, cytoplasmic creatine phosphokinase, and creatine phosphokinase isoform ratios. *Biol Reprod.* **56**(4), pp.1020-4.
- Huszar, G.Stone, K.Dix, D. and Vigue, L. 2000. Putative creatine kinase M-isoform in human sperm is identified as the 70-kilodalton heat shock protein HspA2. *Biol Reprod.* **63**(3), pp.925-32.
- Huszar, G.Willetts, M. and Corrales, M. 1990. Hyaluronic acid (Sperm Select) improves retention of sperm motility and velocity in normospermic and oligospermic specimens. *Fertil Steril.* **54**(6), pp.1127-34.
- Ickowicz, D.Finkelstein, M. and Breitbart, H. 2012. Mechanism of sperm capacitation and the acrosome reaction: role of protein kinases. *Asian J Androl.* **14**(6), pp.816-21.
- Ikawa, M.Inoue, N.Benham, A.M. and Okabe, M. 2010. Fertilization: a sperm's journey to and interaction with the oocyte. *J Clin Invest.* **120**(4), pp.984-94.
- Inaba, K. 2011. Sperm flagella: comparative and phylogenetic perspectives of protein components. *Mol Hum Reprod.* **17**(8), pp.524-38.
- J. Necas, L.B., P. Brauner, J. Kolar. 2008. Hyaluronic acid (hyaluronan): a review. *Veterinarni Medicina* **53**(8), pp.397-411.
- Jackson, R.E.Bormann, C.L.Hassun, P.A.Rocha, A.M.Motta, E.L.Serafini, P.C. and Smith, G.D. 2010. Effects of semen storage and separation techniques on sperm DNA fragmentation. *Fertil Steril.* **94**(7), pp.2626-30.
- Jagan Mohanarao, G. and Atreja, S.K. 2011. Identification of capacitation associated tyrosine phosphoproteins in buffalo (*Bubalus bubalis*) and cattle spermatozoa. *Anim Reprod Sci.* **123**(1-2), pp.40-7.
- Jaiswal, B.S.Cohen-Dayag, A.Tur-Kaspa, I. and Eisenbach, M. 1998. Sperm capacitation is, after all, a prerequisite for both partial and complete acrosome reaction. *FEBS Lett.* **427**(2), pp.309-13.
- Jakab, A.Sakkas, D.Delpiano, E.Cayli, S.Kovanci, E.Ward, D.Revelli, A. and Huszar, G. 2005. Intracytoplasmic sperm injection: a novel selection method for sperm with normal frequency of chromosomal aneuploidies. *Fertil Steril.* **84**(6), pp.1665-73.
- Jaleel, R. and Khan, A. 2013. Paternal factors in spontaneous first trimester miscarriage. *Pak J Med Sci.* **29**(3), pp.748-52.

- Jameel, T. 2008. Sperm swim-up: a simple and effective technique of semen processing for intrauterine insemination. *J Pak Med Assoc.* **58**(2), pp.71-4.
- Jayaraman, V.Upadhy, D.Narayan, P.K. and Adiga, S.K. 2012. Sperm processing by swim-up and density gradient is effective in elimination of sperm with DNA damage. *J Assist Reprod Genet.* **29**(6), pp.557-63.
- Jenkins, T.G.Aston, K.I.Hotaling, J.M.Shamsi, M.B.Simon, L. and Carrell, D.T. 2016a. Teratozoospermia and asthenozoospermia are associated with specific epigenetic signatures. *Andrology.* **4**(5), pp.843-9.
- Jenkins, T.G.Aston, K.I.Meyer, T.D.Hotaling, J.M.Shamsi, M.B.Johnstone, E.B.Cox, K.J.Stanford, J.B.Porucznik, C.A. and Carrell, D.T. 2016b. Decreased fecundity and sperm DNA methylation patterns. *Fertility and Sterility.* **105**(1), pp.51-57e3.
- Jenkins, T.G. and Carrell, D.T. 2012. The sperm epigenome and potential implications for the developing embryo. *Reproduction.* **143**(6), pp.727-734.
- Jha, K.N.Shumilin, I.A.Digilio, L.C.Chertihin, O.Zheng, H.Schmitz, G.Visconti, P.E.Flickinger, C.J.Minor, W. and Herr, J.C. 2008. Biochemical and structural characterization of apolipoprotein A-I binding protein, a novel phosphoprotein with a potential role in sperm capacitation. *Endocrinology.* **149**(5), pp.2108-20.
- Jimenez-Rabadan, P.Ramon, M.Garcia-Alvarez, O.Maroto-Morales, A.del Olmo, E.Perez-Guzman, M.D.Bisbal, A.Fernandez-Santos, M.R.Garde, J.J. and Soler, A.J. 2012. Effect of semen collection method (artificial vagina vs. electroejaculation), extender and centrifugation on post-thaw sperm quality of Blanca-Celtiberica buck ejaculates. *Anim Reprod Sci.* **132**(1-2), pp.88-95.
- Jin, J.M.Hou, C.C.Tan, F.Q. and Yang, W.X. 2016. The potential function of prohibitin during spermatogenesis in Chinese fire-bellied newt *Cynops orientalis*. *Cell Tissue Res.* **363**(3), pp.805-22.
- Jin, S.K. and Yang, W.X. 2017. Factors and pathways involved in capacitation: how are they regulated? *Oncotarget.* **8**(2), pp.3600-3627.
- Jones, R. 1989. Membrane remodelling during sperm maturation in the epididymis. *Oxf Rev Reprod Biol.* **11**, pp.285-337.
- Jones, R. 1998. Plasma membrane structure and remodelling during sperm maturation in the epididymis. *J Reprod Fertil Suppl.* **53**, pp.73-84.
- Jono, H. and Ando, Y. 2010. Midkine: a novel prognostic biomarker for cancer. *Cancers (Basel).* **2**(2), pp.624-41.
- Kahmann, J.D.O'Brien, R.Werner, J.M.Heinegard, D.Ladbury, J.E.Campbell, I.D. and Day, A.J. 2000. Localization and characterization of the hyaluronan-binding site on the link module from human TSG-6. *Structure.* **8**(7), pp.763-74.
- Kamel, R.M. 2013. Assisted reproductive technology after the birth of louise brown. *J Reprod Infertil.* **14**(3), pp.96-109.
- Katoh, M. and Katoh, M. 2003. Identification and characterization of human ZPBP-like gene in silico. *Int J Mol Med.* **12**(3), pp.399-404.
- Katz, D.F.Overstreet, J.W.Samuels, S.J.Niswander, P.W.Bloom, T.D. and Lewis, E.L. 1986. Morphometric analysis of spermatozoa in the assessment of human male fertility. *J Androl.* **7**(4), pp.203-10.
- Kawakami, E.Nishizono, Y.Miyata, C.Hirano, T.Hori, T. and Tsutsui, T. 2006. Effects of hyaluronic acid on Ca(2+) influx, lactate dehydrogenase activity, and cyclic AMP synthesis in canine ejaculated sperm during In Vitro capacitation. *J Vet Med Sci.* **68**(2), pp.119-23.
- Khazamipour, N.Noruzinia, M.Fatehmanesh, P.Keyhanee, M. and Pujol, P. 2009. MTHFR promoter hypermethylation in testicular biopsies of patients with non-obstructive azoospermia: the role of epigenetics in male infertility. *Hum Reprod.* **24**(9), pp.2361-4.



- Kheirollahi-Kouhestani, M.Razavi, S.Tavalaee, M.Deemeh, M.R.Mardani, M.Moshtaghian, J. and Nasr-Esfahani, M.H. 2009. Selection of sperm based on combined density gradient and Zeta method may improve ICSI outcome. *Hum Reprod.* **24**(10), pp.2409-16.
- Kim, E.Yamashita, M.Kimura, M.Honda, A.Kashiwabara, S. and Baba, T. 2008. Sperm penetration through cumulus mass and zona pellucida. *Int J Dev Biol.* **52**(5-6), pp.677-82.
- Kim, H.S.Kang, M.J.Kim, S.A.Oh, S.K.Kim, H.Ku, S.Y.Kim, S.H.Moon, S.Y. and Choi, Y.M. 2013. The utility of sperm DNA damage assay using toluidine blue and aniline blue staining in routine semen analysis. *Clin Exp Reprod Med.* **40**(1), pp.23-8.
- Kim, T.Oh, J.Woo, J.M.Choi, E.Im, S.H.Yoo, Y.J.Kim, D.H.Nishimura, H. and Cho, C. 2006. Expression and relationship of male reproductive ADAMs in mouse. *Biol Reprod.* **74**(4), pp.744-50.
- Kimura, M.Kim, E.Kang, W.Yamashita, M.Saigo, M.Yamazaki, T.Nakanishi, T.Kashiwabara, S. and Baba, T. 2009. Functional roles of mouse sperm hyaluronidases, HYAL5 and SPAM1, in fertilization. *Biol Reprod.* **81**(5), pp.939-47.
- Kimura, N.Hoshino, Y.Totsukawa, K. and Sato, E. 2007. Cellular and molecular events during oocyte maturation in mammals: molecules of cumulus-oocyte complex matrix and signalling pathways regulating meiotic progression. *Soc Reprod Fertil Suppl.* **63**, pp.327-42.
- Kinoshita, T. and Fujita, M. 2016. Biosynthesis of GPI-anchored proteins: special emphasis on GPI lipid remodeling. *J Lipid Res.* **57**(1), pp.6-24.
- Kohda, D.Morton, C.J.Parkar, A.A.Hatanaka, H.Inagaki, F.M.Campbell, I.D. and Day, A.J. 1996. Solution structure of the link module: a hyaluronan-binding domain involved in extracellular matrix stability and cell migration. *Cell.* **86**(5), pp.767-75.
- Kongmanas, K.Kruevaisayawan, H.Saewu, A.Sugeng, C.Fernandes, J.Souda, P.Angel, J.B.Faull, K.F.Aitken, R.J.Whitelegge, J.Hardy, D.Berger, T.Baker, M.A. and Tanphaichitr, N. 2015. Proteomic Characterization of Pig Sperm Anterior Head Plasma Membrane Reveals Roles of Acrosomal Proteins in ZP3 Binding. *J Cell Physiol.* **230**(2), pp.449-63.
- Koppers, A.J.De luliis, G.N.Finnie, J.M.McLaughlin, E.A. and Aitken, R.J. 2008. Significance of mitochondrial reactive oxygen species in the generation of oxidative stress in spermatozoa. *J Clin Endocrinol Metab.* **93**(8), pp.3199-207.
- Kornovski, B.S.McCoshen, J.Kredentser, J. and Turley, E. 1994. The regulation of sperm motility by a novel hyaluronan receptor. *Fertil Steril.* **61**(5), pp.935-40.
- Kota, V.Dhople, V.M. and Shivaji, S. 2009. Tyrosine phosphoproteome of hamster spermatozoa: role of glycerol-3-phosphate dehydrogenase 2 in sperm capacitation. *Proteomics.* **9**(7), pp.1809-26.
- Kotaja, N. 2014. MicroRNAs and spermatogenesis. *Fertil Steril.* **101**(6), pp.1552-62.
- Kouvidi, K.Berdiaki, A.Nikitovic, D.Katonis, P.Afratis, N.Hascall, V.C.Karamanos, N.K. and Tzanakakis, G.N. 2011. Role of receptor for hyaluronic acid-mediated motility (RHAMM) in low molecular weight hyaluronan (LMWHA)-mediated fibrosarcoma cell adhesion. *J Biol Chem.* **286**(44), pp.38509-20.
- Kratzschmar, J.Haendler, B.Eberspaecher, U.Roosterman, D.Donner, P. and Schleuning, W.D. 1996. The human cysteine-rich secretory protein (CRISP) family. Primary structure and tissue distribution of CRISP-1, CRISP-2 and CRISP-3. *Eur J Biochem.* **236**(3), pp.827-36.
- Krausz, C. and Chianese, C. 2010. The role of aging on fecundity in the male. *Paternal Influences on Human Reproductive Success.* Cambridge University Press, pp.70-81.
- Krisfalusi, M.Miki, K.Magyar, P.L. and O'Brien, D.A. 2006. Multiple glycolytic enzymes are tightly bound to the fibrous sheath of mouse spermatozoa. *Biol Reprod.* **75**(2), pp.270-8.
- Kumar, D.Upadhyaya, D.Salian, S.R.Rao, S.B.Kalthur, G.Kumar, P. and Adiga, S.K. 2013a. The extent of paternal sperm DNA damage influences early post-natal survival of first generation mouse offspring. *Eur J Obstet Gynecol Reprod Biol.* **166**(2), pp.164-7.

- Kumar, D.Upadhyaya, D.Uppangala, S.Salian, S.R.Kalthur, G. and Adiga, S.K. 2013b. Nuclear DNA fragmentation negatively affects zona binding competence of Y bearing mouse spermatozoa. *J Assist Reprod Genet.* **30**(12), pp.1611-5.
- Kumar, K.Deka, D.Singh, A.Mitra, D.K.Vanitha, B.R. and Dada, R. 2012a. Predictive value of DNA integrity analysis in idiopathic recurrent pregnancy loss following spontaneous conception. *Journal of Assisted Reproduction and Genetics.* **29**(9), pp.861-867.
- Kumar, K.Thilagavathi, J.Deka, D. and Dada, R. 2012b. Unexplained early pregnancy loss: role of paternal DNA. *Indian J Med Res.* **136**(2), pp.296-8.
- Kumar, M.Kumar, K.Jain, S.Hassan, T. and Dada, R. 2013c. Novel insights into the genetic and epigenetic paternal contribution to the human embryo. *Clinics (Sao Paulo).* **68 Suppl 1**, pp.5-14.
- Kumar, N. and Singh, A.K. 2015. Trends of male factor infertility, an important cause of infertility: A review of literature. *J Hum Reprod Sci.* **8**(4), pp.191-6.
- Kumar, V.Rangaraj, N. and Shivaji, S. 2006. Activity of pyruvate dehydrogenase A (PDHA) in hamster spermatozoa correlates positively with hyperactivation and is associated with sperm capacitation. *Biol Reprod.* **75**(5), pp.767-77.
- Kupis, L.Dobronski, P.A. and Radziszewski, P. 2015. Varicocele as a source of male infertility - current treatment techniques. *Cent European J Urol.* **68**(3), pp.365-70.
- Kwon W-S.Rahman MS.Kim Y-J.Ryu D-Y. and Kahtun A. 2015. Ferritin Overload Suppresses Male Fertility Via altered Acrosome Reaction. *Reprod Dev Biol* **39**(4), pp.117-125.
- Kwon, W.S.Rahman, M.S.Lee, J.S.Kim, J.Yoon, S.J.Park, Y.J.You, Y.A.Hwang, S. and Pang, M.G. 2014. A comprehensive proteomic approach to identifying capacitation related proteins in boar spermatozoa. *BMC Genomics.* **15**, p897.
- Langlais J. and Roberts KD. 1985. A molecular membrane model of sperm capacitation and the acrosome reaction of mammalian spermatozoa. *Molecular Reproduction and Development.* **12**(2), pp.183-224.
- Larcher, V. 2007. The health of children conceived by assisted reproduction technologies. *Arch Dis Child.* **92**(8), pp.668-9.
- Larsen, E.C.Christiansen, O.B.Kolte, A.M. and Macklon, N. 2013. New insights into mechanisms behind miscarriage. *BMC Med.* **11**, p154.
- Laskowski, R.A. 2001. PDBsum: summaries and analyses of PDB structures. *Nucleic Acids Res.* **29**(1), pp.221-2.
- Laskowski, R.A. 2009. PDBsum new things. *Nucleic Acids Res.* **37**(Database issue), pp.D355-9.
- Laskowski, R.A.Chistyakov, V.V. and Thornton, J.M. 2005. PDBsum more: new summaries and analyses of the known 3D structures of proteins and nucleic acids. *Nucleic Acids Res.* **33**(Database issue), pp.D266-8.
- Laws-King, A.Trounson, A.Sathananthan, H. and Kola, I. 1987. Fertilization of human oocytes by microinjection of a single spermatozoon under the zona pellucida. *Fertil Steril.* **48**(4), pp.637-42.
- Lawson, C.Goupil, S. and Leclerc, P. 2008. Increased activity of the human sperm tyrosine kinase SRC by the cAMP-dependent pathway in the presence of calcium. *Biol Reprod.* **79**(4), pp.657-66.
- Le Lannou, D. and Blanchard, Y. 1988. Nuclear maturity and morphology of human spermatozoa selected by Percoll density gradient centrifugation or swim-up procedure. *J Reprod Fertil.* **84**(2), pp.551-6.
- Leahy, T. and Gadella, B.M. 2011a. Capacitation and capacitation-like sperm surface changes induced by handling boar semen. *Reprod Domest Anim.* **46 Suppl 2**, pp.7-13.
- Leahy, T. and Gadella, B.M. 2011b. Sperm surface changes and physiological consequences induced by sperm handling and storage. *Reproduction.* **142**(6), pp.759-78.

- Ledee, N.Munaut, C.Aubert, J.Serazin, V.Rahmati, M.Chaouat, G.Sandra, O. and Foidart, J.M. 2011. Specific and extensive endometrial deregulation is present before conception in IVF/ICSI repeated implantation failures (IF) or recurrent miscarriages. *J Pathol.* **225**(4), pp.554-64.
- Lee, H.L.Kim, S.H.Ji, D.B. and Kim, Y.J. 2009. A comparative study of Sephadex, glass wool and Percoll separation techniques on sperm quality and IVF results for cryopreserved bovine semen. *J Vet Sci.* **10**(3), pp.249-55.
- Lehti, M.S. and Sironen, A. 2016. Formation and function of the manchette and flagellum during spermatogenesis. *Reproduction.* **151**(4), pp.R43-54.
- Lenormand, H.Deschrevel, B.Tranchepain, F. and Vincent, J.C. 2008. Electrostatic interactions between hyaluronan and proteins at pH 4: how do they modulate hyaluronidase activity. *Biopolymers.* **89**(12), pp.1088-103.
- Lewis, S.E. and Kumar, K. 2015. The paternal genome and the health of the assisted reproductive technology child. *Asian J Androl.* **17**(4), pp.616-22.
- Li, H.Moll, J.Winkler, A.Frappart, L.Brunet, S.Hamann, J.Kroll, T.Verlhac, M.H.Heuer, H.Herrlich, P. and Ploubidou, A. 2015. RHAMM deficiency disrupts folliculogenesis resulting in female hypofertility. *Biol Open.* **4**(4), pp.562-71.
- Li, Y.F.He, W.Mandal, A.Kim, Y.H.Digilio, L.Klotz, K.Flickinger, C.J.Herr, J.C. and Herr, J.C. 2011. CABYR binds to AKAP3 and Ropporin in the human sperm fibrous sheath. *Asian J Androl.* **13**(2), pp.266-74.
- Li, Z.Yang, J. and Huang, H. 2006. Oxidative stress induces H2AX phosphorylation in human spermatozoa. *FEBS Lett.* **580**(26), pp.6161-8.
- Liao, T.T.Xiang, Z.Zhu, W.B. and Fan, L.Q. 2009. Proteome analysis of round-headed and normal spermatozoa by 2-D fluorescence difference gel electrophoresis and mass spectrometry. *Asian J Androl.* **11**(6), pp.683-93.
- Lin, M.H.Lee, R.K.Hwu, Y.M.Lu, C.H.Chu, S.L.Chen, Y.J.Chang, W.C. and Li, S.H. 2008. SPINKL, a Kazal-type serine protease inhibitor-like protein purified from mouse seminal vesicle fluid, is able to inhibit sperm capacitation. *Reproduction.* **136**(5), pp.559-71.
- Lin, Y.N.Roy, A.Yan, W.Burns, K.H. and Matzuk, M.M. 2007. Loss of zona pellucida binding proteins in the acrosomal matrix disrupts acrosome biogenesis and sperm morphogenesis. *Mol Cell Biol.* **27**(19), pp.6794-805.
- Lishko, P.V. and Kirichok, Y. 2010. The role of Hv1 and CatSper channels in sperm activation. *J Physiol.* **588**(Pt 23), pp.4667-72.
- Liu, D.Y.Clarke, G.N. and Baker, H.W. 2006. Tyrosine phosphorylation on capacitated human sperm tail detected by immunofluorescence correlates strongly with sperm-zona pellucida (ZP) binding but not with the ZP-induced acrosome reaction. *Hum Reprod.* **21**(4), pp.1002-8.
- Liu, D.Y.Liu, M.L.Clarke, G.N. and Baker, H.W. 2007. Hyperactivation of capacitated human sperm correlates with the zona pellucida-induced acrosome reaction of zona pellucida-bound sperm. *Hum Reprod.* **22**(10), pp.2632-8.
- Liu, L.K. and Finzel, B. 2014a. High-resolution crystal structures of alternate forms of the human CD44 hyaluronan-binding domain reveal a site for protein interaction. *Acta Crystallogr F Struct Biol Commun.* **70**(Pt 9), pp.1155-61.
- Liu, L.K. and Finzel, B.C. 2014b. Fragment-based identification of an inducible binding site on cell surface receptor CD44 for the design of protein-carbohydrate interaction inhibitors. *J Med Chem.* **57**(6), pp.2714-25.
- Liu, X.G.Hu, H.Y.Guo, Y.H. and Sun, Y.P. 2016. Correlation between Y chromosome microdeletion and male infertility. *Genet Mol Res.* **15**(2).
- Lopez, J.Valdez-Morales, F.J.Benitez-Bribiesca, L.Cerbon, M. and Carranca, A.G. 2013. Normal and cancer stem cells of the human female reproductive system. *Reprod Biol Endocrinol.* **11**, p53.

- Losel, R.Breiter, S.Seyfert, M.Webling, M. and Falkenstein, E. 2005. Classic and non-classic progesterone receptors are both expressed in human spermatozoa. *Horm Metab Res.* **37**(1), pp.10-4.
- Lotfi, S.Mehri, M.Sharafi, M. and Masoudi, R. 2017. Hyaluronic acid improves frozen-thawed sperm quality and fertility potential in rooster. *Anim Reprod Sci.* **184**, pp.204-210.
- Loutradi, K.E.Tarlatzis, B.C.Goulis, D.G.Zepiridis, L.Pagou, T.Chatziioannou, E.Grimbizis, G.F.Papadimas, I. and Bontis, I. 2006. The effects of sperm quality on embryo development after intracytoplasmic sperm injection. *J Assist Reprod Genet.* **23**(2), pp.69-74.
- Luconi, M.Carloni, V.Marra, F.Ferruzzi, P.Forti, G. and Baldi, E. 2004. Increased phosphorylation of AKAP by inhibition of phosphatidylinositol 3-kinase enhances human sperm motility through tail recruitment of protein kinase A. *J Cell Sci.* **117**(Pt 7), pp.1235-46.
- Luconi, M.Muratori, M.Maggi, M.Pecchioli, P.Peri, A.Mancini, M.Filimberti, E.Forti, G. and Baldi, E. 2000. Uteroglobin and transglutaminase modulate human sperm functions. *J Androl.* **21**(5), pp.676-88.
- Luense, L.J.Wang, X.Schon, S.B.Weller, A.H.Lin Shiao, E.Bryant, J.M.Bartolomei, M.S.Coutifaris, C.Garcia, B.A. and Berger, S.L. 2016. Comprehensive analysis of histone post-translational modifications in mouse and human male germ cells. *Epigenetics and Chromatin.* **9**(1).
- Majumdar, G. and Majumdar, A. 2013. A prospective randomized study to evaluate the effect of hyaluronic acid sperm selection on the intracytoplasmic sperm injection outcome of patients with unexplained infertility having normal semen parameters. *J Assist Reprod Genet.* **30**(11), pp.1471-5.
- Malvezzi, H.Sharma, R.Agarwal, A.Abuzenadah, A.M. and Abu-Elmagd, M. 2014. Sperm quality after density gradient centrifugation with three commercially available media: a controlled trial. *Reprod Biol Endocrinol.* **12**, p121.
- Manandhar, G. and Toshimori, K. 2001. Exposure of sperm head equatorin after acrosome reaction and its fate after fertilization in mice. *Biol Reprod.* **65**(5), pp.1425-36.
- Manku, G. and Culty, M. 2015. Mammalian gonocyte and spermatogonia differentiation: recent advances and remaining challenges. *Reproduction.* **149**(3), pp.R139-57.
- Marchesi, D.E.Biederman, H.Ferrara, S.Hershlag, A. and Feng, H.L. 2010. The effect of semen processing on sperm DNA integrity: comparison of two techniques using the novel Toluidine Blue Assay. *Eur J Obstet Gynecol Reprod Biol.* **151**(2), pp.176-80.
- Marchetti, C.Obert, G.Deffosez, A.Formstecher, P. and Marchetti, P. 2002. Study of mitochondrial membrane potential, reactive oxygen species, DNA fragmentation and cell viability by flow cytometry in human sperm. *Hum Reprod.* **17**(5), pp.1257-65.
- Marchlewska, K.Filipiak, E.Walczak-Jedrzejska, R.Oszukowska, E.Sobkiewicz, S.Wojt, M.Chmiel, J.Kula, K. and Slowikowska-Hilczer, J. 2016. Sperm DNA Fragmentation Index and Hyaluronan Binding Ability in Men from Infertile Couples and Men with Testicular Germ Cell Tumor. *Biomed Res Int.* **2016**, p7893961.
- Marco-Jimenez, F.Viudes-de-Castro, M.P.Balasch, S.Moce, E.Silvestre, M.A.Gomez, E.A. and Vicente, J.S. 2006. Morphometric changes in goat sperm heads induced by cryopreservation. *Cryobiology.* **52**(2), pp.295-304.
- Marei, W.F.Ghafari, F. and Fouladi-Nashta, A.A. 2012. Role of hyaluronic acid in maturation and further early embryo development of bovine oocytes. *Theriogenology.* **78**(3), pp.670-7.
- Marei, W.F.Raheem, K.A.Salavati, M.Tremaine, T.Khalid, M. and Fouladi-Nashta, A.A. 2016. Hyaluronan and hyaluronidase, which is better for embryo development? *Theriogenology.* **86**(4), pp.940-8.
- Marei, W.F.Salavati, M. and Fouladi-Nashta, A.A. 2013. Critical role of hyaluronidase-2 during preimplantation embryo development. *Mol Hum Reprod.* **19**(9), pp.590-9.
- Mariappa, D.Aladakatti, R.H.Dasari, S.K.Sreekumar, A.Wolkowicz, M.van der Hoorn, F. and Seshagiri, P.B. 2010. Inhibition of tyrosine phosphorylation of sperm flagellar proteins, outer dense

- fiber protein-2 and tektin-2, is associated with impaired motility during capacitation of hamster spermatozoa. *Mol Reprod Dev.* **77**(2), pp.182-93.
- Marin-Briggiler, C.I.Jha, K.N.Chertihin, O.Buffone, M.G.Herr, J.C.Vazquez-Levin, M.H. and Visconti, P.E. 2005. Evidence of the presence of calcium/calmodulin-dependent protein kinase IV in human sperm and its involvement in motility regulation. *J Cell Sci.* **118**(Pt 9), pp.2013-22.
- Marino-Ramirez, L.Kann, M.G.Shoemaker, B.A. and Landsman, D. 2005. Histone structure and nucleosome stability. *Expert Rev Proteomics.* **2**(5), pp.719-29.
- Marques, M.Sousa, A.P.Paiva, A.Almeida-Santos, T. and Ramalho-Santos, J. 2014. Low amounts of mitochondrial reactive oxygen species define human sperm quality. *Reproduction.* **147**(6), pp.817-24.
- Martegani, M.P.Del Prete, F.Gasbarri, A.Natali, P.G. and Bartolazzi, A. 1999. Structural variability of CD44v molecules and reliability of immunodetection of CD44 isoforms using mAbs specific for CD44 variant exon products. *Am J Pathol.* **154**(1), pp.291-300.
- Martin-DeLeon, P.A. 2006. Epididymal SPAM1 and its impact on sperm function. *Mol Cell Endocrinol.* **250**(1-2), pp.114-21.
- Martin-DeLeon, P.A. 2011. Germ-cell hyaluronidases: their roles in sperm function. *Int J Androl.* **34**(5 Pt 2), pp.e306-18.
- Martinez-Heredia, J.de Mateo, S.Vidal-Taboada, J.M.Ballesca, J.L. and Oliva, R. 2008. Identification of proteomic differences in asthenozoospermic sperm samples. *Hum Reprod.* **23**(4), pp.783-91.
- Martinez, P. and Morros, A. 1996. Membrane lipid dynamics during human sperm capacitation. *Front Biosci.* **1**, pp.d103-17.
- Mayorga, L.S.Tomes, C.N. and Belmonte, S.A. 2007. Acrosomal exocytosis, a special type of regulated secretion. *IUBMB Life.* **59**(4-5), pp.286-92.
- McAlister, G.C.Huttlin, E.L.Haas, W.Ting, L.Jedrychowski, M.P.Rogers, J.C.Kuhn, K.Pike, I.Grothe, R.A.Blethrow, J.D. and Gygi, S.P. 2012. Increasing the multiplexing capacity of TMTs using reporter ion isotopologues with isobaric masses. *Anal Chem.* **84**(17), pp.7469-78.
- McCarthy, F.M.Cooksey, A.M. and Burgess, S.C. 2009. Sequential detergent extraction prior to mass spectrometry analysis. *Methods Mol Biol.* **528**, pp.110-8.
- McDowell, S.Kroon, B.Ford, E.Hook, Y.Glujovsky, D. and Yazdani, A. 2014. Advanced sperm selection techniques for assisted reproduction. *Cochrane Database Syst Rev.* (10), pCD010461.
- McLachlan, R.I.Mallidis, C.Ma, K.Bhasin, S. and de Kretser, D.M. 1998. Genetic disorders and spermatogenesis. *Reprod Fertil Dev.* **10**(1), pp.97-104.
- McLeskey, S.B.Dowds, C.Carballada, R.White, R.R. and Saling, P.M. 1998. Molecules involved in mammalian sperm-egg interaction. *Int Rev Cytol.* **177**, pp.57-113.
- McPherson, S. and Longo, F.J. 1993. Chromatin structure-function alterations during mammalian spermatogenesis: DNA nicking and repair in elongating spermatids. *Eur J Histochem.* **37**(2), pp.109-28.
- McReynolds, S.Dziewiatkowska, M.Stevens, J.Hansen, K.C.Schoolcraft, W.B. and Katz-Jaffe, M.G. 2014. Toward the identification of a subset of unexplained infertility: a sperm proteomic approach. *Fertil Steril.* **102**(3), pp.692-9.
- Mendes Maia, T.Gogendeau, D.Pennetier, C.Janke, C. and Basto, R. 2014. Bug22 influences cilium morphology and the post-translational modification of ciliary microtubules. *Biol Open.* **3**(2), pp.138-51.
- Menezo, Y.Dale, B. and Cohen, M. 2010. DNA damage and repair in human oocytes and embryos: a review. *Zygote.* **18**(4), pp.357-65.
- Meng, D.Cao, M.Oda, T. and Pan, J. 2014. The conserved ciliary protein Bug22 controls planar beating of Chlamydomonas flagella. *J Cell Sci.* **127**(Pt 2), pp.281-7.

- Mengual, L.Ballesca, J.L.Ascaso, C. and Oliva, R. 2003. Marked differences in protamine content and P1/P2 ratios in sperm cells from percoll fractions between patients and controls. *J Androl.* **24**(3), pp.438-47.
- Menkveld, R.El-Garem, Y.Schill, W.B. and Henkel, R. 2003. Relationship between human sperm morphology and acrosomal function. *J Assist Reprod Genet.* **20**(10), pp.432-8.
- Meseguer, M.Martinez-Conejero, J.A.O'Connor, J.E.Pellicer, A.Remohi, J. and Garrido, N. 2008. The significance of sperm DNA oxidation in embryo development and reproductive outcome in an oocyte donation program: a new model to study a male infertility prognostic factor. *Fertil Steril.* **89**(5), pp.1191-9.
- Miah, A.G.Salma, U.Sinha, P.B.Holker, M.Tesfaye, D.Cinar, M.U.Tsujii, H. and Schellander, K. 2011. Intracellular signaling cascades induced by relaxin in the stimulation of capacitation and acrosome reaction in fresh and frozen-thawed bovine spermatozoa. *Anim Reprod Sci.* **125**(1-4), pp.30-41.
- Miah AG.Salma U.Takagi Y.Kohsaka T.Hamano K and H, T. 2008. Effects of relaxin and IGF-I on capacitation, acrosome reaction, cholesterol efflux and utilization of labeled and unlabeled glucose in porcine spermatozoa. *Reprod Med Biol* **7**(1), pp.29-36.
- Miki, K. 2007. Energy metabolism and sperm function. *Soc Reprod Fertil Suppl.* **65**, pp.309-25.
- Miki, K.Qu, W.Goulding, E.H.Willis, W.D.Bunch, D.O.Strader, L.F.Perreault, S.D.Eddy, E.M. and O'Brien, D.A. 2004. Glyceraldehyde 3-phosphate dehydrogenase-S, a sperm-specific glycolytic enzyme, is required for sperm motility and male fertility. *Proc Natl Acad Sci U S A.* **101**(47), pp.16501-6.
- Milburn, D.Laskowski, R.A. and Thornton, J.M. 1998. Sequences annotated by structure: a tool to facilitate the use of structural information in sequence analysis. *Protein Eng.* **11**(10), pp.855-9.
- Miranda, P.V.Brandelli, A. and Tezon, J.G. 1995. Characterization of beta-N-acetylglucosaminidase from human epididymis. *Int J Androl.* **18**(5), pp.263-70.
- Mirza, S.Naaz, S.A. and Alim, S.M. 2016. Assisted Reproductive Technology (ART): A Review *WORLD JOURNAL OF PHARMACY AND PHARMACEUTICAL SCIENCES* **5**(9), pp.608-623.
- Mishra, S.Murphy, L.C. and Murphy, L.J. 2006. The Prohibitins: emerging roles in diverse functions. *J Cell Mol Med.* **10**(2), pp.353-63.
- Misra, S.Hascall, V.C.Markwald, R.R. and Ghatak, S. 2015. Interactions between Hyaluronan and Its Receptors (CD44, RHAMM) Regulate the Activities of Inflammation and Cancer. *Front Immunol.* **6**, p201.
- Misro, M.M. and Ramya, T. 2012. Fuel/Energy Sources of Spermatozoa. In: Parekattil, S.J. and Agarwal, A. eds. *Male Infertility: Contemporary Clinical Approaches, Andrology, ART & Antioxidants.* New York, NY: Springer New York, pp.209-223.
- Mohanty, G.Swain, N. and Samanta, L. 2015. Sperm Proteome: What Is on the Horizon? *Reprod Sci.* **22**(6), pp.638-53.
- Mohanty, S.K. and Singh, R. 2017. *Overview of the Male Reproductive System.* Singapore: Springer.
- Mokanszki, A.Tothne, E.V.Bodnar, B.Tandor, Z.Molnar, Z.Jakab, A.Ujfalusi, A. and Olah, E. 2014. Is sperm hyaluronic acid binding ability predictive for clinical success of intracytoplasmic sperm injection: PICSi vs. ICSI? *Syst Biol Reprod Med.* **60**(6), pp.348-54.
- Moretti, C.Serrentino, M.E.Ialy-Radio, C.Delessard, M.Soboleva, T.Tores, F.Leduc, M.Nitschké, P.Drevet, J.R.Tremethick, D.Vaiman, D.Kocer, A. and Cocquet, J. 2017. SLY regulates genes involved in chromatin remodeling and interacts with TBL1XR1 during sperm differentiation. *Cell Death & differentiation.* pp.1-16.
- Mori, E.Baba, T.Iwamatsu, A. and Mori, T. 1993. Purification and characterization of a 38-kDa protein, sp38, with zona pellucida-binding property from porcine epididymal sperm. *Biochem Biophys Res Commun.* **196**(1), pp.196-202.

- Mori, E.Kashiwabara, S.Baba, T.Inagaki, Y. and Mori, T. 1995. Amino acid sequences of porcine Sp38 and proacrosin required for binding to the zona pellucida. *Dev Biol.* **168**(2), pp.575-83.
- Morris, I.D.Ilott, S.Dixon, L. and Brison, D.R. 2002. The spectrum of DNA damage in human sperm assessed by single cell gel electrophoresis (Comet assay) and its relationship to fertilization and embryo development. *Hum Reprod.* **17**(4), pp.990-8.
- Morrissey, J.H. 1981. Silver stain for proteins in polyacrylamide gels: a modified procedure with enhanced uniform sensitivity. *Anal Biochem.* **117**(2), pp.307-10.
- Mortimer, D. 2000. Sperm preparation methods. *J Androl.* **21**(3), pp.357-66.
- Mortimer, D. and Mortimer, S.T. 2013. Density gradient separation of sperm for artificial insemination. *Methods Mol Biol.* **927**, pp.217-26.
- Moskovtsev, S.I.Jarvi, K.Mullen, J.B.Cadesky, K.I.Hannam, T. and Lo, K.C. 2010. Testicular spermatozoa have statistically significantly lower DNA damage compared with ejaculated spermatozoa in patients with unsuccessful oral antioxidant treatment. *Fertil Steril.* **93**(4), pp.1142-6.
- Mossman, J.A.Pearson, J.T.Moore, H.D. and Pacey, A.A. 2013. Variation in mean human sperm length is linked with semen characteristics. *Hum Reprod.* **28**(1), pp.22-32.
- Mruk, D.D. and Cheng, C.Y. 2010. Tight junctions in the testis: new perspectives. *Philos Trans R Soc Lond B Biol Sci.* **365**(1546), pp.1621-35.
- Munoz, X.Mata, A.Bassas, L. and Larriba, S. 2015. Altered miRNA Signature of Developing Germ-cells in Infertile Patients Relates to the Severity of Spermatogenic Failure and Persists in Spermatozoa. *Sci Rep.* **5**, p17991.
- Muriel, L.Meseguer, M.Fernandez, J.L.Alvarez, J.Remohi, J.Pellicer, A. and Garrido, N. 2006. Value of the sperm chromatin dispersion test in predicting pregnancy outcome in intrauterine insemination: a blind prospective study. *Hum Reprod.* **21**(3), pp.738-44.
- Myles, D.G. and Primakoff, P. 1984a. Localized surface antigens of guinea pig sperm migrate to new regions prior to fertilization. *J Cell Biol.* **99**.
- Myles, D.G. and Primakoff, P. 1984b. Localized surface antigens of guinea pig sperm migrate to new regions prior to fertilization. *J Cell Biol.* **99**(5), pp.1634-41.
- Myles, D.G. and Primakoff, P. 1997. Why did the sperm cross the cumulus? To get to the oocyte. Functions of the sperm surface proteins PH-20 and fertilin in arriving at, and fusing with, the egg. *Biol Reprod.* **56**(2), pp.320-7.
- Naaby-Hansen, S.Mandal, A.Wolkowicz, M.J.Sen, B.Westbrook, V.A.Shetty, J.Coonrod, S.A.Klotz, K.L.Kim, Y.H.Bush, L.A.Flickinger, C.J. and Herr, J.C. 2002. CABYR, a novel calcium-binding tyrosine phosphorylation-regulated fibrous sheath protein involved in capacitation. *Dev Biol.* **242**(2), pp.236-54.
- Nandi, P.Ghosh, S.Jana, K. and Sen, P.C. 2012. Elucidation of the involvement of p14, a sperm protein during maturation, capacitation and acrosome reaction of caprine spermatozoa. *PLoS One.* **7**(1), pe30552.
- Naor, D. 2016. Editorial: Interaction Between Hyaluronic Acid and Its Receptors (CD44, RHAMM) Regulates the Activity of Inflammation and Cancer. *Front Immunol.* **7**, p39.
- Nasr-Esfahani, M.H.Deemeh, M.R. and Tavalae, M. 2012. New era in sperm selection for ICSI. *Int J Androl.* **35**(4), pp.475-84.
- Nasr-Esfahani, M.H. and Marziyeh, T. 2013. Sperm selection for ICSI using the hyaluronic acid binding assay. *Methods Mol Biol.* **927**, pp.263-8.
- Nasr-Esfahani, M.H.Razavi, S.Vahdati, A.A.Fathi, F. and Tavalae, M. 2008. Evaluation of sperm selection procedure based on hyaluronic acid binding ability on ICSI outcome. *J Assist Reprod Genet.* **25**(5), pp.197-203.
- Nassar, A.Mahony, M.Morshedi, M.Lin, M.H.Srisombut, C. and Oehninger, S. 1999. Modulation of sperm tail protein tyrosine phosphorylation by pentoxifylline and its correlation with hyperactivated motility. *Fertil Steril.* **71**(5), pp.919-23.

- Navarro-Costa, P.Nogueira, P.Carvalho, M.Leal, F.Cordeiro, I.Calhaz-Jorge, C.Goncalves, J. and Plancha, C.E. 2010. Incorrect DNA methylation of the DAZL promoter CpG island associates with defective human sperm. *Hum Reprod.* **25**(10), pp.2647-54.
- Navarro, B.Kirichok, Y.Chung, J.J. and Clapham, D.E. 2008. Ion channels that control fertility in mammalian spermatozoa. *Int J Dev Biol.* **52**(5-6), pp.607-13.
- Naz, R.K. and Rajesh, P.B. 2004. Role of tyrosine phosphorylation in sperm capacitation / acrosome reaction. *Reprod Biol Endocrinol.* **2**, p75.
- Necas, J.Bartosikova, L.Brauner, P. and Kolar, J. 2008 Hyaluronic acid (hyaluronan): a review. *Veterinarni Medicina.* **53**(8), pp.397-411.
- Nedvetzki, S.Gonen, E.Assayag, N.Reich, R.Williams, R.O.Thurmond, R.L.Huang, J.F.Neudecker, B.A.Wang, F.S.Turley, E.A. and Naor, D. 2004. RHAMM, a receptor for hyaluronan-mediated motility, compensates for CD44 in inflamed CD44-knockout mice: a different interpretation of redundancy. *Proc Natl Acad Sci U S A.* **101**(52), pp.18081-6.
- Neesen, J.Kirschner, R.Ochs, M.Schmiedl, A.Habermann, B.Mueller, C.Holstein, A.F.Nuesslein, T.Adham, I. and Engel, W. 2001. Disruption of an inner arm dynein heavy chain gene results in asthenozoospermia and reduced ciliary beat frequency. *Hum Mol Genet.* **10**(11), pp.1117-28.
- Nel-Themaat, L.Jang, C.W.Stewart, M.D.Akiyama, H.Viger, R.S. and Behringer, R.R. 2011. Sertoli cell behaviors in developing testis cords and postnatal seminiferous tubules of the mouse. *Biol Reprod.* **84**(2), pp.342-50.
- Nguyen, E.B.Westmuckett, A.D. and Moore, K.L. 2014. SPACA7 is a novel male germ cell-specific protein localized to the sperm acrosome that is involved in fertilization in mice. *Biol Reprod.* **90**(1), p16.
- Nijs, M.Creemers, E.Cox, A.Franssen, K.Janssen, M.Vanheusden, E.De Jonge, C. and Ombelet, W. 2009. Chromomycin A3 staining, sperm chromatin structure assay and hyaluronic acid binding assay as predictors for assisted reproductive outcome. *Reprod Biomed Online.* **19**(5), pp.671-84.
- Nijs, M.Creemers, E.Cox, A.Janssen, M.Vanheusden, E.Van der Elst, J. and Ombelet, W. 2010. Relationship between hyaluronic acid binding assay and outcome in ART: a pilot study. *Andrologia.* **42**(5), pp.291-6.
- Nijs, M.Vanderzwalmen, P.Vandamme, B.Segal-Bertin, G.Lejeune, B.Segal, L.van Roosendaal, E. and Schoysman, R. 1996. Fertilizing ability of immotile spermatozoa after intracytoplasmic sperm injection. *Hum Reprod.* **11**(10), pp.2180-5.
- Nikolic, A.Volarevic, V.Armstrong, L.Lako, M. and Stojkovic, M. 2016. Primordial Germ Cells: Current Knowledge and Perspectives. *Stem Cells Int.* **2016**, p1741072.
- Nixon, B. and Aitken, R.J. 2009. The biological significance of detergent-resistant membranes in spermatozoa. *J Reprod Immunol.* **83**(1-2), pp.8-13.
- Nixon, B.Bromfield, E.G.Dun, M.D.Redgrove, K.A.McLaughlin, E.A. and Aitken, R.J. 2015. The role of the molecular chaperone heat shock protein A2 (HSPA2) in regulating human sperm-egg recognition. *Asian J Androl.* **17**(4), pp.568-73.
- Nunez-Martinez, I.Moran, J.M. and Pena, F.J. 2007. Identification of sperm morphometric subpopulations in the canine ejaculate: do they reflect different subpopulations in sperm chromatin integrity? *Zygote.* **15**(3), pp.257-66.
- O'Doherty, A.M. and McGettigan, P.A. 2015. Epigenetic processes in the male germline. *Reproduction, Fertility and Development.* **27**(5), pp.725-738.
- O'Donnell, L. 2014. Mechanisms of spermiogenesis and spermiation and how they are disturbed. *Spermatogenesis.* **4**(2), pe979623.
- O'Donnell, L.Nicholls, P.K.O'Bryan, M.K.McLachlan, R.I. and Stanton, P.G. 2011. Spermiation: The process of sperm release. *Spermatogenesis.* **1**(1), pp.14-35.



- O'Donnell, L.Stanton, P. and de Kretser, D.M. 2000. Endocrinology of the Male Reproductive System and Spermatogenesis. In: De Groot, L.J., et al. eds. *Endotext*. South Dartmouth (MA).
- O'Flaherty, C. 2015. Redox regulation of mammalian sperm capacitation. *Asian J Androl.* **17**(4), pp.583-90.
- O'Flaherty, C.Beorlegui, N. and Beconi, M.T. 2003. Participation of superoxide anion in the capacitation of cryopreserved bovine sperm. *Int J Androl.* **26**(2), pp.109-14.
- O'Flaherty, C.M.Beorlegui, N.B. and Beconi, M.T. 1999. Reactive oxygen species requirements for bovine sperm capacitation and acrosome reaction. *Theriogenology.* **52**(2), pp.289-301.
- Oakes, C.C.La Salle, S.Smiraglia, D.J.Robaire, B. and Trasler, J.M. 2007. A unique configuration of genome-wide DNA methylation patterns in the testis. *Proc Natl Acad Sci U S A.* **104**(1), pp.228-33.
- Odet, F.Duan, C.Willis, W.D.Goulding, E.H.Kung, A.Eddy, E.M. and Goldberg, E. 2008. Expression of the gene for mouse lactate dehydrogenase C (Ldhc) is required for male fertility. *Biol Reprod.* **79**(1), pp.26-34.
- Okabe, M.Adachi, T.Takada, K.Oda, H.Yagasaki, M.Kohama, Y. and Mimura, T. 1987. Capacitation-related changes in antigen distribution on mouse sperm heads and its relation to fertilization rate in vitro. *J Reprod Immunol.* **11**(2), pp.91-100.
- Oliferenko, S.Kaverina, I.Small, J.V. and Huber, L.A. 2000. Hyaluronic acid (HA) binding to CD44 activates Rac1 and induces lamellipodia outgrowth. *J Cell Biol.* **148**(6), pp.1159-64.
- Oliva, R. 2006. Protamines and male infertility. *Hum Reprod Update.* **12**(4), pp.417-35.
- Oliveira, J.B.Cavagna, M.Petersen, C.G.Mauri, A.L.Massaró, F.C.Silva, L.F.Baruffi, R.L. and Franco, J.G., Jr. 2011. Pregnancy outcomes in women with repeated implantation failures after intracytoplasmic morphologically selected sperm injection (IMSI). *Reprod Biol Endocrinol.* **9**, p99.
- Oliveira, J.B.Massaró, F.C.Mauri, A.L.Petersen, C.G.Nicoletti, A.P.Baruffi, R.L. and Franco, J.G., Jr. 2009. Motile sperm organelle morphology examination is stricter than Tygerberg criteria. *Reprod Biomed Online.* **18**(3), pp.320-6.
- Ooe, H.Taira, T.Iguchi-Arigo, S.M. and Ariga, H. 2005. Induction of reactive oxygen species by bisphenol A and abrogation of bisphenol A-induced cell injury by DJ-1. *Toxicol Sci.* **88**(1), pp.114-26.
- Osheroff, J.E.Visconti, P.E.Valenzuela, J.P.Travis, A.J.Alvarez, J. and Kopf, G.S. 1999. Regulation of human sperm capacitation by a cholesterol efflux-stimulated signal transduction pathway leading to protein kinase A-mediated up-regulation of protein tyrosine phosphorylation. *Mol Hum Reprod.* **5**(11), pp.1017-26.
- Oshio, S.Kaneko, S.Iizuka, R. and Mohri, H. 1987. Effects of gradient centrifugation on human sperm. *Arch Androl.* **19**(1), pp.85-93.
- Osman, A.Alsomait, H.Seshadri, S.El-Toukhy, T. and Khalaf, Y. 2014. The effect of sperm DNA fragmentation on live birth rate after IVF or ICSI: a systematic review and meta-analysis. *Reproductive BioMedicine Online.* (0).
- Osman, A.Alsomait, H.Seshadri, S.El-Toukhy, T. and Khalaf, Y. 2015. The effect of sperm DNA fragmentation on live birth rate after IVF or ICSI: a systematic review and meta-analysis. *Reprod Biomed Online.* **30**(2), pp.120-7.
- Ostermeier, G.C.Sargeant, G.A.Yandell, B.S.Evenson, D.P. and Parrish, J.J. 2001. Relationship of bull fertility to sperm nuclear shape. *J Androl.* **22**(4), pp.595-603.
- Paduch, D.A. 2006. Testicular cancer and male infertility. *Curr Opin Urol.* **16**(6), pp.419-27.
- Pagni, M. and Jongeneel, C.V. 2001. Making sense of score statistics for sequence alignments. *Brief Bioinform.* **2**(1), pp.51-67.
- Palermo, G.Joris, H.Devroey, P. and Van Steirteghem, A.C. 1992. Pregnancies after intracytoplasmic injection of single spermatozoon into an oocyte. *Lancet.* **340**(8810), pp.17-8.

- Parmegiani, L.Cognigni, G.E.Bernardi, S.Troilo, E.Ciampaglia, W. and Filicori, M. 2010a. "Physiologic ICSI": hyaluronic acid (HA) favors selection of spermatozoa without DNA fragmentation and with normal nucleus, resulting in improvement of embryo quality. *Fertil Steril.* **93**(2), pp.598-604.
- Parmegiani, L.Cognigni, G.E.Ciampaglia, W.Pocognoli, P.Marchi, F. and Filicori, M. 2010b. Efficiency of hyaluronic acid (HA) sperm selection. *J Assist Reprod Genet.* **27**(1), pp.13-6.
- Parmegiani, L.Cognigni, G.E. and Filicori, M. 2010c. Risks in injecting hyaluronic acid non-bound spermatozoa. *Reprod Biomed Online.* **20**(3), pp.437-8; author reply 439.
- Patrat, C.Serres, C. and Jouannet, P. 2000. The acrosome reaction in human spermatozoa. *Biol Cell.* **92**(3-4), pp.255-66.
- Patrizio, P.Silber, S.Ord, T.Balmaceda, J.P. and Asch, R.H. 1988. Two births after microsurgical sperm aspiration in congenital absence of vas deferens. *Lancet.* **2**(8624), p1364.
- Peach, R.J.Hollenbaugh, D.Stamenkovic, I. and Aruffo, A. 1993. Identification of hyaluronic acid binding sites in the extracellular domain of CD44. *J Cell Biol.* **122**(1), pp.257-64.
- Perry, K.Haresign, W.Wathes, D.C. and Khalid, M. 2010. Hyaluronan (HA) content, the ratio of HA fragments and the expression of CD44 in the ovine cervix vary with the stage of the oestrous cycle. *Reproduction.* **140**(1), pp.133-41.
- Petersen, C.G.Massarò, F.C.Mauri, A.L.Oliveira, J.B.Baruffi, R.L. and Franco, J.G., Jr. 2010. Efficacy of hyaluronic acid binding assay in selecting motile spermatozoa with normal morphology at high magnification. *Reprod Biol Endocrinol.* **8**, p149.
- Peterson, R.N. and Freund, M. 1971. Factors Affecting Fructose Utilization and Lactic Acid Formation by Human Semen. The Role of Glucose and Pyruvic Acid\*\*This investigation was supported by Grant HD-00488-13 from the National Institute of Child Health and Human Development, National Institutes of Health, United States Public Health Service. *Fertility and Sterility.* **22**(10), pp.639-644.
- Petit, F.M.Serres, C.Bourgeon, F.Pineau, C. and Auer, J. 2013. Identification of sperm head proteins involved in zona pellucida binding. *Hum Reprod.* **28**(4), pp.852-65.
- Phillips, B.T.Gassei, K. and Orwig, K.E. 2010. Spermatogonial stem cell regulation and spermatogenesis. *Philos Trans R Soc Lond B Biol Sci.* **365**(1546), pp.1663-78.
- Piehler, E.Petrunkina, A.M.Ekhlasi-Hundrieser, M. and Topfer-Petersen, E. 2006. Dynamic quantification of the tyrosine phosphorylation of the sperm surface proteins during capacitation. *Cytometry A.* **69**(10), pp.1062-70.
- Pitteloud, N. and Dwyer, A. 2014. Hormonal control of spermatogenesis in men: therapeutic aspects in hypogonadotropic hypogonadism. *Ann Endocrinol (Paris).* **75**(2), pp.98-100.
- Plazinski, W. and Knys-Dziedziuch, A. 2012. Interactions between CD44 protein and hyaluronan: insights from the computational study. *Mol Biosyst.* **8**(2), pp.543-7.
- Ponta, H.Sherman, L. and Herrlich, P.A. 2003. CD44: from adhesion molecules to signalling regulators. *Nat Rev Mol Cell Biol.* **4**(1), pp.33-45.
- Poongothai, J.Gopenath, T.S. and Manonayaki, S. 2009. Genetics of human male infertility. *Singapore Med J.* **50**(4), pp.336-47.
- Porter, M.E. and Sale, W.S. 2000. The 9 + 2 axoneme anchors multiple inner arm dyneins and a network of kinases and phosphatases that control motility. *J Cell Biol.* **151**(5), pp.F37-42.
- Primakoff, P. and Myles, D.G. 2000. The ADAM gene family: surface proteins with adhesion and protease activity. *Trends Genet.* **16**(2), pp.83-7.
- Prinosilova, P.Kruger, T.Sati, L.Ozkavukcu, S.Vigue, L.Kovanci, E. and Huszar, G. 2009. Selectivity of hyaluronic acid binding for spermatozoa with normal Tygerberg strict morphology. *Reprod Biomed Online.* **18**(2), pp.177-83.
- Purcell, B.P.Kim, I.L.Chuo, V.Guinen, T.Dorsey, S.M. and Burdick, J.A. 2014. Incorporation of Sulfated Hyaluronic Acid Macromers into Degradable Hydrogel Scaffolds for Sustained Molecule Delivery. *Biomater Sci.* **2**, pp.693-702.

- Qian, L.Yu, S. and Zhou, Y. 2016. Protective effect of hyaluronic acid on cryopreserved boar sperm. *Int J Biol Macromol.* **87**, pp.287-9.
- Rahman, M.S.Kwon, W.S. and Pang, M.G. 2017. Prediction of male fertility using capacitation-associated proteins in spermatozoa. *Mol Reprod Dev.* **84**(9), pp.749-759.
- Ramaswamy, S. and Weinbauer, G.F. 2014. Endocrine control of spermatogenesis: Role of FSH and LH/ testosterone. *Spermatogenesis.* **4**(2), pe996025.
- Ramos-Ibeas, P.Calle, A.Fernández-González, R.Laguna-Barraza, R.Pericuesta, E.Calero, A.Ramírez, M.A. and Gutiérrez-Adán, A. 2014. Intracytoplasmic sperm injection using DNAFragmented sperm in mice negatively affects embryo-derived embryonic stem cells, reduces the fertility of male offspring and induces heritable changes in epialleles. *PLoS ONE.* **9**(4).
- Ranganathan, S.Bharadwaj, A. and Datta, K. 1995. Hyaluronan mediates sperm motility by enhancing phosphorylation of proteins including hyaluronan binding protein. *Cell Mol Biol Res.* **41**(5), pp.467-76.
- Ranganathan, S.Ganguly, A.K. and Datta, K. 1994. Evidence for presence of hyaluronan binding protein on spermatozoa and its possible involvement in sperm function. *Mol Reprod Dev.* **38**(1), pp.69-76.
- Rao, C.M.Deb, T.B. and Datta, K. 1996. Hyaluronic acid induced hyaluronic acid binding protein phosphorylation and inositol triphosphate formation in lymphocytes. *Biochem Mol Biol Int.* **40**(2), pp.327-37.
- Rebourcet, D.O'Shaughnessy, P.J.Monteiro, A.Milne, L.Cruickshanks, L.Jeffrey, N.Guillou, F.Freeman, T.C.Mitchell, R.T. and Smith, L.B. 2014. Sertoli cells maintain Leydig cell number and peritubular myoid cell activity in the adult mouse testis. *PLoS One.* **9**(8), pe105687.
- Reddy, M., J.Joyce, C. and LJD., Z. 1980. Role of Hyaluronidase in Fertilization: The Antifertility Activity of Myocrisin, a Nontoxic Hyaluronidase Inhibitor. *Journal of Andrology.* **1**(1), pp.28-32.
- Reid, A.T.Redgrove, K.Aitken, R.J. and Nixon, B. 2011. Cellular mechanisms regulating sperm-zona pellucida interaction. *Asian J Androl.* **13**(1), pp.88-96.
- Relucenti, M.Heyn, R.Correr, S. and Familiari, G. 2005. Cumulus oophorus extracellular matrix in the human oocyte: a role for adhesive proteins. *Ital J Anat Embryol.* **110**(2 Suppl 1), pp.219-24.
- Rengan, A.K.Agarwal, A.van der Linde, M. and du Plessis, S.S. 2012. An investigation of excess residual cytoplasm in human spermatozoa and its distinction from the cytoplasmic droplet. *Reprod Biol Endocrinol.* **10**, p92.
- Reynolds, S.Ismail, N.F.B.Calvert, S.J.Pacey, A.A. and Paley, M.N.J. 2017. Evidence for Rapid Oxidative Phosphorylation and Lactate Fermentation in Motile Human Sperm by Hyperpolarized (13)C Magnetic Resonance Spectroscopy. *Sci Rep.* **7**(1), p4322.
- Ribas-Maynou, J.Garcia-Peiro, A.Abad, C.Amengual, M.J.Navarro, J. and Benet, J. 2012a. Alkaline and neutral Comet assay profiles of sperm DNA damage in clinical groups. *Human Reproduction.* **27**(3), pp.652-658.
- Ribas-Maynou, J.Garcia-Peiro, A.Abad, C.Amengual, M.J.Navarro, J. and Benet, J. 2012b. Alkaline and neutral Comet assay profiles of sperm DNA damage in clinical groups. *Hum Reprod.* **27**(3), pp.652-8.
- Ribas-Maynou, J.Garcia-Peiro, A.Fernandez-Encinas, A.Amengual, M.J.Prada, E.Cortes, P.Navarro, J. and Benet, J. 2012c. Double stranded sperm DNA breaks, measured by Comet assay, are associated with unexplained recurrent miscarriage in couples without a female factor. *PLoS One.* **7**(9), pe44679.
- Ricci, G.Perticarari, S.Boscolo, R.Montico, M.Guaschino, S. and Presani, G. 2009. Semen preparation methods and sperm apoptosis: swim-up versus gradient-density centrifugation technique. *Fertil Steril.* **91**(2), pp.632-8.

- Richter, R.P.Hock, K.K.Burkhartsmeier, J.Boehm, H.Bingen, P.Wang, G.Steinmetz, N.F.Evans, D.J. and Spatz, J.P. 2007. Membrane-grafted hyaluronan films: a well-defined model system of glycoconjugate cell coats. *J Am Chem Soc.* **129**(17), pp.5306-7.
- Robinson, L.Gallos, I.D.Conner, S.J.Rajkhowa, M.Miller, D.Lewis, S.Kirkman-Brown, J. and Coomarasamy, A. 2012. The effect of sperm DNA fragmentation on miscarriage rates: a systematic review and meta-analysis. *Hum Reprod.* **27**(10), pp.2908-17.
- Rodriguez Hurtado, I.Stewart, A.J.Wolfe, D.F.Caldwell, F.J.Harrie, M. and Whitley, E.M. 2011. Immunolocalization of the hyaluronan receptor CD44 in the reproductive tract of the mare. *Theriogenology.* **75**(2), pp.276-86.
- Roest, H.P.van Klaveren, J.de Wit, J.van Gurp, C.G.Koken, M.H.Vermeij, M.van Roijen, J.H.Hoogerbrugge, J.W.Vreeburg, J.T.Baarends, W.M.Bootsma, D.Grootegeod, J.A. and Hoeijmakers, J.H. 1996. Inactivation of the HR23B ubiquitin-conjugating DNA repair enzyme in mice causes male sterility associated with chromatin modification. *Cell.* **86**(5), pp.799-810.
- Rogers, B.J.Perreault, S.D.Bentwood, B.J.McCarville, C.Hale, R.W. and Soderdahl, D.W. 1983. Variability in the human-hamster in vitro assay for fertility evaluation. *Fertil Steril.* **39**(2), pp.204-11.
- Romano, F.Tripiciano, A.Muciaccia, B.De Cesaris, P.Ziparo, E.Palombi, F. and Filippini, A. 2005. The contractile phenotype of peritubular smooth muscle cells is locally controlled: possible implications in male fertility. *Contraception.* **72**(4), pp.294-7.
- Roy, S.C. and Atreja, S.K. 2008. Effect of reactive oxygen species on capacitation and associated protein tyrosine phosphorylation in buffalo (*Bubalus bubalis*) spermatozoa. *Anim Reprod Sci.* **107**(1-2), pp.68-84.
- Rybak, J.N.Ettorre, A.Kaissling, B.Giavazzi, R.Neri, D. and Elia, G. 2005. In vivo protein biotinylation for identification of organ-specific antigens accessible from the vasculature. *Nat Methods.* **2**(4), pp.291-8.
- Saegusa, M.Hashimura, M. and Okayasu, I. 1998. CD44 expression in normal, hyperplastic, and malignant endometrium. *J Pathol.* **184**(3), pp.297-306.
- Said, T.M.Agarwal, A.Zborowski, M.Grunewald, S.Glander, H.J. and Paasch, U. 2008. Utility of magnetic cell separation as a molecular sperm preparation technique. *J Androl.* **29**(2), pp.134-42.
- Said, T.M. and Land, J.A. 2011. Effects of advanced selection methods on sperm quality and ART outcome: a systematic review. *Hum Reprod Update.* **17**(6), pp.719-33.
- Sailer, B.L.Jost, L.K. and Evenson, D.P. 1996. Bull sperm head morphometry related to abnormal chromatin structure and fertility. *Cytometry.* **24**(2), pp.167-73.
- Sakairi, A.Tsukise, A. and Meyer, W. 2007. Localization of hyaluronic acid in the seminal vesicles of the miniature pig. *Anat Histol Embryol.* **36**(1), pp.4-9.
- Sakkas, D. 2013. Novel technologies for selecting the best sperm for in vitro fertilization and intracytoplasmic sperm injection. *Fertil Steril.* **99**(4), pp.1023-9.
- Sakkas, D. and Alvarez, J.G. 2010. Sperm DNA fragmentation: mechanisms of origin, impact on reproductive outcome, and analysis. *Fertil Steril.* **93**(4), pp.1027-36.
- Sakkas, D.Manicardi, G.Bizzaro, D. and Bianchi, P.G. 2000a. Possible consequences of performing intracytoplasmic sperm injection (ICSI) with sperm possessing nuclear DNA damage. *Hum Fertil (Camb).* **3**(1), pp.26-30.
- Sakkas, D.Manicardi, G.C.Tomlinson, M.Mandrioli, M.Bizzaro, D.Bianchi, P.G. and Bianchi, U. 2000b. The use of two density gradient centrifugation techniques and the swim-up method to separate spermatozoa with chromatin and nuclear DNA anomalies. *Hum Reprod.* **15**(5), pp.1112-6.

- Sakkas, D.Ramalingam, M.Garrido, N. and Barratt, C.L. 2015. Sperm selection in natural conception: what can we learn from Mother Nature to improve assisted reproduction outcomes? *Hum Reprod Update*. **21**(6), pp.711-26.
- Salas-Huetos, A.Blanco, J.Vidal, F.Grossmann, M.Pons, M.C.Garrido, N. and Anton, E. 2016. Spermatozoa from normozoospermic fertile and infertile individuals convey a distinct miRNA cargo. *Andrology*. **4**(6), pp.1028-1036.
- Saleh, R.A.Agarwal, A.Nada, E.A.El-Tonsy, M.H.Sharma, R.K.Meyer, A.Nelson, D.R. and Thomas, A.J. 2003. Negative effects of increased sperm DNA damage in relation to seminal oxidative stress in men with idiopathic and male factor infertility. *Fertil Steril*. **79 Suppl 3**, pp.1597-605.
- Saling, P.M. and Storey, B.T. 1979. Mouse gamete interactions during fertilization in vitro. Chlortetracycline as a fluorescent probe for the mouse sperm acrosome reaction. *J Cell Biol*. **83**(3), pp.544-55.
- Sandro, C.E. and Sidney, V.J. 2011. Relationship of *in Vitro* Acrosome Reaction to Sperm Function: An Update. *The Open Reproductive Science Journal*. **3**, pp.72-84.
- Santiago-Moreno, J.Castano, C.Coloma, M.A.Gomez-Brunet, A.Toledano-Diaz, A.Lopez-Sebastian, A. and Campo, J.L. 2009. Use of the hypo-osmotic swelling test and aniline blue staining to improve the evaluation of seasonal sperm variation in native Spanish free-range poultry. *Poult Sci*. **88**(12), pp.2661-9.
- Saoud, N.B.Thomas, D.L. and Hohenboken, W.D. 1984. Breed and sire effects on crossbred lamb production from Panama ewes and on spermatozoan midpiece length. *J Anim Sci*. **59**(1), pp.29-38.
- Sati, L.Cayli, S.Delpiano, E.Sakkas, D. and Huszar, G. 2014. The pattern of tyrosine phosphorylation in human sperm in response to binding to zona pellucida or hyaluronic acid. *Reprod Sci*. **21**(5), pp.573-81.
- Sati, L.Ovari, L.Bennett, D.Simon, S.D.Demir, R. and Huszar, G. 2008. Double probing of human spermatozoa for persistent histones, surplus cytoplasm, apoptosis and DNA fragmentation. *Reprod Biomed Online*. **16**(4), pp.570-9.
- Saylan, A. and Duman, S. 2016. Efficacy of Hyaluronic Acid in The Selection of Human Spermatozoa with Intact DNA by The Swim-up Method. *Cell J*. **18**(1), pp.83-8.
- Sbracia, M.Grasso, J.Sayme, N.Stronk, J. and Huszar, G. 1997. Hyaluronic acid substantially increases the retention of motility in cryopreserved/thawed human spermatozoa. *Hum Reprod*. **12**(9), pp.1949-54.
- Schagdarsurengin, U.Paradowska, A. and Steger, K. 2012. Analysing the sperm epigenome: Roles in early embryogenesis and assisted reproduction. *Nature Reviews Urology*. **9**(11), pp.609-619.
- Schagdarsurengin, U. and Steger, K. 2016. Epigenetics in male reproduction: effect of paternal diet on sperm quality and offspring health. *Nature Reviews Urology*.
- Schatten, H. and Sun, Q.Y. 2009. The role of centrosomes in mammalian fertilization and its significance for ICSI. *Mol Hum Reprod*. **15**(9), pp.531-8.
- Scheepers, A.Joost, H.G. and Schurmann, A. 2004. The glucose transporter families SGLT and GLUT: molecular basis of normal and aberrant function. *JPEN J Parenter Enteral Nutr*. **28**(5), pp.364-71.
- Scheurer, S.B.Rybak, J.N.Roesli, C.Brunisholz, R.A.Potthast, F.Schlapbach, R.Neri, D. and Elia, G. 2005. Identification and relative quantification of membrane proteins by surface biotinylation and two-dimensional peptide mapping. *Proteomics*. **5**(11), pp.2718-28.
- Schindler, J. and Nothwang, H.G. 2006. Aqueous polymer two-phase systems: effective tools for plasma membrane proteomics. *Proteomics*. **6**(20), pp.5409-17.
- Schoenfelder, M. and Einspanier, R. 2003. Expression of hyaluronan synthases and corresponding hyaluronan receptors is differentially regulated during oocyte maturation in cattle. *Biol Reprod*. **69**(1), pp.269-77.

- Schulte, R.T.Ohl, D.A.Sigman, M. and Smith, G.D. 2010. Sperm DNA damage in male infertility: etiologies, assays, and outcomes. *J Assist Reprod Genet.* **27**(1), pp.3-12.
- Schwarz, T.Prieler, B.Schmid, J.A.Grzmil, P. and Neesen, J. 2017. Ccdc181 is a microtubule-binding protein that interacts with Hook1 in haploid male germ cells and localizes to the sperm tail and motile cilia. *Eur J Cell Biol.*
- Sebkova, N.Ded, L.Vesela, K. and Dvorakova-Hortova, K. 2014. Progress of sperm IZUMO1 relocation during spontaneous acrosome reaction. *Reproduction.* **147**(2), pp.231-40.
- Secciani, F.Bianchi, L.Ermini, L.Cianti, R.Armini, A.La Sala, G.B.Focarelli, R.Bini, L. and Rosati, F. 2009a. Protein profile of capacitated versus ejaculated human sperm. *J Proteome Res.* **8**(7), pp.3377-89.
- Secciani, F.Bianchi, L.Ermini, L.Cianti, R.Armini, A.La Sala, G.B.Focarelli, R.Bini, L. and Rosati, F. 2009b. Protein profile of capacitated versus ejaculated human sperm. *Journal of Proteome Research.* **8**(7), pp.3377-3389.
- Seli, E. and Sakkas, D. 2005. Spermatozoal nuclear determinants of reproductive outcome: implications for ART. *Hum Reprod Update.* **11**(4), pp.337-49.
- Sellami, A.Chakroun, N.Ben Zarrouk, S.Sellami, H.Kebaili, S.Rebai, T. and Keskes, L. 2013. Assessment of chromatin maturity in human spermatozoa: useful aniline blue assay for routine diagnosis of male infertility. *Adv Urol.* **2013**, p578631.
- Sengupta, A.Banerjee, B.Tyagi, R.K. and Datta, K. 2005. Golgi localization and dynamics of hyaluronan binding protein 1 (HABP1/p32/C1QBP) during the cell cycle. *Cell Res.* **15**(3), pp.183-6.
- Shamsi, M.B.Imam, S.N. and Dada, R. 2011. Sperm DNA integrity assays: diagnostic and prognostic challenges and implications in management of infertility. *J Assist Reprod Genet.* **28**(11), pp.1073-85.
- Sharma, R.Agarwal, A.Rohra, V.K.Assidi, M.Abu-Elmagd, M. and Turki, R.F. 2015. Effects of increased paternal age on sperm quality, reproductive outcome and associated epigenetic risks to offspring. *Reproductive Biology and Endocrinology.* **13**(1).
- Sharma, R.Biedenharn, K.R.Fedor, J.M. and Agarwal, A. 2013. Lifestyle factors and reproductive health: taking control of your fertility. *Reprod Biol Endocrinol.* **11**, p66.
- Shen, C.Kuang, Y.Liu, J.Feng, J.Chen, X.Wu, W.Chi, J.Tang, L.Wang, Y.Fei, J. and Wang, Z. 2013. Prss37 is required for male fertility in the mouse. *Biol Reprod.* **88**(5), p123.
- Shen, H. and Ong, C. 2000. Detection of oxidative DNA damage in human sperm and its association with sperm function and male infertility. *Free Radic Biol Med.* **28**(4), pp.529-36.
- Sheng, K.Liang, X.Huang, S. and Xu, W. 2014. The role of histone ubiquitination during spermatogenesis. *BioMed Research International.* **2014**.
- Sheriff, D.S. and Ali, E.F. 2010. Perspective on plasma membrane cholesterol efflux and spermatozoal function. *J Hum Reprod Sci.* **3**(2), pp.68-75.
- Shivaji, S.Kota, V. and Siva, A.B. 2009. The role of mitochondrial proteins in sperm capacitation. *J Reprod Immunol.* **83**(1-2), pp.14-8.
- Shukla, K.K.Mahdi, A.A. and Rajender, S. 2012. Ion channels in sperm physiology and male fertility and infertility. *J Androl.* **33**(5), pp.777-88.
- Simon, L. 2012. Sperm DNA damage measured by the alkaline Comet assay as an independent predictor of male infertility and in vitro fertilization success (vol 95, pg 652, 2011). *Fertility and Sterility.* **97**(6), pp.1479-1479.
- Simon, L.Brunborg, G.Stevenson, M.Lutton, D.McManus, J. and Lewis, S.E. 2010. Clinical significance of sperm DNA damage in assisted reproduction outcome. *Hum Reprod.* **25**(7), pp.1594-608.
- Simon, L.Liu, L.Murphy, K.Ge, S.Hotaling, J.Aston, K.I.Emery, B. and Carrell, D.T. 2014a. Comparative analysis of three sperm DNA damage assays and sperm nuclear protein content in couples undergoing assisted reproduction treatment. *Hum Reprod.* **29**(5), pp.904-17.

- Simon, L.Lutton, D.McManus, J. and Lewis, S.E. 2011. Sperm DNA damage measured by the alkaline Comet assay as an independent predictor of male infertility and in vitro fertilization success. *Fertil Steril.* **95**(2), pp.652-7.
- Simon, L.Murphy, K.Shamsi, M.B.Liu, L.Emery, B.Aston, K.I.Hotaling, J. and Carrell, D.T. 2014b. Paternal influence of sperm DNA integrity on early embryonic development. *Hum Reprod.* **29**(11), pp.2402-12.
- Simon, L.Proutski, I.Stevenson, M.Jennings, D.McManus, J.Lutton, D. and Lewis, S.E. 2013. Sperm DNA damage has a negative association with live-birth rates after IVF. *Reprod Biomed Online.* **26**(1), pp.68-78.
- Singh, N.P.Muller, C.H. and Berger, R.E. 2003. Effects of age on DNA double-strand breaks and apoptosis in human sperm. *Fertil Steril.* **80**(6), pp.1420-30.
- Smith, B.E. and Braun, R.E. 2012. Germ cell migration across Sertoli cell tight junctions. *Science.* **338**(6108), pp.798-802.
- Soderlund, B. and Lundin, K. 2000. The use of silane-coated silica particles for density gradient centrifugation in in-vitro fertilization. *Hum Reprod.* **15**(4), pp.857-60.
- Song, H.W. and Wilkinson, M.F. 2012. In vitro spermatogenesis: A long journey to get tails. *Spermatogenesis.* **2**(4), pp.238-244.
- Song, N.Liu, J.An, S.Nishino, T.Hishikawa, Y. and Koji, T. 2011. Immunohistochemical Analysis of Histone H3 Modifications in Germ Cells during Mouse Spermatogenesis. *Acta Histochem Cytochem.* **44**(4), pp.183-90.
- Sreenivasa, G.Vineeth, V.Kavitha, P. and Malini, S.S. 2012. Evaluation of acrosome intactness status in male infertility in Mysore, South India. *Int J Appl Basic Med Res.* **2**(1), pp.31-3.
- Steilmann, C.Cavalcanti, M.C.Bartkuhn, M.Pons-Kuhnemann, J.Schuppe, H.C.Weidner, W.Steger, K. and Paradowska, A. 2010. The interaction of modified histones with the bromodomain testis-specific (BRDT) gene and its mRNA level in sperm of fertile donors and subfertile men. *Reproduction.* **140**(3), pp.435-43.
- Steilmann, C.Paradowska, A.Bartkuhn, M.Vieweg, M.Schuppe, H.C.Bergmann, M.Kliesch, S.Weidner, W. and Steger, K. 2011. Presence of histone H3 acetylated at lysine 9 in male germ cells and its distribution pattern in the genome of human spermatozoa. *Reproduction, Fertility and Development.* **23**(8), pp.997-1011.
- Stein, K.K.Go, J.C.Lane, W.S.Primakoff, P. and Myles, D.G. 2006a. Proteomic analysis of sperm regions that mediate sperm-egg interactions. *Proteomics.* **6**(12), pp.3533-43.
- Stein, K.K.Go, J.C.Lane, W.S.Primakoff, P. and Myles, D.G. 2006b. Proteomic analysis of sperm regions that mediate sperm-egg interactions. *Proteomics.* **6**(12), pp.3533-3543.
- Stein, K.K.Primakoff, P. and Myles, D. 2004. Sperm-egg fusion: events at the plasma membrane. *J Cell Sci.* **117**(Pt 26), pp.6269-74.
- Stevanato, J.Bertolla, R.P.Barradas, V.Spaine, D.M.Cedenho, A.P. and Ortiz, V. 2008. Semen processing by density gradient centrifugation does not improve sperm apoptotic deoxyribonucleic acid fragmentation rates. *Fertil Steril.* **90**(3), pp.889-90.
- Stojkovic, M.Krebs, O.Kolle, S.Prelle, K.Assmann, V.Zakhartchenko, V.Sinowatz, F. and Wolf, E. 2003. Developmental regulation of hyaluronan-binding protein (RHAMM/IHABP) expression in early bovine embryos. *Biol Reprod.* **68**(1), pp.60-6.
- Storey, B.T. 2008. Mammalian sperm metabolism: oxygen and sugar, friend and foe. *Int J Dev Biol.* **52**(5-6), pp.427-37.
- Stuppia, L.Franzago, M.Ballerini, P.Gatta, V. and Antonucci, I. 2015. Epigenetics and male reproduction: the consequences of paternal lifestyle on fertility, embryo development, and children lifetime health. *Clin Epigenetics.* **7**, p120.
- Suarez, S.S. 2008. Control of hyperactivation in sperm. *Hum Reprod Update.* **14**(6), pp.647-57.
- Suarez, S.S. and Pacey, A.A. 2006. Sperm transport in the female reproductive tract. *Hum Reprod Update.* **12**(1), pp.23-37.

- Sun, X. and Yang, W. 2010. Mitochondria: transportation, distribution and function during spermiogenesis. *Advances in Bioscience and Biotechnology*. **1**(2), pp.97-109.
- Sun, Y.Zhang, W.J.Zhao, X.Yuan, R.P.Jiang, H. and Pu, X.P. 2014. PARK7 protein translocating into spermatozoa mitochondria in Chinese asthenozoospermia. *Reproduction*. **148**(3), pp.249-57.
- Suzuki, K.Asano, A.Eriksson, B.Niwa, K.Nagai, T. and Rodriguez-Martinez, H. 2002. Capacitation status and in vitro fertility of boar spermatozoa: effects of seminal plasma, cumulus-oocyte-complexes-conditioned medium and hyaluronan. *Int J Androl*. **25**(2), pp.84-93.
- Taira, T.Saito, Y.Niki, T.Iguchi-Ariga, S.M.Takahashi, K. and Ariga, H. 2004. DJ-1 has a role in antioxidative stress to prevent cell death. *EMBO Rep*. **5**(2), pp.213-8.
- Takeda, M.Ogino, S.Umemoto, R.Sakakura, M.Kajiwara, M.Sugahara, K.N.Hayasaka, H.Miyasaka, M.Terasawa, H. and Shimada, I. 2006. Ligand-induced structural changes of the CD44 hyaluronan-binding domain revealed by NMR. *J Biol Chem*. **281**(52), pp.40089-95.
- Tammi, R.Ronkko, S.Agren, U.M. and Tammi, M. 1994. Distribution of hyaluronan in bull reproductive organs. *J Histochem Cytochem*. **42**(11), pp.1479-86.
- Tanphaichitr, N.Kongmanas, K.Kruevaisayawan, H.Saewu, A.Sugeng, C.Fernandes, J.Souda, P.Angel, J.B.Faull, K.F.Aitken, R.J.Whitelegge, J.Hardy, D.Berger, T. and Baker, M. 2015. Remodeling of the plasma membrane in preparation for sperm-egg recognition: roles of acrosomal proteins. *Asian J Androl*. **17**(4), pp.574-82.
- Tarozzi, N.Nadalini, M.Bizzaro, D.Serrao, L.Fava, L.Scaravelli, G. and Borini, A. 2009. Sperm-hyaluronan-binding assay: clinical value in conventional IVF under Italian law. *Reprod Biomed Online*. **19 Suppl 3**, pp.35-43.
- Tasi, Y.C.Chao, H.C.Chung, C.L.Liu, X.Y.Lin, Y.M.Liao, P.C.Pan, H.A.Chiang, H.S.Kuo, P.L. and Lin, Y.H. 2013. Characterization of 3-hydroxyisobutyrate dehydrogenase, HIBADH, as a sperm-motility marker. *J Assist Reprod Genet*. **30**(4), pp.505-12.
- Teerds, K.J.de Rooij, D.G. and Keijer, J. 2011. Functional relationship between obesity and male reproduction: from humans to animal models. *Hum Reprod Update*. **17**(5), pp.667-83.
- Teixeira, D.M.Barbosa, M.A.Ferriani, R.A.Navarro, P.A.Raine-Fenning, N.Nastri, C.O. and Martins, W.P. 2013. Regular (ICSI) versus ultra-high magnification (IMSI) sperm selection for assisted reproduction. *Cochrane Database Syst Rev*. **7**, pCD010167.
- Tengblad, A. 1979. Affinity chromatography on immobilized hyaluronate and its application to the isolation of hyaluronate binding properties from cartilage. *Biochim Biophys Acta*. **578**(2), pp.281-9.
- Teriete, P.Banerji, S.Noble, M.Blundell, C.D.Wright, A.J.Pickford, A.R.Lowe, E.Mahoney, D.J.Tammi, M.I.Kahmann, J.D.Campbell, I.D.Day, A.J. and Jackson, D.G. 2004. Structure of the regulatory hyaluronan binding domain in the inflammatory leukocyte homing receptor CD44. *Mol Cell*. **13**(4), pp.483-96.
- Therien, I.Bousquet, D. and Manjunath, P. 2001. Effect of seminal phospholipid-binding proteins and follicular fluid on bovine sperm capacitation. *Biol Reprod*. **65**(1), pp.41-51.
- Thompson, A.Schafer, J.Kuhn, K.Kienle, S.Schwarz, J.Schmidt, G.Neumann, T.Johnstone, R.Mohammed, A.K. and Hamon, C. 2003. Tandem mass tags: a novel quantification strategy for comparative analysis of complex protein mixtures by MS/MS. *Anal Chem*. **75**(8), pp.1895-904.
- Thorne, R.F.Legg, J.W. and Isacke, C.M. 2004. The role of the CD44 transmembrane and cytoplasmic domains in co-ordinating adhesive and signalling events. *J Cell Sci*. **117**(Pt 3), pp.373-80.
- Tienthai, P.Kimura, N.Heldin, P.Sato, E. and Rodriguez-Martinez, H. 2003. Expression of hyaluronan synthase-3 in porcine oviducal epithelium during oestrus. *Reprod Fertil Dev*. **15**(1-2), pp.99-105.
- Tomlinson, M.J.Moffatt, O.Manicardi, G.C.Bizzaro, D.Afnan, M. and Sakkas, D. 2001. Interrelationships between seminal parameters and sperm nuclear DNA damage before and



- after density gradient centrifugation: implications for assisted conception. *Hum Reprod.* **16**(10), pp.2160-5.
- Tomsu, M.Sharma, V. and Miller, D. 2002. Embryo quality and IVF treatment outcomes may correlate with different sperm comet assay parameters. *Hum Reprod.* **17**(7), pp.1856-62.
- Toole, B.P. 2004. Hyaluronan: from extracellular glue to pericellular cue. *Nat Rev Cancer.* **4**(7), pp.528-39.
- Toole, B.P. 2009. Hyaluronan-CD44 Interactions in Cancer: Paradoxes and Possibilities. *Clin Cancer Res.* **15**(24), pp.7462-7468.
- Torabi, F.Binduraihem, A. and Miller, D. 2016. Sedimentation properties in density gradients correspond with levels of sperm DNA fragmentation, chromatin compaction and binding affinity to hyaluronic acid. *Reprod Biomed Online.*
- Torabi, F.Binduraihem, A. and Miller, D. 2017a. Sedimentation properties in density gradients correspond with levels of sperm DNA fragmentation, chromatin compaction and binding affinity to hyaluronic acid. *Reprod Biomed Online.* **34**(3), pp.298-311.
- Torabi, F.Bogle, O.A.Estanyol, J.M.Oliva, R. and Miller, D. 2017b. Zona pellucida-binding protein 2 (ZBPB2) and several proteins containing BX7B motifs in human sperm may have hyaluronic acid binding or recognition properties. *Mol Hum Reprod.* **23**(12), pp.803-816.
- Toshimori, K.Saxena, D.K.Tanii, I. and Yoshinaga, K. 1998. An MN9 antigenic molecule, equatorin, is required for successful sperm-oocyte fusion in mice. *Biol Reprod.* **59**(1), pp.22-9.
- Tournaye, H. 2003. ICSI: a technique too far? *Int J Androl.* **26**(2), pp.63-9.
- Travis, A.J.Jorgez, C.J.Merdiushev, T.Jones, B.H.Dess, D.M.Diaz-Cueto, L.Storey, B.T.Kopf, G.S. and Moss, S.B. 2001. Functional relationships between capacitation-dependent cell signaling and compartmentalized metabolic pathways in murine spermatozoa. *J Biol Chem.* **276**(10), pp.7630-6.
- Travis, A.J.Tutuncu, L.Jorgez, C.J.Ord, T.S.Jones, B.H.Kopf, G.S. and Williams, C.J. 2004. Requirements for glucose beyond sperm capacitation during in vitro fertilization in the mouse. *Biol Reprod.* **71**(1), pp.139-45.
- Tsunoda, S.Kawano, N.Miyado, K.Kimura, N. and Fujii, J. 2012. Impaired fertilizing ability of superoxide dismutase 1-deficient mouse sperm during in vitro fertilization. *Biol Reprod.* **87**(5), p121.
- Tulsiani, D.R.Abou-Haila, A.Loesser, C.R. and Pereira, B.M. 1998. The biological and functional significance of the sperm acrosome and acrosomal enzymes in mammalian fertilization. *Exp Cell Res.* **240**(2), pp.151-64.
- Turley, E.A.Hossain, M.Z.Sorokan, T.Jordan, L.M. and Nagy, J.I. 1994. Astrocyte and microglial motility in vitro is functionally dependent on the hyaluronan receptor RHAMM. *Glia.* **12**(1), pp.68-80.
- Turley, E.A.Noble, P.W. and Bourguignon, L.Y. 2002. Signaling properties of hyaluronan receptors. *J Biol Chem.* **277**(7), pp.4589-92.
- Underhill, C. 1992. CD44: the hyaluronan receptor. *J Cell Sci.* **103 ( Pt 2)**, pp.293-8.
- Underhill, C.B.Green, S.J.Comoglio, P.M. and Tarone, G. 1987. The hyaluronate receptor is identical to a glycoprotein of Mr 85,000 (gp85) as shown by a monoclonal antibody that interferes with binding activity. *J Biol Chem.* **262**(27), pp.13142-6.
- Urduinguio, R.G.Bayon, G.F.Dmitrijeva, M.Torano, E.G.Bravo, C.Fraga, M.F.Bassas, L.Larriba, S. and Fernandez, A.F. 2015. Aberrant DNA methylation patterns of spermatozoa in men with unexplained infertility. *Hum Reprod.* **30**(5), pp.1014-28.
- Urner, F. and Sakkas, D. 1999. A possible role for the pentose phosphate pathway of spermatozoa in gamete fusion in the mouse. *Biol Reprod.* **60**(3), pp.733-9.
- Urner, F. and Sakkas, D. 2005. Involvement of the pentose phosphate pathway and redox regulation in fertilization in the mouse. *Mol Reprod Dev.* **70**(4), pp.494-503.

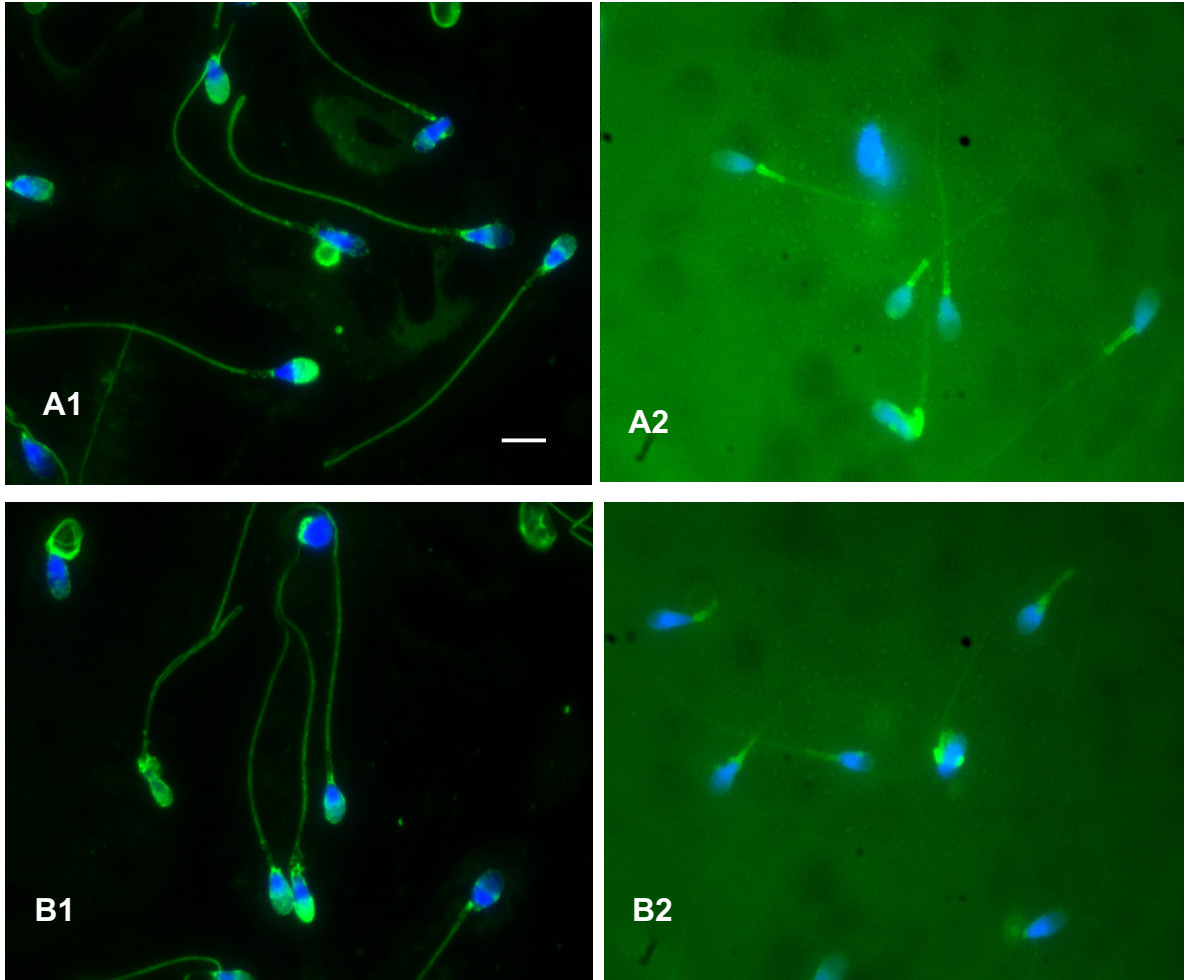
- van Der Horst, G.Seier, J.V.Spinks, A.C. and Hendricks, S. 1999. The maturation of sperm motility in the epididymis and vas deferens of the vervet monkey, *Cercopithecus aethiops*. *Int J Androl.* **22**(3), pp.197-207.
- van Tilburg, M.F.Rodrigues, M.A.Moreira, R.A.Moreno, F.B.Monteiro-Moreira, A.C.Candido, M.J. and Moura, A.A. 2013. Membrane-associated proteins of ejaculated sperm from Morada Nova rams. *Theriogenology.* **79**(9), pp.1247-61.
- Vandevoort, C.A.Cherr, G.N. and Overstreet, J.W. 1997. Hyaluronic acid enhances the zona pellucida-induced acrosome reaction of macaque sperm. *J Androl.* **18**(1), pp.1-5.
- Veeck, L.L.Wortham, J.W., Jr.Witmyer, J.Sandow, B.A.Acosta, A.A.Garcia, J.E.Jones, G.S. and Jones, H.W., Jr. 1983. Maturation and fertilization of morphologically immature human oocytes in a program of in vitro fertilization. *Fertil Steril.* **39**(5), pp.594-602.
- Venkatesh, S.Singh, A.Shamsi, M.B.Thilagavathi, J.Kumar, R.Mitra, D.K. and Dada, R. 2011. Clinical significance of sperm DNA damage threshold value in the assessment of male infertility. *Reprod Sci.* **18**(10), pp.1005-13.
- Vines, C.A.Li, M.W.Deng, X.Yudin, A.I.Cherr, G.N. and Overstreet, J.W. 2001. Identification of a hyaluronic acid (HA) binding domain in the PH-20 protein that may function in cell signaling. *Mol Reprod Dev.* **60**(4), pp.542-52.
- Virant-Klun, I.Tomazevic, T. and Meden-Vrtovec, H. 2002. Sperm single-stranded DNA, detected by acridine orange staining, reduces fertilization and quality of ICSI-derived embryos. *J Assist Reprod Genet.* **19**(7), pp.319-28.
- Visconti, P.E. 2012. Sperm bioenergetics in a nutshell. *Biol Reprod.* **87**(3), p72.
- Visconti, P.E.Galantino-Homer, H.Ning, X.Moore, G.D.Valenzuela, J.P.Jorgez, C.J.Alvarez, J.G. and Kopf, G.S. 1999. Cholesterol efflux-mediated signal transduction in mammalian sperm. beta-cyclodextrins initiate transmembrane signaling leading to an increase in protein tyrosine phosphorylation and capacitation. *J Biol Chem.* **274**(5), pp.3235-42.
- Visconti, P.E.Krapf, D.de la Vega-Beltran, J.L.Acevedo, J.J. and Darszon, A. 2011. Ion channels, phosphorylation and mammalian sperm capacitation. *Asian J Androl.* **13**(3), pp.395-405.
- Wang, C.Thor, A.D.Moore, D.H., 2ndZhao, Y.Kerschmann, R.Stern, R.Watson, P.H. and Turley, E.A. 1998. The overexpression of RHAMM, a hyaluronan-binding protein that regulates ras signaling, correlates with overexpression of mitogen-activated protein kinase and is a significant parameter in breast cancer progression. *Clin Cancer Res.* **4**(3), pp.567-76.
- Wang, C.W.Lai, Y.M.Wang, M.L.Lee, J.D. and Soong, Y.K. 1997. Pregnancy after intracytoplasmic injection of immotile sperm. A case report. *J Reprod Med.* **42**(7), pp.448-50.
- Wang, G.Guo, Y.Zhou, T.Shi, X.Yu, J.Yang, Y.Wu, Y.Wang, J.Liu, M.Chen, X.Tu, W.Zeng, Y.Jiang, M.Li, S.Zhang, P.Zhou, Q.Zheng, B.Yu, C.Zhou, Z.Guo, X. and Sha, J. 2013. In-depth proteomic analysis of the human sperm reveals complex protein compositions. *J Proteomics.* **79**, pp.114-22.
- Wassarman, P.M.Jovine, L. and Litscher, E.S. 2001. A profile of fertilization in mammals. *Nat Cell Biol.* **3**(2), pp.E59-64.
- Weber, R.F.Dohle, G.R. and Romijn, J.C. 2005. Clinical laboratory evaluation of male subfertility. *Adv Clin Chem.* **40**, pp.317-64.
- Weigel, P.H. 2015. Hyaluronan Synthase: The Mechanism of Initiation at the Reducing End and a Pendulum Model for Polysaccharide Translocation to the Cell Exterior. *Int J Cell Biol.* **2015**, p367579.
- Weigel, P.H.Hascall, V.C. and Tammi, M. 1997. Hyaluronan synthases. *J Biol Chem.* **272**(22), pp.13997-4000.
- WHO. 2010a. *WHO laboratory manual for the Examination and processing of human semen*. [Online].
- WHO. 2010b. *WHO laboratory manual for the examination and processing of human semen* 5ed. WHO Press, World Health Organization, Geneva

- Williams, A.C. and Ford, W.C. 2001. The role of glucose in supporting motility and capacitation in human spermatozoa. *J Androl.* **22**(4), pp.680-95.
- Witt, K.D., Beresford, L., Bhattacharya, S., Brian, K., Coomarasamy, A., Cutting, R., Hooper, R., Kirkman-Brown, J., Khalaf, Y., Lewis, S.E., Pacey, A., Pavitt, S., West, R. and Miller, D. 2016. Hyaluronic Acid Binding Sperm Selection for assisted reproduction treatment (HABSelect): study protocol for a multicentre randomised controlled trial. *BMJ Open.* **6**(10), pe012609.
- Witte, T.S. and Schafer-Somi, S. 2007. Involvement of cholesterol, calcium and progesterone in the induction of capacitation and acrosome reaction of mammalian spermatozoa. *Anim Reprod Sci.* **102**(3-4), pp.181-93.
- Woerner, S.M., Givehchian, M., Durst, M., Schneider, A., Costa, S., Melsheimer, P., Lacroix, J., Zoller, M. and Doeberitz, M.K. 1995. Expression of CD44 splice variants in normal, dysplastic, and neoplastic cervical epithelium. *Clin Cancer Res.* **1**(10), pp.1125-32.
- Wolfsberg, T.G., Primakoff, P., Myles, D.G. and White, J.M. 1995. ADAM, a novel family of membrane proteins containing A Disintegrin And Metalloprotease domain: multipotential functions in cell-cell and cell-matrix interactions. *J Cell Biol.* **131**(2), pp.275-8.
- Wolny, P.M., Banerji, S., Gounou, C., Brisson, A.R., Day, A.J., Jackson, D.G. and Richter, R.P. 2010. Analysis of CD44-hyaluronan interactions in an artificial membrane system: insights into the distinct binding properties of high and low molecular weight hyaluronan. *J Biol Chem.* **285**(39), pp.30170-80.
- Wong, A., Chuan, S.S., Patton, W.C., Jacobson, J.D., Corselli, J. and Chan, P.J. 2008. Addition of eosin to the aniline blue assay to enhance detection of immature sperm histones. *Fertil Steril.* **90**(5), pp.1999-2002.
- Wong, M.Y. and Ledger, W.L. 2013. Is ICSI Risky? *Obstet Gynecol Int.* **2013**, p473289.
- Worriolow, K.C., Eid, S., Woodhouse, D., Perloe, M., Smith, S., Witmyer, J., Ivani, K., Khoury, C., Ball, G.D., Elliot, T. and Lieberman, J. 2013. Use of hyaluronan in the selection of sperm for intracytoplasmic sperm injection (ICSI): significant improvement in clinical outcomes--multicenter, double-blinded and randomized controlled trial. *Hum Reprod.* **28**(2), pp.306-14.
- Wright, C., Milne, S. and Leeson, H. 2014. Sperm DNA damage caused by oxidative stress: modifiable clinical, lifestyle and nutritional factors in male infertility. *Reprod Biomed Online.* **28**(6), pp.684-703.
- Wu, W., Shen, O., Qin, Y., Niu, X., Lu, C., Xia, Y., Song, L., Wang, S. and Wang, X. 2010. Idiopathic male infertility is strongly associated with aberrant promoter methylation of methylenetetrahydrofolate reductase (MTHFR). *PLoS One.* **5**(11), pe13884.
- Xu, W., Hu, H., Wang, Z., Chen, X., Yang, F., Zhu, Z., Fang, P., Dai, J., Wang, L., Shi, H., Li, Z. and Qiao, Z. 2012. Proteomic characteristics of spermatozoa in normozoospermic patients with infertility. *J Proteomics.* **75**(17), pp.5426-36.
- Xue, X., Wang, W.S., Shi, J.Z., Zhang, S.L., Zhao, W.Q., Shi, W.H., Guo, B.Z. and Qin, Z. 2014. Efficacy of swim-up versus density gradient centrifugation in improving sperm deformity rate and DNA fragmentation index in semen samples from teratozoospermic patients. *J Assist Reprod Genet.* **31**(9), pp.1161-6.
- Yagci, A., Murk, W., Stronk, J. and Huszar, G. 2010. Spermatozoa bound to solid state hyaluronic acid show chromatin structure with high DNA chain integrity: an acridine orange fluorescence study. *J Androl.* **31**(6), pp.566-72.
- Yamagata, K., Murayama, K., Okabe, M., Toshimori, K., Nakanishi, T., Kashiwabara, S. and Baba, T. 1998. Acrosin accelerates the dispersal of sperm acrosomal proteins during acrosome reaction. *J Biol Chem.* **273**(17), pp.10470-4.
- Yamanaka, M., Tomita, K., Hashimoto, S., Matsumoto, H., Satoh, M., Kato, H., Hosoi, Y., Inoue, M., Nakaoka, Y. and Morimoto, Y. 2016. Combination of density gradient centrifugation and swim-up methods effectively decreases morphologically abnormal sperms. *J Reprod Dev.* **62**(6), pp.599-606.

- Yanagimachi, R. 1969. In vitro capacitation of hamster spermatozoa by follicular fluid. *J Reprod Fertil.* **18**(2), pp.275-86.
- Yanagimachi, R. 1994a. Fertility of mammalian spermatozoa: its development and relativity. *Zygote.* **2**(4), pp.371-2.
- Yanagimachi, R. 1994b. *Mammalian fertilization.* New York.
- Yang, B.Yang, B.L.Savani, R.C. and Turley, E.A. 1994. Identification of a common hyaluronan binding motif in the hyaluronan binding proteins RHAMM, CD44 and link protein. *EMBO J.* **13**(2), pp.286-96.
- Yang, B.Zhang, L. and Turley, E.A. 1993. Identification of two hyaluronan-binding domains in the hyaluronan receptor RHAMM. *J Biol Chem.* **268**(12), pp.8617-23.
- Yetunde, I. and Vasiliki, M. 2013. Effects of advanced selection methods on sperm quality and ART outcome. *Minerva Ginecol.* **65**(5), pp.487-96.
- Yi, Y.J.Zimmerman, S.W.Manandhar, G.Odhiambo, J.F.Kennedy, C.Jonakova, V.Manaskova-Postlerova, P.Sutovsky, M.Park, C.S. and Sutovsky, P. 2012. Ubiquitin-activating enzyme (UBA1) is required for sperm capacitation, acrosomal exocytosis and sperm-egg coat penetration during porcine fertilization. *Int J Androl.* **35**(2), pp.196-210.
- Zaleski, K.J.Kolodka, T.Cywes-Bentley, C.McLoughlin, R.M.Delaney, M.L.Charlton, B.T.Johnson, W. and Tzianabos, A.O. 2006. Hyaluronic acid binding peptides prevent experimental staphylococcal wound infection. *Antimicrob Agents Chemother.* **50**(11), pp.3856-60.
- Zaneveld, L.J.De Jonge, C.J.Anderson, R.A. and Mack, S.R. 1991. Human sperm capacitation and the acrosome reaction. *Hum Reprod.* **6**(9), pp.1265-74.
- Zegers-Hochschild, F.Adamson, G.D.de Mouzon, J.Ishihara, O.Mansour, R.Nygren, K.Sullivan, E.Vanderpoel, S.International Committee for Monitoring Assisted Reproductive, T. and World Health, O. 2009. International Committee for Monitoring Assisted Reproductive Technology (ICMART) and the World Health Organization (WHO) revised glossary of ART terminology, 2009. *Fertil Steril.* **92**(5), pp.1520-4.
- Zeh, J.A.Bonilla, M.M.Adrian, A.J.Mesfin, S. and Zeh, D.W. 2012. From father to son: transgenerational effect of tetracycline on sperm viability. *Sci Rep.* **2**, p375.
- Zhang, H.Morales, C.R.Badran, H.El-Alfy, M. and Martin-DeLeon, P.A. 2004. Spam1 (PH-20) expression in the extratesticular duct and accessory organs of the mouse: a possible role in sperm fluid reabsorption. *Biol Reprod.* **71**(4), pp.1101-7.
- Zhang, S.Chang, M.C.Zylka, D.Turley, S.Harrison, R. and Turley, E.A. 1998. The hyaluronan receptor RHAMM regulates extracellular-regulated kinase. *J Biol Chem.* **273**(18), pp.11342-8.
- Zhang, Y.Wang, H.Wang, L.Zhou, Z.Sha, J.Mao, Y.Cai, L.Feng, T.Yan, Z.Ma, L. and Liu, J. 2008. The clinical significance of sperm DNA damage detection combined with routine semen testing in assisted reproduction. *Mol Med Rep.* **1**(5), pp.617-24.
- Zhao, C.Guo, X.J.Shi, Z.H.Wang, F.Q.Huang, X.Y.Huo, R.Zhu, H.Wang, X.R.Liu, J.Y.Zhou, Z.M. and Sha, J.H. 2009. Role of translation by mitochondrial-type ribosomes during sperm capacitation: an analysis based on a proteomic approach. *Proteomics.* **9**(5), pp.1385-99.
- Zhao, J.Zhang, Q.Wang, Y. and Li, Y. 2014. Whether sperm deoxyribonucleic acid fragmentation has an effect on pregnancy and miscarriage after in vitro fertilization/intracytoplasmic sperm injection: a systematic review and meta-analysis. *Fertil Steril.* **102**(4), pp.998-1005 e8.
- Zheng, H.Mandal, A.Shumilin, I.A.Chordia, M.D.Panneerdoss, S.Herr, J.C. and Minor, W. 2015. Sperm Lysozyme-Like Protein 1 (SLLP1), an intra-acrosomal oolemmal-binding sperm protein, reveals filamentous organization in protein crystal form. *Andrology.* **3**(4), pp.756-71.
- Zheng, Y.Deng, X.Zhao, Y.Zhang, H. and Martin-DeLeon, P.A. 2001. Spam1 (PH-20) mutations and sperm dysfunction in mice with the Rb(6.16) or Rb(6.15) translocation. *Mamm Genome.* **12**(11), pp.822-9.
- Zhuo, L. and Kimata, K. 2001. Cumulus oophorus extracellular matrix: its construction and regulation. *Cell Struct Funct.* **26**(4), pp.189-96.

- Zigo, M.Jonáková, V.Šulc, M. and Maňásková-Postlerová, P. 2013. Characterization of sperm surface protein patterns of ejaculated and capacitated boar sperm, with the detection of ZP binding candidates. *International Journal of Biological Macromolecules*. **61**, pp.322-328.
- Zimmerman, S. and Sutovsky, P. 2009. The sperm proteasome during sperm capacitation and fertilization. *J Reprod Immunol*. **83**(1-2), pp.19-25.
- Zini, A.Bielecki, R.Phang, D. and Zenzes, M.T. 2001. Correlations between two markers of sperm DNA integrity, DNA denaturation and DNA fragmentation, in fertile and infertile men. *Fertil Steril*. **75**(4), pp.674-7.
- Zini, A.Boman, J.M.Belzile, E. and Ciampi, A. 2008. Sperm DNA damage is associated with an increased risk of pregnancy loss after IVF and ICSI: systematic review and meta-analysis. *Hum Reprod*. **23**(12), pp.2663-8.
- Zini, A.Meriano, J.Kader, K.Jarvi, K.Laskin, C.A. and Cadesky, K. 2005. Potential adverse effect of sperm DNA damage on embryo quality after ICSI. *Hum Reprod*. **20**(12), pp.3476-80.
- Zini, A.Nam, R.K.Mak, V.Phang, D. and Jarvi, K. 2000. Influence of initial semen quality on the integrity of human sperm DNA following semen processing. *Fertil Steril*. **74**(4), pp.824-7.
- Zitzmann, M. 2013. Effects of age on male fertility. *Best Practice and Research: Clinical Endocrinology and Metabolism*. **27**(4), pp.617-628.

## Appendices

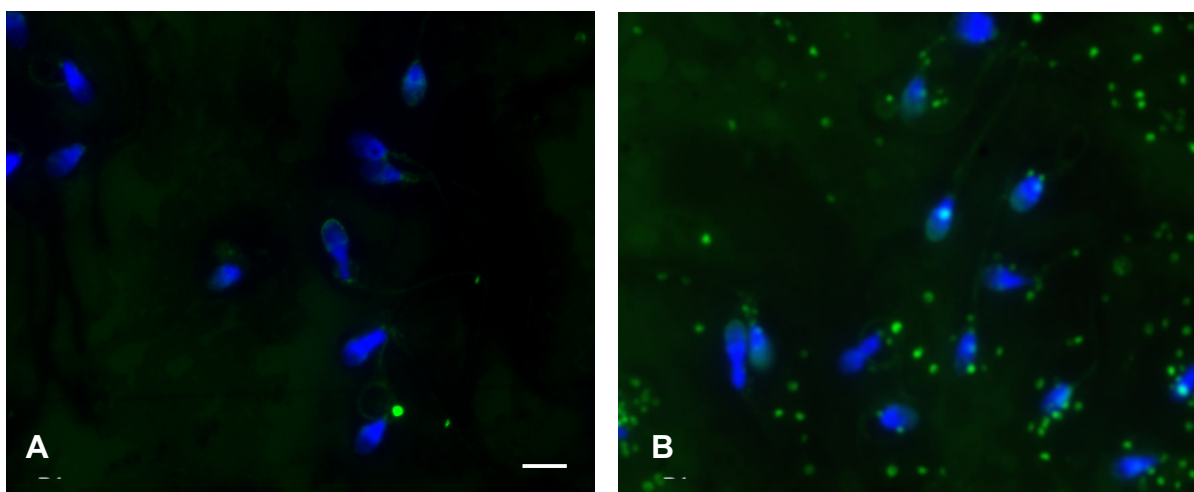


### Appendix Figure 3.1. Optimisation of anti CD44 antibody in human sperm.

Non-capacitated sperm as shown in A1 and B1 were labelled with a biotinylated anti-CD44 at 1/20 and 1/50 dilutions, respectively (90 min at RT). They were then incubated with fixed dilutions of streptavidine-FITC (1/1000), and DAPI (1/5000) for 60 (RT).

A2 and B2 are negative controls incubated with only streptavidine-FITC (1/1000) and DAPI (1/5000) to check the specificity of the antibody

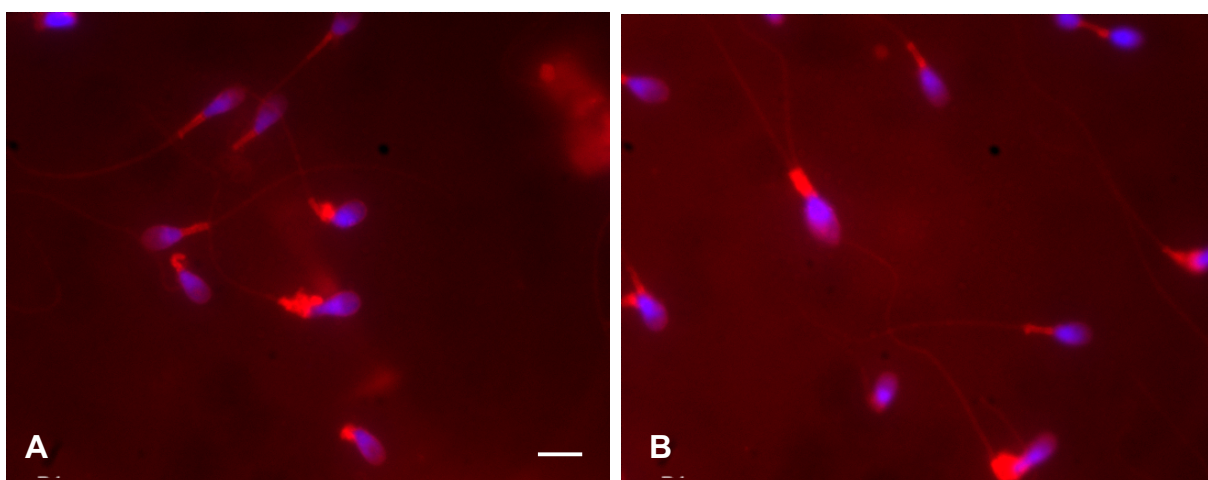
As shown, sperm in both negative controls (A2 and B2) emits green fluorescence that confirms the not all the signal obtained in A1(1/20) and B1 (1/50) is specific and it comes from streptavidin-FITC. Therefore, lower concentrations of the anti-CD44 antibody such as 1/100 and 1/200 had to be examined. The best results were obtained at 1/100 dilution (see Chapter 3). The scale bar is 5  $\mu$ m.



**Appendix Figure 3.2. Optimisation of the right dilution of streptavidin-FITC.**

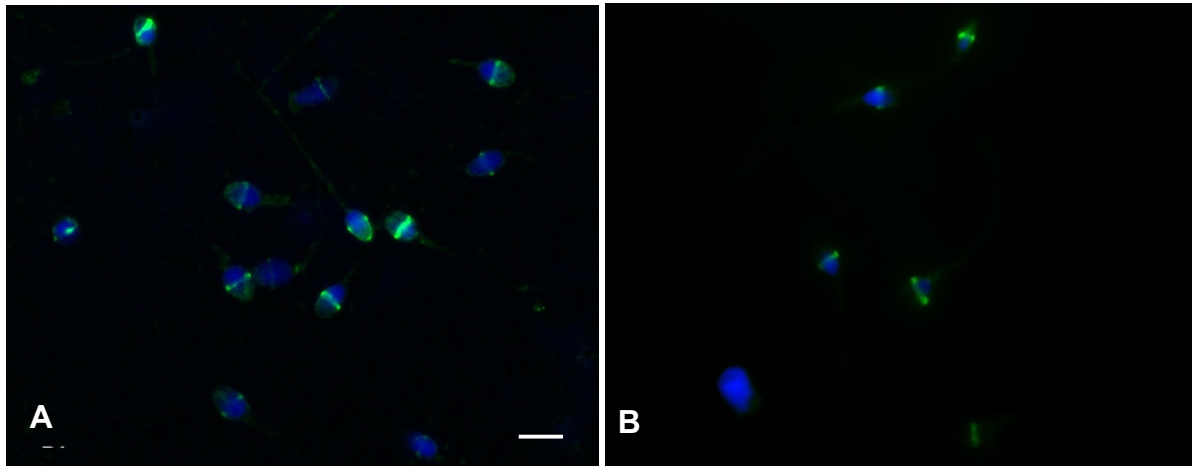
Non-capacitated sperm were labelled with a biotinylated anti-CD44 at 1/100 dilution for 90 min at RT. They were then incubated with streptavidin-FITC at different dilutions of 1/2000 (A) and 1/1500 for 60 min at RT. The nuclei were stained with DAPI (1/5000), fixed dilutions of streptavidin-FITC (1/1000), and DAPI (1/5000) for 60 (RT).

Higher concentrations of streptavidin-FITC such as 1/1000 and 1/500s had to be checked as the obtained green signals at 1/2000 and 1/1500 were not strong enough. The best results were obtained at dilution of 1/100 for anti-CD44 antibody and 1/1000 for streptavidin-FITC. The scale bar is 5  $\mu\text{m}$ .



**Appendix Figure 3.3. Optimisation of HA-TRITC in human sperm.**

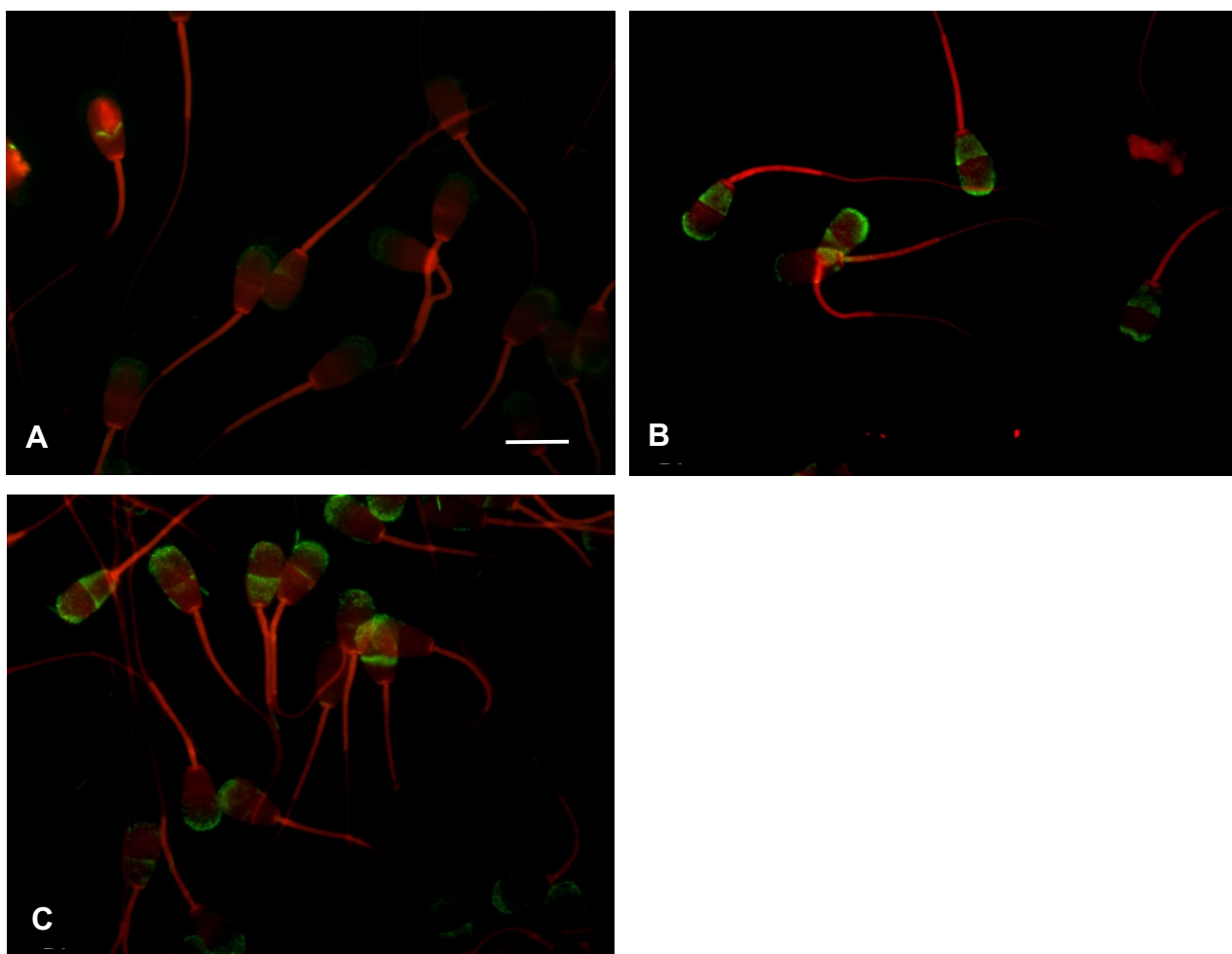
Non-capacitated sperm as shown in A and B were labelled with HA-TRITC at 20 and 50  $\mu\text{g}/\text{mL}$ , respectively for 75 min at RT. As shown the background is very high in both A and B. Therefore, lower concentrations such as 10 and 1  $\mu\text{g}/\text{mL}$  were examined. The best results were obtained at the concentration of 10  $\mu\text{g}/\text{mL}$  (see Chapter 3). The scale bar is 5  $\mu\text{m}$ .



**Appendix Figure 3.4. Optimisation of the anti CD44 antibody using fixation with PFA in human sperm.**

Non-capacitated sperm as shown in B were fixed with 4% PFA. Both non-fixed (A) and fixed (B) sperm were labelled with biotinylated anti CD44 (1/100), streptavidine-FITC (1/1000) and DAPI (1/5000). As seen in B, the green signal from the antibody was significantly reduced by using the fixative. Other fixatives such as methanol were also examined and gave similar results. Therefore, the main experiments were carried out without using any fixative. The scale bar is 5  $\mu$ m.





**Appendix Figure 3.5. Optimisation of the anti CD44 antibody in bovine sperm.**

Non-capacitated sperm as shown in A, B and C were labelled with anti CD44 antibody at dilutions of 1/1000, 1/100 and 1/50. They were then labelled with streptavidine-FITC (1/1000) and DAPI (1/5000). The green signal from 1/100 dilution of the antibody (A) is not strong enough. The signals from 1/100 and 1/50 were very similar and therefore 1/100 dilution was chosen to carry out further experiments. The scale bar is 20  $\mu\text{m}$ .

**Appendix Table 5.1.** Mass spectrometry data for hyaluronic acid-binding fraction (sample D70).

Accession	Description	Score	Coverage	Unique Peptides	Peptides	PSMs	AAs	MW [kDa]	calc. pI
P99999	Cytochrome c	170.64	66.67	9	9	55	105	11.7	9.57
P10323	Acrosin OS	97.90	31.35	10	10	36	421	45.8	9.07
P04279	Semenogelin-1	80.29	35.28	10	13	27	462	52.1	9.29
P13645	Keratin, type I cytoskeletal 10	68.98	38.87	13	15	21	584	58.8	5.21
P04264	Keratin, type II cytoskeletal 1	64.86	25.16	11	13	21	644	66.0	8.12
P06744	Glucose-6-phosphate isomerase	58.94	32.26	12	12	21	558	63.1	8.32
P07205	Phosphoglycerate kinase 2	55.16	46.76	11	14	21	417	44.8	8.54
Q02383	Semenogelin-2	52.39	23.88	7	10	15	582	65.4	9.07
P14618	Pyruvate kinase PKM	48.75	38.79	13	14	18	531	57.9	7.84
P35527	Keratin, type I cytoskeletal 9	48.51	28.09	10	10	15	623	62.0	5.24
P35908	Keratin, type II cytoskeletal 2 epidermal	47.85	31.92	9	12	16	639	65.4	8.00
Q8NEB7	Acrosin-binding protein	36.73	17.13	6	6	10	543	61.3	5.16
P00505	Aspartate aminotransferase, mitochondrial	31.94	26.28	10	10	14	430	47.5	9.01
P54652	Heat shock-related 70 kDa protein 2	27.60	18.62	5	8	10	639	70.0	5.74
Q9UII2	ATPase inhibitor, mitochondrial	25.65	9.43	1	1	7	106	12.2	9.35
Q5JQC9	A-kinase anchor protein 4	24.45	11.71	8	8	8	854	94.4	6.96
Q16836	Hydroxyacyl-coenzyme A dehydrogenase, mitochondrial	24.40	39.17	6	6	7	314	34.3	8.85
P07864	L-lactate dehydrogenase C chain	22.88	27.71	6	7	8	332	36.3	7.46
Q99798	Aconitate hydratase, mitochondrial	20.16	12.05	5	5	5	780	85.4	7.61
P04406	Glyceraldehyde-3-phosphate dehydrogenase	17.03	25.97	4	4	5	335	36.0	8.46
P04259	Keratin, type II cytoskeletal 6B	15.92	6.56	0	3	5	564	60.0	8.00
P25685	DnaJ homolog subfamily B member 1	14.78	15.59	5	6	6	340	38.0	8.63
P04075	Fructose-bisphosphate aldolase A	14.04	23.35	5	5	7	364	39.4	8.09
P13647	Keratin, type II cytoskeletal 5	13.55	6.27	1	3	4	590	62.3	7.74
P20155	Serine protease inhibitor Kazal-type 2	13.22	35.71	2	2	4	84	9.3	9.00
Q7Z4W2	Lysozyme-like protein 2	12.91	26.35	1	2	4	148	16.6	7.84
P40926	Malate dehydrogenase, mitochondrial	12.00	15.98	4	4	5	338	35.5	8.68
P02538	Keratin, type II cytoskeletal 6A	10.76	4.79	0	2	3	564	60.0	8.00
P48668	Keratin, type II cytoskeletal 6C	10.76	4.79	0	2	3	564	60.0	8.00
P06702	Protein S100-A9	10.76	49.12	4	4	4	114	13.2	6.13

<b>P00558</b>	<b>Phosphoglycerate kinase 1</b>	<b>10.76</b>	<b>9.83</b>	<b>0</b>	<b>3</b>	<b>4</b>	<b>417</b>	<b>44.6</b>	<b>8.10</b>
<b>Q9NPJ3</b>	Acyl-coenzyme A thioesterase 13	10.53	44.29	3	3	3	140	15.0	9.14
<b>O75969</b>	A-kinase anchor protein 3	10.13	3.75	2	2	3	853	94.7	6.18
<b>P00761</b>	Trypsin	9.47	14.29	3	3	4	231	24.4	7.18
<b>P02533</b>	Keratin, type I cytoskeletal 14	9.18	7.84	0	4	4	472	51.5	5.16
<b>Q86YZ3</b>	Hornerin	9.15	4.46	3	3	4	2850	282.2	10.04
<b>Q6UWQ5</b>	Lysozyme-like protein 1	8.50	25.00	1	2	3	148	16.6	8.05
<b>Q9BS86</b>	Zona pellucida-binding protein 1	8.24	15.67	3	3	3	351	40.1	9.28
<b>P68363</b>	Tubulin alpha-1B chain	8.15	7.54	0	2	3	451	50.1	5.06
<b>P68366</b>	Tubulin alpha-4A chain	8.15	7.59	0	2	3	448	49.9	5.06
<b>Q13748</b>	Tubulin alpha-3C/D chain	8.15	7.56	0	2	3	450	49.9	5.10
<b>Q6PEY2</b>	Tubulin alpha-3E chain	8.15	7.56	0	2	3	450	49.8	5.14
<b>Q71U36</b>	Tubulin alpha-1A chain	8.15	7.54	0	2	3	451	50.1	5.06
<b>Q9BQE3</b>	Tubulin alpha-1C chain	8.15	7.57	0	2	3	449	49.9	5.10
<b>P40939</b>	Trifunctional enzyme subunit alpha, mitochondrial phospholipase A2 inhibitor and Ly6/PLAUR domain-containing protein	8.14	4.33	2	2	2	763	82.9	9.04
<b>A6NC86</b>		8.10	31.86	3	3	3	204	21.9	7.99
<b>P11142</b>	Heat shock cognate 71 kDa protein	7.76	6.97	0	3	4	646	70.9	5.52
<b>Q6X784</b>	Zona pellucida-binding protein 2	7.68	10.36	2	2	2	338	38.6	7.78
<b>O95678</b>	Keratin, type II cytoskeletal 75	7.45	2.18	0	1	2	551	59.5	7.74
<b>Q5XKE5</b>	Keratin, type II cytoskeletal 79	7.45	3.93	0	2	3	535	57.8	7.20
<b>P00338</b>	L-lactate dehydrogenase A chain	7.34	8.13	1	2	2	332	36.7	8.27
<b>P08779</b>	Keratin, type I cytoskeletal 16	7.10	5.71	0	3	3	473	51.2	5.05
<b>Q9BWH2</b>	FUN14 domain-containing protein 2	7.04	21.69	2	2	2	189	20.7	9.73
<b>Q04695</b>	Keratin, type I cytoskeletal 17	6.78	6.48	0	3	3	432	48.1	5.02
<b>P42785</b>	Lysosomal Pro-X carboxypeptidase	6.69	4.03	2	2	3	496	55.8	7.21
<b>Q00796</b>	Sorbitol dehydrogenase	6.16	4.20	1	1	2	357	38.3	7.97
<b>Q96E40</b>	Uncharacterized protein C9orf9	5.97	22.07	3	3	4	222	25.1	9.13
<b>P55145</b>	Mesencephalic astrocyte-derived neurotrophic factor	5.88	17.58	2	2	2	182	20.7	8.69
<b>Q9UDY4</b>	DnaJ homolog subfamily B member 4	5.81	8.90	1	2	2	337	37.8	8.50
<b>P11021</b>	78 kDa glucose-regulated protein	5.77	4.74	1	2	2	654	72.3	5.16
<b>P62736</b>	Actin, aortic smooth muscle	5.66	9.02	0	2	2	377	42.0	5.39
<b>P63267</b>	Actin, gamma-enteric smooth muscle	5.66	9.04	0	2	2	376	41.8	5.48
<b>P68032</b>	Actin, alpha cardiac muscle 1	5.66	9.02	0	2	2	377	42.0	5.39
<b>P68133</b>	Actin, alpha skeletal muscle	5.66	9.02	0	2	2	377	42.0	5.39
<b>Q6P4A8</b>	Phospholipase B-like 1	5.60	4.16	1	1	1	553	63.2	9.06

<b>O14556</b>	<b>Glyceraldehyde-3-phosphate dehydrogenase, testis-specific</b>	<b>5.19</b>	<b>6.62</b>	<b>2</b>	<b>2</b>	<b>3</b>	<b>408</b>	<b>44.5</b>	<b>8.19</b>
<b>P43155</b>	Carnitine O-acetyltransferase	5.19	4.31	2	2	2	626	70.8	8.44
<b>Q8TDB8</b>	Solute carrier family 2, facilitated glucose transporter member 14	5.16	4.42	1	2	2	520	56.3	7.83
<b>Q9UKX2</b>	Myosin-2	5.01	2.01	0	3	3	1941	222.9	5.82
<b>Q9Y623</b>	Myosin-4	5.01	2.01	0	3	3	1939	222.9	5.85
<b>P13646</b>	Keratin, type I cytoskeletal 13	4.75	4.37	0	2	2	458	49.6	4.96
<b>Q9Y6A4</b>	Cilia- and flagella-associated protein 20	4.71	10.88	2	2	2	193	22.8	9.76
<b>P08727</b>	Keratin, type I cytoskeletal 19	4.69	4.50	0	2	2	400	44.1	5.14
<b>P19012</b>	Keratin, type I cytoskeletal 15	4.69	3.95	0	2	2	456	49.2	4.77
<b>Q9NY65</b>	Tubulin alpha-8 chain	4.25	4.01	0	1	1	449	50.1	5.06
<b>Q6UWM5</b>	GLIPR1-like protein 1	4.24	3.72	1	1	3	242	27.1	8.21
<b>P04350</b>	Tubulin beta-4A chain	4.23	7.88	0	2	2	444	49.6	4.88
<b>P07437</b>	Tubulin beta chain	4.23	7.88	0	2	2	444	49.6	4.89
<b>P68371</b>	Tubulin beta-4B chain	4.23	7.87	0	2	2	445	49.8	4.89
<b>Q13885</b>	Tubulin beta-2A chain	4.23	7.87	0	2	2	445	49.9	4.89
<b>Q9BVA1</b>	Tubulin beta-2B chain	4.23	7.87	0	2	2	445	49.9	4.89
<b>P09622</b>	Dihydrolipoyl dehydrogenase, mitochondrial	4.21	4.91	2	2	2	509	54.1	7.85
<b>Q14CN4</b>	Keratin, type II cytoskeletal 72	4.21	2.35	0	1	1	511	55.8	6.89
<b>Q3SY84</b>	Keratin, type II cytoskeletal 71	4.21	2.29	0	1	1	523	57.3	6.61
<b>Q7RTS7</b>	Keratin, type II cytoskeletal 74	4.21	2.27	0	1	1	529	57.8	7.71
<b>Q86Y46</b>	Keratin, type II cytoskeletal 73	4.21	2.22	0	1	1	540	58.9	7.23
<b>P35663</b>	Cylicin-1	4.19	4.76	2	2	2	651	74.2	9.67
<b>P03973</b>	Antileukoproteinase	4.00	18.94	2	2	2	132	14.3	8.75
<b>Q96HR9</b>	Receptor expression-enhancing protein 6	3.97	7.07	1	1	1	184	20.7	8.56
<b>P21741</b>	Midkine	3.95	13.99	2	2	2	143	15.6	9.79
<b>Q8NBX0</b>	Saccharopine dehydrogenase-like oxidoreductase	3.88	6.76	1	1	1	429	47.1	9.14
<b>P05109</b>	Protein S100-A8	3.87	8.60	1	1	2	93	10.8	7.03
<b>Q5BJF6</b>	Outer dense fiber protein 2	3.87	1.69	1	1	1	829	95.3	7.62
<b>Q7Z794</b>	Keratin, type II cytoskeletal 1b	3.86	2.08	0	1	1	578	61.9	5.99
<b>Q96A08</b>	Histone H2B type 1-A	3.81	11.81	1	1	1	127	14.2	10.32
<b>A4D1T9</b>	Probable inactive serine protease 37	3.72	9.36	1	1	1	235	26.4	8.87
<b>Q96KX0</b>	Lysozyme-like protein 4	3.61	15.07	2	2	2	146	16.4	8.28
<b>P34931</b>	Heat shock 70 kDa protein 1-like	3.45	4.52	0	2	2	641	70.3	6.02
<b>A5A3E0</b>	POTE ankyrin domain family member F	3.18	1.49	0	1	1	1075	121.4	6.20
<b>P60709</b>	Actin, cytoplasmic 1	3.18	4.27	0	1	1	375	41.7	5.48

<b>P63261</b>	<b>Actin, cytoplasmic 2</b>	<b>3.18</b>	<b>4.27</b>	<b>0</b>	<b>1</b>	<b>1</b>	<b>375</b>	<b>41.8</b>	<b>5.48</b>
<b>Q562R1</b>	Beta-actin-like protein 2	3.18	4.26	0	1	1	376	42.0	5.59
<b>Q6S8J3</b>	POTE ankyrin domain family member E	3.18	1.49	0	1	1	1075	121.3	6.20
<b>Q9BYX7</b>	Putative beta-actin-like protein 3	3.18	4.27	0	1	1	375	42.0	6.33
<b>P12882</b>	Myosin-1	3.15	1.50	0	2	2	1939	223.0	5.74
<b>P13535</b>	Myosin-8	3.15	0.93	0	1	1	1937	222.6	5.74
<b>P02788</b>	Lactotransferrin	3.12	2.68	1	1	1	710	78.1	8.12
<b>Q99832</b>	T-complex protein 1 subunit eta	3.04	4.05	1	1	1	543	59.3	7.65
<b>Q16568</b>	Cocaine- and amphetamine-regulated transcript protein	3.02	18.97	2	2	2	116	12.8	8.25
<b>P26640</b>	Valine--tRNA ligase	3.02	0.87	1	1	1	1264	140.4	7.59
<b>P24752</b>	Acetyl-CoA acetyltransferase, mitochondrial	2.92	3.98	1	1	1	427	45.2	8.85
<b>P25705</b>	ATP synthase subunit alpha, mitochondrial	2.90	1.99	1	1	1	553	59.7	9.13
<b>Q9HBV2</b>	Sperm acrosome membrane-associated protein 1	2.87	7.48	1	1	1	294	32.1	4.61
<b>P13667</b>	Protein disulfide-isomerase A4	2.85	1.86	1	1	1	645	72.9	5.07
<b>Q9BUN1</b>	Protein MENT	2.84	4.40	1	1	1	341	36.7	8.59
<b>Q15084</b>	Protein disulfide-isomerase A6	2.78	3.18	1	1	1	440	48.1	5.08
<b>P23786</b>	Carnitine O-palmitoyltransferase 2, mitochondrial	2.75	1.52	1	1	1	658	73.7	8.18
<b>P07195</b>	L-lactate dehydrogenase B chain	2.75	3.59	0	1	1	334	36.6	6.05
<b>Q6ZMR3</b>	L-lactate dehydrogenase A-like 6A	2.75	3.61	0	1	1	332	36.5	6.99
<b>P05976</b>	Myosin light chain 1/3, skeletal muscle isoform	2.71	5.67	1	1	1	194	21.1	5.03
<b>Q8TC27</b>	Disintegrin and metalloproteinase domain-containing protein 32	2.57	2.03	1	1	1	787	87.9	5.55
<b>Q5T9S5</b>	Coiled-coil domain-containing protein 18	2.46	0.69	1	1	1	1454	168.9	5.66
<b>Q7Z3Y7</b>	Keratin, type I cytoskeletal 28	2.40	1.94	0	1	1	464	50.5	5.47
<b>Q7Z3Y8</b>	Keratin, type I cytoskeletal 27	2.40	1.96	0	1	1	459	49.8	5.05
<b>Q7Z3Y9</b>	Keratin, type I cytoskeletal 26	2.40	1.92	0	1	1	468	51.9	4.92
<b>Q7Z3Z0</b>	Keratin, type I cytoskeletal 25	2.40	2.00	0	1	1	450	49.3	5.08
<b>Q8N4P6</b>	Leucine-rich repeat-containing protein 71	2.40	2.33	1	1	1	559	61.8	9.22
<b>Q2M2I5</b>	Keratin, type I cytoskeletal 24	2.38	2.10	0	1	1	525	55.1	4.96
<b>P35900</b>	Keratin, type I cytoskeletal 20	2.37	2.12	0	1	1	424	48.5	5.69
<b>Q8N1A0</b>	Keratin-like protein KRT222	2.37	3.05	0	1	1	295	34.1	5.87
<b>Q6NUT2</b>	Probable C-mannosyltransferase DPY19L2	2.36	2.64	1	1	1	758	87.3	9.10
<b>Q96M98</b>	Parkin coregulated gene protein	2.36	4.73	1	1	1	296	33.3	8.21
<b>Q8N5Q1</b>	Putative protein FAM71E2	2.33	0.98	1	1	1	922	99.9	9.39
<b>Q9BWS9</b>	Chitinase domain-containing protein 1	2.31	6.11	1	1	1	393	44.9	8.63
<b>Q1ZYL8</b>	Izumo sperm-egg fusion protein 4	2.30	6.03	1	1	1	232	26.5	7.46

<b>P07900</b>	<b>Heat shock protein HSP 90-alpha</b>	<b>2.27</b>	<b>1.91</b>	<b>0</b>	<b>1</b>	<b>1</b>	<b>732</b>	<b>84.6</b>	<b>5.02</b>
<b>P08238</b>	Heat shock protein HSP 90-beta	2.27	1.93	0	1	1	724	83.2	5.03
<b>Q12931</b>	Heat shock protein 75 kDa, mitochondrial	2.27	1.99	0	1	1	704	80.1	8.21
<b>P05141</b>	ADP/ATP translocase 2	2.24	3.36	0	1	1	298	32.8	9.69
<b>P12235</b>	ADP/ATP translocase 1	2.24	3.36	0	1	1	298	33.0	9.76
<b>P12236</b>	ADP/ATP translocase 3	2.24	3.36	0	1	1	298	32.8	9.74
<b>Q96QE4</b>	Leucine-rich repeat-containing protein 37B	2.23	1.90	1	1	1	947	105.5	4.91
<b>P11169</b>	Solute carrier family 2, facilitated glucose transporter member 3	2.18	2.22	0	1	1	496	53.9	7.20
<b>Q9Y561</b>	Low-density lipoprotein receptor-related protein 12	2.17	0.93	1	1	1	859	94.9	5.24
<b>Q5T749</b>	Keratinocyte proline-rich protein	2.15	1.55	1	1	1	579	64.1	8.27
<b>Q92820</b>	Gamma-glutamyl hydrolase	2.14	3.77	1	1	1	318	35.9	7.11
<b>Q9H0R5</b>	Guanylate-binding protein 3	2.14	1.51	1	1	1	595	68.1	6.51
<b>Q9BYZ2</b>	L-lactate dehydrogenase A-like 6B	2.14	3.15	1	1	1	381	41.9	8.65
<b>P35237</b>	Serpin B6	2.12	3.99	1	1	1	376	42.6	5.27
<b>Q96PU9</b>	Outer dense fiber protein 3	2.07	5.12	1	1	1	254	27.7	9.89
<b>P81605</b>	Dermcidin	2.07	10.00	1	1	1	110	11.3	6.54
<b>P19367</b>	Hexokinase-1	2.05	1.20	0	1	1	917	102.4	6.80
<b>P52789</b>	Hexokinase-2	2.05	1.20	0	1	1	917	102.3	6.05
<b>Q8WZ59</b>	Transmembrane protein 190	2.01	9.60	1	1	1	177	19.4	5.24
<b>Q14093</b>	Cylicin-2	1.95	4.31	1	1	1	348	39.1	9.74
<b>Q13618</b>	Cullin-3	1.91	1.95	1	1	1	768	88.9	8.48
<b>P0CG47</b>	Polyubiquitin-B	1.82	11.79	0	1	1	229	25.7	7.43
<b>P62979</b>	Ubiquitin-40S ribosomal protein S27a	1.82	5.77	0	1	1	156	18.0	9.64
<b>P62987</b>	Ubiquitin-60S ribosomal protein L40]	1.82	7.03	0	1	1	128	14.7	9.83
<b>P0CG48</b>	Polyubiquitin-C	1.82	11.82	0	1	1	685	77.0	7.66
<b>Q13509</b>	Tubulin beta-3 chain	1.77	2.22	0	1	1	450	50.4	4.93
<b>Q5D862</b>	Filaggrin-2	1.69	0.50	1	1	1	2391	247.9	8.31
<b>O00221</b>	NF-kappa-B inhibitor epsilon	0.00	8.20	1	1	1	500	52.8	6.68
<b>P06576</b>	ATP synthase subunit beta, mitochondrial	0.00	3.02	1	1	1	529	56.5	5.40
<b>P08107</b>	Heat shock 70 kDa protein 1A/1B	0.00	2.03	0	1	1	641	70.0	5.66
<b>P11055</b>	Myosin-3	0.00	0.57	0	1	1	1940	223.8	5.81
<b>P12035</b>	Keratin, type II cytoskeletal 3	0.00	1.43	0	1	1	628	64.4	6.48
<b>P12830</b>	Cadherin-1	0.00	1.02	1	1	1	882	97.4	4.73
<b>P17066</b>	Heat shock 70 kDa protein 6	0.00	2.02	0	1	1	643	71.0	6.14
<b>P30613</b>	Pyruvate kinase PKLR	0.00	1.92	0	1	1	574	61.8	7.74

<b>P46019</b>	<b>Phosphorylase b kinase regulatory subunit alpha, liver isoform</b>	<b>0.00</b>	<b>3.32</b>	<b>1</b>	<b>1</b>	<b>1</b>	<b>1235</b>	<b>138.3</b>	<b>6.44</b>
<b>P48454</b>	Serine/threonine-protein phosphatase 2B catalytic subunit gamma isoform	0.00	2.34	1	1	1	512	58.1	6.98
<b>P48741</b>	Putative heat shock 70 kDa protein 7	0.00	3.54	0	1	1	367	40.2	7.87
<b>P61626</b>	Lysozyme C	0.00	5.41	1	1	1	148	16.5	9.16
<b>Q01546</b>	Keratin, type II cytoskeletal 2 oral	0.00	1.41	0	1	1	638	65.8	8.12
<b>Q5HYC2</b>	Uncharacterized protein KIAA2026	0.00	0.33	1	1	1	2103	227.9	9.04
<b>Q7Z442</b>	Polycystic kidney disease protein 1-like 2	0.00	1.10	1	1	1	2459	272.4	5.82
<b>Q96QH8</b>	Sperm acrosome-associated protein 5	0.00	4.40	1	1	1	159	17.9	6.42
<b>Q9H9Y6</b>	DNA-directed RNA polymerase I subunit RPA2	0.00	3.44	1	1	1	1135	128.1	7.83
<b>Q9UFN0</b>	Protein NipSnap homolog 3A	0.00	4.05	1	1	1	247	28.4	9.16

**Appendix Table 5.2.** Mass spectrometry data for hyaluronic acid non-binding fraction (sample D70).

Accession	Description	Score	Coverage	Unique Peptides	Peptides	PSMs	Area	AAs	MW [kDa]	calc. pI
<b>P06733</b>	Alpha-enolase]	84.18	33.18	3	9	32	1.649E4	434	47.1	7.39
<b>Q5JQC9</b>	A-kinase anchor protein 4	78.68	21.55	13	13	36	1.217E4	854	94.4	6.96
<b>A6NM11</b>	Leucine-rich repeat-containing protein 37A2	67.35	13.65	1	15	24	3.200E4	1700	188.3	5.50
<b>A6NMS7</b>	Leucine-rich repeat-containing protein 37A	65.44	13.06	0	14	23	3.200E4	1700	188.1	5.49
<b>Q8NEB7</b>	Acrosin-binding protein OS=Homo sapiens GN=ACRBP PE=2 SV=1 - [ACRBP_HUMAN]	62.05	27.07	9	9	23	7.398E3	543	61.3	5.16
<b>P04264</b>	Keratin, type II cytoskeletal 1	59.82	22.98	9	13	23	7.405E3	644	66.0	8.12
<b>O60309</b>	Leucine-rich repeat-containing protein 37A3	55.70	12.61	0	13	20	3.200E4	1634	180.5	5.31
<b>Q9XSJ4</b>	Alpha-enolase	54.39	23.04	0	6	17	2.647E3	434	47.3	6.80
<b>P54652</b>	Heat shock-related 70 kDa protein 2	54.29	25.67	1	14	22	7.250E3	639	70.0	5.74
<b>Q9BUN1</b>	Protein MENT	49.44	28.15	6	6	17	6.054E3	341	36.7	8.59
<b>P34933</b>	Heat shock-related 70 kDa protein 2	49.22	20.60	0	12	20	7.250E3	636	69.7	5.59
<b>P04279</b>	Semenogelin-1	46.34	27.27	11	11	17	3.458E3	462	52.1	9.29
<b>P11021</b>	78 kDa glucose-regulated protein	44.69	29.36	1	13	19	1.266E4	654	72.3	5.16
<b>Q0VCX2</b>	78 kDa glucose-regulated protein	42.15	27.02	0	12	17	1.266E4	655	72.4	5.16
<b>P02769</b>	Serum albumin	41.80	21.09	9	10	17	2.528E4	607	69.2	6.18
<b>Q71U36</b>	Tubulin alpha-1A chain	41.30	29.71	0	8	15	8.952E3	451	50.1	5.06
<b>Q2HJ86</b>	Tubulin alpha-1D chain	41.30	29.65	0	8	15	8.952E3	452	50.3	5.03
<b>Q3MHM5</b>	Tubulin beta-4B chain	40.87	18.43	0	7	14	4.721E3	445	49.8	4.89
<b>Q6UW49</b>	Sperm equatorial segment protein 1	40.30	32.29	7	7	14	3.091E3	350	38.9	5.73



<b>P62157</b>	Calmodulin	39.94	44.30	6	7	16	1.399E4	149	16.8	4.22
<b>Q96QE4</b>	Leucine-rich repeat-containing protein 37B	39.83	16.16	10	10	15	6.484E3	947	105.5	4.91
<b>P81947</b>	Tubulin alpha-1B chain	39.38	29.71	0	8	14	8.952E3	451	50.1	5.06
<b>Q13748</b>	Tubulin alpha-3C/D chain	38.93	29.78	0	8	14	8.952E3	450	49.9	5.10
<b>Q6PEY2</b>	Tubulin alpha-3E chain	38.93	29.78	0	8	14	8.952E3	450	49.8	5.14
<b>Q32KN8</b>	Tubulin alpha-3 chain	38.93	29.78	0	8	14	8.952E3	450	49.9	5.10
<b>P13639</b>	Elongation factor 2	38.55	7.81	1	3	12	1.195E4	858	95.3	6.83
<b>Q02383</b>	Semenogelin-2	37.11	23.54	9	9	13	4.842E4	582	65.4	9.07
<b>P60712</b>	Actin, cytoplasmic 1	37.09	35.73	0	6	9	5.979E4	375	41.7	5.48
<b>P63258</b>	Actin, cytoplasmic 2	37.09	35.73	0	6	9	5.979E4	375	41.8	5.48
<b>P68103</b>	Elongation factor 1-alpha 1	36.86	17.10	0	4	11	2.760E4	462	50.1	9.01

<b>Q5VTE0</b>	<b>Putative elongation factor 1-alpha-like 3</b>	<b>36.86</b>	<b>17.10</b>	<b>0</b>	<b>4</b>	<b>11</b>	<b>2.760E4</b>	<b>462</b>	<b>50.2</b>	<b>9.07</b>
<b>Q3SYU2</b>	Elongation factor 2	35.90	4.66	0	2	11	1.195E4	858	95.3	6.83
<b>Q13885</b>	Tubulin beta-2A chain	35.11	15.73	0	6	12	4.721E3	445	49.9	4.89
<b>Q6B856</b>	Tubulin beta-2B chain	35.11	15.73	0	6	12	4.721E3	445	49.9	4.89
<b>P13645</b>	Keratin, type I cytoskeletal 10	35.06	18.15	4	8	14	7.516E3	584	58.8	5.21
<b>P14625</b>	Endoplasmic reticulum chaperone protein	34.22	15.69	2	10	15	8.264E3	803	92.4	4.84
<b>O60664</b>	Perilipin-3	33.07	27.88	8	8	13	8.827E3	434	47.0	5.44
<b>Q32PH8</b>	Elongation factor 1-alpha 2	31.20	11.88	0	3	9	8.930E3	463	50.4	9.03
<b>Q9BQE3</b>	Tubulin alpha-1C chain	30.67	20.71	0	6	11	6.776E3	449	49.9	5.10
<b>Q9Y4L1</b>	Hypoxia up-regulated protein 1	30.56	16.12	11	11	13	5.171E3	999	111.3	5.22
<b>Q3ZCJ7</b>	Tubulin alpha-1C chain	30.48	22.94	0	6	11	6.776E3	449	49.8	5.10
<b>Q2T9S0</b>	Tubulin beta-3 chain	29.26	16.22	0	6	10		450	50.4	4.93
<b>Q3ZBU7</b>	Tubulin beta-4A chain	28.86	18.47	0	7	10	4.721E3	444	49.6	4.88
<b>P07900</b>	Heat shock protein HSP 90-alpha	28.26	15.03	0	9	13	6.115E3	732	84.6	5.02
<b>Q76LV2</b>	Heat shock protein HSP 90-alpha	28.26	15.01	0	9	13	6.115E3	733	84.7	5.01
<b>P07205</b>	Phosphoglycerate kinase 2	27.77	32.37	7	9	14	8.807E3	417	44.8	8.54
<b>Q13561</b>	Dynactin subunit 2	27.10	23.94	3	6	9		401	44.2	5.21
<b>Q2HJ81</b>	Tubulin beta-6 chain	26.65	11.43	0	4	9		446	49.9	4.86
<b>Q9HAT0</b>	Ropporin-1A	25.57	17.92	1	3	9	8.025E3	212	23.9	5.66
<b>P81948</b>	Tubulin alpha-4A chain	25.53	19.87	0	5	9	1.113E4	448	49.9	5.06
<b>P35527</b>	Keratin, type I cytoskeletal 9	24.60	13.96	6	6	10	8.076E3	623	62.0	5.24
<b>P24752</b>	Acetyl-CoA acetyltransferase, mitochondrial	24.47	20.61	2	6	9		427	45.2	8.85
<b>Q95M18</b>	Endoplasmic reticulum chaperone protein	24.10	11.44	0	8	12	8.582E3	804	92.4	4.84
<b>P25705</b>	ATP synthase subunit alpha, mitochondrial	24.04	18.26	1	7	10		553	59.7	9.13
<b>P10909</b>	Clusterin	23.77	10.91	5	5	9	1.153E4	449	52.5	6.27
<b>P15259</b>	Phosphoglycerate mutase 2	22.78	31.62	2	6	9	1.207E4	253	28.7	8.88

<b>Q9BZX4</b>	Ropporin-1B	22.60	12.26	0	2	8	8.025E3	212	23.9	5.15
<b>P19483</b>	ATP synthase subunit alpha, mitochondrial	22.33	15.91	0	6	9		553	59.7	9.19
<b>Q2KJD0</b>	Tubulin beta-5 chain	21.87	14.64	0	6	8	4.721E3	444	49.6	4.89
<b>Q9BUF5</b>	Tubulin beta-6 chain	20.95	11.43	0	4	7		446	49.8	4.88
<b>Q9H4B8</b>	Dipeptidase 3	20.37	9.43	3	3	8		488	53.7	7.96
<b>P30101</b>	Protein disulfide-isomerase A3	20.15	20.00	3	8	9	3.761E3	505	56.7	6.35
<b>Q1ZYL8</b>	Izumo sperm-egg fusion protein 4	19.29	15.09	3	3	7	1.008E4	232	26.5	7.46
<b>P14314</b>	Glucosidase 2 subunit beta	19.26	16.48	6	6	10	2.408E3	528	59.4	4.41
<b>P15289</b>	Arylsulfatase A	19.03	9.27	3	3	7	6.340E3	507	53.6	6.07
<b>Q7L266</b>	Isoaspartyl peptidase/L-asparaginase	18.99	13.96	3	3	6		308	32.0	6.24

<b>P13929</b>	<b>Beta-enolase</b>	<b>18.49</b>	<b>9.22</b>	<b>0</b>	<b>2</b>	<b>5</b>	<b>3.186E3</b>	<b>434</b>	<b>47.0</b>	<b>7.71</b>
<b>P09104</b>	Gamma-enolase	18.49	9.22	0	2	5	3.186E3	434	47.2	5.03
<b>Q3ZC09</b>	Beta-enolase	18.49	9.22	0	2	5	3.186E3	434	47.1	7.72
<b>P40926</b>	Malate dehydrogenase, mitochondrial	17.92	23.67	1	5	7	1.624E4	338	35.5	8.68
<b>P31146</b>	Coronin-1A	17.54	4.56	0	1	5	9.460E3	461	51.0	6.68
<b>Q92176</b>	Coronin-1A	17.54	4.56	0	1	5	9.460E3	461	50.9	6.68
<b>O75969</b>	A-kinase anchor protein 3	17.51	8.79	6	6	8	6.588E3	853	94.7	6.18
<b>Q3ZCF0</b>	Dynactin subunit 2	17.38	12.66	0	3	5		403	44.3	5.16
<b>P61019</b>	Ras-related protein Rab-2A	17.00	25.94	2	4	6		212	23.5	6.54
<b>P10809</b>	60 kDa heat shock protein, mitochondrial	16.87	12.74	2	5	9	6.912E3	573	61.0	5.87
<b>Q29RZ0</b>	Acetyl-CoA acetyltransferase, mitochondrial	16.74	13.74	0	4	6		422	44.9	8.85
<b>Q6S8J3</b>	POTE ankyrin domain family member E	16.49	2.14	0	1	4	9.292E3	1075	121.3	6.20
<b>P04908</b>	Histone H2A type 1-B/E	16.41	43.85	0	3	6	5.849E4	130	14.1	11.05
<b>P0C0S9</b>	Histone H2A type 1	16.41	43.85	0	3	6	5.849E4	130	14.1	10.90
<b>P20671</b>	Histone H2A type 1-D	16.41	43.85	0	3	6	5.849E4	130	14.1	10.90
<b>Q7L7L0</b>	Histone H2A type 3	16.41	43.85	0	3	6	5.849E4	130	14.1	11.05
<b>Q93077</b>	Histone H2A type 1-C	16.41	43.85	0	3	6	5.849E4	130	14.1	11.05
<b>Q96KK5</b>	Histone H2A type 1-H	16.41	44.53	0	3	6	5.849E4	128	13.9	10.89
<b>Q99878</b>	Histone H2A type 1-J	16.41	44.53	0	3	6	5.849E4	128	13.9	10.89
<b>Q3ZBX9</b>	Histone H2A.J	16.41	44.19	0	3	6	5.849E4	129	14.0	10.90
<b>P00338</b>	L-lactate dehydrogenase A chain	16.23	9.04	2	2	6	1.415E4	332	36.7	8.27
<b>P27797</b>	Calreticulin	16.22	16.79	2	4	6	1.188E4	417	48.1	4.44
<b>P12821</b>	Angiotensin-converting enzyme	15.74	5.59	6	6	7	9.300E3	1306	149.6	6.39
<b>P31937</b>	3-hydroxyisobutyrate dehydrogenase, mitochondrial	14.93	14.88	3	3	5		336	35.3	8.13
<b>P18669</b>	Phosphoglycerate mutase 1	14.87	19.69	0	4	6	1.207E4	254	28.8	7.18
<b>Q3SZ62</b>	Phosphoglycerate mutase 1	14.87	19.69	0	4	6	1.207E4	254	28.8	7.18
<b>Q99497</b>	Protein DJ-1	14.53	29.63	0	3	5		189	19.9	6.79
<b>Q5E946</b>	Protein DJ-1	14.53	29.63	0	3	5		189	20.0	7.33
<b>P06744</b>	Glucose-6-phosphate isomerase	13.80	12.72	3	5	6	2.337E3	558	63.1	8.32
<b>Q16698</b>	2,4-dienoyl-CoA reductase, mitochondrial	13.64	15.82	4	4	5	1.478E4	335	36.0	9.28

<b>P30086</b>	Phosphatidylethanolamine-binding protein 1	13.54	28.34	3	3	4	1.009E4	187	21.0	7.53
<b>Q99798</b>	Aconitate hydratase, mitochondrial	13.51	8.97	1	5	7	7.873E3	780	85.4	7.61
<b>P38657</b>	Protein disulfide-isomerase A3	13.28	13.07	0	5	6	3.434E3	505	56.9	6.65
<b>Q8TC56</b>	Protein FAM71B	13.27	8.93	3	3	5		605	64.7	9.48

<b>P35908</b>	<b>Keratin, type II cytoskeletal 2 epidermal</b>	<b>13.06</b>	<b>7.36</b>	<b>3</b>	<b>4</b>	<b>7</b>	<b>5.013E3</b>	<b>639</b>	<b>65.4</b>	<b>8.00</b>
<b>P54709</b>	Sodium/potassium-transporting ATPase subunit beta-3	13.02	17.92	4	4	6	6.669E3	279	31.5	8.35
<b>P80303</b>	Nucleobindin-2	12.98	12.38	4	4	6	1.505E4	420	50.2	5.12
<b>A1A4R1</b>	Histone H2A type 2-C	12.96	21.71	0	2	5		129	14.0	10.90
<b>Q6FI13</b>	Histone H2A type 2-A =3	12.96	21.54	0	2	5		130	14.1	10.90
<b>Q32LG3</b>	Malate dehydrogenase, mitochondrial	12.86	17.16	0	4	5	5.267E3	338	35.6	8.54
<b>P16104</b>	Histone H2AX	12.78	42.66	0	3	5	3.716E4	143	15.1	10.74
<b>Q8IUE6</b>	Histone H2A type 2-B	12.78	46.92	0	3	5	3.716E4	130	14.0	10.89
<b>P05387</b>	60S acidic ribosomal protein P2	12.56	45.22	0	2	4		115	11.7	4.54
<b>P42899</b>	60S acidic ribosomal protein	12.56	45.22	0	2	4		115	11.7	4.61
<b>Q8WW22</b>	DnaJ homolog subfamily A member 4	12.49	11.59	3	3	5		397	44.8	7.59
<b>O95757</b>	Heat shock 70 kDa protein 4L	12.40	3.22	2	2	6	8.961E3	839	94.5	5.88
<b>Q9NY65</b>	Tubulin alpha-8 chain	12.01	10.91	0	3	4	1.113E4	449	50.1	5.06
<b>Q2HJB8</b>	Tubulin alpha-8 chain	12.01	10.91	0	3	4	1.113E4	449	50.0	5.20
<b>P00558</b>	Phosphoglycerate kinase 1	11.94	7.91	0	2	5		417	44.6	8.10
<b>Q3T0P6</b>	Phosphoglycerate kinase 1	11.94	7.91	0	2	5		417	44.5	8.27
<b>P11142</b>	Heat shock cognate 71 kDa protein	11.50	9.60	0	5	5		646	70.9	5.52
<b>P19120</b>	Heat shock cognate 71 kDa protein	11.50	9.54	0	5	5		650	71.2	5.52
<b>P34931</b>	Heat shock 70 kDa protein 1-like	11.36	11.39	0	6	6		641	70.3	6.02
<b>P0CB32</b>	Heat shock 70 kDa protein 1-like	11.36	11.39	0	6	6		641	70.3	6.20
<b>P04075</b>	Fructose-bisphosphate aldolase A	11.34	14.84	3	3	4	3.892E3	364	39.4	8.09
<b>P61603</b>	10 kDa heat shock protein, mitochondrial	11.06	35.29	3	3	5		102	10.9	8.92

<b>P60174</b>	Triosephosphate isomerase	10.97	13.64	2	3	4	5.403E3	286	30.8	5.92
<b>P63103</b>	14-3-3 protein zeta/delta	10.83	17.14	2	3	4	8.093E3	245	27.7	4.79
<b>P02768</b>	Serum albumin	10.76	4.11	1	2	4		609	69.3	6.28
<b>O14556</b>	Glyceraldehyde-3-phosphate dehydrogenase, testis-specific	10.74	9.80	1	3	4	1.319E3	408	44.5	8.19
<b>P15586</b>	N-acetylglucosamine-6-sulfatase	10.52	4.53	0	2	5	1.048E4	552	62.0	8.31
<b>Q1LZH9</b>	N-acetylglucosamine-6-sulfatase	10.52	4.46	0	2	5	1.048E4	560	62.7	8.43
<b>P07195</b>	L-lactate dehydrogenase B chain	10.39	5.99	0	1	3	2.566E3	334	36.6	6.05
<b>Q5E9B1</b>	L-lactate dehydrogenase B chain	10.39	5.99	0	1	3	2.566E3	334	36.7	6.44
<b>P07864</b>	L-lactate dehydrogenase C chain	10.28	18.37	5	5	5	5.922E3	332	36.3	7.46
<b>P78371</b>	T-complex protein 1 subunit beta	10.22	9.72	0	3	5	1.105E4	535	57.5	6.46
<b>Q3ZBH0</b>	T-complex protein 1 subunit beta	10.22	9.72	0	3	5	1.105E4	535	57.4	6.64
<b>O75071</b>	EF-hand calcium-binding domain-containing protein 14	10.14	10.30	4	4	5		495	55.0	6.32

<b>Q8IXA5</b>	<b>Sperm acrosome membrane-associated protein 3</b>	<b>9.91</b>	<b>12.56</b>	<b>2</b>	<b>2</b>	<b>3</b>		<b>215</b>	<b>23.4</b>	<b>7.94</b>
<b>Q8N0Y7</b>	Probable phosphoglycerate mutase 4	9.79	9.45	0	2	4		254	28.8	6.65
<b>P57105</b>	Synaptojanin-2-binding protein	9.70	24.83	0	3	4	8.297E3	145	15.9	6.30
<b>Q3T0C9</b>	Synaptojanin-2-binding protein	9.70	24.83	0	3	4	8.297E3	145	15.8	5.94
<b>P38646</b>	Stress-70 protein, mitochondrial	9.69	2.50	0	1	3	6.993E3	679	73.6	6.16
<b>Q3ZCH0</b>	Stress-70 protein, mitochondrial	9.69	2.50	0	1	3	6.993E3	679	73.7	6.30
<b>P31081</b>	60 kDa heat shock protein, mitochondrial	9.66	8.20	0	3	6		573	61.1	5.74
<b>O75390</b>	Citrate synthase, mitochondrial	9.41	5.79	0	2	3		466	51.7	8.32
<b>Q29RK1</b>	Citrate synthase, mitochondrial	9.41	5.79	0	2	3		466	51.7	8.12
<b>P20674</b>	Cytochrome c oxidase subunit 5A, mitochondrial	9.40	16.00	2	2	4		150	16.8	6.79
<b>Q9HBV2</b>	Sperm acrosome membrane-associated protein 1	9.38	13.61	3	3	5	1.947E3	294	32.1	4.61
<b>Q96QV6</b>	Histone H2A type 1-A	9.33	24.43	0	2	4	1.582E4	131	14.2	10.86
<b>Q9H4A4</b>	Aminopeptidase B	9.31	2.92	1	1	3		650	72.5	5.74
<b>P00918</b>	Carbonic anhydrase 2	9.25	15.38	3	3	6	5.221E3	260	29.2	7.40
<b>P52193</b>	Calreticulin	9.24	11.51	0	2	3	1.314E4	417	48.0	4.46
<b>P30044</b>	Peroxisredoxin-5, mitochondrial	9.19	12.15	1	2	4		214	22.1	8.70
<b>P22695</b>	Cytochrome b-c1 complex subunit 2, mitochondrial	9.07	10.82	2	3	4	1.677E4	453	48.4	8.63
<b>P40939</b>	Trifunctional enzyme subunit alpha, mitochondrial	9.04	3.54	2	2	4		763	82.9	9.04
<b>P50502</b>	Hsc70-interacting protein	8.94	12.74	0	4	5	1.309E4	369	41.3	5.27



<b>P06576</b>	ATP synthase subunit beta, mitochondrial	8.92	19.66	1	7	8	8.961E3	529	56.5	5.40
<b>P00829</b>	ATP synthase subunit beta, mitochondrial	8.92	16.29	0	6	7		528	56.2	5.27
<b>Q8WUD1</b>	Ras-related protein Rab-2B	8.81	11.57	0	2	3		216	24.2	7.83
<b>P13861</b>	cAMP-dependent protein kinase type II-alpha regulatory subunit	8.75	7.43	2	2	3		404	45.5	5.07
<b>P08107</b>	Heat shock 70 kDa protein 1A/1B	8.70	8.89	0	5	5		641	70.0	5.66
<b>Q27965</b>	Heat shock 70 kDa protein 1B	8.70	8.89	0	5	5		641	70.2	5.92
<b>Q27975</b>	Heat shock 70 kDa protein 1A O	8.70	8.89	0	5	5		641	70.2	5.92
<b>P08238</b>	Heat shock protein HSP 90-beta	8.69	4.42	0	3	4		724	83.2	5.03
<b>Q76LV1</b>	Heat shock protein HSP 90-beta	8.69	4.42	0	3	4		724	83.2	5.03
<b>P28838</b>	Cytosol aminopeptidase	8.31	6.74	0	3	4	4.347E3	519	56.1	7.93
<b>P00727</b>	Cytosol aminopeptidase	8.31	6.74	0	3	4	4.347E3	519	56.3	6.48
<b>P14927</b>	Cytochrome b-c1 complex subunit 7	8.29	25.23	2	2	3	2.281E4	111	13.5	8.78

<b>P59282</b>	<b>Tubulin polymerization-promoting protein family member 2</b>	<b>8.22</b>	<b>15.88</b>	<b>1</b>	<b>2</b>	<b>3</b>	<b>4.996E3</b>	<b>170</b>	<b>18.5</b>	<b>9.00</b>
<b>Q7Z794</b>	Keratin, type II cytoskeletal 1b	8.20	4.15	1	2	4	5.013E3	578	61.9	5.99
<b>Q9NQ60</b>	Equatorin	8.16	13.27	3	3	4		294	32.8	5.00
<b>P29401</b>	Transketolase	8.13	3.37	0	1	3		623	67.8	7.66
<b>Q6B855</b>	Transketolase	8.13	3.37	0	1	3		623	67.9	7.65
<b>Q15084</b>	Protein disulfide-isomerase A6	8.01	10.00	3	3	4		440	48.1	5.08
<b>O14950</b>	Myosin regulatory light chain 12B	7.78	11.63	0	1	2		172	19.8	4.84
<b>P19105</b>	Myosin regulatory light chain 12A	7.78	11.70	0	1	2		171	19.8	4.81
<b>Q5E9E2</b>	Myosin regulatory light polypeptide 9	7.78	11.63	0	1	2		172	19.9	4.81
<b>A4IF97</b>	Myosin regulatory light chain 12B	7.78	11.70	0	1	2		171	19.7	4.84
<b>Q14568</b>	Putative heat shock protein HSP 90-alpha Transitional	7.77	6.12	0	2	3	1.278E3	343	39.3	4.65
<b>P55072</b>	endoplasmic reticulum ATPase	7.70	1.61	0	1	3		806	89.3	5.26
<b>Q3ZBT1</b>	Transitional endoplasmic reticulum ATPase	7.70	1.61	0	1	3		806	89.3	5.26
<b>Q9H3G5</b>	Probable serine carboxypeptidase CPVL	7.38	5.88	2	2	4	9.892E3	476	54.1	5.62
<b>Q92820</b>	Gamma-glutamyl hydrolase	7.32	10.69	2	3	4	5.988E3	318	35.9	7.11
<b>P12273</b>	Prolactin-inducible protein	7.31	19.18	2	2	3		146	16.6	8.05
<b>P24534</b>	Elongation factor 1-beta	7.28	6.67	0	1	2		225	24.7	4.67
<b>Q5E983</b>	Elongation factor 1-beta	7.28	6.67	0	1	2		225	24.8	4.67
<b>P48643</b>	T-complex protein 1 subunit epsilon	7.23	3.33	1	1	3	1.258E4	541	59.6	5.66
<b>P31948</b>	Stress-induced-phosphoprotein 1	7.20	4.97	0	2	3	3.457E3	543	62.6	6.80

<b>Q3ZBZ8</b>	Stress-induced-phosphoprotein 1	7.20	4.97	0	2	3	3.457E3	543	62.4	6.43
<b>P31040</b>	Succinate dehydrogenase [ubiquinone] flavoprotein subunit, mitochondrial	7.18	5.27	0	2	3		664	72.6	7.39
<b>P31039</b>	Succinate dehydrogenase [ubiquinone] flavoprotein subunit, mitochondrial	7.18	5.26	0	2	3		665	72.9	7.59
<b>Q3ZBD7</b>	Glucose-6-phosphate isomerase	7.10	5.39	0	2	3	2.337E3	557	62.8	7.71
<b>P50990</b>	T-complex protein 1 subunit theta	7.08	5.11	1	2	5		548	59.6	5.60
<b>Q8TDB8</b>	Solute carrier family 2, facilitated glucose transporter member 14	6.95	4.62	1	2	3	3.651E3	520	56.3	7.83
<b>Q32KV0</b>	Phosphoglycerate mutase 2	6.84	12.65	0	3	3	1.207E4	253	28.7	8.88
<b>P20004</b>	Aconitate hydratase, mitochondrial	6.79	7.18	0	4	4	7.873E3	780	85.3	7.83
<b>Q15506</b>	Sperm surface protein Sp17	6.67	25.83	2	2	2		151	17.4	4.78
<b>A6NNZ2</b>	Tubulin beta-8 chain-like protein LOC260334	6.59	6.53	0	3	3	4.721E3	444	49.5	4.86
<b>Q3ZCM7</b>	Tubulin beta-8 chain	6.59	6.53	0	3	3	4.721E3	444	49.7	4.89

<b>Q7Z6W1</b>	<b>Transmembrane and coiled-coil domain-containing protein 2</b>	<b>6.54</b>	<b>16.48</b>	<b>2</b>	<b>2</b>	<b>2</b>	<b>3.062E4</b>	<b>182</b>	<b>20.1</b>	<b>8.68</b>
<b>Q14697</b>	Neutral alpha-glucosidase AB	6.47	3.71	2	2	2	1.290E4	944	106.8	6.14
<b>Q6BCY4</b>	NADH-cytochrome b5 reductase 2	6.39	15.58	3	3	3	1.713E4	276	31.4	8.50
<b>P06394</b>	Keratin, type I cytoskeletal 10	6.18	6.27	0	3	3	4.859E3	526	54.8	5.11
<b>P04406</b>	Glyceraldehyde-3-phosphate dehydrogenase	6.15	11.64	2	3	3	8.450E3	335	36.0	8.46
<b>P38567</b>	Hyaluronidase PH-20	6.11	2.75	1	1	2		509	57.8	7.01
<b>Q29S21</b>	Keratin, type II cytoskeletal 7	6.09	4.94	0	2	3		466	51.5	5.97
<b>O75952</b>	Calcium-binding tyrosine phosphorylation-regulated protein	6.08	5.88	2	2	2		493	52.7	4.55
<b>Q9P0L0</b>	Vesicle-associated membrane protein-associated protein A	5.87	5.62	0	2	2		249	27.9	8.62
<b>Q0VCY1</b>	Vesicle-associated membrane protein-associated protein A	5.87	5.62	0	2	2		249	27.8	8.60
<b>O15173</b>	Membrane-associated progesterone receptor component 2	5.87	8.52	1	1	2		223	23.8	4.88
<b>Q96KW9</b>	Protein SPACA7	5.81	23.59	3	3	4	3.174E3	195	21.5	4.78
<b>Q8NFI4</b>	Putative protein FAM10A5	5.81	8.94	0	3	4	1.309E4	369	41.4	5.05
<b>Q9BX68</b>	Histidine triad nucleotide-binding protein 2, mitochondrial	5.60	24.54	1	3	4		163	17.2	9.16
<b>O75521</b>	Enoyl-CoA delta isomerase 2, mitochondrial	5.55	3.05	1	1	2		394	43.6	9.00
<b>P20810</b>	Calpastatin	5.55	2.40	1	1	2		708	76.5	5.07
<b>Q15836</b>	Vesicle-associated membrane protein 3	5.34	33.00	0	2	2		100	11.3	8.79
<b>Q2KJD2</b>	Vesicle-associated membrane protein 3	5.34	31.73	0	2	2		104	11.5	8.79
<b>P29692</b>	Elongation factor 1-delta	5.27	8.54	1	2	2		281	31.1	5.01
<b>Q8IYT1</b>	Protein FAM71A	5.25	5.39	2	2	3	7.449E3	594	63.1	9.64
<b>P02662</b>	Alpha-S1-casein	5.24	13.08	2	2	2	1.428E4	214	24.5	5.02
<b>O60884</b>	DnaJ homolog subfamily A member 2	5.20	3.40	0	1	2		412	45.7	6.48
<b>Q2HJ94</b>	DnaJ homolog subfamily A member 2	5.20	3.40	0	1	2		412	45.7	6.48
<b>Q2KJE5</b>	Glyceraldehyde-3-phosphate dehydrogenase, testis-specific	5.07	6.33	0	2	2		395	43.3	8.12
<b>O46375</b>	Transthyretin	4.99	8.84	1	1	2	4.766E3	147	15.7	6.30
<b>P15374</b>	Ubiquitin carboxyl-terminal hydrolase isozyme L3	4.93	6.96	0	1	2		230	26.2	4.92
<b>Q2TBG8</b>	Ubiquitin carboxyl-terminal hydrolase isozyme L3	4.93	6.96	0	1	2		230	26.2	4.92

<b>P11169</b>	<b>Solute carrier family 2, facilitated glucose transporter member 3</b>	<b>4.88</b>	<b>2.22</b>	<b>0</b>	<b>1</b>	<b>2</b>	<b>3.651E3</b>	<b>496</b>	<b>53.9</b>	<b>7.20</b>
<b>P00441</b>	Superoxide dismutase [Cu-Zn]	4.86	16.88	1	2	2	3.241E3	154	15.9	6.13
<b>Q9H0C2</b>	ADP/ATP translocase 4	4.85	8.25	0	2	2		315	35.0	9.89
<b>Q2YDD9</b>	ADP/ATP translocase 4	4.85	8.05	0	2	2		323	35.7	9.55
<b>O75083</b>	WD repeat-containing protein 1	4.84	2.64	1	1	2		606	66.2	6.65
<b>P18859</b>	ATP synthase-coupling factor 6, mitochondrial	4.77	26.85	2	2	2		108	12.6	9.52
<b>Q04837</b>	Single-stranded DNA-binding protein, mitochondrial	4.77	10.14	1	1	2		148	17.2	9.60
<b>P02751</b>	Fibronectin	4.68	0.63	1	1	2	1.138E4	2386	262.5	5.71
<b>Q9BSF0</b>	Small membrane A-kinase anchor protein	4.66	26.32	2	2	2	1.227E4	95	11.0	4.87
<b>P49913</b>	Cathelicidin antimicrobial peptide	4.63	20.00	2	2	2		170	19.3	9.41
<b>P22061</b>	Protein-L-isoaspartate(D-aspartate) O-methyltransferase	4.62	8.37	0	1	2		227	24.6	7.21
<b>P15246</b>	Protein-L-isoaspartate(D-aspartate) O-methyltransferase	4.62	8.37	0	1	2		227	24.5	7.58
<b>P17066</b>	Heat shock 70 kDa protein 6	4.46	3.11	0	2	2		643	71.0	6.14
<b>Q58FF6</b>	Putative heat shock protein HSP 90-beta 4	4.43	1.98	0	1	2		505	58.2	4.73
<b>Q58FF7</b>	Putative heat shock protein HSP 90-beta-3	4.43	1.68	0	1	2		597	68.3	4.79
<b>Q96M98</b>	Parkin coregulated gene protein	4.43	9.12	2	2	3		296	33.3	8.21
<b>Q96E40</b>	Uncharacterized protein C9orf9	4.43	5.86	1	1	2		222	25.1	9.13
<b>P26641</b>	Elongation factor 1-gamma	4.43	2.29	0	1	2		437	50.1	6.67
<b>Q3SZV3</b>	Elongation factor 1-gamma	4.43	2.27	0	1	2		440	50.3	6.57
<b>P21912</b>	Succinate dehydrogenase [ubiquinone] iron-sulfur subunit, mitochondrial	4.42	4.29	0	1	2	1.215E4	280	31.6	8.76
<b>Q3T189</b>	Succinate dehydrogenase [ubiquinone] iron-sulfur subunit, mitochondrial	4.42	4.29	0	1	2	1.215E4	280	31.5	8.60
<b>Q8N4E7</b>	Ferritin, mitochondrial	4.39	9.50	1	1	3		242	27.5	7.27
<b>Q5BJF6</b>	Outer dense fiber protein 2	4.32	2.65	1	2	2	4.091E3	829	95.3	7.62
<b>Q9Y2B0</b>	Protein canopy homolog 2	4.27	8.79	1	1	2		182	20.6	4.92
<b>P05787</b>	Keratin, type II cytoskeletal 8	4.25	2.28	0	1	2		483	53.7	5.59
<b>P08729</b>	Keratin, type II cytoskeletal 7	4.25	2.35	0	1	2		469	51.4	5.48
<b>P14136</b>	Glial fibrillary acidic protein	4.25	2.55	0	1	2		432	49.8	5.52
<b>P19013</b>	Keratin, type II cytoskeletal 4	4.25	2.06	0	1	2		534	57.2	6.61
<b>Q6KB66</b>	Keratin, type II cytoskeletal 80	4.25	2.43	0	1	2		452	50.5	5.67
<b>A0JND2</b>	Keratin, type II cytoskeletal 80	4.25	2.61	0	1	2		422	47.4	5.31
<b>A7YWK3</b>	Keratin, type II cytoskeletal 73	4.25	2.04	0	1	2		540	58.8	7.23

<b>P04263</b>	<b>Keratin, type II cytoskeletal 68 kDa, component IA (Fragment)</b>	<b>4.25</b>	<b>6.04</b>	<b>0</b>	<b>1</b>	<b>2</b>		<b>182</b>	<b>18.1</b>	<b>8.32</b>
<b>Q28115</b>	Glial fibrillary acidic protein	4.25	2.57	0	1	2		428	49.5	5.45
<b>P07108</b>	Acyl-CoA-binding protein	4.18	22.99	1	1	3	2.041E4	87	10.0	6.57
<b>Q9H4B7</b>	Tubulin beta-1 chain	4.18	4.43	0	2	2		451	50.3	5.17
<b>P31930</b>	Cytochrome b-c1 complex subunit 1, mitochondrial	4.10	2.08	1	1	2		480	52.6	6.37
<b>P62739</b>	Actin, aortic smooth muscle	4.09	6.10	0	1	1		377	42.0	5.39
<b>Q3ZC07</b>	Actin, alpha cardiac muscle 1	4.09	6.10	0	1	1		377	42.0	5.39
<b>Q562R1</b>	Beta-actin-like protein 2	4.09	10.90	1	2	2		376	42.0	5.59
<b>P55084</b>	Trifunctional enzyme subunit beta, mitochondrial	3.98	2.74	0	1	2		474	51.3	9.41
<b>O46629</b>	Trifunctional enzyme subunit beta, mitochondrial	3.98	2.74	0	1	2		475	51.3	9.32
<b>Q9NQ48</b>	Leucine zipper transcription factor-like protein 1	3.76	8.70	1	2	2	7.002E3	299	34.6	5.36
<b>O75190</b>	DnaJ homolog subfamily B member 6	3.75	7.06	0	2	2		326	36.1	9.16
<b>Q0III6</b>	DnaJ homolog subfamily B member 6	3.75	9.50	0	2	2		242	26.9	7.61
<b>Q8SQ21</b>	Histidine triad nucleotide-binding protein 2, mitochondrial	3.70	14.72	0	2	3		163	17.1	7.50
<b>P62803</b>	Histone H4	3.67	19.42	2	2	2	1.003E4	103	11.4	11.36
<b>P07954</b>	Fumarate hydratase, mitochondrial	3.67	4.31	2	2	2		510	54.6	8.76
<b>P35579</b>	Myosin-9	3.59	1.07	1	1	1		1960	226.4	5.60
<b>P54727</b>	UV excision repair protein RAD23 homolog B	3.52	4.65	1	2	2		409	43.1	4.84
<b>Q8TC71</b>	Mitochondria-eating protein	3.44	5.20	2	2	2	1.228E4	538	61.1	8.63
<b>O95292</b>	Vesicle-associated membrane protein-associated protein B/C	3.23	4.94	0	1	1		243	27.2	7.30
<b>A2VDZ9</b>	Vesicle-associated membrane protein-associated protein B	3.23	4.94	0	1	1		243	27.1	7.30
<b>P55145</b>	Mesencephalic astrocyte-derived neurotrophic factor	3.20	8.24	1	1	1		182	20.7	8.69
<b>Q8IZP2</b>	Putative protein FAM10A4	3.13	5.83	0	1	1		240	27.4	5.08
<b>P00442</b>	Superoxide dismutase [Cu-Zn]	3.03	7.89	0	1	1	3.241E3	152	15.7	6.32
<b>P07737</b>	Profilin-1	3.01	10.00	1	1	1	1.954E4	140	15.0	8.27
<b>P27708</b>	CAD protein	2.99	1.12	1	1	1		2225	242.8	6.46
<b>P62491</b>	Ras-related protein Rab-11A	2.95	6.02	0	1	1		216	24.4	6.57
<b>Q3MHP2</b>	Ras-related protein Rab-11B	2.95	5.96	0	1	1		218	24.5	5.94

<b>Q2TA29</b>	<b>Ras-related protein Rab-11A</b>	<b>2.95</b>	<b>6.02</b>	<b>0</b>	<b>1</b>	<b>1</b>		<b>216</b>	<b>24.5</b>	<b>6.57</b>
<b>P15311</b>	Ezrin	2.95	3.24	0	1	1	1.096E4	586	69.4	6.27
<b>P26038</b>	Moesin	2.95	3.29	0	1	1	1.096E4	577	67.8	6.40
<b>P35241</b>	Radixin	2.95	3.26	0	1	1	1.096E4	583	68.5	6.37
<b>P31976</b>	Ezrin	2.95	3.27	0	1	1	1.096E4	581	68.7	6.42
<b>Q2HJ49</b>	Moesin	2.95	3.29	0	1	1	1.096E4	577	67.9	6.16
<b>Q32LP2</b>	Radixin	2.95	3.26	0	1	1	1.096E4	583	68.5	6.27
<b>Q8TAD1</b>	Sperm protein associated with the nucleus on the X chromosome E	2.82	11.34	0	1	1	2.254E4	97	11.0	5.26
<b>Q9BXN6</b>	Sperm protein associated with the nucleus on the X chromosome D	2.82	11.34	0	1	1	2.254E4	97	11.0	6.11
<b>Q9NS25</b>	Sperm protein associated with the nucleus on the X chromosome B/F	2.82	10.68	0	1	1	2.254E4	103	11.8	6.15
<b>Q9NS26</b>	Sperm protein associated with the nucleus on the X chromosome A	2.82	11.34	0	1	1	2.254E4	97	11.0	5.10
<b>Q9NY87</b>	Sperm protein associated with the nucleus on the X chromosome C	2.82	11.34	0	1	1	2.254E4	97	11.0	5.10
<b>P0CG47</b>	Polyubiquitin-B	2.79	20.96	0	1	1		229	25.7	7.43
<b>P62992</b>	Ubiquitin-40S ribosomal protein S27a	2.79	10.26	0	1	1		156	18.0	9.64
<b>P63048</b>	Ubiquitin-60S ribosomal protein L40	2.79	12.50	0	1	1		128	14.7	9.83
<b>P0CG48</b>	Polyubiquitin-C	2.79	21.02	0	1	1		685	77.0	7.66
<b>P0CG53</b>	Polyubiquitin-B	2.79	20.98	0	1	1		305	34.3	7.47
<b>P0CH28</b>	Polyubiquitin-C	2.79	20.87	0	1	1		690	77.5	7.66
<b>Q9NUJ1</b>	Mycophenolic acid acyl-glucuronide esterase, mitochondrial	2.79	5.56	1	1	1		306	33.9	8.57
<b>P50991</b>	T-complex protein 1 subunit delta	2.79	2.60	1	1	1		539	57.9	7.83
<b>P06702</b>	Protein S100-A9	2.77	24.56	2	2	2	3.491E3	114	13.2	6.13
<b>Q9H853</b>	Putative tubulin-like protein alpha-4B	2.77	5.81	0	1	1		241	27.5	7.83
<b>Q9HDC9</b>	Adipocyte plasma membrane-associated protein	2.76	2.88	1	1	1	1.217E4	416	46.5	6.16
<b>P17174</b>	Aspartate aminotransferase, cytoplasmic	2.72	3.63	1	1	1	1.764E4	413	46.2	7.01
<b>P04259</b>	Keratin, type II cytoskeletal 6B	2.71	1.77	0	1	1		564	60.0	8.00
<b>O75947</b>	ATP synthase subunit d, mitochondrial	2.70	10.56	1	1	1	1.447E4	161	18.5	5.30
<b>Q5E956</b>	Triosephosphate isomerase	2.67	5.22	0	1	1	3.816E3	249	26.7	6.92
<b>Q00610</b>	Clathrin heavy chain 1	2.65	0.96	0	1	1		1675	191.5	5.69
<b>P49951</b>	Clathrin heavy chain 1	2.65	0.96	0	1	1		1675	191.5	5.69
<b>P48741</b>	Putative heat shock 70 kDa protein 7	2.63	3.00	0	1	1		367	40.2	7.87

<b>P11177</b>	<b>Pyruvate dehydrogenase E1 component subunit beta, mitochondrial</b>	<b>2.60</b>	<b>4.46</b>	<b>0</b>	<b>1</b>	<b>1</b>		<b>359</b>	<b>39.2</b>	<b>6.65</b>
<b>P11966</b>	Pyruvate dehydrogenase E1 component subunit beta, mitochondrial	2.60	4.46	0	1	1		359	39.1	6.65
<b>Q9NZ45</b>	CDGSH iron-sulfur domain-containing protein 1	2.57	13.89	0	1	1	1.905E3	108	12.2	9.09
<b>Q3ZBU2</b>	CDGSH iron-sulfur domain-containing protein 1	2.57	14.15	0	1	1	1.905E3	106	12.0	9.09
<b>P09466</b>	Glycodelin	2.55	7.78	1	1	1		180	20.6	5.57
<b>Q9UBX1</b>	Cathepsin F	2.54	2.07	1	1	1		484	53.3	8.22
<b>Q9UNZ2</b>	NSFL1 cofactor p47	2.54	2.97	0	1	1		370	40.5	5.10
<b>Q3SZC4</b>	NSFL1 cofactor p47	2.54	2.97	0	1	1		370	40.6	5.19
<b>P13667</b>	Protein disulfide-isomerase A4	2.52	1.86	1	1	1		645	72.9	5.07
<b>Q58FF8</b>	Putative heat shock protein HSP 90-beta 2	2.50	2.36	0	1	1		381	44.3	4.84
<b>Q16566</b>	Calcium/calmodulin-dependent protein kinase type IV	2.48	2.96	1	1	1		473	51.9	5.82
<b>Q2T9U2</b>	Outer dense fiber protein 2	2.48	1.83	0	1	1		657	75.5	7.59
<b>P02533</b>	Keratin, type I cytoskeletal 14	2.47	1.91	0	1	1		472	51.5	5.16
<b>P08779</b>	Keratin, type I cytoskeletal 16	2.47	1.90	0	1	1		473	51.2	5.05
<b>Q7Z3Y7</b>	Keratin, type I cytoskeletal 28	2.47	1.94	0	1	1		464	50.5	5.47
<b>Q7Z3Y8</b>	Keratin, type I cytoskeletal 27	2.47	1.96	0	1	1		459	49.8	5.05
<b>Q7Z3Y9</b>	Keratin, type I cytoskeletal 26	2.47	1.92	0	1	1		468	51.9	4.92
<b>Q7Z3Z0</b>	Keratin, type I cytoskeletal 25	2.47	2.00	0	1	1		450	49.3	5.08
<b>Q0P5J4</b>	Keratin, type I cytoskeletal 25	2.47	2.00	0	1	1		450	49.3	5.03
<b>Q0P5J6</b>	Keratin, type I cytoskeletal 27	2.47	1.96	0	1	1		460	49.9	5.10
<b>Q148H6</b>	Keratin, type I cytoskeletal 28	2.47	1.94	0	1	1		464	50.7	5.30
<b>P26640</b>	Valine--tRNA ligase	2.45	1.27	1	1	1		1264	140.4	7.59
<b>Q3SZI4</b>	14-3-3 protein theta	2.44	4.08	0	1	1		245	27.7	4.78
<b>P31946</b>	14-3-3 protein beta/alpha	2.44	4.07	0	1	1		246	28.1	4.83
<b>P31947</b>	14-3-3 protein sigma	2.44	4.03	0	1	1		248	27.8	4.74
<b>P61981</b>	14-3-3 protein gamma	2.44	4.05	0	1	1		247	28.3	4.89
<b>P62261</b>	14-3-3 protein epsilon	2.44	3.92	0	1	1		255	29.2	4.74
<b>Q04917</b>	14-3-3 protein eta	2.44	4.07	0	1	1		246	28.2	4.84
<b>P68509</b>	14-3-3 protein eta	2.44	4.07	0	1	1		246	28.2	4.89
<b>P68250</b>	14-3-3 protein beta/alpha	2.44	4.07	0	1	1		246	28.1	4.87
<b>P68252</b>	14-3-3 protein gamma	2.44	4.05	0	1	1		247	28.2	4.89
<b>Q0VC36</b>	14-3-3 protein sigma	2.44	4.03	0	1	1		248	27.8	4.72



<b>Q3T077</b>	<b>Tubulin polymerization-promoting protein family member 2</b>	<b>2.41</b>	<b>7.60</b>	<b>0</b>	<b>1</b>	<b>1</b>		<b>171</b>	<b>18.6</b>	<b>9.03</b>
<b>Q3LXA3</b>	Bifunctional ATP-dependent dihydroxyacetone kinase/FAD-AMP lyase (cyclizing)	2.40	2.78	1	1	1	8.442E3	575	58.9	7.49
<b>P62820</b>	Ras-related protein Rab-1A	2.40	9.27	0	1	1		205	22.7	6.21
<b>Q9H0U4</b>	Ras-related protein Rab-1B	2.40	9.45	0	1	1		201	22.2	5.73
<b>Q2HJH2</b>	Ras-related protein Rab-1B	2.40	9.45	0	1	1		201	22.2	5.73
<b>P14406</b>	Cytochrome c oxidase subunit 7A2, mitochondrial	2.38	15.66	1	1	1		83	9.4	9.76
<b>P02788</b>	Lactotransferrin	2.37	1.97	1	1	2		710	78.1	8.12
<b>Q16563</b>	Synaptophysin-like protein 1	2.33	4.25	1	1	2		259	28.5	8.43
<b>P81605</b>	Dermcidin	2.31	10.00	1	1	1		110	11.3	6.54
<b>Q8WYR4</b>	Radial spoke head 1 homolog	2.30	5.18	1	1	2		309	35.1	4.63
<b>P21266</b>	Glutathione S-transferase Mu 3	2.29	5.78	1	1	1		225	26.5	5.54
<b>P10515</b>	Dihydrolipoyllysine-residue acetyltransferase component of pyruvate dehydrogenase complex, mitochondrial	2.27	2.63	1	1	1		647	69.0	7.84
<b>Q96C74</b>	Ropporin-1-like protein	2.27	7.83	1	1	1	1.142E4	230	26.1	7.72
<b>A7YWG4</b>	Gamma-glutamyl hydrolase	2.26	3.14	0	1	1	7.389E3	318	35.7	9.06
<b>P00505</b>	Aspartate aminotransferase, mitochondrial	2.25	2.79	1	1	1		430	47.5	9.01
<b>Q8TDM5</b>	Sperm acrosome membrane-associated protein 4	2.23	10.48	1	1	1		124	13.0	5.80
<b>A5D989</b>	Elongation factor 1-delta	2.19	4.29	0	1	1		280	31.1	5.06
<b>Q96JQ2</b>	Calmin	2.17	1.70	1	1	1	1.077E4	1002	111.6	4.94
<b>O95202</b>	LETM1 and EF-hand domain-containing protein 1, mitochondrial	2.14	1.62	0	1	1		739	83.3	6.70
<b>Q0VCA3</b>	LETM1 and EF-hand domain-containing protein 1, mitochondrial	2.14	1.64	0	1	1		732	81.8	6.73
<b>P25686</b>	DnaJ homolog subfamily B member 2	2.14	3.09	0	1	1		324	35.6	5.95
<b>Q8NHS0</b>	DnaJ homolog subfamily B member 8	2.14	9.91	1	2	2		232	25.7	6.42
<b>P10096</b>	Glyceraldehyde-3-phosphate dehydrogenase	2.11	4.20	0	1	1	1.087E4	333	35.8	8.35
<b>Q96IV0</b>	Peptide-N(4)-(N-acetyl-beta-glucosaminy)asparagine amidase	2.09	1.68	1	1	1		654	74.3	6.89
<b>Q9P2E7</b>	Protocadherin-10	2.09	0.96	1	1	1		1040	112.9	4.87
<b>P14174</b>	Macrophage migration inhibitory factor	2.07	7.83	1	1	1		115	12.5	7.88
<b>Q53QW1</b>	Uncharacterized protein C2orf57	2.07	3.80	1	1	1		395	41.6	5.12

<b>P13646</b>	<b>Keratin, type I cytoskeletal 13</b>	<b>2.06</b>	<b>2.40</b>	<b>0</b>	<b>1</b>	<b>1</b>		<b>458</b>	<b>49.6</b>	<b>4.96</b>
<b>Q2M2I5</b>	Keratin, type I cytoskeletal 24	2.06	2.10	0	1	1		525	55.1	4.96
<b>P53396</b>	ATP-citrate synthase	2.04	1.73	0	1	1		1101	120.8	7.33
<b>Q32PF2</b>	ATP-citrate synthase	2.04	1.74	0	1	1		1091	119.7	7.24
<b>Q96T88</b>	E3 ubiquitin-protein ligase UHRF1	2.03	1.26	0	1	1		793	89.8	7.56
<b>A7E320</b>	E3 ubiquitin-protein ligase UHRF1	2.03	1.27	0	1	1		786	88.3	8.00
<b>Q86YB8</b>	ERO1-like protein beta	2.02	2.36	1	1	2		467	53.5	7.99
<b>P61285</b>	Dynein light chain 1, cytoplasmic	2.01	12.36	0	1	1	1.782E3	89	10.4	7.40
<b>Q3MHR3</b>	Dynein light chain 2, cytoplasmic	2.01	12.36	0	1	1	1.782E3	89	10.3	7.37
<b>Q6STE5</b>	SWI/SNF-related matrix-associated actin-dependent regulator of chromatin subfamily D member 3	2.01	4.76	1	1	1		483	55.0	9.35
<b>P30042</b>	ES1 protein homolog, mitochondrial	2.01	9.33	1	1	1		268	28.2	8.27
<b>P46379</b>	Large proline-rich protein BAG6	2.00	1.15	1	1	1		1132	119.3	5.60
<b>Q3ZCI9</b>	T-complex protein 1 subunit theta	1.99	2.01	0	1	2		548	59.6	5.59
<b>Q66GS9</b>	Centrosomal protein of 135 kDa	1.96	0.88	0	1	1		1140	133.4	6.21
<b>O75951</b>	Lysozyme-like protein 6	1.93	6.08	1	1	1		148	16.9	6.14
<b>P25325</b>	3-mercaptopyruvate sulfurtransferase	1.92	4.38	1	1	1		297	33.2	6.60
<b>P04179</b>	Superoxide dismutase [Mn], mitochondrial	1.91	6.31	0	1	1		222	24.7	8.25
<b>P41976</b>	Superoxide dismutase [Mn], mitochondrial	1.91	6.31	0	1	1		222	24.6	8.54
<b>P55854</b>	Small ubiquitin-related modifier 3	1.89	11.65	0	1	1	1.101E4	103	11.6	5.49
<b>P61955</b>	Small ubiquitin-related modifier 2	1.89	12.63	0	1	1	1.101E4	95	10.9	5.50
<b>Q6EEV6</b>	Small ubiquitin-related modifier 4	1.89	12.63	0	1	1	1.101E4	95	10.7	7.18
<b>Q17QV3</b>	Small ubiquitin-related modifier 3	1.89	11.54	0	1	1	1.101E4	104	11.7	5.95
<b>P23786</b>	Carnitine O-palmitoyltransferase 2, mitochondrial	1.86	1.82	0	1	1		658	73.7	8.18
<b>Q2KJB7</b>	Carnitine O-palmitoyltransferase 2, mitochondrial	1.86	1.82	0	1	1		658	74.4	8.13
<b>Q9BY14</b>	Testis-expressed sequence 101 protein	1.85	5.62	1	1	1		249	26.6	4.94
<b>Q08D91</b>	Keratin, type II cytoskeletal 75	1.85	2.21	0	1	1		543	59.0	7.65
<b>Q5XQN5</b>	Keratin, type II cytoskeletal 5	1.85	2.00	0	1	1		601	62.9	7.81
<b>P23004</b>	Cytochrome b-c1 complex subunit 2, mitochondrial	1.82	3.09	0	1	1	1.528E4	453	48.1	8.73
<b>Q9Y371</b>	Endophilin-B1	1.81	3.56	0	1	1		365	40.8	6.04
<b>Q32LM0</b>	Endophilin-B1	1.81	3.56	0	1	1		365	40.8	6.20
<b>P13073</b>	Cytochrome c oxidase subunit 4 isoform 1, mitochondrial	1.81	7.10	1	1	1		169	19.6	9.51

<b>O14645</b>	<b>Axonemal dynein light intermediate polypeptide 1</b>	<b>1.80</b>	<b>11.24</b>	<b>2</b>	<b>2</b>	<b>2</b>	<b>8.760E3</b>	<b>258</b>	<b>29.6</b>	<b>8.50</b>
<b>Q8IYS8</b>	Biorientation of chromosomes in cell division protein 1-like 2	1.80	5.23	1	1	1	8.172E3	172	18.1	5.33
<b>P37198</b>	Nuclear pore glycoprotein p62	1.78	4.60	2	2	2	4.443E3	522	53.2	5.31
<b>O43169</b>	Cytochrome b5 type B	1.78	8.22	1	1	1		146	16.3	4.97
<b>P63027</b>	Vesicle-associated membrane protein 2	1.78	14.66	0	1	1		116	12.7	8.13
<b>P63026</b>	Vesicle-associated membrane protein 2	1.78	14.66	0	1	1		116	12.6	8.13
<b>Q3ZBL4</b>	Leucine zipper transcription factor-like protein 1	1.77	3.68	0	1	1	5.172E3	299	34.6	5.30
<b>Q58FF3</b>	Putative endoplasmic-like protein	1.77	2.51	0	1	1	6.525E3	399	45.8	5.26
<b>Q58FG1</b>	Putative heat shock protein HSP 90-alpha A4	1.76	3.11	0	1	1		418	47.7	5.19
<b>Q86Y82</b>	Syntaxin-12	1.75	5.43	1	1	1		276	31.6	5.59
<b>Q14203</b>	Dynactin subunit 1	1.75	0.94	1	1	1		1278	141.6	5.81
<b>Q9BVL2</b>	Nucleoporin p58/p45	1.75	2.17	1	1	1		599	60.9	9.33
<b>Q29RK4</b>	UV excision repair protein RAD23 homolog B	1.71	2.21	0	1	1		408	43.1	4.84
<b>P10323</b>	Acrosin	1.71	2.14	1	1	1		421	45.8	9.07
<b>P27482</b>	Calmodulin-like protein 3	1.69	5.37	0	1	1		149	16.9	4.42
<b>P25685</b>	DnaJ homolog subfamily B member 1	1.69	6.76	0	2	2		340	38.0	8.63
<b>Q3MI00</b>	DnaJ homolog subfamily B member 1	1.69	6.76	0	2	2		340	38.2	8.63
<b>Q8NHU3</b>	Phosphatidylcholine:ceramide cholinephosphotransferase 2	1.67	2.74	1	1	1		365	42.3	8.81
<b>Q8N0W7</b>	Fragile X mental retardation 1 neighbor protein	1.67	3.53	1	1	1		255	29.2	8.94
<b>Q5VZ72</b>	Izumo sperm-egg fusion protein 3	1.67	3.77	1	1	1	4.288E3	239	27.7	8.29
<b>O43805</b>	Sjogren syndrome nuclear autoantigen 1	1.66	10.92	0	1	1		119	13.6	5.38
<b>Q5E9C3</b>	Sjogren syndrome nuclear autoantigen 1 homolog	1.66	10.92	0	1	1		119	13.6	5.68
<b>Q9BGI1</b>	Peroxiredoxin-5, mitochondrial	1.64	3.65	0	1	1		219	23.2	8.07
<b>P22748</b>	Carbonic anhydrase 4	1.63	4.81	1	1	1		312	35.0	7.83
<b>Q5GAN3</b>	Probable inactive ribonuclease-like protein 13	1.62	7.05	1	1	1		156	17.8	8.59
<b>Q8WWF6</b>	DnaJ homolog subfamily B member 3	1.62	8.97	0	1	1		145	16.5	4.94
<b>P30041</b>	Peroxiredoxin-6	1.62	4.91	0	1	1	1.184E4	224	25.0	6.38
<b>O77834</b>	Peroxiredoxin-6	1.62	4.91	0	1	1	1.184E4	224	25.1	6.38
<b>E9PGG2</b>	Anomalous homeobox protein	0.00	3.43	1	1	1		379	41.7	5.38

<b>O15013</b>	<b>Rho guanine nucleotide exchange factor 10</b>	<b>0.00</b>	<b>1.02</b>	<b>1</b>	<b>1</b>	<b>1</b>		<b>1369</b>	<b>151.5</b>	<b>5.68</b>
<b>O60814</b>	Histone H2B type 1-K	0.00	8.73	0	1	1	5.050E3	126	13.9	10.32
<b>P06899</b>	Histone H2B type 1-J	0.00	8.73	0	1	1	5.050E3	126	13.9	10.32
<b>P0C0S4</b>	Histone H2A.Z	0.00	7.03	0	1	1		128	13.5	10.58
<b>P14618</b>	Pyruvate kinase PKM	0.00	4.33	1	1	2		531	57.9	7.84
<b>P18084</b>	Integrin beta-5	0.00	4.13	1	1	1		799	88.0	6.06
<b>P19367</b>	Hexokinase-1	0.00	1.31	1	1	1		917	102.4	6.80
<b>P23527</b>	Histone H2B type 1-O	0.00	8.73	0	1	1	5.050E3	126	13.9	10.32
<b>P27824</b>	Calnexin	0.00	3.21	1	1	1		592	67.5	4.60
<b>P33778</b>	Histone H2B type 1-B	0.00	8.73	0	1	1	5.050E3	126	13.9	10.32
<b>P48047</b>	ATP synthase subunit O, mitochondrial	0.00	6.57	1	1	1		213	23.3	9.96
<b>P55786</b>	Puromycin-sensitive aminopeptidase	0.00	1.41	1	1	1	8.106E3	919	103.2	5.72
<b>P57053</b>	Histone H2B type F-S	0.00	8.73	0	1	1	5.050E3	126	13.9	10.37
<b>P58876</b>	Histone H2B type 1-D	0.00	8.73	0	1	1	5.050E3	126	13.9	10.32
<b>P62807</b>	Histone H2B type 1-C/E/F/G/I	0.00	8.73	0	1	1	5.050E3	126	13.9	10.32
<b>Q13428</b>	Treacle protein	0.00	2.69	1	1	1		1488	152.0	9.04
<b>Q16543</b>	Hsp90 co-chaperone Cdc37	0.00	4.50	1	1	1		378	44.4	5.25
<b>Q16778</b>	Histone H2B type 2-E	0.00	8.73	0	1	1	5.050E3	126	13.9	10.32
<b>Q5QNW6</b>	Histone H2B type 2-F	0.00	8.73	0	1	1	5.050E3	126	13.9	10.32
<b>Q32LA7</b>	Histone H2A.V	0.00	7.03	0	1	1		128	13.5	10.58
<b>Q86VQ3</b>	Thioredoxin domain-containing protein 2	0.00	2.71	1	1	1		553	60.4	4.87
<b>Q8N257</b>	Histone H2B type 3-B	0.00	8.73	0	1	1	5.050E3	126	13.9	10.32
<b>Q93079</b>	Histone H2B type 1-H	0.00	8.73	0	1	1	5.050E3	126	13.9	10.32
<b>Q96A08</b>	Histone H2B type 1-A	0.00	8.66	0	1	1	5.050E3	127	14.2	10.32
<b>Q96NT0</b>	Coiled-coil domain-containing protein 115	0.00	3.89	1	1	1		180	19.7	6.95
<b>Q99832</b>	T-complex protein 1 subunit eta	0.00	2.21	0	1	1		543	59.3	7.65
<b>Q99877</b>	Histone H2B type 1-N	0.00	8.73	0	1	1	5.050E3	126	13.9	10.32
<b>Q99879</b>	Histone H2B type 1-M	0.00	8.73	0	1	1	5.050E3	126	14.0	10.32
<b>Q99880</b>	Histone H2B type 1-L	0.00	8.73	0	1	1	5.050E3	126	13.9	10.32
<b>Q9P225</b>	Dynein heavy chain 2, axonemal	0.00	0.20	1	1	1		4427	507.4	6.37
<b>A8MVZ5</b>	Butyrophilin-like protein 10	0.00	4.12	1	1	1		291	32.6	8.34
<b>Q2M2T1</b>	Histone H2B type 1-K	0.00	8.73	0	1	1	5.050E3	126	13.9	10.29
<b>Q2NKZ1</b>	T-complex protein 1 subunit eta	0.00	2.21	0	1	1		543	59.4	7.20
<b>Q32L48</b>	Histone H2B type 1-N	0.00	8.73	0	1	1	5.050E3	126	13.9	10.32
<b>Q32L97</b>	Vesicle-associated membrane protein 4	0.00	16.31	1	1	1		141	16.4	7.34

**Appendix Table 5.3.** Mass spectrometry data for hyaluronic acid-binding fraction (sample D31).

Accession	Description	Score	Coverage	Unique Peptides	Peptides	PSMs	AAs	MW [kDa]	calc. pI
P10323	Acrosin	397.02	53.21	18	18	130	421	45.8	9.07
P99999	Cytochrome c	364.45	75.24	14	14	120	105	11.7	9.57
P07205	Phosphoglycerate kinase 2	135.22	62.11	18	21	45	417	44.8	8.54
P06744	Glucose-6-phosphate isomerase	130.00	42.29	17	17	50	558	63.1	8.32
P13645	Keratin, type I cytoskeletal 10	117.06	40.07	17	17	35	584	58.8	5.21
P04264	Keratin, type II cytoskeletal 1	111.18	48.45	17	21	36	644	66.0	8.12
P35908	Keratin, type II cytoskeletal 2 epidermal	84.34	44.91	15	20	28	639	65.4	8.00
P07864	L-lactate dehydrogenase C chain	75.32	60.24	13	14	26	332	36.3	7.46
P14618	Pyruvate kinase PKM	75.30	40.68	14	14	25	531	57.9	7.84
P00505	Aspartate aminotransferase, mitochondrial	57.01	42.56	12	12	20	430	47.5	9.01
P02788	Lactotransferrin	54.29	29.44	15	15	19	710	78.1	8.12
Q9NPJ3	Acyl-coenzyme A thioesterase 13	52.93	62.14	5	5	18	140	15.0	9.14
P35527	Keratin, type I cytoskeletal 9	49.76	29.86	11	11	16	623	62.0	5.24
Q5JQC9	A-kinase anchor protein 4	48.57	19.91	12	12	17	854	94.4	6.96
Q8NEB7	Acrosin-binding protein	45.90	18.23	6	6	14	543	61.3	5.16
Q6UWQ5	Lysozyme-like protein 1	45.58	26.35	2	3	12	148	16.6	8.05
P04075	Fructose-bisphosphate aldolase A	45.16	35.44	8	8	14	364	39.4	8.09
Q02383	Semenogelin-2	44.42	22.16	7	8	15	582	65.4	9.07
Q9UII2	ATPase inhibitor, mitochondrial	42.69	17.92	5	5	15	106	12.2	9.35
P68371	Tubulin beta-4B chain	38.06	41.12	0	10	13	445	49.8	4.89
P04279	Semenogelin-1	38.04	25.76	8	9	13	462	52.1	9.29
Q16836	Hydroxyacyl-coenzyme A dehydrogenase, mitochondrial	33.58	48.41	8	8	10	314	34.3	8.85
P07437	Tubulin beta chain	32.76	31.31	0	8	11	444	49.6	4.89
O14556	Glyceraldehyde-3-phosphate dehydrogenase, testis-specific	30.93	41.91	9	9	13	408	44.5	8.19
P04350	Tubulin beta-4A chain	28.03	33.33	0	8	9	444	49.6	4.88
Q99798	Aconitate hydratase, mitochondrial	26.21	12.44	7	7	11	780	85.4	7.61
Q13509	Tubulin beta-3 chain	25.86	21.78	0	7	10	450	50.4	4.93
Q13885	Tubulin beta-2A chain	24.60	25.17	0	7	9	445	49.9	4.89
Q9BVA1	Tubulin beta-2B chain	24.60	25.17	0	7	9	445	49.9	4.89
Q13748	Tubulin alpha-3C/D chain	23.18	20.67	0	5	7	450	49.9	5.10
Q6PEY2	Tubulin alpha-3E chain	23.18	20.67	0	5	7	450	49.8	5.14

<b>Q71U36</b>	<b>Tubulin alpha-1A chain</b>	<b>23.18</b>	<b>20.62</b>	<b>0</b>	<b>5</b>	<b>7</b>	<b>451</b>	<b>50.1</b>	<b>5.06</b>
<b>P54652</b>	Heat shock-related 70 kDa protein 2	22.59	18.15	6	7	8	639	70.0	5.74
<b>P00558</b>	Phosphoglycerate kinase 1	21.95	9.83	0	3	7	417	44.6	8.10
<b>Q9BS86</b>	Zona pellucida-binding protein 1	20.98	33.05	7	7	8	351	40.1	9.28
<b>Q7Z4W2</b>	Lysozyme-like protein 2	20.85	26.35	2	3	6	148	16.6	7.84
<b>P36969</b>	Phospholipid hydroperoxide glutathione peroxidase, mitochondrial	20.52	35.03	6	6	10	197	22.2	8.37
<b>Q92820</b>	Gamma-glutamyl hydrolase	20.17	21.70	5	5	6	318	35.9	7.11
<b>P68363</b>	Tubulin alpha-1B chain	19.78	17.52	0	4	6	451	50.1	5.06
<b>P68366</b>	Tubulin alpha-4A chain	19.78	17.63	0	4	6	448	49.9	5.06
<b>Q9BQE3</b>	Tubulin alpha-1C chain	17.45	12.25	0	3	5	449	49.9	5.10
<b>Q96E40</b>	Uncharacterized protein C9orf9	17.12	35.14	5	5	6	222	25.1	9.13
<b>P04259</b>	Keratin, type II cytoskeletal 6B	16.98	6.91	0	5	7	564	60.0	8.00
<b>Q5VU65</b>	Nuclear pore membrane glycoprotein 210-like	16.71	5.14	7	7	8	1888	210.5	7.50
<b>P03973</b>	Antileukoprotease	16.71	11.36	2	2	6	132	14.3	8.75
<b>P42785</b>	Lysosomal Pro-X carboxypeptidase	16.50	12.70	4	4	5	496	55.8	7.21
<b>Q7Z794</b>	Keratin, type II cytoskeletal 1b	15.56	3.46	0	2	6	578	61.9	5.99
<b>Q1ZYL8</b>	Izumo sperm-egg fusion protein 4	15.27	24.14	3	3	5	232	26.5	7.46
<b>P07954</b>	Fumarate hydratase, mitochondrial	15.26	20.20	5	5	7	510	54.6	8.76
<b>P07900</b>	Heat shock protein HSP 90-alpha	15.25	8.06	2	5	6	732	84.6	5.02
<b>A6NC86</b>	phospholipase A2 inhibitor and Ly6/PLAUR domain-containing protein	15.10	16.67	2	2	4	204	21.9	7.99
<b>Q96KX0</b>	Lysozyme-like protein 4	14.74	24.66	3	3	5	146	16.4	8.28
<b>P00338</b>	L-lactate dehydrogenase A chain	14.31	11.45	2	3	5	332	36.7	8.27
<b>Q9Y277</b>	Voltage-dependent anion-selective channel protein 3	14.19	13.78	2	2	5	283	30.6	8.66
<b>P04406</b>	Glyceraldehyde-3-phosphate dehydrogenase	13.92	17.61	3	3	4	335	36.0	8.46
<b>P40926</b>	Malate dehydrogenase, mitochondrial	13.65	13.02	3	3	4	338	35.5	8.68
<b>P00761</b>	Trypsin	12.66	16.45	3	3	8	231	24.4	7.18
<b>O75969</b>	A-kinase anchor protein 3	12.58	5.16	3	3	4	853	94.7	6.18
<b>Q6P4A8</b>	Phospholipase B-like 1	12.40	11.93	3	3	3	553	63.2	9.06
<b>Q9Y6C9</b>	Mitochondrial carrier homolog 2	11.70	16.50	3	3	4	303	33.3	7.97
<b>O00233</b>	26S proteasome non-ATPase regulatory subunit 9	11.13	30.49	2	2	3	223	24.7	6.95
<b>P61019</b>	Ras-related protein Rab-2A	10.88	23.58	3	4	4	212	23.5	6.54
<b>Q5BJF6</b>	Outer dense fiber protein 2	10.69	4.58	3	3	4	829	95.3	7.62

<b>P20155</b>	<b>Serine protease inhibitor Kazal-type 2</b>	<b>10.61</b>	<b>26.19</b>	<b>1</b>	<b>1</b>	<b>2</b>	<b>84</b>	<b>9.3</b>	<b>9.00</b>
<b>P25705</b>	ATP synthase subunit alpha, mitochondrial	10.23	5.97	2	2	4	553	59.7	9.13
<b>A6NM11</b>	Leucine-rich repeat-containing protein 37A2	10.18	1.88	0	2	3	1700	188.3	5.50
<b>A6NMS7</b>	Leucine-rich repeat-containing protein 37A	10.18	1.88	0	2	3	1700	188.1	5.49
<b>O60309</b>	Leucine-rich repeat-containing protein 37A3	10.18	1.96	0	2	3	1634	180.5	5.31
<b>P06576</b>	ATP synthase subunit beta, mitochondrial	9.92	10.96	3	3	4	529	56.5	5.40
<b>P19367</b>	Hexokinase-1	9.66	6.54	4	4	4	917	102.4	6.80
<b>P09622</b>	Dihydrolipoyl dehydrogenase, mitochondrial	9.54	6.68	2	2	3	509	54.1	7.85
<b>Q9BUN1</b>	Protein MENT	9.37	6.74	2	2	3	341	36.7	8.59
<b>P02533</b>	Keratin, type I cytoskeletal 14	9.17	8.26	1	3	4	472	51.5	5.16
<b>Q8N5Q1</b>	Putative protein FAM71E2	9.10	2.93	2	2	3	922	99.9	9.39
<b>P45880</b>	Voltage-dependent anion-selective channel protein 2	9.08	13.27	2	2	4	294	31.5	7.56
<b>Q01546</b>	Keratin, type II cytoskeletal 2 oral	8.84	2.82	0	4	4	638	65.8	8.12
<b>P13647</b>	Keratin, type II cytoskeletal 5	8.80	4.58	1	4	4	590	62.3	7.74
<b>P02538</b>	Keratin, type II cytoskeletal 6A	8.69	5.14	0	4	4	564	60.0	8.00
<b>P48668</b>	Keratin, type II cytoskeletal 6C	8.69	5.14	0	4	4	564	60.0	8.00
<b>Q16568</b>	Cocaine- and amphetamine-regulated transcript protein	8.67	14.66	2	2	3	116	12.8	8.25
<b>Q13618</b>	Cullin-3	8.63	1.95	1	1	3	768	88.9	8.48
<b>P31040</b>	Succinate dehydrogenase [ubiquinone] flavoprotein subunit, mitochondrial	8.61	3.77	2	2	3	664	72.6	7.39
<b>Q96QE4</b>	Leucine-rich repeat-containing protein 37B	8.60	4.96	3	3	3	947	105.5	4.91
<b>Q6NUT2</b>	Probable C-mannosyltransferase DPY19L2	8.37	7.65	2	3	3	758	87.3	9.10
<b>P08238</b>	Heat shock protein HSP 90-beta	8.26	3.18	0	2	3	724	83.2	5.03
<b>Q9BUF5</b>	Tubulin beta-6 chain	8.10	9.19	0	3	3	446	49.8	4.88
<b>Q9NY65</b>	Tubulin alpha-8 chain	7.98	8.69	0	2	2	449	50.1	5.06
<b>P04179</b>	Superoxide dismutase [Mn], mitochondrial	7.97	6.76	1	1	3	222	24.7	8.25
<b>P06702</b>	Protein S100-A9	7.66	26.32	2	2	2	114	13.2	6.13
<b>P07195</b>	L-lactate dehydrogenase B chain	7.61	3.59	0	1	3	334	36.6	6.05
<b>Q6ZMR3</b>	L-lactate dehydrogenase A-like 6A	7.61	3.61	0	1	3	332	36.5	6.99
<b>Q86YZ3</b>	Hornerin	7.41	3.79	2	2	4	2850	282.2	10.04
<b>P05787</b>	Keratin, type II cytoskeletal 8	7.06	3.93	0	2	3	483	53.7	5.59
<b>P10909</b>	Clusterin	6.97	8.91	2	2	2	449	52.5	6.27
<b>P55145</b>	Mesencephalic astrocyte-derived neurotrophic factor	6.96	9.34	1	1	4	182	20.7	8.69
<b>P34931</b>	Heat shock 70 kDa protein 1-like	6.94	5.15	1	3	3	641	70.3	6.02

<b>P13929</b>	<b>Beta-enolase</b>	<b>6.81</b>	<b>8.53</b>	<b>0</b>	<b>2</b>	<b>2</b>	<b>434</b>	<b>47.0</b>	<b>7.71</b>
<b>P06733</b>	Alpha-enolase	6.81	8.53	0	2	2	434	47.1	7.39
<b>A6NNZ2</b>	Tubulin beta-8 chain-like protein LOC260334	6.75	9.46	0	2	2	444	49.5	4.86
<b>Q3ZCM7</b>	Tubulin beta-8 chain	6.75	9.46	0	2	2	444	49.7	4.89
<b>P49411</b>	Elongation factor Tu, mitochondrial	6.63	3.76	1	1	2	452	49.5	7.61
<b>P15259</b>	Phosphoglycerate mutase 2	6.54	15.81	2	3	3	253	28.7	8.88
<b>Q16698</b>	2,4-dienoyl-CoA reductase, mitochondrial	6.50	6.57	1	1	2	335	36.0	9.28
<b>O95678</b>	Keratin, type II cytoskeletal 75	6.41	3.09	0	3	3	551	59.5	7.74
<b>Q9BZX4</b>	Ropporin-1B	6.26	12.26	0	2	2	212	23.9	5.15
<b>Q9HAT0</b>	Ropporin-1A	6.26	12.26	0	2	2	212	23.9	5.66
<b>Q16851</b>	UTP--glucose-1-phosphate uridylyltransferase	6.05	2.76	1	1	4	508	56.9	8.15
<b>P26436</b>	Acrosomal protein SP-10	6.05	8.68	2	2	3	265	28.1	4.69
<b>Q6UWU2</b>	Beta-galactosidase-1-like protein	5.79	5.35	4	4	5	654	74.1	8.92
<b>A4D1T9</b>	Probable inactive serine protease 37	5.65	15.32	2	2	3	235	26.4	8.87
<b>P40939</b>	Trifunctional enzyme subunit alpha, mitochondrial	5.58	1.83	1	1	2	763	82.9	9.04
<b>P60174</b>	Triosephosphate isomerase	5.27	9.09	2	2	2	286	30.8	5.92
<b>P21266</b>	Glutathione S-transferase Mu 3	5.20	10.22	2	2	2	225	26.5	5.54
<b>Q9BWH2</b>	FUN14 domain-containing protein 2	5.19	12.70	2	2	2	189	20.7	9.73
<b>P62805</b>	Histone H4	5.15	21.36	2	2	2	103	11.4	11.36
<b>P08729</b>	Keratin, type II cytoskeletal 7	5.08	2.35	0	1	2	469	51.4	5.48
<b>P14136</b>	Glial fibrillary acidic protein	5.08	2.55	0	1	2	432	49.8	5.52
<b>P19013</b>	Keratin, type II cytoskeletal 4	5.08	2.06	0	1	2	534	57.2	6.61
<b>Q6KB66</b>	Keratin, type II cytoskeletal 80	5.08	2.43	0	1	2	452	50.5	5.67
<b>O95563</b>	Mitochondrial pyruvate carrier 2	4.93	9.45	1	1	2	127	14.3	10.43
<b>P08107</b>	Heat shock 70 kDa protein 1A/1B	4.90	3.59	0	2	2	641	70.0	5.66
<b>P08779</b>	Keratin, type I cytoskeletal 16	4.69	4.23	0	2	2	473	51.2	5.05
<b>Q9HBV2</b>	Sperm acrosome membrane-associated protein 1	4.56	9.52	2	2	2	294	32.1	4.61
<b>Q96QH8</b>	Sperm acrosome-associated protein 5	4.44	18.24	2	2	3	159	17.9	6.42
<b>P12036</b>	Neurofilament heavy polypeptide	4.42	0.88	0	2	2	1026	112.4	6.18
<b>Q7RTS7</b>	Keratin, type II cytoskeletal 74	4.42	1.70	0	2	2	529	57.8	7.71
<b>Q86Y46</b>	Keratin, type II cytoskeletal 73	4.42	1.67	0	2	2	540	58.9	7.23
<b>P12035</b>	Keratin, type II cytoskeletal 3	4.42	1.43	0	2	2	628	64.4	6.48
<b>Q9Y6A4</b>	Cilia- and flagella-associated protein 20	4.38	14.51	2	2	2	193	22.8	9.76



<b>P09104</b>	<b>Gamma-enolase</b>	<b>4.35</b>	<b>5.07</b>	<b>0</b>	<b>1</b>	<b>1</b>	<b>434</b>	<b>47.2</b>	<b>5.03</b>
<b>P50990</b>	T-complex protein 1 subunit theta	4.23	3.83	2	2	2	548	59.6	5.60
<b>Q8NBX0</b>	Saccharopine dehydrogenase-like oxidoreductase	4.08	5.36	1	1	1	429	47.1	9.14
<b>P60900</b>	Proteasome subunit alpha type-6	4.07	9.35	2	2	2	246	27.4	6.76
<b>P63167</b>	Dynein light chain 1, cytoplasmic	4.04	24.72	0	2	2	89	10.4	7.40
<b>Q96FJ2</b>	Dynein light chain 2, cytoplasmic	4.04	24.72	0	2	2	89	10.3	7.37
<b>P78371</b>	T-complex protein 1 subunit beta	3.96	5.05	2	2	2	535	57.5	6.46
<b>P55084</b>	Trifunctional enzyme subunit beta, mitochondrial	3.81	4.22	2	2	2	474	51.3	9.41
<b>Q8WUD1</b>	Ras-related protein Rab-2B	3.66	6.02	0	1	1	216	24.2	7.83
<b>Q6NXN4</b>	Putative C-mannosyltransferase DPY19L2P1	3.66	7.85	0	1	1	242	28.0	9.85
<b>Q8N807</b>	Protein disulfide-isomerase-like protein of the testis	3.60	2.23	1	1	1	584	66.6	6.86
<b>Q00796</b>	Sorbitol dehydrogenase	3.54	4.20	1	1	1	357	38.3	7.97
<b>P24539</b>	ATP synthase F(0) complex subunit B1, mitochondrial	3.44	4.69	1	1	1	256	28.9	9.36
<b>P84243</b>	Histone H3.3	3.41	23.53	1	1	1	136	15.3	11.27
<b>P49901</b>	Sperm mitochondrial-associated cysteine-rich protein	3.34	27.59	2	2	2	116	12.8	8.07
<b>P02768</b>	Serum albumin	3.29	2.46	1	1	1	609	69.3	6.28
<b>Q5SRE5</b>	Nucleoporin NUP188 homolog	3.23	0.91	1	1	1	1749	195.9	6.73
<b>P49913</b>	Cathelicidin antimicrobial peptide	3.20	7.65	1	1	1	170	19.3	9.41
<b>O60361</b>	Putative nucleoside diphosphate kinase	3.19	12.41	0	1	2	137	15.5	8.57
<b>P15531</b>	Nucleoside diphosphate kinase A	3.19	11.18	0	1	2	152	17.1	6.19
<b>P22392</b>	Nucleoside diphosphate kinase B	3.19	11.18	0	1	2	152	17.3	8.41
<b>P11142</b>	Heat shock cognate 71 kDa protein	3.13	2.48	0	1	1	646	70.9	5.52
<b>Q8TC27</b>	Disintegrin and metalloproteinase domain-containing protein 32	3.02	2.41	1	1	1	787	87.9	5.55
<b>P13073</b>	Cytochrome c oxidase subunit 4 isoform 1, mitochondrial	2.97	6.51	1	1	1	169	19.6	9.51
<b>Q5FVE4</b>	Long-chain-fatty-acid--CoA ligase ACSBG2	2.68	2.85	1	1	1	666	74.3	8.46
<b>P00414</b>	Cytochrome c oxidase subunit 3	2.67	5.36	1	1	1	261	29.9	7.31
<b>P0CG47</b>	Polyubiquitin-B	2.64	11.79	0	1	1	229	25.7	7.43
<b>P62979</b>	Ubiquitin-40S ribosomal protein S27a	2.64	5.77	0	1	1	156	18.0	9.64
<b>P62987</b>	Ubiquitin-60S ribosomal protein L40	2.64	7.03	0	1	1	128	14.7	9.83
<b>P0CG48</b>	Polyubiquitin-C	2.64	11.82	0	1	1	685	77.0	7.66

<b>Q8WZ59</b>	<b>Transmembrane protein 190</b>	<b>2.64</b>	<b>7.91</b>	<b>1</b>	<b>1</b>	<b>1</b>	<b>177</b>	<b>19.4</b>	<b>5.24</b>
<b>P68104</b>	Elongation factor 1-alpha 1	2.51	2.60	0	1	1	462	50.1	9.01
<b>Q05639</b>	Elongation factor 1-alpha 2	2.51	2.59	0	1	1	463	50.4	9.03
<b>Q5VTE0</b>	Putative elongation factor 1-alpha-like 3	2.51	2.60	0	1	1	462	50.2	9.07
<b>P30042</b>	ES1 protein homolog, mitochondrial	2.48	3.73	1	1	1	268	28.2	8.27
<b>Q6UW49</b>	Sperm equatorial segment protein 1	2.46	3.14	1	1	1	350	38.9	5.73
<b>P23284</b>	Peptidyl-prolyl cis-trans isomerase B	2.45	5.09	1	1	1	216	23.7	9.41
<b>Q6UWM5</b>	GLIPR1-like protein 1	2.41	3.72	1	1	1	242	27.1	8.21
<b>Q58FG0</b>	Putative heat shock protein HSP 90-alpha A5	2.34	4.49	0	1	1	334	38.7	6.57
<b>P14555</b>	Phospholipase A2, membrane associated	2.32	6.94	1	1	1	144	16.1	9.23
<b>P0C8F1</b>	Prostate and testis expressed protein 4	2.30	12.24	1	1	1	98	11.4	8.62
<b>P18669</b>	Phosphoglycerate mutase 1	2.26	4.33	0	1	1	254	28.8	7.18
<b>P35663</b>	Cylicin-1	2.25	2.46	1	1	1	651	74.2	9.67
<b>Q9H4B7</b>	Tubulin beta-1 chain	2.24	2.22	0	1	1	451	50.3	5.17
<b>Q6X784</b>	Zona pellucida-binding protein 2	2.21	2.96	1	1	1	338	38.6	7.78
<b>P14923</b>	Junction plakoglobin	2.21	1.34	1	1	1	745	81.7	6.14
<b>Q18PE1</b>	Protein Dok-7	2.19	2.98	1	1	1	504	53.1	6.89
<b>Q92523</b>	Carnitine O-palmitoyltransferase 1, muscle isoform	2.16	1.42	1	1	1	772	87.7	8.62
<b>P05109</b>	Protein S100-A8	2.15	11.83	1	1	1	93	10.8	7.03
<b>Q58FF6</b>	Putative heat shock protein HSP 90-beta 4	2.14	1.98	0	1	1	505	58.2	4.73
<b>Q58FF7</b>	Putative heat shock protein HSP 90-beta-3	2.14	1.68	0	1	1	597	68.3	4.79
<b>P60709</b>	Actin, cytoplasmic 1	2.14	4.80	0	1	2	375	41.7	5.48
<b>P63261</b>	Actin, cytoplasmic 2	2.14	4.80	0	1	2	375	41.8	5.48
<b>P11021</b>	78 kDa glucose-regulated protein	2.12	1.53	1	1	1	654	72.3	5.16
<b>P13667</b>	Protein disulfide-isomerase A4	2.12	1.24	1	1	1	645	72.9	5.07
<b>P08727</b>	Keratin, type I cytoskeletal 19	2.11	2.25	0	1	1	400	44.1	5.14
<b>P19012</b>	Keratin, type I cytoskeletal 15	2.11	1.97	0	1	1	456	49.2	4.77
<b>Q04695</b>	Keratin, type I cytoskeletal 17	2.11	2.08	0	1	1	432	48.1	5.02
<b>P24752</b>	Acetyl-CoA acetyltransferase, mitochondrial	2.11	2.34	1	1	1	427	45.2	8.85
<b>P30405</b>	Peptidyl-prolyl cis-trans isomerase F, mitochondrial	2.09	3.86	1	1	1	207	22.0	9.38
<b>P30101</b>	Protein disulfide-isomerase A3	2.01	1.78	1	1	1	505	56.7	6.35
<b>O75952</b>	Calcium-binding tyrosine phosphorylation-regulated protein	2.01	4.26	1	1	1	493	52.7	4.55

<b>P17612</b>	<b>cAMP-dependent protein kinase catalytic subunit alpha</b>	<b>1.94</b>	<b>2.56</b>	<b>0</b>	<b>1</b>	<b>1</b>	<b>351</b>	<b>40.6</b>	<b>8.79</b>
<b>P22694</b>	cAMP-dependent protein kinase catalytic subunit beta	1.94	2.56	0	1	1	351	40.6	8.78
<b>P28074</b>	Proteasome subunit beta type-5	1.94	4.56	1	1	1	263	28.5	6.92
<b>Q8N1N4</b>	Keratin, type II cytoskeletal 78	1.93	1.54	0	1	1	520	56.8	6.02
<b>O60814</b>	Histone H2B type 1-K	1.88	8.73	0	1	1	126	13.9	10.32
<b>P06899</b>	Histone H2B type 1-J	1.88	8.73	0	1	1	126	13.9	10.32
<b>P23527</b>	Histone H2B type 1-O	1.88	8.73	0	1	1	126	13.9	10.32
<b>P33778</b>	Histone H2B type 1-B	1.88	8.73	0	1	1	126	13.9	10.32
<b>P57053</b>	Histone H2B type F-S	1.88	8.73	0	1	1	126	13.9	10.37
<b>P58876</b>	Histone H2B type 1-D	1.88	8.73	0	1	1	126	13.9	10.32
<b>P62807</b>	Histone H2B type 1-C/E/F/G/I	1.88	8.73	0	1	1	126	13.9	10.32
<b>Q16778</b>	Histone H2B type 2-E	1.88	8.73	0	1	1	126	13.9	10.32
<b>Q5QNW6</b>	Histone H2B type 2-F	1.88	8.73	0	1	1	126	13.9	10.32
<b>Q8N257</b>	Histone H2B type 3-B	1.88	8.73	0	1	1	126	13.9	10.32
<b>Q93079</b>	Histone H2B type 1-H GN=HIST1H2BH PE=1 SV[	1.88	8.73	0	1	1	126	13.9	10.32
<b>Q96A08</b>	Histone H2B type 1-A	1.88	8.66	0	1	1	127	14.2	10.32
<b>Q99877</b>	Histone H2B type 1-N	1.88	8.73	0	1	1	126	13.9	10.32
<b>Q99879</b>	Histone H2B type 1-M	1.88	8.73	0	1	1	126	14.0	10.32
<b>Q99880</b>	Histone H2B type 1-L	1.88	8.73	0	1	1	126	13.9	10.32
<b>P21741</b>	Midkine	1.86	6.99	1	1	1	143	15.6	9.79
<b>P00918</b>	Carbonic anhydrase 2	1.85	4.62	1	1	1	260	29.2	7.40
<b>Q15363</b>	Transmembrane emp24 domain-containing protein 2	1.75	4.48	1	1	1	201	22.7	5.17
<b>P00403</b>	Cytochrome c oxidase subunit 2	1.74	4.41	1	1	1	227	25.5	4.82
<b>P23786</b>	Carnitine O-palmitoyltransferase 2, mitochondrial	1.71	1.67	1	1	1	658	73.7	8.18
<b>P16104</b>	Histone H2AX	1.69	16.08	0	1	1	143	15.1	10.74
<b>Q8IUE6</b>	Histone H2A type 2-B	1.69	17.69	0	1	1	130	14.0	10.89
<b>Q96QV6</b>	Histone H2A type 1-A	1.69	17.56	0	1	1	131	14.2	10.86
<b>P14625</b>	Endoplasmic	1.65	1.62	1	1	1	803	92.4	4.84
<b>O75122</b>	CLIP-associating protein 2	0.00	1.39	1	1	1	1294	141.0	8.47
<b>P14868</b>	Aspartate--tRNA ligase, cytoplasmic	0.00	2.99	1	1	1	501	57.1	6.55
<b>P16219</b>	Short-chain specific acyl-CoA dehydrogenase, mitochondrial	0.00	2.43	1	1	1	412	44.3	7.99
<b>P25787</b>	Proteasome subunit alpha type-2	0.00	8.12	1	1	1	234	25.9	7.43

<b>Q00325</b>	<b>Phosphate carrier protein, mitochondrial</b>	<b>0.00</b>	<b>1.66</b>	<b>1</b>	<b>1</b>	<b>1</b>	<b>362</b>	<b>40.1</b>	<b>9.38</b>
<b>Q86TL2</b>	Transmembrane protein 110	0.00	15.99	1	1	1	294	33.2	8.15
<b>Q9BYT9</b>	Anoctamin-3	0.00	1.83	1	1	1	981	114.6	8.66
<b>Q9UF56</b>	F-box/LRR-repeat protein 17	0.00	2.57	1	1	1	701	75.6	8.07

**Appendix Table 5.4.** Mass spectrometry data for hyaluronic acid non-binding fraction (sample D31).

Accession	Description	Score	Coverage	Unique Peptides	Peptides	PSMs	Area	AAs	MW [kDa]	calc. pI
P54652	Heat shock-related 70 kDa protein 2	139.86	48.20	2	25	56	3.146E5	639	70.0	5.74
P34933	Heat shock-related 70 kDa protein 2	123.46	41.51	0	22	49	3.146E5	636	69.7	5.59
Q5JQC9	A-kinase anchor protein 4	116.40	31.50	22	22	50	5.026E5	854	94.4	6.96
A6NMS7	Leucine-rich repeat-containing protein 37A	79.66	13.35	1	16	32	1.188E6	1700	188.1	5.49
A6NM11	Leucine-rich repeat-containing protein 37A2	78.06	12.76	0	15	31	1.188E6	1700	188.3	5.50
Q99798	Aconitate hydratase, mitochondrial	68.36	31.54	7	16	25	1.335E5	780	85.4	7.61
O60309	Leucine-rich repeat-containing protein 37A3	64.29	11.32	0	13	26	1.188E6	1634	180.5	5.31
P34931	Heat shock 70 kDa protein 1-like	63.44	30.42	2	14	25	3.175E5	641	70.3	6.02
Q13748	Tubulin alpha-3C/D chain	63.41	34.00	0	9	22	2.421E5	450	49.9	5.10
Q6PEY2	Tubulin alpha-3E chain	63.41	34.00	0	9	22	2.421E5	450	49.8	5.14
Q71U36	Tubulin alpha-1A chain	63.41	33.92	0	9	22	2.421E5	451	50.1	5.06
Q2HJ86	Tubulin alpha-1D chain	63.41	33.85	0	9	22	2.421E5	452	50.3	5.03
Q32KN8	Tubulin alpha-3 chain	63.41	34.00	0	9	22	2.421E5	450	49.9	5.10
Q3MHM5	Tubulin beta-4B chain	63.24	40.22	0	12	23	3.237E5	445	49.8	4.89
Q13885	Tubulin beta-2A chain	61.40	37.53	0	11	22	3.237E5	445	49.9	4.89
Q6B856	Tubulin beta-2B chain	61.40	37.53	0	11	22	3.237E5	445	49.9	4.89
P04279	Semenogelin-1	60.03	35.71	10	13	24	5.795E4	462	52.1	9.29
P07900	Heat shock protein HSP 90-alpha	58.61	25.55	0	17	25	5.664E5	732	84.6	5.02
Q76LV2	Heat shock protein HSP 90-alpha	58.61	25.51	0	17	25	5.664E5	733	84.7	5.01
P11021	78 kDa glucose-regulated protein	57.75	29.36	1	14	23	3.393E5	654	72.3	5.16
P06733	Alpha-enolase	56.92	40.32	4	11	20	3.774E5	434	47.1	7.39
Q0VCX2	78 kDa glucose-regulated protein	55.64	27.02	0	13	22	3.393E5	655	72.4	5.16
P81947	Tubulin alpha-1B chain	55.47	31.04	0	8	18	1.248E5	451	50.1	5.06
Q2KJD0	Tubulin beta-5 chain	55.40	36.49	0	11	21	1.935E5	444	49.6	4.89
Q3ZCJ7	Tubulin alpha-1C chain	55.17	27.17	0	7	18	2.329E5	449	49.8	5.10
P0CB32	Heat shock 70 kDa protein 1-like	54.51	24.49	0	12	22	3.175E5	641	70.3	6.20
O75969	A-kinase anchor protein 3	50.62	27.55	17	18	24	4.435E5	853	94.7	6.18
P06576	ATP synthase subunit beta, mitochondrial	49.67	29.49	1	11	20	2.886E5	529	56.5	5.40

<b>P14625</b>	<b>Endoplasmin</b>	<b>48.97</b>	<b>20.42</b>	<b>4</b>	<b>14</b>	<b>19</b>	<b>8.527E4</b>	<b>803</b>	<b>92.4</b>	<b>4.84</b>
<b>P81948</b>	Tubulin alpha-4A chain	48.55	24.55	0	6	15	1.102E5	448	49.9	5.06
<b>P02788</b>	Lactotransferrin	48.00	21.27	11	11	17	2.377E5	710	78.1	8.12
<b>P08107</b>	Heat shock 70 kDa protein 1A/1B	47.94	23.09	1	10	18	3.175E5	641	70.0	5.66
<b>P00829</b>	ATP synthase subunit beta, mitochondrial	47.79	27.84	0	10	19	2.886E5	528	56.2	5.27
<b>P24752</b>	Acetyl-CoA acetyltransferase, mitochondrial	47.41	38.88	6	11	19	8.252E4	427	45.2	8.85
<b>Q8NEB7</b>	Acrosin-binding protein	45.04	24.49	10	10	21	2.349E6	543	61.3	5.16
<b>Q02383</b>	Semenogelin-2	44.50	31.62	9	12	20	1.056E5	582	65.4	9.07
<b>Q5BJF6</b>	Outer dense fiber protein 2	44.03	16.41	1	12	18	9.159E4	829	95.3	7.62
<b>Q2T9U2</b>	Outer dense fiber protein 2	44.03	19.18	0	11	17	9.159E4	657	75.5	7.59
<b>O75952</b>	Calcium-binding tyrosine phosphorylation-regulated protein	43.49	22.52	8	8	15	4.797E5	493	52.7	4.55
<b>P04264</b>	Keratin, type II cytoskeletal 1	43.45	20.03	9	12	17	8.156E4	644	66.0	8.12
<b>Q3ZBU7</b>	Tubulin beta-4A chain	41.47	33.56	0	10	17	3.019E5	444	49.6	4.88
<b>P62157</b>	Calmodulin	41.28	44.30	6	7	16	7.621E5	149	16.8	4.22
<b>Q96QE4</b>	Leucine-rich repeat-containing protein 37B	41.16	17.21	11	11	16	3.792E5	947	105.5	4.91
<b>P20004</b>	Aconitate hydratase, mitochondrial	40.10	17.82	0	9	13	9.910E4	780	85.3	7.83
<b>Q9Y4L1</b>	Hypoxia up-regulated protein 1	39.55	14.61	9	9	16	6.529E4	999	111.3	5.22
<b>P07205</b>	Phosphoglycerate kinase 2	38.23	29.02	6	8	13	3.113E5	417	44.8	8.54
<b>Q9BQE3</b>	Tubulin alpha-1C chain	37.25	24.94	0	7	14	2.329E5	449	49.9	5.10
<b>Q27965</b>	Heat shock 70 kDa protein 1B	37.19	18.25	0	9	16	3.175E5	641	70.2	5.92
<b>Q27975</b>	Heat shock 70 kDa protein 1A	37.19	18.25	0	9	16	3.175E5	641	70.2	5.92
<b>P78371</b>	T-complex protein 1 subunit beta	35.50	18.32	2	6	12	7.592E4	535	57.5	6.46
<b>P27797</b>	Calreticulin	33.97	22.54	4	6	13	9.550E4	417	48.1	4.44
<b>P30086</b>	Phosphatidylethanolamine-binding protein 1	33.50	35.83	3	4	11	1.132E5	187	21.0	7.53
<b>Q7L266</b>	Isoaspartyl peptidase/L-asparaginase	33.40	39.61	6	7	11	2.337E5	308	32.0	6.24
<b>Q2T9S0</b>	Tubulin beta-3 chain	32.98	23.78	0	8	10	2.105E5	450	50.4	4.93
<b>Q9HAT0</b>	Ropporin-1A	32.75	33.02	1	5	12	1.737E5	212	23.9	5.66
<b>Q6UW49</b>	Sperm equatorial segment protein 1	32.38	27.14	7	7	12	5.448E5	350	38.9	5.73
<b>P40926</b>	Malate dehydrogenase, mitochondrial	32.30	39.64	4	9	15	6.092E5	338	35.5	8.68
<b>P15289</b>	Arylsulfatase A	31.43	14.00	4	4	11	8.825E4	507	53.6	6.07

<b>Q95M18</b>	<b>Endoplasmic</b>	<b>31.42</b>	<b>12.69</b>	<b>0</b>	<b>10</b>	<b>13</b>	<b>2.979E4</b>	<b>804</b>	<b>92.4</b>	<b>4.84</b>
<b>Q9XSJ4</b>	Alpha-enolase	30.93	23.27	0	7	11	3.415E5	434	47.3	6.80
<b>P10809</b>	60 kDa heat shock protein, mitochondrial Homo sapiens	30.91	16.40	3	7	12	1.205E5	573	61.0	5.87
<b>Q8N4E7</b>	Ferritin, mitochondrial	30.85	37.60	6	7	13	3.849E5	242	27.5	7.27
<b>P04075</b>	Fructose-bisphosphate aldolase A	30.37	41.21	10	10	12	1.397E5	364	39.4	8.09
<b>P10909</b>	Clusterin	29.92	23.39	9	9	12	5.095E5	449	52.5	6.27
<b>P31937</b>	3-hydroxyisobutyrate dehydrogenase, mitochondrial	29.83	28.27	4	6	10	1.970E5	336	35.3	8.13
<b>P08238</b>	Heat shock protein HSP 90-beta	29.47	14.78	0	9	13	1.984E5	724	83.2	5.03
<b>P13645</b>	Keratin, type I cytoskeletal 10	29.36	18.15	4	8	12	7.720E4	584	58.8	5.21
<b>P25705</b>	ATP synthase subunit alpha, mitochondrial	29.30	16.82	0	7	10	2.732E5	553	59.7	9.13
<b>P19483</b>	ATP synthase subunit alpha, mitochondrial	29.30	16.82	0	7	10	2.732E5	553	59.7	9.19
<b>P63103</b>	14-3-3 protein zeta/delta	28.65	37.14	5	7	11	2.259E5	245	27.7	4.79
<b>Q9BZX4</b>	Ropporin-1B	28.26	27.83	1	5	10	1.775E5	212	23.9	5.15
<b>Q2HJ81</b>	Tubulin beta-6 chain	28.04	15.25	0	5	8	2.590E5	446	49.9	4.86
<b>P60174</b>	Triosephosphate isomerase	28.00	53.85	3	10	14	1.938E5	286	30.8	5.92
<b>P60712</b>	Actin, cytoplasmic 1	27.78	26.13	0	6	10	6.884E4	375	41.7	5.48
<b>P63258</b>	Actin, cytoplasmic 2	27.78	26.13	0	6	10	6.884E4	375	41.8	5.48
<b>Q76LV1</b>	Heat shock protein HSP 90-beta	27.74	13.12	0	8	12	1.984E5	724	83.2	5.03
<b>P55072</b>	Transitional endoplasmic reticulum ATPase	26.29	12.41	0	6	10	1.167E5	806	89.3	5.26
<b>Q3ZBT1</b>	Transitional endoplasmic reticulum ATPase	26.29	12.41	0	6	10	1.167E5	806	89.3	5.26
<b>P15259</b>	Phosphoglycerate mutase 2	25.94	47.04	3	8	11	3.831E5	253	28.7	8.88
<b>Q13561</b>	Dynactin subunit 2	25.76	22.44	3	6	8	1.114E5	401	44.2	5.21
<b>O14556</b>	Glyceraldehyde-3-phosphate dehydrogenase, testis-specific	25.74	26.23	4	7	12	1.472E5	408	44.5	8.19
<b>P11177</b>	Pyruvate dehydrogenase E1 component subunit beta, mitochondrial	24.40	24.51	4	6	8	6.625E4	359	39.2	6.65
<b>P61019</b>	Ras-related protein Rab-2A	24.23	39.62	4	6	11	2.012E5	212	23.5	6.54
<b>P30044</b>	Peroxiredoxin-5, mitochondrial	23.79	39.25	5	6	8	4.749E4	214	22.1	8.70
<b>P52193</b>	Calreticulin	23.63	11.51	0	2	7	1.201E5	417	48.0	4.46
<b>P19367</b>	Hexokinase-1	23.45	9.27	3	7	10	8.109E4	917	102.4	6.80
<b>P30101</b>	Protein disulfide-isomerase A3	23.11	24.36	4	9	10	3.423E5	505	56.7	6.35

<b>P11142</b>	<b>Heat shock cognate 71 kDa protein</b>	<b>22.36</b>	<b>11.76</b>	<b>0</b>	<b>7</b>	<b>10</b>	<b>5.632E4</b>	<b>646</b>	<b>70.9</b>	<b>5.52</b>
<b>P19120</b>	Heat shock cognate 71 kDa protein	22.36	11.69	0	7	10	5.632E4	650	71.2	5.52
<b>Q29RZ0</b>	Acetyl-CoA acetyltransferase, mitochondrial	21.80	18.48	0	5	9	5.229E4	422	44.9	8.85
<b>Q9NY65</b>	Tubulin alpha-8 chain	21.34	18.49	0	5	7	2.421E5	449	50.1	5.06
<b>Q2HJB8</b>	Tubulin alpha-8 chain	21.34	18.49	0	5	7	2.421E5	449	50.0	5.20
<b>Q3ZBH0</b>	T-complex protein 1 subunit beta	20.78	12.52	0	4	7	7.592E4	535	57.4	6.64
<b>Q92820</b>	Gamma-glutamyl hydrolase	20.16	22.64	5	6	8	1.150E5	318	35.9	7.11
<b>P28838</b>	Cytosol aminopeptidase	20.10	15.41	4	6	10	8.420E4	519	56.1	7.93
<b>P00441</b>	Superoxide dismutase [Cu-Zn]	19.67	32.47	3	4	6	5.830E5	154	15.9	6.13
<b>Q04837</b>	Single-stranded DNA-binding protein, mitochondrial	19.65	38.51	4	4	7	2.278E5	148	17.2	9.60
<b>Q9BX68</b>	Histidine triad nucleotide-binding protein 2, mitochondrial	19.36	47.24	2	5	8	1.968E5	163	17.2	9.16
<b>Q5E956</b>	Triosephosphate isomerase	19.26	46.59	0	7	11	1.485E5	249	26.7	6.92
<b>Q9P0L0</b>	Vesicle-associated membrane protein-associated protein A	19.16	15.66	0	4	7	4.821E5	249	27.9	8.62
<b>Q0VCY1</b>	Vesicle-associated membrane protein-associated protein A	19.16	15.66	0	4	7	4.821E5	249	27.8	8.60
<b>P31948</b>	Stress-induced-phosphoprotein 1	19.14	12.52	1	6	8	2.240E4	543	62.6	6.80
<b>P07954</b>	Fumarate hydratase, mitochondrial	18.48	16.47	6	6	8	2.062E5	510	54.6	8.76
<b>Q32LG3</b>	Malate dehydrogenase, mitochondrial	18.46	21.01	0	5	9	3.016E5	338	35.6	8.54
<b>Q9BUF5</b>	Tubulin beta-6 chain	17.52	11.21	0	4	6	2.133E5	446	49.8	4.88
<b>P59282</b>	Tubulin polymerization-promoting protein family member 2	17.23	27.65	3	3	6	3.471E4	170	18.5	9.00
<b>Q3ZCF0</b>	Dynactin subunit 2	17.10	12.66	0	3	5	7.101E4	403	44.3	5.16
<b>Q16698</b>	2,4-dienoyl-CoA reductase, mitochondrial	16.98	27.16	6	6	7	2.177E5	335	36.0	9.28
<b>Q3ZBZ8</b>	Stress-induced-phosphoprotein 1	16.98	11.23	1	6	8	2.613E4	543	62.4	6.43
<b>Q8TC56</b>	Protein FAM71B	16.96	9.75	4	4	6	7.201E4	605	64.7	9.48
<b>P18669</b>	Phosphoglycerate mutase 1	16.93	24.02	0	5	7	1.283E5	254	28.8	7.18
<b>Q3SZ62</b>	Phosphoglycerate mutase 1	16.93	24.02	0	5	7	1.283E5	254	28.8	7.18
<b>P15586</b>	N-acetylglucosamine-6-sulfatase	16.82	10.33	2	5	7	5.746E4	552	62.0	8.31
<b>Q1ZYL8</b>	Izumo sperm-egg fusion protein 4	16.46	15.09	3	3	7	7.943E5	232	26.5	7.46
<b>Q9HBV2</b>	Sperm acrosome membrane-associated protein 1	16.40	23.81	5	5	7	1.174E5	294	32.1	4.61



<b>P49913</b>	<b>Cathelicidin antimicrobial peptide</b>	<b>16.37</b>	<b>21.76</b>	<b>4</b>	<b>4</b>	<b>7</b>	<b>2.672E4</b>	<b>170</b>	<b>19.3</b>	<b>9.41</b>
<b>P21266</b>	Glutathione S-transferase Mu 3	16.25	32.89	6	6	10	5.312E4	225	26.5	5.54
<b>O60664</b>	Perilipin-3	16.24	14.29	4	4	6	1.000E5	434	47.0	5.44
<b>P16104</b>	Histone H2AX	16.18	42.66	0	3	5	6.383E4	143	15.1	10.74
<b>Q8IU66</b>	Histone H2A type 2-B	16.18	46.92	0	3	5	6.383E4	130	14.0	10.89
<b>P54727</b>	UV excision repair protein RAD23 homolog B	16.11	11.74	1	4	7	8.738E4	409	43.1	4.84
<b>Q8WYR4</b>	Radial spoke head 1 homolog	16.00	18.12	4	4	6	8.430E4	309	35.1	4.63
<b>P13804</b>	Electron transfer flavoprotein subunit alpha, mitochondrial	15.98	12.61	2	3	7	4.781E4	333	35.1	8.38
<b>Q9BUN1</b>	Protein MENT	15.39	9.68	2	2	6	1.410E5	341	36.7	8.59
<b>A6NNZ2</b>	Tubulin beta-8 chain-like protein	14.87	6.31	0	3	9	4.522E4	444	49.5	4.86
<b>Q3ZCM7</b>	Tubulin beta-8 chain	14.87	6.31	0	3	9	4.522E4	444	49.7	4.89
<b>P50990</b>	T-complex protein 1 subunit theta	14.80	13.69	2	6	7	3.970E4	548	59.6	5.60
<b>P61603</b>	10 kDa heat shock protein, mitochondrial	14.59	35.29	3	3	6	1.328E6	102	10.9	8.92
<b>P12273</b>	Prolactin-inducible protein	14.56	24.66	3	3	5	2.948E5	146	16.6	8.05
<b>P35527</b>	Keratin, type I cytoskeletal 9	14.56	11.40	5	5	7	6.261E4	623	62.0	5.24
<b>P07864</b>	L-lactate dehydrogenase C chain	14.51	25.00	7	7	8	1.508E5	332	36.3	7.46
<b>P27595</b>	Hexokinase-1	14.26	5.56	0	4	6	8.109E4	918	103.0	7.03
<b>Q29RK4</b>	UV excision repair protein RAD23 homolog B	14.17	9.31	0	3	6	4.680E4	408	43.1	4.84
<b>P55809</b>	Succinyl-CoA:3-ketoacid coenzyme A transferase 1, mitochondrial	14.11	9.23	2	2	4	5.661E4	520	56.1	7.46
<b>P10323</b>	Acrosin	14.10	10.21	4	4	7	3.523E5	421	45.8	9.07
<b>P31146</b>	Coronin-1A	13.73	4.56	0	1	4	2.298E4	461	51.0	6.68
<b>Q92176</b>	Coronin-1A	13.73	4.56	0	1	4	2.298E4	461	50.9	6.68
<b>Q15084</b>	Protein disulfide-isomerase A6	13.54	10.45	3	3	5	5.444E4	440	48.1	5.08
<b>O95757</b>	Heat shock 70 kDa protein 4L	13.42	8.22	6	6	8	1.011E5	839	94.5	5.88
<b>P24534</b>	Elongation factor 1-beta	13.42	14.67	1	2	4	9.433E4	225	24.7	4.67
<b>Q6BCY4</b>	NADH-cytochrome b5 reductase 2	13.40	26.81	5	5	6	1.325E5	276	31.4	8.50
<b>Q6S8J3</b>	POTE ankyrin domain family member E	13.30	5.21	0	4	5	4.410E4	1075	121.3	6.20
<b>P38657</b>	Protein disulfide-isomerase A3	13.19	13.07	0	5	6	9.113E4	505	56.9	6.65
<b>P11966</b>	Pyruvate dehydrogenase E1 component subunit beta, mitochondrial	13.18	8.91	0	2	4	3.979E4	359	39.1	6.65
<b>Q99832</b>	T-complex protein 1 subunit eta	12.87	8.84	0	3	4	9.525E4	543	59.3	7.65

<b>Q2NKZ1</b>	<b>T-complex protein 1 subunit eta</b>	<b>12.87</b>	<b>8.84</b>	<b>0</b>	<b>3</b>	<b>4</b>	<b>9.525E4</b>	<b>543</b>	<b>59.4</b>	<b>7.20</b>
<b>Q58FF8</b>	Putative heat shock protein HSP 90-beta 2	12.87	11.81	0	4	6	1.536E5	381	44.3	4.84
<b>P31081</b>	60 kDa heat shock protein, mitochondrial	12.77	7.85	0	4	5	7.536E4	573	61.1	5.74
<b>P22695</b>	Cytochrome b-c1 complex subunit 2, mitochondrial	12.72	11.70	3	3	5	3.190E4	453	48.4	8.63
<b>P02768</b>	Serum albumin	12.65	12.64	5	6	6	4.672E4	609	69.3	6.28
<b>P14618</b>	Pyruvate kinase PKM	12.61	11.30	4	4	5		531	57.9	7.84
<b>P50502</b>	Hsc70-interacting protein	12.59	20.05	0	6	8	1.128E5	369	41.3	5.27
<b>P31040</b>	Succinate dehydrogenase [ubiquinone] flavoprotein subunit, mitochondrial	12.53	9.04	1	3	4	2.605E4	664	72.6	7.39
<b>P34932</b>	Heat shock 70 kDa protein 4	12.52	6.31	4	4	6	4.562E4	840	94.3	5.19
<b>P35908</b>	Keratin, type II cytoskeletal 2 epidermal	12.32	6.73	2	4	5	3.224E4	639	65.4	8.00
<b>Q01469</b>	Fatty acid-binding protein, epidermal	12.31	31.85	3	4	5	5.228E4	135	15.2	7.01
<b>P04908</b>	Histone H2A type 1-B/E	12.25	43.85	0	3	5	1.126E5	130	14.1	11.05
<b>P0C0S9</b>	Histone H2A type 1	12.25	43.85	0	3	5	1.126E5	130	14.1	10.90
<b>P20671</b>	Histone H2A type 1-D	12.25	43.85	0	3	5	1.126E5	130	14.1	10.90
<b>Q7L7L0</b>	Histone H2A type 3	12.25	43.85	0	3	5	1.126E5	130	14.1	11.05
<b>Q93077</b>	Histone H2A type 1-C	12.25	43.85	0	3	5	1.126E5	130	14.1	11.05
<b>Q96KK5</b>	Histone H2A type 1-H	12.25	44.53	0	3	5	1.126E5	128	13.9	10.89
<b>Q99878</b>	Histone H2A type 1-J	12.25	44.53	0	3	5	1.126E5	128	13.9	10.89
<b>Q3ZBX9</b>	Histone H2A.J	12.25	44.19	0	3	5	1.126E5	129	14.0	10.90
<b>P49368</b>	T-complex protein 1 subunit gamma	12.22	12.48	0	5	5	1.564E5	545	60.5	6.49
<b>Q3T0K2</b>	T-complex protein 1 subunit gamma	12.22	12.48	0	5	5	1.564E5	545	60.5	6.80
<b>P54709</b>	Sodium/potassium-transporting ATPase subunit beta-3	12.10	17.20	3	3	4	1.332E5	279	31.5	8.35
<b>P30042</b>	ES1 protein homolog, mitochondrial	12.08	23.13	3	3	5	5.363E4	268	28.2	8.27
<b>P40939</b>	Trifunctional enzyme subunit alpha, mitochondrial	12.08	3.80	2	2	5	6.150E4	763	82.9	9.04
<b>Q58FG0</b>	Putative heat shock protein HSP 90-alpha A5	11.98	7.49	0	2	4	8.937E4	334	38.7	6.57
<b>P04406</b>	Glyceraldehyde-3-phosphate dehydrogenase	11.90	17.91	3	4	5	1.460E5	335	36.0	8.46

<b>P07108</b>	<b>Acyl-CoA-binding protein</b>	<b>11.78</b>	<b>50.57</b>	<b>2</b>	<b>3</b>	<b>6</b>	<b>1.004E5</b>	<b>87</b>	<b>10.0</b>	<b>6.57</b>
<b>P17174</b>	Aspartate aminotransferase, cytoplasmic	11.48	14.04	4	4	5	2.364E4	413	46.2	7.01
<b>Q9Y230</b>	RuvB-like 2	11.43	10.15	1	5	5	3.360E4	463	51.1	5.64
<b>O75976</b>	Carboxypeptidase D	11.11	5.94	4	4	5	2.921E4	1380	152.8	6.05
<b>P17066</b>	Heat shock 70 kDa protein 6	11.10	5.13	0	3	5		643	71.0	6.14
<b>P17987</b>	T-complex protein 1 subunit alpha	11.02	8.81	0	3	4	5.971E4	556	60.3	6.11
<b>Q32L40</b>	T-complex protein 1 subunit alpha	11.02	8.81	0	3	4	5.971E4	556	60.2	6.11
<b>Q32KV0</b>	Phosphoglycerate mutase 2	10.88	17.39	0	4	5	1.336E5	253	28.7	8.88
<b>Q3ZC19</b>	T-complex protein 1 subunit theta	10.77	7.85	0	4	5	3.493E4	548	59.6	5.59
<b>Q15506</b>	Sperm surface protein Sp17	10.63	35.76	4	4	4	2.869E5	151	17.4	4.78
<b>P00558</b>	Phosphoglycerate kinase 1	10.45	7.91	0	2	3	1.349E5	417	44.6	8.10
<b>Q3T0P6</b>	Phosphoglycerate kinase 1	10.45	7.91	0	2	3	1.349E5	417	44.5	8.27
<b>P12821</b>	Angiotensin-converting enzyme	10.37	3.45	4	4	5	1.373E5	1306	149.6	6.39
<b>P61285</b>	Dynein light chain 1, cytoplasmic	10.34	24.72	0	2	5	1.518E5	89	10.4	7.40
<b>Q3MHR3</b>	Dynein light chain 2, cytoplasmic	10.34	24.72	0	2	5	1.518E5	89	10.3	7.37
<b>Q1LZH9</b>	N-acetylglucosamine-6-sulfatase	10.23	6.25	0	3	4	6.029E4	560	62.7	8.43
<b>Q9UBX1</b>	Cathepsin F	10.07	7.85	4	4	5	7.783E4	484	53.3	8.22
<b>Q2KJE5</b>	Glyceraldehyde-3-phosphate dehydrogenase, testis-specific	10.04	9.87	0	3	4	1.037E5	395	43.3	8.12
<b>Q8WW22</b>	DnaJ homolog subfamily A member 4	9.77	11.59	3	3	4	1.270E5	397	44.8	7.59
<b>P50991</b>	T-complex protein 1 subunit delta	9.62	13.17	2	4	5	1.090E5	539	57.9	7.83
<b>Q2TBU9</b>	RuvB-like 2	9.59	7.56	0	4	4	2.606E4	463	51.1	5.76
<b>Q8WUD1</b>	Ras-related protein Rab-2B	9.57	11.57	0	2	4	2.463E5	216	24.2	7.83
<b>Q58FF7</b>	Putative heat shock protein HSP 90-beta-3	9.50	5.70	0	3	5	1.536E5	597	68.3	4.79
<b>P14314</b>	Glucosidase 2 subunit beta	9.49	10.61	4	4	7	1.094E5	528	59.4	4.41
<b>P25685</b>	DnaJ homolog subfamily B member 1	9.44	9.71	1	3	4	6.780E4	340	38.0	8.63
<b>P17980</b>	26S protease regulatory subunit 6A	9.08	10.25	3	3	5	7.994E4	439	49.2	5.24
<b>P48741</b>	Putative heat shock 70 kDa protein 7	9.06	6.54	0	2	4		367	40.2	7.87
<b>Q9UJZ1</b>	Stomatin-like protein 2, mitochondrial	9.01	4.78	0	1	3	4.079E4	356	38.5	7.39
<b>Q32LL2</b>	Stomatin-like protein 2, mitochondrial	9.01	4.78	0	1	3	4.079E4	356	38.7	8.32
<b>P06744</b>	Glucose-6-phosphate isomerase	8.89	10.22	2	4	4	1.591E5	558	63.1	8.32

<b>P57105</b>	<b>Synaptojanin-2-binding protein</b>	<b>8.88</b>	<b>17.93</b>	<b>0</b>	<b>2</b>	<b>3</b>	<b>1.378E5</b>	<b>145</b>	<b>15.9</b>	<b>6.30</b>
<b>Q3T0C9</b>	Synaptojanin-2-binding protein	8.88	17.93	0	2	3	1.378E5	145	15.8	5.94
<b>P31039</b>	Succinate dehydrogenase [ubiquinone] flavoprotein subunit, mitochondrial	8.85	4.66	0	2	3	2.605E4	665	72.9	7.59
<b>P37198</b>	Nuclear pore glycoprotein p62	8.64	9.20	3	3	4	1.045E5	522	53.2	5.31
<b>P62191</b>	26S protease regulatory subunit 4	8.63	4.55	1	1	2		440	49.2	6.21
<b>Q7Z4H3</b>	HD domain-containing protein 2	8.63	22.06	2	3	4	2.824E4	204	23.4	5.49
<b>P48643</b>	T-complex protein 1 subunit epsilon	8.35	7.58	2	2	3	9.123E4	541	59.6	5.66
<b>Q14568</b>	Putative heat shock protein HSP 90-alpha A2	8.35	9.62	0	3	4		343	39.3	4.65
<b>Q16543</b>	Hsp90 co-chaperone Cdc37	8.34	10.05	1	2	3	9.712E4	378	44.4	5.25
<b>P52209</b>	6-phosphogluconate dehydrogenase, decarboxylating	8.16	6.21	2	2	3	5.419E4	483	53.1	7.23
<b>P08559</b>	Pyruvate dehydrogenase E1 component subunit alpha, somatic form, mitochondrial	8.15	8.46	0	3	4		390	43.3	8.06
<b>A7MB35</b>	Pyruvate dehydrogenase E1 component subunit alpha, somatic form, mitochondrial	8.15	8.46	0	3	4		390	43.4	8.03
<b>Q5E983</b>	Elongation factor 1-beta	8.14	6.67	0	1	2	9.433E4	225	24.8	4.67
<b>P18859</b>	ATP synthase-coupling factor 6, mitochondrial	7.99	22.22	2	2	3	1.681E5	108	12.6	9.52
<b>Q9H3G5</b>	Probable serine carboxypeptidase CPVL	7.96	12.18	4	4	5	1.665E5	476	54.1	5.62
<b>Q96JQ2</b>	Calmin	7.95	2.79	2	2	3	3.358E4	1002	111.6	4.94
<b>Q8NF14</b>	Putative protein FAM10A5	7.95	11.65	0	4	5	1.762E4	369	41.4	5.05
<b>Q8IXA5</b>	Sperm acrosome membrane- associated protein 3	7.55	17.67	3	3	3		215	23.4	7.94
<b>Q96S96</b>	Phosphatidylethanolamine-binding protein 4	7.46	14.10	2	2	3	4.996E4	227	25.7	6.54
<b>Q2KJE4</b>	Electron transfer flavoprotein subunit alpha, mitochondrial	7.45	4.80	0	1	3	9.192E4	333	34.9	8.56
<b>P07195</b>	L-lactate dehydrogenase B chain	7.42	5.99	0	1	3	2.004E4	334	36.6	6.05
<b>Q5E9B1</b>	L-lactate dehydrogenase B chain	7.42	5.99	0	1	3	2.004E4	334	36.7	6.44
<b>Q99497</b>	Protein DJ-1	7.35	29.63	0	3	3		189	19.9	6.79
<b>Q5E946</b>	Protein DJ-1	7.35	29.63	0	3	3		189	20.0	7.33
<b>P14927</b>	Cytochrome b-c1 complex subunit	7.31	11.71	1	1	2	7.861E4	111	13.5	8.78

<b>O14950</b>	<b>Myosin regulatory light chain 12B</b>	<b>7.27</b>	<b>11.63</b>	<b>0</b>	<b>1</b>	<b>2</b>	<b>5.300E4</b>	<b>172</b>	<b>19.8</b>	<b>4.84</b>
<b>P19105</b>	Myosin regulatory light chain 12A	7.27	11.70	0	1	2	5.300E4	171	19.8	4.81
<b>Q5E9E2</b>	Myosin regulatory light polypeptide 9	7.27	11.63	0	1	2	5.300E4	172	19.9	4.81
<b>A4IF97</b>	Myosin regulatory light chain 12B	7.27	11.70	0	1	2	5.300E4	171	19.7	4.84
<b>A5A3E0</b>	POTE ankyrin domain family member F	7.19	3.07	0	3	3	1.760E4	1075	121.4	6.20
<b>Q2HJD7</b>	3-hydroxyisobutyrate dehydrogenase, mitochondrial	7.14	13.69	1	3	3	9.693E3	336	35.4	8.13
<b>Q9NZ45</b>	CDGSH iron-sulfur domain-containing protein 1	7.08	13.89	0	1	2	2.234E4	108	12.2	9.09
<b>Q3ZBU2</b>	CDGSH iron-sulfur domain-containing protein 1	7.08	14.15	0	1	2	2.234E4	106	12.0	9.09
<b>O75947</b>	ATP synthase subunit d, mitochondrial	7.06	26.09	2	3	4	6.982E4	161	18.5	5.30
<b>O75390</b>	Citrate synthase, mitochondrial	7.02	3.43	0	1	2		466	51.7	8.32
<b>Q29RK1</b>	Citrate synthase, mitochondrial	7.02	3.43	0	1	2		466	51.7	8.12
<b>Q86Y82</b>	Syntaxin-12	6.99	14.13	3	3	3	4.822E4	276	31.6	5.59
<b>P05387</b>	60S acidic ribosomal protein P2	6.94	45.22	0	2	2	2.184E4	115	11.7	4.54
<b>P42899</b>	60S acidic ribosomal protein P2	6.94	45.22	0	2	2	2.184E4	115	11.7	4.61
<b>Q8IYT1</b>	Protein FAM71A	6.89	5.39	2	2	4	7.643E4	594	63.1	9.64
<b>O43805</b>	Sjogren syndrome nuclear autoantigen 1	6.86	20.17	1	2	3	8.416E3	119	13.6	5.38
<b>Q8NHS0</b>	DnaJ homolog subfamily B member 8	6.86	9.91	1	2	3	2.497E3	232	25.7	6.42
<b>Q3MI00</b>	DnaJ homolog subfamily B member 1	6.65	6.76	0	2	3	6.780E4	340	38.2	8.63
<b>Q96QV6</b>	Histone H2A type 1-A	6.65	24.43	0	2	3	5.395E4	131	14.2	10.86
<b>Q2YDI9</b>	Ferritin, mitochondrial	6.63	5.37	0	1	3	8.235E4	242	27.3	7.33
<b>A2A3N6</b>	Putative PIP5K1A and PSMD4-like protein	6.54	1.97	0	1	2	9.150E4	862	95.0	5.71
<b>P55036</b>	26S proteasome non-ATPase regulatory subunit 4	6.54	4.51	0	1	2	9.150E4	377	40.7	4.79
<b>Q58DA0</b>	26S proteasome non-ATPase regulatory subunit 4	6.54	4.45	0	1	2	9.150E4	382	41.4	4.79
<b>Q96EP5</b>	DAZ-associated protein 1	6.51	3.93	1	1	2	4.636E4	407	43.4	8.56
<b>Q8IZP2</b>	Putative protein FAM10A4	6.48	17.08	0	3	4	1.505E5	240	27.4	5.08
<b>P55084</b>	Trifunctional enzyme subunit beta, mitochondrial	6.43	6.12	1	3	3	6.108E3	474	51.3	9.41

<b>Q9Y265</b>	<b>RuvB-like 1</b>	<b>6.33</b>	<b>5.48</b>	<b>2</b>	<b>2</b>	<b>3</b>	<b>2.953E4</b>	<b>456</b>	<b>50.2</b>	<b>6.42</b>
<b>O15173</b>	Membrane-associated progesterone receptor component 2	6.29	8.52	1	1	2	5.591E4	223	23.8	4.88
<b>P68103</b>	Elongation factor 1-alpha 1	6.29	9.31	0	3	3	2.247E5	462	50.1	9.01
<b>Q5VTE0</b>	Putative elongation factor 1-alpha-like 3	6.29	9.31	0	3	3	2.247E5	462	50.2	9.07
<b>Q9BS86</b>	Zona pellucida-binding protein 1	6.26	9.69	3	3	4	5.802E4	351	40.1	9.28
<b>P21912</b>	Succinate dehydrogenase [ubiquinone] iron-sulfur subunit, mitochondrial	6.25	12.50	1	3	3	1.768E4	280	31.6	8.76
<b>P22061</b>	Protein-L-isoaspartate(D-aspartate) O-methyltransferase	6.25	19.82	1	3	3	9.113E3	227	24.6	7.21
<b>P36957</b>	Dihydrolipoyllysine-residue succinyltransferase component of 2-oxoglutarate dehydrogenase complex, mitochondrial	6.19	3.09	0	1	2	1.155E5	453	48.7	8.95
<b>P11179</b>	Dihydrolipoyllysine-residue succinyltransferase component of 2-oxoglutarate dehydrogenase complex, mitochondrial	6.19	3.08	0	1	2	1.155E5	455	48.9	8.95
<b>P0C7P4</b>	Putative cytochrome b-c1 complex subunit Rieske-like protein 1	6.18	9.19	0	1	2	1.182E5	283	30.8	8.87
<b>P47985</b>	Cytochrome b-c1 complex subunit Rieske, mitochondrial	6.18	9.49	0	1	2	1.182E5	274	29.6	8.32
<b>Q56K14</b>	60S acidic ribosomal protein P1	6.14	14.04	1	1	3	4.839E4	114	11.5	4.32
<b>Q3LXA3</b>	Bifunctional ATP-dependent dihydroxyacetone kinase/FAD-AMP lyase (cyclizing)	6.14	5.04	2	2	3	3.369E4	575	58.9	7.49
<b>P10096</b>	Glyceraldehyde-3-phosphate dehydrogenase	6.08	6.31	0	1	2		333	35.8	8.35
<b>Q8TAD1</b>	Sperm protein associated with the nucleus on the X chromosome E	6.08	11.34	0	1	2		97	11.0	5.26
<b>Q9BXN6</b>	Sperm protein associated with the nucleus on the X chromosome D	6.08	11.34	0	1	2		97	11.0	6.11
<b>Q9NS25</b>	Sperm protein associated with the nucleus on the X chromosome B/F	6.08	10.68	0	1	2		103	11.8	6.15
<b>Q9NS26</b>	Sperm protein associated with the nucleus on the X chromosome A	6.08	11.34	0	1	2		97	11.0	5.10

<b>Q9NY87</b>	<b>Sperm protein associated with the nucleus on the X chromosome C</b>	<b>6.08</b>	<b>11.34</b>	<b>0</b>	<b>1</b>	<b>2</b>		<b>97</b>	<b>11.0</b>	<b>5.10</b>
<b>P02743</b>	Serum amyloid P-component	6.03	9.42	2	2	3	3.826E4	223	25.4	6.54
<b>P13861</b>	cAMP-dependent protein kinase type II-alpha regulatory subunit	6.00	7.18	1	2	2	4.202E4	404	45.5	5.07
<b>P30041</b>	Peroxiredoxin-6	5.96	11.61	2	2	3		224	25.0	6.38
<b>P29803</b>	Pyruvate dehydrogenase E1 component subunit alpha, testis-specific form, mitochondrial	5.96	10.05	2	4	4	1.129E4	388	42.9	8.46
<b>Q3ZBD7</b>	Glucose-6-phosphate isomerase	5.96	5.39	0	2	2	1.316E5	557	62.8	7.71
<b>Q5EAC6</b>	Hsp90 co-chaperone Cdc37	5.95	5.53	0	1	2	7.339E4	380	44.6	5.17
<b>O43247</b>	Testis-expressed sequence 33 protein	5.92	6.07	1	1	2		280	30.7	7.99
<b>Q7Z6W1</b>	Transmembrane and coiled-coil domain-containing protein 2	5.89	8.79	1	1	2	1.100E5	182	20.1	8.68
<b>P0CG47</b>	Polyubiquitin-B	5.89	20.96	0	1	2	1.686E4	229	25.7	7.43
<b>P62992</b>	Ubiquitin-40S ribosomal protein S27a	5.89	10.26	0	1	2	1.686E4	156	18.0	9.64
<b>P63048</b>	Ubiquitin-60S ribosomal protein L40	5.89	12.50	0	1	2	1.686E4	128	14.7	9.83
<b>P0CG48</b>	Polyubiquitin-C	5.89	21.02	0	1	2	1.686E4	685	77.0	7.66
<b>P0CG53</b>	Polyubiquitin-B	5.89	20.98	0	1	2	1.686E4	305	34.3	7.47
<b>P0CH28</b>	Polyubiquitin-C	5.89	20.87	0	1	2	1.686E4	690	77.5	7.66
<b>P26436</b>	Acrosomal protein SP-10	5.84	6.04	1	1	2	3.546E4	265	28.1	4.69
<b>P31930</b>	Cytochrome b-c1 complex subunit 1, mitochondrial	5.80	4.58	2	2	3	5.024E4	480	52.6	6.37
<b>P23434</b>	Glycine cleavage system H protein, mitochondrial	5.68	11.56	1	1	2	2.053E4	173	18.9	4.88
<b>Q562R1</b>	Beta-actin-like protein 2	5.61	9.04	1	2	2	4.672E4	376	42.0	5.59
<b>P02751</b>	Fibronectin	5.61	0.63	1	1	2		2386	262.5	5.71
<b>P13929</b>	Beta-enolase	5.60	7.60	0	2	2	8.964E5	434	47.0	7.71
<b>P09104</b>	Gamma-enolase	5.60	7.60	0	2	2	8.964E5	434	47.2	5.03
<b>Q3ZC09</b>	Beta-enolase	5.60	7.60	0	2	2	8.964E5	434	47.1	7.72
<b>P62739</b>	Actin, aortic smooth muscle	5.55	6.90	0	2	2	2.463E4	377	42.0	5.39
<b>Q5E9B5</b>	Actin, gamma-enteric smooth muscle GN=ACTG2 PE=2	5.55	6.91	0	2	2	2.463E4	376	41.8	5.48
<b>Q3ZC07</b>	Actin, alpha cardiac muscle 1	5.55	6.90	0	2	2	2.463E4	377	42.0	5.39
<b>P68138</b>	Actin, alpha skeletal muscle	5.55	6.90	0	2	2	2.463E4	377	42.0	5.39

<b>P41222</b>	<b>Prostaglandin-H2 D-isomerase</b>	<b>5.50</b>	<b>17.37</b>	<b>2</b>	<b>2</b>	<b>2</b>		<b>190</b>	<b>21.0</b>	<b>7.80</b>
<b>Q92526</b>	T-complex protein 1 subunit zeta-2	5.47	6.98	2	2	3	7.760E4	530	57.8	7.24
<b>Q58FG1</b>	Putative heat shock protein HSP 90-alpha A4	5.31	3.11	0	1	2		418	47.7	5.19
<b>P61981</b>	14-3-3 protein gamma	5.21	9.72	0	2	2	1.536E5	247	28.3	4.89
<b>P68252</b>	14-3-3 protein gamma	5.21	9.72	0	2	2	1.536E5	247	28.2	4.89
<b>P62333</b>	26S protease regulatory subunit 10B	5.18	6.43	1	2	2	7.092E4	389	44.1	7.49
<b>O95292</b>	Vesicle-associated membrane protein-associated protein B/C	5.11	9.47	0	2	2	2.466E5	243	27.2	7.30
<b>A2VDZ9</b>	Vesicle-associated membrane protein-associated protein B	5.11	9.47	0	2	2	2.466E5	243	27.1	7.30
<b>P10515</b>	Dihydrolipoyllysine-residue acetyltransferase component of pyruvate dehydrogenase complex, mitochondrial	5.08	2.63	1	1	2		647	69.0	7.84
<b>P52789</b>	Hexokinase-2	5.06	1.20	0	1	2	3.519E4	917	102.3	6.05
<b>Q2YDE4</b>	Proteasome subunit alpha type-6	5.03	8.94	2	2	3	4.957E4	246	27.4	6.76
<b>O75071</b>	EF-hand calcium-binding domain- containing protein 14	5.03	6.06	2	2	2	5.973E4	495	55.0	6.32
<b>P62491</b>	Ras-related protein Rab-11A	5.00	10.19	0	2	2	1.122E4	216	24.4	6.57
<b>Q3MHP2</b>	Ras-related protein Rab-11B	5.00	10.09	0	2	2	1.122E4	218	24.5	5.94
<b>Q2TA29</b>	Ras-related protein Rab-11A	5.00	10.19	0	2	2	1.122E4	216	24.5	6.57
<b>Q5E9C3</b>	Sjogren syndrome nuclear autoantigen 1 homolog	4.99	10.92	0	1	2		119	13.6	5.68
<b>Q9BSF0</b>	Small membrane A-kinase anchor protein	4.95	32.63	2	2	2	1.078E4	95	11.0	4.87
<b>Q9UFH2</b>	Dynein heavy chain 17, axonemal	4.94	0.58	2	2	2	2.658E4	4485	511.5	5.77
<b>P29692</b>	Elongation factor 1-delta	4.90	8.54	1	2	2		281	31.1	5.01
<b>Q5E9F9</b>	26S protease regulatory subunit 7	4.89	11.09	3	3	3	5.850E4	433	48.6	5.95
<b>P25325</b>	3-mercaptopyruvate sulfurtransferase	4.88	13.47	2	2	2	8.313E3	297	33.2	6.60
<b>Q8TAA3</b>	Proteasome subunit alpha type-7- like	4.81	5.86	1	1	2	2.465E4	256	28.5	8.98
<b>Q9BYZ2</b>	L-lactate dehydrogenase A-like 6B	4.81	6.82	2	2	2	3.755E4	381	41.9	8.65
<b>Q9UI46</b>	Dynein intermediate chain 1, axonemal	4.63	5.29	2	2	2	3.027E4	699	79.2	6.87
<b>Q9H0B3</b>	Uncharacterized protein KIAA1683	4.61	2.88	2	2	2	2.628E4	1180	127.6	10.23



<b>Q8N0Y7</b>	<b>Probable phosphoglycerate mutase 4</b>	<b>4.54</b>	<b>9.45</b>	<b>0</b>	<b>2</b>	<b>2</b>		<b>254</b>	<b>28.8</b>	<b>6.65</b>
<b>P13667</b>	Protein disulfide-isomerase A4	4.51	4.19	1	2	2	7.127E4	645	72.9	5.07
<b>P59910</b>	DnaJ homolog subfamily B member 13	4.44	7.91	2	2	2	6.217E4	316	36.1	7.87
<b>P04179</b>	Superoxide dismutase [Mn], mitochondrial	4.35	12.61	1	2	2	1.236E4	222	24.7	8.25
<b>P06394</b>	Keratin, type I cytoskeletal 10	4.31	6.27	0	3	3	5.391E4	526	54.8	5.11
<b>Q9H4B7</b>	Tubulin beta-1 chain	4.25	2.22	0	1	2	4.979E4	451	50.3	5.17
<b>Q3T189</b>	Succinate dehydrogenase [ubiquinone] iron-sulfur subunit, mitochondrial	4.21	6.79	0	2	2	1.848E4	280	31.5	8.60
<b>O46629</b>	Trifunctional enzyme subunit beta, mitochondrial	4.17	4.21	0	2	2	8.652E3	475	51.3	9.32
<b>P55145</b>	Mesencephalic astrocyte-derived neurotrophic factor	4.16	13.74	1	2	2	3.829E4	182	20.7	8.69
<b>P26641</b>	Elongation factor 1-gamma	4.11	5.49	2	2	2	1.115E5	437	50.1	6.67
<b>P00727</b>	Cytosol aminopeptidase	4.09	4.62	0	2	2	8.444E4	519	56.3	6.48
<b>Q5SRN2</b>	Uncharacterized protein C6orf10	4.03	4.26	2	2	2	4.425E4	563	61.6	9.25
<b>Q32PH8</b>	Elongation factor 1-alpha 2	4.01	4.10	0	2	2	8.604E4	463	50.4	9.03
<b>Q6UWQ5</b>	Lysozyme-like protein 1	3.97	8.11	0	1	2		148	16.6	8.05
<b>Q7Z4W2</b>	Lysozyme-like protein 2	3.97	8.11	0	1	2		148	16.6	7.84
<b>P62194</b>	26S protease regulatory subunit 8	3.95	4.43	1	1	1	6.132E4	406	45.6	7.55
<b>P42126</b>	Enoyl-CoA delta isomerase 1, mitochondrial	3.92	4.97	1	1	2	7.706E4	302	32.8	8.54
<b>Q9UNN5</b>	FAS-associated factor 1	3.91	1.69	1	1	2		650	73.9	4.88
<b>P00918</b>	Carbonic anhydrase 2	3.88	13.08	3	3	3	9.047E4	260	29.2	7.40
<b>P49773</b>	Histidine triad nucleotide-binding protein 1	3.82	15.87	1	1	2		126	13.8	6.95
<b>P02533</b>	Keratin, type I cytoskeletal 14	3.80	3.81	0	2	2		472	51.5	5.16
<b>P08779</b>	Keratin, type I cytoskeletal 16	3.80	3.81	0	2	2		473	51.2	5.05
<b>P0CG38</b>	POTE ankyrin domain family member I	3.79	1.58	0	2	2	6.149E3	1075	121.2	6.21
<b>P0CG39</b>	POTE ankyrin domain family member J	3.79	1.64	0	2	2	6.149E3	1038	117.3	5.97
<b>P00515</b>	cAMP-dependent protein kinase type II-alpha regulatory subunit	3.76	4.24	0	1	1	4.202E4	401	45.1	4.93
<b>Q8SQ21</b>	Histidine triad nucleotide-binding protein 2, mitochondrial	3.61	26.99	0	3	3	2.521E5	163	17.1	7.50

<b>Q99536</b>	<b>Synaptic vesicle membrane protein VAT-1 homolog</b>	<b>3.47</b>	<b>4.33</b>	<b>1</b>	<b>1</b>	<b>2</b>	<b>1.754E4</b>	<b>393</b>	<b>41.9</b>	<b>6.29</b>
<b>P11310</b>	Medium-chain specific acyl-CoA dehydrogenase, mitochondrial	3.46	4.28	1	1	1	4.903E4	421	46.6	8.37
<b>Q9NQ60</b>	Equatorin	3.41	8.50	2	2	2	9.178E3	294	32.8	5.00
<b>Q9BYX7</b>	Putative beta-actin-like protein 3	3.40	4.27	0	1	1	4.049E4	375	42.0	6.33
<b>P15246</b>	Protein-L-isoaspartate(D-aspartate) O-methyltransferase	3.37	14.98	0	2	2	9.113E3	227	24.5	7.58
<b>Q0P565</b>	HD domain-containing protein 2	3.32	8.78	0	1	1	3.816E4	205	23.3	5.16
<b>Q5THR3</b>	EF-hand calcium-binding domain-containing protein 6	3.17	1.33	1	1	1	4.724E4	1501	172.8	8.40
<b>Q7Z794</b>	Keratin, type II cytoskeletal 1b	3.17	2.08	0	1	1	5.205E3	578	61.9	5.99
<b>Q12931</b>	Heat shock protein 75 kDa, mitochondrial	3.13	1.99	0	1	1	1.660E5	704	80.1	8.21
<b>Q2TBI4</b>	Heat shock protein 75 kDa, mitochondrial	3.13	1.99	0	1	1	1.660E5	703	79.3	7.14
<b>Q2T9X2</b>	T-complex protein 1 subunit delta	3.11	7.38	0	2	2	9.300E4	542	58.2	7.33
<b>Q9H4B8</b>	Dipeptidase 3	3.05	3.89	1	1	1	5.382E4	488	53.7	7.96
<b>Q9UBS4</b>	DnaJ homolog subfamily B member 11	2.97	4.47	0	1	1		358	40.5	6.18
<b>Q3ZBA6</b>	DnaJ homolog subfamily B member 11	2.97	4.47	0	1	1		358	40.5	6.32
<b>O95473</b>	Synaptogyrin-4	2.96	6.41	1	1	1	2.075E4	234	25.8	7.75
<b>Q8TF09</b>	Dynein light chain roadblock-type 2	2.94	16.67	0	1	1	1.707E5	96	10.8	7.50
<b>Q32P85</b>	Dynein light chain roadblock-type 2	2.94	16.67	0	1	1	1.707E5	96	10.8	7.44
<b>P13639</b>	Elongation factor 2	2.92	2.80	0	1	1	6.702E3	858	95.3	6.83
<b>Q3SYU2</b>	Elongation factor 2	2.92	2.80	0	1	1	6.702E3	858	95.3	6.83
<b>Q8TDM5</b>	Sperm acrosome membrane-associated protein 4	2.90	10.48	1	1	1		124	13.0	5.80
<b>Q9NR28</b>	Diablo homolog, mitochondrial	2.88	4.18	1	1	1	7.327E4	239	27.1	5.90
<b>P00442</b>	Superoxide dismutase [Cu-Zn]	2.81	7.89	0	1	1		152	15.7	6.32
<b>Q3SZI4</b>	14-3-3 protein theta	2.78	7.76	0	2	2	1.524E5	245	27.7	4.78
<b>P31946</b>	14-3-3 protein beta/alpha	2.78	7.72	0	2	2	1.524E5	246	28.1	4.83
<b>P31947</b>	14-3-3 protein sigma	2.78	4.03	0	1	1	2.972E5	248	27.8	4.74
<b>P62261</b>	14-3-3 protein epsilon	2.78	3.92	0	1	1	2.972E5	255	29.2	4.74
<b>Q04917</b>	14-3-3 protein eta	2.78	4.07	0	1	1	2.972E5	246	28.2	4.84
<b>P68509</b>	14-3-3 protein eta	2.78	4.07	0	1	1	2.972E5	246	28.2	4.89
<b>P68250</b>	14-3-3 protein beta/alpha	2.78	7.72	0	2	2	1.524E5	246	28.1	4.87

<b>Q0VC36</b>	<b>14-3-3 protein sigma</b>	<b>2.78</b>	<b>4.03</b>	<b>0</b>	<b>1</b>	<b>1</b>	<b>2.972E5</b>	<b>248</b>	<b>27.8</b>	<b>4.72</b>
<b>Q2KIW6</b>	26S protease regulatory subunit 10B	2.74	3.60	0	1	1	1.355E5	389	44.0	7.20
<b>A1A4R1</b>	Histone H2A type 2-C	2.72	21.71	0	2	3	1.514E5	129	14.0	10.90
<b>Q6FI13</b>	Histone H2A type 2-A	2.72	21.54	0	2	3	1.514E5	130	14.1	10.90
<b>Q96C74</b>	Ropporin-1-like protein	2.71	7.83	1	1	1	3.536E4	230	26.1	7.72
<b>Q8NBX0</b>	Saccharopine dehydrogenase-like oxidoreductase	2.68	3.03	1	1	1	2.048E5	429	47.1	9.14
<b>Q8N427</b>	Thioredoxin domain-containing protein 3	2.66	2.89	1	1	1	5.120E4	588	67.2	4.97
<b>Q9BVL2</b>	Nucleoporin p58/p45	2.62	2.84	1	1	1		599	60.9	9.33
<b>Q9H0C2</b>	ADP/ATP translocase 4	2.58	4.13	0	1	1		315	35.0	9.89
<b>Q2YDD9</b>	ADP/ATP translocase 4	2.58	4.02	0	1	1		323	35.7	9.55
<b>P09622</b>	Dihydrolipoyl dehydrogenase, mitochondrial	2.56	2.55	1	1	1		509	54.1	7.85
<b>O95202</b>	LETM1 and EF-hand domain-containing protein 1, mitochondrial	2.55	5.28	1	2	2	4.061E4	739	83.3	6.70
<b>Q0VCA3</b>	LETM1 and EF-hand domain-containing protein 1, mitochondrial	2.55	1.64	0	1	1	2.802E4	732	81.8	6.73
<b>Q9BY14</b>	Testis-expressed sequence 101 protein	2.53	5.62	1	1	1	1.136E5	249	26.6	4.94
<b>Q3T064</b>	Ropporin-1	2.51	4.25	0	1	1		212	24.0	5.27
<b>P13646</b>	Keratin, type I cytoskeletal 13	2.51	2.40	0	1	1	5.819E4	458	49.6	4.96
<b>Q2M2I5</b>	Keratin, type I cytoskeletal 24	2.51	2.10	0	1	1	5.819E4	525	55.1	4.96
<b>P15374</b>	Ubiquitin carboxyl-terminal hydrolase isozyme L3	2.51	6.96	0	1	1		230	26.2	4.92
<b>Q2TBG8</b>	Ubiquitin carboxyl-terminal hydrolase isozyme L3	2.51	6.96	0	1	1		230	26.2	4.92
<b>Q96HR9</b>	Receptor expression-enhancing protein 6	2.50	7.07	1	1	1		184	20.7	8.56
<b>P15104</b>	Glutamine synthetase	2.50	4.56	1	1	1		373	42.0	6.89
<b>O75521</b>	Enoyl-CoA delta isomerase 2, mitochondrial	2.50	3.05	1	1	1	2.038E5	394	43.6	9.00
<b>Q58FF3</b>	Putative endoplasmic-like protein	2.50	2.51	0	1	2	9.379E3	399	45.8	5.26
<b>Q8N1F7</b>	Nuclear pore complex protein Nup93	2.49	3.17	0	1	1	5.712E4	819	93.4	5.72
<b>A5PJZ5</b>	Nuclear pore complex protein Nup93 ]	2.49	3.17	0	1	1	5.712E4	819	93.4	5.72
<b>P04259</b>	Keratin, type II cytoskeletal 6B	2.48	1.77	0	1	1	3.295E4	564	60.0	8.00

<b>P42785</b>	<b>Lysosomal Pro-X carboxypeptidase</b>	<b>2.48</b>	<b>2.82</b>	<b>1</b>	<b>1</b>	<b>1</b>		<b>496</b>	<b>55.8</b>	<b>7.21</b>
<b>P00505</b>	Aspartate aminotransferase, mitochondrial	2.47	3.26	1	1	1	6.630E4	430	47.5	9.01
<b>O60884</b>	DnaJ homolog subfamily A member 2	2.46	6.55	0	2	2	9.562E4	412	45.7	6.48
<b>Q2HJ94</b>	DnaJ homolog subfamily A member 2	2.46	6.55	0	2	2	9.562E4	412	45.7	6.48
<b>Q6P2I3</b>	Fumarylacetoacetate hydrolase domain-containing protein 2B	2.46	5.41	0	1	1	9.859E4	314	34.6	7.75
<b>Q96GK7</b>	Fumarylacetoacetate hydrolase domain-containing protein 2A	2.46	5.41	0	1	1	9.859E4	314	34.6	8.24
<b>Q96LK8</b>	Spermatogenesis-associated protein 32	2.45	4.95	1	1	1	8.276E4	384	42.3	4.77
<b>Q9BGI1</b>	Peroxioredoxin-5, mitochondrial	2.44	3.65	0	1	1	9.084E4	219	23.2	8.07
<b>P55854</b>	Small ubiquitin-related modifier 3	2.43	11.65	0	1	1		103	11.6	5.49
<b>P61955</b>	Small ubiquitin-related modifier 2	2.43	12.63	0	1	1		95	10.9	5.50
<b>Q6EEV6</b>	Small ubiquitin-related modifier 4	2.43	12.63	0	1	1		95	10.7	7.18
<b>Q17QV3</b>	Small ubiquitin-related modifier 3	2.43	11.54	0	1	1		104	11.7	5.95
<b>P41976</b>	Superoxide dismutase [Mn], mitochondrial	2.42	6.31	0	1	1		222	24.6	8.54
<b>Q5VZ72</b>	Izumo sperm-egg fusion protein 3	2.41	3.77	1	1	1	1.325E4	239	27.7	8.29
<b>Q32LE5</b>	Isoaspartyl peptidase/L- asparaginase	2.40	3.90	0	1	1		308	32.0	7.40
<b>Q86VQ3</b>	Thioredoxin domain-containing protein 2	2.39	8.14	2	2	2		553	60.4	4.87
<b>Q9HAE3</b>	EF-hand calcium-binding domain- containing protein 1	2.36	5.21	1	1	1	3.218E4	211	24.5	5.06
<b>Q96BH3</b>	Epididymal sperm-binding protein 1	2.34	5.83	1	1	1		223	26.1	6.62
<b>P20674</b>	Cytochrome c oxidase subunit 5A, mitochondrial	2.34	6.00	1	1	1	1.770E4	150	16.8	6.79
<b>Q14697</b>	Neutral alpha-glucosidase AB	2.34	1.59	1	1	1	5.476E4	944	106.8	6.14
<b>P56597</b>	Nucleoside diphosphate kinase homolog 5	2.33	8.49	1	1	1		212	24.2	6.29
<b>P28070</b>	Proteasome subunit beta type-4	2.32	3.79	0	1	1		264	29.2	5.97
<b>Q3T108</b>	Proteasome subunit beta type-4	2.32	3.79	0	1	1		264	29.0	5.67
<b>Q96GG9</b>	DCN1-like protein 1	2.32	6.56	1	1	1	7.175E3	259	30.1	5.34
<b>P09496</b>	Clathrin light chain A	2.32	3.63	0	1	1	2.940E3	248	27.1	4.51
<b>P04973</b>	Clathrin light chain A =1 -	2.32	3.70	0	1	1	2.940E3	243	26.7	4.51
<b>P02769</b>	Serum albumin	2.31	2.47	0	1	1	4.697E4	607	69.2	6.18

<b>Q16563</b>	<b>Synaptophysin-like protein 1</b>	<b>2.29</b>	<b>4.25</b>	<b>1</b>	<b>1</b>	<b>1</b>		<b>259</b>	<b>28.5</b>	<b>8.43</b>
<b>P36542</b>	ATP synthase subunit gamma, mitochondrial	2.27	4.03	1	1	1	4.119E4	298	33.0	9.22
<b>Q99417</b>	C-Myc-binding protein	2.25	25.24	0	2	2		103	12.0	5.91
<b>Q2TBP7</b>	C-Myc-binding protein	2.25	25.24	0	2	2		103	12.0	5.91
<b>O14645</b>	Axonemal dynein light intermediate polypeptide 1	2.24	6.59	1	1	2	7.518E4	258	29.6	8.50
<b>Q5EA85</b>	Semaphorin-4A	2.23	2.36	1	1	1		762	83.6	6.54
<b>Q58FF6</b>	Putative heat shock protein HSP 90-beta 4	2.23	3.76	0	2	2	2.628E5	505	58.2	4.73
<b>P52565</b>	Rho GDP-dissociation inhibitor 1	2.21	7.35	1	1	1	2.587E4	204	23.2	5.11
<b>P30046</b>	D-dopachrome decarboxylase	2.19	9.32	1	1	1	4.206E4	118	12.7	7.30
<b>P34949</b>	Mannose-6-phosphate isomerase	2.18	3.78	1	1	1		423	46.6	5.95
<b>Q9Y4F5</b>	Centrosomal protein of 170 kDa protein B	2.17	0.69	1	1	1	1.316E5	1589	171.6	6.84
<b>A5D989</b>	Elongation factor 1-delta	2.17	4.29	0	1	1		280	31.1	5.06
<b>P54725</b>	UV excision repair protein RAD23 homolog A	2.17	2.20	0	1	1	2.971E4	363	39.6	4.58
<b>A3KMV2</b>	UV excision repair protein RAD23 homolog A	2.17	2.21	0	1	1	2.971E4	362	39.6	4.58
<b>Q9BVM2</b>	Protein DPCD	2.16	4.93	1	1	1	2.046E4	203	23.2	9.03
<b>P29144</b>	Tripeptidyl-peptidase 2	2.15	0.88	1	1	1		1249	138.3	6.32
<b>Q9NQC3</b>	Reticulon-4	2.11	0.92	1	1	1	5.728E3	1192	129.9	4.50
<b>Q2NKU6</b>	Protein dpy-30 homolog	2.10	9.09	1	1	1		99	11.2	4.88
<b>P24539</b>	ATP synthase F(0) complex subunit B1, mitochondrial	2.10	4.69	1	1	1	1.218E4	256	28.9	9.36
<b>P02545</b>	Prelamin-A/C	2.09	1.36	1	1	1	8.717E3	664	74.1	7.02
<b>P25786</b>	Proteasome subunit alpha type-1	2.09	5.70	0	1	1		263	29.5	6.61
<b>Q3T0X5</b>	Proteasome subunit alpha type-1	2.09	5.70	0	1	1		263	29.6	6.61
<b>P35968</b>	Vascular endothelial growth factor receptor 2	2.09	0.66	1	1	1		1356	151.4	5.85
<b>P27824</b>	Calnexin	2.09	2.03	1	1	1	1.845E4	592	67.5	4.60
<b>Q15435</b>	Protein phosphatase 1 regulatory subunit 7	2.08	5.28	1	2	2	2.950E4	360	41.5	4.91
<b>O75951</b>	Lysozyme-like protein 6	2.06	6.08	1	1	1	5.879E4	148	16.9	6.14
<b>Q29RV1</b>	Protein disulfide-isomerase A4	2.04	2.33	0	1	1	1.023E5	643	72.5	5.12
<b>Q9H1X1</b>	Radial spoke head protein 9 homolog	2.04	11.23	2	2	2	3.263E4	276	31.3	5.43

<b>P04792</b>	<b>Heat shock protein beta-1</b>	<b>2.03</b>	<b>4.88</b>	<b>0</b>	<b>1</b>	<b>1</b>		<b>205</b>	<b>22.8</b>	<b>6.40</b>
<b>Q3T149</b>	Heat shock protein beta-1	2.03	4.98	0	1	1		201	22.4	6.40
<b>Q9H853</b>	Putative tubulin-like protein alpha-4B	2.01	5.81	0	1	1	3.616E4	241	27.5	7.83
<b>O00330</b>	Pyruvate dehydrogenase protein X component, mitochondrial	2.00	3.39	0	1	1	4.838E4	501	54.1	8.66
<b>P22439</b>	Pyruvate dehydrogenase protein X component	2.00	3.39	0	1	1	4.838E4	501	53.9	8.44
<b>Q9Y2B0</b>	Protein canopy homolog 2	2.00	8.79	1	1	1	4.430E4	182	20.6	4.92
<b>Q7Z3Y7</b>	Keratin, type I cytoskeletal 28	1.99	1.94	0	1	1		464	50.5	5.47
<b>Q7Z3Y8</b>	Keratin, type I cytoskeletal 27	1.99	1.96	0	1	1		459	49.8	5.05
<b>Q7Z3Y9</b>	Keratin, type I cytoskeletal 26	1.99	1.92	0	1	1		468	51.9	4.92
<b>Q7Z3Z0</b>	Keratin, type I cytoskeletal 25	1.99	2.00	0	1	1		450	49.3	5.08
<b>Q0P5J4</b>	Keratin, type I cytoskeletal 25	1.99	2.00	0	1	1		450	49.3	5.03
<b>Q0P5J6</b>	Keratin, type I cytoskeletal 27	1.99	1.96	0	1	1		460	49.9	5.10
<b>Q148H6</b>	Keratin, type I cytoskeletal 28	1.99	1.94	0	1	1		464	50.7	5.30
<b>O77797</b>	A-kinase anchor protein 3	1.97	1.17	0	1	1	1.760E4	858	94.6	6.71
<b>Q9BUR5</b>	Apolipoprotein O	1.95	5.56	1	1	1	5.789E4	198	22.3	9.13
<b>O75190</b>	DnaJ homolog subfamily B member 6	1.95	3.07	0	1	1	2.497E3	326	36.1	9.16
<b>P25686</b>	DnaJ homolog subfamily B member 2	1.95	3.09	0	1	1	2.497E3	324	35.6	5.95
<b>Q0III6</b>	DnaJ homolog subfamily B member 6	1.95	4.13	0	1	1	2.497E3	242	26.9	7.61
<b>Q96RQ9</b>	L-amino-acid oxidase	1.94	1.76	1	1	1	6.345E4	567	62.8	8.68
<b>Q8TE73</b>	Dynein heavy chain 5, axonemal	1.93	0.17	1	1	1		4624	528.7	6.10
<b>Q8N387</b>	Mucin-15	1.93	2.99	1	1	1		334	36.3	5.08
<b>Q14203</b>	Dynactin subunit 1	1.92	0.94	1	1	1		1278	141.6	5.81
<b>O43242</b>	26S proteasome non-ATPase regulatory subunit 3	1.92	2.06	0	1	1		534	60.9	8.44
<b>Q2KJ46</b>	26S proteasome non-ATPase regulatory subunit 3	1.92	2.06	0	1	1		534	60.9	8.60
<b>P27482</b>	Calmodulin-like protein 3	1.91	5.37	0	1	1	4.226E5	149	16.9	4.42
<b>Q8IYS0</b>	GRAM domain-containing protein 1C	1.88	1.21	1	1	1	4.697E3	662	76.0	7.24
<b>P46379</b>	Large proline-rich protein BAG6	1.88	2.03	2	2	2	1.105E5	1132	119.3	5.60
<b>P28072</b>	Proteasome subunit beta type-6	1.88	4.60	1	1	1	2.213E4	239	25.3	4.92
<b>Q6UXV1</b>	Izumo sperm-egg fusion protein 2	1.86	6.33	1	1	1	3.072E4	221	24.8	8.79

<b>A5PKW4</b>	<b>PH and SEC7 domain-containing protein 1</b>	<b>1.86</b>	<b>1.07</b>	<b>1</b>	<b>1</b>	<b>1</b>	<b>3.813E4</b>	<b>1024</b>	<b>109.5</b>	<b>6.87</b>	
<b>P08727</b>	Keratin, type I cytoskeletal 19	1.81	2.25	0	1	1			400	44.1	5.14
<b>P19012</b>	Keratin, type I cytoskeletal 15	1.81	1.97	0	1	1			456	49.2	4.77
<b>Q04695</b>	Keratin, type I cytoskeletal 17	1.81	2.08	0	1	1			432	48.1	5.02
<b>A1L595</b>	Keratin, type I cytoskeletal 17	1.81	2.04	0	1	1			441	48.7	5.15
<b>P08728</b>	Keratin, type I cytoskeletal 19	1.81	2.26	0	1	1			399	43.9	5.01
<b>Q6J272</b>	Protein FAM166A	1.81	3.79	1	1	1		2.195E4	317	36.1	7.81
<b>Q9BQP9</b>	BPI fold-containing family A member 3	1.81	3.54	1	1	1			254	28.4	6.65
<b>P48047</b>	ATP synthase subunit O, mitochondrial	1.80	5.63	1	1	1			213	23.3	9.96
<b>Q92896</b>	Golgi apparatus protein 1	1.79	1.10	1	1	1			1179	134.5	6.90
<b>P07107</b>	Acyl-CoA-binding protein	1.78	9.20	0	1	1		2.045E5	87	10.0	6.57
<b>P13696</b>	Phosphatidylethanolamine-binding protein 1	1.77	7.49	0	1	1		1.209E5	187	21.0	7.49
<b>P14174</b>	Macrophage migration inhibitory factor	1.75	7.83	1	1	1		2.094E5	115	12.5	7.88
<b>Q5JVL4</b>	EF-hand domain-containing protein 1	1.74	1.25	1	1	1		2.528E4	640	73.9	6.16
<b>Q15046</b>	Lysine--tRNA ligase	1.72	2.01	1	1	1			597	68.0	6.35
<b>Q15631</b>	Translin	1.71	4.39	0	1	1		5.379E3	228	26.2	6.44
<b>Q08DM8</b>	Translin	1.71	4.39	0	1	1		5.379E3	228	26.2	6.44
<b>O60814</b>	Histone H2B type 1-K	1.66	8.73	0	1	3		1.930E4	126	13.9	10.32
<b>P06899</b>	Histone H2B type 1-J	1.66	8.73	0	1	3		1.930E4	126	13.9	10.32
<b>P23527</b>	Histone H2B type 1-O	1.66	8.73	0	1	3		1.930E4	126	13.9	10.32
<b>P33778</b>	Histone H2B type 1-B	1.66	8.73	0	1	3		1.930E4	126	13.9	10.32
<b>P57053</b>	Histone H2B type F-S	1.66	8.73	0	1	3		1.930E4	126	13.9	10.37
<b>P58876</b>	Histone H2B type 1-D	1.66	8.73	0	1	3		1.930E4	126	13.9	10.32
<b>P62807</b>	Histone H2B type 1-C/E/F/G/I	1.66	8.73	0	1	3		1.930E4	126	13.9	10.32
<b>Q16778</b>	Histone H2B type 2-E	1.66	8.73	0	1	3		1.930E4	126	13.9	10.32
<b>Q5QNW6</b>	Histone H2B type 2-F	1.66	8.73	0	1	3		1.930E4	126	13.9	10.32
<b>Q8N257</b>	Histone H2B type 3-B	1.66	8.73	0	1	3		1.930E4	126	13.9	10.32
<b>Q93079</b>	Histone H2B type 1-H	1.66	8.73	0	1	3		1.930E4	126	13.9	10.32
<b>Q96A08</b>	Histone H2B type 1-A	1.66	8.66	0	1	3		1.930E4	127	14.2	10.32
<b>Q99877</b>	Histone H2B type 1-N	1.66	8.73	0	1	3		1.930E4	126	13.9	10.32
<b>Q99879</b>	Histone H2B type 1-M	1.66	8.73	0	1	3		1.930E4	126	14.0	10.32
<b>Q99880</b>	Histone H2B type 1-L	1.66	8.73	0	1	3		1.930E4	126	13.9	10.32

<b>Q2M2T1</b>	<b>Histone H2B type 1-K</b>	<b>1.66</b>	<b>8.73</b>	<b>0</b>	<b>1</b>	<b>3</b>	<b>1.930E4</b>	<b>126</b>	<b>13.9</b>	<b>10.29</b>
<b>Q32L48</b>	Histone H2B type 1-N	1.66	8.73	0	1	3	1.930E4	126	13.9	10.32
<b>Q99490</b>	Arf-GAP with GTPase, ANK repeat and PH domain-containing protein 2	1.65	0.67	0	1	1		1192	124.6	9.89
<b>O94905</b>	Erlin-2	1.64	3.54	1	1	1	7.960E3	339	37.8	5.62
<b>P80513</b>	Mesencephalic astrocyte-derived neurotrophic factor	1.63	5.59	0	1	1		179	20.3	8.54
<b>P00338</b>	L-lactate dehydrogenase A chain	1.62	6.02	1	1	1	2.796E3	332	36.7	8.27
<b>A7YWG4</b>	Gamma-glutamyl hydrolase	1.62	3.14	0	1	1		318	35.7	9.06
<b>P55052</b>	Fatty acid-binding protein, epidermal	1.61	6.67	0	1	1		135	15.1	7.69
<b>B2RXF5</b>	Zinc finger and BTB domain-containing protein 42	0.00	3.08	1	1	1	6.901E3	422	46.5	8.47
<b>O60232</b>	Sjogren syndrome/scleroderma autoantigen 1	0.00	4.02	1	1	1	2.285E4	199	21.5	5.24
<b>P00492</b>	Hypoxanthine-guanine phosphoribosyltransferase	0.00	4.59	1	1	1	2.227E4	218	24.6	6.68
<b>P0C0S4</b>	Histone H2A.Z	0.00	7.03	0	1	1		128	13.5	10.58
<b>P11169</b>	Solute carrier family 2, facilitated glucose transporter member 3	0.00	1.81	0	1	1		496	53.9	7.20
<b>P18754</b>	Regulator of chromosome condensation	0.00	3.56	1	1	1	5.592E4	421	44.9	7.52
<b>P20810</b>	Calpastatin	0.00	2.40	1	1	1	4.461E4	708	76.5	5.07
<b>P23786</b>	Carnitine O-palmitoyltransferase 2, mitochondrial	0.00	1.82	0	1	1	1.942E4	658	73.7	8.18
<b>P28074</b>	Proteasome subunit beta type-5	0.00	4.56	1	1	1	7.885E3	263	28.5	6.92
<b>P29218</b>	Inositol monophosphatase 1	0.00	7.94	2	2	2	2.115E4	277	30.2	5.26
<b>P45880</b>	Voltage-dependent anion-selective channel protein 2	0.00	3.40	0	1	1		294	31.5	7.56
<b>P49748</b>	Very long-chain specific acyl-CoA dehydrogenase, mitochondrial	0.00	2.90	1	1	1	3.976E4	655	70.3	8.75
<b>P53597</b>	Succinyl-CoA ligase [ADP/GDP-forming] subunit alpha, mitochondrial	0.00	4.34	1	1	1		346	36.2	8.79
<b>P54107</b>	Cysteine-rich secretory protein 1	0.00	8.03	1	1	1	6.720E4	249	28.5	5.91
<b>Q15785</b>	Mitochondrial import receptor subunit TOM34	0.00	2.91	1	1	1	1.556E4	309	34.5	8.98
<b>Q32LA7</b>	Histone H2A.V	0.00	7.03	0	1	1		128	13.5	10.58



<b>A7MBJ5</b>	<b>Cullin-associated NEDD8-dissociated protein 1</b>	<b>0.00</b>	<b>1.06</b>	<b>1</b>	<b>1</b>	<b>1</b>	<b>1.109E5</b>	<b>1230</b>	<b>136.3</b>	<b>5.78</b>
<b>Q8NAM6</b>	Zinc finger and SCAN domain-containing protein 4	0.00	2.08	1	1	1		433	48.9	6.95
<b>Q8TDB8</b>	Solute carrier family 2, facilitated glucose transporter member 14	0.00	1.73	0	1	1		520	56.3	7.83
<b>Q96E40</b>	Uncharacterized protein C9orf9	0.00	10.36	2	2	2		222	25.1	9.13
<b>Q96KW9</b>	Protein SPACA7	0.00	5.13	1	1	1	3.939E3	195	21.5	4.78
<b>Q9BYC2</b>	Succinyl-CoA:3-ketoacid coenzyme A transferase 2, mitochondrial	0.00	5.22	1	1	1	6.651E4	517	56.1	7.14
<b>Q9C0H9</b>	SRC kinase signaling inhibitor 1	0.00	1.42	1	1	1		1055	112.4	9.29
<b>Q9H0K4</b>	Radial spoke head protein 6 homolog A	0.00	1.81	1	1	1	1.168E4	717	80.9	4.39
<b>Q9NVE4</b>	Coiled-coil domain-containing protein 87	0.00	0.82	1	1	1		849	96.3	8.59
<b>Q9P1Z2</b>	Calcium-binding and coiled-coil domain-containing protein 1	0.00	1.01	0	1	1		691	77.3	4.82
<b>Q9UJ68</b>	Mitochondrial peptide methionine sulfoxide reductase	0.00	6.38	1	1	1	2.974E4	235	26.1	8.09
<b>Q9UNZ2</b>	NSFL1 cofactor p47	0.00	3.24	0	1	1		370	40.5	5.10
<b>P13620</b>	ATP synthase subunit d, mitochondrial	0.00	5.59	0	1	1	7.300E4	161	18.7	6.24
<b>P58352</b>	Solute carrier family 2, facilitated glucose transporter member 3	0.00	1.82	0	1	1		494	54.0	5.60
<b>P68002</b>	Voltage-dependent anion-selective channel protein 2	0.00	3.40	0	1	1		294	31.6	7.55
<b>Q2KIL1</b>	Uncharacterized protein C1orf141 homolog	0.00	3.95	1	1	1		430	49.7	9.73
<b>Q2KJ21</b>	Calcium-binding and coiled-coil domain-containing protein 1	0.00	1.03	0	1	1		680	75.6	4.93
<b>Q2KJB7</b>	Carnitine O-palmitoyltransferase 2, mitochondrial	0.00	1.82	0	1	1	1.942E4	658	74.4	8.13
<b>Q3SZC4</b>	NSFL1 cofactor p47	0.00	3.24	0	1	1		370	40.6	5.19
<b>Q3T0W4</b>	Protein phosphatase 1 regulatory subunit 7	0.00	2.78	0	1	1		360	41.4	4.96

**Appendix Table 5.5.** Proteins found in both non-binding fractions and no overlap with HA-binding fractions (ND: Not detected).

<b>UniProt/SwissProt Accession</b>	<b>Description</b>	<b>Uniprot Gene Name</b>	<b>Potential HA- binding domain (N)</b>
<u><a href="#">O14645</a></u>	dynein axonemal light intermediate chain 1	<u><a href="#">DNALI1</a></u>	BX7B (1)
<u><a href="#">O15173</a></u>	progesterone receptor membrane component 2	<u><a href="#">PGRMC2</a></u>	BX7B (1)
<u><a href="#">O43805</a></u>	SS nuclear autoantigen 1	<u><a href="#">SSNA1</a></u>	N/D
<u><a href="#">O60664</a></u>	perilipin 3	<u><a href="#">PLIN3</a></u>	N/D
<u><a href="#">O75071</a></u>	EF-hand calcium binding domain 14	<u><a href="#">EFCAB14</a></u>	N/D
<u><a href="#">O75521</a></u>	enoyl-CoA delta isomerase 2	<u><a href="#">ECI2</a></u>	BX7B (3)
<u><a href="#">O75947</a></u>	ATP synthase, H <sup>+</sup> transporting, mitochondrial Fo complex subunit D	<u><a href="#">ATP5H</a></u>	N/D
<u><a href="#">O75951</a></u>	lysozyme like 6	<u><a href="#">LYZL6</a></u>	N/D
<u><a href="#">O95202</a></u>	leucine zipper and EF-hand containing transmembrane protein 1	<u><a href="#">LETM1</a></u>	N/D
<u><a href="#">O95757</a></u>	heat shock protein family A (Hsp70) member 4 like	<u><a href="#">HSPA4L</a></u>	BX7B (1)
<u><a href="#">P00441</a></u>	superoxide dismutase 1, soluble	<u><a href="#">SOD1</a></u>	N/D
<u><a href="#">P02751</a></u>	fibronectin 1	<u><a href="#">FN1</a></u>	BX7B (4)
<u><a href="#">P07108</a></u>	diazepam binding inhibitor, acyl-CoA binding protein	<u><a href="#">DBI</a></u>	N/D
<u><a href="#">P10515</a></u>	dihydrolipoamide S-acetyltransferase	<u><a href="#">DLAT</a></u>	N/D
<u><a href="#">P10809</a></u>	heat shock protein family D (Hsp60) member 1	<u><a href="#">HSPD1</a></u>	N/D
<u><a href="#">P12273</a></u>	prolactin induced protein	<u><a href="#">PIP</a></u>	N/D
<u><a href="#">P12821</a></u>	angiotensin I converting enzyme	<u><a href="#">ACE</a></u>	N/D
<u><a href="#">P13639</a></u>	eukaryotic translation elongation factor 2	<u><a href="#">EEF2</a></u>	N/D
<u><a href="#">P13861</a></u>	protein kinase cAMP-dependent type II regulatory subunit alpha	<u><a href="#">PRKAR2A</a></u>	N/D
<u><a href="#">P14174</a></u>	macrophage migration inhibitory factor (glycosylation-inhibiting factor)	<u><a href="#">MIF</a></u>	N/D
<u><a href="#">P14314</a></u>	protein kinase C substrate 80K-H	<u><a href="#">PRKCSH</a></u>	N/D
<u><a href="#">P14927</a></u>	ubiquinol-cytochrome c reductase binding protein	<u><a href="#">UQCRB</a></u>	N/D
<u><a href="#">P15289</a></u>	arylsulfatase A	<u><a href="#">ARSA</a></u>	N/D
<u><a href="#">P17174</a></u>	glutamic-oxaloacetic transaminase 1	<u><a href="#">GOT1</a></u>	N/D
<u><a href="#">P18859</a></u>	ATP synthase, H <sup>+</sup> transporting, mitochondrial Fo complex subunit F6	<u><a href="#">ATP5J</a></u>	N/D
<u><a href="#">P20674</a></u>	cytochrome c oxidase subunit 5A	<u><a href="#">COX5A</a></u>	N/D
<u><a href="#">P20810</a></u>	calpastatin	<u><a href="#">CAST</a></u>	BX7B (2)

<b><u>P22695</u></b>	ubiquinol-cytochrome c reductase core protein II	<b><u>UQCRC2</u></b>	N/D
<b><u>P25325</u></b>	mercaptopyruvate sulfurtransferase	<b><u>MPST</u></b>	N/D
<b><u>P27797</u></b>	calreticulin	<b><u>CALR</u></b>	BX7B (1)
<b><u>P27824</u></b>	calnexin	<b><u>CANX</u></b>	BX7B (1)
<b><u>P29692</u></b>	eukaryotic translation elongation factor 1 delta	<b><u>EEF1D</u></b>	N/D
<b><u>P30044</u></b>	peroxiredoxin 5	<b><u>PRDX5</u></b>	N/D
<b><u>P30086</u></b>	phosphatidylethanolamine binding protein 1	<b><u>PEBP1</u></b>	BX7B (1)
<b><u>P31930</u></b>	ubiquinol-cytochrome c reductase core protein I	<b><u>UQCRC1</u></b>	N/D
<b><u>P31937</u></b>	3-hydroxyisobutyrate dehydrogenase	<b><u>HIBADH</u></b>	N/D
<b><u>P37198</u></b>	nucleoporin 62	<b><u>NUP62</u></b>	N/D
<b><u>P46379</u></b>	BCL2 associated athanogene 6	<b><u>BAG6</u></b>	BX7B (2)
<b><u>P48047</u></b>	ATP synthase, H <sup>+</sup> transporting, mitochondrial F1 complex, O subunit	<b><u>ATP5O</u></b>	BX7B (1)
<b><u>P48643</u></b>	chaperonin containing TCP1 subunit 5	<b><u>CCT5</u></b>	N/D
<b><u>P50991</u></b>	chaperonin containing TCP1 subunit 4	<b><u>CCT4</u></b>	BX7B (1)
<b><u>P54709</u></b>	ATPase Na <sup>+</sup> /K <sup>+</sup> transporting subunit beta 3	<b><u>ATP1B3</u></b>	BX7B (3)
<b><u>P54727</u></b>	RAD23 homolog B, nucleotide excision repair protein	<b><u>RAD23B</u></b>	N/D
<b><u>P59282</u></b>	tubulin polymerization promoting protein family member 2	<b><u>TPPP2</u></b>	N/D
<b><u>P62491</u></b>	RAB11A, member RAS oncogene family	<b><u>RAB11A</u></b>	N/D
<b><u>Q04837</u></b>	single stranded DNA binding protein 1	<b><u>SSBP1</u></b>	N/D
<b><u>Q13561</u></b>	dynactin subunit 2	<b><u>DCTN2</u></b>	N/D
<b><u>Q14203</u></b>	dynactin subunit 1	<b><u>DCTN1</u></b>	BX7B (3)
<b><u>Q14697</u></b>	glucosidase II alpha subunit	<b><u>GANAB</u></b>	N/D
<b><u>Q15506</u></b>	sperm autoantigenic protein 17	<b><u>SPA17</u></b>	N/D
<b><u>Q16543</u></b>	cell division cycle 37	<b><u>CDC37</u></b>	BX7B (1)
<b><u>Q16563</u></b>	synaptophysin like 1	<b><u>SYPL1</u></b>	N/D
<b><u>Q3LXA3</u></b>	triokinase and FMN cyclase	<b><u>TKFC</u></b>	N/D
<b><u>Q5VZ72</u></b>	IZUMO family member 3	<b><u>IZUMO3</u></b>	BX7B (1)
<b><u>Q6BCY4</u></b>	cytochrome b5 reductase 2	<b><u>CYB5R2</u></b>	N/D
<b><u>Q7L266</u></b>	asparaginase like 1	<b><u>ASRGL1</u></b>	N/D
<b><u>Q7Z6W1</u></b>	transmembrane and coiled-coil domains 2	<b><u>TMCO2</u></b>	BX7B (1)
<b><u>Q86VQ3</u></b>	thioredoxin domain containing 2	<b><u>TXNDC2</u></b>	N/D
<b><u>Q86Y82</u></b>	syntaxin 12	<b><u>STX12</u></b>	N/D

<u>Q8IXA5</u>	<b>sperm acrosome associated 3</b>	<u>SPACA3</u>	<b>N/D</b>
<u>Q8IYT1</u>	family with sequence similarity 71 member A	<u>FAM71A</u>	BX7B (3)
<u>Q8N4E7</u>	ferritin mitochondrial	<u>FTMT</u>	BX7B (1)
<u>Q8NHS0</u>	DnaJ heat shock protein family (Hsp40) member B8	<u>DNAJB8</u>	BX7B (1)
<u>Q8TC56</u>	<b>family with sequence similarity 71 member B</b>	<u>FAM71B</u>	<b>BX7B (2)</b>
<u>Q8TDM5</u>	sperm acrosome associated 4	<u>SPACA4</u>	N/D
<u>Q8WW22</u>	DnaJ heat shock protein family (Hsp40) member A4	<u>DNAJA4</u>	N/D
<u>Q8WYR4</u>	radial spoke head 1 homolog	<u>RSPH1</u>	BX7B (2)
<u>Q96C74</u>	rhopilin associated tail protein 1 like	<u>ROPN1L</u>	N/D
<u>Q96JQ2</u>	calmin	<u>CLMN</u>	BX7B (3)
<u>Q96KW9</u>	sperm acrosome associated 7	<u>SPACA7</u>	N/D
<u>Q9BSF0</u>	chromosome 2 open reading frame 88	<u>C2orf88</u>	N/D
<u>Q9BVL2</u>	nucleoporin 58	<u>NUP58</u>	BX7B (1)
<u>Q9BX68</u>	histidine triad nucleotide binding protein 2	<u>HINT2</u>	N/D
<u>Q9BY14</u>	testis expressed 101	<u>TEX101</u>	N/D
<u>Q9H3G5</u>	carboxypeptidase, vitellogenic like	<u>CPVL</u>	N/D
<u>Q9H4B8</u>	dipeptidase 3	<u>DPEP3</u>	BX7B (1)
<u>Q9NQ60</u>	equatorin	<u>EQTN</u>	N/D
<u>Q9UBX1</u>	cathepsin F	<u>CTSF</u>	BX7B (2)
<u>Q9Y2B0</u>	canopy FGF signaling regulator 2	<u>CNPY2</u>	N/D
<u>Q9Y4L1</u>	hypoxia up-regulated 1	<u>HYOU1</u>	BX7B (3)
<u>Q8IZP2</u>	Putative protein FAM10A4	<u>ST13P4</u>	BX7B (1)

